University of Southampton

Faculty of Medicine

Human Development and Health

Microbiota-independent effects of galactooligosaccharide fibres on human peripheral blood mononuclear cells

By

Stefania Del Fabbro

Thesis for the degree of Doctor of Philosophy

January 2022

University of Southampton

Abstract

Faculty of Medicine

Human Development and Health

Thesis for the degree of Doctor of Philosophy

Microbiota-independent effects of galactooligosaccharide fibres on human peripheral blood mononuclear cells

Galactooligosaccharides (GOS) are prebiotic fibres known for their role in supporting intestinal health through modulation of the gut microbiota. GOS reach the colon intact and are fermented by commensal bacteria, resulting in the production of short-chain fatty acids with immunomodulatory properties. Supplementation with GOS is associated with reduced symptoms of gastrointestinal disorders and lower systemic and mucosal inflammation.

Prebiotics may bypass the gut barrier in individuals with pathologies that disrupt gut permeability (*e.g.* inflammatory bowel diseases, IBD) as well as in healthy subjects exposed to life-style associated stressors, and directly interact with intestinal and systemic immune cells. Among these cells, mucosal-associated invariant T (MAIT) cells play a key role in immune surveillance. Alterations in their blood frequencies and functions have been linked with inflammatory diseases, including IBD. More evidence is needed to understand whether GOS affect immunity solely via their prebiotic action on the microbiota or whether they also directly interact with immune cells.

The research described in this thesis investigates the effects of GOS upon phenotypes, soluble mediators, activation markers and toll-like receptors of *ex-vivo* peripheral blood mononuclear cells (PBMCs) and MAIT cells from healthy donors and those with IBD. Commercially available GOS (B-GOS®), which contain whole GOS as well as free sugars deriving from GOS production, and pure isolated GOS fractions were tested either alone or in combination with other inflammatory stimuli.

GOS consistently exerted anti-inflammatory effects on healthy PBMCs when combined with other immune challenges (riboflavin metabolite, lipopolysaccharide or polyinosinic:polycytidylic acid), as measured by a reduction in the levels of both pro-inflammatory mediators and activation markers. IBD PBMCs failed to respond to stimulation with a selected inflammatory stimulus (riboflavin metabolite) co-administered with GOS which is likely to relate to their significantly

higher baseline inflammation compared to healthy PBMCs. These data highlight the importance of performing donor immunophenotyping before assessing the effects of GOS on diseased donors.

When tested alone, GOS exerted direct immunomodulatory effects on healthy PBMCs and IBD PBMCs by enhancing the activation of T helper cells and by inducing the secretion of a wide range of anti-inflammatory as well as pro-inflammatory mediators. The effects of GOS were chain-length dependent, with fractions at lower degree of polymerisation inducing the strongest responses. The residual free sugars contained in B-GOS® displayed pro-inflammatory effects such as an increase in CD69 expression and IL-8 secretion by both healthy monocytes and IBD monocytes. These results suggest that the amount of free sugars present in commercially available prebiotics should be minimised to avoid pro-inflammatory responses by *ex-vivo* immune cells. Although further research is required to identify the pathways of GOS signalling, no involvement of toll-like receptor 4 was identified. Based on secreted cytokine data and activated cells, a mechanism via toll-like receptor 2 is proposed. Overall, this research confirms for the first time that GOS exert immunological effects on *ex-vivo* adult PBMCs with mechanisms that are independent from the action of the gut microbiota, and provide an insight into the cell types and potential pathways involved in their action.

By

Stefania Del Fabbro

Table of Contents

Table of Tables

Table of Tables

Table of Tables

Table of Figures

Table of Figures

Table of Figures

Table of Figures

Research Thesis: Declaration of Authorship

Print name: Stefania Del Fabbro

Title of thesis: Microbiota-independent effects of galactooligosaccharide fibres on human peripheral blood mononuclear cells

I declare that this thesis and the work presented in it are my own and has been generated by me as the result of my own original research. I confirm that:

1. This work was done wholly or mainly while in candidature for a research degree at this University;
2. Where any part of this thesis has previously been submitted for a degree or any other qualification at this University or any other institution, this has been clearly stated;
3. Where I have consulted the published work of others, this is always clearly attributed;
4. Where I have quoted from the work of others, the source is always given. With the exception of such quotations, this thesis is entirely my own work;
5. I have acknowledged all main sources of help;
6. Where the thesis is based on work done by myself jointly with others, I have made clear exactly what was done by others and what I have contributed myself;
7. Parts of this work have been published as:

Del Fabbro S, Calder PC, Childs CE. (2020) Microbiota-independent immunological effects of non-digestible oligosaccharides in the context of inflammatory bowel diseases. Proc Nutr Soc, 1-11.

Del Fabbro S, Calder PC, Childs CE. (2021) Galactooligosaccharide fibres exert immunomodulatory properties and interfere with riboflavin derivatives in an *ex-vivo* study. Proc Nutr Soc.

Del Fabbro S, Calder PC, Childs CE. (2018) Immunological effects of prebiotic B-GOS® on adult peripheral blood mononuclear cells. XI International Conference on Immunonutrition 2018: ISIN. Ann Nutr Metab 73, 184-226.

Signature: ..... Date:.....

Acknowledgements

Firstly, I would like to thank my supervisors Caroline Childs and Philip Calder for believing in me from the start and for giving me the opportunity to work at this project. Caroline, I am extremely grateful for the endless support I received from you throughout my PhD. Thanks for always being there when I needed, for sharing your expertise with generosity and for your contagious optimism. You taught me so much by being an excellent role model. I always felt happier and more motivated after a chat with you. Philip, a special thanks for always finding the time for a meeting with me, for your insightful feedbacks and for teaching me to never forget 'the bigger picture'. Thanks for being there the first time I presented at a conference, it meant a lot to me.

I would also like to thank Clasado Biosciences for the financial support to this project. Lucien Harthoorn and Aleksandra Maruszak, I am grateful for all the trust you gave me throughout the PhD and I very much enjoyed collaborating with you. A special thanks to Nicola Englyst and Judith Holloway for letting me use the Attune NxT flow cytometer and to the WISH lab for the help with the Bioplex machine. Thank you to Christopher Byrne and Jaswinder Sethi for the opportunity to work at the INSYTE study.

Many thanks to all my colleagues within the Nutrition & Metabolism Group, and in particular to Annette for always being helpful in the lab, to Ella for looking at my data, making me laugh and being a good friend, to Vivian, Loreana and Noora for making my time in Southampton much more enjoyable and to Liset, for being an excellent Master's student and offering to help when things were hectic. A special thanks to Luke and Josie for kindly offering to host me during the last phases of my PhD. You are wonderful friends and I really had a great time living with you! I would also like to thank Liz for always being kind and supportive; Chris, for all our chats in the lab; Carina and Helena, for always being there when I needed; Lucinda, Melissa, Adrian and Kate for their technical help.

I would also like to thank Michelle and Sponge for all practical and emotional support, you have become my Southampton family and I will never forget the time spent together! A special thanks goes to all my friends in the UK, Belgium and Italy, and in particular to Eliana for always being present even if far away.

Grazie di cuore alla mia famiglia per tutti i sacrifici fatti affinchè io avessi un'ottima istruzione, per avermi lasciata libera di inseguire le mie passioni ed essermi sempre stata vicina durante questo percorso. Grazie ad Antonia e Gianni per aver sempre creduto in me ed avermi appoggiata in ogni

scelta. Un grazie speciale a Moreno per essermi stato vicino durante uno dei periodi più stressanti del dottorato.

Finally, I would like to express my deepest gratitude to my wonderful husband Mattia. You have been the best partner and mentor that I could ever have imagined. Thanks for all the love and support you gave me, and for believing in me when I was doubting myself. Thanks for teaching me that with the right attitude, perseverance and hard work anything can be achieved. You are the most amazing listener and motivator and I would not have completed this work without you.

Definitions and Abbreviations

AOS	Arabinooligosaccharide
APC	Antigen-presenting cell
APC-R700	Allophycocyanin-R700
ASD	Autism spectrum disorder
BB (515/700)	BD Horizon Brilliant™ blue (515/700)
BCP	B cell progenitor
BCR	B cell receptor
B-GOS®	Bimuno® galactooligosaccharides
BSA	Bovine serum albumin
BV(421/450/510/605/650/711)	Brilliant™ violet (421/450/510/605/650/711)
Caco-2 cells	Continuous line of heterogeneous human epithelial colorectal adenocarcinoma cells
CBMC	Cord blood mononuclear cell
CBTC	Cord blood T cell
CCL	Chemokine ligand
CCR	Chemokine receptor
CD	Cluster of differentiation
CD62L	L-selectin
CKD	Chronic kidney disease
CLP	Common lymphoid progenitor
CLR	C-type lectin receptor
CMP	Common myeloid progenitor
Con A	Concanavalin A
CRP	C-reactive protein
CXCL	C-X-C motif ligand
DAMP	Damage-associated molecular pattern
DC	Dendritic cell
DMSO	Dimethyl sulfoxide
DN	Double negative

DP	Double positive
ENA-78/CXCL5	Epithelial neutrophil activating peptide/ C-X-C motif chemokine 5
EU	Endotoxin unit
FAE	Follicle-associated epithelium
FBS	Foetal bovine serum
FDA	Food and Drug Administration
FGF basic	Basic fibroblast growth factor
FITC	Fluorescein isothiocyanate
FOS	Fructooligosaccharide
FMO	Fluorescence minus one
FSC	Forward scatter
FVS (510/780)	BD Horizon™ Fixable Viability Stain (510/780)
GALT	Gut-associated lymphoid tissue
G-CSF	Granulocyte colony-stimulating factor
GOS	Galactooligosaccharide
GM-CSF	Granulocyte-macrophage colony-stimulating factor
GMO	Goat-milk oligosaccharide
GMP	Granulocyte/macrophage progenitor
GRO	Growth-related oncogene
HAT	Hypoxanthine aminopterin thymidine
HEPES	4-(2-hydroxyethyl)-1-piperazineethanesulfonic acid
HMO	Human milk oligosaccharide
HUVEC	Human umbilical vein endothelial cells
IBD	Inflammatory bowel diseases
IBS	Irritable bowel syndrome
IEC	Intestinal epithelial cell
IEL	Intraepithelial lymphocyte
IFN	Interferon
Ig	Immunoglobulin

ILF	Isolated lymphoid follicles
IL-	Interleukin
IRF	Interferon regulatory factor
IQR	Interquartile range
KLRG-1	Lectin-like receptor subfamily G member 1
LAL assay	Limulus amoebocyte lysate assay
LBP	LPS-binding protein
lcFOS	Long chain fructooligosaccharides
LPS	Lipopolysaccharide
LRR	Leucine-rich-repeat
M cell	Microfold cell
MAdCAM-1	Mucosal addressin cell adhesion molecule 1
MAIT	Mucosal-associated invariant T (cell)
MALT	Mucosal-associated lymphoid tissue
MAPK	Mitogen-activated protein kinase
MCP-1/CCL2	Monocyte chemoattractant protein-1/chemokine (C-C motif) ligand 2
MDM	Monocyte-derived macrophage
MD-2	Myeloid differentiation factor-2
MEP	Megakaryocyte/erythrocyte progenitor
MG	Methylglyoxal
MHC	Major histocompatibility complex
MIP-1α/CCL3	Macrophage inflammatory protein 1-alpha/chemokine (C-C motif) ligand 3
MIP-1β/CCL4	Macrophage inflammatory protein 1-beta/chemokine (C-C motif) ligand 4
MLN	Mesenteric lymph node
Mo-DC	Monocyte derived dendritic cell
MOS	Mannanooligosaccharide
MR1	Major histocompatibility complex-related protein 1
MyD88	Myeloid differentiation primary-response protein 88

NDO	Non-digestible oligosaccharide
NF-κB	Nuclear factor kappa-light-chain enhancer of activated B cells
NK cells	Natural killer cells
NKT cells	Natural killer T cells
NLR	Nucleotide-binding oligomerisation domain-like receptor
OOR	Out of range
pNA	P-nitroaniline
PAMP	Pathogen-associated molecular pattern
PBMC	Peripheral blood mononuclear cell
PBS	Phosphate-buffered saline
PE	Phycoerythrin
PerCP-Cy®5.5	Peridinin chlorophyll protein complex-cyanine® 5.5
PE-Cy 7®	Phycoerythrin-cyanine 7®
PHSC	Pluripotent haematopoietic stem cells
PI	Propidium iodide
PKC	Protein kinase C
PMA	Phorbol 12-myristate 13-acetate
PMB	Polymyxin B
Poly(I:C)	Polyinosinic-polycytidylic acid
POS	Pectic oligosaccharide
PP	Peyer's patch
PRR	Pattern recognition receptor
RANTES/CCL5	Chemokine (C-C motif) ligand 5
REC	Research Ethics Committee
RLR	Retinoic acid-inducible gene-1 like receptor
RL-6-Me-7-OH	7-hydroxy-6-methyl-8-ribityllumazine
RL-6,7-diMe	6,7-dimethyl-8-ribityllumazine
ROS	Reactive oxygen species
RPMI	Roswell Park Memorial Institute (medium)

rRL-6-CH_2OH	Reduced 6-(hydroxymethyl)-8-ribityllumazine
scGOS	Short chain galactooligosaccharide
SCFA	Short chain fatty acid
SD	Standard deviation
SI	Separation index
SSC	Side scatter
Streptavidin-PE	Streptavidin-phycoerythrin
TCA	T cell activator via binding to CD3 CD8 CD2
TB	Trypan blue
TJ	Tight junction
TCM	Central-memory T (cell)
TCR	T cell receptor
TEM	Effector-memory T (cell)
TGF-β	Transforming growth factor beta
Th	T helper (cell)
TIR	Toll/IL-1 receptor
TLR-	Toll-like receptor-
TNF-	Tumour necrosis factor-
TNKP	T cell and natural killer progenitor
TRIF	TIR domain-containing adaptor inducing IFN-β
VEGF-A	Vascular endothelial growth factor A
XOS	Xylooligosaccharide
5-OE-RU	5-(2-oxoethylideneamino)-6-D-ribitylaminouracil
5-OP-RU	5-(2-oxopropylideneamino)-6-D-ribitylaminouracil

Chapter 1 INTRODUCTION AND LITERATURE REVIEW

1.1 General statement

The positive role of prebiotics in supporting gut health via modulation of the intestinal microbiota is well understood. Prebiotics are dietary fibres that reach the colon intact and are fermented by commensal bacteria, resulting in the production of short chain fatty acids with immunomodulatory properties. Alongside the known microbiota-mediated effects, prebiotics may directly interact with immune cells in the gut-associated lymphoid tissue as well as with systemic immune cells, particularly in individuals with gut barrier disruptions.

This project investigates whether prebiotic galactooligosaccharides exert any direct immunological effects on peripheral blood mononuclear cells from healthy donors and inflammatory bowel disease donors. The effects of galactooligosaccharide fibres upon phenotypes, soluble mediators, activation markers and toll-like receptors will be investigated in detail.

To the aim of the study, this literature review will provide a general overview of the immune system, including a description of its main organs and cells. A greater insight on gut immunity, mucosal-associated invariant T cells and the gut microbiota will be given. Information on prebiotic fibres including sources, structures, mechanisms of action and potential use as a support therapy in inflammatory bowel diseases will be provided. The mechanisms of action of prebiotics, and in particular of galactooligosaccharides, through modulation of the gut microbiota and through direct interaction with immune cells will be discussed.

1.2 The immune system

1.2.1 Innate and adaptive immunity

The main function of the immune system is to defend the body against external challenges, such as pathogenic bacteria, viruses and parasites, or internal threats, such as malignant and auto-reactive cells formed within the body. The first line of defence against pathogens is the innate immune system, which includes physical and chemical barriers as well as specialised innate cells. Skin, mucus layers and tight junctions between epithelial cells all constitute physical barriers that block the entrance of pathogens. Defensins released by innate cells and epithelial cells bind to the cell membrane of microbes and create pores that cause the efflux of ions and nutrients,

ultimately resulting in their cell death. If microbes evade these barriers, for example by adhering to the epithelial barrier and degrading its structure, innate cells called antigen-presenting cells (APCs) are able to quickly recognise, present and destroy pathogen structures called pathogen-associated molecular patterns (PAMPs).

Molecular structures deriving from foreign compounds or generated inside the body that trigger adaptive immunity are called antigens. APCs (*e.g.* macrophages and dendritic cells, DCs) engulf exogenous antigens in a process called phagocytosis, break them down into smaller fragments and load them onto major histocompatibility complex (MHC) class II molecules that then migrate to their cell surface. Digested antigens are presented to the receptor of adaptive immune cells, such as T helper cells, which become activated and stimulate macrophages, B cells and cytotoxic T cells to eliminate the pathogenic fractions. Antigens generated within the body, such as cancer cells or virus-infected cells, are recognised by cytotoxic T cells following interaction with MHC class I molecules and destroyed by their release of cytotoxic compounds.

While the innate immunity provides a rapid (within hours) and unspecific response to external and internal threats, the adaptive immunity requires up to 10 days to become fully activated and to generate antigen-specific adaptive cells (effector cells). While innate cells recognise structures shared by many pathogens, adaptive cells recognise specific antigen sequences. After encountering the antigen for the first time, some antigen-stimulated adaptive cells differentiate into long-lived memory cells. Immune memory allows the host to respond more quickly and effectively in case of a second infection by the same agent.

1.2.2 Discrimination between self and non-self: PAMPs and PRRs

If antigens break through the host's barriers, innate cells recognise pathogen's structures via their surface receptors and cytoplasmic sensors called pattern recognition receptors (PRRs). PRRs are mainly expressed on DCs, macrophages, monocytes and neutrophils but also present on lymphocyte subsets [1] and have the function to identify pathogen-associated molecular patterns (PAMPs) or damage-associated molecular patterns (DAMPs). A PAMP is a conserved molecular structure present in many pathogenic microbes, including bacteria, viruses and fungi, able to induce an immune response. PAMPs are often structural components of the microorganism's cell wall and include, for example, lipopolysaccharide (LPS), peptidoglycan and β-glucan [2]. DAMPs are, instead, intracellular molecules released by damaged tissues or dying cells. They can be of protein origin, such as the heat-shock proteins produced by cells in response to stress, or non-protein origin, such as purine metabolites (*e.g.* adenosine) released by damaged cells [3].

There are several classes of PRRs, including toll-like receptors (TLRs), C-type lectin receptors (CLRs), nucleotide-binding oligomerisation domain-like receptors (NLRs) and retinoic acid-inducible gene (RIG)-1 like receptors (RLRs), which differ in terms of localisation, ligands that they recognise and type of pathways activated [4]. Further information on PRRs in general [5] and on CLRs [6], NLRs [7] and RLRs [8] are available elsewhere.

TLRs are transmembrane proteins that recognise structures from exogenous pathogens or from infected cells. In humans, there are 10 types of TLRs (TLR1 – TLR10) classified upon their localisation. TLRs expressed on the cell surface of immune cells are TLR1, TLR2, TLR4, TLR5, TLR6, TLR10, while TLRs localised intracellularly in endosomes are TLR3, TLR7, TLR8, TLR9 [9]. While surface TLRs recognise lipids, proteins or carbohydrates found on the cell membranes of microbes, intracellular TLRs sense viral and bacterial nucleic acids. Table 1.1 provides an overview of the 10 human TLRs, including their location, ligands and expression on immune cells.

Table 1.1 Human TLRs and their location, ligands and expression on immune cells [1, 10].

TLR	**Location**	**Ligand**	**TLR-expressing immune cell**
TLR1	Cell surface	Triacyl lipoprotein from bacteria	B cells, DCs
TLR2	Cell surface	Lipoprotein from bacteria, viruses, parasites	DCs, monocytes, T cells
TLR3	Intracellular	Double-stranded RNA from viruses	DCs, NK cells, T cells
TLR4	Cell surface	LPS from Gram-negative bacteria	DCs, macrophages, T cells
TLR5	Cell surface	Flagellin from bacteria	DCs, monocytes, NK cells, T cells
TLR6	Cell surface	Diacyl lipoprotein from bacteria and viruses	B cells, DCs
TLR7	Intracellular	Single-stranded RNA from bacteria and viruses	B cells, DCs, monocytes, T cells
TLR8	Intracellular	Single-stranded RNA from bacteria and viruses	DCs, monocytes
TLR9	Intracellular	Double-stranded DNA from bacteria and viruses	B cells, DCs, macrophages, NK cells
TLR10	Cell surface	Unknown	B cells

TLRs are constituted by an ectodomain with leucine-rich repeats (LRRs) specific for PAMP recognition and comprising glycan moieties that serve as a binding site for ligands, a trasmembrane domain with a role in signal transduction and a cytoplasmic toll/IL-1 receptor (TIR) domain involved in the initiation of downstream signalling [11]. Once the PAMP is bound to the TLR, adaptor molecules containing the TIR domain are recruited to ensure functional signalling. These include the myeloid differentiation primary-response protein 88 (MyD88) and the TIR domain-containing adaptor inducing IFN-β (TRIF). All receptors except TLR3 use the MyD88-dependent pathway, which ultimately leads to the activation of nuclear factor kappa-light-chain enhancer of activated B cells (NF-κB) that promotes the release of pro-inflammatory cytokines and chemokines (*e.g.* TNF-α, IL-1β, IL-6, IL-8 and IL-10). TLR3, but also TLR4, use the TRIF-dependent pathway that activates interferon regulatory factors (IRFs) resulting in the secretion of type I interferons (IFNs) [11].

LPS is a component of the outer membrane of Gram-negative bacteria with a role in protecting the microorganism's cell against dangerous substances. The name LPS refers to the structure of this endotoxin, which is made by a lipid portion called lipid A, a core oligosaccharide, and an O-polysaccharide chain called O-antigen (Figure 1.1) [12, 13].

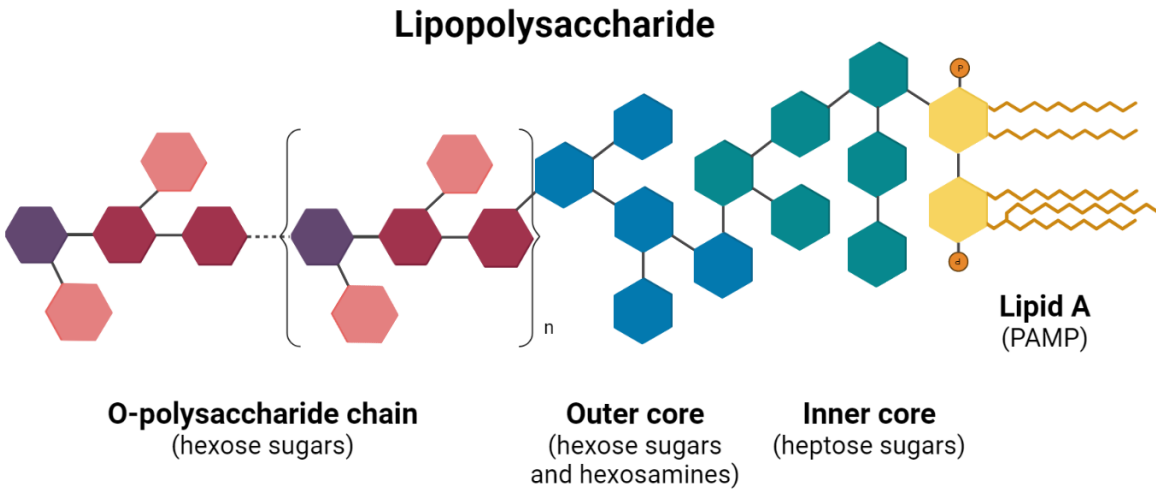

Figure 1.1 Structure of lipopolysaccharide (LPS) from Gram-negative bacteria.

LPS is made by a lipid fraction bound to a saccharide fraction. The endotoxicity of the molecule is given by lipid A (PAMP), which is linked to a highly conserved core made by oligosaccharides and a more variable polysaccharide chain.

The endotoxic activity of LPS is given by the lipid A portion, which is a PAMP recognised by TLR4 [14]. The saccharide fraction of the molecule is made by a core, constituted by heptose sugars (inner core), hexose sugars and hexosamines (outer core), and by an O-polysaccharide chain made by common hexoses. This latter is involved in the activation and responsiveness of innate immune cells, and its composition is highly variable amongst Gram-negative species [15]. The sugars constituting the outer core are primarily hexose sugars such as glucose, mannose, galactose, N-acetyl galactosamine and N-acetyl glucosamine and have a role in modulating the activity and endotoxicity of lipid A [16].

LPS is first recognised in serum by the soluble acute phase protein LPS binding protein (LBP), which binds to the lipid A moiety and enhances the response of immune cells expressing the cluster of differentiation (CD) 14 to LPS. LBP transports LPS to CD14, which in turn mediates the transfer of LPS to the TLR4/myeloid differentiation factor 2 (MD-2) receptor complex [17, 18]. MD-2 is a protein that associates with TLR4 to allow functional downstream signalling via MyD88-dependent or MyD88-independent pathways, resulting in the secretion of pro-inflammatory mediators (*e.g.* TNF-α, IL-1β, IL-6, IL-8 and IL-10) or IFNs, respectively [19]. As a consequence of cytokine release, LPS enhances the expansion of T cells and their differentiation into effector cells and upregulates the expression of the activation markers CD25 and CD69 on their surface [15, 20]. Specific TLR are also able to recognise a wider range of ligands following a process called heterodimerisation. This refers to the formation of a complex between different types of receptors [21]. For example, the CLR dectin-1 expressed on DCs, monocytes and T cells and involved in the recognition of carbohydrates (β-glucans) interacts with TLR2 and TLR4 to amplify their cytokine production [22].

PRRs are not only present as cell receptors on the surface or within the endosomes of immune cells, but are also found as soluble receptors in blood. These are referred to as the complement system, which include around 20 proteins that are activated in a cascade sequence. Complement proteins are responsible for the binding of pathogens, lysis of bacteria, recruitment of phagocytes and stimulation of immune cells. There are three pathways of complement activation, namely the classical pathway (triggered by antigen-antibody binding), the lectin pathway (activated by mannose-lectin reactions) and the alternative pathway (started by polysaccharides from pathogens). After a series of cascade proteolytic reactions, C3a, C3b, C5, C6, C7, C8 and C9 molecules are produced. These peptides promote inflammation by attracting other immune cells (chemotaxis) and by forming pores in bacterial membranes, leading to elimination of the pathogen [23]. An example of complement activation via the classical pathway is that induced by C-reactive protein (CRP) produced by liver cells and immune cells (*e.g.* macrophages,

lymphocytes) in response to inflammation. Binding of CRP to microbial structure or to ligands on damaged cells results in complement activation and phagocytosis [24].

Molecular patterns recognised by PRRs are often present not only on pathogens, but also on commensal bacteria. While it is unclear whether and how PRRs alone distinguish between the two groups, tolerance mechanisms are in place to ensure that an inflammatory response is mounted only against pathogens. A clear example is the downregulation of TLR4 and MD-2, which are both needed for a correct response to LPS, on intestinal epithelial cells (IECs). Since IECs are constantly exposed to host microbiota and food antigens, constant inflammation is avoided by reducing their responsiveness to LPS [25]. While commensals do not normally cross the intestinal epithelium, pathogens break through the gut barrier exploiting their virulence factors and are recognised by TLRs expressed on immune cells of the lamina propria, which initiate protective pro-inflammatory responses [26]. The discrimination between self (host) and non-self (foreign) is pivotal for the maintenance of body homeostasis. Failure to distinguish self from non-self often results in auto-immune diseases, which are characterised by the presence of auto-reactive T cells that bind to self-antigens and, once activated, lead to the destruction of the host healthy tissues [27]. Type 1 diabetes mellitus is an example of auto-immune disease where auto-reactive T helper cells and cytotoxic T cells drive the loss of insulin-producing β cells [28].

1.2.3 Organs of the immune system

The main role of immune organs is to orchestrate the production, maturation and function of immune cells. Immune organs are classified in primary lymphoid organs, which are sites of lymphocyte formation and maturation, and secondary lymphoid organs, which are where mature lymphocytes interact with antigens. Primary lymphoid organs are the bone marrow and the thymus, whereas secondary lymphoid organs are the spleen, lymph nodes and mucosal-associated lymphoid tissue (MALT) [29]. The bone marrow is a spongy tissue that contains hematopoietic stem cell from which all immune cells are generated. It is also the site where B cells undergo maturation, as opposed to T cells that mature in the thymus [30]. The thymus is a gland made by two lobes, each one presenting an external cortex and an inner medulla where different steps of T cell maturation occur [31]. These include processes called positive and negative selection. The spleen is a secondary lymphoid organ located in the abdomen. It has the function of identifying infections in blood, removing old red blood cells and storing platelets. Antibody-producing lymphocytes and monocytes formed in primary lymphoid organs are stored in the spleen and have a role in detecting and eliminating blood antigens. Another secondary lymphoid organ is constituted by the lymph nodes, which are clusters of lymphoid tissue located throughout the body and functioning as lymphatic fluid filters. Immune cells contained within the

lymph nodes, such as T cells, B cells, macrophages and DCs, detect and eliminate pathogens carried in the lymph [32]. Secondary lymphoid organs include the MALT, which are a diffuse system of lymphoid tissue distributed throughout mucosal membranes. The primary role of MALT is to provide immune defence against antigens that enter the body following inhalation or ingestion. According to their location in the body, different MALTs can be distinguished: bronchus-associated lymphoid tissue, nasal-associated lymphoid tissue, salivary gland duct-associated lymphoid tissue, conjunctiva-associated lymphoid tissue, lacrimal duct-associated lymphoid tissue and gut-associated lymphoid tissue [33].

1.2.4 Cells of the immune system

Pluripotent haematopoietic stem cells (PHSC) are immature cells in the bone marrow that differentiate into all types of blood cells, including red blood cells (erythrocytes), white blood cells (leukocytes) and platelets. From a PHSC, a common myeloid progenitor (CMP) and a common lymphoid progenitor (CLP) are generated. From the CMP, a megakaryocyte/erythrocyte progenitor (MEP) and a granulocyte/macrophage progenitor (GMP) are formed. Erythrocytes and platelets are produced from the MEP, while monocytes and granulocytes are generated from the GMP. From the CLP, a T cell and natural killer (NK) cell progenitor (TNKP) as well as a B cell progenitor (BCP) are formed. The main cell types resulting from the haematopoietic process are summarised in Figure 1.2.

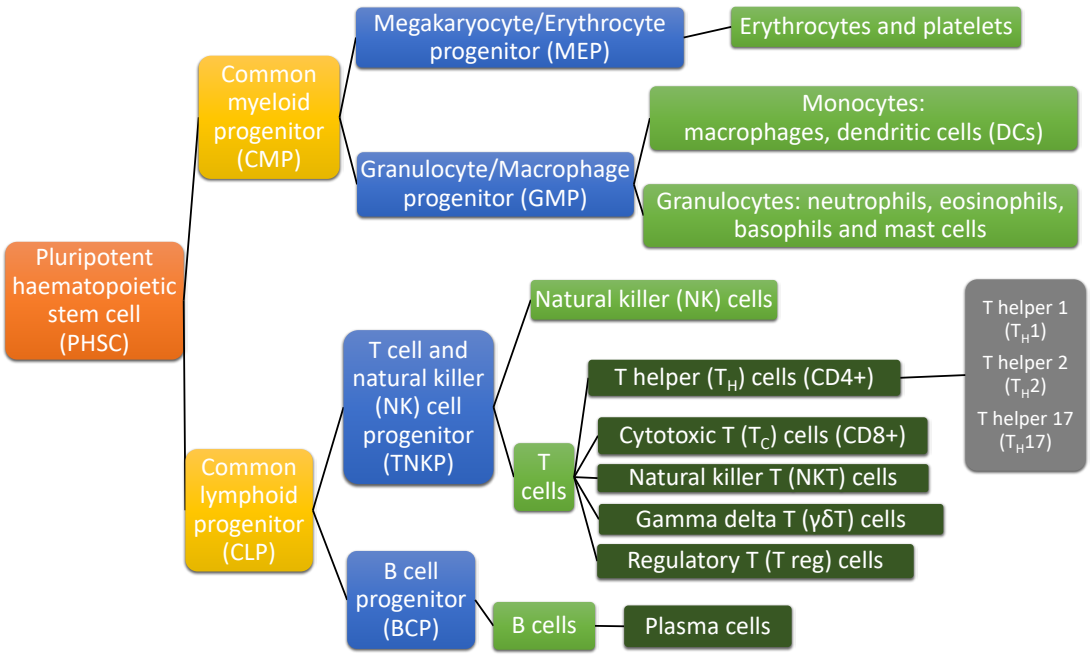

Figure 1.2 Cells deriving from pluripotent hematopoietic stem cells (PHSC).

Innate cells

Innate cells comprise granulocytes (neutrophils, eosinophils, basophils and mast cells), monocytes (macrophages and myeloid lineage DCs) and a subset of lymphocytes called natural killer (NK) cells [23, 31, 34-36].

Granulocytes

Granulocytes are named after the granules located in their cytoplasm. These vesicles contain antimicrobial molecules such as lysozyme, acid hydrolases and defensins. The largest group of granulocytes is constituted by neutrophils, which are the first players in the early immune response. Neutrophils are short-lived cells rapidly recruited from the blood to the site of infection by macrophages, soluble proteins with chemoattractant properties and PAMPs. Neutrophils engulf and kill pathogens by forming a structure called 'phagolysosome', which contains proteases and lipases as well reactive oxygen species (ROS). The presence of hydrolytic enzymes together with the release of high levels of ROS (respiratory burst) creates an inhospitable environment for the pathogens, ultimately leading to their death. Neutrophils also trap microbes in a sticky net by ejecting their own chromatin, in a process that causes the elimination not only of the pathogen but of the neutrophil itself. Mast cells and basophils are similar cells expressing immunoglobulin E (IgE) receptors on their surface. IgE are antibodies secreted by plasma cells (activated B cells) in response to parasitic infections. After IgE binding to the the IgE receptor and its cross-linking with the antigen, signals are sent for the release of histamine by mast cells and basophils. Histamine affects blood vessel dilation and allows the recruitment of other immune cells to the infected tissue. Uncontrolled immune responses to IgE are often seen in allergies (*e.g.* asthma).

Monocytes

Monocytes are nucleated cells that are classified into three subsets based on their cell surface receptors, namely $CD14^{++}CD16^{-}$ (classical monocytes), $CD14^{dim}CD16^{++}$ (non-classical monocytes) and $CD14^{++}CD16^{+}$ (intermediate monocytes) [37]. The most represented group in human blood, which constitutes up to 90% of peripheral blood monocytes, is the classical subset. This latter is distinguished from the other subsets for the secretion of high levels of IL-1β, IL-6, IL-8 and TNF-α following TLR stimulation [38]. Monocytes exert phagocytic functions and, thanks to the expression of PRRs on their surface, recognise different types of PAMPs. They also express chemokine receptors that provide signals for their migration to the site of infection or inflammation, where they differentiate into monocyte-derived macrophages (MDMs) and monocyte-derived DCs (Mo-DCs) and secrete pro-inflammatory mediators that lead to the elimination of the pathogen and to the recruitment of other immune cells.

Natural killer (NK) cells

NK cells are generated from a lymphoid progenitor and present the same morphology as lymphocytes, but are classified within the innate arm of immunity because they lack antigen-specific cell surface receptors [39]. NK cells are phenotypically defined as $CD3^-$ $CD56^+$ lymphocytes and express a wide range of mediators, including IFN-γ, GM-CSF, TNF-α, IL-4, IL-10 and MIP-1β, which promote anti-viral activity and enhance adaptive immune responses. As their name implies, NK cells exert cytotoxic activity mainly through the release of perforin and IFN-γ and are involved in the recognition and elimination of virus-infected cells and tumour cells [40].

Adaptive cells

Lymphocytes, and specifically B cells and T cells, are the main players in adaptive immunity. An overview on the different classes and functions of lymphocytes is provided here. The main resources consulted for the description of B cells and T cells are [32] and [41-43], respectively. More information on T cell responses are available in [44-46].

B lymphocytes

B lymphocytes are the only immune cells able to express and secrete antibodies, also called immunoglobulins (Igs). There are five types of Igs in humans, namely IgA, IgD, IgE, IgG and IgM. Their main function is to bind and coat pathogens for phagocytosis, a process known as opsonisation, and to activate complement proteins. Before being secreted, Igs are present on the cell surface of early-stage B cells functioning as B cell receptors (BCRs). They recognise antigens and present them to T cells, which in turn secrete cytokines that promote the maturation of B cells into plasma cells [23] IgD and IgM are the first antibodies acting as receptors on naïve B cells [36]. IgM is also present in a secreted form and it is involved in complement activation. Following a series of DNA rearrangements known as class switching, IgG, IgA and IgE are produced from IgM. IgG is the most abundant immunoglobulin in plasma [29, 32] and its function is to activate complement proteins and contribute to the opsonisation of pathogens. IgG is also responsible for passive immunity of the foetus, since some of its subsets are transported across the placenta and are secreted in mother's milk. IgA is localised in mucosal surfaces and found in secretion such as saliva and tears. It contributes to host defence against pathogens in the gastrointestinal, urogenital and respiratory tracts. IgA is found in human milk and provides passive immunity to newborns. IgE is present at very low levels in serum and is involved in immune responses to parasites and has a role in allergic disease.

B cells begin to mature in the bone marrow and then move into secondary lymphoid organs to complete the process. Within the spleen and lymph nodes, B cells become mature and start

expressing IgM and IgD. B lymphocytes that are localised in mucosal tissues differ from other B cells because they mainly express IgA, which plays a role in protection against microbes. B cells also express a B cell receptor (BCR) that allows them to bind to antigens. After antigen ligation, B cells multiply and differentiate into plasma cells, B cells which are able to produce Igs that then bind to pathogens leading to their neutralisation. Memory B cells are formed after antigen stimulation, resulting in a stronger immune response in case of a second infection by the same pathogen. Finally, B cells communicate with other immune cells, such as T helper cells, and recruit them to the site of infection.

T lymphocytes

T cells are transported from the bone marrow to the thymus to complete their development, which occurs via a process called thymopoiesis. During thymopoiesis, T lymphocytes differentiate into specialised cells expressing different cell surface markers (receptors and co-receptors). Cell surface markers are proteins or carbohydrates expressed on the cell membranes and having different roles, such as transporting/recognising molecules and mediating the communication with other immune cells. Lymphocytes are classified using cluster of differentiation (CD) nomenclature, which identifies cell types based on their cell surface molecules. Thymocyte progenitors do not express CD3, CD4 and CD8 cell surface markers and hence are defined triple negative. Following a process called β-selection, double positive ($CD4^+CD8^+$) population of lymphocytes expressing naïve T cell receptors (TCRs) are formed. T cell receptors are essential for the recognition of antigens by T cells following interaction with APCs.

TCRs are generated following molecular arrangements within the thymus. In the majority of T cells, TCRs are constituted by an α chain and a β chain, but around 5% of T cells, called gamma delta T cells, present TCRs made by a δ chain and a γ chain. Every chain presents two domains, one variable (V) and one constant (C). The variable region is the part of the receptor that binds to the antigen presented by the MHC on the surface of APCs. The TCR is also associated with accessory chains constituting the CD3 complex, made by the membrane proteins ε/δ and γ/ε and the ζ homodimer. Whilst the membrane proteins ε/δ and γ/ε play a role in sending intracellular signals for T cell activation, the ζ homodimer is an intracellular protein necessary for TCR expression and functioning. Figure 1.3 illustrates a TCR receptor made by αβ chains.

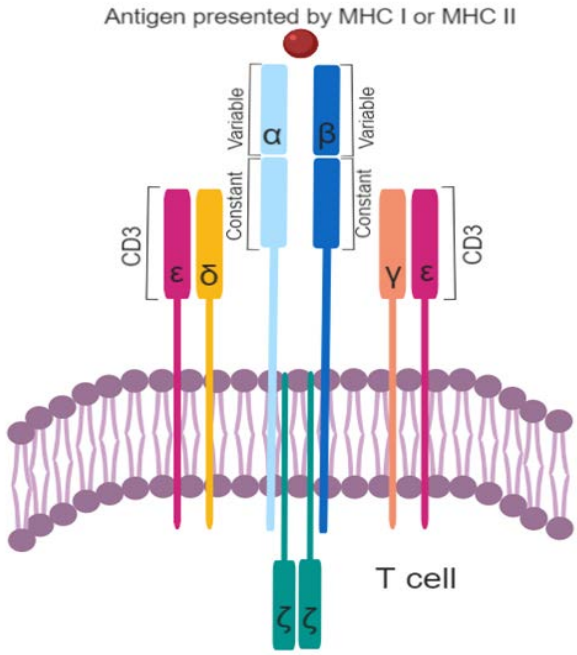

Figure 1.3 Structure of an αβ T cell receptor (TCR) expressed on T lymphocytes.The scheme depicts the interaction between the variable region of the TCR and an antigen presented by the major histocompatibility complex (MHC). Variable regions can either be present as α/β or γ/δ chains (here α/β TCR chains are displayed). The T cell receptor is associated with CD3 membrane proteins, which are required to send intracellular signals for cell activation. The ζ homodimer is an intracellular protein necessary for TCR expression and functioning. Created with BioRender (https://biorender.com/).

Additionally, CD4 and CD8 co-receptor molecules are found in association with the TCRs with the aim of increasing the sensitivity of T cells to the presented antigens. Following thymic selection of the functioning TCRs, single positive cells expressing either the co-receptor CD4 or the co-receptor CD8 are formed. T cells expressing the CD4 or CD8 co-receptors migrate from the thymus to the periphery as naïve T cells and differentiate into T helper cells ($CD4^+$), cytotoxic T cells ($CD8^+$) and regulatory T cells ($CD4^+$) after encountering their cognate antigens. Although T cell activation is initiated by the interaction between a ligand with the TLR, other co-stimulatory receptors (*e.g.* CD2 and CD28) are required for its full activation. CD2 is a glycoprotein expressed on T cells that binds to CD58 on the surface of APCs and reduces the minimum required affinity of the TCR for the antigen bound to the MHCs, thus enhancing T cell activation [47]. Similarly, the CD28 protein expressed on T cells interacts with the membrane protein B7 on APCs to provide a strong co-stimulatory signal that amplifies T cell activation [48]. Activated T cells present upregulated expression of the early activation marker CD69 in the 3–24 h after TCR-dependent activation and of the late activation marker CD25 in the 24–72 h after TCR-dependent activation [49].

CD4 and CD8 co-receptors interact with structurally different MHCs on the surface of APCs. MHC class I (expressed by all nucleated cells) presents viral antigens to cells bearing the CD8 co-receptor, whereas MHC class II (expressed on B cells, DCs, monocytes and macrophages) presents bacterial antigens to cells bearing the CD4 co-receptor. MHCs capture the antigens and expose them to the TCRs, which recognise different epitopes (specific part of the antigen that interacts with TCRs/antibodies) from the same antigen and mount an immune response. The specific interaction between MHC and CD4/CD8 co-receptors is important in determining the elimination of pathogens via cytotoxic activity, mediated by cytotoxic T cells, or through the recruitment of other immune cells, carried out by T helper cells. Whilst T helper cells recognise the antigens and communicate with phagocytes, cytotoxic T cells secrete cytotoxic compounds such as perforin and granzyme B that eliminate the foreign microbes. Regulatory T cells have a role in suppressing the immune responses and restoring the homeostasis. Following antigen elimination, memory T cells expressing CD45RO on their surface are formed. The CD45 family comprises several isoforms, which are similar forms of a protein produced from a single gene, including high molecular mass CD45RA and low molecular mass CD45RO. As naïve T cells become mature T cells or memory T cells, they start expressing CD45RO instead of CD45RA [50]. Memory cells are divided into central-memory T (TCM) cells and effector memory T (TEM) cells. While TCM cells present interleukin 7 (IL-7), chemokine receptor 7 (CCR7), adhesion markers CD44 and L-selectin (CD62L) on their surface, TEM cells express killer cell lectin-like receptor subfamily G member 1 (KLRG-1) molecule. These receptors assist T cells to mount a quicker immune response in case of re-infection from the same pathogen.

T helper cells are further classified in specialised subsets (Th1, Th2 and Th17) based on their function and ability to secrete soluble mediators. Th1 cells are involved in protection against intracellular bacteria and viruses and mainly secrete interferon gamma (IFN-γ), interleukin 2 (IL-2) and tumour necrosis factor alpha (TNF-α). Th2 cells are the main players in protecting the body from parasites. Their signature mediators are interleukin 4 (IL-4), interleukin 5 (IL-5) and interleukin 13 (IL-13), but they also produce TNF-α and interleukin 9 (IL-9). Th17 cells respond to extracellular bacteria and fungi and primarily secrete interleukin 17A (IL-17A), interleukin 17F (IL-17F) and interleukin 22 (IL-22). There is a degree of overlap among Th1, Th2 and Th17 subsets, which present flexibility in the types of mediators secreted. The balance between Th1, Th2 and Th17 responses is crucial in maintaining homeostasis. Alterations in Th1 and Th17 response have been associated with autoimmune diseases, whereas shifts towards a more pronounced Th2 response have been linked to allergies.

Natural killer T (NKT) cells are a subset of T cells showing similarities with NK cells and therefore classified in between the innate and adaptive immunity. They express CD3, CD16 and CD56 and

have a unique αβ TCR that allow them to interact with an unconventional MHC molecule called CD1d, which conversely to MHC (that binds to protein antigens) recognises lipid antigens.

1.2.5 Secreted mediators: cytokines, chemokines, growth factors and proteases

Cytokines, chemokines and growth factors are protein messengers secreted by immune and non-immune cells acting as a bridge between innate and adaptive immunity. They bind to cell receptors and initiate a cascade of signals that induce changes in gene regulation. These signals stimulate the differentiation, activation and movement of immune cells. Secreted mediators allow communication between cells and can have anti-inflammatory or pro-inflammatory effects. The balance between pro-inflammatory and anti-inflammatory mediators is important to maintain immunological homeostasis, and shifts in this balance are associated with allergies and auto-immune diseases. Generally, IFN-γ, IL-1, IL-6, IL-22, TNF-α, MCP-1, MIP-1α and RANTES are classified as pro-inflammatory, whereas IL-4, IL-10, IL-13 and TGF-β are considered anti-inflammatory [51]. Proteases are enzymes that break down the peptide bonds of proteins. An example of protease is granzyme B, which is found in the granules of NK cells and cytotoxic T cells. Granzyme B enters the cytoplasm of the target cells and induces cell death by apoptosis [52]. A summary of the main types of soluble mediators, their cell sources and functions are presented in Table 1.2.

Table 1.2 Cell sources and main functions of cytokines, chemokines, growth factors and proteases secreted by immune cells. Modified from [51].

Class		**Analyte**	**Function**
Cytokines	**Th1**	IL-1α	Activation of T cell, pro-inflammatory
		IL-1β	Activation of T cell, pro-inflammatory
		IL-2	Differentiation of T cells
		IFN-γ	Inhibition of virus replication, activation of macrophages, pro-inflammatory, anti-allergic
		TNF-α	Pyrogen, induction of apoptosis, anti-infectious, anti-tumour, pro-inflammatory, angiogenic
	Th2	IL-1ra	Antagonist of IL-1
		IL-4	Differentiation of B cells into plasma cells, B cell class switch to IgE, anti-inflammatory
		IL-5	Eosinophil differentiation factor, enhancement of IgA production
		IL-6	Support of B cell functions, mediator of fever, both anti- and pro-inflammatory
	Th1/Th2	IL-10	Anti-inflammatory
	Th17	IL-17A	Anti-microbial defence
Chemokines		CCL2/MCP-1	Chemotactic for monocytes
		CCL3/MIP-1α	Macrophage inflammatory protein
		CCL4/MIP-1β	Macrophage inflammatory protein
		CCL5/RANTES	Regulated upon activation, normal T cell expressed and secreted. Inflammatory
		CXCL5/ENA-78	Epithelial derived neutrophil attractant, angiogenic
		CXCL8/IL-8	Chemotactic, stimulation of angiogenesis, pro-inflammatory
Growth factors		FGF basic	Basic fibroblast growth factor, anti-infectious
		G-CSF	Granulocyte chemoattractant protein, anti-infectious
		GM-CSF	Granulocyte-macrophage colony-stimulating factor, anti-infectious
		VEGF-A	Vascular endothelial growth factor, angiogenic
Proteases		Granzyme B	Mediation of apoptosis in target cells

1.3 Immunity in the gut

1.3.1 The gut-associated lymphoid tissue

The gut-associated lymphoid tissue (GALT) is the largest immune organ of the body and its main function is to regulate immunity in the intestinal mucosa (Figure 1.4). The GALT protects the host from invading pathogens while showing tolerance to commensal bacteria and food antigens [53]. The GALT is found throughout the entire intestine and it is separated from the intestinal lumen by a layer of epithelial cells called follicle-associated epithelium (FAE), comprising enterocytes, goblet cells, Paneth cells and microfold (M) cells [54]. Enterocytes absorb nutrients from food and act as physical barriers against the entrance of pathogens. Enterocytes are kept in close contact between each other by tight junctions (TJs), which are proteins that regulate intestinal permeability. Goblet cells and Paneth cells prevent the breach of pathogens into the epithelial barrier by secreting mucins and antimicrobial compounds, respectively. M cells are responsible for sampling the luminal content and activating immune cells in the GALT [55, 56]. To do so, M cells phagocytose antigens in the lumen and transport them across the epithelial layer in a process called 'transcytosis'.

The GALT is constituted by different lymphoid tissues, including Peyer's patches (PPs), isolated lymphoid follicles (ILFs), intraepithelial lymphocytes (IELs) and mesenteric lymph nodes (MLNs). PPs, IELs and MLNs constitute important induction sites where T cells and B cells are activated in an antigen-specific manner and are transported through effector sites, such as the lamina propria [33]. PPs are organised aggregations of lymphoid follicles located in the small intestine. They contain DCs, follicle-compartmentalised B lymphocytes and T lymphocytes, which are in a naïve status before entering in contact with the antigens sampled by M cells. After thymic egress, lymphocytes are transported by the blood and lymph throughout the body and they enter the PPs localising in follicles (B cells) or outside the follicles (T cells and DCs). When M cells take up an antigen from the lumen, follicle associated epithelial cells secrete chemokines to attract DCs. DCs phagocyte the antigen and present it on their MHC to the lymphocytes, which become effector cells. Activated $CD4^+$ T cells and $CD8^+$ T cells, as well as effector B cells secreting IgA, also called plasma cells, are formed. Following secretion of retinoic acid by DCs, T and B lymphocytes start expressing homing receptors such as integrin $\alpha_4\beta_7$ and chemokine receptor 9 (CCR9). This means that lymphocytes, after being transported to other tissues via lymphatic circulation, home back to the lamina propria where integrin $\alpha_4\beta_7$ expressed on their surface binds to mucosal addressin cell adhesion molecule 1 (MAdCAM-1) found in intestinal venules. Similarly, CCR9 is a receptor found on the surface of lymphocytes that binds to chemokine ligand 25 (CCL25) on intestinal epithelial cells and allows the lymphocytes to home back to the intestinal mucosa [29, 31, 33, 57-59].

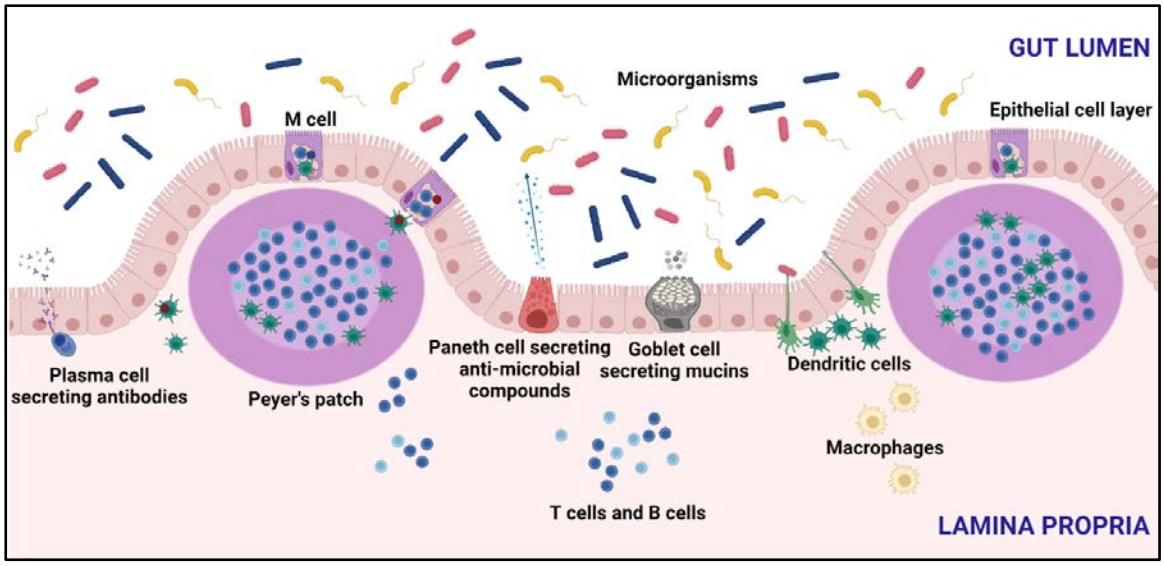

Figure 1.4 A schematic of the gut associated lymphoid tissue (GALT). Created with BioRender (https://biorender.com/).

1.4 Mucosal-associated invariant T (MAIT) cells

1.4.1 MAIT cell location and frequencies in humans

MAIT cells are an evolutionarily conserved subset of lymphocytes with putative crucial effects on both systemic and gut-associated immune systems. MAIT cells play a role in the defence against orally acquired pathogens and in the control of the gut immune responses. Alterations in their numbers are associated with a range of inflammatory disorders [60-63]. As their name suggests, MAIT cells are mainly found in mucosal tissues, such as the gut lamina propria and the respiratory tract mucosa. They are also found in kidney, lymphoid organs and in the liver [64]. In peripheral blood of healthy adults, the frequency of MAIT cells can vary widely, with values ranging from 0.19% to 21.7% (median 2.12%, IQR 0.25–14.7%) of total $CD3^{+}TCR\gamma\delta^{-}$ lymphocytes [65]. This is likely due to differences in age, as MAIT cell numbers rise steadily after birth until adulthood, and differences in gender, as women of reproductive age present higher MAIT cell numbers than men of the same age [66].

1.4.2 MAIT cell biology and phenotype

Unlike other adaptive cells and similarly to NKT cells, MAIT cells present a limited number of receptors and therefore recognise only restricted sets of antigens. This is due to the presence of a semi-invariant TCRα chain, made up by the invariant Vα 7.2 segment paired with the semi-invariant Jα 33, Jα 12 or Jα 20 domains [67, 68]. MAIT cells are considered a bridge between the innate and the adaptive immunity, and for this reason called innate lymphocytes. On one hand, they are capable of rapidly responding to immune challenge and recognise a limited variety of antigens, like innate immune cells. On the other hand, they express antigen receptors and present an effector-memory phenotype ($CD45RA^{-}$ $CD45RO^{+}$ $CD95^{hi}$ $CD62L^{lo}$), like adaptive immune cells [63, 64, 69].

Based on their cell surface receptors, MAIT cells are defined as $CD3^{+}$ Vα 7.2^{+} $CD161^{++}$ and are either $CD8^{+}$ or double negative (DN) $CD4^{-}CD8^{-}$ [70], with recent studies also identifying a minor proportion of $CD4^{+}$ MAIT cells (1.3%) and $CD4^{+}CD8^{+}$ (double positive, DP) MAIT cells (1.3%) [71]. MAIT cells also express the gut homing marker $\alpha_4\beta_7$ integrin, which indicates a preferential migration of MAIT cells from the periphery to the intestine [72]. MAIT cells are produced within the thymus and subsequently migrate to the periphery bearing a naïve phenotype ($CD45RA^{+}$ $CD27^{+}$) until they encounter B cells and commensal bacteria, which are required for their expansion in an antigen-dependent process [67, 73]. MAIT cells interact with the antigen presenting cell class-I like receptor called MHC-related protein 1 (MR1), which is ubiquitously expressed on many cell types including DCs, monocytes, macrophages, B cells and epithelial cells [74-76]. The MR1 presents antigens to MAIT cells, which recognise the specific ligands thanks to the expression of a TCR on their surface (Figure 1.5).

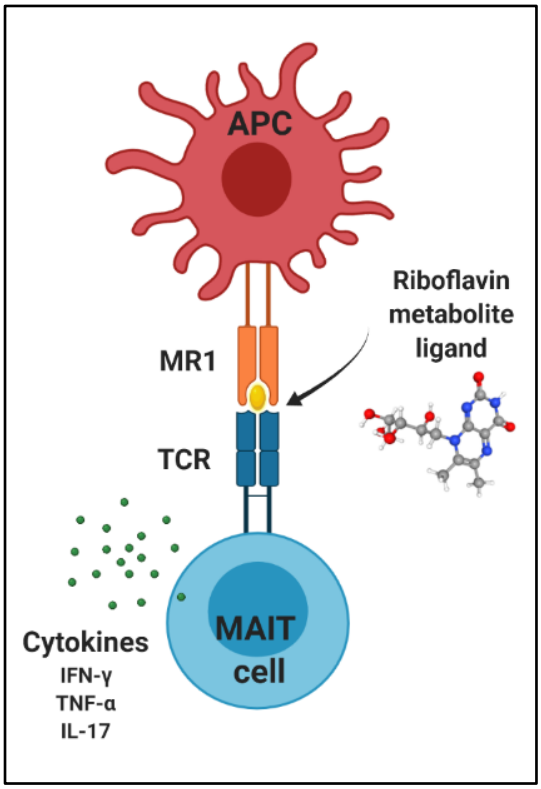

Figure 1.5 Presentation of a riboflavin metabolite ligand by an antigen presenting cell (APC)to a mucosal associated invariant T (MAIT) cell. MAIT cells express a T cell receptor (TCR) and are restricted by the MHC-related protein 1 (MR1). Activation of MAIT cells results in the release of pro-inflammatory cytokines. Created with BioRender (https://biorender.com/).

Full activation of MAIT cells also requires co-stimulatory molecules, such as cytokines and TLR agonists [76]. For example, IL-7, IL-12 and IL-18 cytokines enhance MAIT cell activation and cytotoxicity in response to bacterial infections [77-80], and TLR1, TLR2 and TLR6 agonists indirectly increase MAIT cell activation through their action on APCs and consequent upregulation of MR1 presentation on their surface [78, 81]. While MR1-TCR-mediated activation of MAIT cells is associated with bacterial infections, viruses are unable to synthesise MAIT cell ligands as they lack the riboflavin biosynthesis pathway [82]. Nevertheless, MAIT cells can detect virus-infected cells and become activated in a MR1-independent manner through exposure to their secreted mediators, such as type-I IFNs [83, 84]. MAIT cells activated in a MR1-TCR-dependent manner secrete multiple pro-inflammatory cytokines including IL-17, IFN-γ and TNF-α. Activation in a MR1-TCR-independent manner leads to the release of cytotoxic compounds by MAIT cells, such as perforin and granzyme B, and it is characterised by an IFN-γ-dominated response [76]. Activated MAIT cells present upregulated CD25 and CD69 expression [72, 85, 86] and are more prone to apoptosis compared to other T cell subsets [87].

1.4.3 MAIT cell ligands

Several hydrophilic ligands deriving from the riboflavin pathway were identified as MAIT cell activators. These include 6,7-dimethyl-8-ribityllumazine (RL-6,7-diMe), 7-hydroxy-6-methyl-8-ribityllumazine (RL-6-Me-7-OH), reduced 6-(hydroxymethyl)-8-ribityllumazine (rRL-6-CH_2OH), 5-(2-oxoethylideneamino)-6-D-ribitylaminouracil (5-OE-RU) and the most potent activator 5-(2-oxopropylideneamino)-6-D-ribitylaminouracil (5-OP-RU) [85]. While lumazines are intermediates formed during bacterial synthesis of riboflavin, pyrimidines 5-OE-RU and 5-OP-RU result from the reaction between 5-A-RU of microbial origin and host-derived glyoxal (5-OE-RU) or methylglyoxal (5-OP-RU) formed during glycolysis [73, 88]. A schematic of the chemical structures of identified MAIT cell ligands is provided in Figure 1.6.

Vitamin metabolites acting as MAIT cell ligands are widely produced both by commensals and by pathogenic bacteria. Bacteria lacking the riboflavin-biosynthesis pathway do not activate MAIT cells via MR1-TCR [89]. Riboflavin metabolites may act as a danger signal for MAIT cells, indicating the presence of non-self products [82], although it is still unclear whether MAIT cells can discern between ligands deriving from commensals and ligands from pathogens. More recently, a subset of MAIT cells was shown to recognise a non-activating ligand from the folate pathway [71]. Additionally, evidence suggests that unknown metabolites from dietary probiotics also modulate T cell and MAIT cell functions [90, 91]. Molecules present in lactobacilli cell-free supernatants directly dampened IFN-γ expression in immune-challenged MAIT cells *in vitro* [91], paving the way for the search of new MAIT cell ligands.

LUMAZINES

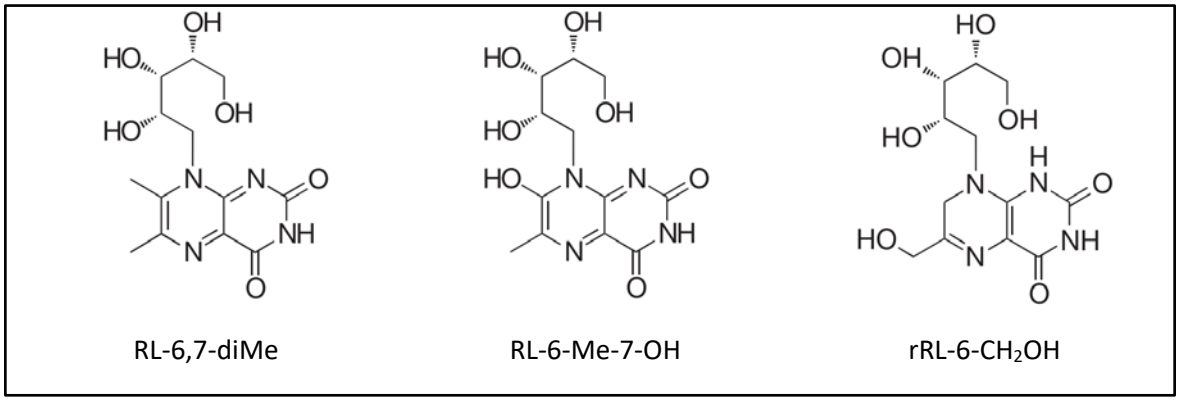

PYRIMIDINES

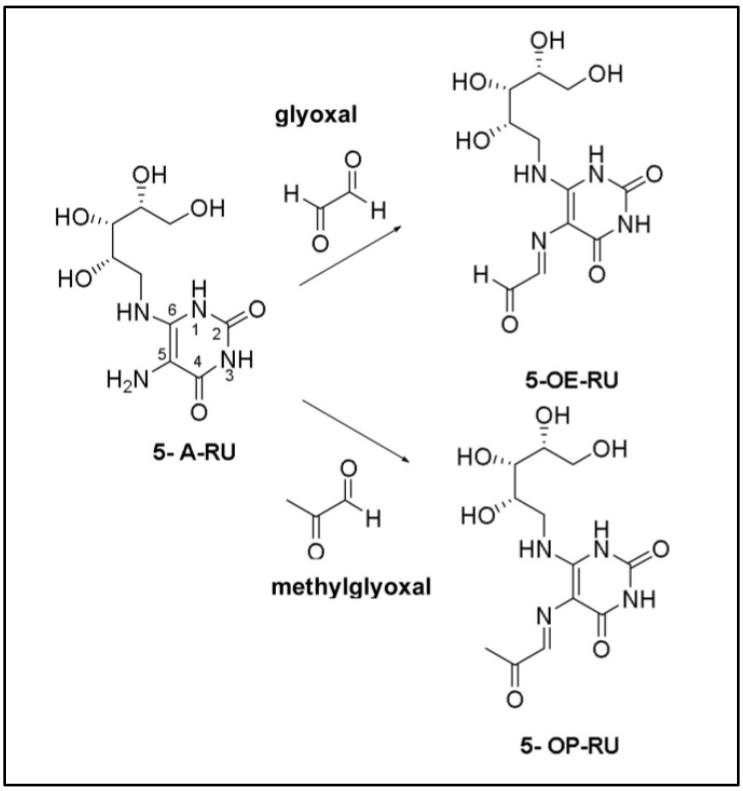

Figure 1.6 A schematic of the chemical structures of lumazines and pyrimidines identified as MAIT cell ligands. Adapted from [85, 86, 88].

1.4.4 MAIT cells in health and disease: a focus on inflammatory bowel diseases

MAIT cells exert a protective role against bacterial infections by releasing pro-inflammatory molecules (*e.g.* TNF-α, IFN-γ) ultimately leading to the death of infected cells. They also contribute to eliminate virus-infected cells by secreting cytotoxic compounds (*e.g.* perforin, granzyme B) after activation in a MR1-independent manner by APC mediators [60, 63, 92]. Recent studies highlighted a relationship between the frequencies and functions of MAIT cells and a wider range of diseases, including immune-mediated diseases, metabolic diseases, malignant diseases and liver diseases. Overall, a general reduction in the numbers of circulating MAIT cells, an accumulation at the inflammation site, a shift in cytokine profiles and an increased expression of activation markers were observed in diseased individuals, as reported in Table 1.3 and Table 1.4.

Individuals affected by Crohn's disease and ulcerative colitis, who have extensive mucosal inflammation in the gastrointestinal tract, present lower frequencies of MAIT cells in peripheral blood compared to healthy controls. These changes are likely due to migration of MAIT cells to the inflamed mucosa of IBD patients. Indeed, higher frequencies of MAIT cells were seen in the ileal tissue and intestinal mucosa of Crohn's disease and ulcerative colitis patients, respectively [87, 93-95]. While there are contrasting results on the direction of change (increase *vs* decrease) of soluble mediators secreted by MAIT cells in IBD, possibly due to different experimental settings used, all studies highlighted a shift in IL-17, IL-22 and IFN-γ cytokine profiles in blood, together with an increased expression of the activation marker CD69.

The role of IL-17 in IBD has not been fully defined yet. IL-17 is a pro-inflammatory cytokine with a protective role against invading pathogens at mucosal sites. It acts by stimulating the release of neutrophil chemoattractant molecules and antimicrobial peptides by epithelial cells, while also enhancing gut barrier integrity through the induction of tight junction proteins [96]. Despite there being higher levels of IL-17 in the inflamed mucosa of IBD patients compared to healthy controls, blocking its production was ineffective in Crohn's disease [96] and even led to aggravation of Crohn's disease symptoms in another study [97].

Conversely, administration of IL-22 to mice with experimental colitis reduced their gut inflammation, suggesting a potential protective role [96]. IL-22 displays both pro-inflammatory and anti-inflammatory effects, such as the release of defensins and other antimicrobial molecules and the promotion of cell proliferation and tissue regeneration in the damaged epithelium [98].

IFN-γ is generally understood to be a pro-inflammatory cytokine involved in antiviral responses, although it also exerts many other functions including stimulation of antigen presentation, macrophage activation and regulation of cell proliferation and apoptosis [99]. Contrasting results are available for the role of IFN-γ in IBD, with some studies suggesting a causative role in the initiation and progression of the disease [100] and others indicating a protective function via regulation of Th17 responses [101].

CD69 is an early marker of cell activation and it is upregulated on lymphocytes and monocytes from as early as 2 h after stimulation to a peak at 24 h [102, 103]. CD69 is highly expressed on infiltrated lymphocytes at inflammatory sites as well as on regulatory T cells in the gut. Upregulation of CD69 expression in the gut is induced by the microbiota and it is thought to play an important role in preserving the homeostasis between inflammatory responses against pathogens and immune tolerance towards commensal bacteria [104]. However, the exact function of CD69 in IBD is yet to be clarified, as a pro-inflammatory role was demonstrated in *in vitro* studies using mouse models [105] but not confirmed [106] or even disproved [107] *in vivo*.

Overall, it is unclear whether MAIT cells directly or via their secreted mediators exert a protective or pathological role in IBD. Both genetic and environmental factors lead to impaired gut barrier function in IBD, resulting in the translocation of commensal bacteria and their product from the lumen to the inside of the gut wall [108]. MAIT cells may exert a protective role by eliminating the microbes that cause immune cell activation in the disrupted intestine of IBD individuals, or alternatively may exacerbate inflammation by releasing pro-inflammatory cytokines in the gut, such as IL-17 and IFN-γ.

Table 1.3 Changes in mucosal associated invariant T (MAIT) cell frequencies, soluble mediators and activation status in immune-mediated diseases and metabolic diseases.

Human MAIT cells	IMMUNE-MEDIATED DISEASES									METABOLIC DISEASES
	Inflammatory bowel disease		Auto-immune diseases					Pulmonary diseases		
	Crohn's disease	Ulcerative colitis	Multiple sclerosis*	Systemic lupus erythematosus*	Rheumatoid arthritis*	Psoriasis	Coeliac disease	Asthma*	Chronic obstructive pulmonary disease*	Obesity/type 2 diabetes mellitus
Frequencies in blood	↓	↓	Contrasting results	↓	Contrasting results	↓	↓	↓	↓	↓
Frequencies at site of disease	↑ (in ileal tissue)	↑ (in intestinal mucosa)	↑ (in brain lesions)	N/A	↑ (in synovial fluid)	↑ (in psoriatic skin)	↓ (in lamina propria)	↓ (in sputum and bronchial biopsies)	↓ (in bronchial biopsies from corticosteroids patients)	↑ (in adipose tissue)
Soluble mediators in blood	Contrasting results on IL-17, IL-22 and IFN-γ	Contrasting results on IL-17 and IL-22	↓ INF-γ	↓ INF-γ	N/A	↑ IL-17	N/A	N/A	N/A	↑ IFN-γ, IL-2, granzyme B and IL-17A
Activation status	↑ CD69 expression	↑ CD69 expression	N/A	↑ CD69 expression	N/A	N/A	N/A	N/A	N/A	↑ CD25 and CD69 expression
References	[67, 87, 89, 93-95]	[67, 87, 93-95]	[67, 89, 109-111]	[111-113]	[111, 114, 115]	[67, 116]	[64, 111, 117]	[67, 111]	[67, 118]	[67, 111, 119]

*MAIT cells are susceptible to corticosteroid use, which causes a decrease in their blood frequencies.

Table 1.4 Changes in mucosal associated invariant T (MAIT) cell frequencies, soluble mediators and activation status in bacterial infections, viral infections, malignant diseases and liver diseases.

Human MAIT cells	BACTERIAL INFECTIONS			VIRAL INFECTIONS			MALIGNANT DISEASES		LIVER DISEASES	
	Gastrointestinal infections	Pulmonary infections	Sepsis	Chronic hepatitis C virus	Human immunodeficiency virus	Dengue	Brain/kidney/colon tumour	Chronic lymphocyte leukaemia	Alcoholic liver diseases	Cirrhosis
Frequencies in blood	↓ (*H. pilori*) ↓ (*V. cholerae 01*) ↓ (*S. dysenteriae-1*)	↓ (in patients with active tuberculosis)	↓	↓	↓	↓	↔ (colorectal cancer)	↓	↓ (but relative increase in proportions of $CD4^+$ MAIT cells)	N/A
Frequencies at site of disease	↑ (suggested recruitment to infection site)	↑ (in lung lesions of patients with active infection)	N/A	↑ (in liver)	↓ (in lymph nodes and colon. Same $CD8^+$ MAIT cell frequencies in colon but loss of $CD4^+$ subset)	N/A	↑ (at tumour site in brain, kidney and colon)	N/A	Contrasting results	↑ (in liver)
Soluble mediators in blood	↑ secretion of Th1 and Th17 cytokines (*H. pilori*)	Contrasting results on INF-γ, TNF-α, IL-17 and granzyme B	N/A	↓ INF-γ	↓ INF-γ, TNF-α and IL-17	N/A	↑ IL-17 ↓ INF-γ	N/A	N/A	N/A
Activation status	↑ CD25 and CD69 expression (*S. dysenteriae-1 and V. cholerae 01)*	N/A	N/A	N/A	↑ activation status of MAIT cells in HIV^+ patients, correlated with ↓ blood frequencies	N/A	↑ CD69 expression (colorectal cancer)	N/A	N/A	N/A
References	[67, 120-122]	[63, 67, 82, 123, 124]	[67, 84, 125]	[89, 92, 126]	[67, 77, 89, 127, 128]	[83]	[67, 89, 129-131]	[67, 132]	[89, 133]	[89, 134]

1.5 The gut microbiota

1.5.1 Definition of gut microbiota

The term gut microbiota refers to the ensemble of living microorganisms including bacteria, constituting the vast majority of gut microbial cells [135], archaea and eukarya residing in the human intestine [136]. It is estimated that more than 10^{14} cells constitute the intestinal microbiota, and among these, more than 5,000 different species of bacteria are present [137]. Through evolution, a mutualistic relationship has been developed between the host and its microbiota. While the latter receives nutrients from the host and gains a stable habitat where to thrive, in turn it metabolises undigested carbohydrates, synthesises vitamins and exerts immunoregulatory functions helping the host in maintaining a healthy state [138]. Although it is challenging to provide a definition for a 'normal' or 'healthy' microbiota due to the complexity of studying the gut eco-physiology and the high inter-individual variability, a balance or 'homeostasis' between particular microbial species is generally associated with positive health outcomes. On the other hand, 'dysbiosis' is characterised by the loss of beneficial bacteria (*e.g.* bacteriodes and lactobacilli), a reduction in microbiota diversity and a rise in potentially pathogenic bacteria or 'pathobionts' [139].

1.5.2 Location and composition of gut microbiota

The majority of gut microbiota is located in the large intestine, where the growth of bacteria is supported by the higher pH and the lower oxygen levels compared to those found in the small intestine. In the colon, the most represented bacteria are anaerobic and aerobic facultative bacteria belonging to the *Bacteroidetes, Firmicutes (*now also known as *Bacillota)* and *Actinobacteria* phyla [136, 140]. While the gut of breast-fed infants is dominated by bifidobacteria belonging to the *Actinobacteria* phylum, the most represented phyla in the adult gut and constituting up to 90% of the total microbiota are *Bacteroidetes* and *Firmicutes*, which include the bacteroides and lactobacilli genera, respectively [141]. Despite being found in lower abundance in adulthood compared to childhood, lactobacilli and bifidobacteria are present in stable numbers in healthy individuals [142]. Perturbations in their numbers have been linked with a number of diseases, including metabolic diseases, inflammatory diseases, immune disorders and malignancies [34, 143, 144].

1.5.3 Gut flora development

Microorganisms start to colonise the sterile intestine of new-borns immediately after birth [136, 143]. The mode of delivery itself has an important impact on the pattern of species found in the intestine. Vaginally-delivered children displayed higher numbers of lactobacilli compared to children born via caesarean delivery [145]. Breast feeding, early antibiotic use, probiotic and prebiotic consumption during and after pregnancy all influence the colonisation mechanisms in infants [143]. During the first years of life, the gut microbiota undergoes major changes before becoming more stable around the age of two, following the introduction of solid food [143]. While the microbiota of healthy adults is characterised by high diversity in terms of genera and stable numbers of beneficial bacteria, ageing is associated with a decrease in bifidobacteria and an overrepresentation of pathobionts [146]. In addition to age, many other individual and environmental factors can shape the quantity and quality of microorganisms in the adult gut (Figure 1.7). Antibiotics, stress, sedentary lifestyles and alcohol consumption have all been linked to dysbiosis [136]. Among the environmental factors, diet plays a pivotal role in shaping the gut flora. Non-digestible dietary fibres have bifidogenic effects on the microbiota, meaning that they selectively support the growth and activity of bifidobacteria in the intestine [147].

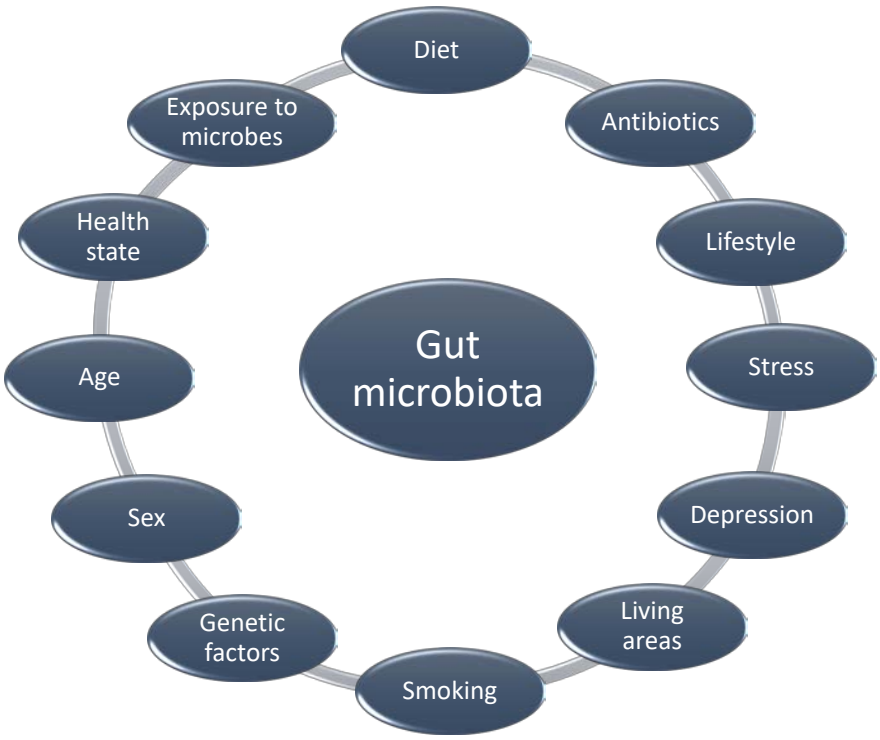

Figure 1.7 Individual and environmental factors influencing microbiota composition.

1.5.4 Functions of the gut microbiota

Many functions are fulfilled by the gut microbiota, including fermentation of undigested carbohydrates, competition with pathogens, biosynthesis of vitamins and immune system regulation [31, 34, 43, 145, 148, 149]. Additionally, the intestinal flora has a role in supporting bone health [137] and neurodevelopment [148]. Gut bacteria are responsible for the fermentation of non-digestible fibres that reach the colon intact because they are not metabolised by human enzymes. Degradation of dietary fibres results in the production of short chain fatty acids (SCFAs) such as acetate, propionate and butyrate (3:1:1 to 10:2:1), which display antimicrobial, metabolic and immunomodulatory effects. Acetate is the most abundant SCFA and is essential in supporting the growth of microbial populations in the gut. Additionally, it is involved in lipid metabolism by promoting fat oxidation and in appetite regulation by changing the expression profiles of neuropeptides that promote appetite suppression [150, 151]. After absorption by passive diffusion in the large intestine, propionate and butyrate become energy sources for intestinal cells. Butyrate displays anti-cancer activity by inducing apoptosis of tumour cells, by regulating gene expression, by reducing cell proliferation and by exerting anti-inflammatory effects [152]. Similarly to acetate, propionate displays anti-lipogenic and cholesterol-lowering effects and, like butyrate, it shows anti-carcinogenic effects on colon cancer cells [153].

Production of SCFAs leads to a reduction in intestinal pH, which results in a better selection of beneficial species against acid-sensitive and pathogenic strains [154]. Beneficial bacteria also directly protect the host by competing with pathogens for space and nutrition [145]. Additionally, the gut flora is responsible for the synthesis of group K and group B vitamins, such as cobalamin, biotin, folate, nicotinic acid, pantothenic acid, riboflavin, pyridoxine and thiamine. Up to half of vitamin K daily intake and over a quarter of vitamin B daily intake are produced by the gut microbiota [154, 155]. Vitamins are used as nutrients by both gut bacteria and host and are also known to exert immunomodulatory functions. For instance, the pyrimidine compounds derived from the riboflavin precursor 5-amino-6-D-ribitylaminouracil are potent activators of MAIT cells. In homeostatic conditions, ligation of riboflavin metabolites from commensal bacteria to the TCR of MAIT cells results in the production of IL-17 and IL-22 cytokines, which promote barrier integrity. However, when the same ligands bind to MAIT cells in dysbiotic conditions where also other immunostimulatory molecules (*e.g.* LPS) are present, pro-inflammatory cytokines such as IFN-γ and TNF-α are released [156].

Studies in germ-free mice demonstrated that the gut flora is essential for immune modulation and absence of it is associated with defective immunity. Commensal bacteria have a role in the development of T lymphocytes and are responsible of regulating the secretion of IgA in the lumen [149]. SCFAs produced by the gut microbiota exert anti-inflammatory effects by inhibiting NF-κB signalling in neutrophils and therefore reducing their release of pro-inflammatory mediators, such as TNF-α [157]. SCFAs also affect the activation and function of T cells by stimulating the differentiation of regulatory T cells and reducing the differentiation of Th17 cells [158]. The microbiota may indirectly regulate bone homeostasis via the production of SCFAs, which lower the pH increasing the amount of absorbable calcium as well as interfere with the signalling pathways involved in bone mineralisation [137]. Lastly, the gut flora has an impact on neurological development via the production of metabolites, such as SCFAs and neurotransmitters (*e.g.* serotonin and dopamine), which bind to receptors involved in brain functions [159].

1.5.5 Mechanisms to prevent the contact between microorganisms and immune cells

Physical barriers are in place to segregate microbes present in the gut lumen from hosts' immune cells in the lamina propria. These include two layers of mucus produced by goblet cells against the invasion of pathogens or endotoxins, and one layer of epithelial cells kept close together by tight junctions [160]. While commensals do not enter in contact with the intestinal epithelial cells (IECs) and remain confined to the outer mucus in normal conditions, pathogens have evasive mechanisms that allow them to adhere to the gut epithelium, degrade tight junction proteins (*e.g.* occludins, claudins) and breach through the gut barrier [161]. IECs recognise molecular structures from bacteria, such as peptidoglycan, LPS and β-glucans, thanks to the expression of TLRs. Due to the constant exposure to bacterial product, TLR expression is often downregulated in IECs to avoid chronic inflammation [25]. However, if pathogens cross the epithelial barrier, mechanisms are in place to upregulate the expression of TLRs and other co-stimulatory molecules on immune cells of the lamina propria [25]. For example, LPS is extracted by LPS binding protein (LBP) from bacterial cells and transferred to CD14 on monocytes, which splits LPS into monomeric units and present them to the TLR4-MD2 complex. The formation of this complex activates the NF-κB pathway, which leads to the production of IL-1β, IL-6, IL-8, TNF-α cytokines that promote inflammation and ultimately result in the elimination of the antigen [162]. DCs present fragments from pathogenic bacteria to plasma cells, which in turn produce IgA that passes through the epithelial layer and bind to the microorganisms preventing their transfer across the gut barrier [58]. Since colonic microbes are found both in the lumen and in the mucus covering the intestinal epithelium, recent studies have stressed the importance of performing both mucus and stool sampling when assessing microbiota alterations in diseases [163].

1.5.6 Alterations in gut microbiota and link to diseases

Disruptions in microbiota composition have been observed in many pathologies, such as gastrointestinal disorders, chronic inflammatory diseases, diabetes and obesity [34]. Overall, a damaged gut barrier or 'leaky gut', a depletion in bacterial diversity and a shift in gut flora populations are frequently observed in these conditions. Obese people present fewer numbers of *Bacteroidetes* and higher numbers of *Firmicutes* compared to normal-weight controls [143]. In the same manner, malnourished children displayed disruptions in microbiota composition opposed to healthy subjects [136, 149]. Abnormalities in gut bacteria composition are also associated with allergic diseases, atopic diseases and autism spectrum disorders (ASDs). Children affected by ASDs often experience abdominal pain, diarrhoea and constipation, which were linked to the lower numbers of bifidobacteria and higher numbers of Clostridium spp. in their gut [148]. Alterations in the early colonisation of the intestine have a role in the onset of eczema, atopic dermatitis and allergies developed in adulthood [149]. Shifts in microbial composition are found in people affected by chronic inflammatory diseases, such as IBD. Individuals affected by ulcerative colitis and Crohn's disease have reduced numbers of *Firmicutes* and *Bacteroidetes* [143, 164]. Chronic kidney disease (CKD) and irritable bowel syndrome (IBS) have both been linked with gut dysbiosis. IBS patients displayed an excessive growth of bacteria in the small intestine compared to healthy controls, which also correlated with the severity of symptoms [136, 165]. Asthma patients showed fewer numbers of *Bifidobacterium adolescentis* compared to those found in the intestine of healthy people [166]. Overall, there are associations between the composition of the gut microbiota and the occurrence of a wide range of diseases.

1.6 Inflammatory bowel diseases

Inflammatory bowel diseases (IBD) are chronic and relapsing conditions affecting the gastrointestinal tract. Common symptoms of IBD include abdominal pain, diarrhoea, rectal bleeding and weight loss [167]. In the 21st century, IBD has become a major burden in Western countries, with over 1.5 million and 2 million people affected in North America and Europe, respectively [168]. Based on the location of inflammation, IBD are classified as Crohn's disease or ulcerative colitis. While Crohn's disease is associated with deep inflammation in any part of the gastrointestinal tract, ulcerative colitis is linked to severe damage of the colonic and rectal mucosa [43].

Endoscopic procedures, such as colonoscopy, flexible sigmoidoscopy and upper endoscopy, combined with histological assessments are generally used to diagnose and classify IBD [169]. Based on the disease severity and disease activity, mild, moderate and severe forms of IBD are distinguished. While individuals with mild forms of Crohn's disease display normal appetite, minor weight loss (< 10%) and no fever, subjects with severe forms present very low BMI (< 18 kg/m^2) significant weight loss, persistent symptoms despite treatment, high fever and increased levels of CRP in blood, which is produced by liver cells in response to acute inflammation. More detailed information on the clinical features of each form can be found in [170].

Although the exact pathogenesis is unclear, there is evidence that IBD develop in genetically susceptible individuals who have been exposed to environmental insults that lead to an aberrant immune response to commensal gut microbiota and chronic inflammation [171]. Despite both Crohn's disease and ulcerative colitis having a genetic basis, ulcerative colitis is more strongly affected by environmental factors than genetic factors, compared to Crohn's disease [172]. Relevant environmental factors include lifestyle (*e.g.* smoking, diet and stress), host microbiota (dysbiosis), pharmacologic agents (*e.g.* antibiotics), ecological factors (*e.g.* pollution) and surgery (*e.g.* appendectomy), with smoking having the greatest level of evidence for association with IBD than other factors according to the 2009 Oxford Centre for Evidence-based Medicine levels of Evidence [171].

Genetic and environmental factors drive alterations to the gut immune response, leading to reduced ability to clear pathogenic bacteria [173], lower levels of goblet cells, Paneth cell dysfunction and increased secretion of inflammatory mediators [174]. While Crohn's disease is driven by Th1/Th17 responses in which upregulation of IL-1β, IL-6, IL-12, IL-17, IL-23, TNF-α and IFN-γ is observed, ulcerative colitis is mainly driven by Th2-like responses characterised by increased IL-5, IL-10 and IL-13, but not IL-4, production [43, 175]. These changes in innate and adaptive immune responses cause damage to the intestinal epithelium, which becomes permeable and susceptible to the microbiota and their metabolites. Whereas in healthy conditions the gut microbes live in mutualistic relationship with the host (homeostasis), in IBD this balance is altered (dysbiosis) and the host responds to the commensal bacteria with an aberrant immune response.

Unfortunately, there is no current cure for IBD, but maintenance treatments including anti-inflammatory drugs, immunosuppressants, antibiotics and biologic therapies (*e.g.* TNF-α blockers) are often used to mitigate the symptoms [176]. In recent years, alongside the suggestion to use probiotics as a preventive or support therapy in IBD [177], prebiotics have been studied for their

role in maintaining gut health, supporting the growth of health-promoting bacteria and positively affecting gut immunity [178].

1.7 Non-digestible oligosaccharides (NDOs) and their role as prebiotics

1.7.1 Definition and classes of prebiotics

NDOs are fermentable dietary fibres with a role as prebiotics. According to the International Scientific Association for Probiotics and Prebiotics consensus statement [179], prebiotics are "substrates that are selectively utilised by host microorganisms conferring a health benefit". Fructooligosaccharides (FOS), inulin and galactooligosaccharides (GOS) are the most researched prebiotics. Additionally, lactulose-derived oligosaccharides, human milk oligosaccharides (HMOs), arabinooligosaccharides (AOS), mannanoligosaccharides (MOS), xylooligosaccharides (XOS), pectic oligosaccharides (POS) and glucose-derived oligosaccharides are emerging prebiotics, as the level of evidence of their health benefits is lower than for FOS, inulin and GOS [179-181]. NDOs are carbohydrates usually made up by 3 to 10 monosaccharide units, usually glucose, galactose, fructose, and xylose. The number of monomeric units constituting NDOs is also referred to as the degree of polymerisation (DP). The carbons of the monosaccharide units are linked by covalent β-glycosidic bonds rather than by α-glycosidic bonds found in digestible oligosaccharides. This β configuration of the bonds makes NDOs indigestible by human salivary and digestive enzymes [182]. With the exception of HMOs, which are found at high concentration in human milk (12-15 mg/mL) [183], dietary sources of NDOs are plants and include chicory, garlic, Jerusalem artichoke, leeks, onions, bananas, barley and wheat [184]. The levels of NDOs contained in natural sources varies considerably and ranges between 0.3% and 20% of the product's fresh weight [182]. Alongside extraction from food sources, NDOs are industrially produced via chemical or enzymatic synthesis using monosaccharide and disaccharide sugars [182]. For the aim of this work, the production and structure of GOS fibres will be discussed in more detail. Further information on NDOs is available elsewhere [180, 181, 185, 186].

1.7.2 Galactooligosaccharide (GOS) fibres: production and structure

GOS are constituted by chains of galactose units, usually DP2-DP8, linked by β-(1,3), β-(1,4) or β-(1,6) glycosidic bonds and terminating with a glucosyl residue linked by β-(1,4) bonds [185], as displayed in Figure 1.8. GOS are produced by transgalactosylation reaction (Figure 1.9), which involves the action of β-galactosidases enzymes on the substrate lactose. β-galactosidases

hydrolyse lactose and transfer the resulting galactose to another carbohydrate, usually lactose, leading to the production of an oligosaccharide with higher DP [187, 188]. Since the reactions of lactose hydrolysis and GOS synthesis are competitive processes, a high concentration of lactose and low concentration of water are required to produce GOS [185].

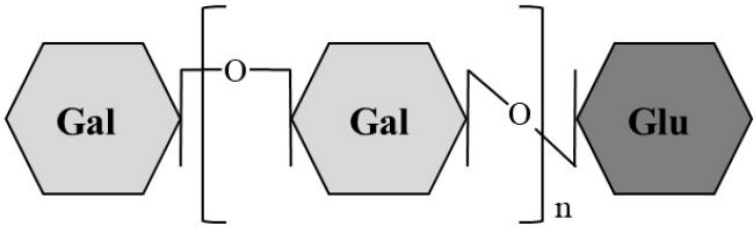

Figure 1.8 Chemical structure of galactooligosaccharides (GOS). GOS are made by galactopyranosyl units linked by β-(1,4) or β-(1,6) bonds and terminating with a glucosyl residue linked by β-(1,4) bonds. Gal, galactose; Glu, glucose. Created with BioRender (https://biorender.com/).

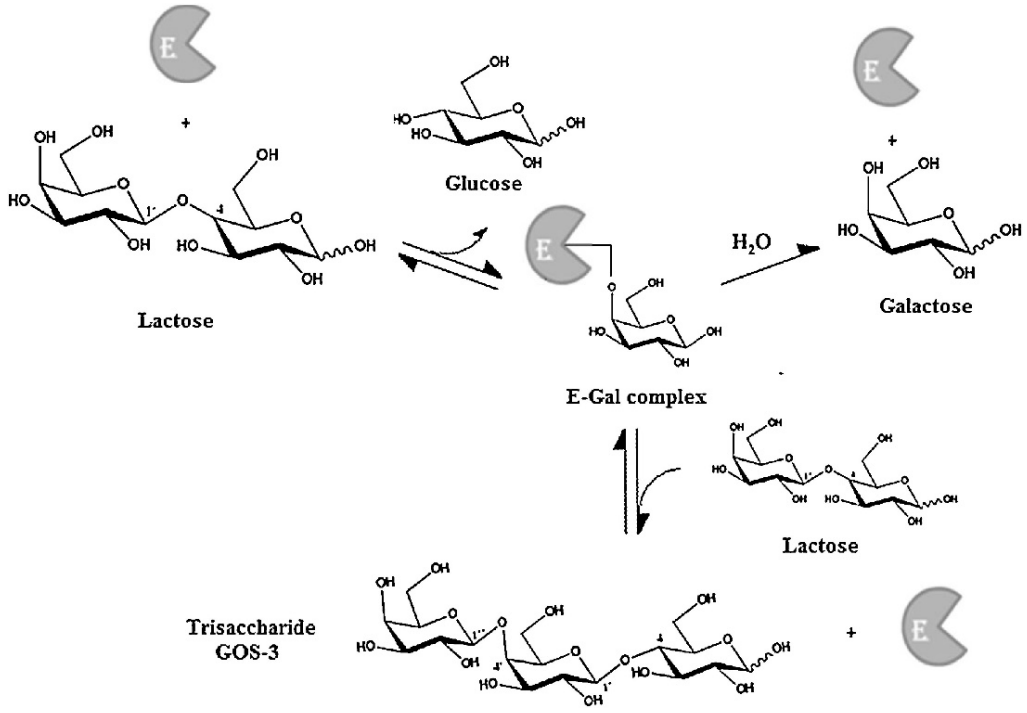

Figure 1.9 Schematic of the transgalactosylation of lactose catalysed by the enzyme β-galactosidase. Image re-adapted from [189].

β-galactosidases enzymes are derived from various bacteria, fungi and yeasts including the probiotic species *Lactobacillus* and *Bifidobacterium*, which have been widely used for the industrial production of GOS [190]. Based on the type of enzyme used for GOS synthesis and the conversion degree of lactose, GOS fractions of different DP are formed [191].

Examples of GOS fractions include the disaccharide allolactose (β-d-Gal (1→6)-d-Glc), trisaccharide 3-galactosyllactose (β-d-Gal (1→3)-β-d-Gal-(1→4)-d-Glc) and tetrasaccharide 4'-digalactosyllactose (β-d-Gal (1→4)-β-d-Gal-(1→4)-β-d-Gal-(1→4)-d-Glc). Among these, the trisaccharide 3-galactosyllactose is of particular interest as it is also found in human breast milk, it is a favoured substrate for bifidobacteria and it contributes to immunomodulation by attenuating TLR3 signalling [192-194].

Due to their health-promoting effects which are potentially linked to their structural similarity with HMOs, GOS alone or mixtures of GOS and FOS have been widely used in infant milk formula as well as in food supplements to promote the growth and activity of beneficial gut bacteria, such as bifidobacteria [194-196].

1.7.3 Health-promoting effects of GOS

The positive health effects associated with GOS consumption have been mainly linked to their bifidogenic activity on the gut microbiota. Evidence from human supplementation studies and *in-vitro* models indicate that GOS support gut homeostasis by selectively increasing the abundance of beneficial gut bifidobacteria [197-201] and exerting anti-pathogenic effects against invading microbes [202, 203]. In a double-blind, randomised controlled study on healthy adults, supplementation with GOS was linked with a reduction in the incidence and severity of travellers' diarrhoea [203], which is caused by the consumption of food or water contaminated with enteropathogens (*e.g. Escherichia coli*) [204]. The protective action of GOS against pathogens was confirmed by an *in-vitro* study, which indicated a strong inhibitory effect of GOS against the adhesion of enteropathogens to intestinal epithelial cell lines [205]. Controlled clinical trials on healthy individuals experiencing gastrointestinal discomfort [206] and on subjects with irritable bowel syndrome [144] showed that supplementation with GOS reduced abdominal pain, bloating and flatulence. GOS displayed immunomodulatory effects on mucosal barrier function *in vitro* by stimulating the production of mucins by goblet cell lines [207]. Increased IL-10, IL-8, NK cell activity and CRP and lower IL-1β were observed in elderly subjects after a 10-week supplementation with GOS in a double-blind, randomised controlled study [200]. Data from human clinical trials and animal models suggest that supplementation with prebiotic mixtures

(including GOS) in early life may reduce the risk of developing atopic dermatitis [208, 209], food allergy [210, 211] and allergic asthma [166, 212]. Finally, data from a controlled clinical study on healthy volunteers indicate that GOS may affect brain health by reducing stress hormone levels and anxiety [213]. Although there is preliminary evidence of a potential therapeutic or preventive use of prebiotics, more research is needed to clarify their mechanism of action. To date, only inulin received a favourable opinion from EFSA on its contribution to normal bowel function by increasing stool frequency. In order to achieve the claimed effect, 12 g of native chicory inulin should be consumed daily [214]. Conversely, EFSA concluded that there is currently not enough scientific evidence to make health claims on GOS, as larger clinical trials are needed to prove their effectiveness in the wider population [215, 216].

1.7.4 Prebiotic mechanism of action

Prebiotic NDOs resist low gastric pH and hydrolytic enzymes due to their chemical structure and reach the colon virtually intact, where they are degraded by the gut microbiota [217]. Lactobacilli and bifidobacteria break down NDOs via saccharolytic reactions and use them as energy sources to support their growth. In doing so, SCFAs are generated as volatile end-products of the fermentation process. These SCFAs, which include acetate, propionate and butyrate [136], exert beneficial health effects for the host such as inhibition of pathogens, maintenance of gut barrier integrity, regulation of glucose and lipid metabolism and modulation of immunity [218-222].

Traditionally, immunomodulatory effects of prebiotics were thought to result exclusively from the actions of SCFAs and other metabolites (*e.g.* bactericidal molecules) produced by the microbiota. For example, SCFAs are known to modulate cytokine production and immune cell functions of DCs and T cells as well as to inhibit several pro-inflammatory pathways, as extensively reviewed elsewhere [149, 178, 223, 224].

There is growing interest in understanding whether NDOs can also modulate immunity in a non-prebiotic manner, especially in those individuals with increased gut permeability, by directly interacting with systemic and gut immune cells (Figure 1.10).

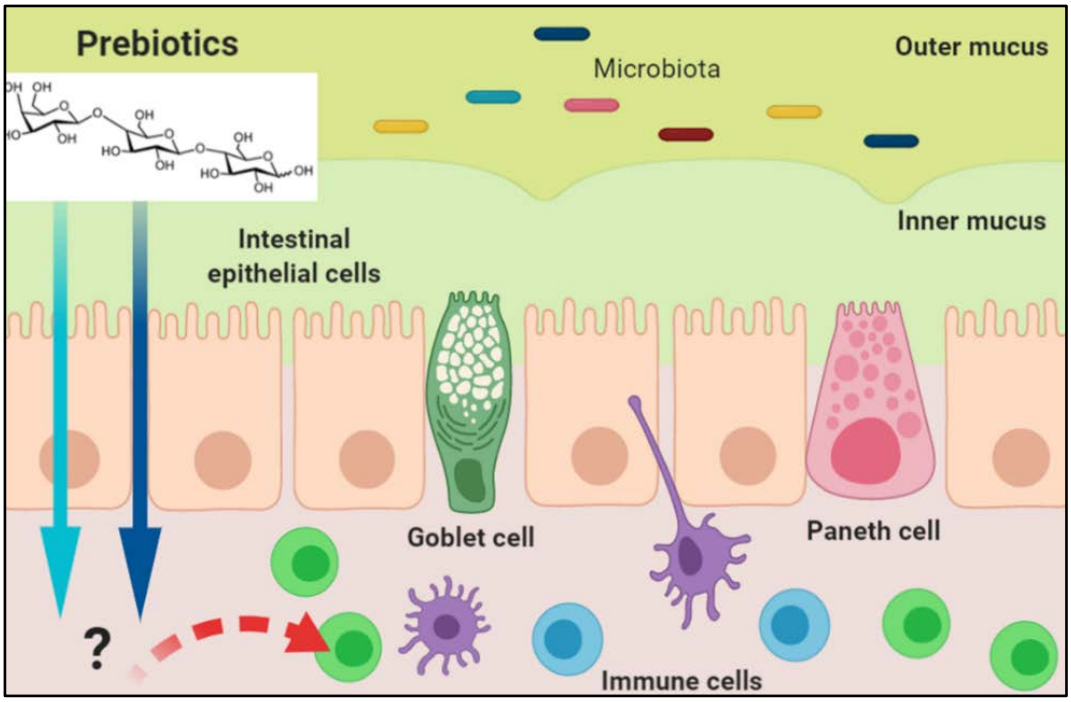

Figure 1.10 Proposed mechanism of action of prebiotic NDOs via direct interaction with immune cells. Created with BioRender (https://biorender.com/).

1.7.5 Microbiota-independent effects of NDOs on immunity

1.7.4.1. Evidence for intestinal transportation

Prebiotics may pass through the gut barrier and enter in direct contact with gut and systemic immune cells when the gut is immature, such as is the case in infants [225, 226] and other situations characterised by increased gut permeability, including IBD [227], obesity [228, 229], type I diabetes [230] and non-alcoholic fatty liver disease [231]. It is conceivable that NDOs may also be transported across the intestinal barrier in individuals exposed to lifestyle-associated stressors that have been linked to alterations in gut permeability, such as high fat Western diet, alcohol consumption and use of medications [232]. Studies *in vitro* demonstrated that neutral and acidic HMOs are transported across a Caco-2 monolayer via transcellular and/or paracellular pathways [233] and that short chain GOS/long chain FOS (scGOS/lcFOS) are transferred with rates of 4-14% depending on their molecular size and structure [234]. In human supplementation studies, HMOs, FOS and GOS with a DP between 3 and 9 were found in plasma, urine and stool of infants fed with supplemented human milk or formula containing FOS or GOS [235, 236], confirming transport of intact oligosaccharides across the intestinal epithelium, as summarised in Table 1.5 and Table 1.6. It is plausible that prebiotics are similarly transported across the intestinal epithelium in adults with increased gut permeability, but it remains as an important gap in the current research field to test this hypothesis.

Table 1.5 *In vitro* studies providing evidence for intestinal transportation of prebiotics.

Reference	Treatment	*In vitro* model	Study design	Findings
[233]	Neutral and acidic HMOs fractions (5 mg/mL)	Caco-2 cells	Caco-2 cells grown on filter inserts in minimal essential medium. 200 µL of transport buffer with neutral and acidic HMOs fractions applied. HPLC-MS analysis of HMO in basolateral compartment	Neutral HMOs use transcellular and paracellular pathways to cross Caco-2 monolayer; acidic components use only paracellular pathways
[234]	scGOS/lcFOS	Caco-2 cells	Transfer of scGOS/lcFOS via Caco-2 monolayer measured by HPAEC-PAD. Sample preparation as in [233]	Transfer of scGOS/lcFOS detected with rate of transfer of 4-14%, depending on molecular size and structure

Abbreviations: HMO, human milk oligosaccharides; Caco-2 cells, human epithelial colorectal adenocarcinoma cells; HPLC-MS, high performance liquid chromatography mass spectrometry; scGOS/lcFOS, short chain galactooligosaccharides/long chain fructooligosaccharides; HPAEC-PAD, high-pH anion exchange chromatography with pulsed amperometric detection.

Table 1.6 Human studies supporting evidence for intestinal transportation of prebiotics.

Reference	Treatment	Population	Study design	Findings
[235]	Infant formula with FOS (3 g/L)	Term infants (*n*= 84) aged 1 to 8 (± 3) days	Controlled, randomised and blinded clinical study to determine safety of use of FOS and ability to detect oligosaccharides in urine and plasma of infants randomised to receive FOS-enriched formula, control formula or breast-feeding for 16 weeks. Anthropometric measures, urine, stool and plasma samples taken	No adverse effects with FOS supplementation. Prebiotic effect of FOS on lactobacilli. FOS with DP= 4 in plasma and urine of infants fed with FOS-enriched formula
[236]	HMOs; fortified human milk; infant formula with FOS; infant formula with GOS or *B. animalis*	Mother-preterm infant dyads (*n*= 4)	Clinical study where preterm infants received human milk with Similac® Human Milk Fortifier or unsupplemented human milk followed by human milk with fortifier Prolact+4® or formula milk Similac® Special Care® 24 High Protein either with GOS or with *B. animalis*. Samples of milk, urine and stool collected for analysis by nanoflow LC-TOFMS	HMOs and oligosaccharides with $3 < DP < 9$ identified and quantified in urine and stool of infants

Abbreviations: FOS, fructooligosaccharides; DP, degree of polymerisation; HMO, human milk oligosaccharides; GOS, galactooligosaccharides; B. animalis, Bifidobacterium animalis; LC-TOFMS, liquid chromatography time-of-flight mass spectrometry.

1.7.4.2. Evidence for direct effects on immunity

Twelve *in vitro* studies involving human or animal cell lines and/or primary cultures and one *in vivo* study using germ-free mice were reviewed to assess whether NDOs could directly affect immunity (Table 1.7 – Table 1.9). Three out of thirteen studies focused on HMOs [194, 237, 238], whereas the other studies focused on other NDOs including FOS, inulin, GOS and/or a combination of these [195, 239-244].

Of those studies that looked at effects of NDOs on human cell lines, HMO acidic fractions (12.5-125 μg/mL) showed anti-inflammatory effects by dose-dependently inhibiting leukocyte rolling and adhesion, which are two inflammatory processes involved in tissue damage, to human umbilical vein endothelial cells (HUVEC) [237]. Treatment with HMOs and GOS (both 5 g/L) attenuated TNF-α-, IL-1β- and pathogen-induced inflammatory cytokines (IL-8, MCP-1 and MIP-3α) in H4 cells, a cell model for human immature intestine [194]. When the same experiment was conducted on T84 and NCM-460 cell lines to mimic mature intestinal cells, TNF-α-induced MIP-3α was reduced by HMO and GOS treatment. However, TNF-α-induced IL-8 was inhibited in NCM-460, but not T84, cells only by HMOs [194]. Inflammatory NF-κB signalling was attenuated in H4 and NCM-460 cell lines [194]. A reduction in the expression of pro-inflammatory IL-8, as well as IL-12 and TNF-α, was seen after treatment of human epithelial colorectal adenocarcinoma cells (Caco-2 cells) with α3-sialyllactose HMO (50 mg/L) and FOS (50 g/L), whose anti-inflammatory effects are likely linked to the induction of PPARγ [239]. When the same cell line was incubated with lower concentrations (5 g/L) of FOS, inulin, GOS and goat milk oligosaccharides (GMOs), reduced production of MCP-1, but not IL-8, was observed. However, in the same study, stimulation with FOS, inulin and GMOs but not GOS resulted in a higher IL-8 production by human colon cancer cell lines (HT-29), in contrast to the studies on H4, NCM-460 and Caco-2 cells [242].

Overall, *in vitro* work conducted on cell lines consistently supports the hypothesis that NDOs are able to modulate cytokine production (*e.g.* IL-8, MCP-1) in a microbiota-independent manner. However, their anti-inflammatory effects appear to be cell-line specific and the various NDO structures, doses and stimulation times used in the studies may contribute to the different outcomes observed.

Among the *in vitro* studies that used animal cell cultures, when GOS and GOS/FOS were tested at higher concentrations (5 – 20 g/L) on LPS-challenged equine PBMCs, an increase in TNF-α was found. However, a mixture of GOS/FOS/AOS showed a biphasic effect when used at different doses, with a reduction in TNF-α and IL-10 at higher concentrations and an increase in the same mediators at lower concentrations [243]. Stimulation of rat splenic macrophages and T cells with

FOS, inulin and GOS (all 5 g/L) increased the levels of TNF-α, IL-6, and IL-10 and reduced the levels of LPS-induced IFN-γ and IL-17, with effects that may be related to the modulation of TLR4 [241]. Research conducted on rat small intestinal cell lines (IEC18 cells) confirmed the hypothesis that FOS, GOS and GMOs may act as TLR4 ligands. Indeed, there was a reduction in cytokine secretion (GRO-α, MCP-1 and MIP-2) after treatment with FOS, GOS and GMOs (5 g/L) when the TLR4 gene was knocked down in IEC18 cells [242]. Interaction between NDOs and TLR4 was demonstrated not only in rat intestinal cells but also in mouse-derived bone marrow DCs, whose maturation and cytokine secretion (TNF-α, IL-6, IL-10 and IL-12) were enhanced by treatment with feruloylated oligosaccharides from rice bran tested at different concentrations (6.25-100 μg/mL) [245].

One *in vivo* study on germ-free mice receiving short chain or long chain β2→1 fructans for 5 days showed that the immunomodulatory effects seen were partially mediated by the microbiota and partially microbiota-independent. Both short chain and long chain fructans increased the numbers of T helper cells in the Peyer's patches. Short chain fructans increased regulatory T cells and $CD11b^-$ $CD103^-$ DCs in the mesenteric lymph node and reduced their CD80 expression in the Peyer's patches, whereas long chain fructans modulated the B cell responses. These effects were independent from the gut microbiota and/or their SCFA production [246].

Research performed on human primary cells revealed that treatment of cord blood mononuclear cells with acidic HMOs (1 μg/mL) lead to an increase in IFN-γ- and IL-13-producing T helper and/or cytotoxic T cells and stimulated T helper cell maturation, as shown by higher expression of the activation marker CD25 [238]. Culture with FOS and inulin (5 g/L) increased IL-10 and TNF-α, but not IL-1β and IL-8, production by adult peripheral blood monocytes compared to control, and an upregulation in the response to LPS was seen when those cells were co-stimulated with NDOs and LPS [241]. Higher levels of IL-10 were found after stimulation of human immature monocyte-derived DCs (MoDCs) from peripheral blood with 5 g/L of scGOS/lcFOS, through a mechanism that involved NDO binding to toll-like receptor 4 (TLR4) [195].

Table 1.7 *In vitro* studies with human cell cultures showing direct effects of oligosaccharides on immunity.

Reference	Treatment	Human cells cultured	Study design	LPS testing	Findings
[237]	HMO fractions (12.5 - 125 µg/mL)	Monocytes, lymphocytes and neutrophils from PB + HUVEC	Monocytes, lymphocytes and neutrophils passed over TNF-α-activated HUVEC. Effects of HMO determined by video-microscopy	Yes (QC LAL assay)	Acidic fraction dose-dependently inhibited leukocyte rolling and adhesion to endothelial cells (125 µg/mL, $P < 0.001$; 87.5 µg/mL, $P < 0.001$; 50 µg/mL, $P < 0.001$; 25 µg/mL, $P < 0.001$)
[238]	Neutral HMO (10 µg/mL) and acidic HMO (1 µg/mL)	Term new born CBMC	CBMC cultured with HMO. Intracellular cytokines (IL-4, IL-6, IL-10, IL-13 and IFN-γ) and surface markers of T cells and maturation (CD3, CD4,CD8 and CD25) analysed by flow cytometry	Yes (LAL assay)	Acidic HMO ↑ % IFN-γ-producing T helper and cytotoxic T cells ($P < 0.05$), as well as IL-13 by cytotoxic T cells ($P < 0.05$). Acidic HMO ↑ CD25 expression on T helper cells ($P < 0.05$)
[239]	a3-sialyllactose (10, 50, or 100 mg/L) or FOS Raftilose p95 (0.05, 0.5, 1, 10, or 50 g/L) or a combination (50 mg/L a3-sialyllactose + 50 g/L Raftilose p95)	Caco-2 cells	Caco-2 cells cultured with a3-sialyllactose or Raftilose p95 or combination. Effects of treatments tested on expression of PGlyRP3, PPARγ and pro-inflammatory cytokines	None reported	a3-sialyllactose and Raftilose p95 ↓ IL-12, IL-8 and TNF-α ($P < 0.05$). Both induced ↑ PGlyRP3 expression ($P < 0.05$ for 50 mg/L and 50 g/L), linked to the induction of PPARγ

Abbreviations: LPS, lipopolysaccharide; HMOs, human milk oligosaccharides; PB, peripheral blood; HUVEC, human umbilical vein endothelial cells; QC, quantitative chromogenic; TNF, tumour necrosis factor; LAL, Limulus Amoebocyte Lysate; CBMC, cord blood mononuclear cells; IL, interleukin; IFN, interferon; Caco-2 cells, human epithelial colorectal adenocarcinoma cells; PGlyRP3, peptidoglycan recognition protein 3; PPARγ, peroxisome proliferator-activated receptor γ;

Table 1.7 *In vitro* studies with human cell cultures showing direct effects of oligosaccharides on immunity.

Reference	Treatment	Human cells cultured	Study design	LPS testing	Findings
[240]	Fructans (1 μg/mL or 100 μg/mL) at different DP	Adult PBMC (*n*= 6) and TLR-engineered cell lines (*n*= 11)	PBMC stimulated with fructans. Effects on cytokines (IL-1Ra, IL-1β, IL-6, IL-10, IL-12p70, and TNF-α) evaluated. TLR-engineered cell lines stimulated with fructans. Cell activation measured	Yes (quantitative LAL assay)	Cytokine production dependent on dose and chain length of fructans. SC fructans (DP up to 10) induced regulatory cytokine balance *vs* to LC fructans (DP up to 60), as seen by IL-10/IL-12 ratio ($P < 0.05$ for PBMC stimulated with 1 μg/mL or 100 μg/mL fructans). Activation of TLR-engineered cell lines showed signalling was TLR-dependent
[241]	FOS, inulin, GOS and GMO (5 g/L)	Adult PB monocytes (*n*= 10)	PB monocytes pre-stimulated with LPS (1 μg/mL) or unstimulated, then cultured with NDO. Supernatants collected for cytokine analysis (IL-1β, IL-8, IL-10 and TNF-α) by ELISA	None reported	Treatment with FOS and inulin ↑ IL-10 and TNF-α ($P < 0.05$) but not IL-1β and IL-8. NDO ↑ LPS response when the cells where co-treated
[242]	FOS, inulin, GOS and GMO (5 g/L)	HT29 and Caco-2 cells	LPS (1-5 μg/mL) used for reference or as co-treatment. Cytokine secretion (IL-8 and MCP-1) measured by ELISA	None reported	FOS, inulin, and GMO, but not GOS, ↑ IL-8 production by HT29 cells ($P < 0.05$). No changes in IL-8 after treatment of Caco-2 lines. MCP-1 ↓after treatment of Caco-2 cells with NDO ($P < 0.05$)

Abbreviations: DP, degree of polymerisation; PBMC, peripheral blood mononuclear cells; TLR, toll-like receptor; SC, short chain; LC, long chain; FOS, fructooligosaccharides; GOS, galactooligosaccharides; GMO, goat milk oligosaccharides; ELISA, enzyme-linked immunosorbent assay; HT29 cells, human colorectal adenocarcinoma cells; MCP-1, monocyte chemoattractant protein-1;

Table 1.7 *In vitro* studies with human cell cultures showing direct effects of oligosaccharides on immunity.

Reference	Treatment	Human cells cultured	Study design	LPS testing	Findings
[195]	scGOS/lcFOS (5 g/L)	Immature MoDC and T cells from PB	Immature MoDC stimulated with scGOS/lcFOS in presence or absence of LAB. IL-1α, IL-1β, IL-6, TNF-α, MIP-3α, IL-10 and IL-12p70 measured by ELISA and Luminex assay. MoDC co-cultured with naïve T cells, and Foxp3 expression evaluated by flow cytometry. Experiments with TLR4 antagonist included	Yes (quantitative LAL assay)	scGOS/lcFOS promoted IL-10 release by MoDC ($P < 0.01$). Blocking TLR4 abrogated IL-10 increase, suggesting that NDO act via TLR4. scGOS/lcFOS showed a tendency to ↑ regulatory T cells ($Foxp3^+$)
[194]	HMO (5 g/L) and GOS (5 g/L)	Immature H4 and mature T84, NCM-460 enterocyte cell lines	H4, T84 and NCM-460 cell lines treated with TNF-α or IL-1β or infected with *Salmonella* or *Listeria* and/or with HMO or GOS. Induction of IL-8, MCP-1 and MIP-3α by ELISA and mRNA by qPCR	None reported	HMO and GOS ↓ TNF-α-, IL-1β- and pathogen-induced IL-8, MCP-1 and MIP-3α in H4 cells ($P < 0.001$). In T84 and NCM-460 cells, HMO and GOS ↓ TNF-α-induced MIP-3α ($P < 0.0005$). TNF-□–mediated IL-8 induction was ↓ by HMO in NCM-460 ($P < 0.0005$) but not in T84 cells. Galactosyllactosein HMO and GOS ↓ inflammatory NF-κB signalling in H4 and NCM-460 cell lines ($P < 0.0005$)

Abbreviations: scGOS/lcFOS, short chain galactooligosaccharides/long chain fructooligosaccharides; MoDC, monocyte-derived dendritic cells; LAB, Lactic Acid Bacteria; MIP-3α, macrophage inflammatory protein-3 alpha; H4 cells, human normal foetal intestinal epithelial cells; T84 cells, human metastatic colonic epithelial cells; NCM-460 cells, human normal colon mucosal epithelial cells; mRNA, messenger ribonucleic acid; qPCR, quantitative polymerase chain reaction.

Table 1.8 *In vitro* studies with animal cell cultures showing direct effects of oligosaccharides on immunity.

Reference	Treatment	Cell culture	Study design	LPS testing	Findings
[243]	GOS, GOS+FOS and GOS+FOS+AOS (5 - 20 g/L)	Equine PBMC (*n*= 22)	Equine PBMC pre-incubated with oligosaccharides, then incubated with medium with 1 µg/mL LPS + oligosaccharides. IL-10 and TNF-α measured by ELISA	Yes (quantitative LAL assay)	Exposing PBMC to GOS or GOS+FOS caused a dose-dependent ↑ of TNF-α in LPS-challenged PBMC ($P < 0.05$ for 20 g/L dose of GOS or GOS+FOS vs LPS). Incubation with GOS/FOS/AOS dose-dependently ↓ TNF-α and IL-10 following LPS challenge ($P < 0.05$ for 20 g/L dose of GOS+FOS+AOS vs LPS). Mono- and disaccharide control fractions stimulated inflammatory response in LPS-challenged PBMC, though to a lesser extent than NDO
[241]	FOS, inulin, GOS and GMO (5 g/L)	Rat splenic T cells (*n*= 28) and WT/TLR4 KO mouse splenocytes (*n*= 10)	Rat splenic T cells and WT/TLR4 KO mouse splenocytes pre-stimulated with LPS 1 µg/mL, then cultured with oligosaccharides. Cell signalling inhibitors added prior to treatment with NDO. Supernatants collected for cytokine analysis (rat cytokines: IL-1β, IL-2, IL-6, IL10, GRO-α, IFN-γ, TNF-α and mouse cytokines: IL-6, IL-10, IL-17, IFN-γ, and TNF-α) by ELISA	None reported	Prebiotics ↑ TNF-α, IL-6, and IL-10 secretion by mouse splenocytes ($P < 0.05$) but ↓LPS-induced IFN-γ and IL-17 ($P < 0.05$). Inulin ↑LPS-induced IL-10 ($P < 0.05$). TLR4 KO splenocytes had a depressed response. Prebiotics are TLR4 ligands/modulators in monocytes

Abbreviations: LPS, lipopolysaccharide; GOS, galactooligosaccharides; FOS, fructooligosaccharides; AOS, acidic oligosaccharides; PBMC, peripheral blood mononuclear cells;; IL, interleukin; TNF, tumour necrosis factor; ELISA, enzyme-linked immunosorbent assay; LAL, Limulus Amoebocyte Lysate; GMO, goat milk oligosaccharides; WT/TLR4 KO mice, wild type/toll like receptor 4 knockout mice; NDO, non-digestible oligosaccharides; GRO-α, growth-related oncogene-alpha; IFN, interferon; TLR, toll-like receptor;

Table 1.8 *In vitro* studies with animal cell cultures showing direct effects of oligosaccharides on immunity.

Reference	Treatment	Cell culture	Study design	LPS testing	Findings
[242]	FOS, inulin, GOS and GMO (5 g/L)	Rat IEC18 cells	LPS used for reference or as co-treatment with prebiotics. Cytokine secretion (IL-6, IL-8, MIP-2, MCP-1, GRO-α) measured by ELISA	None reported	IEC18 cells secreted GRO-α, MCP-1 and MIP-2 ($P < 0.05$) following treatment with prebiotics, with an efficacy similar to LPS-stimulated cells. Response was ↓ by TLR4 gene knockdown. Prebiotics are TLR4 ligands in IEC
[244]	Feruloylated oligosaccharides from rice bran (6.25-100 µg/mL)	Bone marrow DC from C3H/HeN or C57BL/6 mouse with normal or mutated TLR4 and TLR2	DC cultured with LPS or feruloylated oligosaccharides. Cytokines and chemokines (IL-6, IL-10, IL-12, MCP-1, TNF-α and RANTES) analysed by ELISA. Surface markers analysed by flow cytometry. Activity assaysfor NF-κB	Yes (QC LAL assay)	Feruloylated oligosaccharides induced maturation of DC, as shown by ↑ CD40, CD80/CD86 expression ($P < 0.01$ and $P < 0.001$, respectively) as well as ↑ TNF-α, IL-6, IL-10 and IL-12 (at the highest dose tested, $P < 0.001$ for all cytokines) via TLR4 and/or TLR2. This may be related to ↑ NF-κB activity

Abbreviations: IEC18 cells, nontransformed rat small intestinal epithelial cells; MCP-1, monocyte chemoattractant protein-1; MIP-2, macrophage inflammatory protein-2; IEC, intestinal epithelial cells; DC, dendritic cells; RANTES, regulated on activation, normal T cell expressed and secreted; NF-κB, nuclear factor κB; QC, quantitative chromogenic.

Table 1.9 *In vivo* study on germ-free mice showing direct effects of oligosaccharides on immunity.

Reference	Treatment	Study design	Duration	Findings
[246]	SC or LC β2→1-fructans	Conventional C57BL/6OlaHsd male mice or C57BL/6OlaHsd male GF mice (both 8 weeks old) received SC or LC β2→1-fructans. Immune cells in spleen, MLN and PP analysed by flow cytometry. Gene expression in ileum measured with microarray. Gut microbiota composition analysed with 16S rRNA sequencing of faecal samples	5 days	β2→1-fructans modulated immunity by microbiota and microbiota-independent effects. Effects dependent on chain length of fructans. Both SC and LC fructans ↑ Th1 cells in PP (both $P < 0.05$). SC fructans ↑ regulatory T cells and CD11b− CD103− DCs in MLN ($P < 0.01$). ↑ 2-α-l-fucosyltransferase 2 expression in ileum of conventional mice. Effects not associated with shifts in gut microbiota or SCFA. SC fructan induced ↓ CD80 expression by CD11b− CD103− DC in PP ($P < 0.05$), LC fructan modulated B cell responses in GF mice

Abbreviations: SC, short chain; LC, long chain; GF, germ free; MLN, mesenteric lymph nodes; PP, Peyer's patches; rRNA, ribosomial RNA; Th1, T helper 1; DC, dendritic cells; SCFA, short chain fatty acids;

Overall, there is evidence to conclude that NDOs can exert direct, microbiota-independent effects on immune cells. HMOs, FOS, inulin and GOS were consistently shown to directly modulate cytokine production (IL-6, IL-8, IL-10, IL-12, MCP-1, MIP-3α and TNF-α) and immune cell maturation (lymphocytes, DCs) in *in vitro* models, with mechanisms that seem to involve TLR ligation. One *in vivo* study on germ-free mice reinforced the *in vitro* evidence for microbiota-independent effects of NDOs on immunity. However, not all NDOs appear to have the same effect (anti-inflammatory *vs* pro-inflammatory) and within a class of NDOs inconsistent effects have been reported. Whereas HMOs displayed clear anti-inflammatory properties *in vitro*, which might at least partially explain their protective effects against allergy and infection *in vivo*, FOS, inulin and GOS showed various outcomes on immunity, including anti-inflammatory as well as pro-inflammatory effects.

The use of different doses and types of prebiotics as well as various cell culture models may explain the differences in cytokine production observed *in vitro*. Additionally, the chain length of oligosaccharides appears to have an important role in inducing either anti-inflammatory or pro-inflammatory responses. Vogt *et al.* [240] demonstrated that short chain FOS (2-5 units) elicited the production of anti-inflammatory cytokines to a greater extent than long chain FOS (>8 units). Additionally, only half of the studies assessed the LPS content of oligosaccharide fractions used in culture [195, 234, 237, 238, 243, 245]. Because the binding of LPS to TLR4 on monocytes, macrophages and B cells leads to strong, pro-inflammatory responses including the secretion of TNF-α, IL-1β, IL-6, IL-8, IL-10, IL-12, IL-15 and TGF-β [247], it is important to determine whether the direct effects of oligosaccharides on cytokines are due to the action of the oligosaccharide fractions or to the presence of LPS within prepared fractions.

Although dietary oligosaccharides bind and signal via TLR4 in monocytes, macrophages and intestinal epithelial cells [195, 240, 242, 245] often eliciting a pro-inflammatory cytokine production *in vitro*, they are not necessarily pro-inflammatory *in vivo*. This is most likely due to differences between *in vitro* and *in vivo* conditions. Therefore, more research needs to be carried out to understand the mechanisms through which oligosaccharides affect immunity.

1.7.6 Effects of prebiotics on inflammatory bowel diseases: animal models and human clinical trials

IBD patients have lower numbers of bifidobacteria and lactobacilli in the gut, lower concentrations of faecal SCFAs and high mucosal inflammation primarily induced by pro-inflammatory cytokines [248]. Prebiotics are promising in the management of IBD for their role in restoring gut microbiota homeostasis and affecting cytokine production and immune cell maturation. In recent years, animal and human studies on the role of prebiotics in IBD have been extensively reviewed [249-253].

Murine experimental models of colitis associated either with epithelial barrier disruption or with immune cell defects have been developed to mimic IBD in humans [254]. Rodent experimental colitis models showed that both short term (<1 week) and long term (>1 month) treatment with prebiotics including lactulose, inulin and GMOs reduced colonic damage and inflammation, whereas no convincing reduction of inflammation was seen in animal studies that used GOS or FOS [251]. When GOS and FOS were used in association with other soluble and insoluble polysaccharides, a decrease in inflammatory cytokines as well as an increase in IL-10 and regulatory T cells in the mesenteric lymph nodes were observed [255]. Together, these results indicate that various prebiotics may have different potential in attenuating inflammation, and that more studies using the experimental colitis model are needed [251].

Human clinical trials on prebiotic use in IBD have mostly been conducted using FOS and inulin, while only one study is available for GOS (Table 1.10). In a double-blind placebo controlled trial on individuals with chronic pouchitis (an inflammation in the lining of an artificial rectum created after UC surgery), treatment with 24 g/d inulin for 3 weeks resulted in lower endoscopic and histological inflammation, higher faecal butyrate concentration and a tendency for lower concentrations of secondary bile acids in faeces [256]. Similarly, patients with active UC receiving 12 g/d oligofructose-enriched inulin for 2 weeks displayed a reduction in disease activity and in faecal calprotectin (a marker of intestinal inflammation) but no changes in circulating inflammatory mediators (*e.g.* IL-8), compared to control [257]. In an open-label study on patients with active UC, supplementation with 2.8 g/d GOS did not decrease clinical scores or inflammation but normalised stools and increased the proportions of health-promoting gut bacteria (*e.g. Bifidobacterium*) in individuals with less active disease [253]. In another double-blind randomised control trial, supplementation with 10 g/d inulin for 4 weeks increased the numbers of bifidobacteria, lead to higher concentrations of faecal acetaldehyde and butyrate and decreased disease activity in CD patients, although there was a higher dropout rate for those undergoing supplementation compared to placebo [258]. In an open-label trial, treatment with 15

g/d FOS for 3 weeks reduced disease activity in individuals with active ileo-colonic CD and increased the numbers of bifidobacteria as well as the numbers of DCs from rectal biopsies expressing IL-10, TLR2 and TLR4 [259]. These results were only partially confirmed by a larger double-blind randomised control trial, where patients with active CD supplemented 15 g/d FOS for 4 weeks showed higher numbers of IL-10^{+} DCs from rectal biopsies but no differences in disease activity, numbers of bifidobacteria and levels of faecal calprotectin [260]. Several studies conducted on other non-prebiotic dietary fibres, such as ispaghula husk [261] and germinated barley foodstuff [262-264], showed that also these two polysaccharides may have a potential in attenuating UC and/or CD clinical symptoms. Overall, while inulin appears promising in reducing IBD symptoms and inflammation, there are currently few studies of FOS and GOS in IBD. More research using standardised methods needs to be conducted to explore the potential preventive and/or therapeutic use of prebiotics in the management of IBD.

Table 1.10 Human studies of prebiotic use for the management of IBD.

Reference	Treatment	Study design	Duration	Condition	Findings
[256]	Inulin 24 g/d	Double-blind placebo controlled trial (*n*= 20)	3 weeks	Chronic pouchitis	↓ endoscopic and histological inflammation, ↑ in faecal butyrate ($P < 0.01$), ↓ in faecal pH ($P = 0.02$), tendency in ↓ secondary bile acids in faeces
[259]	FOS 15 g/d	Open-label trial (*n*= 10)	3 weeks	Active ileocolonic CD	↓ disease activity ($P < 0.01$), ↑ in faecal bifidobacteria ($P < 0.001$), ↑numbers of dendritic cells expressing IL-10, TLR2 ($P < 0.08$) and TLR4 ($P < 0.001$) from rectal biopsies
[260]	FOS 15 g/d	Double-blind randomised control trial (*n*= 103)	4 weeks	Active CD	No difference in disease activity, ↑ flatulence ($P = 0.004$) and abdominal pain ($P = 0.048$) than placebo. No difference in bifidobacteria, serum C-reactive protein or faecal calprotectin. ↑ in IL-10^+ DC from rectal biopsies ($P < 0.05$)
[258]	Oligofructose-inulin (1:1) 10 g/d	Double-blind randomised control trial (*n*= 67)	4 weeks	Inactive or moderately active CD	↓ disease activity ($P < 0.048$), but ↑ dropout rate than placebo. ↑ in bifidobacteria ($P = 0.03$) and faecal acetaldehyde ($P = 0.0008$) and butyrate ($P = 0.0011$) concentrations
[257]	Oligofructose-enriched inulin 12 g/d	Double-blind randomised controlled trial (*n*= 19)	2 weeks	Active UC	↓ disease activity ($P < 0.05$), ↓ in faecal calprotectin ($P < 0.05$) after just 1 week, no changes in inflammatory mediator release (IL-8, PGE-2)
[253]	GOS 2.8 g/d	Open-label study (*n*= 17)	6 weeks	Active UC	No differences in clinical scores, faecal calprotectin, SCFAs and pH. ↑ normal stool proportion and ↓ severity of loose stools and urgency (all $P < 0.05$). ↑ proportions of *Bifidobacterium* and *Christensenellaceae* only in patients with less active disease

Abbreviations: FOS, fructooligosaccharides; CD, Crohn's disease; IL, interleukin; TLR, toll-like receptor; DC, dendritic cells; UC, ulcerative colitis; PGE-2, prostaglandin-E2; SCFAs, short chain fatty acids.

1.8 Rationale, hypothesis and aims

1.8.1 Rationale

Supplementation with prebiotics including GOS has been associated with positive health benefits, such as maintaining gut health and improving the symptoms of gastrointestinal disorders. To date, it is unclear whether the effects of GOS on health and immunity are exerted exclusively through modulation of the intestinal microbiota or whether they can directly interact with immune cells. There is evidence from *in vitro* models using intestinal cell lines and human supplementation studies that prebiotics are transported across the intestinal epithelium and are found in plasma, urine and stools of infants and of those with disrupted intestinal permeability. It is likely that GOS pass through the gut barrier of adults with a leaky gut due to inflammatory conditions or to life-style associated stressors and enter in contact with GALT and systemic immune cells. *In vitro* studies on human or animal cell lines and primary cell cultures demonstrated that prebiotics modulate cytokine production in a microbiota-independent manner both in unchallenged and immune-challenged cells, with mechanism that may involve TLR signalling. While HMOs showed clear anti-inflammatory effects, other prebiotics including GOS displayed anti-inflammatory as well as pro-inflammatory effects. Because most studies failed to perform quality controls on prebiotic compounds before application to cell cultures, some pro-inflammatory effects might have been due to LPS contamination or to an effect of residual free sugars from the production process. Inconsistent data in the literature may have been caused also by different prebiotic doses, prebiotic structures and cell culture models used. In terms of oligosaccharide structure, the chain length of prebiotic fractions were shown to directly affect the direction of inflammatory responses by immune cells, leading to either anti-inflammatory (short-chain FOS) or pro-inflammatory (long-chain FOS) outcomes. So far, the microbiota-independent effects of GOS upon phenotypes and inflammatory cytokines of human adult PBMCs have not been studied. There is limited information in the literature on the immunological effects of GOS fractions with different chain length. Convincing preliminary data support the use of prebiotics as immunomodulators for the management of IBD, but there are currently no *in vitro* studies on the immunological effects of GOS on immune cells from IBD donors. MAIT cells are thought to play an important role in auto-immune and inflammatory diseases, such as IBD. MAIT cells are depleted in peripheral blood and recruited to the inflamed mucosa in patients with IBD. Vitamin metabolites produced by the gut microbiota are known to activate MAIT cells via binding to their TCR. Activation and accumulation of these cells at the inflammation site depends not only on microbial ligands but also on co-stimulatory signals, such as TLRs. The search for new MAIT cells ligands has been identified as a research priority, and prebiotics may be involved in MAIT cell activation either via

direct binding to their TCR or by indirectly modulating the TLRs on other cell types. This research will provide evidence for the immunological effects of GOS upon PBMCs and MAIT cells from healthy donors and those with IBD. If effects upon immune functions are observed, this will have the potential to inform future nutritional or therapeutic studies among healthy individuals and those with IBD.

1.8.2 Aim and objectives

The aim of this research is to investigate whether GOS fibres exert direct immunomodulatory effects on human PBMCs from healthy donors and from IBD donors *ex vivo*, and the role of MAIT cells in this response. The specific objectives are to:

-Optimise an *ex vivo* model using adult PBMCs from healthy donors to study the direct immunological effects of GOS. Four different GOS batches will be screened by Limulus Amoebocyte Lysate (LAL) assay to ensure suitability for cell culture applications. The optimal concentrations and incubation times for culturing PBMCs with GOS or other inflammatory stimuli for pre-incubation and co-culture experiments will be identified based on their effects on cell viability and secreted cytokines;

-Assess the effects of GOS upon cell viability, cell frequencies, activation markers and soluble mediators of PBMCs from healthy donors and those with IBD, and compare the immune responses between the two PBMC groups. Additionally, to provide an insight into the mechanisms of GOS action first by investigating the role of TLRs (TLR2, TLR4) in cytokine secretion following culture with GOS, and secondly by evaluating the PBMC response to GOS in presence of LPS challenge;

-Evaluate the effects of culturing healthy PBMCs with isolated GOS fractions at different degree of polymerisation on the frequencies of PBMC subsets, on the expression of activation markers and on a panel of secreted cytokines, and compare the results with those of whole GOS. Additionally, to select the most potent GOS fraction and assess its ability to affect TLR3-mediated inflammation, as measured by changes in the expression levels of activation markers and secreted cytokines;

-Optimise a gating strategy to identify MAIT cells in PBMCs and evaluate the effects of culturing with GOS and/or a vitamin B metabolite on total PBMC viability and on the expression of surface markers, intracellular cytokines and CD69 by MAIT cells and other T cell subsets, using cells from healthy donors and those with IBD. Additionally, to assess the effects of culturing with GOS

and/or a selected vitamin B metabolite on a panel of secreted cytokines chosen for their role in IBD.

1.8.3 Hypothesis

It is hypothesised that GOS will induce changes in the levels of activation markers and soluble mediators of PBMCs and MAIT cells *in vitro*, with mechanisms that may involve signalling through TLR4. While the direction of change (anti-inflammatory *vs* pro-inflammatory) is likely to vary according to the dose and structure of GOS used, it is expected that GOS will promote immunostimulation *in vitro* by increasing the amounts of secreted cytokines and by stimulating immune cell activation. It is expected that isolated GOS fractions at lower degree of polymerisation will have the strongest immunological effects. The immunostimulatory effects of GOS will be measured in terms of changes in the frequencies and expression levels of cell surface and intracellular markers of PBMC subsets by flow cytometry and in the levels of secreted mediators by Luminex assays compared to unstimulated controls. It is speculated that PBMCs from IBD donors will respond differently to stimulation with GOS compared to PBMCs from healthy donors due to differing levels of inflammation at baseline and genetic variation. Specifically, it is hypothesised that IBD PBMCs will respond more strongly to GOS due to their likely higher inflammation at baseline. Although it is expected that GOS will signal via TLR4 as shown for other NDOs in *in-vitro* models using monocytes, macrophages and intestinal epithelial cells, often eliciting a pro-inflammatory cytokine production *in vitro*, they are not expected to be pro-inflammatory *in vivo.* Instead, it is expected that GOS will reduce inflammation induced by other inflammatory stimuli (*e.g.* LPS, riboflavin metabolite) when tested in co-cultures, which are more representative of the physiological conditions in the gut, by competing with them for binding sites on cells or by coating them and blocking their signalling.

Chapter 2 MATERIALS AND METHODS

2.1 *Ex vivo* human peripheral blood mononuclear cells

2.1.1 Ethics statement

The purchase of previously-collected, non-identifiable human peripheral blood mononuclear cells (PBMCs) from Stemcell Technologies (Cambridge, UK) for this study obtained a favourable ethical opinion from the Derby Research Ethics Committee (REC reference: 17/EM/0462). PBMCs were collected by Stemcell Technologies following approval from Western Institutional Review Boards. Information sheets were provided to the participants and consent forms for the blood donation were signed by donors. Samples were linked anonymous and researchers did not have access to coding information nor to any participant information beyond basic characterisation data. PBMCs were stored at the Institute of Developmental Sciences, University of Southampton, Southampton General Hospital in accordance with the Human Tissue Authority requirements. Research data were backed up to University of Southampton secure storage and the research outputs uploaded to the University of Southampton Institutional Research Repository.

2.1.2 Peripheral blood mononuclear cells from healthy donors

Healthy PBMCs were isolated by Stemcell Technologies from peripheral blood leukapheresis samples using density gradient separation or red blood cell lysis. Peripheral blood was collected using acid-citrate-dextrose solution A as the anticoagulant. Cells were characterised for age, sex, ethnicity, obesity status and smoking status of the donors and delivered frozen on dry ice in CryoStor® CS10 cryopreservation medium, which contained 10% dimethyl sulfoxide (DMSO). On receipt, PBMC cryovials (1 x 10^8 cells/vial, Cat. No. 70025) were immediately stored in liquid nitrogen. Healthy PBMCs were selected to match the characteristics of Crohn's disease PBMCs (see section 2.1.3) by age (41.4 *vs* 44.1 years), sex (64.3% *vs* 62.5% male) and ethnicity (71.4% *vs* 75% Caucasian). It was not possible to match the donors for obesity status (21.4% *vs* 37.5% obese) and smoking status (14.3% *vs* 0% smokers) due to limited inventory. A list of selected healthy donors and their characteristics is presented in Table 2.1. Five additional donors were selected for the work on isolated GOS fractions (Chapter 5), which was conducted exclusively on healthy PBMCs (Table 2.2).

Table 2.1 List of chosen healthy donors and their age, sex, ethnicity, obesity status and smoking status.

Lot number	Age	Sex	Ethnicity	Obesity (BMI> 30 kg/m^2)	Smoker
1805140180	38	M	Caucasian	NO	YES
1802210244	29	M	Hispanic	NO	NO
1805090103	57	M	Caucasian	NO	NO
1809140196	49	F	African American	YES	NO
1804230207	25	F	Caucasian	NO	NO
1807160152	63	M	Caucasian	YES	NO
1903060075	47	M	Caucasian	NO	NO
1910401003	26	F	Caucasian	NO	NO
1606200170	47	M	Caucasian	NO	YES
1702070039	30	M	African American	NO	NO
1703170126	41	M	African American	NO	NO
1707170061	45	F	Caucasian	YES	NO
1712130101	61	F	Caucasian	NO	NO
1903110116	22	M	Caucasian	NO	NO

Table 2.2 Five healthy donors selected for use in experiments on isolated GOS fractions.

Lot number	Age	Sex	Ethnicity	Obesity (BMI> 30 kg/m^2)	Smoker
1903040034	31	M	Caucasian	NO	NO
200271301C	44	M	Caucasian	NO	NO
2003425001	20	M	Caucasian	NO	NO
2011412001	52	M	Caucasian	NO	NO
210172901C	35	M	Caucasian	NO	NO

2.1.3 Peripheral blood mononuclear cells from Crohn's disease donors

Crohn's disease PBMCs were isolated by Stemcell Technologies from peripheral blood of patients with Crohn's disease using density gradient separation or red blood cell lysis. Peripheral blood was collected using citrate-phosphate-dextrose-adenine 1, acid-citrate-dextrose solution A, acid-citrate-dextrose solution B or ethylenediaminetetraacetic acid as an anticoagulant. Cells were characterised as described for healthy PBMCs. No information on disease status (e.g. active disease, under medication, in remission) was available. Cells were delivered frozen on dry ice in CryoStor® CS10 cryopreservation medium (10% DMSO), and cryovials (1 x 10^7 cells/vial, Cat. No. 70052) were immediately stored in liquid nitrogen. A list of chosen Crohn's disease donors and their characteristics is reported in Table 2.3.

Table 2.3 List of chosen Crohn's disease donors and their age, sex, ethnicity, obesity status and smoking status.

Lot number	Age	Sex	Ethnicity	Obesity(BMI> 30 kg/m^2)	Smoker
1010113267	50	F	Caucasian	NO	NO
1010113278	28	M	Caucasian	NO	NO
1010113287	50	M	Caucasian	YES	NO
1010113291	73	M	Caucasian	YES	NO
1010113300	39	F	African American	NO	NO
1010113306	25	F	African American	NO	NO
1010113308	50	M	Caucasian	NO	NO
1010113318	38	M	Caucasian	YES	NO

PBMCs were thawed according to Stemcell Technologies' recommended protocol [265] using sterile techniques. Cells were transported from the liquid nitrogen store to the tissue culture laboratory on dry ice. Cell counts and viability measurements were performed before and after the washing steps to confirm the number of cells provided and to assess the quality of recovery. The washing steps were carried out using complete Roswell Park Memorial Institute (RPMI)-1640 medium, containing 20 mM 4-(2-hydroxyethyl)-1-piperazineethanesulfonic acid (HEPES) and 20 mM L-glutamine, without sodium bicarbonate, sterile-filtered and supplemented with 10% foetal bovine serum (FBS) and 1% penicillin/streptomycin (Sigma Aldrich). The cell suspension was incubated for 15 minutes at room temperature with 1 mg/mL DNase I solution (Stemcell Technologies) to prevent cell clumping. After the washing steps, PBMCs were centrifuged at 200 x g for 10 minutes and the cell pellet was resuspended in 1 mL of complete RPMI-1640 medium. Cells not immediately used for downstream applications were cryopreserved in 10% DMSO cell-freezing medium (Sigma Aldrich). Cryovials were kept on ice and transferred rapidly into a Mr. Frosty™ freezing container filled with 100% isopropyl alcohol (Sigma Aldrich). The container was placed in a -80°C freezer overnight and the cells were transported on dry ice for long-term storage in liquid nitrogen.

2.2 *In vitro* human monocytic cell line THP-1

THP-1 is a human monocytic cell line derived from the peripheral blood of a 1-year-old male with acute monocytic leukaemia. THP-1 cells were obtained from the European Collection of Authenticated Cell Cultures (ECACC – 88081201). Cells were thawed and subcultured according to supplier's instructions. Cells were cultured at 5-7 x 10^5 cells/mL in RPMI-1640 medium supplemented with 10% FBS, 0.4 mM L-glutamine, 1% penicillin/streptomycin and HAT (100 µM hypoxanthine, 0.4 µM aminopterin and 16 µM thymidine), and incubated at 37°C, 5% CO_2. Passages used for assays ranged from 8 to 25. Cells were grown in T-175 flasks until confluent.

2.3 Cell culture conditions

Unless otherwise stated, 2.5 x 10^6 PBMCs or THP-1 cells/mL in complete RPMI-1640 medium (Sigma Aldrich) were seeded in 48-well suspension plates (Greiner Cellstar®) in a final culture volume of 500 µL/well. Specific stimulation conditions and incubation times used in each experiment will be presented within each study chapter. An overview of the main stimuli used in cell cultures is presented here.

2.3.1 Bimuno® galactooligosaccharide

Bimuno® galactooligosaccharide (B-GOS®) batches were supplied by Clasado Biosciences either in a powder (batch A and batch B) or in a syrup format (batch C and batch D). The B-GOS® powders contained on average 80% (w/w) pure GOS and approximately 20% (w/w) free sugars, including glucose (5.3% w/w), galactose (0.5% w/w) and lactose (11.6% w/w). B-GOS® syrup batch C was constituted by 47.8% (w/v) pure GOS, 28.2% (w/v) glucose, 15.2% (w/v) galactose and 7.6% (w/v) lactose, while B-GOS® syrup batch D was constituted by 66.1% (w/v) pure GOS, 22.9% (w/v) glucose, 1.7% (w/v) galactose and 8.2% (w/v) lactose. Concentrations of B-GOS® used in cell cultures were selected based upon previous *in vitro* research conditions used by Vendrig *et al*. [243] and with reference to the instructions for daily intake if orally consumed (approximately 12 mg/mL pure GOS). For B-GOS® powders (batches A and B), the highest dose of product was a final concentration of 15 mg/mL, corresponding to 12 mg/mL of pure GOS (80% w/w). A medium dose of 5 mg/mL B-GOS® product (4 mg/mL pure GOS) and a low dose of 1 mg/mL B-GOS® product (0.8 mg/mL pure GOS) were prepared by further diluting the highest dose with RPMI-1640 medium. In order to use the same final concentrations of pure GOS in cultures (0.8 mg/mL, 4 mg/mL and 12 mg/mL) when using the B-GOS® syrups, a stock solution (1 g/mL) was prepared taking into account their water content (25.6% and 24.1% water in B-GOS® syrup batches C and D, respectively). Dilutions of the stock solution were made to obtain a high dose (25.1 mg/mL and 18.2 mg/mL), medium dose (8.4 mg/mL and 6.1 mg/mL) and low dose (1.7 mg/mL and 1.2 mg/mL) of B-GOS® syrup batches C and D, respectively. B-GOS® solutions were aliquoted to avoid multiple freeze-thaw cycles and stored at -20°C. Concentrations of pure GOS rather than of B-GOS® product (powder or syrup) will be referred to throughout this work. A summary of B-GOS® batches used in cell cultures and their relative nomenclature is reported in Table 2.4.

Table 2.4 Concentrations of B-GOS® batches used in cell cultures and their relative nomenclature.

Product	Format	Final concentration of product in culture	Final concentration of pure GOS in culture	Abbreviation
B-GOS® batch A	Powder (80% pure GOS)	1 mg/mL 5 mg/mL 15 mg/mL	0.8 mg/mL 4 mg/mL 12 mg/mL	GOS A 0.8 GOS A 4 GOS A 12
B-GOS® batch B	Powder (80% pure GOS)	1 mg/mL 5 mg/mL 15 mg/mL	0.8 mg/mL 4 mg/mL 12 mg/mL	GOS B 0.8 GOS B 4 GOS B 12
B-GOS® batch C	Syrup (47.8% pure GOS)	1.7 mg/mL 8.4 mg/mL 25.1 mg/mL	0.8 mg/mL 4 mg/mL 12 mg/mL	GOS C 0.8 GOS C 4 GOS C 12
B-GOS® batch D	Syrup (66.1% pure GOS)	1.2 mg/mL 6.1 mg/mL 18.2 mg/mL	0.8 mg/mL 4 mg/mL 12 mg/mL	GOS D 0.8 GOS D 4 GOS D 12

Because B-GOS® batches contain pure GOS as well as residual mono- and di- saccharides deriving from their enzymatic production, controls were included to quantify and discriminate the effects of glucose, galactose and lactose from those of pure GOS. Concentrations of free sugars were chosen to correspond to the quantity of glucose, galactose and lactose contained in the highest dose tested of B-GOS® batch C (25.1 mg/mL, corresponding to 12 mg/mL pure GOS), which was the batch that presented the highest content of free sugars. Glucose (7.1 mg/mL), galactose (3.8 mg/mL) and lactose (1.9 mg/mL) were assessed in combination or individually at their original concentration in the product. Glucose, galactose and lactose were also tested at a reference concentration (1.9 mg/mL) to enable comparison of each single sugar at the same concentration. Controls were prepared using cell-culture grade D-(+)-glucose, D-(+)-galactose and α-lactose powders (Sigma Aldrich), and dilutions were carried out in RPMI-1640 supplemented media. Sugar controls were aliquoted to avoid multiple freeze-thaw cycles and stored at -20°C.

2.3.2 Mitogens, protein kinase C activator, toll-like receptor 3 agonist and riboflavin derivatives

In order to gain insight into cell types and/or signalling pathways activated by GOS and to identify potential stimuli to use in co-culture and pre-incubation experiments, a range of mitogens, a protein kinase C (PKC) activator, a TLR-3 agonist and riboflavin derivatives were utilised. Depending on the aim of the experiment, stimuli were used either as a positive control indicating functional cell activation or as an immune challenge in co-culture and pre-incubation settings.

Mitogens are substances that promote cell division or 'mitosis', which is when the replicated chromosomes are divided into two new nuclei. Mitogens act by promoting the activation of mitogen-activated protein kinase (MAPK) pathways, which transduce extracellular signals to cellular responses including cell proliferation, differentiation and inflammatory responses [266, 267]. Concanavalin A (Con A) is a lectin mitogen that binds to the mannose moiety of cell surface glycoproteins including the T cell receptor TCR. The binding of Con A to the TCR triggers intracellular signalling that results in T cell activation and proliferation [268]. Lipopolysaccharide (LPS) is a non-lectin mitogen that forms a complex with LPS-binding protein (LBP), cluster of differentiation (CD) 14, myeloid differentiation factor 2 (MD2) and TLR4 resulting in the activation of B cells, monocytes and macrophages and the induction of inflammatory cytokines [15, 269]. Phorbol 12-myristate 13-acetate (PMA) is a phorbol ester that binds to the C1 domain of PKC and causes the enzyme to translocate to the cell surface. PMA is often used in association with ionomycin, an ionophore that binds Ca^{2+} ions and facilitates their transport across membranes [268, 270]. Activation of PKC by PMA and ionomycin triggers a cascade of cellular responses, resulting in T cell activation and cytokine production. The CD3 CD28 CD2 T cell activator (TCA) consists of soluble antibody complexes that bind CD3, CD28 and CD2, therefore providing primary and co-stimulatory signals for T cell activation. 6,7-dimethylribityl lumazine (RL-6,7-DiMe) and 5-amino-6-D-ribitylaminouracil (5-A-RU) are intermediates in bacterial riboflavin synthesis. Both activate mucosal-associated invariant T (MAIT) cells in a major histocompatibility complex class I-related (MR1)-dependent manner, with different levels of potency [271]. 5-A-RU reacts with small ubiquitous metabolites, such as methylglyoxal (MG), to form the potent MAIT cell activator 5-(2-oxopropylideneamino)-6-D-ribitylaminouracil (5-OP-RU) [272]. Polyinosinic-polycytidylic acid (poly(I:C)) is a synthetic analogue of viral dsRNA that binds to the TLR3 of dendritic cells (DCs) and macrophages, resulting in the activation of TNF receptor-associated factors (TRAF3 and TRAF6) that trigger the production of pro-inflammatory cytokines [273]. Concentrations of mitogens, PKC activator, TLR3 agonist and riboflavin derivatives were established based on similar studies with PBMCs found in the literature [85, 86, 200, 243, 274-280]. Con A, LPS, PMA, ionomycin and MG were purchased from Sigma Aldrich, TCA from Stemcell Technologies, poly(I:C) from InvivoGen, RL-6,7-DiMe and 5-A-RU from 2BScientific. A summary of the concentrations and nomenclature used is presented in Table 2.5. Negative or 'unstimulated' controls were always cultured under the same experimental conditions as the stimulated cells, but without GOS or other immune challenges.

Table 2.5 Concentrations of mitogens, protein kinase C activator, TLR3 agonist and riboflavin derivatives used in cell cultures and their relative nomenclature.

Reagent	Final concentration in culture	Abbreviation
Concanavalin A from *Canavalia ensiformis*	5 µg/mL 50 µg/mL	Con A 5 Con A 50
Lipopolysaccharide from *Escherichia coli* O111:BA	0.1 µg/mL 1 µg/mL	LPS 0.1 LPS 1
Phorbol 12-myristate 13-acetate + ionomycin	10 ng/mL + 1 µg/mL 25 ng/mL + 1 µg/mL 50 ng/mL + 1 µg/mL	PMA 10 PMA 25 PMA 50
CD3 CD28 CD2 T cell activator	25 µg/mL	TCA
Polyinosinic-polycytidylic acid	10 µg/mL	Poly(I:C)
6,7-dimethylribityl lumazine	75 µM	RL-6,7-DiMe
5-amino-6-D-ribitylaminouracil + methylglyoxal	0.18 µM + 1 µM	5-A-RU + MG

2.4 Cell counts

The cell counting method is based on the Coulter principle, in which nonconductive particles suspended in electrolytes cause an increase in the electrical resistance of the liquid. Therefore, the number of cells contained in a given volume of electrolyte (buffered saline solution) can be quantified by measuring changes in current. Cell suspensions were diluted 1:500 in Isoton® II Diluent (Beckman Coulter) and counted on a Beckman-Coulter counter. Fresh Isoton® II Diluent was used to rinse the probe and wash the system in between readings from different samples. Cells were counted before and after the washing steps to check cell numbers and ensure optimal recovery (Appendix A).

2.5 Cell viability

To ensure that culture with B-GOS® and/or other stimuli (mitogens, PKC activator, TLR3 agonist and riboflavin derivatives) did not damage immune cells under the tested conditions, cell viability measurements were performed using membrane leakage assays. Membrane leakage assays are based on the principle that viable cells possess an intact plasma membrane that excludes the dye, which instead passes through the damaged membrane of dead cells and stains their cytoplasm. Stained dead cells can be distinguished from clear live cells either using microscopy (trypan blue, TB) or flow cytometry (propidium iodide, PI; fixable viability stains). Viability assays by flow cytometry generally have higher sensitivity due to increased sample size and allow for inclusion in other assays, such as immunophenotyping panels [281]. The level of correlation between viability measures obtained by microscopy (TB) and flow cytometry (PI) was calculated to validate the use of flow cytometry. To ensure optimal separation between viable and non-viable cells, BD

Horizon™ fixable viability stains 510 (FVS510) and 780 (FVS780) were titrated before use. Results from validation and titration experiments can be found in Appendix B. For TB assay, cell suspensions (2.5 x 10^6 cells/mL) were stained 1:1 with a 0.4% solution of TB in PBS (Thermo Fisher Scientific). Solutions were allowed to settle in the haemocytometer for 10 seconds before counting. Dead cells and total cells were counted within the 4 corner squares using a 10 X objective. Cells were only counted when within a square or on the right-hand or bottom boundary line. Cell viability (%) was calculated by dividing the live cell count by the total cell count and multiplying by 100. In matched samples, viability was also evaluated using PI staining. 200 µL of cell suspension (2.5 x 10^6 cells/mL) were mixed with 5 µL of 1 mg/mL PI solution (Thermo Fisher Scientific) and analysed on a FACS Calibur flow cytometer (Becton Dickinson Immunocytometry Systems). Unstained cells were included to take into account auto-fluorescence of samples. In order to have more flexibility in multicolour flow cytometry panels and minimise spillover when using multiple fluorochromes, FVS510 or FVS780 were used instead of PI. The choice between FVS510 and FVS780 was dictated by channel availability and compatibility with other dyes. FVS510 and FVS780 dyes were reconstituted according to the manufacturer's instructions [282, 283] and used at a final concentration in cell suspension of 1:500 and 1:1000, respectively. 100 µL cells (4 x 10^5 cells/FACS tube) were incubated with 10 µL of FVS510 or FVS780 for 15 minutes, protected from light. Cells were washed twice with a washing solution constituted by 1% bovine serum albumin (BSA) and 0.1% sodium azide in phosphate-buffered saline, PBS (Sigma Aldrich), then centrifuged at 450 x g for 5 minutes and resuspended in 300 µL PBS. Data were collected on an Attune NxT flow cytometer (Thermo Fisher Scientific) and viability was expressed as percentage of gated PBMCs following doublet exclusion. Measurements were performed at baseline and after treatment with stimuli.

2.6 Cell culture supernatant collection

After incubation with B-GOS® and/or inflammatory stimuli, PBMC suspensions were centrifuged at 300 x g for 10 minutes at room temperature. Cell-free cell culture supernatants (300 µL) were collected in Eppendorf tubes and stored at -80°C for the analysis of secreted mediators by Luminex assay.

2.7 Flow cytometry

2.7.1 Principle of flow cytometry

Flow cytometry is a technique used to detect and measure the characteristics of cells or other particles flowing in a fluid stream. Flow cytometers are comprised of fluidics, optics and electronics systems (Figure 2.1) that function together to collect and measure the characteristics of single particles (events) in suspension when they pass through a laser beam.

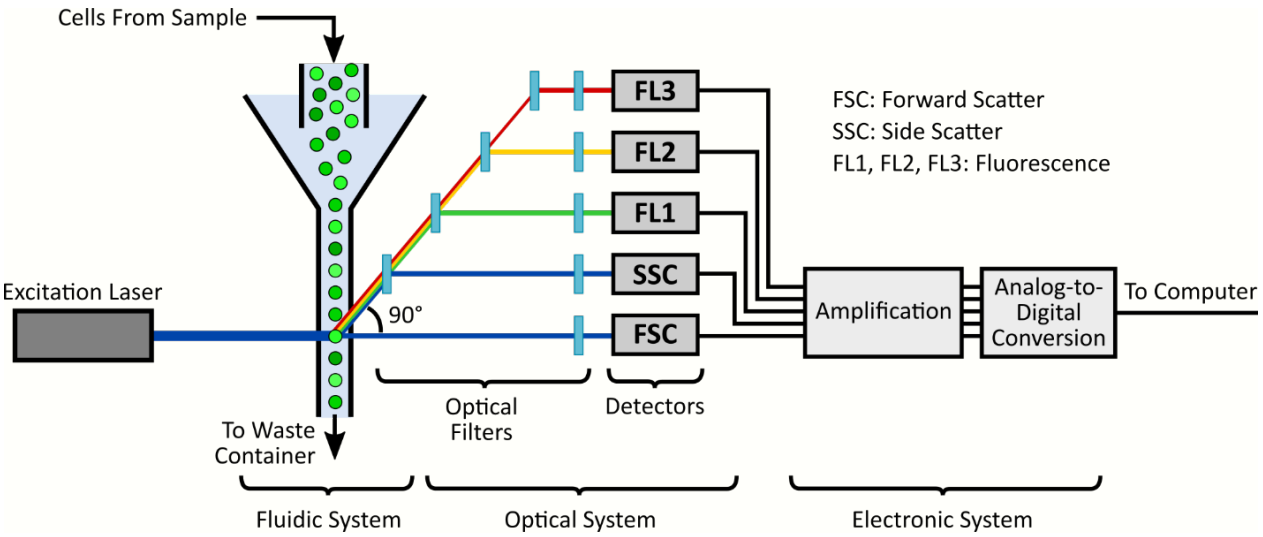

Figure 2.1 Schematic of the fluidic, optic and electronic systems of a flow cytometer. Cells are transported in a single row by the sheath fluid to the 'interrogation point', where they are excited by a laser light (fluidic system). Following interrogation, light scatter and fluorescence emission are collected by collection lenses and directed to optical filters and detectors (optical system). Optical signals are amplified and converted into proportional digital signals, in a process called 'analog-to-digital conversion' (electronic system). Data are collected by computers as .FCS files. From [284].

The fluidics transports the cells to the 'interrogation point', which is where the laser beam intersects with the sample. It also ensures that the cells move in a single row in a pressurised fluid stream within the flow chamber, in a process called 'hydrodynamic focus'. Ensuring that the sample pressure is set correctly is important for the quality of the analysis. If the sample pressure is too high, multiple cells can pass through the interrogation point at the same time, resulting in lower resolution. The passage of two particles (doublet) through the laser is undesirable because

it can lead to inaccurate data collection. Acoustic-assisted hydrodynamic focusing is a technology that minimises the impact of higher pressure and higher flow rates on the ability to collect single cell data.

The optics is required to produce and collect light signals. The optics components include lasers to illuminate the stream of samples, lenses to focus laser light and collect light scatter/fluorescence, mirrors to direct light to the detectors, and filters to restrict the light introduced into the detectors. Once it reaches the interrogation point, light emitted by the laser is scattered by the particles based on their physical properties. Light scatter is collected at two angles, the forward scatter (FSC) and the side scatter (SSC). The FSC is related to the characteristic of size of the particle (i.e. the higher the FSC values the higher the particle size), whilst SSC is related to the granularity or complexity of the particle (e.g. neutrophils have higher SSC than lymphocytes because they present higher nucleus complexity). FSC and SCC allow the identification of different cell types based on their physical and structural properties. To distinguish cells with similar FSC and SSC properties, fluorescent molecules called 'fluorophores' or 'fluorochromes' are used as markers. Fluorochromes are excited by the laser at a specific wavelength and re-emit light at a longer wavelength. In immunophenotyping, fluorochromes are conjugated with antibodies that are specific for a certain antigen, allowing to distinguish different cell types based on their fluorescence. Emitted light is collected by collection lenses and directed to optical filters and detectors.

The electronics amplifies the optical signals and converts them into proportional digital signals, in a process called 'analog-to-digital conversion'. Data are collected by computers as .FCS files readable by software such as BD CellQuest™ Pro Software (BD Biosciences) and FlowJo (FlowJo LLC).

In this project, an Attune NxT acoustic focusing flow cytometer (Thermo Fisher Scientific) with a 13-parameter capacity was used. The cytometer was equipped with three lasers, namely a violet laser (405 nm) with VL1-VL4 detectors, a blue laser (488 nm) with BL1-BL4 detectors and a red laser (637 nm) with RL1-RL3 detectors. The instrument was used for immunophenotyping, which is the analysis of cell populations by flow cytometry in order to identify the presence and proportions of determined subsets of immune cells [285].

2.7.2 Cell surface staining

PBMCs were either single-stained (compensation controls) or multi-stained (samples) with the antibodies of interest for the analysis of cell surface markers. Compensation was performed using single-stained cells for high expressing antigens and antibody-capture beads (BD™ CompBeads, BD Biosciences) for low expressing antigens or normally absent antigens. Unstained cells were used to monitor the background staining and auto-fluorescence of cells, whereas isotype controls were used to control for non-specific binding and validate the Fc blocking step. Fluorescence minus one (FMO) controls, which refer to the experimental cells stained with all fluorochromes except one, were used to take into account fluorescence spread when setting the gates. Because dead cells tend to bind non-specifically to antibodies leading to false positive results, viability dyes were used before surface staining in order to identify and allow for exclusion of dead cells. Cells were washed twice with a washing solution constituted by 1% bovine serum albumin (BSA) and 0.1% sodium azide in phosphate-buffered saline, PBS (Sigma Aldrich), then centrifuged at 450 x g for 5 minutes and resuspended in 100 µL PBS. 5 µL Human BD Fc Block™ (BD Biosciences) were added to the cells undergoing staining in order to minimise the non-specific binding of antibodies to Fc receptors present on B cells, natural killer cells and macrophages. After 10 minutes incubation, 50 µL of BD Horizon Brilliant™ Stain Buffer (BD Biosciences) were added to reduce the formation of staining artefacts in multi-stained samples.

Three antibody panels (PBMC panel, MAIT cell panel and monocyte/TLR panel) were designed to study into detail the frequencies and activation status of PBMC subsets (Table 2.6 and Table 2.7), the frequencies and activation status of MAIT cells and their subsets (Table 2.8 and Table 2.9) and the frequencies of monocytes and expression of TLRs (Table 2.10 and Table 2.11).

Table 2.6 List of antibodies for cell surface staining included in PBMC panel and their relative staining volumes.

Fluorochrome-labeled antibody	Isotype	Clone	Staining volume
Mouse anti-human CD45 FITC	Mouse IgG1, k	HI30	20 µL/test
Mouse anti-human CD56 PE	Mouse IgG1, k	B159	20 µL/test
Mouse anti-human CD14 PE-Cy 7®	Mouse IgG2a, k	M5E2	5 µL/test
Mouse anti-human CD3 PerCP-Cy®5.5	Mouse IgG1, k	UCHT1	5 µL/test
Mouse anti-human CD4 BV605	Mouse IgG1, k	RPA-T4	5 µL/test
Mouse anti-human CD8 V450	Mouse IgG1, k	RPA-T8	5 µL/test
Mouse anti-human CD19 BV711	Mouse BALB/c IgG1, k	SJ25C1	5 µL/test
Mouse anti-human CD69 APC-R700	Mouse IgG1, k	FN50	5 µL/test

Table 2.7 List of isotype controls for cell surface staining included in PBMC panel and their relative staining volumes.

Fluorochrome-labeled isotype control	**Clone**	**Staining volume**
Mouse anti-human IgG1, κ FITC	MOPC-21	20 µL/test
Mouse anti-human IgG1, κ PE	MOPC-21	20 µL/test
Mouse anti-human IgG2a, κ PE-Cy 7®	G155-178	5 µL/test
Mouse anti-human IgG1, κ PerCP-Cy®5.5	MOPC-21	5 µL/test
Mouse anti-human IgG1, κ BV605	X40	5 µL/test
Mouse anti-human IgG1, κ V450	MOPC-21	5 µL/test
Mouse anti-human IgG1, κ BV711	X40	5 µL/test
Mouse anti-human IgG1, κ APC-R700	X40	5 µL/test

Table 2.8 List of antibodies for cell surface staining included in MAIT cell panel and their relative staining volumes.

Fluorochrome-labeled antibody	**Isotype**	**Clone**	**Staining volume**
Mouse anti-human CD161 APC	Mouse IgG1, k	DX12	20 µL/test
Mouse anti-human CD14 PE-Cy 7®	Mouse IgG2a, k	M5E2	5 µL/test
Mouse anti-human CD3 PerCP-Cy®5.5	Mouse IgG1, k	UCHT1	5 µL/test
Mouse anti-human CD4 BV605	Mouse IgG1, k	RPA-T4	5 µL/test
Mouse anti-human CD8 V450	Mouse IgG1, k	RPA-T8	5 µL/test
Mouse anti-human TCR Vα7.2 PE	Mouse IgG1, k	OF-5A12	5 µL/test
Mouse anti-human CD69 APC-R700	Mouse IgG1, k	FN50	5 µL/test

Table 2.9 List of isotype controls for cell surface staining included in MAIT cell panel and their relative staining volumes.

Fluorochrome-labeled isotype control	**Clone**	**Staining volume**
Mouse anti-human IgG1, κ APC	DX12	20 µL/test
Mouse anti-human IgG2a, κ PE-Cy 7®	G155-178	5 µL/test
Mouse anti-human IgG1, κ PerCP-Cy®5.5	MOPC-21	5 µL/test
Mouse anti-human IgG1, κ BV605	X40	5 µL/test
Mouse anti-human IgG1, κ V450	MOPC-21	5 µL/test
Mouse anti-human IgG1, κ PE	MOPC-21	5 µL/test
Mouse anti-human IgG1, κ APC-R700	X40	5 µL/test

Table 2.10 List of antibodies for cell surface staining included in monocyte/TLR panel and their relative staining volumes.

Fluorochrome-labeled antibody	Isotype	Clone	Staining volume
Mouse anti-human CD282 Alexa Fuor® 647	Mouse IgG1, k	11G7	20 µL/test
Mouse anti-human CD14 PE-Cy 7®	Mouse IgG2a, k	M5E2	5 µL/test
Mouse anti-human CD284 BV421	Mouse IgG1, k	TF901	5 µL/test

Table 2.11 List of isotype controls for cell surface staining included in monocyte/TLR panel and their relative staining volumes.

Fluorochrome-labeled isotype control	Clone	Staining volume
Mouse anti-human IgG1, k Alexa Fuor® 647	MOPC-21	20 µL/test
Mouse anti-human IgG2a, κ PE-Cy 7®	G155-178	5 µL/test
Mouse anti-human IgG1, k BV421	X40	5 µL/test

PBMCs were stained with the fluorescent antibodies or corresponding isotype controls at the manufacturer's recommended volume/test (all BD Biosciences). After 20 minutes incubation at room temperature protected from light, cells were washed twice with a washing solution constituted by 1% bovine serum albumin (BSA) and 0.1% sodium azide in phosphate-buffered saline, PBS (Sigma Aldrich), then centrifuged at 450 x g for 5 minutes and resuspended in 300 µL PBS, giving a final working concentration of 1.3 x 10^6 cells/mL. PBMCs were analysed using a three-laser Attune NxT flow cytometer with data from 10,000 events/sample (300,000 events/sample for MAIT cells) recorded using the Attune™ NxT Software. Instrument settings and compensation matrixes are reported in Appendix C.

2.7.3 Intracellular staining

Cell surface staining was performed prior to fixation, permeabilisation and staining for intracellular antigens to prevent damage to surface markers. Fixation of cells is important to preserve the morphology of cells before the permeabilisation step, which is required to disrupt the plasma membrane and allow penetration of the antibodies. For intracellular cytokine and chemokine detection, the protein transport inhibitor brefeldin A (5 µg/mL) was added in cell cultures to block protein secretory/transport pathways [286]. Brefeldin A was selected over another commonly used inhibitor, monensin, because it was better tolerated by cells as measured by flow cytometry staining using a viability dye (Appendix D).

In addition to blank and isotype control samples, controls stained exclusively for surface markers were included to ensure that they did not stain non-specifically with the antibodies targeted towards intracellular markers. After the final washing step for cell surface staining, 0.5 mL/tube of Fixation Buffer were added instead of PBS, and cells were incubated in the dark for 20 minutes at room temperature. Cells were centrifuged at 350 x g for 5 minutes and supernatants were discarded. Cell were washed twice with 0.5 mL/tube Cell Staining Buffer and centrifuged as described above. Fixed cells were resuspended in 0.5 mL/tube 1x Intracellular Staining Permeabilisation Wash Buffer and washed/centrifuged twice at 350 x g for 10 minutes. Fixed/permeabilised cells were resuspended in residual 1x Intracellular Staining Permeabilisation Wash Buffer and stained for 20 minutes in the dark with the fluorochromes of interest at the manufacturer's recommended volume/test (Table 2.12 – Table 2.15). Cells were washed twice with 2 mL/tube of 1x Intracellular Staining Permeabilisation Wash Buffer and centrifuged at 350 x g for 5 minutes. Cells were resuspended in 300 µL Cell Staining Buffer and analysed as described in section 2.7.2. All reagents for intracellular staining were purchased from BioLegend, with the exception of the fluorochrome-conjugated antibodies and isotype controls (BD Biosciences).

Table 2.12 List of antibodies for intracellular staining included in MAIT cell panel and their relative staining volumes.

Fluorochrome-labeled antibody	Isotype	Clone	Staining volume
Mouse anti-human IFN-γ FITC	Mouse IgG1, k	4S.B3	20 µL/test
Mouse anti-human IL-8 BV510	Mouse IgG2b	G265-8	5 µL/test
Mouse anti-human IL-17A BV650	Mouse IgG1, k	N49-653	5 µL/test

Table 2.13 List of isotype controls for intracellular staining included in MAIT cell panel and their relative staining volumes.

Fluorochrome-labeled isotype control	Clone	Staining volume
Mouse anti-human IgG1, κ FITC	MOPC-21	20 µL/test
Mouse anti-human IgG2a, κ BV510	G155-178	5 µL/test
Mouse anti-human IgM, κ BV650	G155-228	5 µL/test

Table 2.14 List of antibodies for intracellular staining included in monocyte/TLR panel and their relative staining volumes.

Fluorochrome-labeled antibody	Isotype	Clone	Staining volume
Mouse anti-human IL-1β FITC	Mouse IgG1, k	AS10	20 µL/test
Mouse anti-human IL-10 BB700	Rat IgG2a, κ	JES3-19F1	5 µL/test
Mouse anti-human IL-8 BV510	Mouse IgG2b	G265-8	5 µL/test

Table 2.15 List of isotype controls for intracellular staining included in monocyte/TLR panel and their relative staining volumes.

Fluorochrome-labeled isotype control	Clone	Staining volume
Mouse anti-human IgG1, κ FITC	MOPC-21	20 µL/test
Rat anti-human IgG2a BB700	R35-95	5 µL/test
Mouse anti-human IgG2a, κ BV510	G155-178	5 µL/test

2.8 Evaluation of secreted cytokines

Luminex® assays enable the detection of multiple cytokines within a sample. Luminex® assays are based on the interaction of the analytes with specific capture antibodies, which are pre-coated with colour-coded magnetic beads. Biotinylated detection antibodies specific for the analytes of interest are added and form an antibody-antigen sandwich. Samples are then incubated with streptavidin-phycoerythrin (PE), which binds to the biotinylated detection antibodies. The plate is read on a flow-based detection instrument equipped with two lasers to allow identification of beads and therefore of specific bound-analytes and quantification of streptavidin-PE fluorescence, which is proportional to the amount of analyte bound [287]. A schematic of the multiplex assay principle is shown in Figure 2.2.

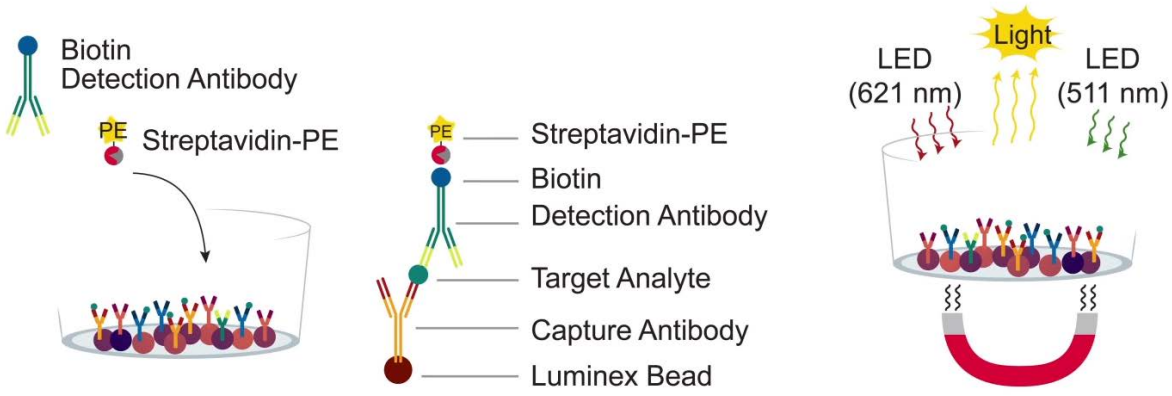

Figure 2.2 Schematic of multiplex assay principle. The analyte binds to a capture antibody embedded with colour-coded magnetic beads. A biotinylated detection antibody binds to the analyte forming an antibody-antigen sandwich. Streptavidin-phycoerythin (PE) forms a complex with the biotinylated detection antibody. A dual-laser flow-based detection instrument allows to identify and quantify the analyte of interest. From [287].

Mediators (cytokines, chemokines, growth factors and proteases) secreted in cell culture supernatants were analysed using Premixed Magnetic Luminex® Assays (R&D Systems). Following preparation of reagents and standards according to the manufacturer's instructions [287], 50 µL/well of each standard or sample were added to a black 96-well plate. 50 µL of capture antibodies coated with colour-coded magnetic beads were added to each well, and the plate was incubated for 3 hours on a horizontal orbital microplate shaker (Thermo Fisher Scientific) set at 800 ± 50 rpm, protected from light. The plate was attached on a magnetic support and washed three times with 100 µL/well washing buffer. One minute was allowed in between washes before removing the liquid. 50 µL/well of biotinylated detection antibodies were added and the plate was incubated for 1 hour. Following other washings, 50 µL/well of streptavidin-PE were added and the plate was incubated for 30 minutes. After washings, 100 µL of washing buffer were added to each well and the plate was incubated for 2 minutes on the shaker. The plate was read within 90 minutes on a Bioplex® 200 reader using a Luminex® 200 technology (Bio-Rad). Particles were resupended immediately prior to reading by shaking the plate for 5 minutes on the plate shaker at 800 ± 50 rpm. Firstly, a range of cytokines, chemokines, growth factors and proteases were analysed on undiluted samples of culture medium in a 22-plex explorative study to determine the optimal dilution factors. As a result, MIP-1α, ENA-78, MIP-1β and IL-1ra were analysed on 1:10-diluted samples; MCP-1, IL-1β, IL-8, granzyme B and IL-6 were analysed on 1:100-diluted samples; RANTES, FGF basic, G-CSF, GM-CSF, IFN-γ, IL-1α, IL-2, IL-4, IL-5, IL-10, IL-17A, TNF-α and VEGF-A were analysed on undiluted samples. When required, calibration diluent RD6-52 (R&D Systems) was used to perform dilutions. A full list of analytes and their main function, sensitivity and maximum standard value (pg/mL) is reported in Table 2.16.

In order to ensure precision and repeatability of results, intra- and inter- assay coefficients of variation (CV) were calculated and reported here for one sample mediator (IL-8). THP-1 cell supernatants from 5 different stimulation conditions were plated in duplicate on the same Luminex assay plate. As shown in Table 2.17, the intra-assay CV for IL-8 readings was equal to 7.7%, meaning that the variation between duplicates was within the acceptable limit of 10% [288]. Due to the necessity of running the samples on multiple Luminex assay plates, inter-assay CV was calculated to ensure plate-to-plate consistency. Healthy PBMC supernatants from 6 different stimulation conditions/donors were plated twice using separate plates and the levels of secreted IL-8 were assessed by Luminex assay. The inter-assay CV (*n*= 6) was 9.9 %, which was within the acceptable limit of 15% [288], as shown in Table 2.18.

Table 2.16 List of 22 cytokines, chemokines, growth factors and proteases analysed by Premixed Magnetic Luminex® Assays (R&D Systems) and their main source in blood, function, sensitivity and maximum standard value. The main sources of reference for the functions of analysed mediators are [23, 51, 289, 290].

Class		Analyte	Main source in blood	Function	Sensitivity (pg/mL)	Max standard (pg/mL)
Cytokines	Th1	Interleukin 1α (IL-1α)	Monocytes, macrophages, B cells and Th1 cells	Activation of inflammatory processes	0.9	1270
		Interleukin 1β (IL-1β)	Monocytes, macrophages, DCs, B cells, NK cells and Th1 cells	Activation of inflammatory processes	0.8	4744
		Interleukin 2 (IL-2)	Th1 cells, naïve $CD8^+$ T cells, DCs	Activation and differentiation of T cells. Response against microbial infection and recognition of non-self *vs* self	1.8	7200
		Interleukin 6 (IL-6)	Monocytes, macrophages, T cells, B cells and mast cells	Regulation of T cell and B cell growth, acute-phase responses, mediator of fever	1.7	1154
		Interferon γ (IFN-γ)	NK cells, NKT cells, Th1 cells and $CD8^+$ T cells	Activation of macrophages, differentiation of T cells, promotion of IgG2a production by B cells, responses against viral and bacterial infections	0.40	14209
		Tumour necrosis factor α (TNF-α)	Macrophages, monocytes, T cells, B cells and NK cells	Immune activation, inhibition of viral replication, induction of tumour necrosis	1.2	2359
	Th2	Interleukin 1 receptor antagonist (IL-1ra)	Monocytes and macrophages	Antagonist of IL-1α and IL-1β. Modulation of IL-1-induced responses	18.0	6793
		Interleukin 4 (IL-4)	Mast cells, Th2 cells, basophils, eosinophils and NK cells	Differentiation of T cells, inhibition of IFN-γ action, promotion of IgE	9.3	3550
		Interleukin 5 (IL-5)	Th2 cells, NK cells, basophils, eosinophils and mast cells	Eosinophil maturation, B cell growth, IgA production	0.5	1610

Table 2.16 Continued.

Class		Analyte	Main source in blood	Function	Sensitivity (pg/mL)	Max standard (pg/mL)
Cytokines	Th1/Th2	Interleukin 10 (IL-10)	Monocytes, macrophages, Th2 cells, T regs, $CD8^+$ T cells, B cells and mast cells	Inhibition of Th1 cytokines, downregulation of antigen presentation, reduction of monocyte/macrophage activation	1.6	1162
	Th17	Interleukin 17A (IL-17A)	Activated $CD4^+$ and $CD8^+$ memory T cells, invariant NKT cells, eosinophils, neutrophils and monocytes	Anti-microbial defence, induction of IL-6, ENA-78, IL-8 and GM-CSF, neutrophil chemoattractant	1.8	3100
Chemokines		Monocyte chemoattractant protein 1 (MCP-1), also known as chemokine C-C motif ligand 2 (CCL2)	Monocytes and macrophages	Recruitment of monocytes, NKT cells, memory T cells and DCs	9.9	8017
		Macrophage inflammatory protein α (MIP-1α), also known as chemokine C-C motif ligand 3 (CCL3)	Monocytes and macrophages	Recruitment of monocytes and T cells	16.2	24580
		Macrophage inflammatory protein β (MIP-1β), also known as chemokine C-C motif ligand 4 (CCL4)	Monocytes, macrophages, endothelial cells, T and B cells	Recruitment of monocytes and $CD8^+$ T cells	5.8	36493
		RANTES, also known as chemokine C-C motif ligand 5 (CCL5)	Platelets and T cells	Recruitment of monocytes, memory T cells, NKT cells and eosinophils	1.8	5020
		Epithelial-neutrophil activating peptide (ENA-78), also known as C-X-C motif chemokine 5 (CXCL5)	Eosinophils	Recruitment of neutrophils	8.2	11660
		Interleukin 8 (IL-8), also known as C-X-C motif ligand 8 (CXCL8)	Monocytes and macrophages	Recruitment of neutrophils and naïve T cells, stimulation of phagocytosis, promotion of angiogenesis	1.8	1255

Table 2.16 Continued.

Class	Analyte	Main source in blood	Function	Sensitivity (pg/mL)	Max standard (pg/mL)
Growth factors	Basic fibroblast growth factor (FGF basic)	N/A	Proliferation and differentiation of cells, angiogenic	6.5	440
	Granulocyte colony- stimulating factor (G-CSF)	Monocytes and macrophages	Promotion of myeloid cell growth	4.1	5840
	Granulocyte-macrophage colony-stimulating factor (GM-CSF)	T cells, NK cells, macrophages, eosinophils and mast cells	Neutrophil proliferation and maturation, eosinophil activation and apoptosis	4.1	2970
	Vascular endothelial growth factor A (VEGF-A)	Macrophages, neutrophils and eosinophils	Vascular endothelial growth factor, angiogenic, eosinophil chemoattractant	2.1	2051
Proteases	Granzyme B	NK cells, $CD8^+$ T cells and MAIT cells	Mediation of apoptosis, stimulation of cytokine release	1.42	4300

Table 2.17 Intra-assay coefficient of variability (CV) for IL-8 readings.

THP-1 cell stimulation condition	Replicate 1 IL-8 reading (pg/mL)	Replicate 2 IL-8 reading (pg/mL)	Mean	SD	% CV	Intra-assay CV (*n*= 5)
Unstimulated	366.8	366.8	366.8	0.0	0.0	7.7%
Free sugars control	531.1	663.8	597.5	93.8	15.7	
Galactose 5.7 mg/mL	517.7	422.4	470.0	67.4	14.3	
LPS 0.1 µg/mL	150446.0	142529.4	146487.7	5597.9	3.8	
GOS C 18 mg/mL	394.7	422.4	408.5	19.6	4.8	

Table 2.18 Inter-assay coefficient of variability (CV) for IL-8 readings.

Donor ID	Stimulation condition	Plate 1 IL-8 reading (pg/mL)	Plate 2 IL-8 reading (pg/mL)	Mean	SD	% CV	Inter-assay CV (*n*= 6)
1809140196	Unstimulated	1644.0	1498.6	1571.3	102.8	6.5	9.9 %
1805090103	Unstimulated	2473.0	2395.5	2434.3	54.9	2.3	
1809140196	LPS 1 µg/mL	69938.8	71770.8	70854.8	1295.4	1.8	
1805090103	LPS 1 µg/mL	101158.4	197471.6	149315.0	68103.8	45.6	
1809140196	PMB 30 µg/mL	3034.0	3038.9	3036.4	3.5	0.1	
1805090103	PMB 30 µg/mL	2746.0	2868.0	2807.0	86.3	3.1	

2.9 Lipopolysaccharide quantification, removal and blocking

2.9.1 Lipopolysaccharide limit for cell culture applications

Mammalian blood cells such as monocytes, macrophages and B cells are highly sensitive to LPS and release pro-inflammatory cytokines, such as IL-1β, IL-6, IL-8 and TNF-α, following LPS recognition [14]. LPS is a strong immunostimulant that when present at high levels in circulation can cause acute inflammation, fever and ultimately septic shock [13]. For this reason, the FDA established a limit of 0.5 endotoxin units (EU)/mL for products that directly or indirectly enter in contact with the cardiovascular and lymphatic system [291], whilst the limit for *in vitro* cell culture applications generally corresponds to 0.1 EU/mL. The conversion between EU and units of weight depends on the source of LPS. The same amounts of LPS from different Gram-negative bacteria can have very different levels of biological activity. Nevertheless, 10 EU/mL of LPS can be approximately converted to 1 ng/mL [292]. While there are no safety limits for LPS in food supplements [13], prebiotic products may contain LPS arising from manufacturing or packaging processes. Therefore, LPS levels were assessed in B-GOS® batches prior to their use *in vitro* due to experimental settings.

2.9.2 Lipopolysaccharide quantification by Limulus Amoebocyte Lysate assay

The Limulus Amoebocyte Lysate (LAL) assay is used for the detection of bacterial LPS in quantities as low as 0.01 EU/mL. The method is based on the reaction between an aqueous extract of blood cells (amoebocytes) from the Atlantic horseshoe crab (*Limulus polyphemus*) and LPS. Two types of LAL assays have been developed for the quantitative detection of LPS. The turbidimetric method, which correlates the amount of LPS to the level of turbidity of the analysed sample, and the chromogenic method, which quantifies LPS based on the intensity of colour developed from a series of enzymatic reactions. A chromogenic LAL assay was carried out using Pierce™ Chromogenic Endotoxin Quant Kit (Thermo Fisher Scientific). When LPS encounters the amoebocyte lysate, enzymatic reactions leading to the activation of a pro-clotting enzyme are initiated. This enzyme promotes the release of p-nitroaniline (pNA) from a chromogenic substrate, causing the colourless solution to turn yellow. The intensity of colour is proportional to the amount of LPS present in the sample and is quantified by absorbance reading at 405 nm. The correlation between the value of absorbance and the LPS concentration is linear in the 0.01-0.1 EU/mL and 0.1-1.0 EU/mL range. Unknown concentrations of LPS in the samples are then calculated using a standard curve [293].

Samples and reagents were equilibrated at room temperature before use, and the 96-well reaction plate was maintained at 37 ± 1°C throughout the assay. *Escherichia coli* Endotoxin Standard (potency= 15 EU) was reconstituted by adding 1.5 mL of Endotoxin-Free Water, leading to a final concentration of 10 EU/mL. The solution was placed on a plate shaker for 15 minutes to allow for reconstitution of the powder. The rehydrated Endotoxin Standard Solution was used to prepare the standards in the 0.01-0.1 EU/mL range. LAL was reconstituted immediately before use with 1.7 mL of Endotoxin-Free Water and the pH of the samples was verified using litmus paper to ensure it remained between 6 and 8, as required for optimal performance. In each well, 50 µL of endotoxin standards/samples/controls were added, followed by 50 µL/well of reconstituted LAL. The plate was incubated for 30 minutes at 37 ± 1°C. After reconstitution of the Chromogenic Substrate with 3.4 mL Endotoxin-Free Water, 100 µL/well of solution were added and the plate was incubated for 6 minutes at 37 ± 1°C. The reaction was stopped with 50 µL/well of Stop Solution, and the absorbance was read at 405 nm on a GloMax® Discover Microplate Reader (Promega) immediately after assay completion.

LAL assay was performed on B-GOS® batches as a quality control prior to use in cell culture. Negative controls (RPMI-1640 medium) and a positive control (LPS from *E. coli* O111:BA) were included.

2.9.3 Lipopolysaccharide removal with Polymyxin B coated chromatographic columns

The Detoxi-Gel™ Endotoxin Removing Gel (Thermo Fisher Scientific) was used to remove LPS if detected in the samples. The method employs chromatographic columns pre-packed with a gel of immobilised Polymyxin B (PMB) [294]. PMB is an antibiotic that binds with high affinity to the lipid A portion of LPS. The sample is loaded into the column and any LPS present in the sample is bound to the PMB gel. The purified sample is eluted from the column using a pyrogen-free buffer or water. The chromatographic column was regenerated by washing with five resin-bed volumes of 1% sodium deoxycholate (Sigma Aldrich), followed by 3-5 resin-bed volumes of water to remove the detergent. The resin was then equilibrated with 3-5 resin-bed volumes of a water. 1 mL of sample was applied to the column and incubated for 1 hour to allow for the binding of LPS to PMB. After incubation, the sample was eluted from the column with 2 mL of water and stored in a sealed tube to prevent contamination (Figure 2.3). Purified samples were lyophilised for 72 h to remove residual elution water and then rehydrated to the desired working concentration.

Figure 2.3 LPS removal using Detoxi-Gel™ Endotoxin Removing Gel (Thermo Fisher Scientific). Samples were loaded into a pre-packed column containing polymyxin B gel. After 1 hour incubation, which allows binding of LPS to polymyxin B, purified Samples were eluted from the column with 2 mL water.

2.9.4 Blocking of lipopolysaccharide-induced effects by Polymyxin B

Samples were pre-incubated with or without PMB (30 µg/mL, Sigma Aldrich) for 24 h and then tested at three concentrations (0.8 mg/mL, 4 mg/mL and 12 mg/mL) in healthy PBMC cultures. LPS (1 µg/mL)-stimulated cells and unstimulated cells were used as positive and negative controls, respectively. After 24 h incubation, viability was assessed by flow cytometry using FVS780 and cell culture supernatants were collected for the analysis of secreted mediators (IL-8, IL-10 and TNF-α) by Luminex® assay.

2.10 Statistical analysis

Flow cytometry raw data, expressed as percentage of gated cells and/or MFI, were used only if >100 events/gate were present and if viability of healthy PBMCs was above 70% under all stimulation conditions. Crohn's disease PBMC viability was often <70% at baseline, therefore, viability was coded as a covariate when performing the statistical tests in order to maintain the study power and to remove the bias of viability as a confounding variable.

When out of range (OOR) Luminex data were present and it was not possible to repeat the experiment using more diluted/more concentrated samples due to limited sample volume, "OOR<" values were substituted with the lowest detection limit extrapolated from the standard curve fit (*value) divided by 2, and "OOR>" values were substituted with the highest detection limit extrapolated from the curve multiplied by 2. Extrapolated concentrations (*values) were used for those values below the lowest standard or above the highest standard of the assay but not OOR (lower or above asymptote of equation) [295]. Statistical analysis was performed using GraphPad Prism software (version 8) and IBM SPSS Statistics (version 24.0). Power calculations were conducted with G*Power software version 3.1.9.4.

Graphical tests using quantile-quantile (QQ) plots and Shapiro-Wilk tests were carried out to assess whether data followed a Gaussian (normal) distribution. Non-normally distributed data were $\log_{10}$-transformed to achieve a normal distribution. Normally-distributed data were expressed as mean ± standard deviation (SD), whereas non-normally distributed data were expressed as median ± interquartile range (IQR). When the sample size was <5, for example during optimisation or pilot experiments, a more conservative approach was used by carrying out non-parametric tests. Outliers were detected using a combination of graphical and statistical methods. Outliers were revealed graphically using boxplots, which are summary plots of the dataset depicting the median, 1st quartile (25th percentile), 3rd quartile (75th percentile), IQR and whiskers (lines that extend from the 1st and 3rd quartiles with values no greater than 1.5 X IQ). Outliers were defined as those data falling outside the 3rd quartile + 1.5 X IQR or the 1st quartile –

1.5 X IRQ. Values outside the 3rd quartile + 3 X IQR or the 1st quartile – 3 X IRQ were classified as extreme outliers. The ROUT method, which is a statistical approach that combines robust regression and outlier removal, was used to identify and remove outliers. ROUT coefficient Q was set at 1% in order to have at least 99% actual outliers and no more than 1% false outliers. Data sets were carefully screened to investigate the causes of outliers (e.g. data entry or measurement errors *vs* biological variability) before removing extreme values. Details on the removed outliers as well as the sample size before and after outlier removal were included within presented results.

Correlations: according to data distribution, Pearson's correlation test or Spearman non-parametric correlation test were used to compute correlation coefficients (r). Correlation was considered significant when $p < 0.05$.

Differences between two independent groups: assessed by two-tailed unpaired t test (parametric) or two-tailed unpaired Mann-Whitney test (non-parametric). When equal SDs could not be assumed following an F test, two-tailed unpaired t test with Welch's correction was used.

Differences between more than two independent groups (one independent variable): assessed by one-way analysis of variance (ANOVA) or Kruskal-Wallis test depending upon data distribution. When a covariate was present, one-way analysis of covariance (ANCOVA) was performed in order to adjust the means for the confounding variable. Welch's ANOVA test was used when equal SDs could not be assumed following the Brown-Forsythe test.

Differences between more than two independent groups (two independent variables): two-way ANOVA was used to compare the mean differences between groups that have been split on two independent variables, or "factors". When a significant interaction between the factors was present, the simple main effects were reported. When no interaction was present, the *post-hoc* results were interpreted in the context of the significant independent variable alone.

Corrections for multiple comparisons: corrections were applied based upon experimental design to limit the type I error rate, which refers to the acceptance of a false positive result. Dunnett's (parametric) or Dunn's (non-parametric) corrections were applied when comparing the mean of each group with the mean of a control group. Bonferroni correction was applied when comparing the means of selected groups. When equal SDs could not be assumed, Dunnett T3 correction was used.

Across all statistical analyses, a significance level (α) of 0.05 was used and p values $< \alpha$ were considered significantly different.

Chapter 3 DEVELOPMENT OF AN *EX VIVO* PBMC MODEL TO STUDY THE MICROBIOTA-INDEPENDENT EFFECTS OF GALACTOOLIGOSACCHARIDES

3.1 Introduction

Galactooligosaccharides (GOS) reach the large intestine intact and are fermented by bifidobacteria and lactobacilli, which utilise GOS as an energy source and in turn produce short chain fatty acids (SCFAs) as end-products [201]. SCFAs affect immunity by modulating immune cell functions including cytokine production (*e.g.* IL-10 and TNF-α) and by inhibiting pro-inflammatory pathways, such as the NF-κB pathway [149, 178, 223, 224, 296].

In addition to the SCFA-mediated effects, GOS affect gut and systemic immunity in a microbiota-independent manner. *In vitro* models using human intestinal cell lines and human supplementation studies showed that intact GOS, as well as fructooligosaccharides (FOS), are transported across the intestinal epithelium with rates of 4-14% [234] and are found in plasma, urine and stool of infants [236].

In one human study, a small fraction of prebiotic FOS corresponding to around 0.12 ± 0.04% of the ingested dose was recovered in the urine of healthy adults. It was hypothesised that the excretion of intact FOS resulted from their absorption in the small intestine, as previously documented for the sugar lactulose [297]. A fraction of FOS was hydrolysed in the upper gastrointestinal tract and absorbed as glucose and fructose. Most of the ingested FOS (89.0 ± 8.3%) were fermented by the colonic microbiota and therefore not detected in stools [298].

Adults affected by chronic inflammatory conditions, such as inflammatory bowel disease (IBD), and healthy adults exposed to lifestyle-associated stressors (*e.g.* high-fat Western diet, alcohol and medications) display increased gut permeability to microbes and macromolecules from food [227, 232, 299]. Despite there being a lack of transportation studies on adults, it is plausible that GOS pass through the epithelium not only of infants with an immature gut but also of adults with a “leaky” gut.

In vitro studies involving human or animal cell lines and/or primary cell cultures demonstrated that GOS directly modulate cytokine production in unchallenged and immune-challenged cells, with mechanism that may involve toll-like receptor (TLR) signalling [241, 242]. The immunomodulatory effects of GOS on mediators such as IL-6, IL-8, IL-10, IL-17, IFN-γ, MCP-1, MIP-

3α and TNF-α have been studied in a range of model systems, including rat and human intestinal epithelial cells, human peripheral blood monocytes, rat splenic T cells and equine peripheral blood mononuclear cells (PBMCs) [194, 241-243, 300]. Overall, treatment with GOS resulted in various outcomes on immunity, including anti-inflammatory as well as pro-inflammatory effects, perhaps reflecting the heterogeneity of cell models and GOS doses used (5 – 20 mg/mL). Additionally, only one study assessed the lipopolysaccharide (LPS) content of GOS prior to its use in cell culture [243]. Since LPS is a strong immunostimulant that binds to monocytes, macrophages and B cells and stimulates the secretion of pro-inflammatory mediators (e.g. TNF-α, IL-1β, IL-6, IL-8, IL-10) [247], it is important to perform LPS testing to ensure that the effects seen are due to GOS and not due to the presence of LPS.

To date, there are limited studies on the microbiota-independent effects of GOS upon phenotypes and inflammatory cytokines of human adult PBMCs. While it is possible to study the direct effects of oligosaccharides on immune cells using germ-free animal models [246, 301], it is not ethical to conduct these experiments in humans. Based upon the evidence that GOS are partially transported across the intestine and can therefore come into contact with immune cells, *ex vivo* adult PBMCs were chosen as a model for the investigation of the immunomodulatory effects of B-GOS®.

An advantage of using this *ex vivo* model is that primary PBMCs are more likely to capture the variability of potential responses in humans compared with homogeneous and standardised immune cell lines. Using *ex vivo* PBMC cultures allows exploration of the complex interplay between cell subsets, which is not possible in experiments with isolated cell populations.

The limitation of using an *ex vivo* model instead of cell lines is that the intrinsic biological variability can affect statistical power during hypothesis testing. A sensitivity analysis performed before conducting the study indicated that a sample size of 5 donors per group would enable detection of effect sizes >2 (80% power, $p< 0.05$, G*Power software version 3.1.9.4). Differences of ≥ 0.8 standard deviations are considered large effect sizes [302]. Animal *ex-vivo* studies indicate that culturing PBMCs with GOS results in higher production of secreted cytokines compared to unstimulated control, with effect sizes of up to 8 [243].

3.2 Aim and objectives

The aim of the work described in this chapter was to develop and optimise an *ex vivo* model using adult PBMCs from healthy donors to study the direct immunological effects of GOS.

The specific objectives were to:

- Assess the LPS content of 4 different batches of B-GOS® using the Limulus Amoebocyte Lysate (LAL) assay

- Identify the optimal incubation time for PBMC culturing with B-GOS® or with LPS, concanavalin A (Con A), phorbol 12-myristate 13-acetate (PMA) and ionomycin or CD3/CD28/CD2 T cell activator (TCA) and select the best stimuli to use in co-culture/pre-incubation experiments based upon observed effects on cell viability and secreted cytokines

3.3 Methods

B-GOS® batches, LPS, Con A, PMA and ionomycin and TCA were prepared as detailed in section 2.3. The LAL assay was carried out as described in section 2.9.2. Healthy PBMCs were cultured as explained in section 2.3. Purification of B-GOS® batches by chromatography and pre-incubation experiments with PMB were conducted as detailed in sections 2.9.3 and 2.9.4, respectively. Cell viability was measured by flow cytometry using fixable viability stains (FVS510 or FVS780) as reported in section 2.5. Mediators (IL-1α, IL-1β, IL-8, IL-10, TNF-α and granzyme B) secreted in cell culture supernatants were analysed using Premixed Magnetic Luminex® Assays. Further details on the Luminex method and the dilution factors used can be found in section 2.8. A graphical summary of the methods used in this chapter is provided in Figure 3.1.

A

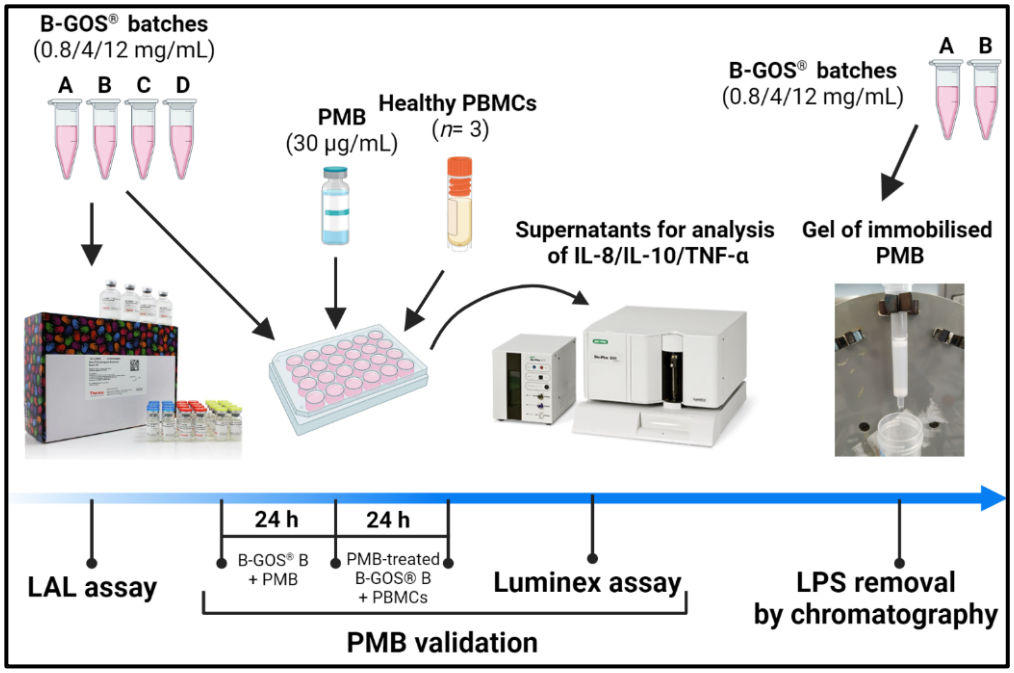

B

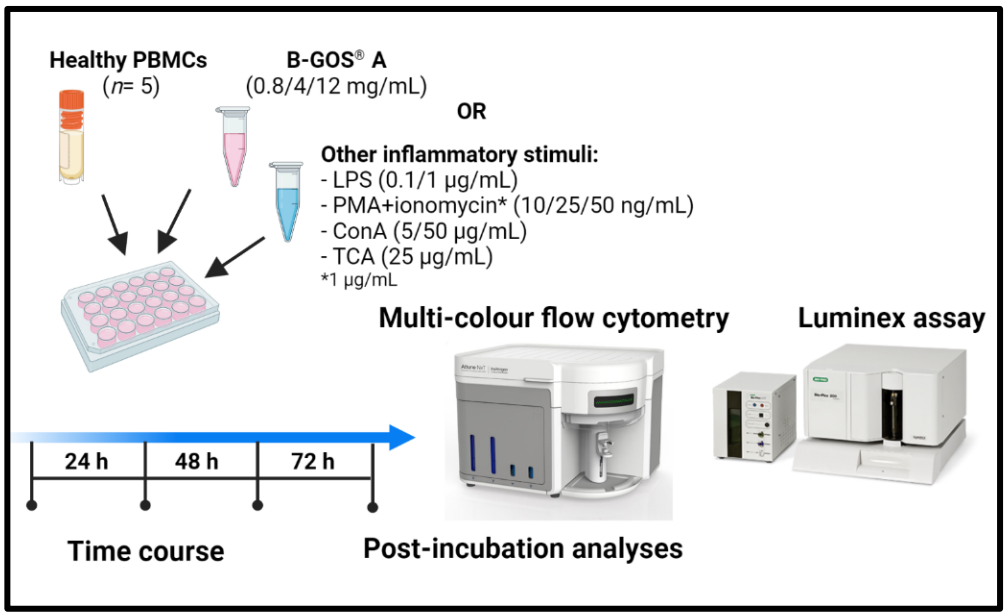

Figure 3.1 Graphical summary of the methods used for A) the screening of B-GOS® batches by LAL assay followed by validation by polymyxin B (PMB) and LPS removal by chromatography; and B) the determination of optimal incubation time for stimulation with B-GOS® and other inflammatory stimuli.

3.4 Results

3.4.1 Screening of B-GOS® batches by LAL assay

B-GOS® batches A – D were quality checked by the LAL assay before direct application to *ex-vivo* cell cultures. The assay was conducted on all prepared concentrations of B-GOS® batches (0.8 mg/mL, 4 mg/mL and 12 mg/mL). A negative control (RPMI-1640 medium) and a positive control (LPS from *E. coli* O111:BA; 0.1 µg/mL and 1 µg/mL) were included in the assay. B-GOS® batches and the positive control were diluted 10 times and 5 times, respectively, in LPS-free water prior to testing with a dilution factor determined by pilot experiments. Each sample was tested in triplicate. The average absorbance of the readings minus the average absorbance of the blank was used to calculate unknown LPS concentrations from a standard curve in the 0.01-0.1 EU/mL range (Figure 3.2).

B-GOS® batch A contained low but detectable levels of LPS, proportional to the concentration tested. B-GOS® batch B contained levels of LPS above the 0.1 EU/mL limit for cell culture applications at all concentration tested. B-GOS® batches C and D and the negative control did not contain any detectable LPS. The positive control presented quantities of LPS above the cell culture limit for both concentrations tested (Figure 3.2).

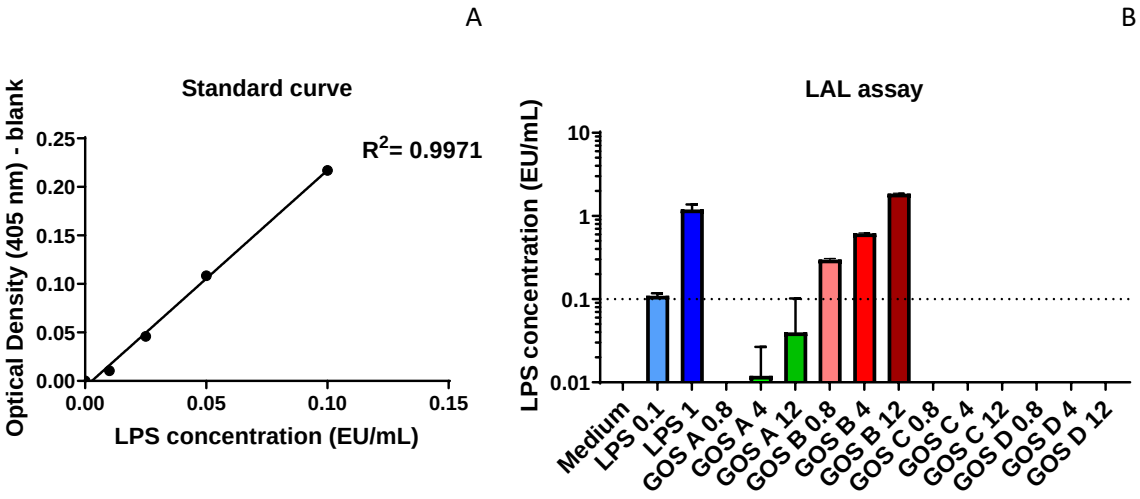

Figure 3.2 A) Standard curve in the 0.01-0.1 EU/mL range for the quantitation of LPS in samples by the LAL assay. B) Levels of LPS (EU/mL) in B-GOS® batches and controls. LAL assay was conducted with technical replicates. Data are expressed as mean ± SD (*n*= 3). The dotted line at Y= 0.1 refers to the limit of LPS for cell culture applications.

3.4.2 Validation of LAL assay results by polymyxin B treatment

Prior to validation of LAL assay results by polymyxin B (PMB) treatment, the viability of PBMCs exposed to B-GOS® batch B (0.8 mg/mL, 4 mg/mL and 12 mg/mL), PMB (30 µg/mL) or LPS (1 µg/mL) was measured to ensure that the chosen stimuli and concentrations were not cytotoxic. Viability was above 90% for all conditions tested. Incubation of PBMCs with LPS (p= 0.0107) and with B-GOS® batch B (0.8 mg/mL, p= 0.0076; 4 mg/mL, p= 0.0156) resulted in even higher viability than for the negative control (Table 3.1).

Table 3.1 Total viability of PBMCs from healthy donors in different culture conditions. PBMC viability was assessed by flow cytometry using a live/dead stain.

Stimulus	**Viability (%) Mean ± IQR (n= 3†)**	**Kruskal-Wallis p value**
NC	93.1 ± 1.7	**0.0057**
LPS 1 µg/mL	96.3 ± 1.9*	
PMB 30 µg/mL	95.9 ± 3.8	
GOS B 0.8 mg/mL	96.5 ± 0.5**	
GOS B 4 mg/mL	96.5 ± 2.1*	
GOS B 12 mg/mL	95.1 ± 1.9	

†Except for GOS B 0.8 (n= 2)
*Significantly different from NC (Dunn's *post-hoc* test, p< 0.05)
**Significantly different from NC (Dunn's *post-hoc* test, p< 0.01)

B-GOS® batch B (0.8 mg/mL, 4 mg/mL and 12 mg/mL) was pre-treated for 24 h with or without PMB (30 µg/mL) and then applied for 24 h to healthy PBMC cultures (n= 3). The ability of PMB to neutralise the effects of LPS was evaluated by measuring changes in secreted mediators, namely LPS-induced IL-8, IL-10 and TNF-α [303-305]. PMB concentration was chosen based on a similar study assessing the effects of polysaccharide extracts on mononuclear cells [303]. B-GOS® batch B was selected because it presented the highest levels of LPS among the tested batches. LPS (1 µg/mL)-stimulated PBMCs and unstimulated PBMCs were used as positive control and negative control, respectively. Both controls were pre-treated with or without PMB.

PBMCs incubated with LPS or B-GOS® batch B (0.8 mg/mL, 4 mg/mL and 12 mg/mL) presented higher secretion of IL-8 compared to the negative control (p= 0.0053, p= 0.0220, p= 0.0023, p< 0.0001). Similarly, PBMCs stimulated with B-GOS® batch B (12 mg/mL) secreted significantly more

TNF-α than the negative control (p= 0.0016). Higher levels of IL-10 were seen after stimulation of PBMCs with B-GOS® batch B, despite not reaching significance due to wide variation among donors. *Post-hoc* analyses on the effects of PMB showed that pre-treatment with PMB significantly reduced the secretion of IL-10 (p= 0.0434) and TNF-α (p= 0.0009), but not IL-8, by PBMCs (Table 3.2).

These results suggest that while the increased production of IL-10 and TNF-α was likely to be an effect of the LPS contained in B-GOS® batch B, the higher secretion of IL-8 observed in B-GOS® batch B-stimulated cells was at least partially attributable to B-GOS® itself. In order to confirm this and to further study the immunostimulatory effects of B-GOS®, it was decided to purify the batches with detectable levels of LPS (B-GOS® batches A and B) and to re-assess their effects in PBMC cultures.

Table 3.2 Levels of soluble mediators secreted by PBMCs from healthy donors after culture with GOS or LPS, as measured by Luminex assay.

Secreted mediator	**NC**		**LPS 1 µg/mL**		**GOS B 0.8 mg/mL**		**GOS B 4 mg/mL**		**GOS B 12 mg/mL**		**Two-way ANOVA *p* value**		
	Mean ± SD (*n*= 3)		Mean ± SD (*n*= 3)		Mean ± SD (*n*= 2)		Mean ± SD (*n*= 3)		Mean ± SD (*n*= 2)				
	-PMB	+PMB	-PMB	+PMB	-PMB	+PMB	-PMB	+PMB	-PMB	+PMB	PMB	Stimuli	PMB*Stimuli
IL-8 (ng/mL)	3.4 ± 3.1	2.7 ± 0.6	127.6 ± 65.0	65.4 ± 74.1	76.2 ± 15.7	92.3 ± 97.2	150.3 ± 65.6	59.2 ± 77.4	188.2 ± 54.7	153.2 ± 60.7	0.0551	**<0.0001**	0.3109
IL-10 (pg/mL)	0.8 ± 0.0	1.5 ± 1.4	1231.0 ± 660.2	81.8 ± 98.2	763.6 ± 132.3	63.8 ± 42.3	1522.0 ± 811.7	91.8 ± 92.9	1415.0 ± 1454.0	164.6 ± 151.2	**0.0003**	0.1201	0.2434
TNF-α (pg/mL)	1.4 ± 0.0	3.7 ± 3.2	866.7 ± 357.7	80.3 ± 72.5	692.5 ± 50.1	96.7 ± 9.4	924.7 ± 190.1	143.9 ± 134.0	2791.0 ± 2037.0	426.0 ± 524.9	**0.0024**	**0.0059**	0.0672

Significant main effect of *Stimuli* – Dunnett's *post-hoc* test for multiple comparison:

IL-8 – LPS, GOS B 0.8, GOS B 4 and GOS B 12 all significantly different from NC (*p*= 0.0053, *p*= 0.0220, *p*= 0.0023, *p*< 0.0001)

TNF-α – GOS 12 significantly different from NC (*p*= 0.0016)

Significant main effect of *PMB* – Bonferroni's *post-hoc* test for multiple comparison:

IL-10 – Without PMB significantly different from with PMB (*p*= 0.0434)

TNF-α – Without PMB significantly different from with PMB (*p*= 0.0009)

LPS was removed from B-GOS® batches A and B by using chromatographic columns pre-packed with a gel of immobilised PMB, with no detectable LPS after filtration (Figure 3.3).

However, healthy PBMCs (*n*= 5) incubated for 24 h with 12 mg/mL purified B-GOS® batch A had poor viability compared to those cells incubated with non-purified B-GOS® batch A (average % viability 15.0 ± 6.0 *vs* 96.5 ± 1.1, *p*< 0.0001). Similar results were seen for purified B-GOS® batch B-stimulated cells (Figure 3.3).

The increase in cell death observed with the purified B-GOS® batches A and B was possibly due to residual sodium deoxycholate deriving from the purification process.

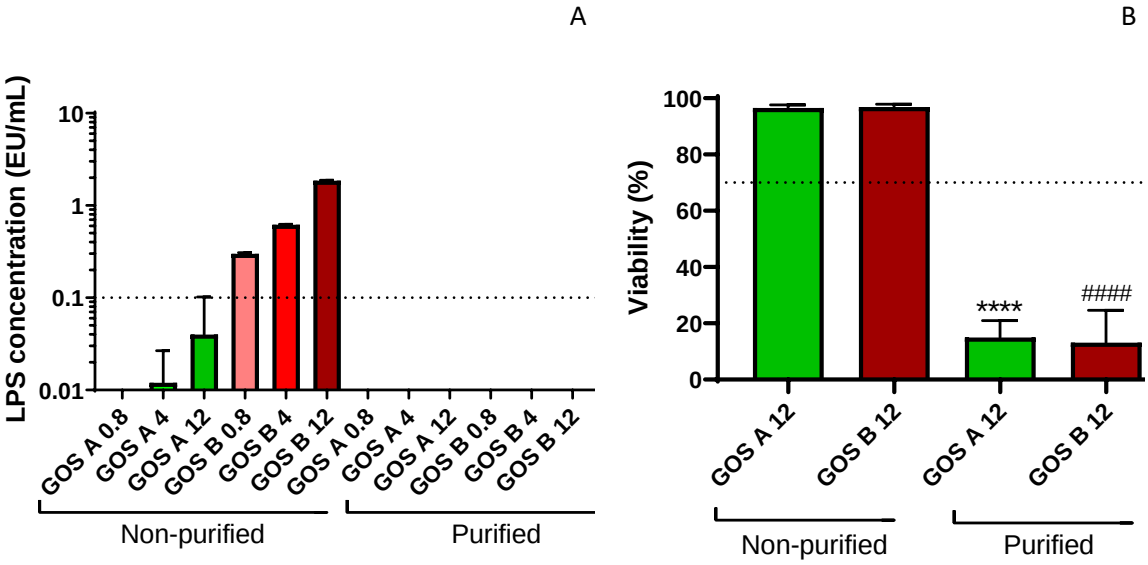

Figure 3.3 A) Levels of LPS in B-GOS® batches before and after purification by chromatography, as assessed by LAL assay.LAL assay was conducted with technical replicates. Data are expressed as mean ± SD (*n*= 3). B) Viability of healthy PBMCs (*n*= 5) stimulated for 24 h with purified or non-purified B-GOS® batches. Data are expressed as mean ± SD. One-way ANOVA followed by Bonferroni's *post-hoc* test was performed. ****Purified GOS A 12 *vs* non-purified GOS A 12 (*p*< 0.0001); ####Purified GOS B 12 *vs* non-purified GOS B 12 (*p*< 0.0001).

While B-GOS® batch B had been excluded from further experiments due to its levels of LPS above the limit for cell culture, and while it was not possible to use the purified B-GOS® batches due to their negative effects on PBMC viability, B-GOS® batch A (which contained levels of LPS below the threshold) was utilised for a time-course study to determine the optimal incubation time for PBMC stimulation.

3.4.3 Time-course study to determine the optimal incubation time for stimulation with B-GOS® and/or other inflammatory stimuli

Healthy PBMCs were incubated with B-GOS® batch A (0.8 mg/mL, 4 mg/mL and 12 mg/mL) or other inflammatory stimuli (LPS 0.1 µg/mL and 1 µg/mL; PMA and ionomycin 10 ng/mL, 25 ng/mL, 50 ng/mL and 1 µg/mL; Con A 5 µg/mL and 50 µg/mL; TCA 25 µg/mL) for 24 h, 48 h or 72 h. Mitogens and PKC activators were included to gain insight into cell types and/or signalling pathways activated by B-GOS® and to identify potential stimuli to use in subsequent co-culture and pre-incubation experiments. The effects on PBMC viability and secreted mediators (IL-8, IL-10 and TNF-α) were measured at each time point. The chosen time range (24 h – 72 h) was in line with similar prebiotic studies in literature [238, 240, 245, 306].

Viability was always above 90% except for PBMCs stimulated with 50 µg/mL Con A, which presented lower viability compared to unstimulated control (p< 0.0001) and to PBMCs stimulated with 5 µg/mL Con A (p< 0.0001). The highest concentration of Con A (50 µg/mL) was therefore not used in further experiments because of its cytotoxic effects (Figure 3.4 and Table 3.3).

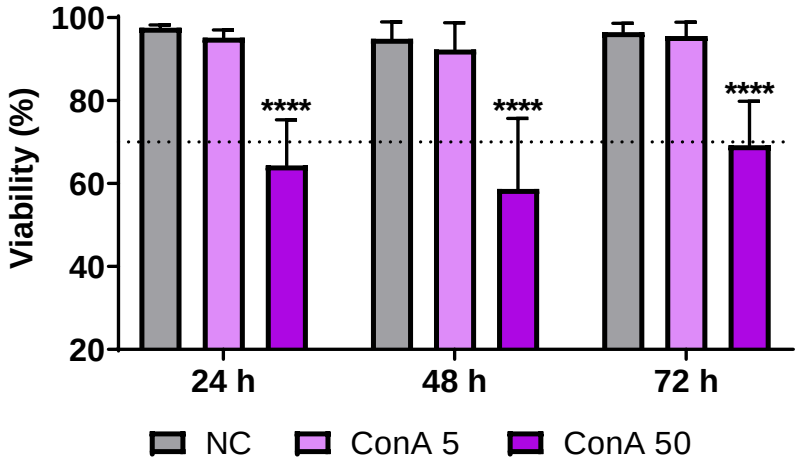

Figure 3.4 Total viability of PBMCs from healthy donors (n= 5) cultured with two concentration of Con A for different incubation times. PBMC viability was assessed by flow cytometry using a live/dead stain. Data are expressed as mean ± SD. Two-way ANOVA followed by Bonferroni's *post-hoc* test was performed. ****Indicate differences between Con A 50 and NC (p< 0.0001) or Con A 5 (p< 0.0001).

No significant effect of concentration on viability was observed for GOS-, LPS-, PMA- or TCA-stimulated PBMCs. Time showed a significant effect upon viability both in GOS-stimulated cells (p= 0.0103) and in LPS-stimulated cells (p= 0.0300). *Post-hoc* analyses on the effects of time revealed that 24 h incubation resulted in better viability than 48 h incubation both in GOS-stimulated (p= 0.0084) and in LPS-stimulated (p= 0.0290) PBMCs. There was no effect of incubation time on the viability of PMA-, TCA-stimulated PBMCs. Results are summarised in Table 3.3.

Table 3.3 Total viability of PBMCs in different culture conditions and at different incubation times. Healthy PBMCs were cultured for 24 h, 48 h or 72 h with B-GOS® batch A, LPS, PMA and ionomycin, Con A or TCA. PBMC viability was assessed by flow cytometry using a live/dead stain.

Stimuli	**Viability (%)**			**Two-way ANOVA *p* value**		
	24 h	**48 h**	**72 h**			
	Mean ± SD (n= 5)	Mean ± SD (n= 5)	Mean ± SD (n= 5)	Time	Stimuli	Time*Stimuli
Control **GOS A 0.8 mg/mL** **GOS A 4 mg/mL** **GOS A 12 mg/mL**	97.6 ± 0.7 97.1 ± 1.1 97.4 ± 1.0 96.5 ± 1.2	94.9 ± 4.0 94.6 ± 3.4 95.5 ± 2.2 96.3 ± 1.9	96.5 ± 2.2 95.8 ± 2.4 96.5 ± 2.2 97.0 ± 1.1	**0.0103**	0.6751	0.8088
Control **LPS 0.1 µg/mL** **LPS 1 µg/mL**	97.6 ± 0.7 96.9 ± 1.1 97.2 ± 0.8	94.9 ± 4.0 94.1 ± 4.4 95.2 ± 3.5	96.5 ± 2.2 95.5 ± 3.4 94.6 ± 3.8	**0.0300**	0.6381	0.8792
Control **PMA 10 ng/mL** **PMA 25 ng/mL** **PMA 50 ng/mL**	97.6 ± 0.7 96.2 ± 1.5 94.8 ± 4.2 96.1 ± 1.7	94.9 ± 4.0 93.8 ± 3.4 94.0 ± 3.4 93.6 ± 3.1	96.5 ± 2.2 95.1 ± 4.5 95.1 ± 3.4 94.3 ± 4.0	0.0574	0.2957	0.9790
Control **ConA 5 µg/mL** **ConA 50 µg/mL**	97.6 ± 0.7 95.2 ± 1.8 64.4 ± 11.0	94.9 ± 4.0 92.3 ± 6.5 58.7 ± 17.1	96.5 ± 2.2 95.6 ± 3.4 69.2 ± 10.6	0.1190	**<0.0001**	0.6527
Control **TCA 25 µg/mL**	97.6 ± 0.7 97.2 ± 1.1	94.9 ± 4.0 92.0 ± 7.3	96.5 ± 2.2 95.2 ± 4.9	0.0509	0.2319	0.7182

Significant main effect of *Time* – Bonferroni's *post-hoc* test for multiple comparison:
GOS A – 24 h significantly different from 48 h (p= 0.0084)
LPS – 24 h significantly different from 48 h (p= 0.0290)

Significant main effect of *Stimuli* – Bonferroni's *post-hoc* test for multiple comparison:
ConA – ConA 50 significantly different from NC (p< 0.0001) and from ConA 5 (p< 0.0001)

In GOS-stimulated PBMCs, a significant effect of stimuli was observed on secreted IL-8 (p= 0.02). Incubation of PBMCs with 12 mg/mL B-GOS® batch A led to higher IL-8 secretion compared to unstimulated control (p= 0.0249, Figure 3.5 and Table 3.4). Although an increase in secreted IL-8 was seen following incubation with LPS, PMA, Con A and TCA, this was not statistically significant compared to control. IL-8 levels in GOS-stimulated cells did not change significantly over time, indicating that most IL-8 production occurred within the first 24 h of stimulation (Table 3.4).

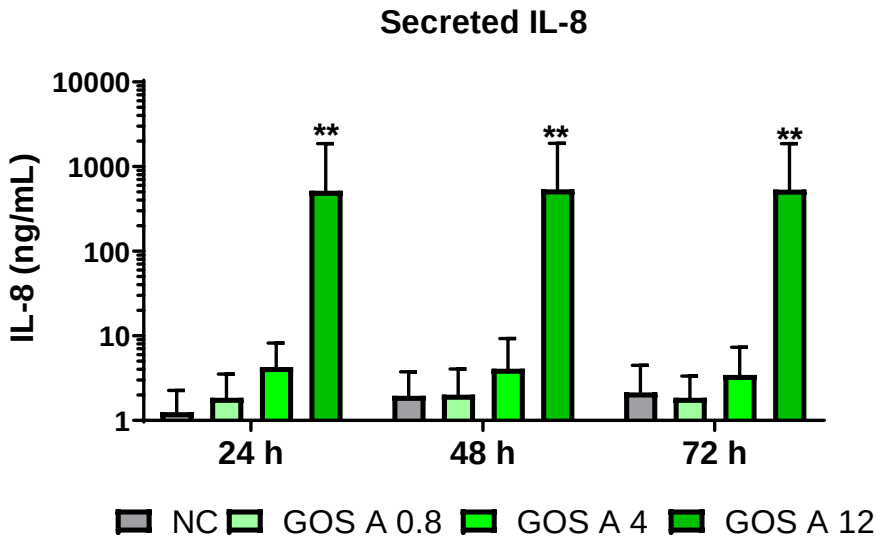

Figure 3.5 Levels of IL-8 secreted by healthy PBMCs (n= 5) after culture with B-GOS® batch A at different incubation times. Data are expressed as mean ± SD. Two-way ANOVA followed by Dunnett's *post-hoc* test was performed. **Indicate differences between GOS A 12 and NC (p= 0.0249).

Table 3.4 Levels of IL-8 secreted by healthy PBMCs after culture with different stimuli, concentrations and incubation times. Secreted IL-8 was measured by Luminex assay.

Stimuli	**IL-8 (ng/mL)**			**Two-way ANOVA *p* value**		
	24 h	**48 h**	**72 h**			
	Mean ± SD (*n*= 5)	Mean ± SD (*n*= 5)	Mean ± SD (*n*= 5)	Time	Stimuli	Time*Stimuli
Control **GOS A 0.8 mg/mL** **GOS A 4 mg/mL** **GOS A 12 mg/mL**[†]	0.9 ± 1.0 1.7 ± 2.1 5.1 ± 4.5 907.3 ± 1778.7	1.9 ± 2.2 1.9 ± 2.5 4.8 ± 6.1 751.7 ± 1579.2	1.7 ± 2.5 1.7 ± 1.8 4.0 ± 4.6 748.9 ± 1580.4	0.9844	**0.0200**	>0.9999
Control **LPS 0.1 µg/mL** **LPS 1 µg/mL**	0.9 ± 1.0 121.9 ± 49.0 162.1 ± 49.6	1.9 ± 2.2 197.5 ± 122.8 257.4 ± 123.8	1.7 ± 2.5 855.4 ± 1522.3 915.4 ± 1489.9	0.1286	0.1915	0.7055
Control **PMA 10 ng/mL** **PMA 25 ng/mL** **PMA 50 ng/mL**	0.9 ± 1.0 4.5 ± 3.3 16.6 ± 23.2 3.4 ± 2.0	1.9 ± 2.2 33.9 ± 63.8 81.1 ± 171.1 4.0 ± 1.6	1.7 ± 2.5 131.3 ± 287.5 106.0 ± 219.3 19.1 ± 34.6	0.2994	0.3155	0.8850
Control **ConA 5 µg/mL** **TCA 25 µg/mL**	0.9 ± 1.0 79.2 ± 48.2 81.8 ± 40.9	1.9 ± 2.2 829.5 ± 1534.9 284.5 ± 204.7	1.7 ± 2.5 874.9 ± 1510.2 242.2 ± 243.0	0.3915	0.0890	0.7212

[†]*n*= 4 at 72 h time point

Significant main effect of *Stimuli* – Dunnett's *post-hoc* test for multiple comparison:
GOS A 12 significantly different from NC (*p*= 0.0249)

No differences in secreted IL-10 were seen after stimulation of PBMCs with B-GOS® batch A, PMA, Con A or TCA at any of the time points tested. A significant interaction of time and stimuli was observed when PBMCs were incubated with LPS (Figure 3.6). At 24 h, PBMCs stimulated either with 0.1 µg/mL LPS or 1 µg/mL LPS secreted significantly more IL-10 than the unstimulated control (*p*= 0.0357 and *p*< 0.0001, respectively). The amount of secreted IL-10 was higher for PBMCs stimulated with 1 µg/mL LPS at 24 h than at 48 h or 72 h (both *p*< 0.0001). Results for secreted IL-10 are presented in Table 3.5.

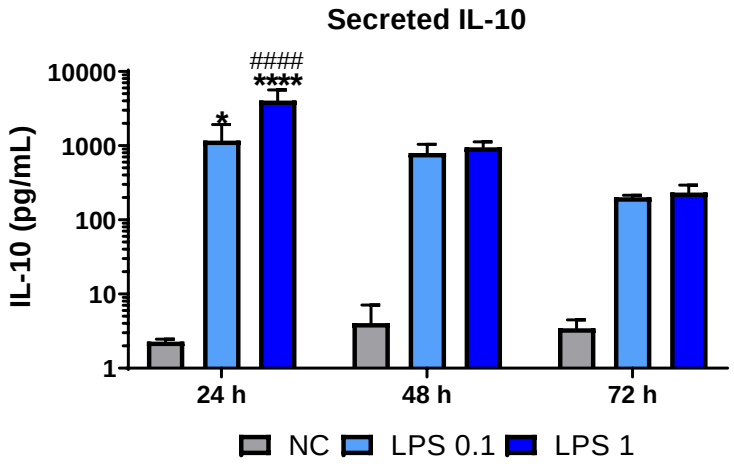

Figure 3.6 Levels of IL-10 secreted by healthy PBMCs (*n*= 3) after culture with LPS at different incubation times. Data are expressed as mean ± SD. Two-way ANOVA followed by Dunnett's or Bonferroni's *post-hoc* test was performed depending upon groups compared. *LPS 0.1 24 h *vs* NC 24 h; ****LPS 1 24 h *vs* NC 24 h; $^{\#\#\#\#}$LPS 1 24 h *vs* LPS 1 48 h and LPS 1 72 h.

Table 3.5 Levels of IL-10 secreted by health PBMCs after culture with different stimuli, concentrations and incubation times. Secreted IL-10 was measured by Luminex assay.

Stimuli	**IL-10 (pg/mL)**			**Two-way ANOVA** ***p* value**		
	24 h	**48 h**	**72 h**			
	Mean ± SD (*n*= 3)	Mean ± SD (*n*= 3)	Mean ± SD (*n*= 3)	Time	Stimuli	Time*Stimuli
Control **GOS A 0.8 mg/mL** **GOS A 4 mg/mL** **GOS A 12 mg/mL**	2.3 ± 0.2 3.0 ± 0.8 4.5 ± 1.9 4.0 ± 1.5	4.1 ± 3.0 4.0 ± 0.8 6.6 ± 1.8 6.5 ± 1.4	3.5 ± 1.0 8.3 ± 6.6 5.5 ± 3.1 7.1 ± 3.9	0.0772	0.2178	0.6648
Control **LPS 0.1 µg/mL** **LPS 1 µg/mL**	2.3 ± 0.2 1173.0 ± 761.4 4058.0 ± 1590.0	4.1 ± 3.0 799.6 ± 247.3 950.8 ± 176.9	3.5 ± 1.0 202.5 ± 12.9 234.2 ± 59.7	**<0.0001**	**<0.0001**	**0.0002**
Control **PMA 10 ng/mL** **PMA 25 ng/mL** **PMA 50 ng/mL**	2.3 ± 0.2 2.7 ± 0.6 10.9 ± 11.3 3.6 ± 1.3	4.1 ± 3.0 3.9 ± 2.6 79.8 ± 131.6 2.9 ± 0.7	3.5 ± 1.0 2.9 ± 1.1 14.6 ± 19.2 2.9 ± 1.3	0.4598	0.2306	0.6207
Control **ConA 5 µg/mL** **TCA 25 µg/mL**	2.3 ± 0.2 983.2 ± 957.0 777.6 ± 806.5	4.1 ± 3.0 379.9 ± 167.0 2086.0 ± 2554.0	3.5 ± 1.0 89.0 ± 51.6 531.9 ± 702.2	0.4217	0.0741	0.4495

Significant interaction *Time*Stimuli*:
Dunnett's *post-hoc* test for multiple comparison – at 24 h, LPS 0.1 and LPS 1 significantly different from NC (p= 0.0357 and p< 0.0001, respectively); Bonferroni's *post-hoc* test for multiple comparison – LPS 1 24 h significantly different from LPS 1 48 h and LPS 1 72 h (both p< 0.0001)

PBMCs cultured with B-GOS® batch A (12 mg/mL), LPS (0.1 µg/mL and 1 µg/mL) and TCA (25 µg/mL) showed higher levels of secreted TNF-α compared to unstimulated control (p= 0.0014, p= 0.0084, p= 0.0044 and p< 0.0001), as shown in Figure 3.7. No differences between incubation times were observed. Incubation with PMA and ionomycin did not alter TNF-α levels at any of the concentrations and time points tested (Table 3.6).

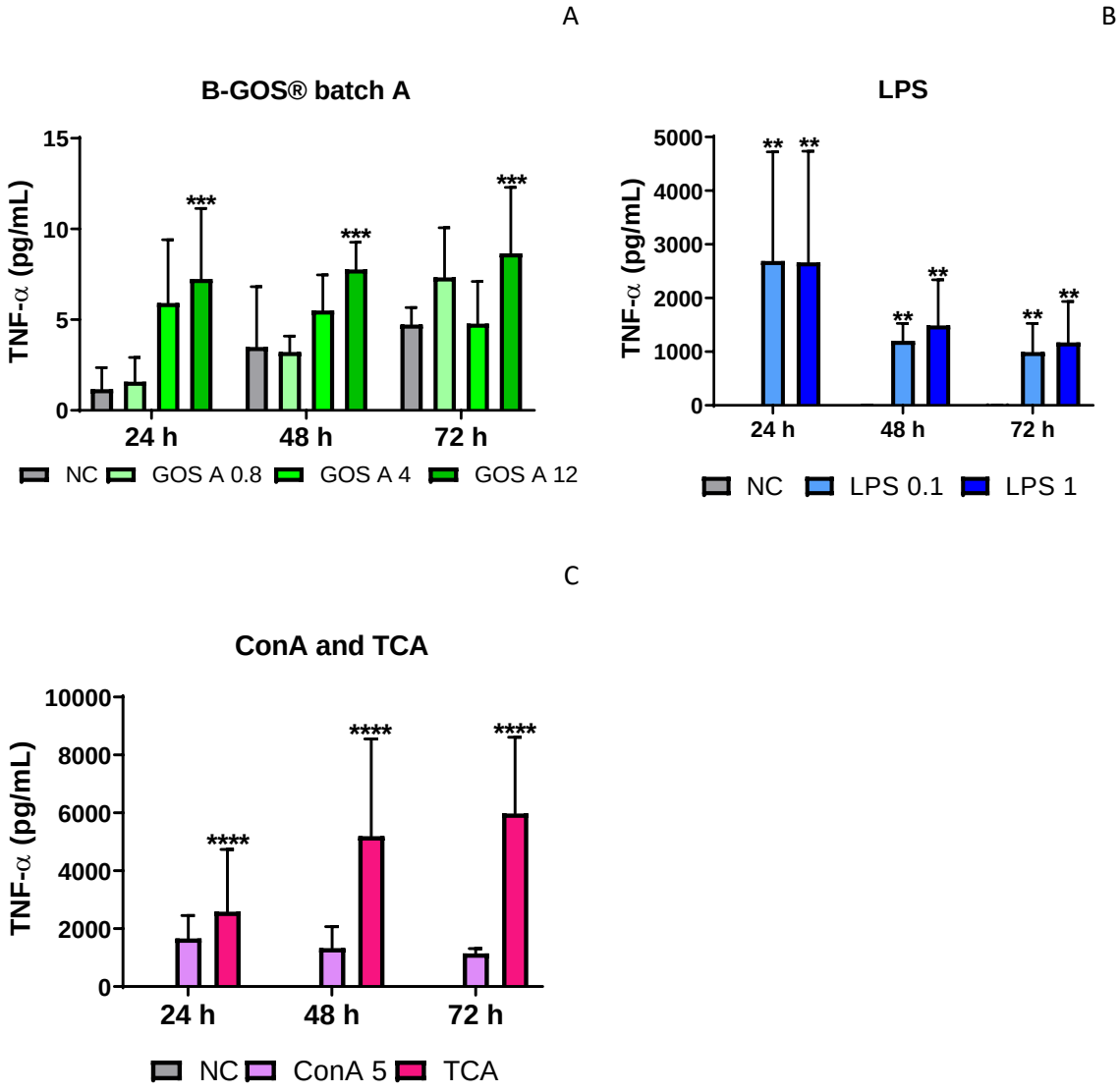

Figure 3.7 Levels of TNF-α secreted by healthy PBMCs (n= 3) after culture with different stimulation conditions at different incubation times. Data are expressed as mean ± SD. Two-way ANOVA followed by Dunnett's *post-hoc* test was performed.

Table 3.6 Levels of TNF-α secreted by healthy PBMCs after culture with different stimuli, concentrations and incubation times. Secreted TNF-α was measured by Luminex assay.

Stimuli	**TNF-α (pg/mL)**			**Two-way ANOVA *p* value**		
	24 h	**48 h**	**72 h**			
	Mean ± SD (*n*= 3)	Mean ± SD (*n*= 3)	Mean ± SD (*n*= 3)	Time	Stimuli	Time*Stimuli
Control **GOS A 0.8 mg/mL** **GOS A 4 mg/mL** **GOS A 12 mg/mL**	1.2 ± 1.2 1.6 ± 1.3 5.9 ± 3.5 7.2 ± 3.9	3.5 ± 3.3 3.2 ± 0.9 5.5 ± 2.0 7.8 ± 1.5	4.7 ± 0.9 7.3 ± 2.7 4.8 ± 2.3 8.7 ± 3.6	0.0832	**0.0030**	0.3775
Control **LPS 0.1 µg/mL** **LPS µg/mL**	1.2 ± 1.2 2688.0 ± 2034.0 2665.0 ± 2070.0	3.5 ± 3.3 1201.0 ± 328.3 1488.0 ± 850.7	4.7 ± 0.9 992.3 ± 536.1 1173.0 ± 761.4	0.1023	**0.0038**	0.6217
Control **PMA 10 ng/mL** **PMA 25 ng/mL** **PMA 50 ng/mL**	1.2 ± 1.2 10.3 ± 6.0 859.8 ± 1462.0 20.6 ± 28.2	3.5 ± 3.3 210.4 ± 318.3 3035.0 ± 5222.0 12.4 ± 4.8	4.7 ± 0.9 23.5 ± 8.5 2930.0 ± 4956.0 54.6 ± 50.7	0.7565	0.0836	0.9576
Control **ConA 5 µg/mL** **TCA 25 µg/mL**	1.2 ± 1.2 1659.0 ± 793.5 2591.0 ± 2147.0	3.5 ± 3.3 1331.0 ± 740.7 5194.0 ± 3362.0	4.7 ± 0.9 1149.0 ± 167.0 5978.0 ± 2636.0	0.4388	**<0.0001**	0.2840

Significant main effect of *Stimuli* – Dunnett's *post-hoc* test for multiple comparison:
GOS A 12 significantly different from NC (*p*= 0.0014)
LPS 0.1 and LPS 1 significantly different from NC (*p*= 0.0084 and *p*= 0.0044, respectively)
TCA significantly different from NC (*p*< 0.0001)

Overall, the 24 h time point was selected as the optimal incubation time for stimulation with B-GOS® because it presented the highest viability and no higher cytokine production was observed at later time points. LPS was chosen among the other inflammatory stimuli because it induced the strongest cytokine response from PBMCs. Depending upon the aim of the experiment, LPS will be used in PBMC cultures as a positive control indicating functional cell activation or as an immune challenge in co-culture and pre-incubation settings.

A detailed time course of a range of LPS-induced mediators (IL-1α, IL-1β, IL-8, IL-10 and granzyme B) was studied in order to understand the best timing for LPS stimulation to use in pre-incubation experiment with B-GOS® batches. Healthy PBMCs (*n*= 2) were stimulated with LPS (0.1 µg/mL and 1 µg/mL) for up to 24 h. Supernatants were collected at different time intervals (2 h, 4 h, 6 h, 10 h, 20 h and 24 h) and stored at -80°C until ready for analysis by Luminex assay.

For all measured mediators, no significant differences between LPS-stimulated cells and unstimulated cells were observed before 6 h stimulation. The lower (0.1 μg/mL) and higher (1 μg/mL) concentrations of LPS had similar effects on secreted mediators.

Higher levels of IL-1α (LPS 0.1 *vs* control, p= 0.0007; LPS 1 *vs* control, p= 0.0009), IL-1β (LPS 0.1 *vs* control, p= 0.0028; LPS 1 *vs* control, p= 0.0018) and IL-8 (LPS 0.1 *vs* control, p= 0.0214; LPS 1 *vs* control, p= 0.0249) were observed after 6 h incubation compared to unstimulated control. Significantly higher levels of IL-1α, IL-1β and IL-8 following PBMC stimulation with LPS (0.1 and 1 μg/mL) were also seen at 10 h, 20 h and 24 h compared to unstimulated control (all p< 0.0001).

Increased levels of IL-10 and granzyme B were seen only after 20 h stimulation. Despite there not being a significant interaction between time and stimuli for IL-10, PBMCs incubated with LPS for 20 h secreted more IL-10 compared to those incubated for 2 h, 4 h or 6 h (p= 0.0185, p= 0.0194 and p= 0.0243). Additionally, PBMCs stimulated with 0.1 μg/mL LPS and 1 μg/mL LPS presented significantly higher IL-10 than control (p= 0.0264 and p= 0.0219). Increased amounts of secreted granzyme B were found after 20 h (LPS 0.1 *vs* control, p= 0.0008; LPS 1 *vs* control, p= 0.0010) and 24 h (LPS 0.1 and LPS 1 *vs* control, p< 0.0001) incubation with LPS. A summary of the results for IL-1α, IL-1β, IL-8, IL-10 and granzyme B is given in Figure 3.8.

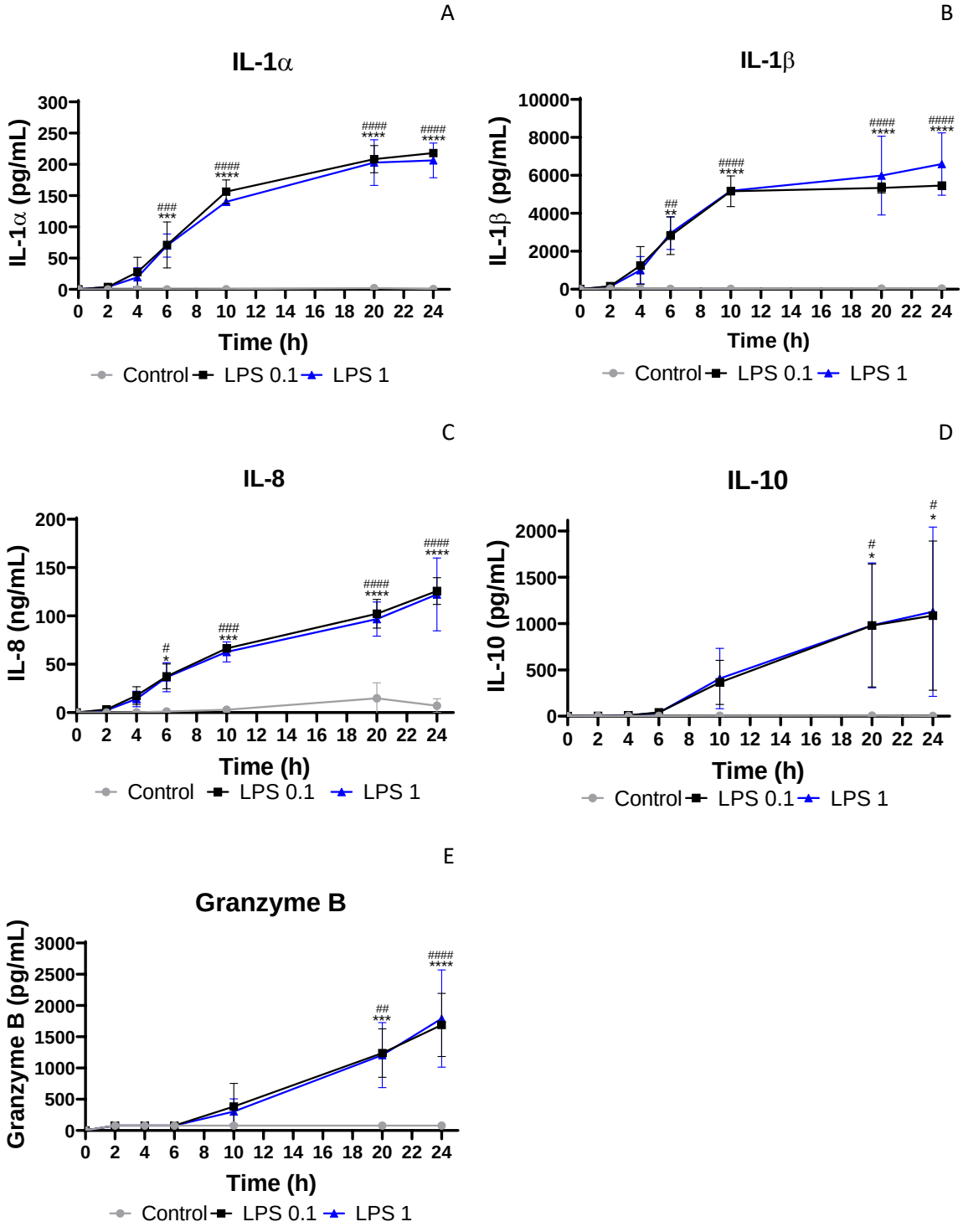

Figure 3.8 24 h time course for a range of LPS-induced mediators secreted by healthy PBMCs (*n*= 2).A) IL-1α (pg/mL); B) IL-1β (pg/mL); C) IL-8 (ng/mL); D) IL-10 (pg/mL) and E) Granzyme B (pg/mL). Data are expressed as mean ± SD. Two-way ANOVA followed by Bonferroni's or Dunnett's *post-hoc* test was performed depending upon groups compared. *Indicates differences between LPS 0.1 and NC, while #indicates differences between LPS 1 and NC.

3.5 Discussion

The aim of the research described in this chapter was to develop an *ex-vivo* PBMC model using cells from adult healthy donors to investigate the direct immunological effects of GOS. Results from the LAL assay revealed that two out of four batches contained detectable levels of LPS, which were above the limit for cell culture applications in B-GOS® batch B. While there are no requirements on LPS absence when prebiotics are consumed orally, it is important to ensure that B-GOS® batches do not contain LPS when tested in experimental settings in direct contact with immune cells because it may lead to immunostimulation and thus to misinterpretation of potential GOS effects.

Since PMB is able to inhibit the effects of LPS, including the release of pro-inflammatory mediators, results were validated by pre-incubating B-GOS® batch B with or without PMB before use in cultures. This confirmed that the secretion of high levels of IL-10 and TNF-α was mainly due to the LPS contained in B-GOS® batch B. However, pre-treatment with PMB did not affect IL-8 secretion, which is therefore likely an effect of GOS itself.

B-GOS® batches A and B were purified by affinity chromatography, which successfully removed LPS. Unfortunately, low viability was observed when the purified batches were used in PBMCs cultures, possibly due to the presence of residual sodium deoxycholate from the purification process. B-GOS® batch C or D did not contain detectable LPS and presented negligible batch-to batch-variability between them according to manufacturer's instructions. Therefore, only B-GOS® batch C data is presented in further experiments within this thesis. It was chosen to test B-GOS® batch C at a range of concentrations (0.8 mg/mL, 4 mg/mL and 12 mg/mL) in all experiments in order to capture its effects both at lower and higher doses.

The importance of testing for LPS and removing LPS when researching the immunological effects of oligosaccharide preparations has been previously highlighted in the literature [307] and represents a key advantage of this model. Failure to take into account the contribution of LPS has previously resulted in an erroneous interpretation of the direct immunostimulatory effects of 3-sialyllactose, a prebiotic found in human milk, on DCs [307].

PBMCs tolerated up to 72 h stimulation with B-GOS® or other inflammatory stimuli including LPS, PMA and ionomycin, Con A and TCA. Viability was always well above the acceptable limit of 70% for cryopreserved cells [308] for all concentration tested, except for the highest dose of Con A (50 µg/mL) that showed cytotoxic effects and was excluded from further experiments.

The optimal incubation time for PBMC stimulation with B-GOS® was identified as 24 h based upon data on viability and secreted mediators. The 24 h time point will be used in later chapters to

assess the immune effects of GOS upon PBMCs from healthy donors and donors with Crohn's disease.

Among the mitogens and PKC activators tested, LPS was chosen as the best stimulus to use in cultures, as it induced the strongest cytokine response by PBMCs. IL-1α, IL-1β and IL-8 were the first cytokines to be secreted after stimulation of PBMCs with LPS, followed by IL-10 and granzyme B. This was in line with other studies found in literature [309, 310]. Monocytes are the first to be activated by LPS stimulation, and are indeed the main cells responsible for the secretion of IL-1α, IL-1β and IL-8. Since preliminary data on the effects of B-GOS® on secreted IL-8 (Figure 3.4 and Table 3.4) support the hypothesis that GOS may act via monocytes, and given that the chemokine IL-8 is among the first mediators being secreted after stimulation with LPS, the 6 h time point was chosen as the optimal stimulation time for further pre-incubation studies.

LPS will be applied in PBMC cultures for 24 h when used as a positive control indicating functional stimulation or for 6 h in preventive setting experiments where PBMCs will be pre-incubated with B-GOS® for 24 h before the LPS challenge. A summary of the conditions chosen for co-culture and pre-incubation experiments presented in the next chapters is provided in Table 3.7.

Table 3.7 Stimuli, concentrations and time points chosen for co-culture and pre-incubation of PBMCs with GOS and LPS.

Stimuli	**Concentration**	**Time point co-cultures GOS + LPS**	**Time point pre-incubation with GOS + LPS challenge**	**Reason for choice**
B-GOS® batch C	0.8 mg/mL 4 mg/mL 12 mg/mL	24 h	24 h	✓ LPS-free batch ✓ Wide range of concentration to capture effects both at lower and higher doses ✓ Better viability
LPS	1 µg/mL	24 h	6 h	✓ Strongest inducer of cytokines ✓ Better viability ✓ Significant effects on release of early-time mediators

Data from LPS-stimulated PBMCs provided a useful insight on the possible mechanisms of GOS action. LPS binds to the TLR4 and through the recruitment of adaptor proteins (MyD88, IL-1R kinase, TNFR associated factor 6 and NADPH oxidase) leads to activation of NF-κB, ultimately resulting in the release of pro-inflammatory cytokines, such as IL-8 [311]. Within PBMCs, monocytes are the predominant subset expressing TLR4 [19], although B cells were also shown to express TLR4 following stimulation with IL-4 [312]. Intracellular cytokine staining will be used in Chapter 4 to determine what cell type is responsible for the upregulated IL-8 production.

In-vitro work using cell lines and human supplementation studies consistently support the hypothesis that GOS may modulate IL-8 production in a microbiota-independent manner [313]. While incubation with human milk oligosaccharides (HMOs) generally reduced the expression of pro-inflammatory IL-8 [239], FOS and inulin but not GOS led to higher IL-8 production by human colon cancer cell lines [242]. In another *in-vitro* study, human colorectal adenocarcinoma cell lines (HT-29) stimulated with LPS secreted lower levels of IL-8 following incubation with cell-free supernatants from probiotic strains [314], suggesting that microbial metabolites may have immunomodulatory properties per se. Human supplementation studies also showed that GOS may affect the IL-8 pathway. In a randomised, double-blind, placebo-controlled, cross-over study on elderly adults, supplementation with GOS (5.5 g/d) for 10 weeks led to significantly higher levels of IL-8 secreted by PBMCs [200]. Similarly, upregulation of the gene CXCL8 which encodes IL-8 was observed in adults with active ulcerative colitis who received 2.8 g/d of GOS for 6 weeks [253].

From the preliminary results presented in this chapter, B-GOS® directly affected IL-8 production by healthy PBMCs. The increase in secreted IL-8 suggests that B-GOS® may promote immunostimulation. Further experiments using GOS fractions isolated from B-GOS® (Chapter 5) will be conducted to better understand the mechanism of GOS action.

Chapter 4 EFFECTS OF GOS UPON IMMUNE PARAMETERS OF *EX VIVO* PBMCs FROM HEALTHY DONORS AND THOSE WITH CROHN'S DISEASE

4.1 Introduction

Non-digestible oligosaccharides (NDOs), including GOS, directly modulate cytokine production (IL-6, IL-8, IL-10, MCP-1, MIP-3α and TNF-α) and immune cell activation (T cells, DCs) *in vitro*, with mechanisms that seem to involve TLR ligation [313]. Anti-inflammatory as well as pro-inflammatory effects were observed in the literature after stimulation with GOS [194, 195, 241-243].

Inconsistent effects reported in the literature were likely due to different GOS concentrations, GOS structures and cell culture models used. Additionally, most studies did not take into account the contribution of mono- (glucose and galactose) and di- saccharides (lactose) deriving from the enzymatic production of GOS. High glucose conditions directly activate human monocytes via upregulation of TLRs (TLR2 and TLR4), resulting in the activation of NF-κB and the release of pro-inflammatory cytokines [315, 316]. Despite there not being studies on the effects on PBMCs, galactose has been used in mice models to increase the lung pro-inflammatory status [317] and to mimic immune changes that occur with aging [318]. Lactose exerts immunostimulatory properties by blocking the galectin-9 pathway, which is involved in the modulation of T cell responses, inhibiting the downregulation of Th1-Th17 immune responses [319]. Overall, because glucose, galactose and lactose directly affect immune cells, it is essential to include them as a control when assessing the effects of GOS products.

Convincing preliminary data support the use of NDOs as immunomodulators for the management of inflammatory bowel diseases (IBD) [313]. While *in vitro* studies and human clinical trials on prebiotic use in IBD are available for FOS and inulin [256-260], no such studies have been conducted for GOS. As a model of IBD, *ex-vivo* Crohn's disease PBMCs will be used in this study to assess the immunological effects of GOS. In IBD, PBMC subsets including monocytes and T cells are more prone to migrate to the inflamed mucosa. Circulating PBMCs are generally more activated and secrete increased amounts of pro-inflammatory cytokines compared to healthy PBMCs [320]. Abnormalities in T cell and B cell numbers and activation status have often been observed in Crohn's disease PBMCs [321-323].

4.2 Aim and objectives

The aim of the work described in this chapter was to assess the effects of GOS on phenotypes, activation markers and secreted/intracellular cytokines of PBMCs from healthy donors and Crohn's disease donors, and to compare the responses between the two PBMC groups. The second aim was to provide an insight into the mechanisms of GOS action by investigating the involvement of TLRs and the interaction of GOS with LPS.

The specific objectives were to:

- Assess the effects of GOS on cell viability, cell frequencies (lymphocytes, monocytes, T cells, B cells, NK cells, NKT cells, T helper cells and cytotoxic T cells), activation markers (CD25 and CD69), secreted mediators (*e.g.* IL-1α, IL-1β, IL-6, IL-8, IL-10, IFN-γ TNF-α), intracellular mediators (IL-8) and TLR expression (TLR2 and TLR4) of PBMCs from healthy donors and Crohn's disease donors

- Investigate the mechanisms of GOS action through TLR4 by blocking the signalling via the receptor with penta-acylated LPS from *Rhodobacter sphaeroides* (TLR4 antagonist), using PBMCs from healthy donors as well as THP-1 monocytic cell lines

- Investigate the role of mono- (glucose and galactose) and di- saccharides (galactose) contained in GOS product upon secreted IL-8 and CD69 expression by healthy PBMCs and Crohn's disease PBMCs

- Evaluate the effects of 24 h culture of healthy PBMCs with GOS and LPS, or the effects of 24 h pre-incubation of healthy PBMCs with GOS followed by 6 h LPS challenge, upon cell viability, phenotypes and secreted mediators

Based on the preliminary data showed in Chapter 3 and on the reviewed literature, it is hypothesised that B-GOS® will promote immunostimulation on healthy PBMCs via the TLR4 receptor (*e.g.* increased secretion of pro-inflammatory cytokines, increased cell activation), and that mono- and di-saccharides within B-GOS® will be important contributors to this effect. In co-culture settings, it is hypothesised that B-GOS® will block LPS signalling via TLR4, either by binding to the TLR4 instead of LPS or by indirectly interfering with the TLR4, resulting in lower levels of LPS-induced cytokines but higher levels of B-GOS®-induced cytokines.

4.3 Methods

B-GOS® batch C and free sugars controls were prepared as detailed in section 2.3. Healthy PBMCs and Crohn's disease PBMCs were cultured as explained in section 2.1, while THP-1 cell lines were cultured as detailed in section 2.2. Unless otherwise stated in this chapter, cell culture conditions were carried out as indicated in section 2.3. Cell viability was measured by flow cytometry using a fixable viability stain (FVS780) as reported in section 2.5. Cell surface staining and intracellular staining by flow cytometry were performed as described in sections 2.7.2 and 2.7.3, respectively. Data were either displayed in FSC/SSC plots or in fluorescence plots and analysed using FlowJo Single Cell Analysis Software version 10.0 (FlowJo LLC). Unstained cells, isotype controls and fluorescence minus one (FMO) controls were used as indicated in section 2.7.2. Doublets were excluded on FSC-H vs FSC-A graphs using a polygonal gate. Within the singlets, a polygonal gate was drawn around PBMCs to exclude debris. Within the PBMC gate, a bisector gate was used to determine the percentages of live cells ($FVS780^-$) and dead cells ($FVS780^+$) in a FVS780-A histogram. Within the live PBMCs, lymphocytes were identified using a polygonal gate in a SSC-A vs FSC-A plot based on their size and complexity while monocytes were determined by gating the $CD14^+$ cells in a SSC-A vs CD14-PE-Cy7®-A graph. Since CD3 and CD19 staining is mutually exclusive, T cells ($CD3^+$ $CD19^-$) and B cells ($CD3^-$ $CD19^+$) were identified using a quadrant gate within the lymphocyte population in a CD19-BV711-A *vs* CD3-PerCP-Cy®5.5-A graph. Within the T cell population, subset analysis of T helper cells and cytotoxic T cells was carried out. T helper cells were defined as $CD3^+CD4^+CD8^-$ cells and cytotoxic T cells as $CD3^+CD8^+CD4^-$ cells in CD8-V450-A *vs* CD4-BV605-A plots. Natural killer cells ($CD3^-CD56^+$) and natural killer T cells ($CD3^+CD56^+$) percentages were calculated within the lymphocyte population in CD56-R-PE-A *vs* CD3-PerCP-Cy5.5-A graphs using a quadrant gate. Mediators secreted in cell culture supernatants were analysed using Premixed Magnetic Luminex® Assays. Further details on the Luminex method and the dilution factors used can be found in section 2.8. A graphical summary of the methods used in this chapter is provided in Figure 4.1 and Figure 4.2.

A

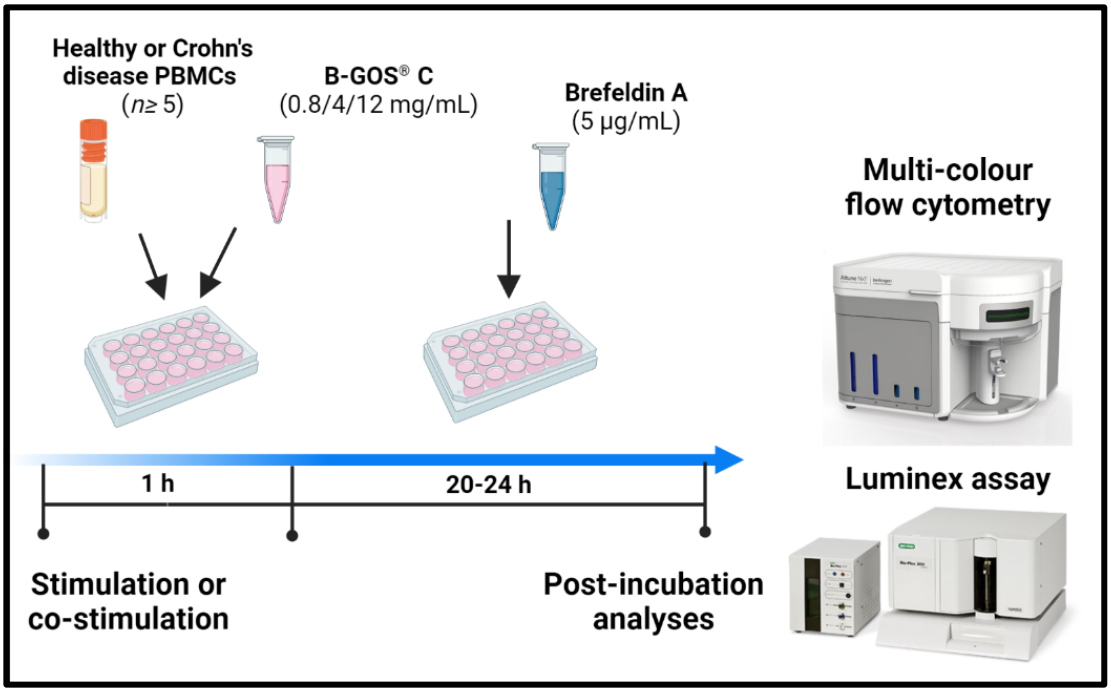

B

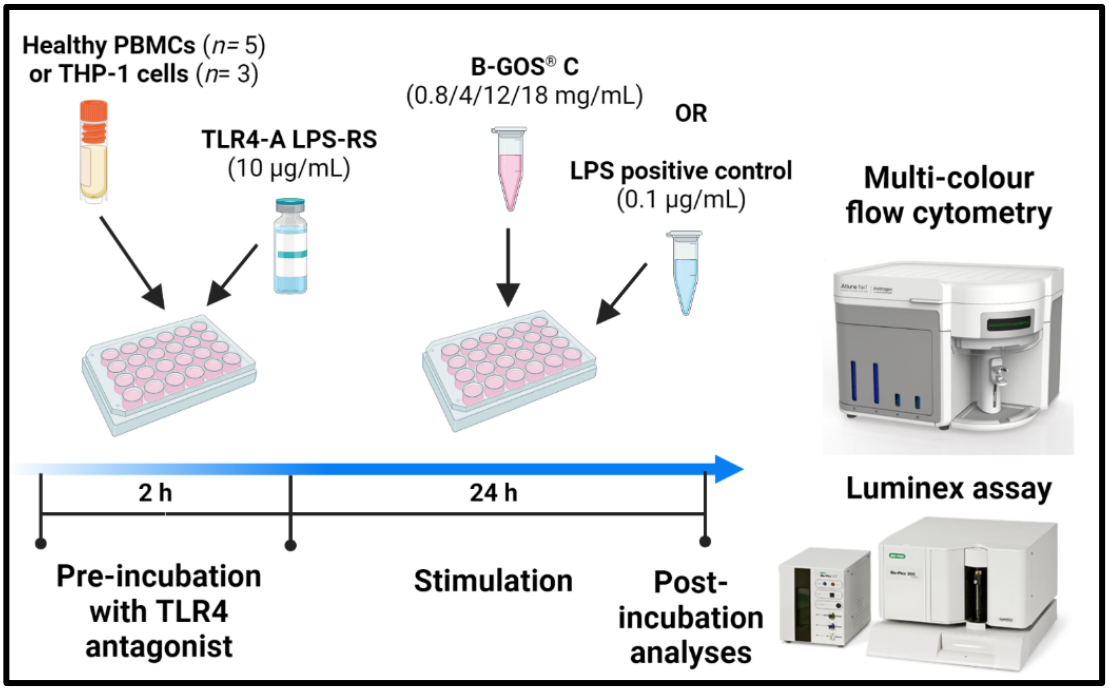

Figure 4.1 Graphical summary of the methods used for A) the assessment of the effects of B-GOS® batch C upon viability, phenotypes, activation markers and cytokines of PBMCs from healthy donors and Crohn's disease donors; and B) the assessment of the involvement of TLR4 in cytokine secretion following stimulation of PBMCs and THP-1 monocytic cell lines with B-GOS® batch C.

A

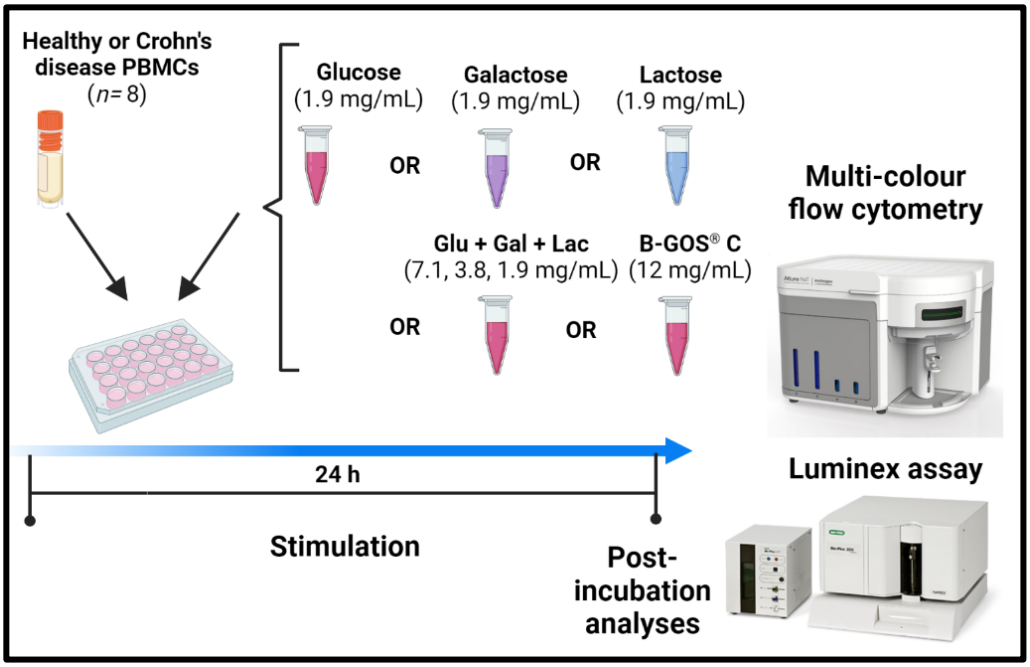

B

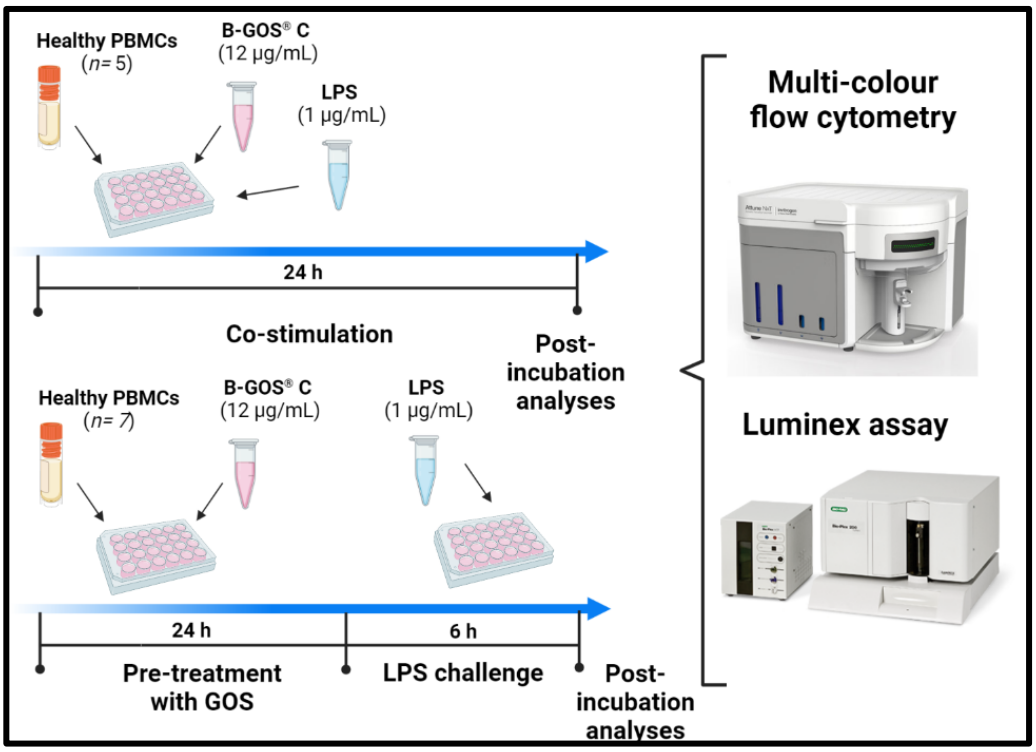

Figure 4.2 Graphical summary of the methods used for A) the investigation of the role of free sugars galactose, lactose and glucose contained in B-GOS® batch C upon secreted cytokines and activation markers; and B) assessing the effects of co-stimulation or pre-treatment with B-GOS® batch C and LPS upon viability, phenotypes and cytokines from healthy PBMCs.

4.4 Results

4.4.1 Baseline differences between PBMCs from healthy donors and Crohn's disease donors

Unstimulated Crohn's disease PBMCs showed significantly lower viability than unstimulated healthy PBMCs both in the absence (p= 0.0003) and in the presence (p= 0.0112) of brefeldin A 5 µg/mL (Figure 4.3). In order to allow comparisons between healthy and Crohn's disease donors, increase the power and remove the bias of having a confounding variable, viability was coded as a covariate and included in all further analyses.

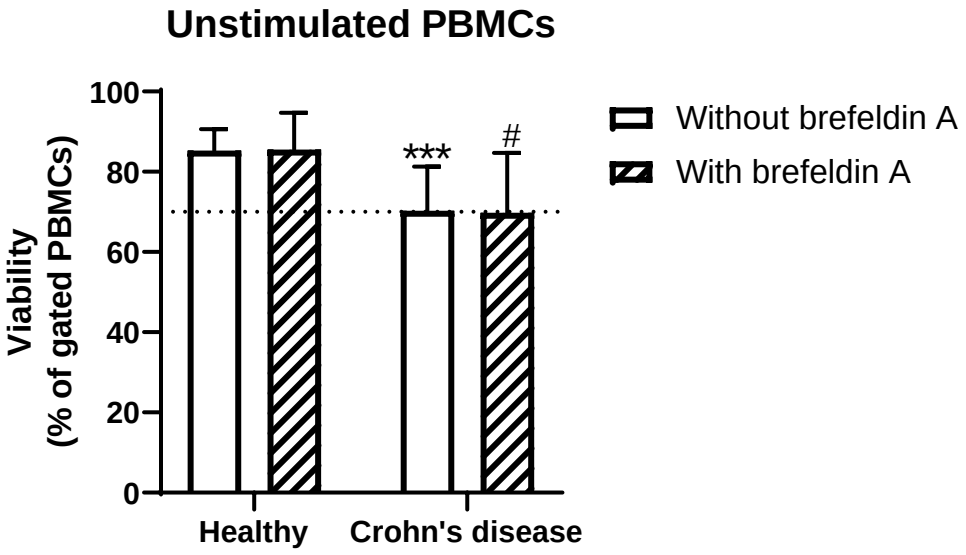

Figure 4.3 Viability of unstimulated PBMCs from healthy donors and Crohn's disease donors in the presence (n= 8 and n= 5, respectively) and in the absence (n= 13 and n= 8, respectively) of brefeldin A (5 µg/mL). Viability was measured by flow cytometry using a fixable viability stained (FVS780) and expressed as % of $FVS780^-$ cells within the PBMC gate. Data are expressed as mean ± SD. Two-way ANOVA followed by Bonferroni's *post-hoc* test was performed. Significant differences between healthy and Crohn's disease PBMCs in presence and in absence of brefeldin A are marked with an hash and with an asterisk, respectively.

Unstimulated Crohn's disease PBMCs presented higher numbers of NKT cells and lower numbers of T helper cells compared to unstimulated healthy PBMCs (Table 4.1 and Figure 4.4).

Table 4.1 Differences in cell frequencies between unstimulated healthy PBMCs and unstimulated Crohn's disease PBMCs measured by flow cytometry. Data were expressed as mean ± SD. One-way ANCOVA followed by Bonferroni's *post-hoc* test was performed. Cell viability was coded as a covariate.

Cell frequencies	**Unstimulated healthy PBMCs**	**Unstimulated Crohn's disease PBMCs**	**One-way ANCOVA *p* value**
	Mean ± SD (*n*= 14)	Mean ± SD (*n*= 8)	
Lymphocytes (% of live PBMCs)	86.8 ± 5.8	88.1 ± 9.6	0.288
Monocytes (% of live PBMCs)	7.4 ± 4.3	4.0 ± 5.1	0.221
B cells (% of lymphocytes)*	10.2 ± 3.6	4.1 ± 3.1	0.061
NK cells (% of lymphocytes)*	2.6 ± 2.0	4.6 ± 2.6	0.102
NKT cells (% of lymphocytes)*	0.4 ± 0.4	2.8 ± 1.9	**0.026**
T cells (% of lymphocytes)	80.2 ± 4.3	81.5 ± 8.2	0.587
T helper cells (% of T cells)**	74.8 ± 8.3	62.8 ± 12.9	**0.048**
Cytotoxic T cells (% of T cells)	21.5 ± 7.1	26.8 ± 11.1	0.113

**n*= 6 and *n*= 9 for healthy PBMCs and for CD PBMCs, respectively; ***n*= 10 for both.

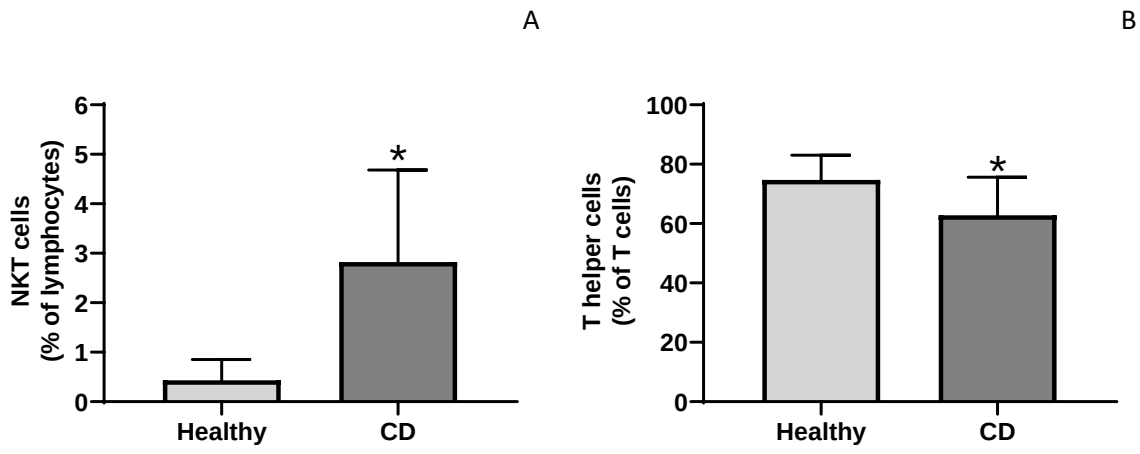

Figure 4.4 Differences in cell frequencies between unstimulated healthy PBMCs (*n*= 6 in graph A and *n*= 10 in graph B) and unstimulated Crohn's disease PBMCs (*n*= 9 in graph A and *n*= 10 in graph B) measured by flow cytometry.A) NKT cells (% of lymphocytes); B) T helper cells (% of T cells). Data were expressed as mean ± SD. One-way ANCOVA followed by Bonferroni's *post-hoc* test was performed. Cell viability was coded as a covariate. Significant differences between healthy *vs* Crohn's disease PBMCs are marked with an asterisk (*$p < 0.05$).

Overall, unstimulated Crohn's disease PBMCs presented higher percentages of activated lymphocytes, T cells and cytotoxic T cells and a tendency for lower frequencies of activated B cells compared to healthy PBMCs (Table 4.2 and Figure 4.5). CD69 expression in Crohn's disease donors was negatively correlated with the frequencies of monocytes (r= -0.5028, p= 0.0239), indicating that, when there were less monocytes within PBMCs, they were more activated and expressed higher levels of CD69. Interestingly, this correlation was not seen in monocytes from healthy PBMCs (Figure 4.6).

Table 4.2 Differences in the frequencies of CD69-expressing cells between unstimulated healthy PBMCs and unstimulated Crohn's disease PBMCs. Percentages of $CD69^+$ cells were quantified by flow cytometry. One-way ANCOVA followed by Bonferroni's *post-hoc* test was performed. Cell viability was coded as a covariate.

CD69 expression (%)	**Unstimulated healthy PBMCs**	**Unstimulated Crohn's disease PBMCs**	**One-way ANCOVA *p* value**
	Mean ± SD (*n*= 12)	Mean ± SD (*n*= 6)	
$CD69^+$ lymphocytes (% of lymphocytes)	9.3 ± 8.1	19.6 ± 4.3	**0.023**
$CD69^+$ T cells (% of T cells)	4.9 ± 3.8	16.3 ± 5.0	**0.004**
$CD69^+$ T helper cells (% of T helper cells)	12.7 ± 21.4	15.0 ± 5.3	0.727
$CD69^+$ cytotoxic T cells (% of cytotoxic T cells)	7.6 ± 5.6	20.6 ± 5.7	**0.002**
$CD69^+$ B cells (% of B cells)*	50.7 ± 11.1	37.1 ± 4.5	0.055
$CD69^+$ monocytes (% of monocytes)*	13.9 ± 8.5	13.3 ± 6.6	0.414

**n*= 5 for unstimulated healthy PBMCs;

A

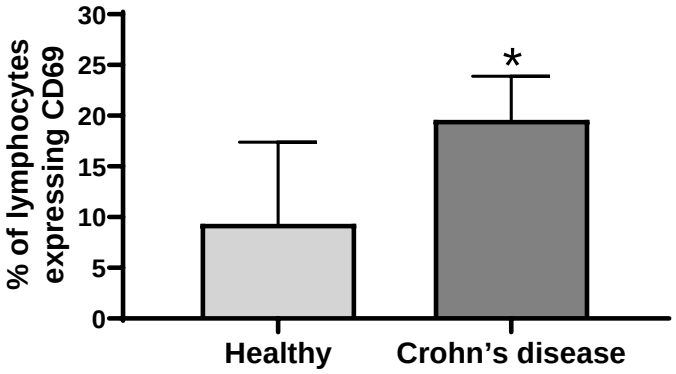

B

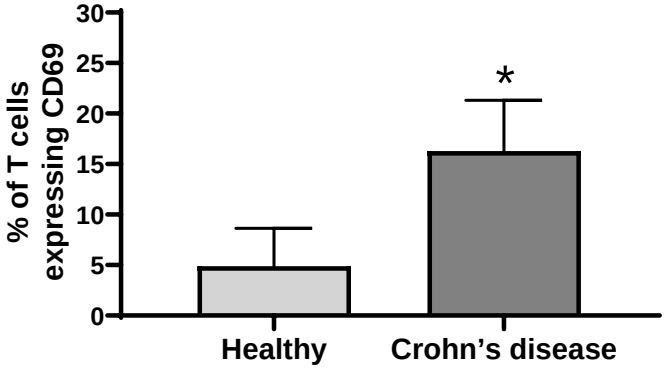

C

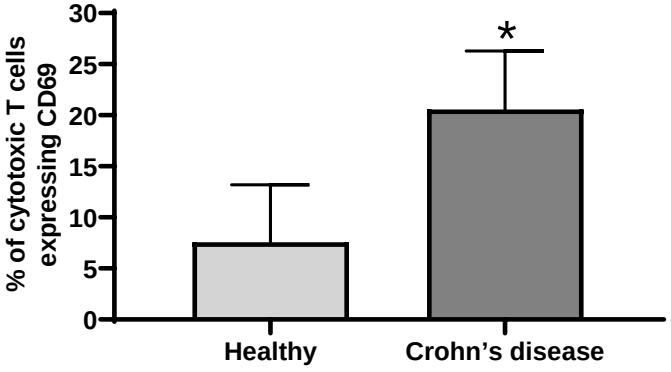

Figure 4.5 Differences in the frequencies of CD69-expressing A) lymphocytes B) T cells and C) cytotoxic T cells between unstimulated healthy PBMCs and unstimulated Crohn's disease PBMCs (all *n*= 12 and *n*= 6, respectively) measured by flow cytometry. Data were expressed as mean ± SD. One-way ANCOVA followed by Bonferroni's *post-hoc* test was performed. Cell viability was coded as a covariate. Significant differences between healthy *vs* Crohn's disease PBMCs are marked with an asterisk (*p< 0.05).

A

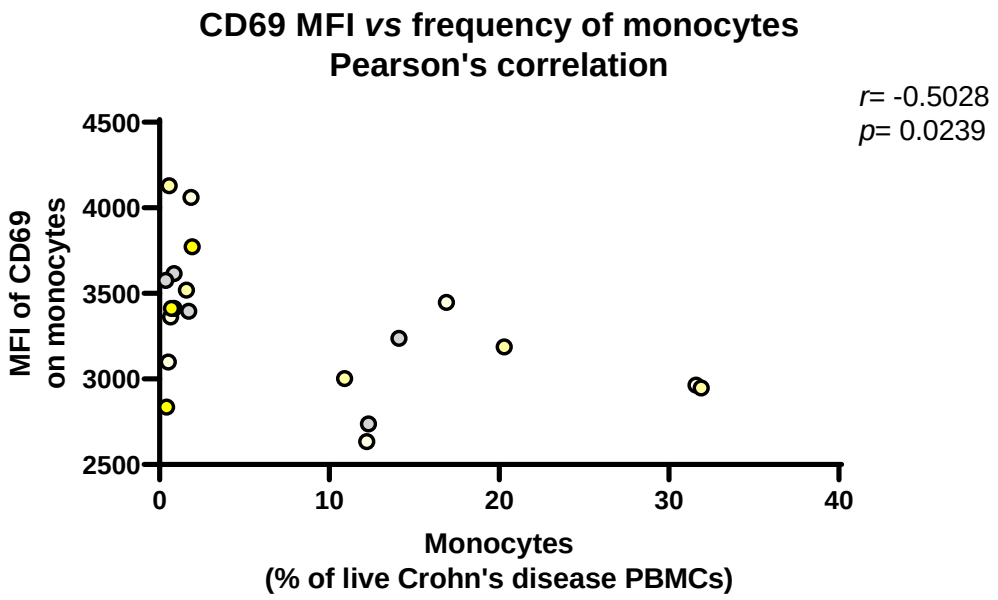

B

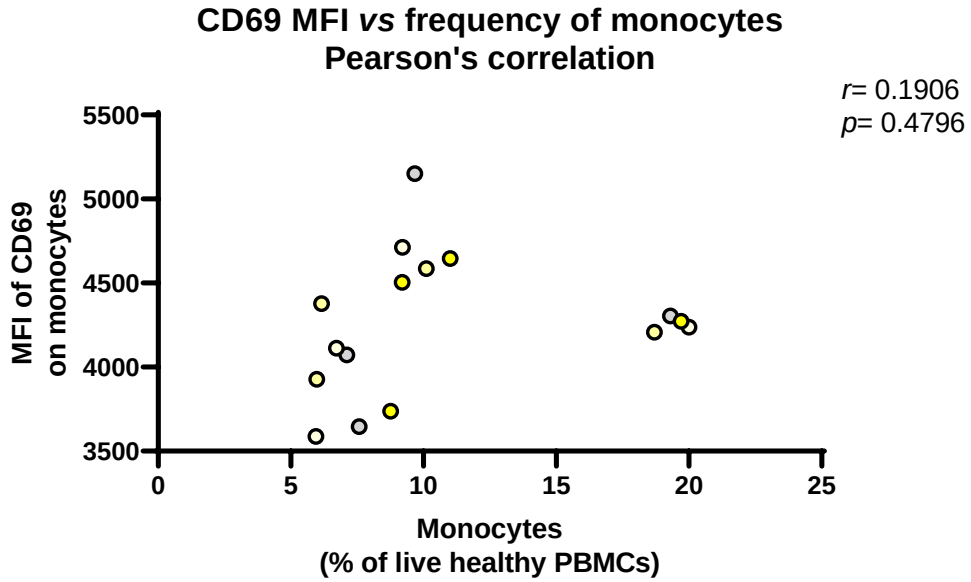

Figure 4.6 Pearson's correlation analysis between the levels of CD69 expression (MFI) on monocytes and their frequencies (%) within live PBMCs. Data refer to unstimulated (gray circles) or B-GOS® batch C (yellow circles)-stimulated A) Crohn's disease PBMCs (*n*= 20); B) Healthy PBMCs (*n*= 16).

Unstimulated Crohn's disease PBMCs secreted higher levels of the pro-inflammatory cytokines IL-1β and IL-6 but lower amounts of the anti-inflammatory IL-10 compared to healthy PBMCs (Table 4.3 and Figure 4.7).

Table 4.3 Differences in the levels of mediators secreted by unstimulated healthy PBMCs unstimulated Crohn's disease PBMCs. Secreted mediators were quantified by Luminex assay. One-way ANCOVA followed by Bonferroni's *post-hoc* test was performed. Cell viability was coded as a covariate.

Secreted cytokines (pg/10^6 cells)	**Unstimulated healthy PBMCs** Mean ± SD (*n*= 12)	**Unstimulated Crohn's disease PBMCs** Mean ± SD (*n*= 12)	**One-way ANCOVA *p* value**
IL-1α	0.7 ± 1.0	0.4 ± 0.0	0.391
IL-1β	1.4 ± 1.2	81.1 ± 29.7	**<0.0001**
IL-6	1.5 ± 1.7	6.2 ± 0.0	**0.001**
IL-8[†]	0.9 ± 1.2	0.4 ± 0.4	0.870
IL-10	1.2 ± 0.6	0.3 ± 0.4	**0.009**
IL-12p70	6.9 ± 4.7	4.9 ± 4.6	0.288
IL-17A	0.7 ± 0.6	0.1 ± 0.0	0.171
IFN-γ	3.0 ± 3.2	1.9 ± 1.7	0.605
TNF-α	2.1 ± 1.5	0.7 ± 0.6	0.128
Granzyme B	42.5 ± 27.3	102.0 ± 46.2	0.382
IL-1ra[†]	0.6 ± 0.4	337.5 ± 178.2	0.470

[†]ng/10^6 cells;

Healthy PBMCs: *n*= 10 for IL-6; *n*= 8 for IL-12p70. Crohn's disease PBMCs: *n*= 6 for IL-1α, IL-6, granzyme B, IL-1ra

A

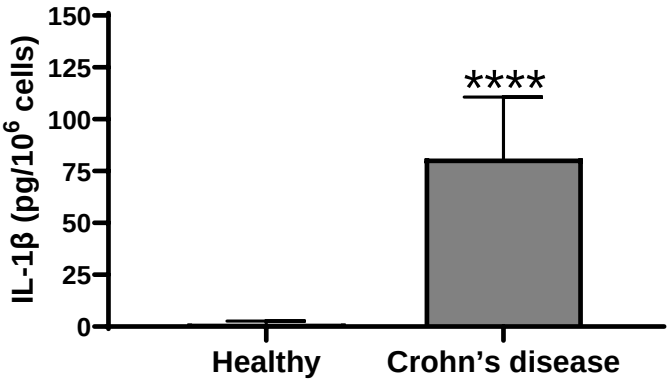

B

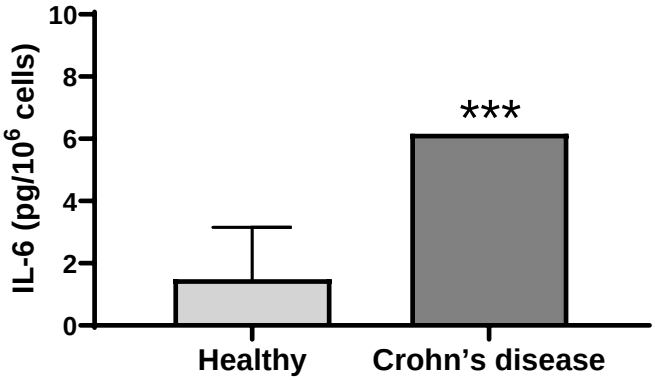

C

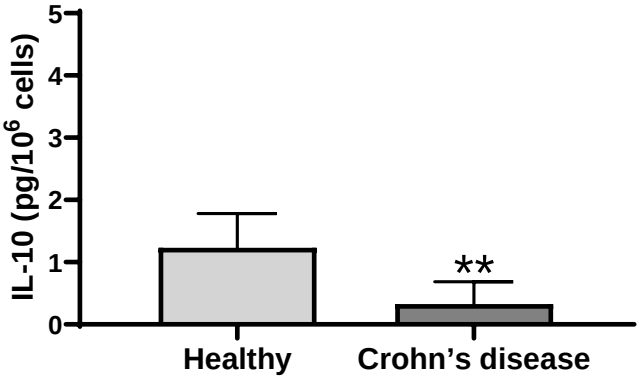

Figure 4.7 Differences in the levels of mediators secreted by unstimulated healthy PBMCs and unstimulated Crohn's disease PBMCs after 20 – 24 h culture. Secreted A) IL-1β (both *n*= 12) B) IL-6 (*n*= 10 for healthy PBMCs and *n*= 6 for Crohn's disease PBMCs) and C) IL-10 (both *n*= 12) were quantified by Luminex assay. Data were expressed as mean ± SD. One-way ANCOVA followed by Bonferroni's *post-hoc* test was performed. Cell viability was coded as a covariate. Significant differences are marked with an asterisk (****$p < 0.0001$; ***$p < 0.001$; **$p < 0.01$).

4.4.2 Effects of B-GOS® batch C upon viability of PBMCs from healthy donors and Crohn's disease donors

The viability of PBMCs cultured for 20 – 24 h with B-GOS® batch C (0.8 mg/mL, 4 mg/mL and 12 mg/mL) in presence or in absence of brefeldin A (5 μg/mL) was measured to ensure that the chosen concentrations were tolerated by the cells. Healthy PBMCs presented viability above 80% at all the tested conditions, both when cultured without (Table 4.4) and with (Table 4.5) brefeldin A. No differences in cell viability were observed between B-GOS® batch C-stimulated healthy PBMCs and unstimulated control (Table 4.4 and Table 4.5). Similarly, no differences were observed B-GOS® batch C-stimulated Crohn's disease PBMCs and unstimulated control (Table 4.6 and Table 4.7). Overall, B-GOS® batch C was tolerated by healthy and Crohn's disease PBMCs at all concentrations tested.

Table 4.4 Viability of healthy PBMCs cultured for 20 – 24 h with different concentrations of B-GOS® batch C in absence of brefeldin A.

Healthy PBMCs	**NC**	**GOS C 0.8 mg/mL**	**GOS C 4 mg/mL**	**GOS C 12 mg/mL**	**Kruskal-Wallis *p* value**
	Median ± IQR (*n*= 13)	Median ± IQR (*n*= 14)	Median ± IQR (*n*= 14)	Median ± IQR (*n*= 13)	
Viability (%) without brefeldin A	85.9 ± 19.2	85.5 ± 37.7	85.0 ± 34.6	84.7 ± 24.8	0.824

Table 4.5 Viability of healthy PBMCs cultured for 20 – 24 h with different concentrations of B-GOS® batch C in presence of brefeldin A.

Healthy PBMCs	**NC**	**GOS C 0.8 mg/mL**	**GOS C 4 mg/mL**	**GOS C 12 mg/mL**	**Kruskal-Wallis *p* value**
	Median ± IQR (*n*= 8)	Median ± IQR (*n*= 8)	Median ± IQR (*n*= 8)	Median ± IQR (*n*= 8)	
Viability (%) with brefeldin A	89.3 ± 27.3	89.7 ± 28.1	89.6 ± 29.0	85.2 ± 32.3	0.555

Table 4.6 Viability of Crohn's disease PBMCs cultured for 20 – 24 h with different concentrations of B-GOS® batch C in absence of brefeldin A.

Crohn's disease PBMCs	**NC**	**GOS C 0.8 mg/mL**	**GOS C 4 mg/mL**	**GOS C 12 mg/mL**	**One-way ANOVA *p* value**
	Mean ± SD (*n*= 8)	Mean ± SD (*n*= 6)	Mean ± SD (*n*= 6)	Mean ± SD (*n*= 8)	
Viability (%) without brefeldin A	70.3 ± 11.1	70.5 ± 13.1	68.6 ± 14.1	60.8 ± 13.6	0.267

Table 4.7 Viability of Crohn's disease PBMCs cultured for 20 – 24 h with B-GOS® batch C in presence of brefeldin A.

Crohn's disease PBMCs	**NC**	**GOS C 12 mg/mL**	**Unpaired t test with Welch's correction *p* value**
	Mean ± SD (*n*= 5)	Mean ± SD (*n*= 6)	
Viability (%) with brefeldin A	69.8 ± 14.9	61.8 ± 11.1	0.355

4.4.3 Effects of B-GOS® batch C upon healthy and Crohn's disease PBMC phenotypes

Healthy and Crohn's disease PBMC subsets including lymphocytes, monocytes, T cells, B cells, NK cells, NKT cells, T helper cells and cytotoxic T cells were studied by multi-colour flow cytometry. A summary of the gating strategy used in this work is reported in Figure 4.8. An example of flow cytometry graphs from a single healthy donor stimulated for 24 h with B-GOS® batch C (0.8 mg/mL) is given in Figure 4.9. Gates were confirmed by back-gated cells (Figure 4.10), isotype controls and unstained samples (Figure 4.11).

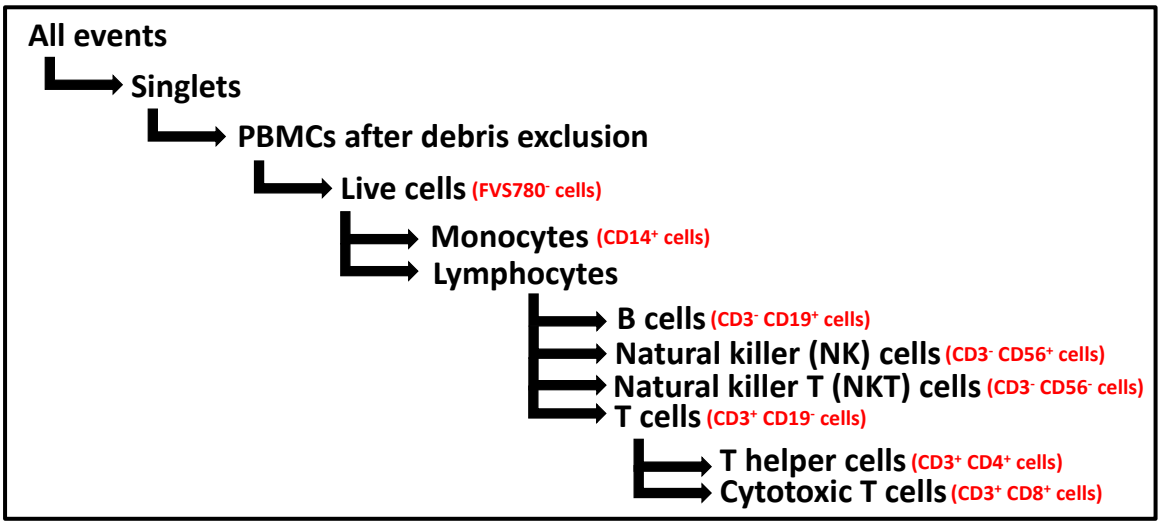

Figure 4.8 Summary of the gating strategy used to analyse PBMC subsets and their relative phenotypes (in red).

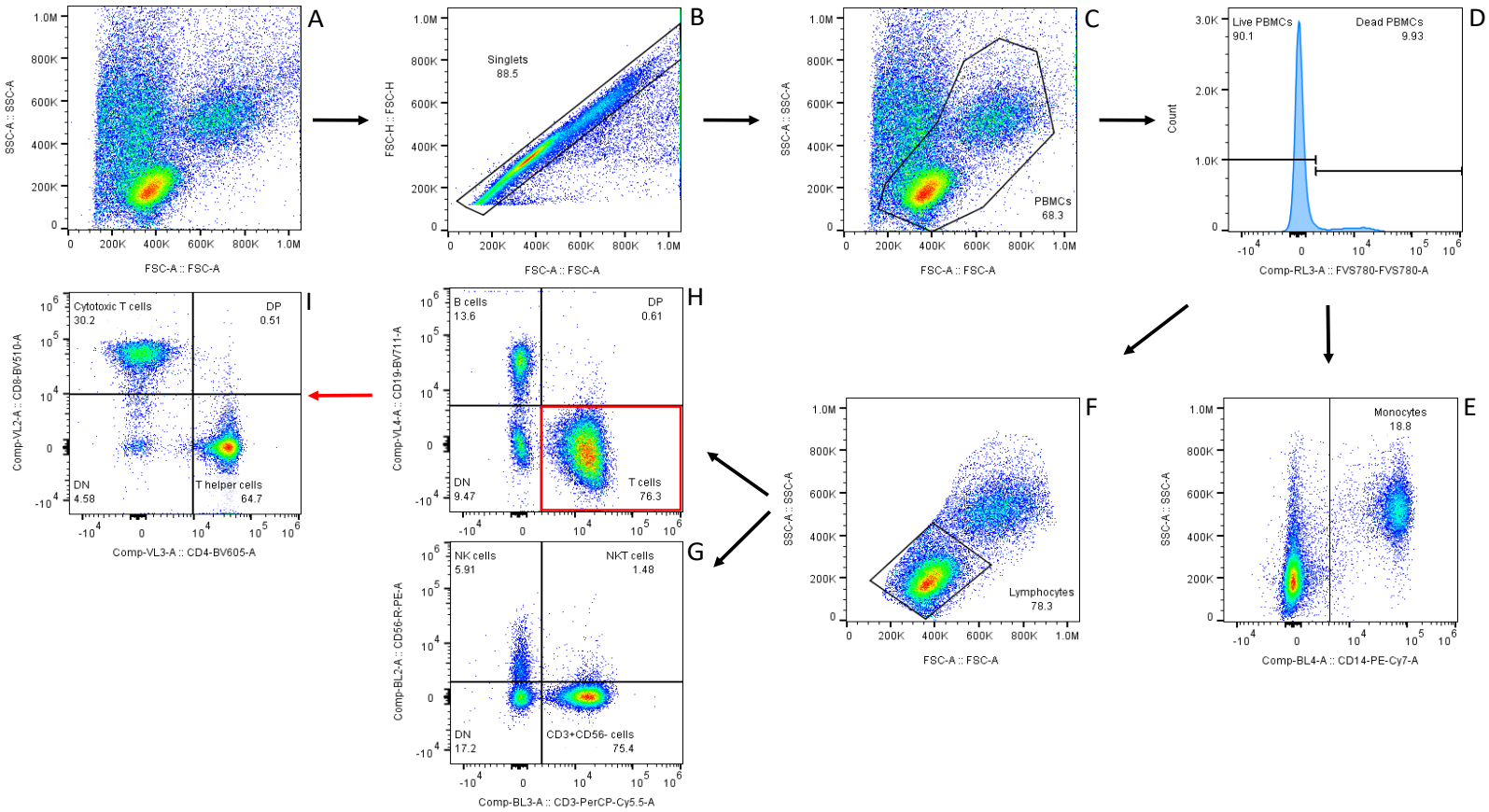

Figure 4.9 Example of flow cytometry graphs from a single healthy donor stimulated for 24 h with B-GOS® batch C (0.8 mg/mL). A) All events; B) Singlets gated from all events; C) PBMCs gated from singlets; D) Live PBMCs gated from PBMCs; E) Monocytes ($CD14^+$) gated from live PBMCs; F) Lymphocytes gated from live PBMCs; G) NK cells and NKT cells gated from lymphocytes; H) B cells and T cells gated from lymphocytes; I) Cytotoxic T cells and T helper cells gated from T cells.

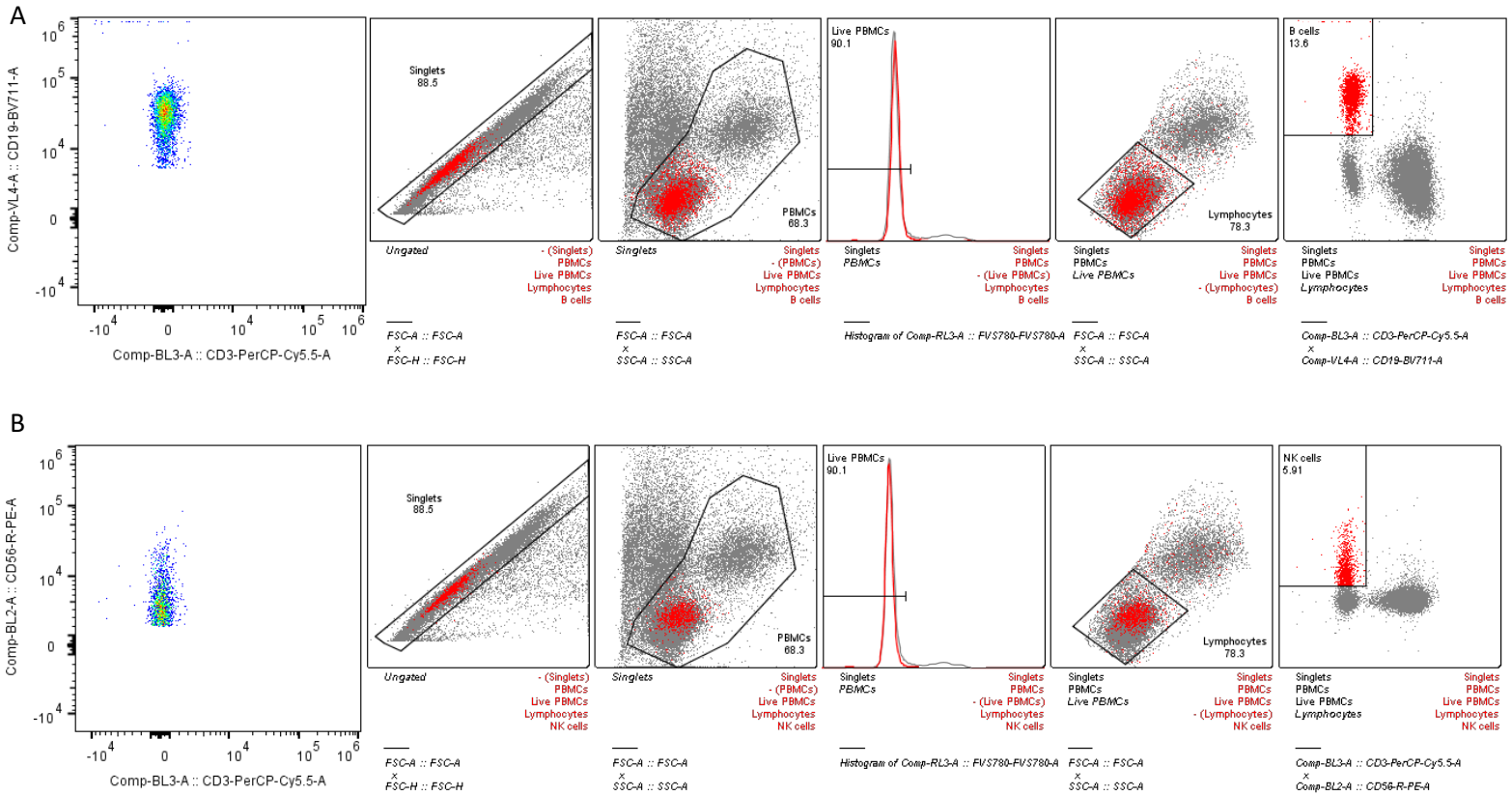

Figure 4.10 Examples of back-gating applied to confirm the gating strategy. A) B cells were identified as $CD3^{-}CD19^{+}$ events gated from lymphocytes/live PBMCs/PBMCs excluded debris/singlets/all events; B) NK cells were identified as $CD3^{-}CD56^{+}$ events gated from lymphocytes/live PBMCs/PBMCs excluded debris/singlets/all events.

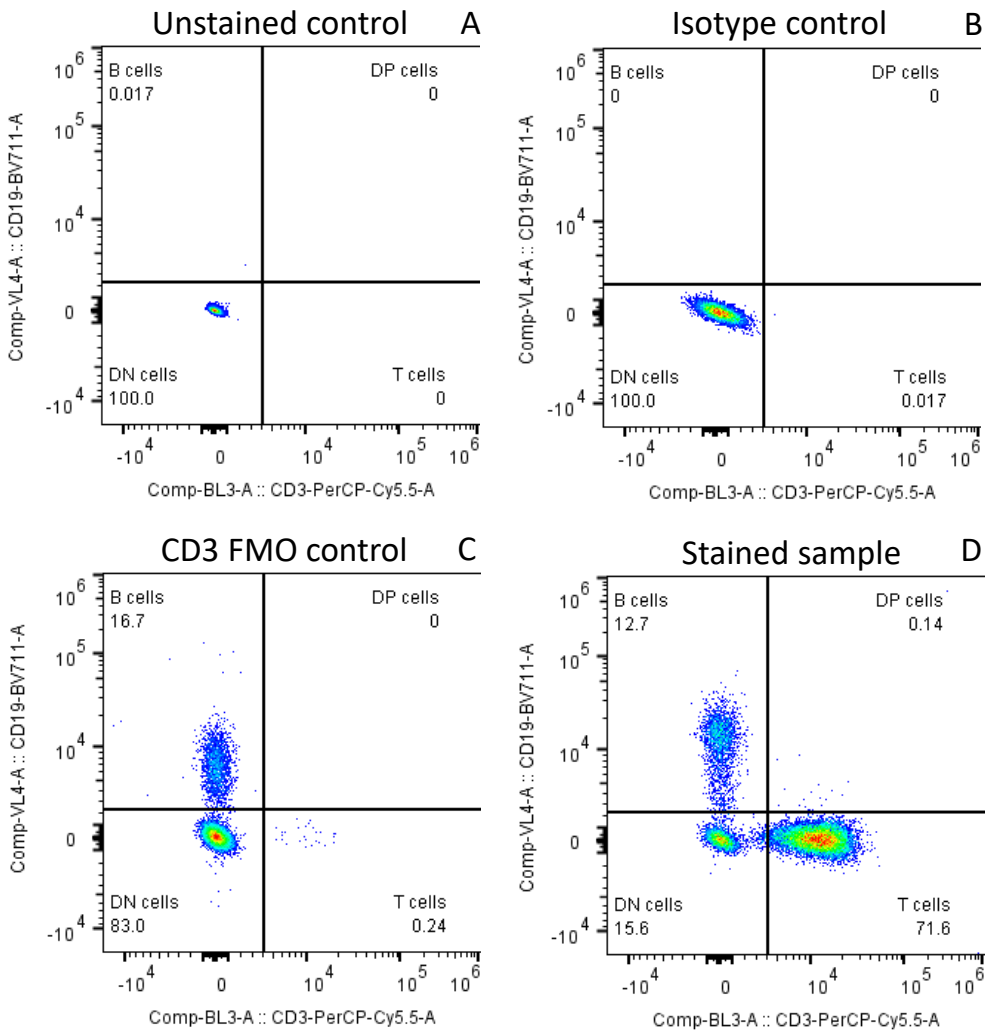

Figure 4.11 Example of A) unstained control, B) isotype control and C) FMO control used for setting up the gates for the D) stained sample.

Culture of healthy PBMCs (Table 4.8) or Crohn's disease PBMCs (Table 4.9) with B-GOS® batch C for 20 – 24 h did not affect the frequencies (or recovery) of any cell subsets compared to unstimulated control.

Table 4.8 Frequencies of PBMC subsets from healthy donors following 20 – 24 h culture with B-GOS® batch C. Percentages of cells were quantified by flow cytometry. Cell viability was coded as a covariate.

Healthy PBMCs	**NC**	**GOS C 0.8 mg/mL**	**GOS C 4 mg/mL**	**GOS C 12 mg/mL**	**One-way ANCOVA *p* value**
	Mean ± SD (*n*= 14)	Mean ± SD (*n*= 14)	Mean ± SD (*n*= 14)	Mean ± SD (*n*= 14)	
Lymphocytes (% of live PBMCs)	86.8 ± 5.8	87.5 ± 5.9	87.4 ± 6.3	86.6 ± 6.3	0.963
Monocytes (% of live PBMCs)	7.4 ± 4.3	6.8 ± 4.5	7.0 ± 4.8	8.1 ± 4.7	0.686
B cells (% of lymphocytes)*	10.2 ± 3.6	10.0 ± 3.8	10.4 ± 3.9	10.2 ± 3.6	0.992
NK cells (% of lymphocytes)*	2.6 ± 2.0	2.6 ± 2.0	2.5 ± 2.0	2.0 ± 1.5	0.956
NKT cells (% of lymphocytes)*	0.4 ± 0.4	0.3 ± 0.3	0.3 ± 0.2	0.3 ± 0.2	0.737
T cells (% of lymphocytes)	80.2 ± 4.3	80.5 ± 4.5	80.5 ± 4.2	80.7 ± 3.9	0.979
T helper cells (% of T cells)**	74.8 ± 8.3	74.5 ± 8.3	75.3 ± 8.2	74.9 ± 7.6	0.993
Cytotoxic T cells (% of T cells)	21.5 ± 7.1	21.2 ± 7.4	20.7 ± 7.1	21.4 ± 6.7	0.995

**n*= 9 for all stimulation conditions; ***n*= 10 for all stimulation conditions.

Table 4.9 Frequencies of PBMC subsets from Crohn's disease donors following 20 – 24 h culture with B-GOS® batch C. Percentages of cells were quantified by flow cytometry. Cell viability was coded as a covariate.

Crohn's disease PBMCs	**NC**	**GOS C 0.8 mg/mL**	**GOS C 4 mg/mL**	**GOS C 12 mg/mL**	**One-way ANCOVA *p* value**
	Mean ± SD (*n*= 8)	Mean ± SD (*n*= 6)	Mean ± SD (*n*= 6)	Mean ± SD (*n*= 8)	
Lymphocytes (% of live PBMCs)	88.1 ± 9.6	85.4 ± 14.6	85.3 ± 14.9	86.8 ± 10.9	0.068
Monocytes (% of live PBMCs)	4.0 ± 5.1	10.6 ± 12.3	11.0 ± 12.8	3.1 ± 3.9	0.065
B cells (% of lymphocytes)*	4.1 ± 3.1	4.1 ± 2.9	3.9 ± 2.7	3.4 ± 2.4	0.972
NK cells (% of lymphocytes)*	4.6 ± 2.6	4.4 ± 2.3	4.3 ± 2.2	4.0 ± 1.8	0.989
NKT cells (% of lymphocytes)*	2.8 ± 1.9	2.6 ± 1.6	2.5 ± 1.7	2.3 ± 1.5	0.593
T cells (% of lymphocytes)	81.5 ± 8.2	81.9 ± 8.3	81.8 ± 9.4	80.4 ± 9.2	0.084
T helper cells (% of T cells)	62.8 ± 12.9	65.1 ± 12.4	65.7 ± 13.4	63.6 ± 13.4	0.968
Cytotoxic T cells (% of T cells)	26.8 ± 11.1	25.9 ± 12.1	26.2 ± 13.0	26.6 ± 11.0	0.998

**n*= 6 for all stimulation conditions.

4.4.4 Effects of B-GOS® batch C upon healthy and Crohn's disease PBMC activation markers

Multi-colour flow cytometry was used to assess the effects of 20 – 24 h culture with B-GOS® batch C on healthy PBMC and Crohn's disease PBMC activation markers (CD69 and CD25). An example of gating strategy applied to identify CD69-expressing lymphocytes from Crohn's disease PBMCs is reported in Figure 4.12. Back-gating was performed to ensure correct gate position (Figure 4.13).

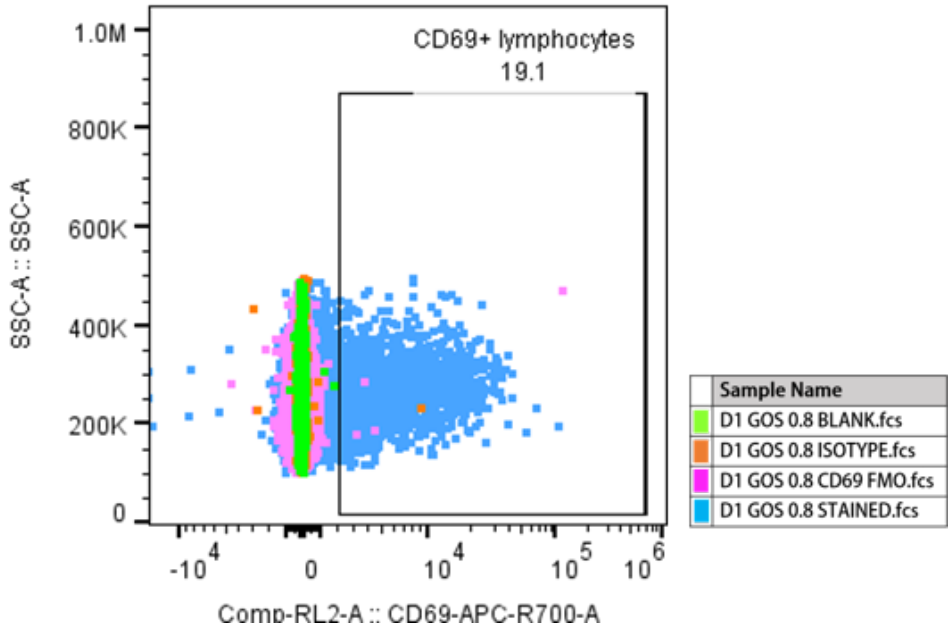

Figure 4.12 Example of gating strategy used to identify $CD69^+$ lymphocytes using unstained control (blank), isotype control and CD69 FMO control.Data are from one single Crohn's disease donor stimulated for 24 h with B-GOS® batch C (0.8 mg/mL).

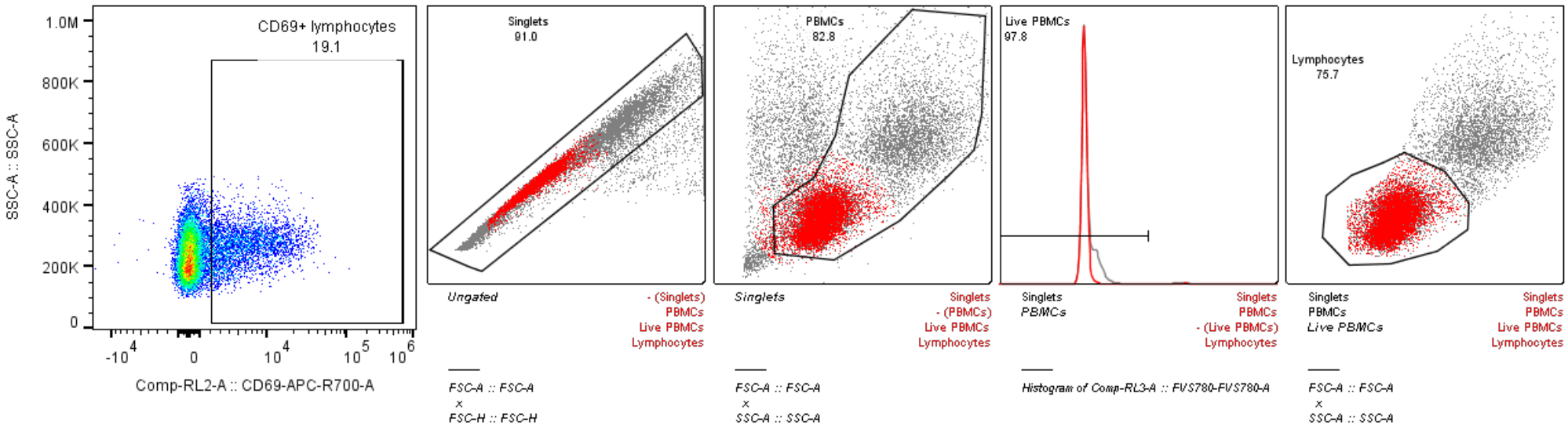

Figure 4.13 Example of back-gating applied to confirm the gating strategy of CD69-expressing lymphocytes.CD69-expressing lymphocytes were identified as $CD69^{+}$ cells gated from lymphocytes/live PBMCs/PBMCs excluded debris/singlets. Data are from one single Crohn's disease donor stimulated for 24 h with B-GOS® batch C (0.8 mg/mL).

Incubation for 20 – 24 h with B-GOS® batch C did not affect the percentages of healthy PBMC subsets expressing CD69 nor did it change their CD69 expression levels (Table 4.10 and Table 4.11). Similarly, there were no differences in the frequencies of CD25-expressing PBMC subsets from healthy donors nor in their expression levels of CD25 (Table 4.12 and Table 4.13).

Higher percentages of CD69-expressing lymphocytes (p= 0.011), T cells (p= 0.022) and T helper cells (p= 0.003) were observed after incubation of Crohn's disease PBMCs with the highest concentration of B-GOS® batch C compared to unstimulated control (Table 4.14). These three cell subsets also presented increased CD69 (MFI) expression on their surface after stimulation with B-GOS® batch C (Table 4.15). These results may indicate that B-GOS® exert direct immunostimulatory properties on Crohn's disease PBMCs at the highest concentration used.

Table 4.10 Frequencies of CD69-expressing PBMC subsets from healthy donors following 20 – 24 h culture with B-GOS® batch C.Percentages of $CD69^+$ cells were quantified by flow cytometry. Cell viability was coded as a covariate.

CD69 expression healthy PBMCs (%)	**NC**	**GOS C 0.8 mg/mL**	**GOS C 4 mg/mL**	**GOS C 12 mg/mL**	**One-way ANCOVA *p* value**
	Mean ± SD (n= 12)	Mean ± SD (n= 12)	Mean ± SD (n= 12)	Mean ± SD (n= 12)	
$CD69^+$ lymphocytes (% of lymphocytes)	9.3 ± 8.1	9.7 ± 8.3	9.8 ± 8.9	11.4 ± 10.5	0.925
$CD69^+$ T cells (% of T cells)	4.9 ± 3.8	5.1 ± 4.0	5.2 ± 4.3	6.2 ± 5.6	0.853
$CD69^+$ T helper cells (% of T helper cells)	12.7 ± 21.4	13.5 ± 22.3	13.9 ± 22.7	13.9 ± 21.1	0.993
$CD69^+$ cytotoxic T cells (% of cytotoxic T cells)	7.6 ± 5.6	7.8 ± 6.0	7.8 ± 6.3	8.1 ± 7.3	0.979
$CD69^+$ B cells (% of B cells)*	50.7 ± 11.1	51.7 ± 12.6	57.4 ± 12.0	72.0 ± 9.1	0.149
$CD69^+$ monocytes (% of monocytes)*	13.9 ± 8.5	13.5 ± 10.8	14.7 ± 11.7	12.0 ± 4.2	0.859

*n= 5 for all stimulation conditions;

Table 4.11 Median fluorescence intensity (MFI) of CD69 on PBMC subsets from healthy donors following 20 – 24 h culture with B-GOS® batch C.CD69 (MFI) expression was quantified by flow cytometry. Cell viability was coded as a covariate.

CD69 expression healthy PBMCs (MFIs)	**NC**	**GOS C 0.8 mg/mL**	**GOS C 4 mg/mL**	**GOS C 12 mg/mL**	**One-way ANCOVA *p* value**
	Mean ± SD (*n*= 12)	Mean ± SD (*n*= 12)	Mean ± SD (*n*= 12)	Mean ± SD (*n*= 12)	
CD69 on lymphocytes	11,568 ± 4,983	11,577 ± 4,945	11,382 ± 4,790	11,105 ± 4,547	0.982
CD69 on T cells	11,779 ± 5,243	11,726 ± 5,113	11,535 ± 5,012	11,069 ± 4,791	0.966
CD69 on T helper cells	11,587 ± 4,205	11,717 ± 4,391	11,471 ± 4,246	11,033 ± 4,094	0.963
CD69 on cytotoxic T cells	12,165 ± 5,323	12,211 ± 5,195	12,098 ± 5,097	11,634 ± 4,940	0.979
CD69 on B cells*	4,535 ± 348	4,495 ± 444	4,682 ± 444	5,069 ± 496	0.425
CD69 on monocytes*	4,293 ± 634	4,163 ± 463	4,275 ± 279	4,290 ± 399	0.883

**n*= 5 for all stimulation conditions;

Table 4.12 Frequencies of CD25-expressing PBMC subsets from healthy donors following 20 – 24 h culture with B-GOS® batch C.Percentages of $CD25^+$ cells were quantified by flow cytometry. Cell viability was coded as a covariate.

CD25 expression healthy PBMCs (%)	**NC**	**GOS C 0.8 mg/mL**	**GOS C 4 mg/mL**	**GOS C 12 mg/mL**	**One-way ANCOVA *p* value**
	Mean ± SD (*n*= 5)	Mean ± SD (*n*= 5)	Mean ± SD (*n*= 5)	Mean ± SD (*n*= 5)	
$CD25^+$ lymphocytes (% of lymphocytes)	1.9 ± 0.8	1.6 ± 0.6	1.6 ± 0.8	1.4 ± 0.7	0.145
$CD25^+$ T cells (% of T cells)	1.4 ± 0.6	1.3 ± 0.4	1.2 ± 0.6	1.1 ± 0.6	0.414
$CD25^+$ T helper cells (% of T helper cells)	1.3 ± 0.9	0.9 ± 0.5	1.1 ± 0.5	0.7 ± 0.6	0.810
$CD25^+$ cytotoxic T cells (% of cytotoxic T cells)	0.9 ± 0.7	0.8 ± 0.6	0.9 ± 0.7	0.8 ± 0.6	0.837
$CD25^+$ B cells (% of B cells)	5.1 ± 2.2	3.7 ± 1.0	3.3 ± 1.3	2.9 ± 1.2	0.117
$CD25^+$ monocytes (% of monocytes)	3.0 ± 1.9	2.4 ± 0.9	2.8 ± 1.2	2.4 ± 1.2	0.312

Table 4.13 Median fluorescence intensity (MFI) of CD25 on PBMC subsets from healthy donors following 20 – 24 h culture with B-GOS® batch C. CD25 (MFI) expression was quantified by flow cytometry. Cell viability was coded as a covariate.

CD25 expression healthy PBMCs (MFIs)	**NC**	**GOS C 0.8 mg/mL**	**GOS C 4 mg/mL**	**GOS C 12 mg/mL**	**One-way ANCOVA *p* value**
	Mean ± SD (*n*= 5)	Mean ± SD (*n*= 5)	Mean ± SD (*n*= 5)	Mean ± SD (*n*= 5)	
CD25 on lymphocytes	16,902 ± 1,147	16,754 ± 956	16,950 ± 1,443	17,425 ± 1,220	0.964
CD25 on T cells	15,982 ± 1,548	16,290 ± 962	16,104 ± 874	15,798 ± 1,364	0.951
CD25 on B cells	15,701 ± 523	15,845 ± 1,576	16,177 ± 1,410	16,572 ± 1,763	0.551

Table 4.14 Frequencies of CD69-expressing PBMC subsets from Crohn's disease donors following 20 – 24 h culture with B-GOS® batch C. Percentages of $CD69^+$ cells were quantified by flow cytometry. Cell viability was coded as a covariate.

CD69 expression Crohn's disease PBMCs (%)	**NC**	**GOS C 0.8 mg/mL**	**GOS C 4 mg/mL**	**GOS C 12 mg/mL**	**One-way ANCOVA *p* value**
	Mean ± SD (*n*= 6)	Mean ± SD (*n*= 6)	Mean ± SD (*n*= 6)	Mean ± SD (*n*= 6)	
$CD69^+$ lymphocytes (% of lymphocytes)	19.6 ± 4.3	20.1 ± 3.7	22.3 ± 4.5	35.8 ± 11.0	**0.005**
$CD69^+$ T cells (% of T cells)	16.3 ± 5.0	16.9 ± 4.3	19.1 ± 5.7	34.3 ± 12.8	**0.009**
$CD69^+$ T helper cells (% of T helper cells)	15.0 ± 5.3	15.6 ± 5.0	18.5 ± 6.3	37.4 ± 13.7	**0.001**
$CD69^+$ cytotoxic T cells (% of cytotoxic T cells)	20.6 ± 5.7	21.0 ± 5.9	22.8 ± 6.7	33.0 ± 13.9	0.069
$CD69^+$ B cells (% of B cells)	37.1 ± 4.5	38.4 ± 4.8	41.7 ± 4.5	45.2 ± 5.4	0.112
$CD69^+$ NK cells (% of NK cells)	30.2 ± 8.4	31.8 ± 7.9	31.8 ± 9.7	32.2 ± 7.9	0.499
$CD69^+$ NKT cells (% of NKT cells)	35.0 ± 19.1	35.5 ± 20.0	33.3 ± 18.6	39.3 ± 21.5	0.386
$CD69^+$ monocytes (% of monocytes)	13.3 ± 6.6	15.1 ± 7.5	11.8 ± 6.3	18.3 ± 10.8	0.666

$CD69^+$ lymphocytes – GOS 12 significantly different from NC, GOS 0.8 and GOS 4 (Bonferroni's *post-hoc* test, *p*= 0.011, *p*= 0.010 and *p*= 0.027, respectively)

$CD69^+$ T cells – GOS 12 significantly different from NC, GOS 0.8 and GOS 4 (Bonferroni's *post-hoc* test, *p*= 0.022, *p*= 0.017 and *p*= 0.039, respectively)

$CD69^+$ T helper cells – GOS 12 significantly different from NC, GOS 0.8 and GOS 4 (Bonferroni's *post-hoc* test, *p*= 0.003, *p*= 0.002 and *p*= 0.006, respectively)

Table 4.15 Median fluorescence intensity (MFI) of CD69 on PBMC subsets from Crohn's disease donors following 20 – 24 h culture with B-GOS® batch C. CD69 (MFI) expression was quantified by flow cytometry. One-way ANCOVA followed by Bonferroni's *post-hoc* test was performed. Cell viability was coded as a covariate.

CD69 expression Crohn's disease PBMCs (MFIs)	**NC**	**GOS C 0.8 mg/mL**	**GOS C 4 mg/mL**	**GOS C 12 mg/mL**	**One-way ANCOVA *p* value**
	Mean ± SD (*n*= 6)	Mean ± SD (*n*= 6)	Mean ± SD (*n*= 6)	Mean ± SD (*n*= 6)	
CD69 on lymphocytes	4,830 ± 647	4,867 ± 745	4,941 ± 718	5,366 ± 446	**0.002**
CD69 on T cells	4,625 ± 614	4,689 ± 713	4,757 ± 645	5,459 ± 457	**0.001**
CD69 on T helper cells	4,076 ± 276	4,158 ± 308	4,293 ± 189	5,398 ± 414	**< 0.0001**
CD69 on cytotoxic T cells	4,982 ± 1,301	4,996 ± 1,479	5,045 ± 1,480	5,103 ± 945	0.156
CD69 on B cells	7,017 ± 807	7,242 ± 1,144	7,197 ± 743	6,025 ± 431	0.384
CD69 on monocytes	3,253 ± 350	3,261 ± 488	3,366 ± 435	3,130 ± 407	0.226

MFI of CD69 on lymphocytes – GOS 12 significantly different from NC, GOS 0.8 and GOS 4 (Bonferroni's *post-hoc* test, p= 0.002, p= 0.007 and p= 0.025, respectively)

MFI of CD69 on T cells – GOS 12 significantly different from NC, GOS 0.8 and GOS 4 (Bonferroni's *post-hoc* test, p= 0.001, p= 0.003 and p= 0.007, respectively)

MFI of CD69 on T helper cells – GOS 12 significantly different from NC, GOS 0.8 and GOS 4 (Bonferroni's *post-hoc* test, all p< 0.0001)

4.4.5 Effects of B-GOS® batch C upon secreted and intracellular cytokines from healthy and Crohn's disease PBMCs

Healthy PBMCs incubated for 20 – 24 h with B-GOS® batch C secreted higher amounts of IL-6 (p= 0.011) and IL-8 (p< 0.0001) at the highest concentration of prebiotic used compared to unstimulated control. No changes were observed in any of the other cytokines and chemokines measured (Table 4.16). Increased levels of secreted IL-8 (p= 0.003) and TNF-α (p= 0.026) were observed in Crohn's disease PBMCs after stimulation with the highest dose of B-GOS® batch C, while lower amounts of IL-12p70 (p= 0.033) were seen at lower doses of B-GOS® batch C (Table 4.17).

Since both healthy and Crohn's disease PBMCs presented higher IL-8 secretion following culture with B-GOS® batch C, the groups were compared both in unstimulated and stimulated conditions to understand whether the disease status might affect IL-8 secretion. While, overall, the differences between the secretion levels of IL-8 from healthy PBMCs and Crohn's disease PBMCs were not significant when also considering the control, healthy PBMCs secreted nearly twice the amount of IL-8 in response to B-GOS® stimulation (Figure 4.14).

Table 4.16 Levels of mediators secreted by healthy PBMCs following culture with B-GOS® batch C for 20 – 24 h. Secreted mediators were quantified by Luminex assay. One-way ANCOVA followed by Bonferroni's *post-hoc* test was performed. Cell viability was coded as a covariate.

Healthy PBMCs **Secreted cytokines (pg/10^6 cells)**	**NC**	**GOS C 0.8 mg/mL**	**GOS C 4 mg/mL**	**GOS C 12 mg/mL**	**One-way ANCOVA *p* value**
	Mean ± SD (*n*= 12)	Mean ± SD (*n*= 12)	Mean ± SD (*n*= 12)	Mean ± SD (*n*= 12)	
IL-1α	0.7 ± 1.0	0.2 ± 0.1	0.2 ± 0.1	0.2 ± 0.1	0.110
IL-1β	1.4 ± 1.2	0.8 ± 0.5	0.9 ± 0.3	0.9 ± 0.5	0.139
IL-6*	1.5 ± 1.7	1.1 ± 1.1	10.8 ± 13.5	14.5 ± 14.5[#]	**0.011**
IL-8[†]	0.9 ± 1.2	0.9 ± 1.1	1.3 ± 1.6	14.5 ± 14.9[#]	**<0.0001**
IL-10	1.2 ± 0.6	1.1 ± 0.5	1.0 ± 0.5	1.0 ± 0.6	0.528
IL-12p70**	6.9 ± 4.7	8.8 ± 4.9	3.3 ± 3.4	6.4 ± 6.7	0.269
IL-17A	0.7 ± 0.6	1.1 ± 1.2	0.6 ± 0.6	0.3 ± 0.4	0.080
IFN-γ	3.0 ± 3.2	3.4 ± 3.1	3.9 ± 4.0	1.4 ± 1.2	0.186
TNF-α	2.1 ± 1.5	2.0 ± 1.9	1.5 ± 0.9	2.6 ± 1.9	0.298
Granzyme B	42.5 ± 27.3	56.9 ± 43.1	49.1 ± 45.2	66.0 ± 52.7	0.436
IL-1ra[†]	0.6 ± 0.4	0.4 ± 0.2	0.4 ± 0.2	0.5 ± 0.2	0.444
MIP-1α	61.6 ± 60.8	58.8 ± 60.4	63.9 ± 65.5	115.2 ± 106.5	0.100
MIP-1β***	9.2 ± 0.0	9.2 ± 0.0	9.2 ± 0.0	9.2 ± 0.0	N/A
IL-5***	0.1 ± 0.1	0.1 ± 0.0	0.1 ± 0.0	0.1 ± 0.0	N/A
MCP-1***	118.7 ± 136.3	9.3 ± 11.1	16.3 ± 24.7	38.1 ± 39.3	0.094
FGF basic***	2.8 ± 0.4	2.9 ± 0.6	3.3 ± 0.1	2.8 ± 0.3	0.182
G-CSF***	1.1 ± 2.0	< DL	0.7 ± 0.9	0.7 ± 1.1	0.505
GM-CSF***	1.3 ± 0.5	1.4 ± 0.9	1.0 ± 0.5	1.6 ± 0.7	0.579
IL-2***	1.5 ± 1.6	0.5 ± 0.9	1.8 ± 2.3	0.1 ± 0.1	0.368
IL-4***	3.2 ± 3.5	2.9 ± 3.2	5.0 ± 4.8	2.5 ± 2.9	0.468
VEGF***	5.8 ± 3.7	5.4 ± 5.2	3.3 ± 3.1	5.3 ± 3.1	0.701

**n*= 10 for all stimulation conditions; ***n*= 8 for all stimulation conditions; ****n*= 6 for all stimulation conditions; [†]ng/10^6 cells; < DL= below detection limit of the method; [#]significantly different from NC.

IL-6 – GOS 12 significantly different from NC and GOS 0.8 (Bonferroni's *post-hoc* test, *p*= 0.041 and *p*= 0.040, respectively)

IL-8 – GOS 12 significantly different from NC, GOS 0.8 and GOS 4 (Bonferroni's *post-hoc* test, all *p*< 0.0001)

Table 4.17 Levels of mediators secreted by Crohn's disease PBMCs following culture with B-GOS® batch C for 20 – 24 h. Secreted mediators were quantified by Luminex assay. One-way ANCOVA followed by Bonferroni's *post-hoc* test was performed. Cell viability was coded as a covariate.

Crohn's disease PBMCs Secreted cytokines (pg/10^6 cells)	**NC**	**GOS C 0.8 mg/mL**	**GOS C 4 mg/mL**	**GOS C 12 mg/mL**	**One-way ANCOVA *p* value**
	Mean ± SD (*n*= 12)	Mean ± SD (*n*= 6)	Mean ± SD (*n*= 6)	Mean ± SD (*n*= 12)	
IL-1α*	0.4 ± 0.0	N/A	N/A	0.5 ± 0.2	**0.040**
IL-1β	81.1 ± 29.7	60.9 ± 16.4	63.6 ± 21.8	90.3 ± 35.6	0.174
IL-6*	6.2 ± 0.0	13.3 ± 12.9	6.2 ± 0.0	6.2 ± 0.0	0.199
IL-8†	0.4 ± 0.4	1.4 ± 2.4	4.0 ± 4.3	7.0 ± 8.5#	**0.004**
IL-10	0.3 ± 0.4	0.4 ± 0.6	0.2 ± 0.2	0.2 ± 0.1	0.461
IL-12p70	4.9 ± 4.6	0.4 ± 0.0	0.4 ± 0.0	4.9 ± 4.6	**0.033**
IL-17A	0.1 ± 0.0	0.1 ± 0.0	0.1 ± 0.0	0.1 ± 0.0	N/A
IFN-γ	1.9 ± 1.7	0.4 ± 0.0	0.4 ± 0.0	2.0 ± 2.0	0.062
TNF-α	0.7 ± 0.6	0.8 ± 1.1	1.9 ± 2.0	2.5 ± 2.5#	**0.022**
Granzyme B*	102.0 ± 46.2	N/A	N/A	173.1 ± 211.2	0.724
IL-1ra*	337.5 ± 178.2	N/A	N/A	442.8 ± 278.2	0.803

**n*= 6 for all stimulation conditions; †ng/10^6 cells; #significantly different from NC.

IL-8 – GOS 12 significantly different from NC and GOS 0.8 (Bonferroni's *post-hoc* test, *p*= 0.003 and *p*= 0.035)

TNF-α – GOS 12 significantly different from NC (Bonferroni's *post-hoc* test, *p*= 0.026)

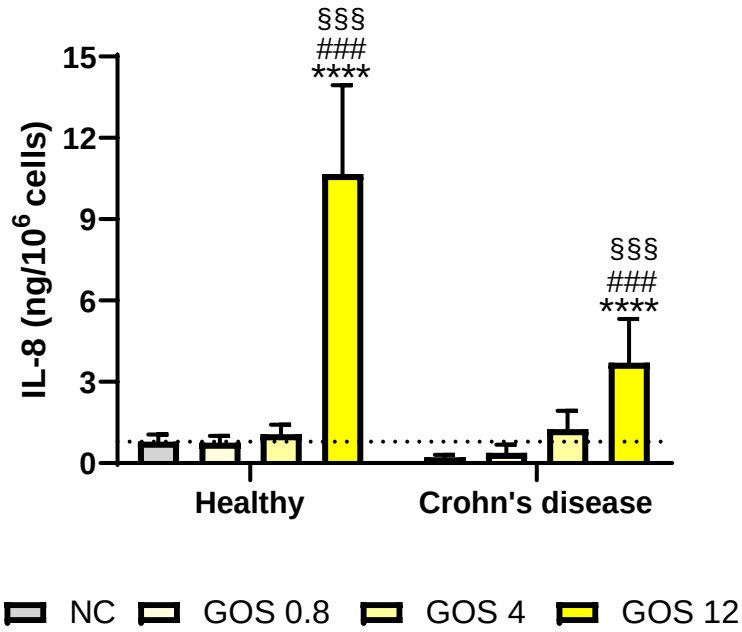

Figure 4.14 Comparison between the levels of IL-8 secreted by healthy PBMCs (*n*= 12) and Crohn's disease PBMCs (*n*= 6) after 20 – 24 h culture with different concentrations of B-GOS® batch C. Secreted IL-8 was quantified by Luminex assay. Two-way ANCOVA followed by Bonferroni's *post-hoc* test was performed. Cell viability was coded as a covariate. Significant differences between GOS 12 and NC, GOS 12 and GOS 0.8, GOS 12 and GOS 4 are marked with an asterisk (****p< 0.0001), hash ($^{###}p$< 0.001) or section ($^{§§§}p$< 0.001).

In order to understand which cell types were responsible for the higher IL-8 secretion observed after B-GOS® stimulation both in healthy PBMCs and in Crohn's disease PBMCs, intracellular cytokine staining was performed. Monocytes expressed the highest levels of intracellular IL-8 expression within PBMCs and were the main producers of IL-8. When healthy PBMCs were stimulated with the highest concentration of B-GOS® (12 mg/mL), there were significantly higher percentages of monocytes expressing IL-8 compared to unstimulated control (p= 0.010). Furthermore, the expression levels of IL-8 on monocytes from healthy donors was significantly upregulated as a result of B-GOS® stimulation (12 mg/mL *vs* control, p< 0.0001), as shown in Table 4.18.

Table 4.18 Intracellular IL-8 expression on monocytes from healthy PBMCs after 20 – 24 h culture with different concentrations of B-GOS® batch C. Intracellular IL-8 was quantified by flow cytometry. One-way ANCOVA followed by Bonferroni's *post-hoc* test was performed. Cell viability (values with brefeldin A) was coded as a covariate.

Healthy PBMCs Intracellular IL-8	**NC**	**GOS C 0.8 mg/mL**	**GOS C 4 mg/mL**	**GOS C 12 mg/mL**	**One-way ANCOVA *p* value**
	Mean ± SD (*n*= 6)	Mean ± SD (*n*= 6)	Mean ± SD (*n*= 6)	Mean ± SD (*n*= 6)	
IL-8$^+$ monocytes (% of monocytes)	68.2 ± 11.7	68.8 ± 14.1	70.2 ± 14.9	91.3 ± 2.4	**0.010**
MFI of IL-8 on monocytes	12,644 ± 1,472	11,757 ± 932	15,010 ± 3,955	36,301 ± 9,971	**<0.0001**

IL-8$^+$ monocytes – GOS 12 significantly different from NC, GOS 0.8 and GOS 4 (Bonferroni's *post-hoc* test, p= 0.019, p= 0.019 and p= 0.047)

MFI of IL-8 on monocytes – GOS 12 significantly different from NC, GOS 0.8 and GOS 4 (Bonferroni's *post-hoc* test, all p< 0.0001)

Unfortunately, due to the lower numbers of PBMCs available from Crohn's disease donors and the consequent lower recovery of monocytes, there were not sufficient events to quantify intracellular IL-8 expression on Crohn's disease monocytes. However, it was possible to compare the frequencies of IL-8-expressing healthy PBMCs and Crohn's disease PBMCs as well as their IL-8 expression levels (Figure 4.15) to have an insight into possible differences in cytokine responses between the two groups.

Overall, no significant differences were seen between the frequencies of IL-8-expressing PBMCs from healthy donors and Crohn's disease donors in unstimulated and stimulated conditions. Nevertheless, in line with what observed for secreted IL-8, the percentages of IL-8-expressing PBMCs from healthy donors after B-GOS® stimulation were nearly twice those of IL-8 expressing PBMCs from Crohn's disease donors (Figure 4.15). Interestingly, Crohn's disease PBMCs presented higher IL-8 expression (MFI) on their surface compared to healthy PBMCs (p< 0.0001), both in unstimulated conditions and in presence of B-GOS® (Figure 4.15).

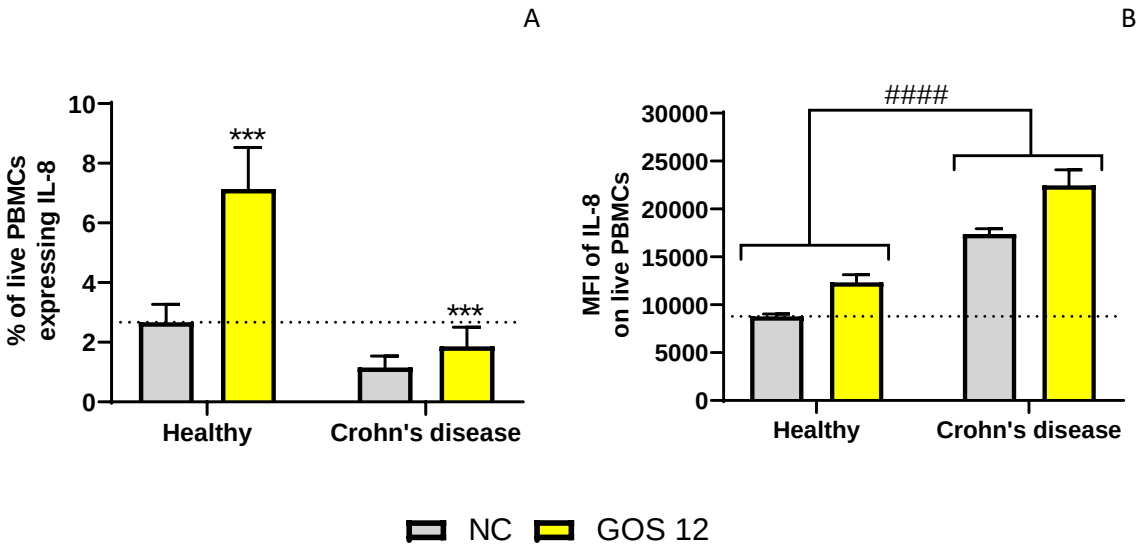

Figure 4.15 Comparison between the levels of intracellular IL-8 expression by healthy PBMCs and Crohn's disease PBMCs (both *n*= 6) after 20 – 24 h culture with the highest concentration of B-GOS® batch C. Intracellular IL-8 was quantified by flow cytometry. A) Percentages of live PBMCs expressing IL-8; B) MFI of IL-8 on live PBMCs. Two-way ANCOVA followed by Bonferroni's *post-hoc* test was performed. Cell viability (values with brefeldin A) was coded as a covariate. Significant differences between GOS 12 and NC or between healthy PBMCs and Crohn's disease PBMCs are marked with an asterisk (***p= 0.001) or with a hash ($^{\#\#\#\#}p$< 0.0001).

4.4.6 Investigation of the involvement of TLR4 in cytokine secretion following stimulation of PBMCs and THP-1 monocytic cell lines with B-GOS® batch C

Since incubation with the highest concentration of B-GOS® batch C (12 mg/mL) led to higher secretion of pro-inflammatory IL-6, IL-8 and TNF-α by PBMCs, and since other studies associated similar increases in soluble mediators with TLR4 activation [195, 241, 242, 324], experiments to determine the involvement of TLR4 in the release of IL-6, IL-8 and TNF-α were conducted.

Penta-acylated LPS from *Rhodobacter sphaeroides*, a TLR4 antagonist, was used to block the signalling via TLR4 by its binding to the myeloid differentiation factor 2 (MD-2) before stimulation of PBMCs or THP-1 cells with B-GOS®.

PBMCs from healthy donors (*n*= 5) or THP-1 cells (*n*= 3) were seeded at 2.5 X 10^6 cells/mL and pre-incubated with or without the antagonist (TLR4-A, LPS-RS Ultrapure, Invivogen) for 2 h. TLR4-A was used at a 100-fold excess (10 µg/mL) relative to positive control LPS (0.1 µg/mL) to achieve complete inhibition. After 2 h pre-incubation in presence or absence of the antagonist, cells were stimulated for 24 h with a wide range of B-GOS® batch C concentrations (0.1 mg/mL, 0.8 mg/mL, 4

mg/mL, 12 mg/mL and 18 mg/mL). LPS (0.1 µg/mL) was used as positive control indicating functional stimulation, whereas unstimulated cells were used as negative control. Cell viability and secreted mediators (IL-6, IL-8 and TNF-α) were measured by multi-colour flow cytometry and Luminex assay, respectively.

A quality check was performed to confirm the expression of CD14 on THP-1 cells. CD14 is required for optimal response to LPS, as it chaperones the formation of the LPS/MD-2/TLR4 compex allowing for intracellular signalling ultimately leading to cytokine production [325]. Approximately 95% unstimulated THP-1 cells expressed CD14 (Figure 4.16).

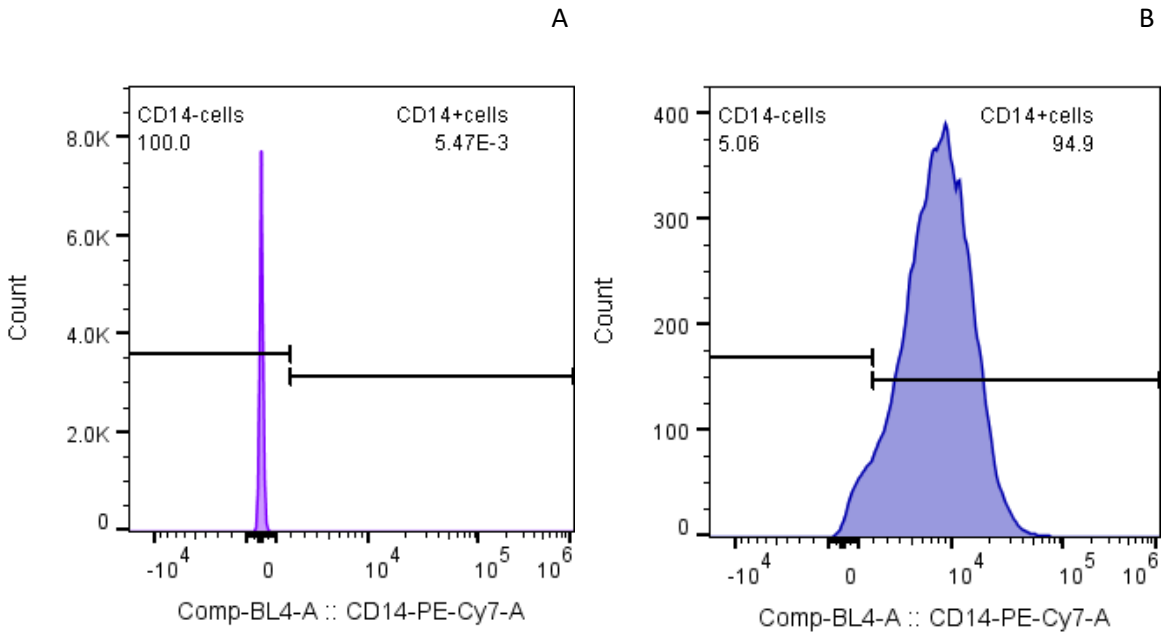

Figure 4.16 Expression of CD14 on the surface of unstimulated THP-1 cells measured by flow cytometry. $CD14^+$ cells were gated within the singlet population. A) Unstained control; B) CD14-PE-Cy®7-stained THP-1 cells.

Average THP-1 cell viability was always above 70% (Figure 4.17). THP-1 cells stimulated with LPS or with B-GOS® batch C 18 mg/mL in absence of TLR4-A had lower viability compared to unstimulated control (p< 0.0001 and p= 0.0003, respectively). LPS-stimulated THP-1 cells pre-incubated with TLR4-A presented higher viability than those not pre-incubated with the antagonist (p< 0.0001), while the opposite was observed for cells stimulated with B-GOS® batch C 0.1 mg/mL (p= 0.0416). These results may indicate that LPS and the highest dose of B-GOS® batch C are slightly cytotoxic to THP-1 cells, although cell viability was always above the acceptable limit for all conditions tested.

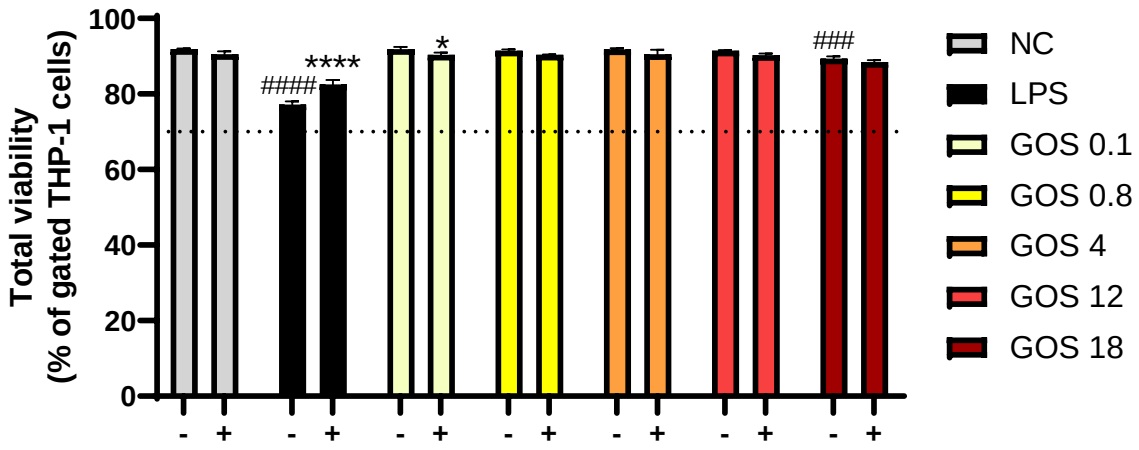

Figure 4.17 Viability of THP-1 monocytic cell line measured by flow cytometry. THP-1 cells (*n*= 3) were pre-incubated with or without TLR4-A for 2 h, then stimulated with B-GOS® batch C for 24 h. LPS (0.1 µg/mL) and unstimulated cells were used as positive and negative controls, respectively. Data are expressed as mean ± SD. Two-way ANOVA followed by Bonferroni's or Dunnett's *post-hoc* test was performed. Differences between conditions with or without TLR4-A (+/- in the graphs) are marked with *p< 0.05; ****p< 0.0001. Differences between cells stimulated with B-GOS® or LPS *vs* unstimulated control (NC) are marked with $^{\#\#\#}p$< 0.001; $^{\#\#\#\#}p$< 0.0001.

Stimulation of THP-1 cells with LPS resulted in increased secretion of IL-6, IL-8 and TNF-α compared to unstimulated control (all p< 0.0001) (Figure 4.18). Pre-treatment of LPS-stimulated THP-1 cells with the antagonist resulted in a significant reduction of all secreted mediators (IL-6, IL-8 and TNF-α, all p< 0.0001). Stimulation with B-GOS® batch C did not increase the secretion of any mediators by THP-1 cells, which were released at concentrations similar to those of unstimulated cells. Because the amount of secreted IL-6, IL-8 and TNF-α was very low in B-GOS® batch C-stimulated cells and unstimulated control, no further reduction was caused by pre-incubation with TLR4-A (Figure 4.18).

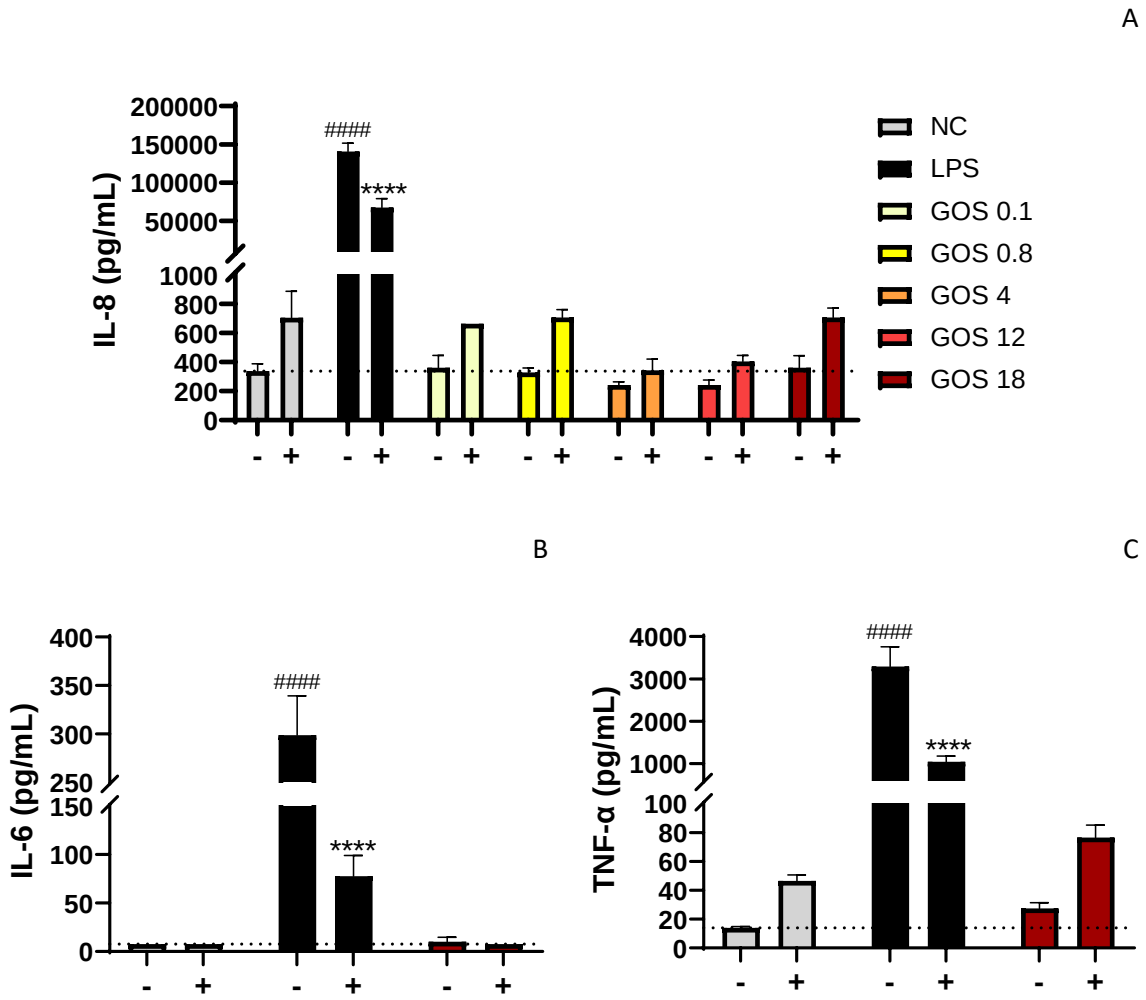

Figure 4.18 Levels of secreted mediators in stimulated THP-1 cells pre-incubated with or without TLR4-A. THP-1 cells (*n*= 3) were pre-incubated with or without TLR4-A for 2 h, then stimulated for 24 h with B-GOS® batch C. LPS (0.1 µg/mL) and unstimulated cells were used as positive and negative controls, respectively. Data are expressed as mean ± SD. Two-way ANOVA followed by Bonferroni's or Dunnett's *post-hoc* test was performed. Differences between conditions with or without TLR4-A (+/- in the graphs) are marked with ***p*< 0.01; *****p*< 0.0001. Differences between cells stimulated with B-GOS® or LPS *vs* unstimulated control (NC) are marked with $^{\#\#\#\#}p$< 0.0001.

PBMCs also presented average cell viability always above 70% (Figure 4.19). No differences were seen between B-GOS®- or LPS- stimulated cells and unstimulated control, meaning that PBMCs tolerated the stimuli and concentrations used. Pre-incubation with TLR4-A did not affect cell viability.

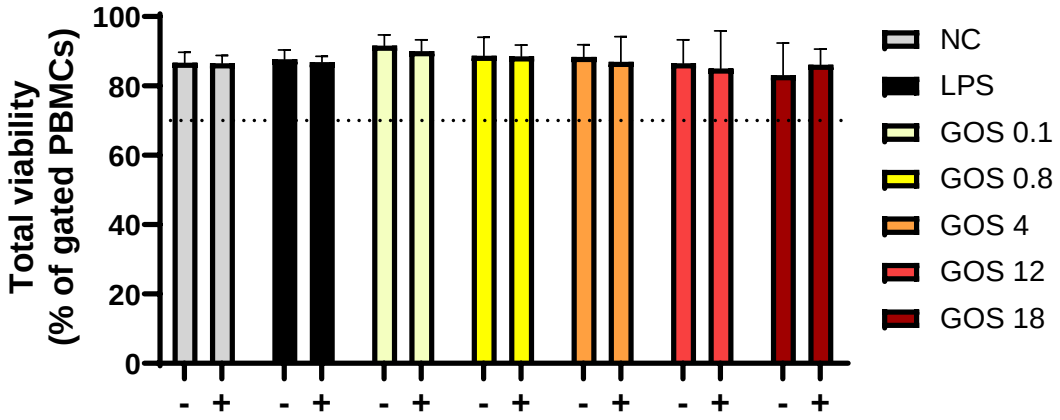

Figure 4.19 Viability of PBMCs measured by flow cytometry. Healthy PBMCs (*n*= 5) were pre-incubated with or without TLR4-A for 2 h, then stimulated for 24 h with B-GOS® batch C. LPS (0.1 µg/mL) and unstimulated cells were used as positive and negative controls, respectively. Data are expressed as mean ± SD.

Significantly higher IL-8 was secreted by LPS-stimulated PBMCs compared to unstimulated control (p= 0.0007) and by B-GOS®-stimulated PBMCs compared to unstimulated control (18 mg/mL, p= 0.0300). Pre-treatment of LPS-stimulated cells or of B-GOS®-stimulated cells with TLR4-A did not reduce the amount of secreted IL-8 (Figure 4.20).

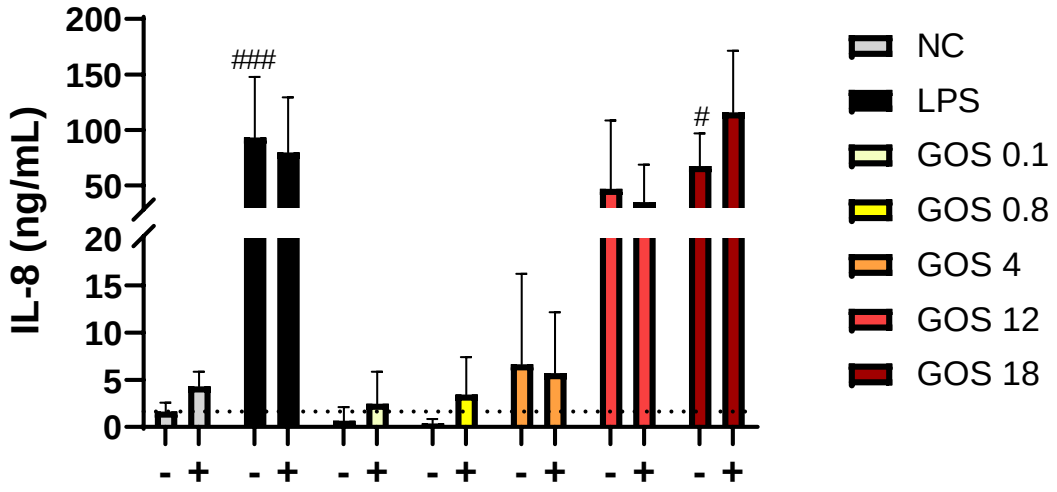

Figure 4.20 Levels of IL-8 in stimulated PBMCs pre-incubated with or without TLR4-A. Healthy PBMCs (n= 5) were pre-incubated with or without TLR4-A for 2 h, then stimulated for 24 h with B-GOS® batch C. LPS (0.1 µg/mL) and unstimulated cells were used as positive and negative controls, respectively. Data are expressed as mean ± SD. Two-way ANOVA followed by Bonferroni's or Dunnett's *post-hoc* test was performed. Differences between cells stimulated with B-GOS® or LPS *vs* unstimulated control (NC) are marked with $^{###}p$< 0.001.

4.4.7 Investigation on the role of galactose, lactose and glucose contained in B-GOS® batch C upon secreted IL-8 and CD69 expression

In order to clarify the mechanism of GOS action upon secreted cytokines and activation markers and to discern the effects of GOS from those of residual mono- and di- saccharides also present in B-GOS® batch C product, experiments using free sugars controls were performed. The effects of free sugars were assessed on secreted and intracellular IL-8, which was selected among the other soluble mediators because it was upregulated both in healthy PBMCs and in Crohn's disease PBMCs. The effects of free sugars on CD69 expression were evaluated only in Crohn's disease PBMCs, as B-GOS® batch C did not affect cell activation in healthy PBMCs. Concentrations of free sugars were chosen to correspond to the quantity of glucose, galactose and lactose contained in the highest dose tested of B-GOS® batch C (25.1 mg/mL), corresponding to 12 mg/mL pure GOS. Glucose (7.1 mg/mL), galactose (3.8 mg/mL) and lactose (1.9 mg/mL) were therefore assessed in

combination at their original concentration in the product. Glucose, galactose and lactose were also tested individually and at a reference concentration (1.9 mg/mL) to understand the effect of each sugar in isolation and to enable comparison between sugars at the same concentration. Details on the preparation of free sugar controls are described in Chapter 2. PBMCs (*n*= 8) from healthy and Crohn's disease donors were stimulated for 24 h with the free sugars mixture or with the highest concentration of B-GOS® batch C. The effects on secreted IL-8 were evaluated by Luminex assay, while the effects on intracellular IL-8 and on CD69 expression were assessed by flow cytometry.

As previously observed in section 4.4.5, stimulation of healthy PBMCs with the highest dose of B-GOS® batch C led to higher IL-8 secretion. Interestingly, these effects were mainly due to the free sugars (LAC+GAL+GLU *vs* NC, *p*= 0.0025) contained in the product rather than to GOS itself (GOS 12 *vs* NC, *p*= 0.0125) (Figure 4.21). While glucose and lactose contributed minimally to the effects on secreted IL-8 induced by the free sugars mixture, galactose had the strongest effect (GAL 3.8 *vs* NC, *p*< 0.0001). Indeed, when the free sugars were tested individually at the same dose (1.9 mg/mL), significantly higher IL-8 secretion was observed only after stimulation with galactose (Figure 4.21).

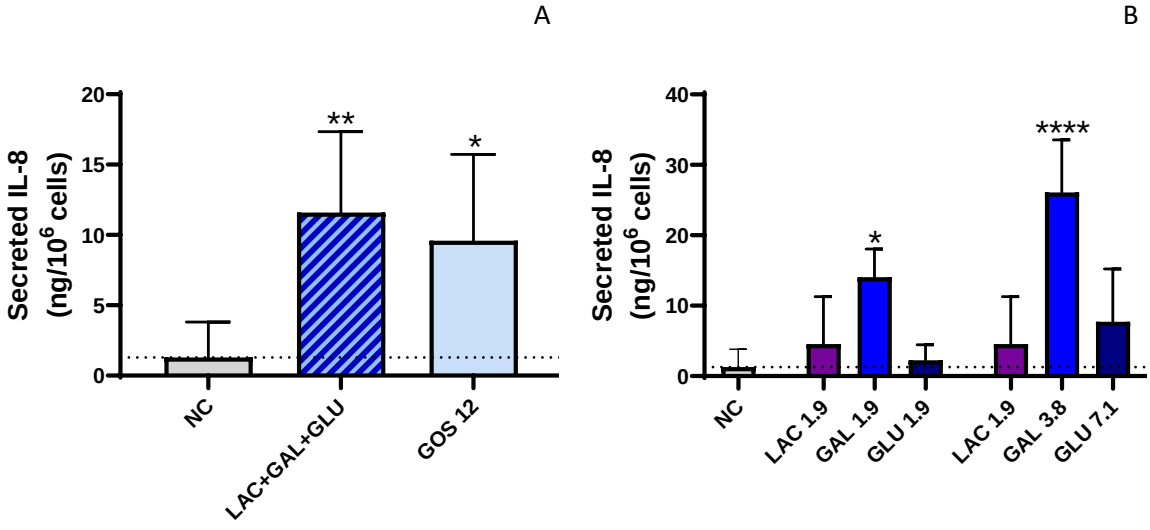

Figure 4.21 Levels of IL-8 secreted by healthy PBMCs (*n*= 8) following 24 h stimulation with B-GOS® batch C or with free sugars controls tested A) in combination or B) in isolation. Healthy PBMCs were stimulated for 24 h with B-GOS® batch C (12 mg/mL) or with glucose (7.1 mg/mL), galactose (3.8 mg/mL) and lactose (1.9 mg/mL) tested in combination or individually. Each sugar was also tested at a reference concentration of 1.9 mg/mL. Data are expressed as mean ± SD. One-way ANOVA followed by Dunnett's *post-hoc* test was performed. Differences between stimulated cells *vs* unstimulated control (NC) are marked with an asterisk (*p< 0.05; **p< 0.01; ****p< 0.0001).

An example of gating strategy used to identify IL-8-expressing monocytes from one single healthy PBMC donor stimulated with B-GOS® batch C at 12 mg/mL is reported. Back-gating was performed to ensure correct gate position (Figure 4.22 and Figure 4.23). Intracellular cytokine staining of IL-8 by flow cytometry supported the findings from data on secreted IL-8 measured by Luminex assay. Higher percentages of IL-8-expressing monocytes were observed following culture of healthy PBMCs with B-GOS® batch C compared to unstimulated control (GOS 12 *vs* NC, p= 0.0050). As reported for secreted IL-8, it was mainly the free sugars (LAC+GAL+GLU vs NC, p= 0.0004) contained in the product, rather than GOS, that caused an increase in the frequencies of IL-8-expressing monocytes. Similarly, the main contributors to the upregulation in IL-8 expression by monocytes were the free sugars contained in B-GOS® product (LAC+GAL+GLU *vs* NC, p< 0.0001) (Figure 4.24).

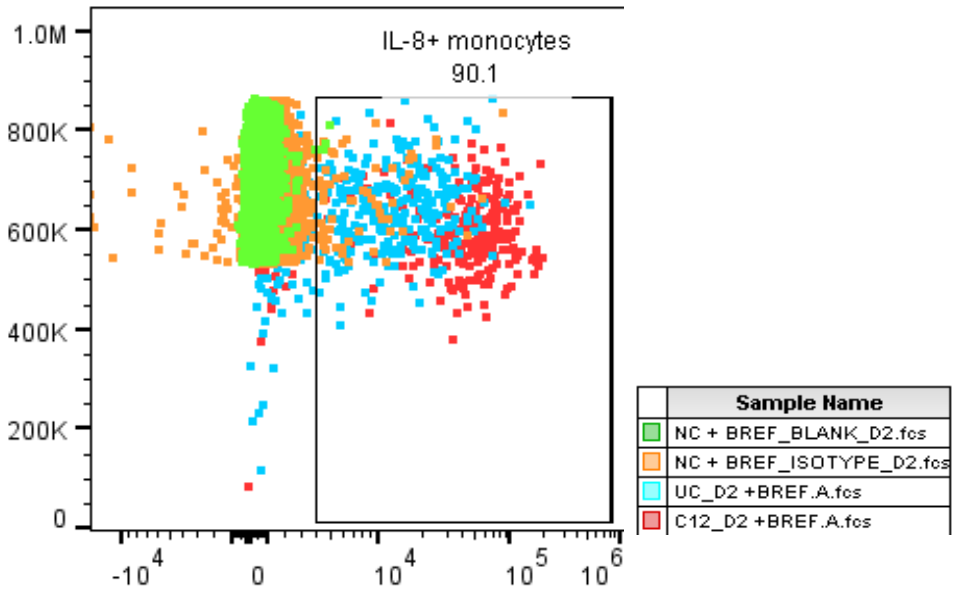

Figure 4.22 Example of gating strategy used to identify IL-8$^+$ monocytes from one single healthy PBMC donor stimulated with B-GOS® batch C at 12 mg/mL is reported.

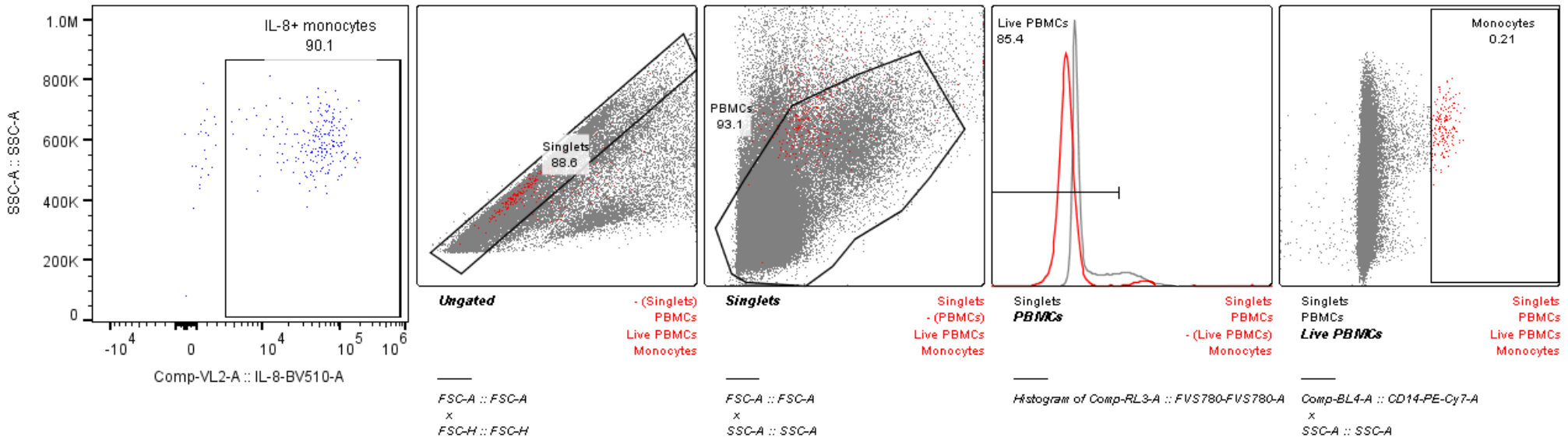

Figure 4.23 Example of back-gating applied to confirm the gating strategy of IL-8-expressing monocytes. IL-8-expressing monocytes were identified as IL-8^{+} cells gated from monocytes/live PBMCs/PBMCs excluded debris/singlets. Data are from one single healthy donor stimulated for 24 h with B-GOS® batch C (12 mg/mL).

A

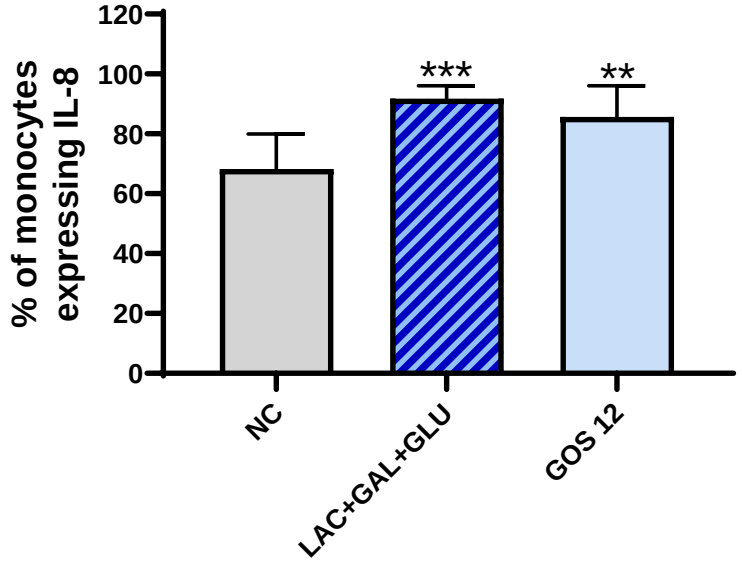

B

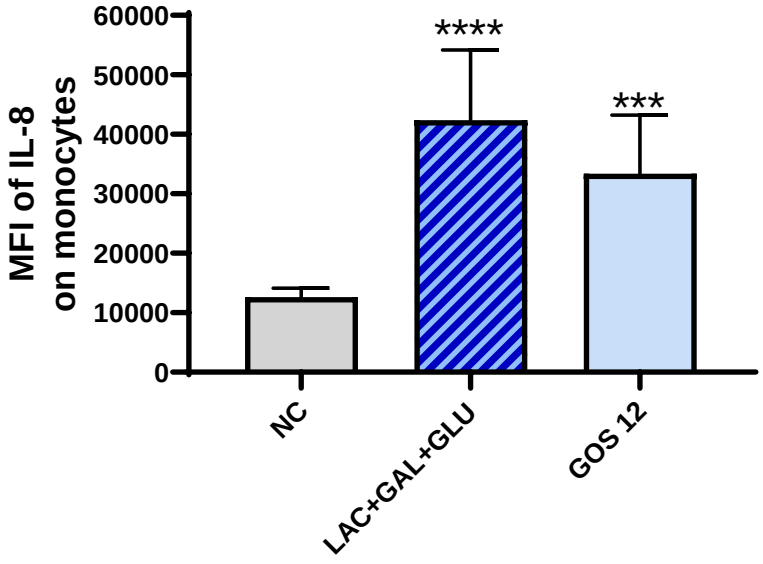

Figure 4.24 Levels of intracellular IL-8 expression by monocytes from healthy PBMCs (*n*= 8) after 24 h culture with B-GOS® batch C or with free sugars control. Intracellular IL-8 was quantified by flow cytometry. A) Percentages of monocytes expressing IL-8; B) MFI of IL-8 on monocytes. One-way ANOVA followed by Dunnett's *post-hoc* test was performed. Significant differences between GOS 12 and NC or between healthy PBMCs and CD PBMCs are marked with an asterisk (***p= 0.001) or with a hash ($^{\#\#\#\#}p$< 0.0001).

In line with what seen in healthy PBMCs, incubation of Crohn's disease PBMCs with the highest dose of B-GOS® batch C led to higher IL-8 secretion. The observed effects were mainly due to the free sugars (LAC+GAL+GLU *vs* NC, p= 0.0100; GOS 12 *vs* NC, p= 0.0100), as shown in Figure 4.25.

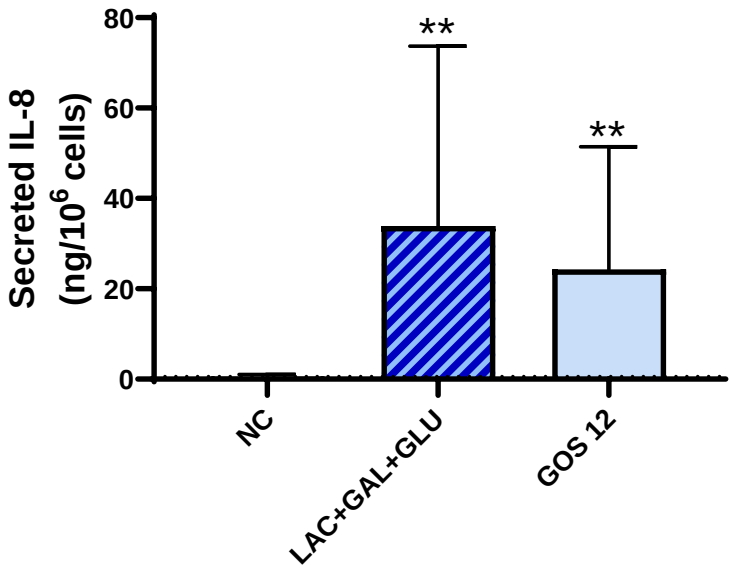

Figure 4.25 Levels of IL-8 secreted by Crohn's disease PBMCs (n= 8) following 24 h stimulation with B-GOS® batch C or with free sugars controls. Crohn's disease PBMCs were stimulated for 24 h with B-GOS® batch C (12 mg/mL) or with glucose (7.1 mg/mL), galactose (3.8 mg/mL) and lactose (1.9 mg/mL) tested in combination. Data are expressed as median ± IQR. Kruskal-Wallis test followed by Dunn's *post-hoc* test was performed. Differences between stimulated cells *vs* unstimulated control (NC) are marked with an asterisk (**p< 0.01).

Interestingly, the effects of B-GOS® batch C on CD69 expression were at least partially attributed to GOS rather than the to free sugars. Stimulation with B-GOS® batch C resulted in significantly higher frequencies of lymphocytes (p= 0.0044), T cells (p= 0.0064) and T helper cells (p= 0.0023) expressing CD69, while the free sugars alone had no effect (Figure 4.26). Similarly, higher CD69 (MFI) expression was observed on T cells (p= 0.0243) and T helper cells (p< 0.0001) after stimulation with B-GOS® batch C, while the free sugars had only minor stimulatory effects on T helper cells (p= 0.0066) (Figure 4.27).

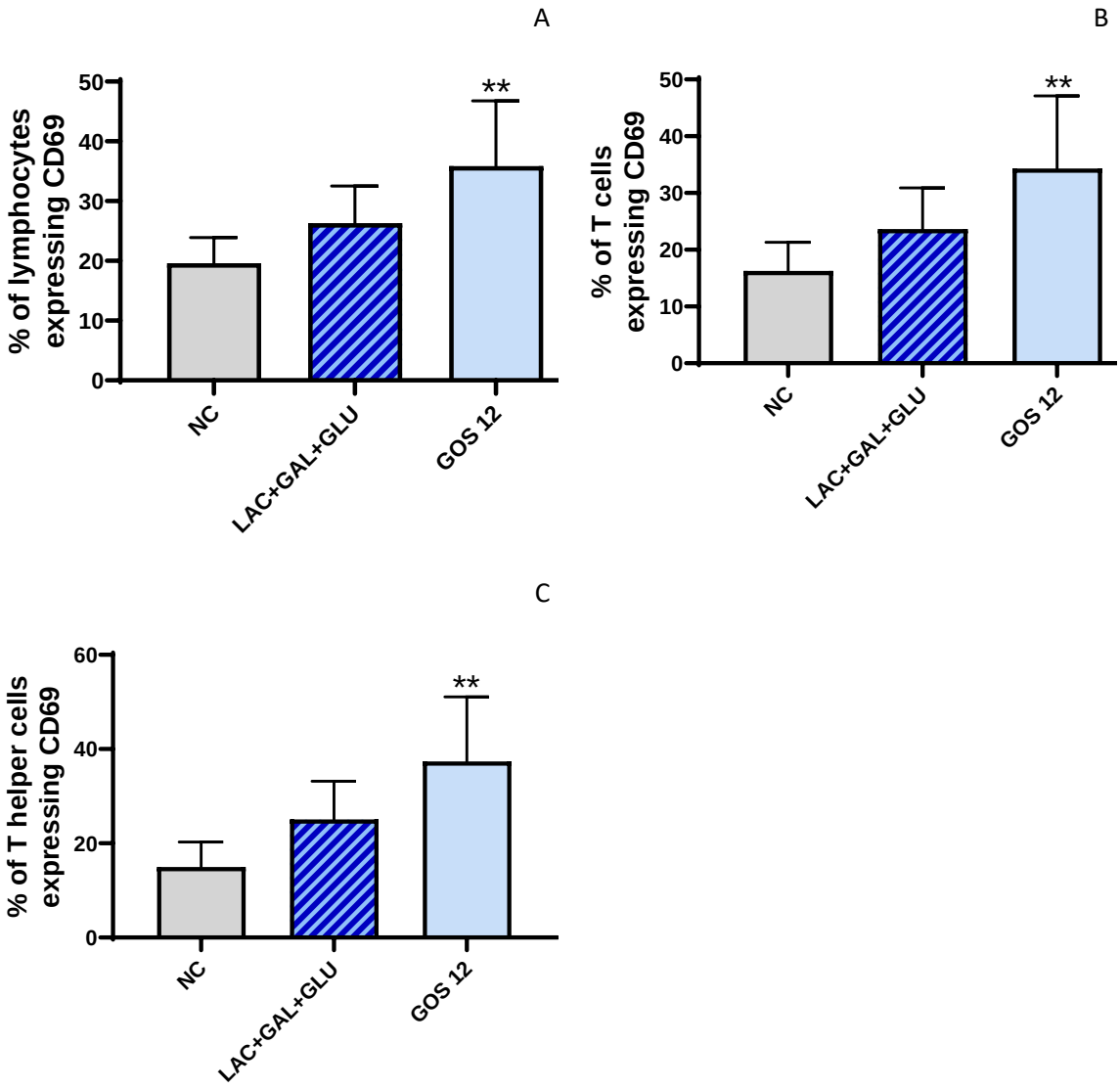

Figure 4.26 Percentages of CD69-expressing cells from Crohn's disease PBMCs (*n*= 8) after 24 h culture with B-GOS® batch C or with free sugars control. CD69 expression was quantified by flow cytometry. A) Percentages of lymphocytes expressing CD69; B) Percentages of T cells expressing CD69; C) Percentages of T helper cells expressing CD69. One-way ANOVA followed by Dunnett's *post-hoc* test was performed. Significant differences between stimulated cells and unstimulated control are marked with an asterisk (**p< 0.01).

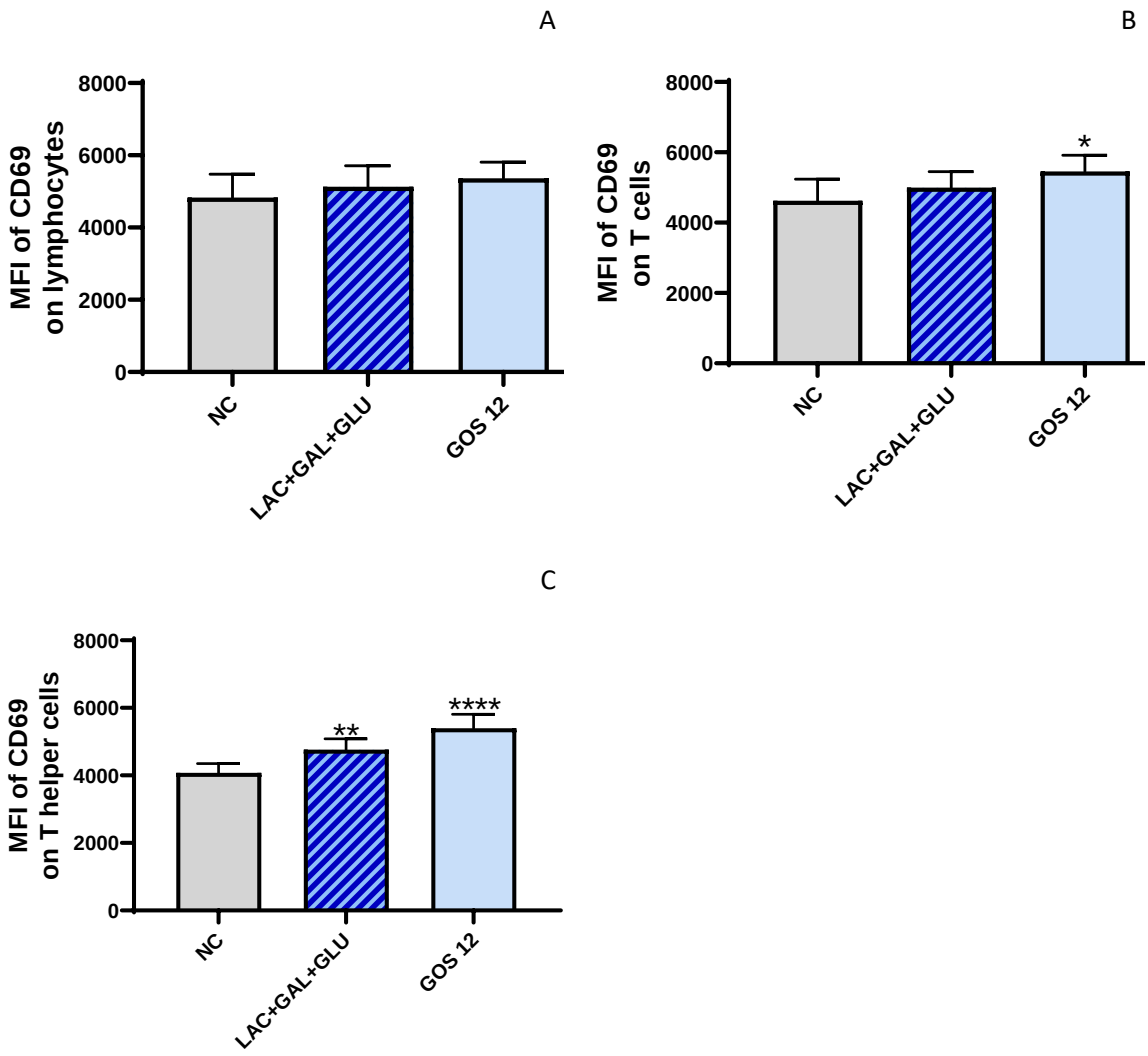

Figure 4.27 Levels of CD69 (MFI) expression by lymphocytes, T cells and T helper cells from Crohn's disease PBMCs (*n*= 8) after 24 h culture with B-GOS® batch C or with free sugars control. CD69 expression was quantified by flow cytometry. A) MFI of CD69 on lymphocytes; B) MFI of CD69 on T cells; C) MFI of CD69 on T helper cells. One-way ANOVA followed by Dunnett's *post-hoc* test was performed. Significant differences between stimulated cells and unstimulated control are marked with an asterisk (*p< 0.05; **p< 0.01; ****p< 0.0001).

4.4.8 Effects of co-stimulation with B-GOS® batch C and LPS upon viability, phenotypes and cytokines from healthy PBMCs

PBMCs from healthy donors (*n*= 5) were co-stimulated for 24 h with B-GOS® batch C (12 mg/mL) and LPS (1 µg/mL) to understand whether B-GOS® interferes with LPS and whether immune cells respond differently to immune challenge in presence of B-GOS®. Cell viability measurement and phenotypic analysis of lymphocytes, monocytes, T cells, B cells, NK cells, NKT cells, T helper cells and cytotoxic T cells were conducted by flow cytometry. Luminex assay was performed to quantify a panel of secreted mediators (IL-1α, IL-1β, IL-1ra, IL-6, IL-8, IL-10, granzyme B, IFN-γ and MIP-1α).

Co-treatment with LPS and B-GOS® batch C was tolerated by healthy PBMCs, with cell viability above 70% and no significant differences compared to unstimulated control or to LPS alone (Figure 4.28). Co-incubation with LPS, B-GOS® batch C or the combination of both did not lead to changes in the frequency (or recovery) of any PBMC subsets (Figure 4.29).

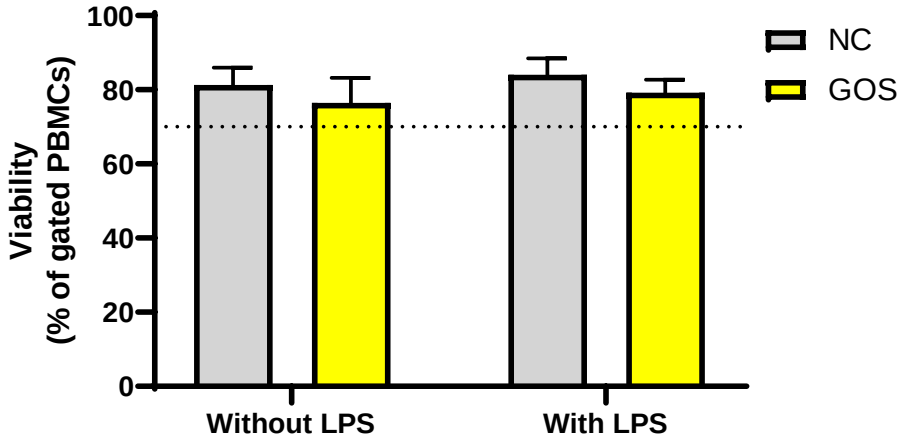

Figure 4.28 Viability of PBMCs from healthy donors (*n*= 5) stimulated with LPS, B-GOS® batch C or co-stimulated with both. Viability was measured by flow cytometry using a fixable viability stained (FVS780) and expressed as % of $FVS780^-$ cells within the PBMC gate. Data are expressed as mean ± SD.

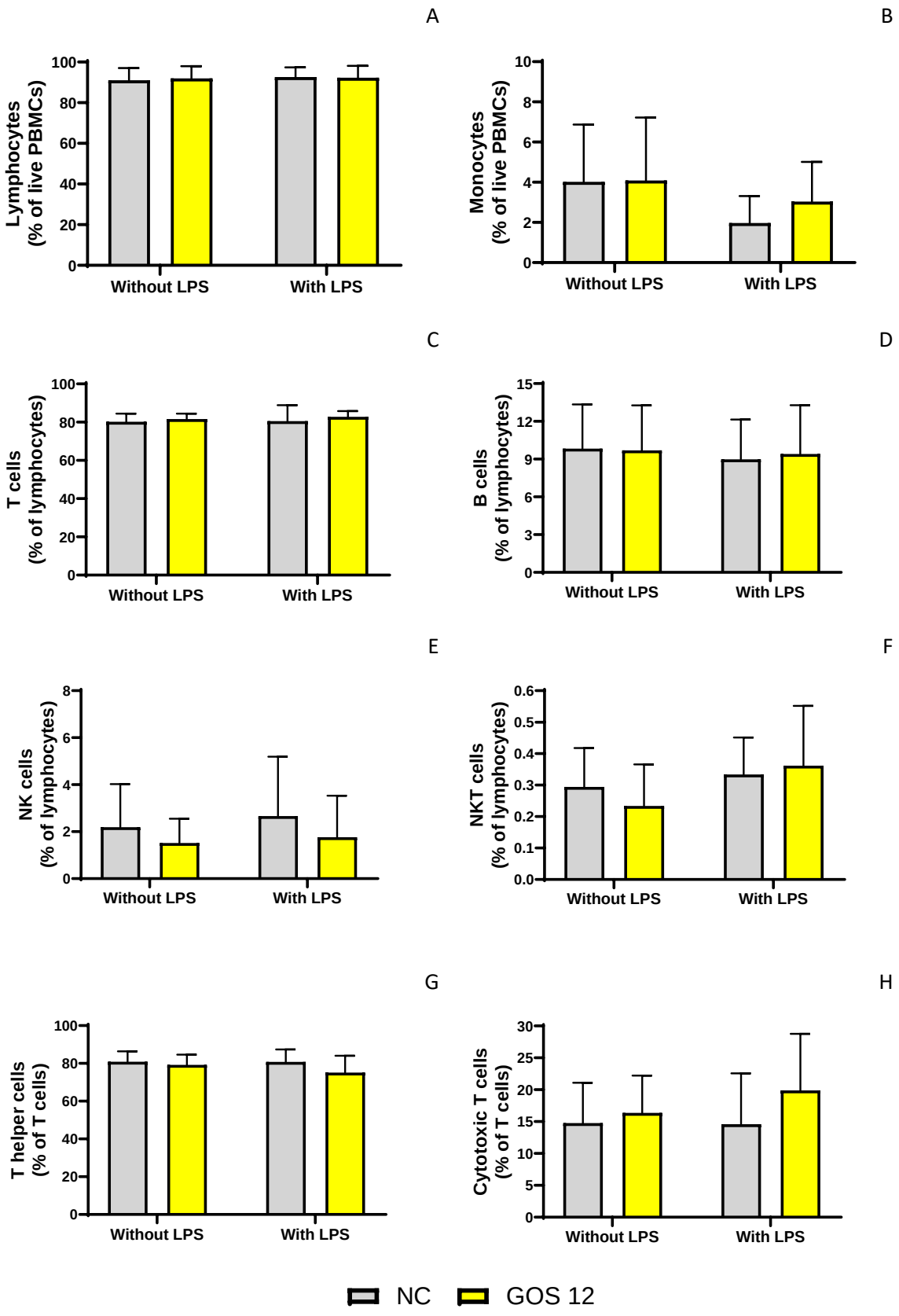

Figure 4.29 Cell frequencies of A) lymphocytes, B) monocytes, C) T cells, D) B cells, E) NK cells, F) NKT cells, G) T helper cells and H) cytotoxic T cells from healthy donors (*n*= 5) after stimulation with LPS, B-GOS® batch C or after co-stimulation with both, as measured by flow cytometry. Data were expressed as mean ± SD.

Overall, incubation with LPS alone led to increased secretion of all measured mediators compared to unstimulated control. This was significant for IL-1β (p= 0.0042), IL-1ra (p< 0.0001), IL-10 (p= 0.0038), granzyme B (p< 0.0001) and IFN-γ (p= 0.0032), as shown in Figure 4.30. Stimulation with B-GOS® batch C alone led to higher IL-6 and IL-8 secretion compared to unstimulated control, as previously observed in section 4.4.5. Co-incubation of healthy PBMCs with B-GOS® batch C and LPS resulted in lower secretion of IL-1β (p= 0.0071), IL-ra (p< 0.0001), IL-10 (p= 0.0349), granzyme B (p= 0.0010) and IFN-γ (p= 0.0188) compared to LPS alone. No changes were observed in levels of other soluble mediators. (Figure 4.30).

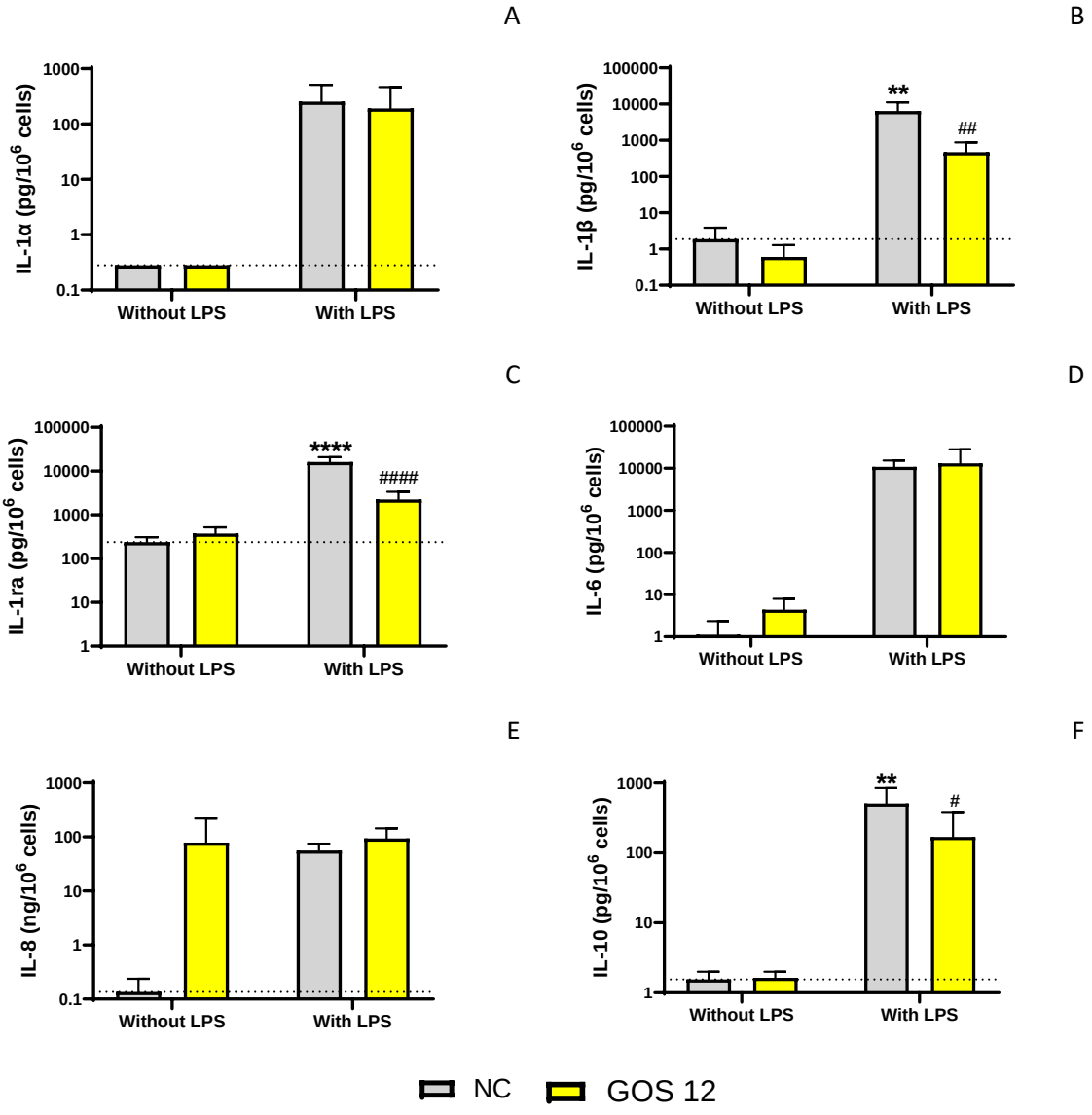

Figure 4.30 Levels of soluble mediators secreted by healthy PBMCs (n= 5) after 24 h culture with LPS alone, B-GOS® batch C alone or with both. Secreted mediators were quantified by Luminex assay. Two-way ANOVA followed by Bonferroni's *post-hoc* test was performed. Significant differences between LPS alone *vs* NC are marked with an asterisk (**p< 0.01; ****p< 0.0001). Significant differences between B-GOS® batch C + LPS *vs* LPS are marked with a hash ($^{\#}p$< 0.05; $^{\#\#}p$< 0.01; $^{\#\#\#}p$< 0.001; $^{\#\#\#\#}p$< 0.0001).

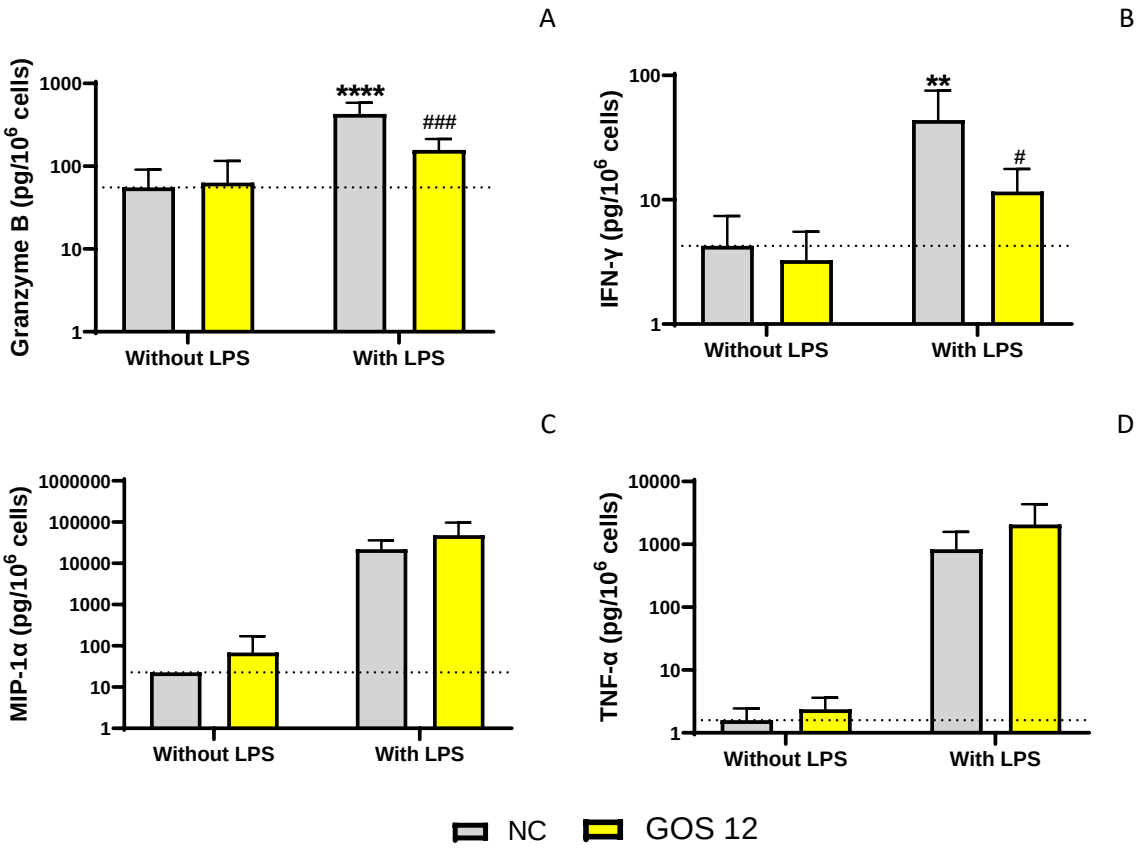

Figure 4.30_Continued Levels of soluble mediators secreted by healthy PBMCs (*n*= 5) after 24 h culture with LPS alone, B-GOS® batch C alone or with both. Secreted mediators were quantified by Luminex assay. Two-way ANOVA followed by Bonferroni's *post-hoc* test was performed. Significant differences between LPS alone *vs* NC are marked with an asterisk (***p*< 0.01; *****p*< 0.0001). Significant differences between B-GOS® batch C + LPS *vs* LPS are marked with a hash ($^{\#}p$< 0.05; $^{\#\#}p$< 0.01; $^{\#\#\#}p$< 0.001; $^{\#\#\#\#}p$< 0.0001).

4.4.9 Effects of pre-treatment with B-GOS® batch C before LPS challenge upon viability, phenotypes and secreted cytokines from healthy PBMCs

In order to study the effects of B-GOS® in preventive settings, healthy PBMCs (*n*= 7) were pre-incubated for 24 h with B-GOS® batch C before a 6 h immune challenge with LPS. Secreted soluble mediators (IL-1α, IL-1β, IL-1ra, IL-8, IL-10, IFN-γ, TNF-α and granzyme B) were measured by Luminex assay. Multi-colour flow cytometry was performed to assess changes in viability and in the expression of CD14, TLR2 (CD282) and TLR4 (CD284) markers.

PBMC mean viability was above 70% for all conditions tested, with no differences between cells pre-incubated with B-GOS® batch C and LPS alone (Figure 4.31). There were no significant changes

in the percentage of monocytes ($CD14^+$ cells) or in their CD14 (MFI) expression levels between PBMCs pre-incubated with B-GOS® and LPS alone (Figure 4.32).

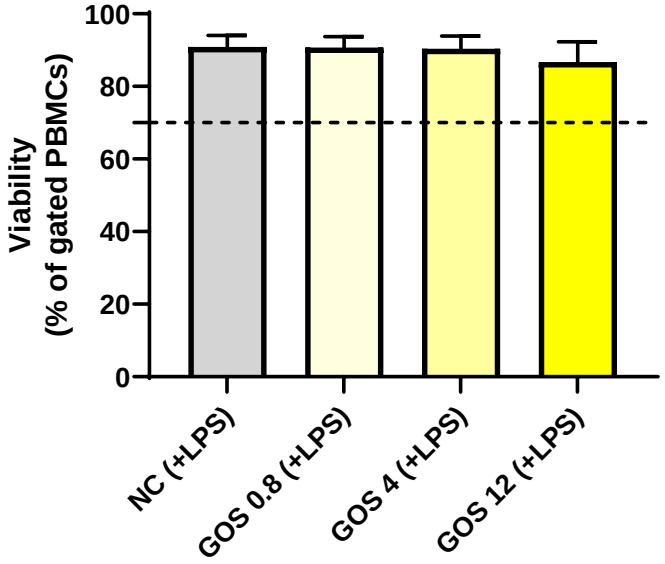

Figure 4.31 Viability of PBMCs from healthy donors (*n*= 7) pre-incubated for 24 h with B-GOS® batch C and then challenged for 6 h with LPS. Viability was measured by flow cytometry using a fixable viability stained (FVS780) and expressed as % of $FVS780^-$ cells within the PBMC gate. Data are expressed as mean ± SD.

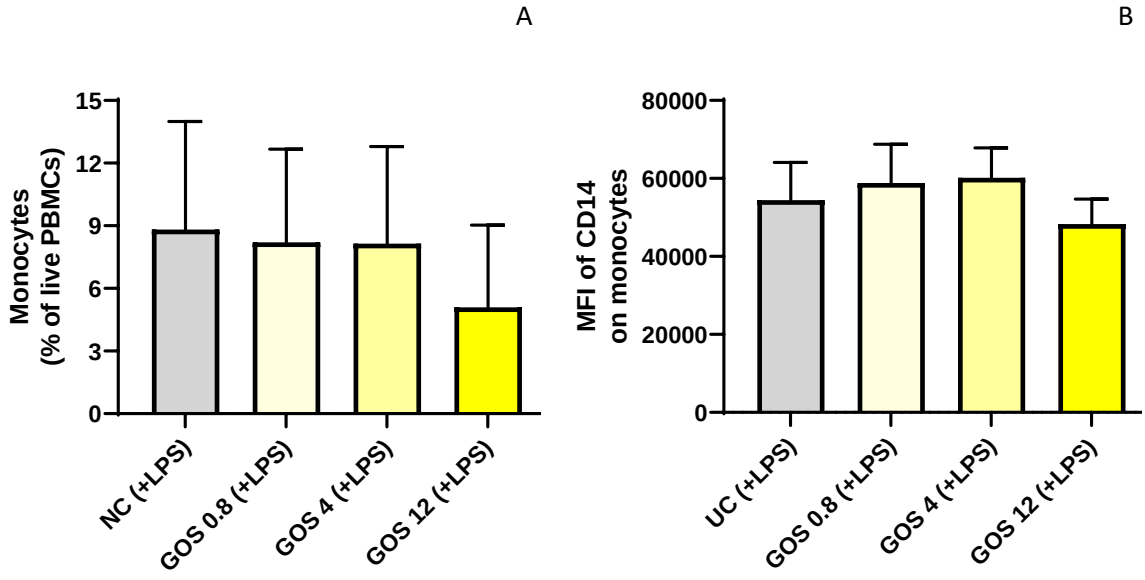

Figure 4.32 A) Frequencies of monocytes and B) CD14 (MFI) expression on monocytes measured by flow cytometry on healthy PBMC donors (*n*= 7) pre-incubated for 24 h with B-GOS® batch C and then challenged for 6 h with LPS. Data were expressed as mean ± SD.

Virtually all monocytes were found to express TLR2 (overall average 99.3 ± 1.0). This was in line with the TLR2 values for peripheral blood monocytes found in literature [326]. Pre-incubation with B-GOS® batch C did not alter the numbers of $TLR2^+$ monocytes, but there was a trend (p= 0.0553) for an increase in TLR2 (MFI) expression after pre-incubation with the highest dose of the prebiotic followed by LPS challenge compared to LPS challenge alone (Figure 4.33). Pre-incubation with B-GOS® batch C followed by LPS challenge did not affect the proportions of monocytes expressing TLR4 nor their levels of TLR4 (MFI) expression (Figure 4.33).

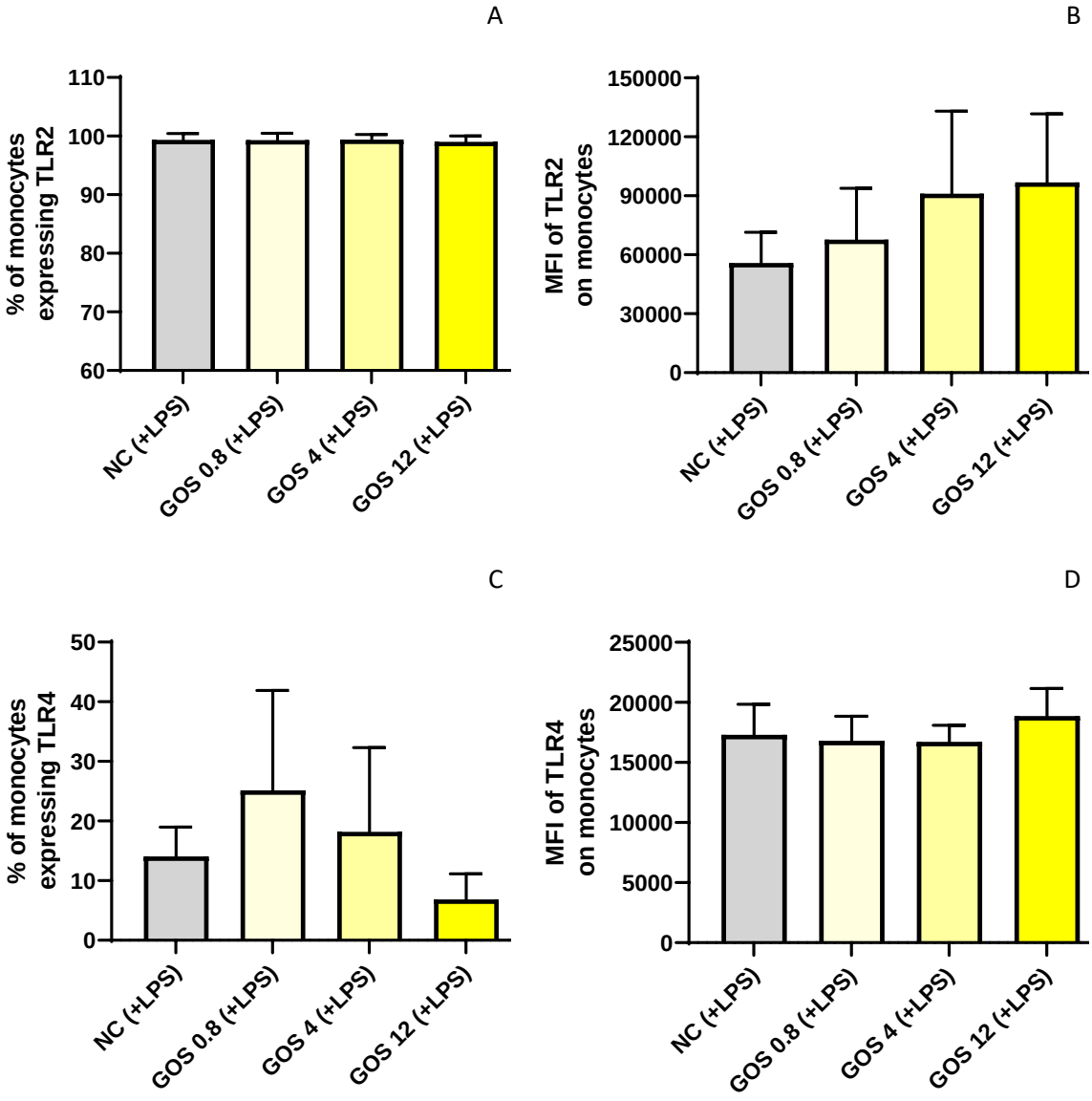

Figure 4.33 A) Frequencies of monocytes expressing TLR2 and TLR4 (graphs A and C) and relative MFIs (graphs B and D) after 24 h pre-incubation of healthy PBMCs (n= 7) with B-GOS® batch C followed by 6 h LPS challenge. TLR2 and TLR4 expression was measured by flow cytometry. Data were expressed as mean ± SD.

Pre-incubation with B-GOS® batch C before LPS challenge did not affect the levels of secreted IL-1α, IL-1β, IL-1ra, IFN-γ, TNF-α or granzyme B (Figure 4.34). A synergic effect was observed on IL-8 secretion when cells were incubated with B-GOS® batch C and LPS compared to LPS alone (p= 0.0004). This was in agreement with previously presented data (section 4.4.5), which showed a direct effect of B-GOS® batch C on IL-8 secretion (Figure 4.34). Pre-treatment with the prebiotic led to a dose-dependent reduction (GOS 4, p= 0.0228; GOS 12, p= 0.0007) in the amounts of secreted IL-10 compared to LPS alone (Figure 4.34), as observed in co-stimulatory settings (section 4.4.8).

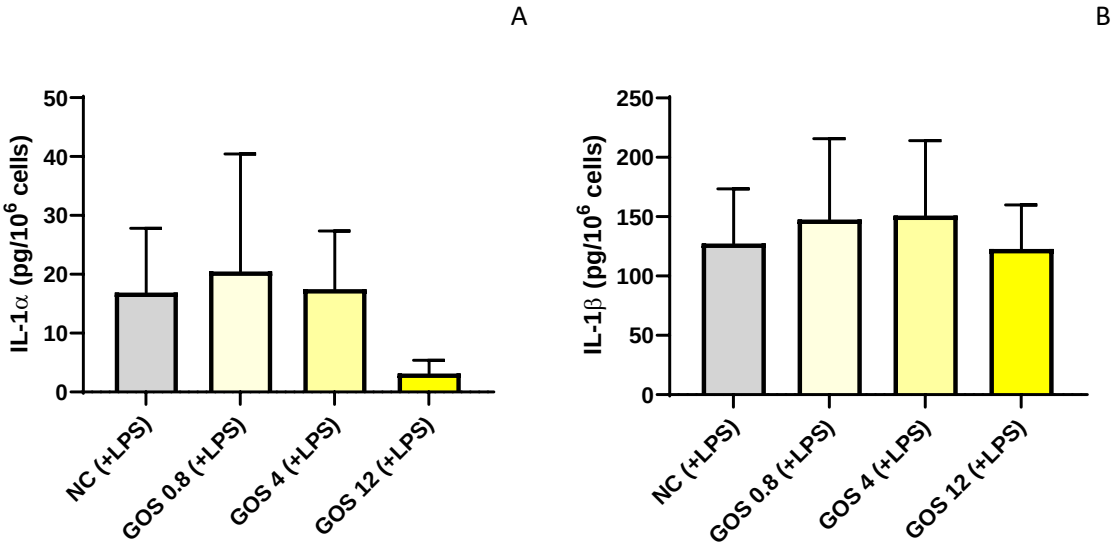

Figure 4.34 Levels of soluble mediators secreted by healthy PBMCs (n= 7) after 24 h pre-incubation of healthy PBMCs (n= 7) with B-GOS® batch C followed by 6 h LPS challenge. Secreted mediators were quantified by Luminex assay. One-way ANOVA followed by Dunnett's *post-hoc* test was performed. Significant differences between B-GOS® batch C + LPS *vs* LPS are marked with an asterisk (*p< 0.05; ***p< 0.001).

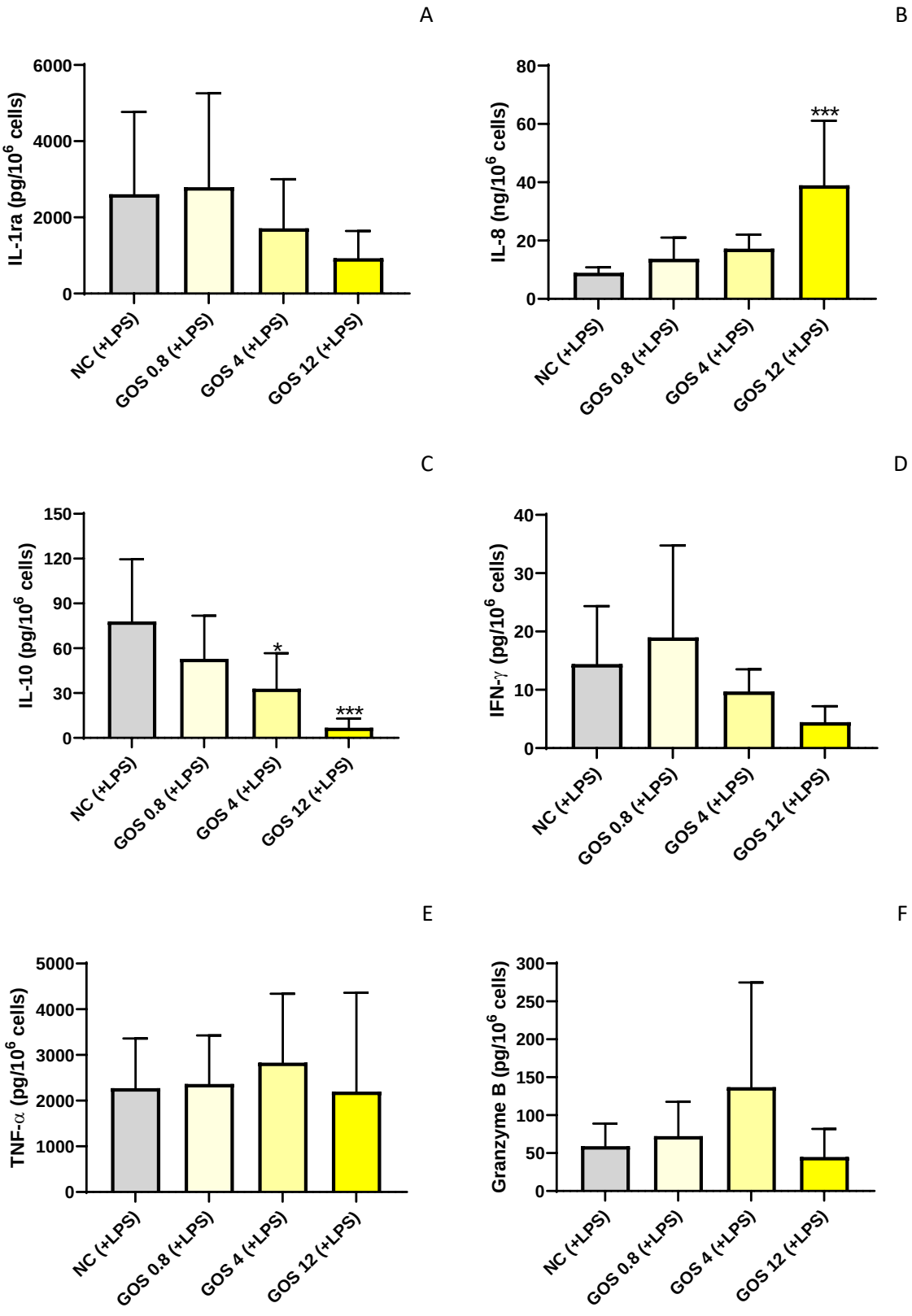

Figure 4.34_Continued Levels of soluble mediators secreted by healthy PBMCs (*n*= 7) after 24 h pre-incubation of healthy PBMCs (*n*= 7) with B-GOS® batch C followed by 6 h LPS challenge. Secreted mediators were quantified by Luminex assay. One-way ANOVA followed by Dunnett's *post-hoc* test was performed. Significant differences between B-GOS® batch C + LPS *vs* LPS are marked with an asterisk (*p< 0.05; ***p< 0.001).

4.5 Discussion

In unstimulated conditions, Crohn's disease PBMCs showed lower viability and presented a more pro-inflammatory phenotype compared to healthy PBMCs, with higher frequencies of activated cells in circulation, such as CD69-expressing lymphocytes, T cells and cytotoxic T cells. Additionally, they secreted higher amounts of pro-inflammatory IL-β and IL-6 and lower amounts of anti-inflammatory IL-10 compared to healthy PBMCs. Higher numbers of NKT cells and lower numbers of T helper cells were seen in unstimulated Crohn's disease PBMCs compared to unstimulated healthy PBMCs. Crohn's disease donors with low numbers of monocytes presented a more activated phenotype. Overall, these changes in the frequencies and activation of circulating lymphocytes and monocytes are likely due to systemic inflammation of Crohn's disease donors and suggest a migration of certain cell subsets to the inflammation site.

Alterations in NKT cell numbers and functions have been previously associated with the pathogenesis of IBD; however, it is still unclear whether they exert a pathogenic or a protective role [327]. In the literature, and in contrast with what observed here, lower proportions of NKT cells were seen in the peripheral blood of Crohn's disease and ulcerative colitis patients [328]. Different subsets of NKT cells include type I (or invariant) NKT cells and type II (or variant) NKT cells. While type I NKT cells show both protective and pro-inflammatory effects, type II NKT cells generally promote inflammation [329, 330]. Although it was not possible to include additional markers to study into more detail NKT subsets, it is plausible that the higher numbers of total NKT cells observed in this study were due to increased proportions of the pro-inflammatory NKT cell subset in the blood of Crohn's disease donors.

Together with NKT cells, T helper cells also have a key function in mediating intestinal inflammation and have been implicated in the pathogenesis of IBD. Children affected by Crohn's disease displayed lower levels of T helper cells in blood, which directly associated with disease-related clinical parameters [331]. In this study, the observed lower frequencies of T helper cells in the blood of Crohn's disease donors are likely due to their migration to the inflamed mucosa and may associate with the severity of the disease [332].

Differences in CD69 expression between unstimulated healthy and Crohn's disease PBMCs were in line with other studies available in the literature, which found increased proportions of activated T cells in the blood of IBD patients and reduced frequencies of circulating activated B cells in individuals with Crohn's disease [321-323]. In inflammatory diseases such as IBD, circulating lymphocytes are activated, present an effector phenotype and are ready to migrate from peripheral blood to the inflamed mucosa [322]. CD69 is expressed on infiltrated lymphocytes at inflammatory sites [102] and, although its precise function is yet to be clarified, it may play an

important role in the pathogenesis of IBD, as demonstrated in an animal model of induced chronic colitis [105]. While there are studies in the literature on the expression of CD69 on Crohn's disease lymphocytes, to the author's knowledge this is the first study to have looked into detail at the CD69 expression on monocytes from adult Crohn's disease patients.

It was hypothesised that healthy PBMC and Crohn's disease PBMCs would respond differently to B-GOS® stimulation due to their different levels of inflammation at baseline. Indeed, while B-GOS® failed to induce any changes in the expression of CD25 or CD69 on healthy PBMCs, in Crohn's disease PBMCs it led to higher percentages of lymphocytes, T cells and T helper cells expressing CD69 as well as to increased CD69 (MFI) expression on their surface. These immunostimulatory effects on Crohn's disease donors were stronger at the highest concentration of B-GOS® tested and were at least partially attributed to GOS itself, as the free sugars alone failed to induce significant increases in CD69 expression. It is not fully clear from the literature whether the induction of increased levels of CD69 expression on Crohn's disease PBMCs may lead to even higher inflammation or whether it could promote immune regulation. In a study assessing the role of CD69 in the pathogenesis of dextran sulphate sodium-induced colitis, CD69-deficient mice showed lower lethality, weight loss and clinical signs and better histological characteristics than wild-type mice, indicating that CD69 may play an important role in the pathogenesis of the disease [105]. In another study, higher levels of CD69 expression were observed on peripheral blood of patients with acute severe ulcerative colitis compared to healthy controls and was associated with higher rates of treatment failure [333]. However, other studies on transgenic mice found that CD69 can also exert regulatory functions and that absence of CD69 expression may lead to impaired oral tolerance, reduced regulatory T cell induction and may even exacerbate the severity of IBD [104, 334].

The preliminary data on secreted IL-8 showed in Chapter 3 were confirmed by the work presented in this chapter, highlighting that the effects of GOS on IL-8 persist without the presence of LPS. As expected, B-GOS® displayed immunostimulatory effects inducing the secretion of pro-inflammatory cytokines by healthy PBMCs (IL-6 and IL-8) and Crohn's disease PBMCs (IL-8 and TNF-α), with stronger effects at the highest concentration used and showing a trend for a dose-dependent response. Healthy PBMCs appeared more sensitive to stimulation with the prebiotic and responded more strongly to it than Crohn's disease PBMCs, releasing high amounts of IL-8. Crohn's disease PBMCs, on the other hand, presented higher surface expression of IL-8 than healthy PBMCs even in unstimulated conditions, suggesting a more pro-inflammatory profile. Interestingly, incubation with low concentrations of B-GOS® led to a reduction in the levels of IL-12p70 secreted by Crohn's disease PBMCs. IL-12p70 is a Th1 cytokine that is synthesised during active Crohn's disease and is a key driver of inflammation in IBD [335]. A reduction in the levels of

IL-12p70 induced by B-GOS® could be beneficial for Crohn's disease patients, considering that anti-IL-12 monoclonal antibodies are currently used to down-regulate its pro-inflammatory activity [335].

In this chapter, it was also demonstrated that the effects on secreted IL-8 were mainly due to the free sugars, and in particular the galactose fraction, contained in the prebiotic product rather than to GOS itself. Galactose is known to exert pro-inflammatory effects in mouse models [317] and to modulate LPS endotoxicity as one of the sugars present in its outer core [16]. Intracellular staining revealed that monocytes were the main contributors to IL-8 production. It is important to stress that the pro-inflammatory effects of the free sugars observed *in vitro* may not reflect the *in-vivo* situation. In normal conditions, galactose is not in direct contact with immune cells as it is absorbed by active transport across the intestinal epithelium into the bloodstream for transport to the liver, where it is then converted into glucose [336]. While lowering the amount of galactose contained B-GOS® could be helpful in reducing the inflammatory risk in *ex-vivo* Crohn's disease PBMCs and should be taken into account in *in-vitro* studies, it does not represent a matter of concern when the prebiotic is consumed orally. Unfortunately, it was not possible to discriminate the effects of glucose, galactose and lactose upon IL-6 and TNF-α from those of GOS, but it is likely that the free sugars upregulate TLR2/TLR4 expression on monocytes, leading to NF-κB activation and the release of pro-inflammatory cytokines. It is unclear whether the increased activation of T cells and T helper cells observed in Crohn's disease PBMCs is a consequence of monocyte activation by the free sugars or whether GOS exert an independent direct effect on T cells *per se*.

Interestingly, in co-culture settings of healthy PBMCs, despite B-GOS® causing an even stronger increase in IL-6 and IL-8, probably due to the free sugars' effects on monocytes, it also led to lower secretion of other LPS-induced mediators including granzyme B, IFN-γ, IL-10, IL-1β and IL-1ra. This suggests that GOS may physically coat LPS impeding its binding to the receptor or may affect TLR2/TLR4 expression indirectly and block LPS binding. Since these effects on secreted cytokines were almost totally lost when PBMCs were pre-incubated with B-GOS® before LPS challenge, it is most likely that GOS interferes with LPS rather than with TLR receptors.

Experiments using a TLR4 antagonist (TLR4-A) were conducted to assess the involvement of TLR4 in cytokine secretion following stimulation of PBMCs and THP-1 cell lines with B-GOS®. Whereas cytokine levels were significantly reduced after pre-treating THP-1 cells with TLR4 antagonist, indicating functional inhibition, no changes were seen in pre-treated PBMCs. This may indicate that much higher doses of the antagonist, or alternative antagonists, are required when pre-treating PBMCs rather than THP-1 cells, which are known to produce significantly lower cytokines (*e.g.* IL-8) compared to PBMCs and isolated monocytes [337]. The fact that pre-treatment with

TLR4-A did not lead to a reduction in the levels of IL-8 at any B-GOS® concentrations may indicate that B-GOS® promotes IL-8 secretion via different mechanisms or that alternative antagonists should be tested. Future work should assess the involvement of other receptors (*e.g.* TLR2, TLR5, TLR7, TLR8, complement receptor 3 and C-type lectin receptors) on IL-8 production by B-GOS®-stimulated PBMCs and THP-1 cells. Furthermore, cytokine secretion might have been induced by potential TLR2 agonist contained in LPS itself. Due to limited volume of supernatants from PBMC cultures, it was not possible to evaluate the effect of pre-incubating with TLR4-A on the release of IL-6 and TNF-α, as assessed for THP-1 cells. The effects of blocking the TLR4 in PBMCs should be evaluated in the future also on these mediators. Increasing doses of the antagonist could also be tested on PBMCs in order to block the action of LPS and, potentially, of B-GOS®. Finally, the antagonising effects of TLR4-A should be evaluated on different types of LPS, whose immune stimulatory potency differ largely among different bacteria [338].

To confirm the findings of the experiments with the TLR4 antagonist, TLR2 and TLR4 expression levels were assessed by flow cytometry. While pre-incubation with B-GOS® did not affect TLR4 expression on monocytes, there was a trend for an increase in TLR2 expression at the highest concentration used. These results suggest that GOS may act through TLR2, although further studies with increased sample size (n= 9, α= 0.05; 1-β= 0.80) might be required.

Overall, this is the first *ex-vivo* study to have looked at the immunological effects of GOS on PBMCs from Crohn's disease donors. The data presented in this chapter highlighted the importance of minimising the content of galactose in B-GOS® products when used *in-vitro* to avoid pro-inflammatory effects in Crohn's disease PBMCs, and also demonstrated that GOS may be useful to decrease the levels of pro-inflammatory IL-12p70. Additionally, co-culture experiments indicated that GOS could be used to block the action of LPS and therefore to reduce the levels of LPS-induced cytokines.

Chapter 5 EFFECTS OF ISOLATED GOS FRACTIONS WITH DIFFERENT DEGREE OF POLYMERISATION UPON IMMUNE PARAMETERS OF HEALTHY PBMCs

5.1 Introduction

Galactooligosaccharides (GOS) consist of chains of galactose units with a terminal glucose monomer and mainly β(1–3) and β(1–4) and β(1–6) glycosidic linkages [339]. These chains, or GOS fractions, have different degree of polymerisation (DP), which refers to the number of monomeric units in the polymer.

Disaccharide allolactose (β-d-Gal (1→6)-d-Glc), trisaccharide 3-galactosyllactose (β-d-Gal (1→3)-β-d-Gal-(1→4)-d-Glc) and tetrasaccharide 4'- digalactosyllactose (β-d-Gal (1→4)-β-d-Gal-(1→4)-β-d-Gal-(1→4)-d-Glc) are all examples of GOS fractions [340]. The type of enzyme used for the transgalactosylation reaction and the conversion degree of lactose determine the DP of the fractions [191]. In the transgalactosylation process (Figure 5.1), β-galactosidases hydrolyse lactose and transfer galactose to another carbohydrate (lactose), resulting in an oligosaccharide with higher DP [187, 188].

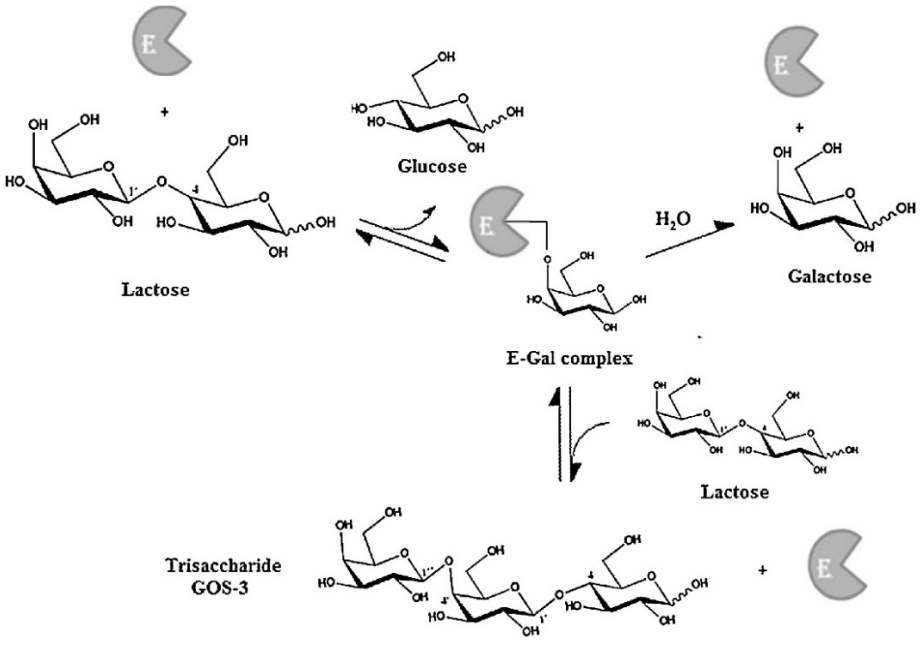

Figure 5.1 Schematic of the transgalactosylation of lactose catalysed by the enzyme β-galactosidase. Image from [189].

In the work presented in this thesis, B-GOS® was produced from an enzyme isolated from Bifidobacterium bifidum NCIMB 41171 on lactose [339] and consisted of DP2-DP8 fractions [144]. DP2 and DP3 are the most represented fractions, followed by DP4 and DP5, whereas DP6-DP8 are present in much lower abundance (< 2%). The various oligosaccharide fractions were achieved from whole B-GOS® by gel filtration on a BioGel P2 column using water as eluent. Chromatographic analysis was conducted to ensure that molecules with the same DP were pooled [202, 341]. Clasado Biosciences was the provider of the isolated B-GOS® fractions.

The chain length of prebiotic fractions has been shown to directly affect the direction of inflammatory responses (anti-inflammatory *vs* pro-inflammatory) by immune cells. Vogt and colleagues [240] demonstrated that short-chain fructooligosaccharides (FOS, DP2-DP3) elicited the production of anti-inflammatory cytokines by *ex-vivo* human PBMCs to a greater extent than long-chain FOS (>DP8). Cytokine production was both dose- and chain length-dependent. Isolated DP2 and DP3 GOS fractions significantly prevented barrier disruption induced by a fungal toxin on Caco-2 cells, whereas larger fractions (≥ DP4) showed no effects [300]. The immunomodulatory effects of DP2 and DP3 GOS fractions could be due to their different interaction with cell receptors compared to higher DP fractions or, when whole GOS is tested, to their higher abundance in the product. Vogt and colleagues [240] hypothesised that lower DP fractions activate a few distant receptors at a time, while higher DP fractions activate larger numbers of receptors by clustering them in a LPS-like manner and eliciting a stronger response. In an *in-vivo* animal study, rats fed with fructans at a lower DP (DP4) presented increased IFN-γ and IL-10 production compared to higher DP (DP16), which also correlated with higher lactobacilli counts [342].

One of the most interesting GOS fractions in terms of potential immunomodulatory effects is DP3, which is specifically found in B-GOS®. DP3 presents the same structure as the human milk oligosaccharide (HMO) 3'-galactosyllactose (3'-GL) [192, 193, 343], which is depicted in Figure 5.2. 3'-GL is found at high concentrations in human colostrum and contributes to immune modulation by attenuating TLR3 signalling, as demonstrated in cultured human enterocytes [194, 344]. Within PBMCs, TLR3 is expressed on dendritic cells (DCs) and macrophages and it recognises double-stranded RNA (dsRNA) from viruses. A synthetic analogue of viral dsRNA is the polyinosinic-polycytidylic acid (poly(I:C)), which binds to TLR3 resulting in the activation of TNF receptor-associated factors (TRAF3 and TRAF6) that trigger the production of pro-inflammatory cytokines (*e.g.* IL-6, IL-8, IFN-γ and TNF-α). HMO 3'-GL was shown to exert anti-inflammatory effects by reducing poly(I:C)-induced IL-8 secretion by *ex-vivo* immature intestinal cells [193].

There is limited information in the literature on the immunological effects of GOS fractions at different DP. No studies have yet assessed the effects of whole GOS or DP3 GOS fraction on poly(I:C)-challenged *ex-vivo* PBMCs from healthy donors.

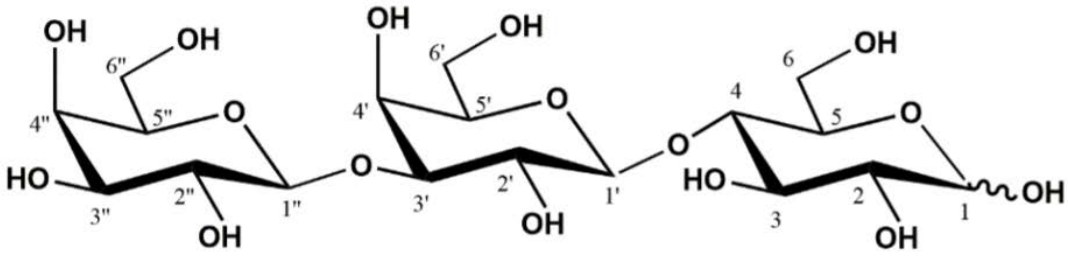

Figure 5.2 Chemical structure of the HMO 3-galactosyllactose . Image from [345].

5.2 Aim and objectives

The purpose of this chapter is to understand whether the most abundant B-GOS® fractions DP2-DP5 exert immunological effects when tested in isolation and whether differences in their chain length (DP) elicit a different response. Additionally, pre-incubation experiments using whole B-GOS®, DP3 B-GOS® fraction or 3'-GL followed by poly(I:C) challenge will be conducted to understand whether B-GOS® and/or DP3 B-GOS® fraction affect TLR3-mediated inflammation.

The specific objectives were to:

- Perform LAL assay upon four isolated B-GOS® fractions (DP2, DP3, DP4 and DP5) provided by Clasado Biosciences

- Assess the potential cytotoxicity of DP2-DP5 B-GOS® GOS fractions and 3'-GL, in presence and in absence of poly(I:C), on PBMC cultures

- Evaluate the effects of culturing healthy PBMCs with DP2-DP5 B-GOS® GOS fractions on the frequencies of PBMC subsets (lymphocytes, monocytes, T cells, B cells, NK cells, NKT cells, cytotoxic T cells and T helper cells), on the expression of CD69 and on a panel of secreted cytokines (IL-1α, IL-1β, IL-1ra, IL-6, IL-8, IL-10, granzyme B, IFN-γ, MIP-1α and TNF-α), and compare the results with those of whole B-GOS® and 3'-GL

- Evaluate the ability of DP3 B-GOS® fraction, whole B-GOS® and 3'-GL to affect TLR3-mediated inflammation induced by poly(I:C), as assessed by changes in the expression

levels of the activation marker CD69 and secreted cytokines (IL-1α, IL-1β, IL-1ra, IL-6, IL-8, IL-10, granzyme B, IFN-γ, MIP-1α and TNF-α)

The first hypothesis is that different B-GOS® fractions will have different immunological effects on PBMCs, with DP2 and DP3 expected to have the strongest effects. The second hypothesis is that both whole B-GOS®, which mainly contains DP3, and the isolated DP3 B-GOS® fraction will interfere with TLR3-mediated inflammation elicited by poly(I: C).

5.3 Methods

Whole B-GOS® (batch C) and isolated DP2 – DP5 B-GOS® fractions were prepared as detailed in section 2.3. LAL assay was carried out as described in section 2.9.2. Healthy PBMCs were cultured as explained in section 2.3. Cell viability was measured by flow cytometry using a fixable viability stain (FVS780) as reported in 2.5. Cell surface staining by flow cytometry was performed as described in 2.7.2. Mediators (IL-1α, IL-1β, IL-1ra, IL-6, IL-8, IL-10, granzyme B, IFN-γ, MIP-1α and TNF-α) secreted in cell culture supernatants were analysed using Premixed Magnetic Luminex® Assays. Further details on the Luminex method and the dilution factors used can be found in 2.8. A graphical summary of the methods used in this chapter is provided in Figure 5.3.

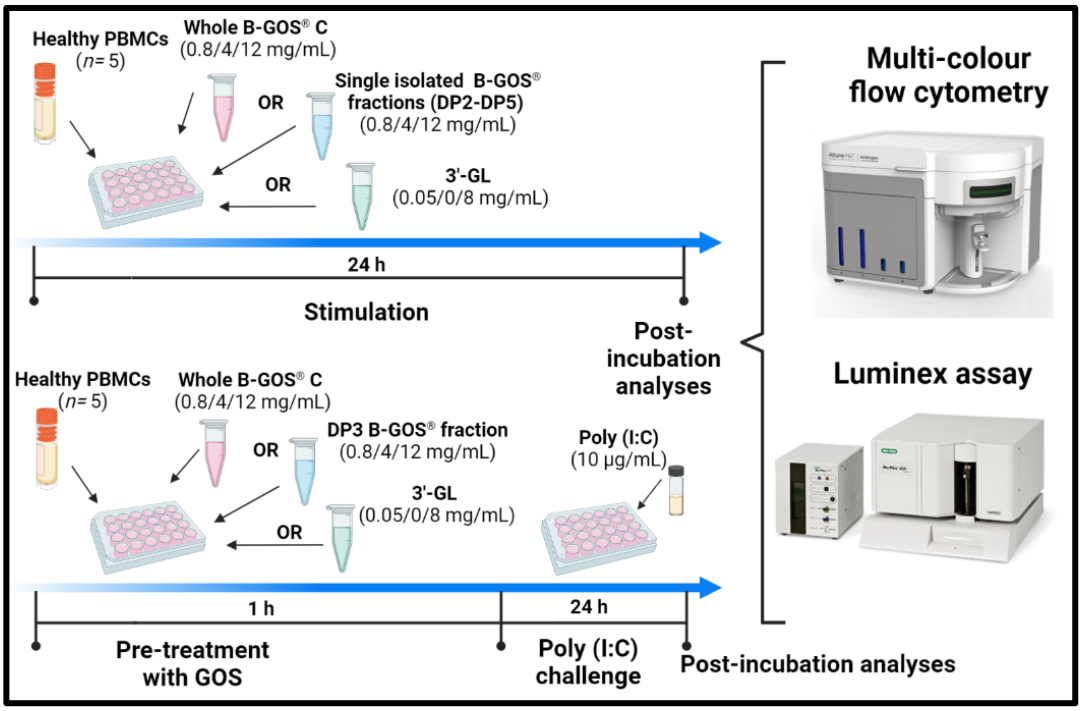

Figure 5.3 Graphical summary of the methods used for the assessment of the effects of B-GOS® fractions, 3'-GL and whole B-GOS® in presence and in absence of poly(I:C) upon PBMC viability, phenotypes, activation markers and secreted cytokines.

5.4 Results

5.4.1 Quality control of isolated B-GOS® fractions and 3'-GL by LAL assay and pre-treatment with PMB

B-GOS® fractions (DP2 – DP5) and 3'-GL were quality checked by the LAL assay before direct application to *ex-vivo* cell cultures. A negative control (RPMI-1640 medium) and a positive control (LPS from *E. coli* O111:BA, 0.05 µg/mL) were included in the assay. Each sample was tested in triplicate at 0.8 mg/mL, 4 mg/mL and 12 mg/mL. 3'-GL was tested at 0.05 mg/mL and 0.8 mg/mL. The average absorbance of the readings minus the average absorbance of the blank was used to calculate unknown LPS concentrations from a standard curve in the 0.01-0.1 EU/mL range (Figure 5.4).

All fractions contained levels of LPS above the 0.1 EU/mL limit for cell culture applications at all concentration tested, whereas 3'-GL presented low but detectable levels of LPS at both concentrations tested. The negative control did not contain any detectable LPS, while the positive control presented LPS above the cell culture limit (Figure 5.4).

A

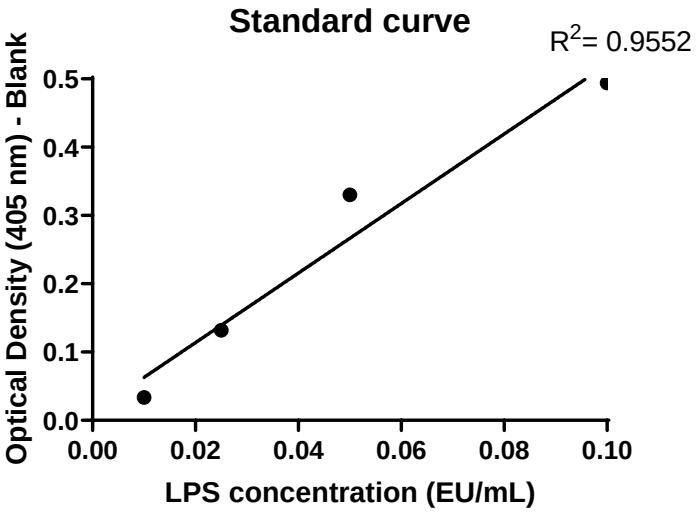

B

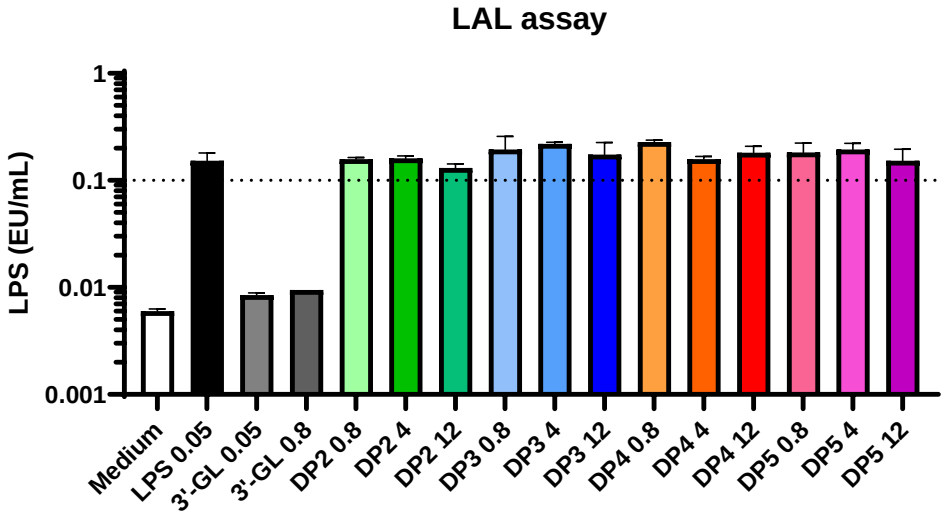

Figure 5.4 A) Standard curve in the 0.01-0.1 EU/mL range for the quantitation of LPS in samples by LAL assay. B) Levels of LPS in B-GOS® fractions (DP2-DP5) and 3'-GL. A negative control (RPMI-1640 medium) and a positive control (LPS from *E. coli* O111:BA) were included. LAL assay was conducted with technical replicates. Data are expressed as mean ± SD (*n*= 3). The dotted line at Y= 0.1 refers to the limit of LPS (EU/mL) for cell culture applications.

While it was acceptable to use 3'-GL in direct contact with immune cells, DP2 – DP5 B-GOS® fractions were pre-treated for 24 h with PMB at the maximum dose (30 μg/mL) advised for use in PBMC cultures in order to neutralise the effects of LPS. The effects of PMB pre-treatment were evaluated on a range of LPS-induced mediators (IL-1α, IL-1β, IL-6, IL-8, IL-10 and TNF-α). Stimulation of PBMCs with LPS (positive control, 1 μg/mL) or with B-GOS® fractions (0.8 mg/mL, 4 mg/mL and 12 mg/mL) resulted in increased levels of all secreted mediators compared to unstimulated control, although this was statistically significant only for B-GOS® fractions (Figure 5.5–Figure 5.7). Incubation with DP2 – DP5 B-GOS® fractions led to higher production of IL-1α (all $p< 0.005$), IL-1β (all $p< 0.005$), IL-6 (all $p< 0.002$), IL-8 (all $p< 0.01$), IL-10 (all $p< 0.05$) and TNF-α (all $p< 0.05$) compared to unstimulated control (Figure 5.5–Figure 5.7). The effects on secreted cytokines were dose-dependent, and lower DP fractions (DP2 – DP3) seemed to have stronger effects compared to higher DP fractions (DP5). Pre-incubation of LPS with PMB significantly reduced the secretion of all mediators to the levels observed for the unstimulated control. PMB-treated LPS-stimulated cells produced lower IL-1α ($p= 0.0214$), IL-1β ($p= 0.0067$), IL-6 ($p= 0.0076$), IL-8 ($p= 0.0039$), IL-10 ($p= 0.0252$) and TNF-α ($p= 0.0244$) compared to untreated LPS-stimulated cells, meaning that the antibiotic was effective in inhibiting the action of LPS (Figure 5.5–Figure 5.7). LPS elicited a cytokine response that was the same order of magnitude of B-GOS® fractions at approximately 0.8 mg/mL. However, while PMB completely neutralised the effects of LPS to levels similar to the unstimulated control, it did not show any inhibitory effects on the B-GOS® fractions. Therefore, the effects on secreted cytokines were most likely due to the B-GOS® fractions themselves rather than to LPS. PMB-treated B-GOS® fractions will be used for all further experiments presented in this chapter.

A

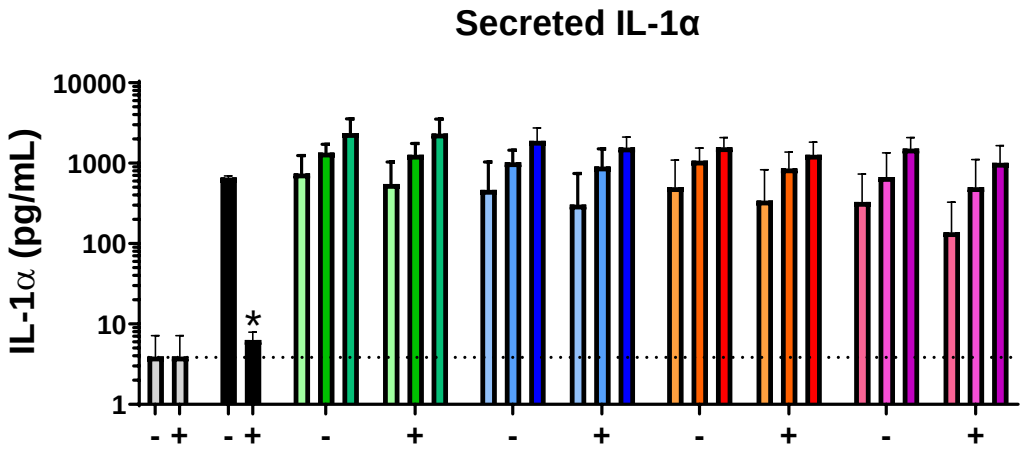

B

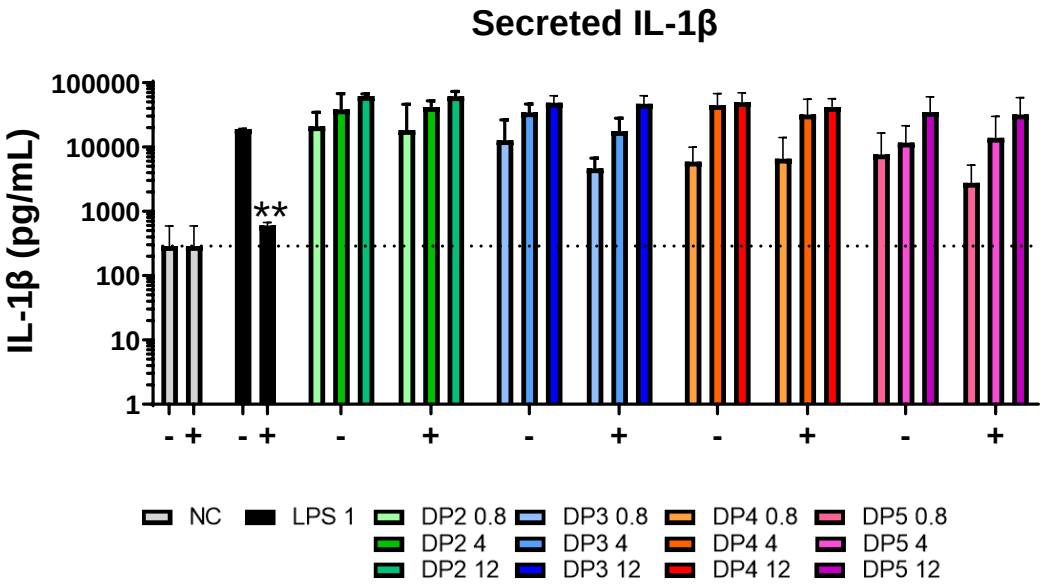

Figure 5.5 Effects of pre-treating B-GOS® DP2 – DP5 fractions or LPS positive control with (+) or without (-) PMB for 24 h on Th1 cytokines IL-1α and IL-1β. Healthy PBMCs (*n*= 5) were incubated for 24 h with DP2 – DP5 B-GOS® fractions or LPS, pre-treated with or without PMB. Unstimulated cells (NC) were used as control. Data are expressed as mean ± SD. Two-way ANOVA followed by Bonferroni's *post-hoc* test was performed. Because all B-GOS® fractions caused a significant increase in all secreted mediators, only significant differences between conditions with or without PMB (+/-) are represented. A) *p= 0.0214. B) *p= 0.0067.

A

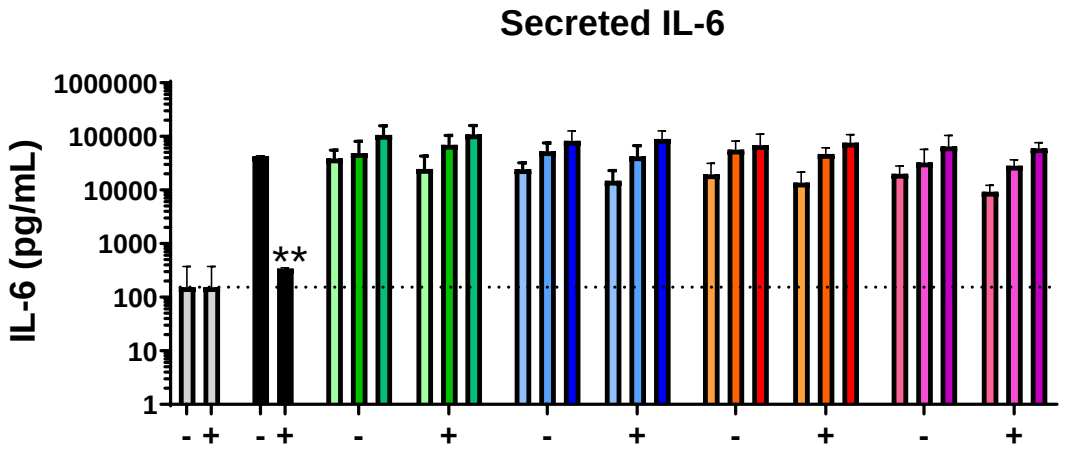

B

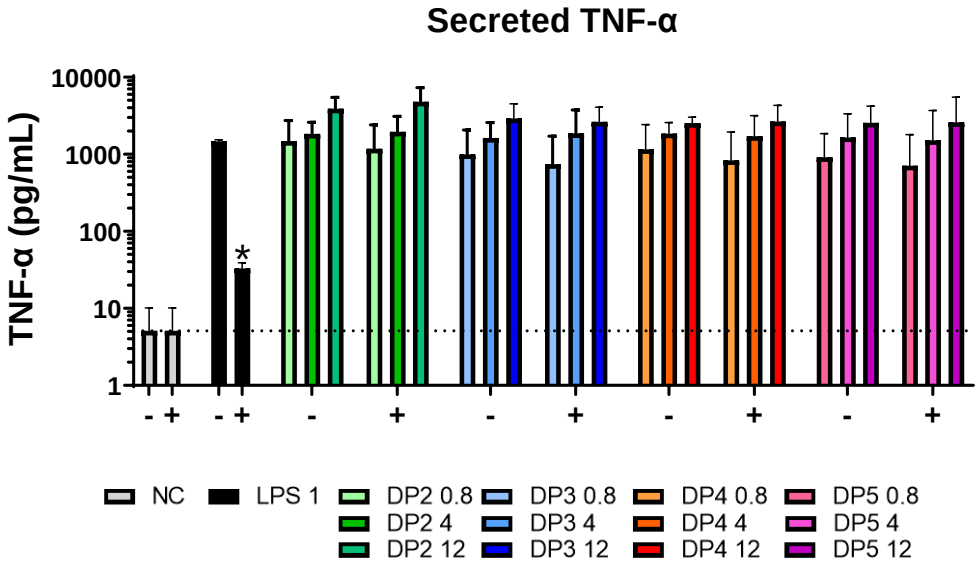

Figure 5.6 Effects of pre-treating B-GOS® DP2 – DP5 fractions or LPS positive control with (+) or without (-) PMB for 24 h on Th1 cytokines IL-6 and TNF-α. Healthy PBMCs (*n*= 5) were incubated for 24 h with DP2 – DP5 B-GOS® fractions or LPS, pre-treated with or without PMB. Unstimulated cells (NC) were used as control. Data are expressed as mean ± SD. Two-way ANOVA followed by Bonferroni's *post-hoc* test was performed. Because all B-GOS® fractions caused a significant increase in all secreted mediators, only significant differences between conditions with or without PMB (+/-) are represented. A) *p= 0.0076. B) *p= 0.0244.

A

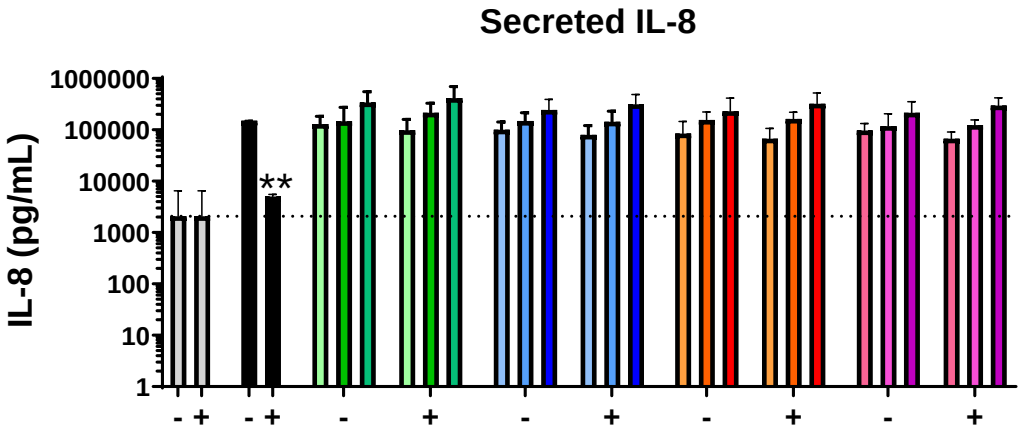

B

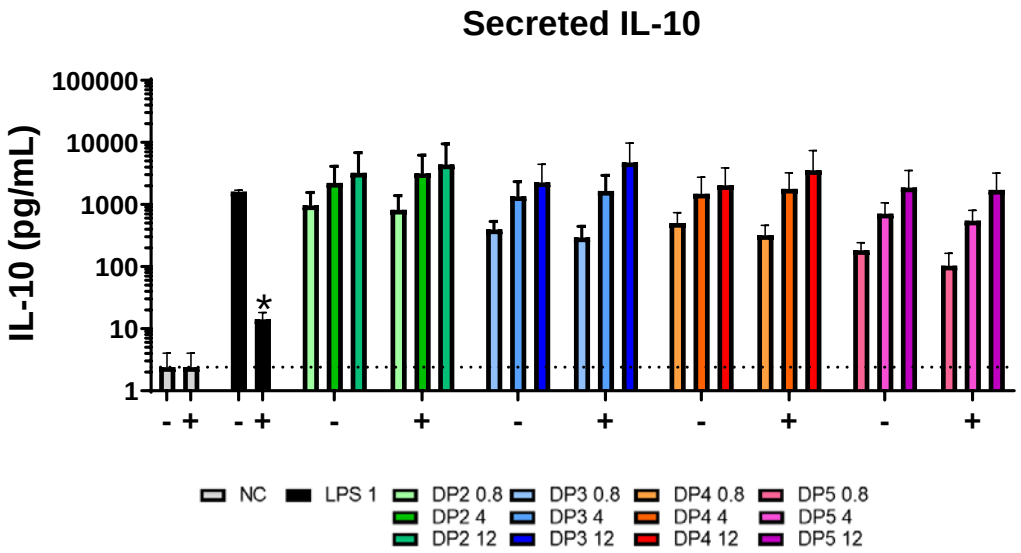

Figure 5.7 Effects of pre-treating B-GOS® DP2 – DP5 fractions or LPS positive control with (+) or without (-) PMB for 24 h on the chemokines (IL-8) and Th1/Th2 cytokines (IL-10). Healthy PBMCs (*n*= 5) were incubated for 24 h with DP2 – DP5 B-GOS® fractions or LPS, pre-treated with or without PMB. Unstimulated cells (NC) were used as control. Data are expressed as mean ± SD. Two-way ANOVA followed by Bonferroni's *post-hoc* test was performed. Because all B-GOS® fractions caused a significant increase in all secreted mediators, only significant differences between conditions with or without PMB (+/-) are represented. A) **p*= 0.0039. B) **p*= 0.0252.

5.4.2 Effects of B-GOS® fractions, 3'-GL and whole B-GOS® in presence and in absence of poly(I:C) upon PBMC viability

PBMCs tolerated 24 h stimulation with DP2 – DP5 B-GOS® fractions, 3'-GL or whole B-GOS®, with viability always above the acceptable limit for cryopreserved cells (≥ 70%). No differences were seen between stimulated PBMCs compared to unstimulated PBMCs, nor between PBMCs pre-treated with DP3 B-GOS® fraction, 3'-GL or whole B-GOS® for 1 h and then cultured for 24 h with poly(I:C) at 10 µg/mL compared to those cultured in absence of poly(I:C), as shown in Figure 5.8.

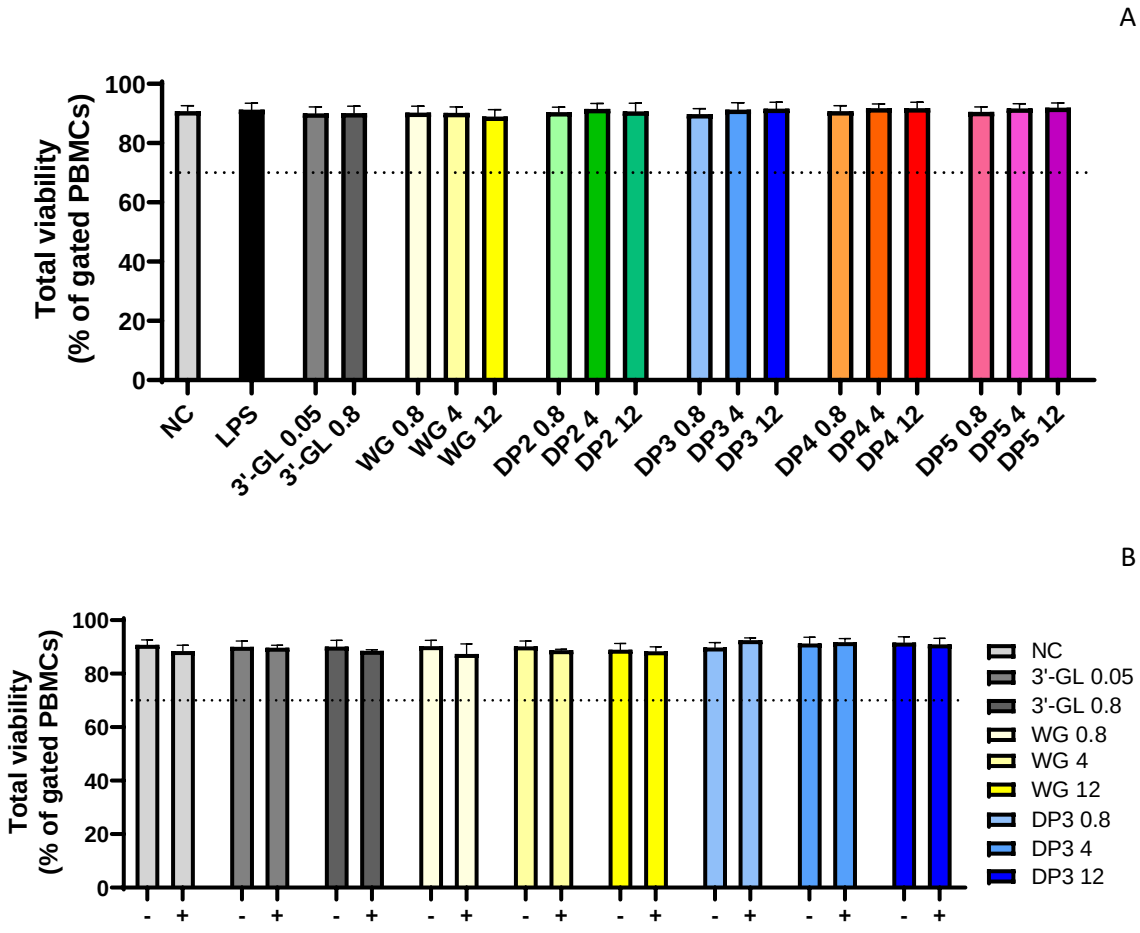

Figure 5.8 Total viability of healthy PBMCs cultured with B-GOS® fractions, 3'-GL or whole B-GOS®, in presence (+) or in absence (-) of poly(I:C). A) Healthy PBMCs (*n*= 5) were incubated for 24 h with DP2 – DP5 B-GOS® fractions, 3'-GL, whole B-GOS® or LPS. B) Healthy PBMCs (*n*= 5) were pre-treated for 1 h with DP3 B-GOS® fraction, 3'-GL or whole B-GOS® and then stimulated for 24 h with (+) or without (-) poly(I:C). Unstimulated cells (NC) were used as control. Data are expressed as mean ± SD.

5.4.3 Effects of B-GOS® fractions, 3'-GL and whole B-GOS® in presence and in absence of poly(I:C) upon PBMC phenotypes

Incubation of PBMCs for 24 h with DP2 – DP5 B-GOS® fractions, 3'-GL or whole B-GOS® did not affect the frequencies (or recovery) of any cell subsets compared to unstimulated control (Figure 5.9 – Figure 5.11). Similarly, when PBMCs were pre-incubated with DP3 B-GOS® fraction, 3'-GL or whole B-GOS® for 1 h before 24 h challenge with poly(I:C) or when they were stimulated with poly(I:C) alone, no changes in the frequencies of any PBMC subsets were observed (Figure 5.12 and Figure 5.13). Analysed PBMC subsets included lymphocytes and monocytes (both expressed as % of live PBMCs), T cells, B cells, natural killer (NK) cells and NKT cells (all expressed as % of lymphocytes), cytotoxic T cells and T helper cells (expressed as % of T cells).

A

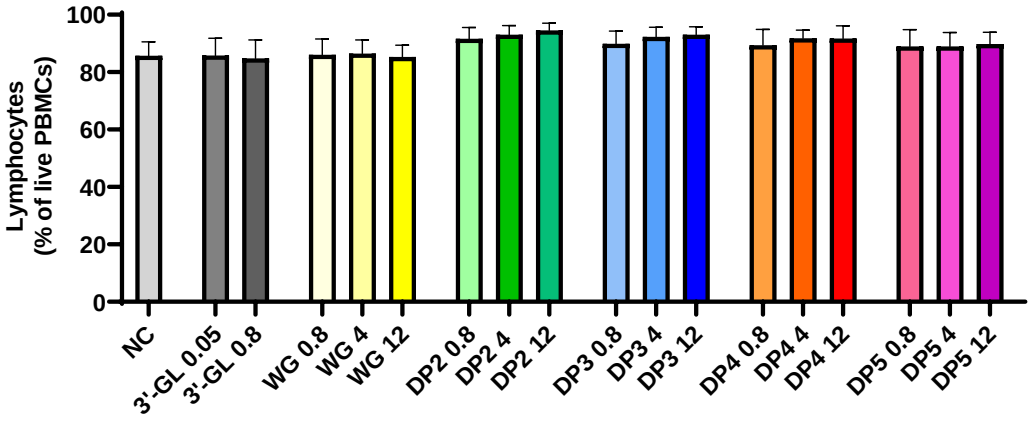

B

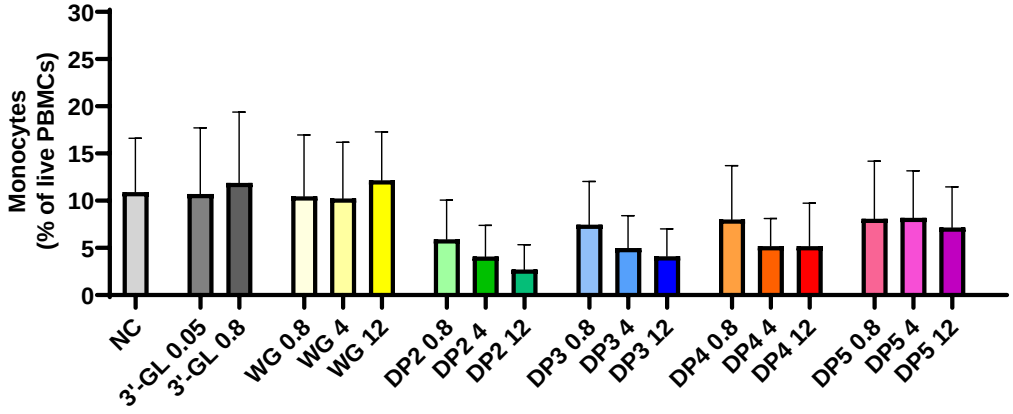

Figure 5.9 Frequencies of lymphocytes and monocytes from healthy PBMCs (*n*= 5) following 24 h culture with DP2 – DP5 B-GOS® fractions, 3'-GL or whole B-GOS®. Unstimulated cells (NC) were used as control. Data are expressed as mean ± SD.

A

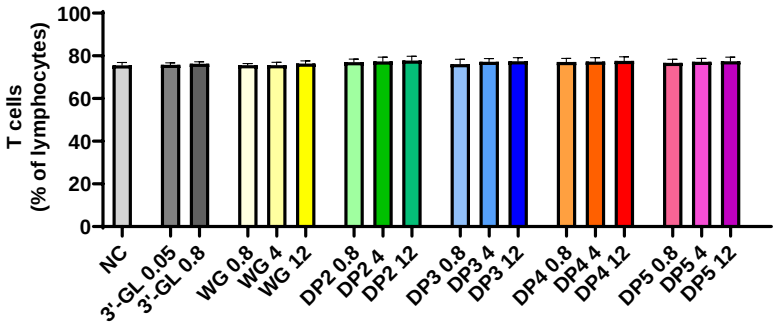

B

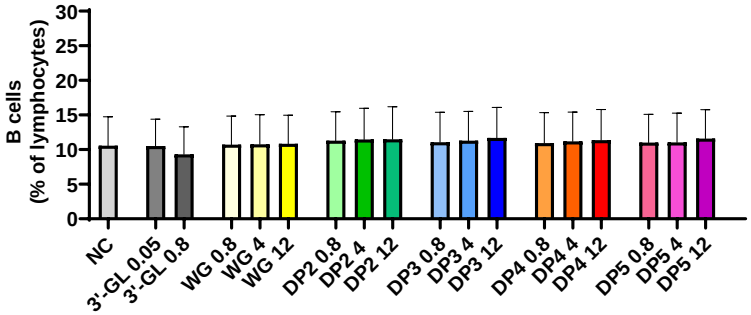

C

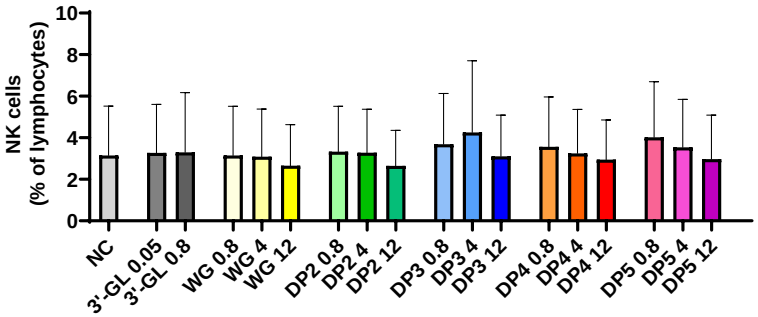

D

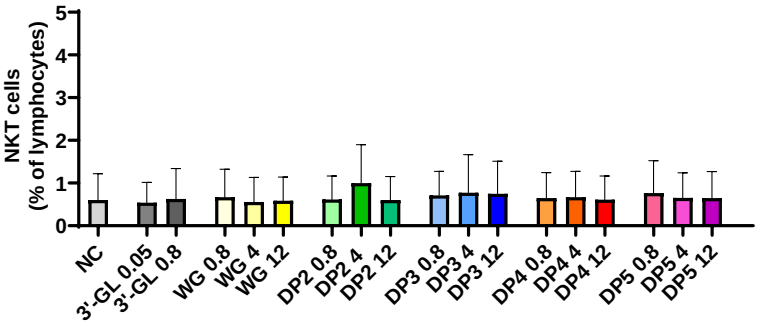

Figure 5.10 Frequencies of T cells, B cells, NK cells and NKT cells from healthy PBMCs (*n*= 5) following 24 h culture with DP2 – DP5 B-GOS® fractions, 3'-GL or whole B-GOS®. Unstimulated cells (NC) were used as control. Data are expressed as mean ± SD.

A

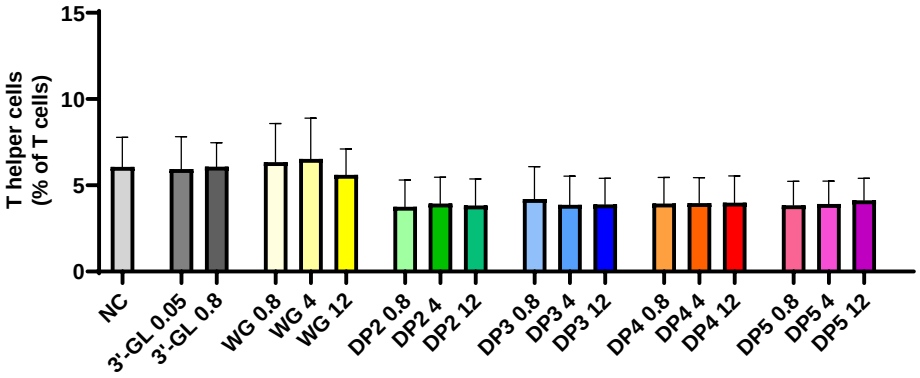

B

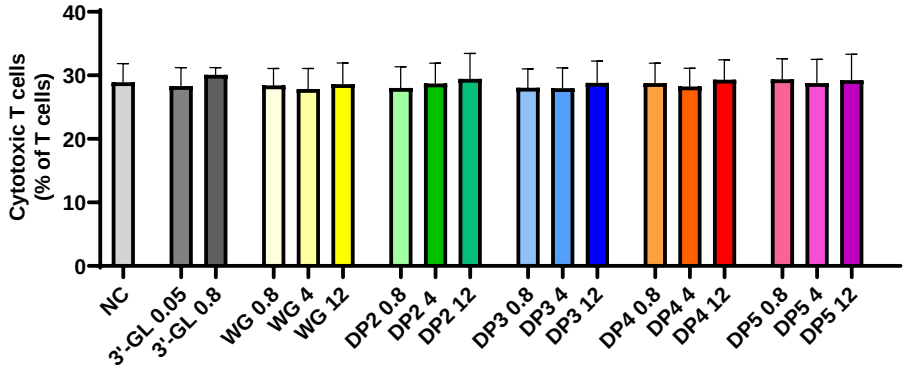

Figure 5.11 Frequencies of T helper cells and cytotoxic T cells from healthy PBMCs (*n*= 5) following 24 h culture with DP2 – DP5 B-GOS® fractions, 3'-GL or whole B-GOS®. Unstimulated cells (NC) were used as control. Data are expressed as mean ± SD.

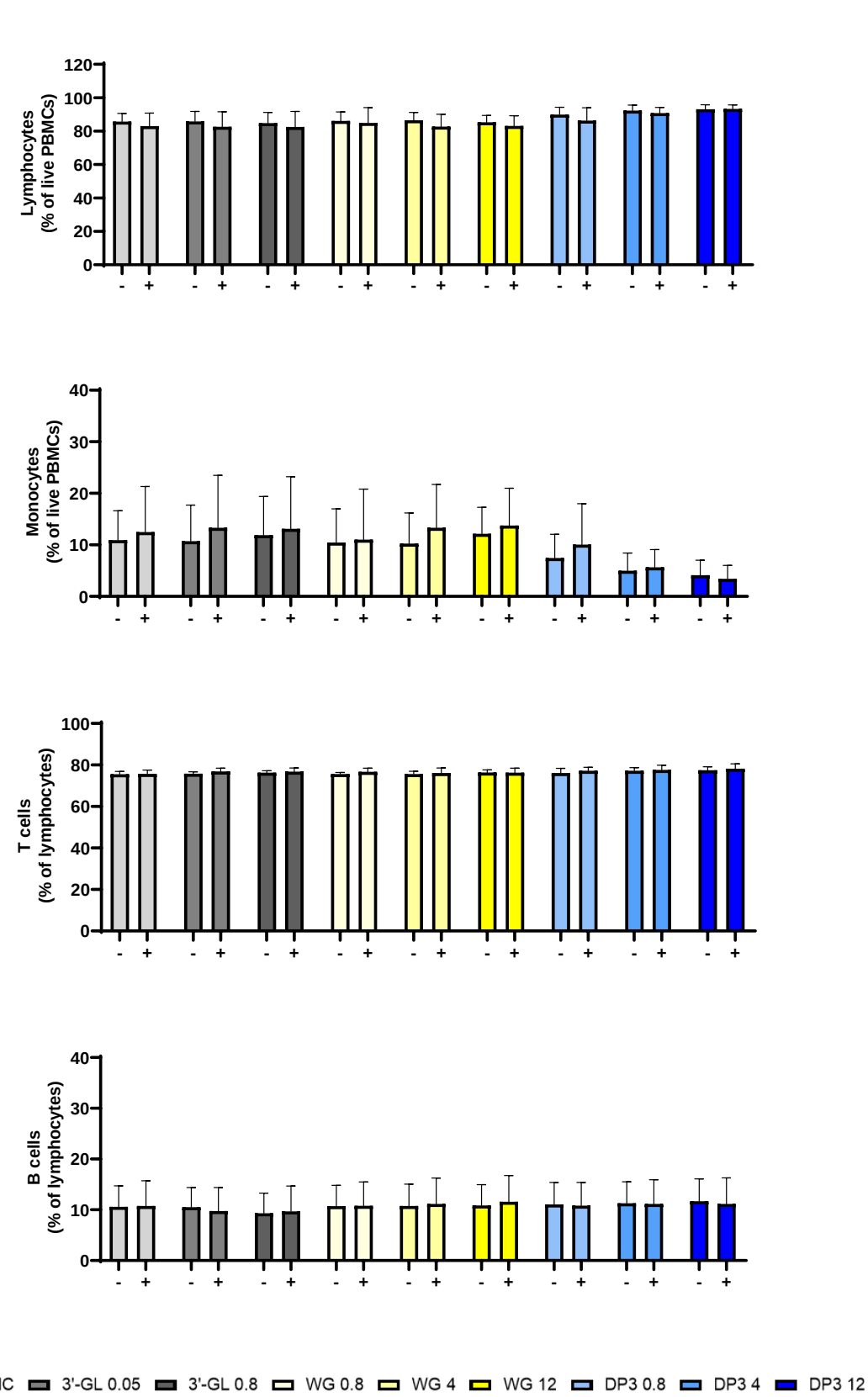

Figure 5.12 Frequencies of lymphocytes, monocytes, T cells and B cells from healthy PBMCs (*n*= 5) after 1 h pre-incubation with DP2 – DP5 B-GOS® fractions, 3'-GL or whole B-GOS® followed by 24 challenge with (+) or without (-) poly(I:C). Unstimulated cells (NC) were used as control. Data are expressed as mean ± SD.

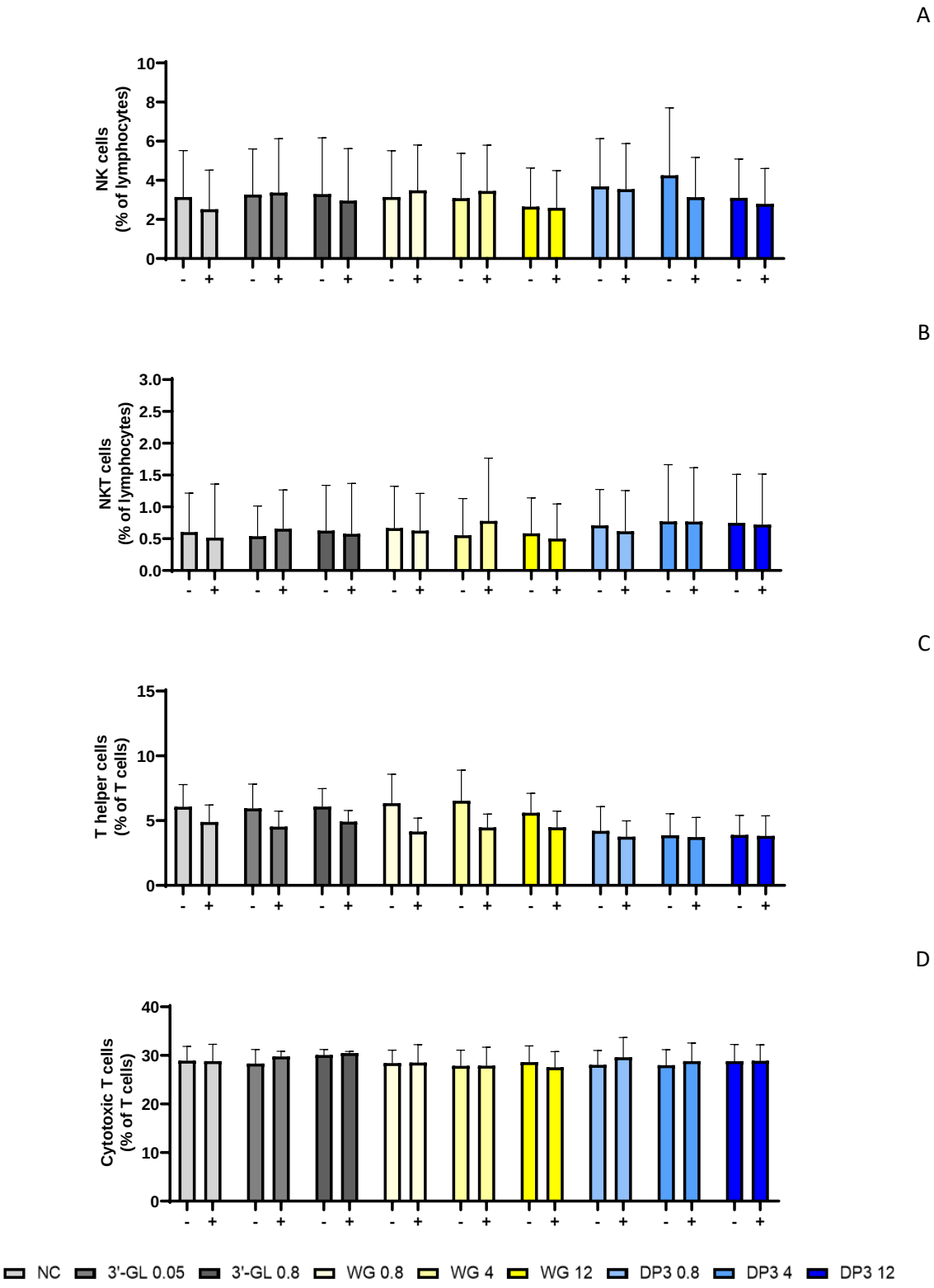

Figure 5.13 Frequencies of NK cells, NKT cells, T helper cells and cytotoxic T cells from healthy PBMCs (*n*= 5) after 1 h pre-incubation with DP2 – DP5 B-GOS® fractions, 3'-GL or whole B-GOS® followed by 24 challenge with (+) or without (-) poly(I:C). Unstimulated cells (NC) were used as control. Data are expressed as mean ± SD. B) For DP3 0.8 without poly(I:C), *n*= 4 (1 outlier was removed).

5.4.4 Effects of isolated B-GOS® fractions, 3'-GL and whole B-GOS® in presence and in absence of poly(I:C) upon the activation marker CD69

Stimulation for 24 h with DP2 – DP5 B-GOS® fractions alone resulted in higher percentages of lymphocytes (DP2, DP3, DP4 and DP5, all $p< 0.01$), T cells (DP2, DP3, DP4 and DP5, all $p< 0.05$), B cells (DP2, DP3 and DP4, all $p< 0.05$), cytotoxic T cells (DP2, DP3 and DP4, all $p< 0.05$) and T helper cells (DP2 and DP3, all $p< 0.05$) expressing CD69 compared to unstimulated control (Figure 5.14 and Figure 5.15). Not only there were higher percentages of cells expressing CD69 following stimulation with B-GOS® fractions, but they also presented higher CD69 (MFI) expression, as shown in lymphocytes (DP2 and DP3, both $p< 0.05$), monocytes (DP4, $p< 0.05$) and B cells (DP2, DP3 and DP4, all $p< 0.01$) compared to unstimulated control (Figure 5.16 and Figure 5.17). While all B-GOS® fractions promoted T cell activation, incubation with whole B-GOS® or with 3'-GL did not alter the frequencies of any CD69-expressing cells (Figure 5.14 and Figure 5.15) nor it did affect their expression levels (Figure 5.16 and Figure 5.17).

A

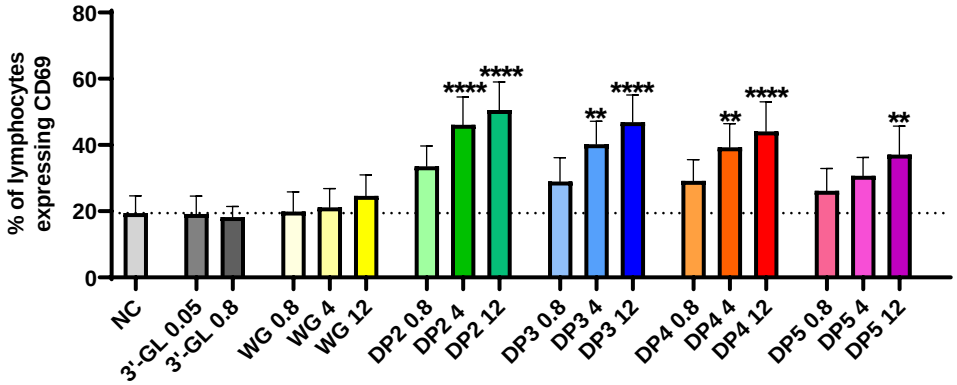

B

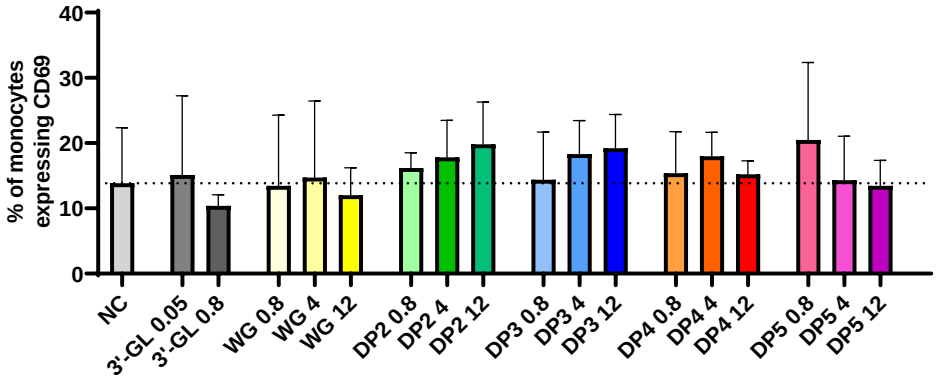

Figure 5.14 Frequencies of CD69-expressing lymphocytes and monocytes from healthy PBMCs (*n*= 5) following 24 h culture with DP2 – DP5 B-GOS® fractions, 3'-GL or whole B-GOS®. Unstimulated cells (NC) were used as control. Data are expressed as mean ± SD. One-way ANOVA followed by Dunnett's *post-hoc* test was performed. Significant differences between stimulated cells *vs* unstimulated control (NC) are marked with an asterisk (**p< 0.01; ****p< 0.0001).

A

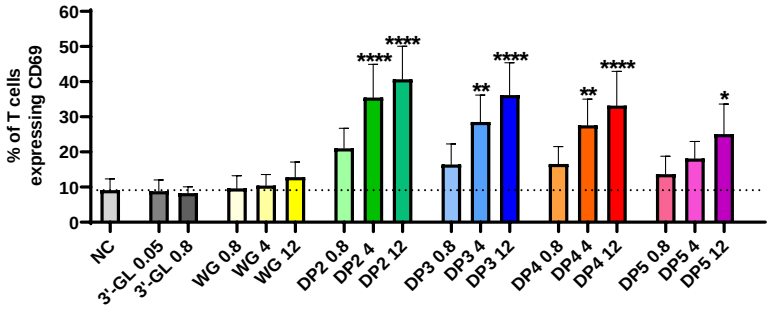

B

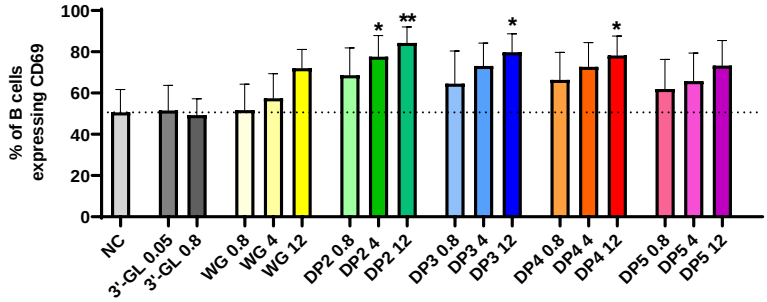

C

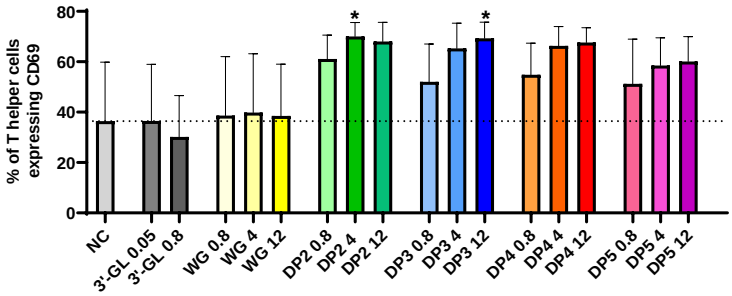

D

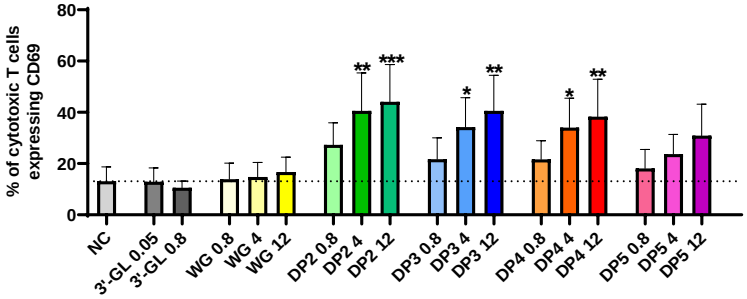

Figure 5.15 Frequencies of CD69-expressing T cells, B cells, T helper cells and cytotoxic T cells from healthy PBMCs (*n*= 5) following 24 h culture with DP2 – DP5 B-GOS® fractions, 3'-GL or whole B-GOS® Unstimulated cells (NC) were used as control. Data are expressed as mean ± SD. One-way ANOVA followed by Dunnett's *post-hoc* test was performed. Significant differences between stimulated cells *vs* unstimulated control (NC) are marked with an asterisk (**p*< 0.05; ***p*< 0.01; ****p*< 0.001; *****p*< 0.0001).

A

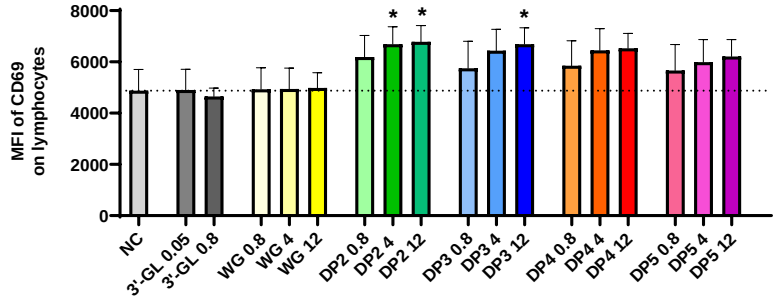

B

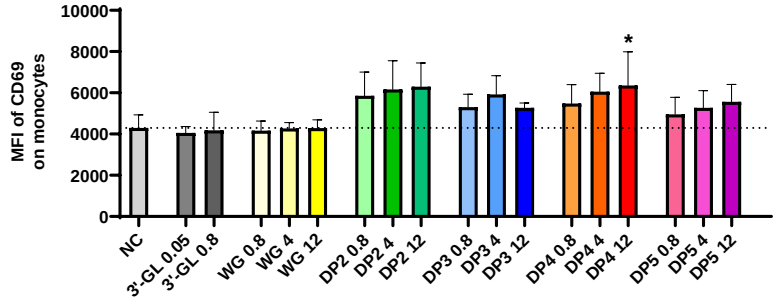

C

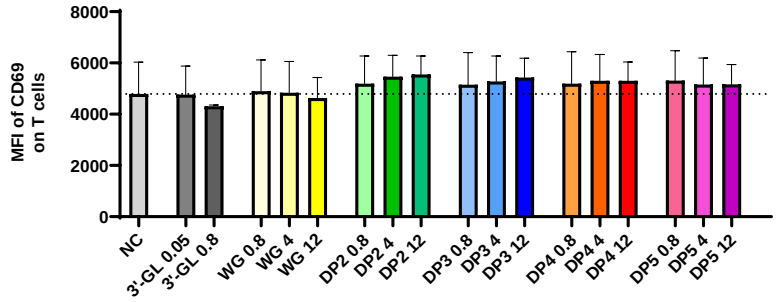

D

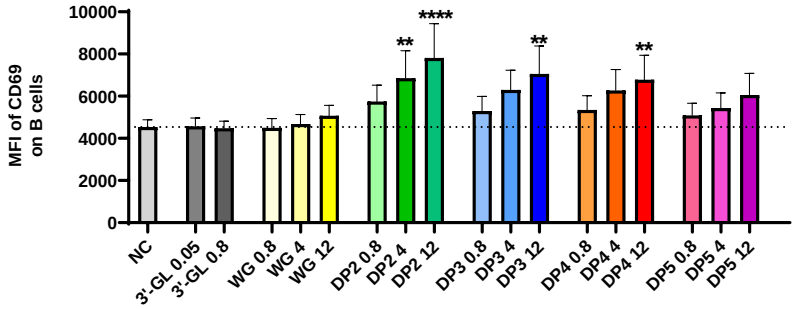

Figure 5.16 CD69 (MFI) expression on lymphocytes, monocytes, T cells and B cells from healthy PBMCs (*n*= 5) following 24 h culture with DP2 – DP5 B-GOS® fractions, 3'-GL or whole B-GOS®. Unstimulated cells (NC) were used as control. Data are expressed as mean ± SD. One-way ANOVA followed by Dunnett's *post-hoc* test was performed. Significant differences between stimulated cells *vs* unstimulated control (NC) are marked with an asterisk (*p< 0.05; **p< 0.01; ****p< 0.0001).

A

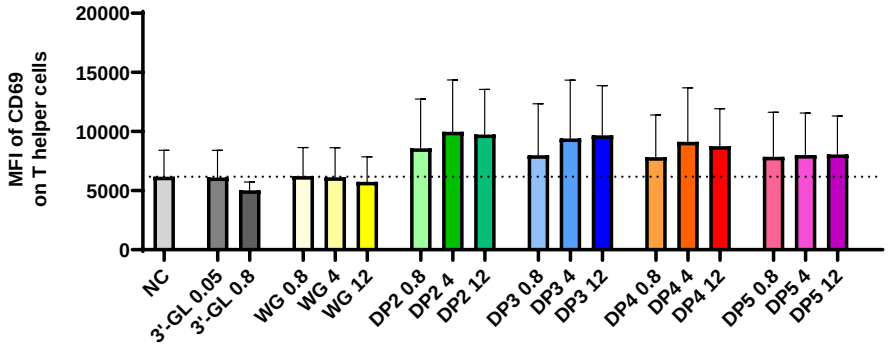

B

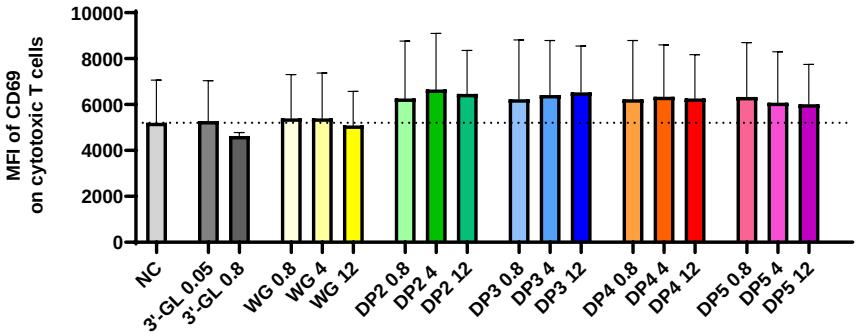

Figure 5.17 CD69 (MFI) expression on T helper cells and cytotoxic T cells from healthy PBMCs (*n*= 5) following 24 h culture with DP2 – DP5 B-GOS® fractions, 3'-GL or whole B-GOS®. Unstimulated cells (NC) were used as control. Data are expressed as mean ± SD.

Challenge with the TLR3-agonist poly(I:C) alone led to higher percentages of lymphocytes (p< 0.0001), monocytes (p< 0.0001), T cells (p= 0.0005) and B cells (p= 0.0122) expressing CD69 compared to unstimulated control (Figure 5.18 and Figure 5.19) as well as to an increased CD69 (MFI) expression in lymphocytes (p= 0.0465), monocytes (p= 0.0015) and B cells (p= 0.0402) (Figure 5.20 and Figure 5.21). Pre-incubation of PBMCs with 3'-GL failed to decrease poly(I:C)-induced CD69 expression, both in terms of percentages of cells expressing CD69 (Figure 5.18 and Figure 5.19) and brightness (MFI) of CD69 expression (Figure 5.20 and Figure 5.21). Pre-incubation of cells with DP3 B-GOS® fraction before poly(I:C) challenge led to even higher percentages of lymphocytes (DP3 4 and DP3 12, both p< 0.01) and T cells (DP3 4 and DP3 12, both p< 0.01) expressing CD69 but lower percentages of monocytes (DP3 0.8, DP3 4 and DP3 12, all p< 0.0001) expressing CD69 compared to poly(I:C) challenge alone (Figure 5.18 and Figure 5.19). While no changes in CD69 (MFI) expression were seen on lymphocytes and T cells, monocytes expressed less CD69 when pre-incubated with DP3 B-GOS® fraction and challenged with poly(I:C) (DP3 0.8, p= 0.0051) compared to poly(I:C) alone (Figure 5.20). Lower frequencies of monocytes expressing CD69 were seen when PBMCs were pre-incubated with whole B-GOS® before poly(I:C) addition (WG 12, p= 0.0188), compared to poly(I:C) alone (Figure 5.18).

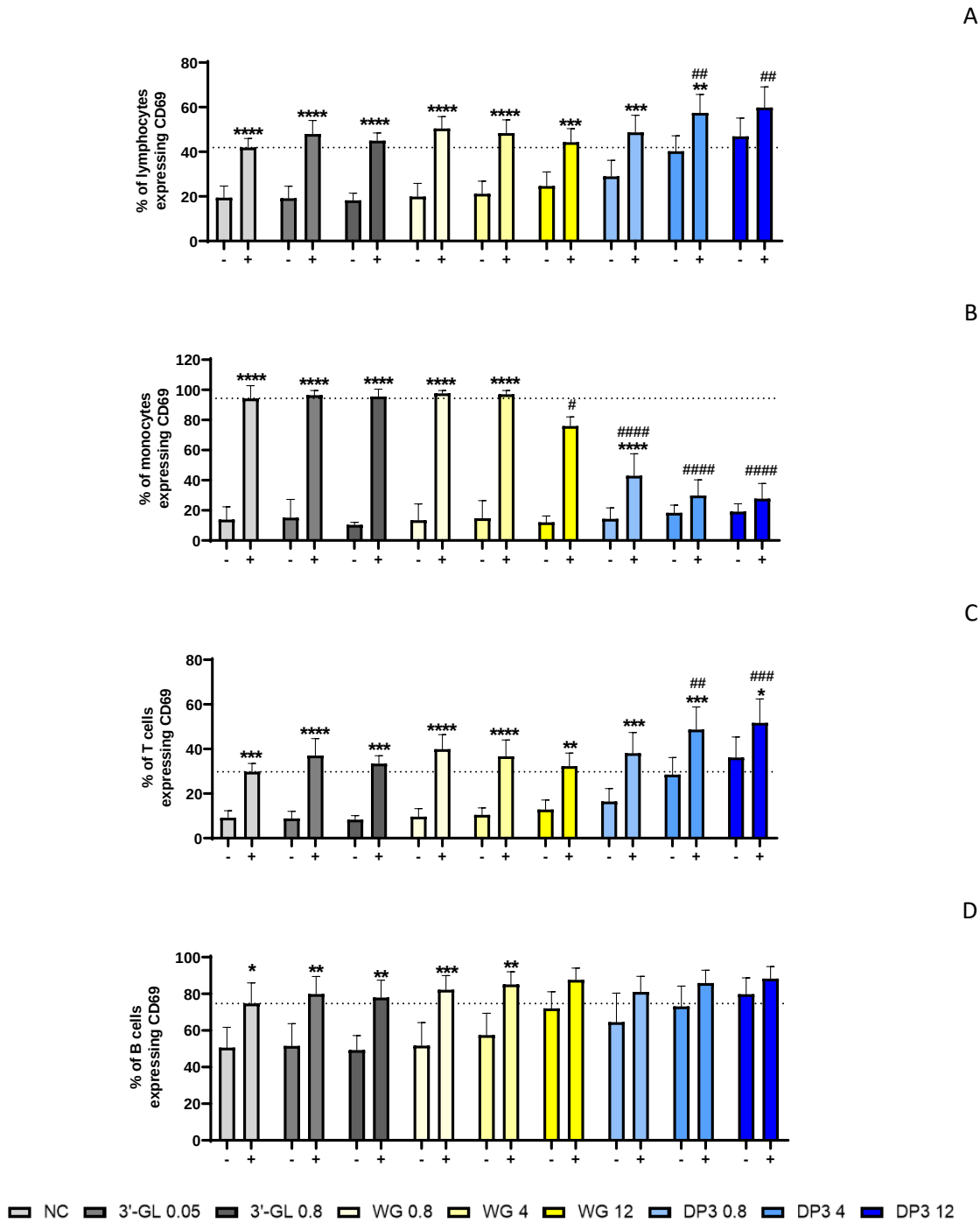

Figure 5.18 Frequencies of CD69-expressing lymphocytes, monocytes, T cells and B cells from healthy PBMCs (*n*= 5) after 1 h pre-incubation with DP2 – DP5 B-GOS® fractions, 3'-GL or whole B-GOS® followed by 24 challenge with (+) or without (-) poly(I:C). Unstimulated cells (NC) were used as control. Data are expressed as mean ± SD. Two-way ANOVA followed by Bonferroni's or Dunnett's *post-hoc* test was performed. Significant differences between conditions with (+) or without (-) poly(I:C) are marked with an asterisk: *p< 0.05; **p< 0.01; ***p< 0.001; ****p< 0.0001. Significant differences between pre-incubated cells challenged with poly(I:C) *vs* poly(I:C) alone are marked with a hash: $^{\#\#}p$< 0.01; $^{\#\#\#}p$< 0.001; $^{\#\#\#\#}p$< 0.0001.

A

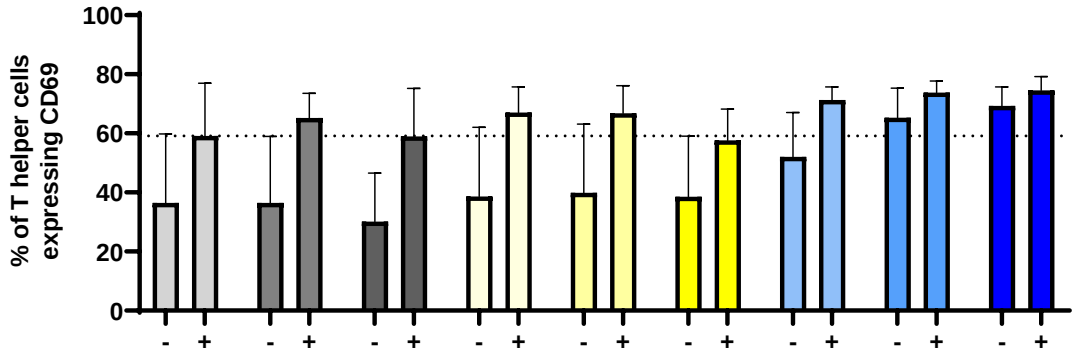

B

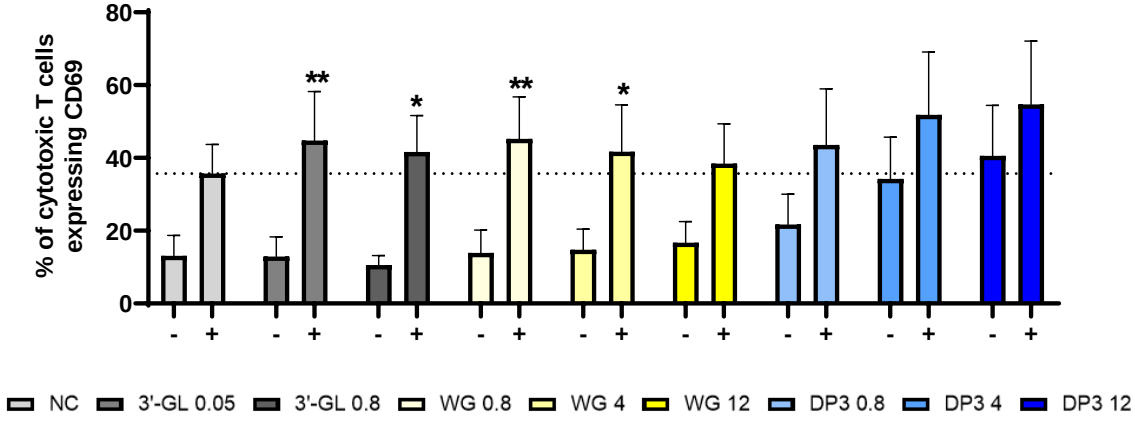

Figure 5.19 Frequencies of CD69-expressing T helper cells and cytotoxic T cells from healthy PBMCs (*n*= 5) after 1 h pre-incubation with DP2 – DP5 B-GOS® fractions, 3'-GL or whole B-GOS® followed by 24 challenge with (+) or without (-) poly(I:C). Unstimulated cells (NC) were used as control. Data are expressed as mean ± SD. Two-way ANOVA followed by Bonferroni's or Dunnett's *post-hoc* test was performed. Significant differences between conditions with (+) or without (-) poly(I:C) are marked with an asterisk: *p< 0.05; **p< 0.01.

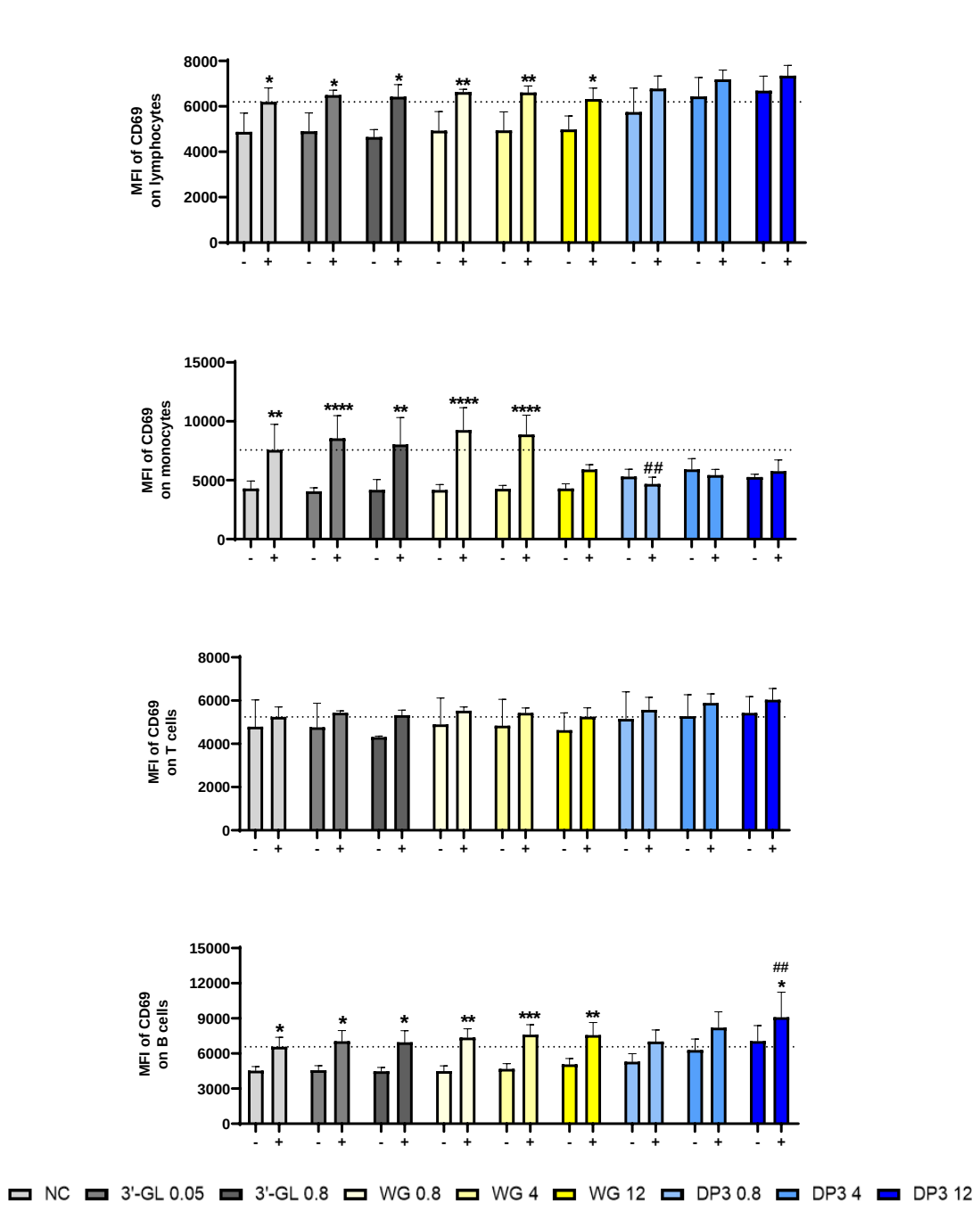

Figure 5.20 CD69 (MFI) expression on lymphocytes, monocytes, T cells and B cells from healthy PBMCs (*n*= 5) after 1 h pre-incubation with DP2 – DP5 B-GOS® fractions, 3'-GL or whole B-GOS® followed by 24 challenge with (+) or without (-) poly(I:C). Unstimulated cells (NC) were used as control. Data are expressed as mean ± SD. Two-way ANOVA followed by Bonferroni's or Dunnett's *post-hoc* test was performed. Significant differences between conditions with (+) or without (-) poly(I:C) are marked with an asterisk: *p< 0.05; **p< 0.01; ***p< 0.001; ****p< 0.0001. Significant differences between pre-incubated cells challenged with poly(I:C) *vs* poly(I:C) alone are marked with a hash: $^{\#\#}p$< 0.01.

A

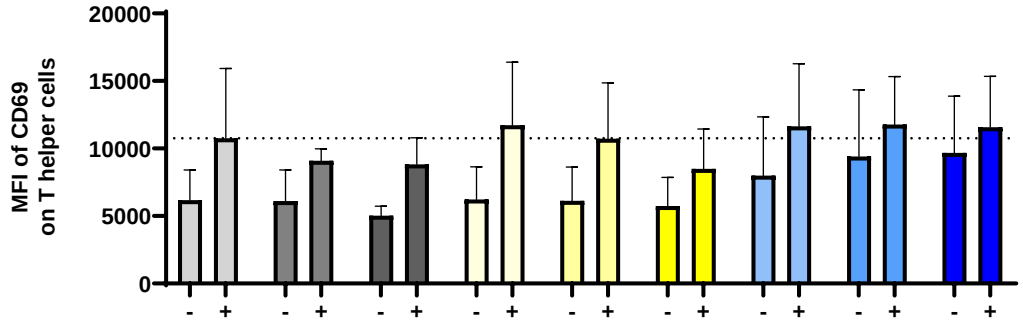

B

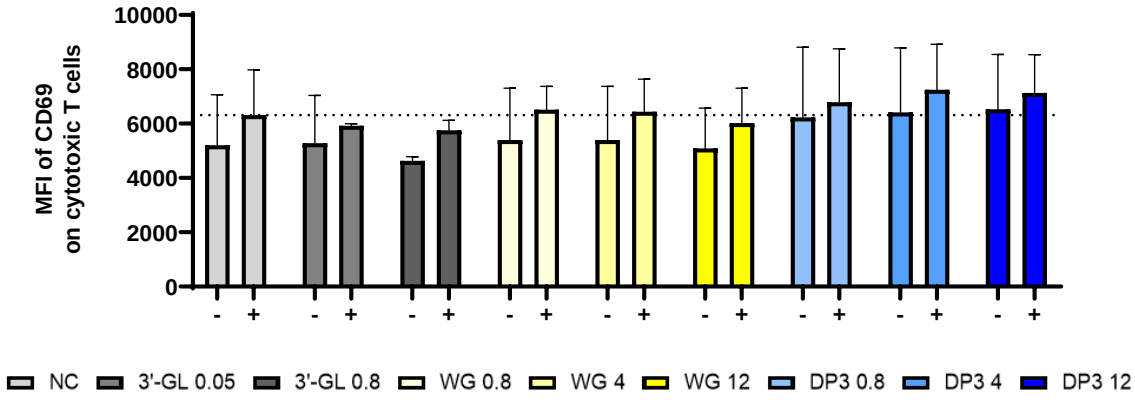

Figure 5.21 CD69 (MFI) expression on T helper cells and cytotoxic T cells from healthy PBMCs (*n*= 5) after 1 h pre-incubation with DP2 – DP5 B-GOS® fractions, 3'-GL or whole B-GOS® followed by 24 challenge with (+) or without (-) poly(I:C). Unstimulated cells (NC) were used as control. Data are expressed as mean ± SD.

Table 5.1 and Table 5.2 summarise the results on CD69 expression. Overall, culture with B-GOS® fractions significantly increased the percentage of lymphocytes and their subsets expressing CD69, with lower DP fractions having the most effects, particularly on T helper cells. This was also associated with increased relative expression of CD69 on B cells, but not upon T lymphocytes. The TLR3-agonist poly(I:C) was effective in inducing PBMC activation, as seen by higher percentages of PBMCs subsets expressing CD69 together with an increased relative expression of CD69 on lymphocytes, monocytes and B cells. Pre-incubation with DP3 B-GOS® fraction before poly(I:C) challenge enhanced the effects of the TLR3 agonist on the percentages of lymphocytes and T cells expressing CD69 as well as on the relative expression of CD69 on B cells. Conversely, it led to lower percentages of monocytes expressing CD69, which was also associated with lower relative expression of CD69 on their surface, when compared to poly(I:C) challenge alone. Lower frequencies of monocytes expressing CD69 were seen also when PBMCs were pre-incubated with whole B-GOS® compared to poly(I:C) challenge alone.

Table 5.1 Direction of changes in the frequencies of CD69-expressing cells following culture with DP2 – DP5 B-GOS® fractions, 3'-GL or whole B-GOS®, in presence or in absence of poly(I:C).

	% of PBMC subsets expressing CD69												
	Stimuli vs NC						*With Poly(I:C) vs without Poly(I:C)*				*Stimuli + Poly(I:C) vs Poly(I:C)*		
	3'-GL	WG	DP2	DP3	DP4	DP5	Poly(I:C)	3'-GL	WG	DP3	3'-GL	WG	DP3
Lymphocytes	↔	↔	↑	↑	↑	↑	↑	↑	↑	↑	↔	↔	↑
Monocytes	↔	↔	↔	↔	↔	↔	↑	↑	↑	↑	↔	↓	↓
T cells	↔	↔	↑	↑	↑	↑	↑	↑	↑	↑	↔	↔	↑
B cells	↔	↔	↑	↑	↑	↔	↑	↑	↑	↔	↔	↔	↔
Cytotoxic T cells	↔	↔	↑	↑	↑	↔	↔	↑	↑	↔	↔	↔	↔
T helper cells	↔	↔	↑	↑	↔	↔	↔	↔	↔	↔	↔	↔	↔

Arrows indicate an increase (↑, in yellow), decrease (↓, in blue) or no changes (↔) in the frequencies of PBMC subsets expressing CD69 following stimulation.

Table 5.2 Direction of changes in CD69 (MFI) expression following culture with DP2 – DP5 B-GOS® fractions, 3'-GL or whole B-GOS®, in presence or in absence of poly(I:C).

	MFI of CD69 on PBMC subsets												
	Stimuli vs NC						*With Poly(I:C) vs without Poly(I:C)*				*Stimuli + Poly(I:C) vs Poly(I:C)*		
	3'-GL	WG	DP2	DP3	DP4	DP5	Poly(I:C)	3'-GL	WG	DP3	3'-GL	WG	DP3
Lymphocytes	↔	↔	↑	↑	↔	↔	↑	↑	↑	↔	↔	↔	↔
Monocytes	↔	↔	↔	↔	↑	↔	↑	↑	↑	↔	↔	↔	↓
T cells	↔	↔	↔	↔	↔	↔	↔	↔	↔	↔	↔	↔	↔
B cells	↔	↔	↑	↑	↑	↔	↑	↑	↑	↑	↔	↔	↑
Cytotoxic T cells	↔	↔	↔	↔	↔	↔	↔	↔	↔	↔	↔	↔	↔
T helper cells	↔	↔	↔	↔	↔	↔	↔	↔	↔	↔	↔	↔	↔

Arrows indicate an increase (↑, in yellow), decrease (↓, in blue) or no changes (↔) in CD69 (MFI) expression on PBMC subsets following stimulation.

5.4.5 Effects of B-GOS® fractions, 3'-GL and whole B-GOS® upon secreted cytokines

Stimulation of PBMCs with the TLR3-agonist poly(I:C) alone did not increase the levels of any of the studied cytokines compared to unstimulated control, as shown for IL-6 and TNF-α (Figure 5.22 and Appendix F). For this reason, only the effects of isolated B-GOS® fractions, 3'-GL and whole B-GOS® alone and not the co-culture data with poly(I:C) were presented.

While stimulation with whole B-GOS® or 3'-GL did not cause significant changes in secreted cytokines, incubation with PMB-treated DP2 – DP5 B-GOS® fractions led to higher production of IL-1α, IL-1β, IL-6, IL-8, IL-10, granzyme B, MIP-1α and TNF-α by PBMCs compared to unstimulated control (Section 5.4.1 and Appendix F). Consistent with observations of changes in cellular activation markers, the effects on secreted mediators were more pronounced in presence of B-GOS® fractions with smaller DP (*e.g.* DP2 *vs* DP5).

Since there was an increase in both pro-inflammatory and anti-inflammatory cytokines after culture with B-GOS® fractions, pro-inflammatory to anti-inflammatory cytokine ratios were calculated to better understand the direction of change (immunostimulation *vs* immunomodulation, which refer to the increased activity of the immune system or its regulation to restore homeostasis, respectively). The amounts of secreted IL-1α, IL-1β, IL-6, IL-8, granzyme B, MIP-1α or TNF-α were divided by the amount of secreted IL-10 to achieve pro-inflammatory to anti-inflammatory ratios. Interestingly, only whole B-GOS® but not isolated B-GOS® fractions significantly increased cytokine ratios. Higher IL-8 : IL-10 (WG 12, $p < 0.0001$) and granzyme B : IL-10 (WG 12, $p < 0.001$) were observed in PBMCs stimulated with whole B-GOS® compared to unstimulated control (Figure 5.23 and Figure 5.24). While B-GOS® fractions induced the release of pro-inflammatory cytokines, they also promoted the secretion of high levels of anti-inflammatory IL-10 that contributed to maintain immune balance (Figure 5.23 and Figure 5.24). There was a trend for lower granzyme B : IL-10 in PBMCs incubated with B-GOS® fractions compared to unstimulated control (DP2, DP3 and DP4, all $p = 0.09$) (Figure 5.24).

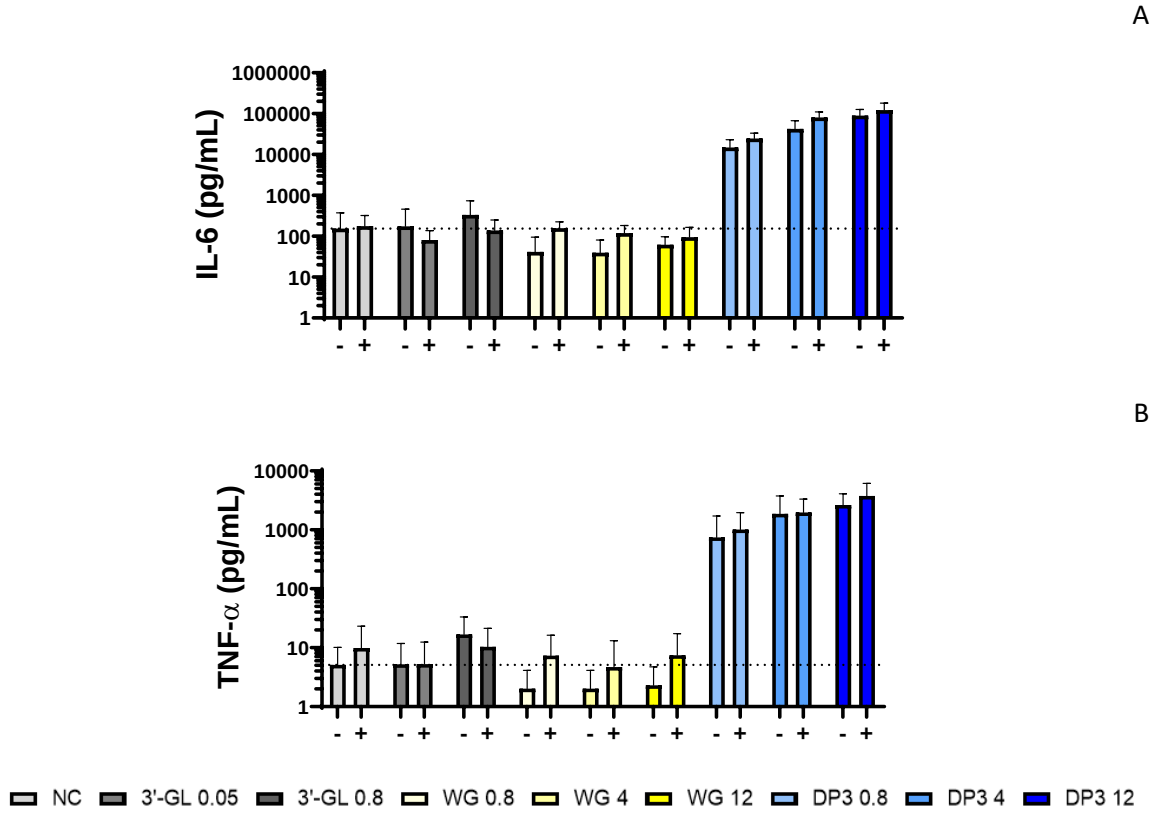

Figure 5.22 Levels of IL-6 and TNF-α secreted by healthy PBMCs ($n = 5$) after 1 h pre-incubation with DP2 – DP5 B-GOS® fractions, 3'-GL or whole B-GOS® followed by 24 challenge with (+) or without (-) poly(I:C). Unstimulated cells (NC) were used as control. Data are expressed as mean ± SD.

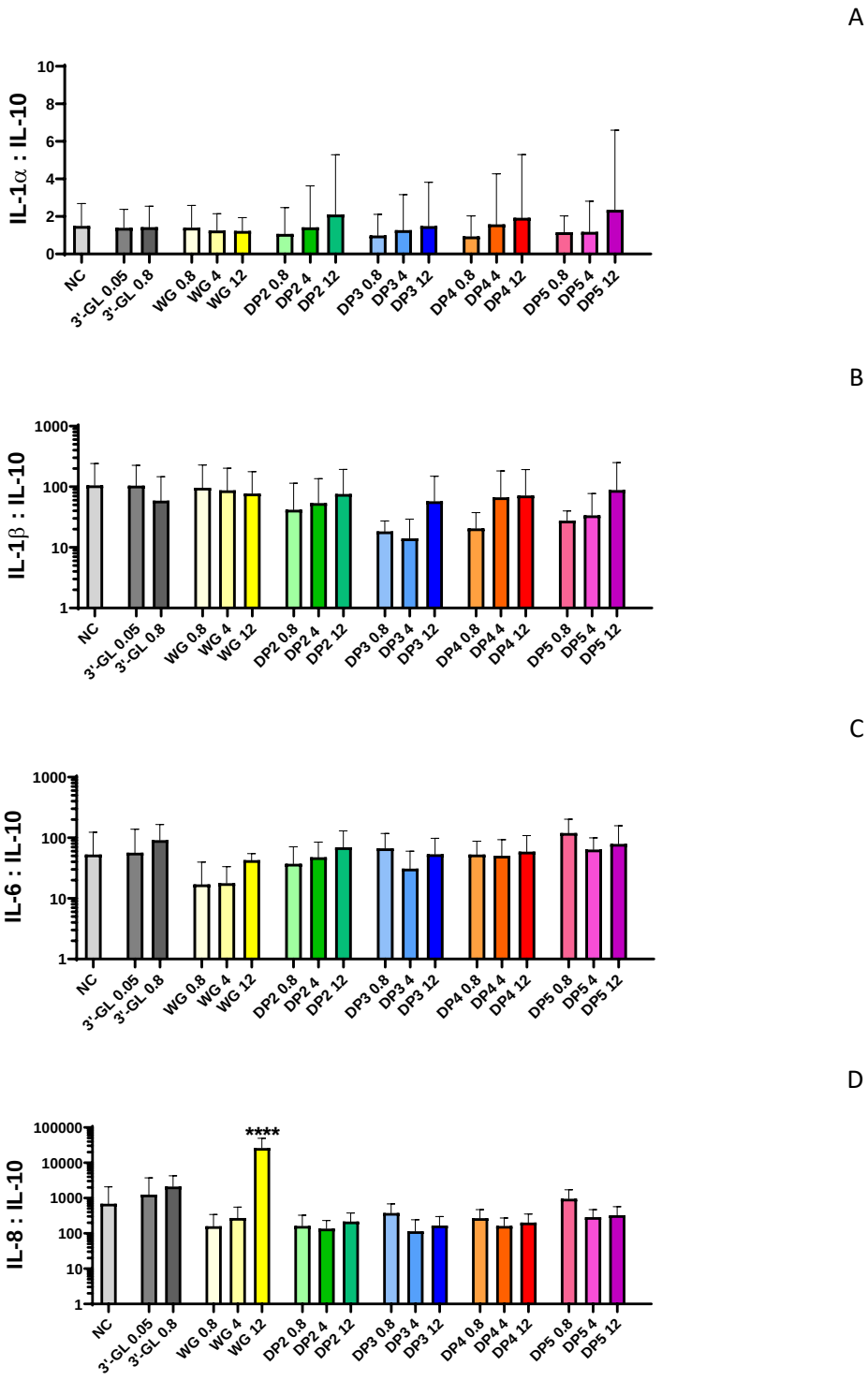

Figure 5.23 Pro-inflammatory to anti-inflammatory cytokine ratios for healthy PBMCs (*n*= 5) cultured with DP2 – DP5 B-GOS® fractions, 3'-GL or whole B-GOS®. Unstimulated cells (NC) were used as control. Data are expressed as mean ± SD. One-way ANOVA followed by Dunnett's *post-hoc* test was performed. Significant differences between stimulated cells *vs* unstimulated control (NC) are marked with an asterisk (****p< 0.0001).

A

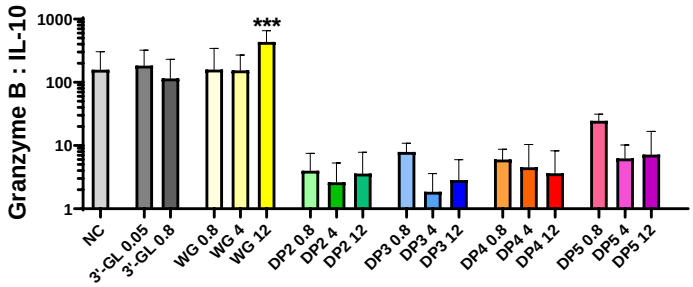

B

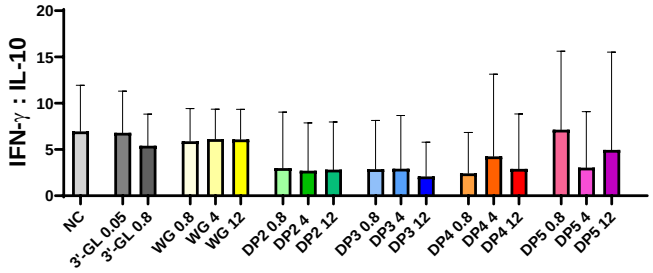

C

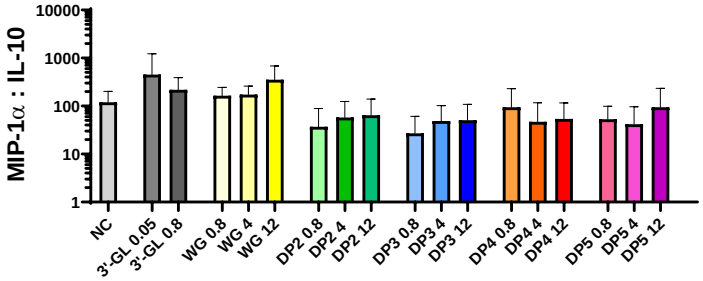

D

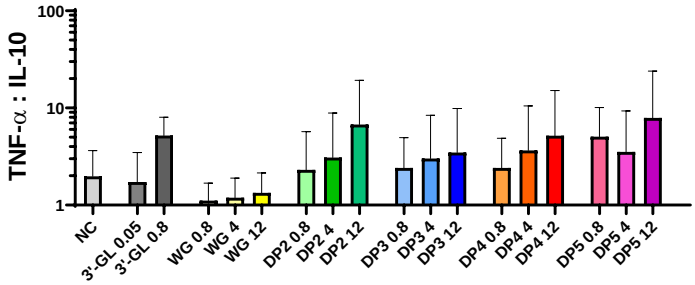

Figure 5.24 Pro-inflammatory to anti-inflammatory cytokine ratios for healthy PBMCs (*n*= 5) cultured with DP2 – DP5 B-GOS® fractions, 3'-GL or whole B-GOS®. Unstimulated cells (NC) were used as control. Data are expressed as mean ± SD. One-way ANOVA followed by Dunnett's *post-hoc* test was performed. Significant differences between stimulated cells *vs* unstimulated control (NC) are marked with an asterisk (***p< 0.001).

5.5 Discussion

The first aim of this work was to assess whether isolated B-GOS® fractions exert any immunological effects on *ex-vivo* healthy PBMCs and whether differences in their chain length elicit a different response. The second aim was to evaluate whether isolated B-GOS® fractions, whole B-GOS® or 3'-GL interfere with TLR3-mediated inflammation induced by poly(I:C).

Because LAL assay revealed LPS levels above the acceptable limit for cell culture, B-GOS® fractions were pre-treated with PMB before use on PBMCs. PBMCs tolerated stimulation with B-GOS®, 3'-GL and whole B-GOS® in presence and in absence of poly(I:C), with viability always above 70%.

Incubation of healthy PBMCs with isolated B-GOS® fractions led to immune activation, as indicated by the higher proportions of lymphocyte subsets expressing CD69 and the increased CD69 expression on total lymphocytes, monocytes and B cells. The strongest effects on the activation marker were seen when lower DP fractions (DP2, DP3) were used.

Overall, pro-inflammatory to anti-inflammatory cytokine ratios revealed that B-GOS® fractions, but not whole B-GOS®, were not pro-inflammatory as significantly higher levels of both anti-inflammatory (*e.g.* IL-1ra, IL-10) and pro-inflammatory (*e.g.* IL-1β, IL-8) cytokines were observed. The strongest effects on CD69 and secreted cytokines were seen in PBMCs stimulated with lower DP fractions (DP2, DP3) compared to higher DP fractions (DP5), in line with the observation that TLR activation by prebiotic fractions is chain-length dependent [240].

3'-GL or whole B-GOS® did not affect CD69 expression when tested alone. Due to experimental settings constraints relative to the cost of the reagent, it was not possible to test 3'-GL at concentrations higher than 0.8 mg/mL, which was the lowest dose of whole B-GOS® and B-GOS® fractions used. Because even for the isolated B-GOS® fractions no effects were observed at the lowest concentration, higher 3'-GL doses may be required in order to observe significant effects. The fact that whole B-GOS® did not promote cell activation could be due to interactions happening among different fractions and free sugars present in the product. Different compounds may neutralise each other's effects or may form complexes that interact differently with cell receptors compared to the purified fractions tested in isolation. Interestingly, whole B-GOS® promoted the secretion of mostly pro-inflammatory cytokines when tested alone, as indicated by higher IL-8:IL-10 and granzyme B:IL-10 ratios. This was in line with previously presented data on secreted and intracellular cytokines after PBMC stimulation with whole B-GOS®, as shown in Chapter 3 and in Chapter 4. Since B-GOS® DP3 fraction was not pro-inflammatory when tested in isolation, whereas free sugars such as galactose were so (Chapter 4), it is likely that the observed effects were due to free sugars contained in whole B-GOS® rather than to GOS itself.

Stimulation with poly(I:C) led to higher CD69 expression by monocytes, lymphocytes, T cells and B cells, but failed to induce a significant increase in cytokine secretion. This could be due to the fact that only few PBMC subsets present in low numbers (*e.g.* DCs, 1-2% of PBMCs) express TLR3, which is the target receptor of poly(I:C), and may therefore have not released significantly higher amounts of cytokines compared to the unstimulated control. Additionally, although stimulation with poly(I:C) activates multiple inflammatory pathways including NF-κB, which ultimately results in the production of mediators such as IL-6 and TNF-α [273] measured in this study, it is also a potent inducer of type I IFNs (*e.g.* IFN-β), which were not included in this work. In comparison, B-GOS® fractions showed much stronger effects on the whole range of cytokines tested, indicating that they might act via a different receptor than TLR3 and affect larger cell subsets (*e.g.* monocytes, 10-20% of PBMCs).

Pre-incubation of poly(I:C)-challenged PBMCs with DP3 B-GOS® fraction led to lower CD69 expression on monocytes, indicating a possible immunomodulatory role. Interestingly, the same reduction in CD69 expression was seen when PBMCs were pre-incubated with whole B-GOS® before poly(I:C) challenge. Since DP3 is the most represented fraction in whole B-GOS®, it is likely that DP3 is responsible for the observed effects. Interestingly, while whole B-GOS® and B-GOS® fractions appear to promote cell activation when tested alone, they both antagonised the pro-inflammatory effects of the TLR3 agonist poly(I:C) in co-culture settings. Indeed, both whole B-GOS® and B-GOS® DP3 fraction showed anti-inflammatory properties when applied to *ex-vivo* immune-challenged PBMCs, as indicated by lower levels of expression of the cell surface marker CD69 and by lower amounts of secreted pro-inflammatory mediators. Similar anti-inflammatory effects were previously observed also in B-GOS® and LPS co-cultures (sections 4.4.8 and 4.4.9 of Chapter 4), suggesting that GOS may help reducing inflammation induced by bacteria or viruses by altering their signalling via TLRs or by impeding their binding to immune cells.

The advantage of using B-GOS® fractions in direct contact with immune cells, compared to whole B-GOS®, is that they do not contain free sugars (*e.g.* galactose) that were shown to activate *ex-vivo* Crohn's disease PBMCs. Among the different fractions, DP3 could be chosen for its interesting anti-inflammatory effects observed when tested in a model of inflammation via TLR3. However, it is important to stress that using whole B-GOS® may not cause cell activation in Crohn's disease patients if the prebiotic is orally consumed, as the free sugars are absorbed in circulation and transported to the liver and do not enter in direct contact with immune cells. Similarly to DP3, whole B-GOS® showed anti-inflammatory effects on poly(I:C)-induced inflammation but it led to even lower lymphocyte activation when tested alone compared to the DP3 fraction. Therefore, whole B-GOS® might be a better option for IBD patients.

Chapter 6 EFFECTS OF GOS AND VITAMIN B METABOLITES ON MUCOSAL-ASSOCIATED INVARIANT T CELLS AND OTHER T CELL SUBSETS

6.1 Introduction

Mucosal-associated invariant T (MAIT) cells are a subset of innate-like T lymphocytes that play a key role in immune surveillance. In humans, high proportions of MAIT cells are found in the liver (20-50% of T cells), colon (10% of T cells), lungs (2-4% of T cells) and peripheral blood (1-10% of T cells) [64]. Alterations in the frequencies and functions of MAIT cells have been associated with ageing [65] and a wide range of diseases [84], as reviewed in Table 1.3 Chapter 1. For the purpose of this thesis, the present chapter will focus specifically on MAIT cells in inflammatory bowel diseases (IBD).

Available literature [87, 93-95, 346, 347] showed a decrease in the frequencies of circulating MAIT cells in IBD, which negatively correlated with the disease activity (Table 6.1). Circulating MAIT cells presented upregulated expression of the activation marker CD69 and altered cytokine secretion (higher IL-17 and lower IFN-γ levels). The recruitment of MAIT cells to the inflamed mucosae was likely the reason for MAIT cell depletion in blood. Lower frequencies of $CD8\alpha^+$ MAIT cells were found in the blood of IBD patients compared to healthy controls [93, 95].

Table 6.1 Alterations in the frequencies and functions of human MAIT cells in IBD.

MAIT cell frequencies in peripheral blood	**MAIT cell frequencies at inflammation site**	**MAIT cell cytokines**	**MAIT cell phenotype**	**MAIT cell activation markers**	**Ref.**
↓ in IBD patients with mild disease activity (1.21 ± 0.64%) and moderate disease activity (0.50 ± 0.29%) *vs* HCs (3.15 ± 1.58%, both $p< 0.001$)	In colon, ↑ in IBD patients with mild disease activity (3.00 ± 0.17%) *vs* HCs (0.92 ± 0.47%, $p= 0.001$)	No difference in secretion patterns between UC and CD patients. ↑ TNF-α and IL-17 in IBD *vs* HCs ($p< 0.05$). No differences in IFN-γ or IL-22	↓ $CD8\alpha^+$ MAIT cells frequencies in blood of IBD patients with moderate disease activity (83.7 ± 10.4%) *vs* HCs (92.0 ± 5.1%, $p< 0.01$)	↑ frequency of MAIT cells expressing CD69 in IBD patients with moderate disease activity (53.3 ± 24.2%) *vs* HCs (31.0 ± 19.4%, $p= 0.021$)	[93]
↓ in UC patients (1.86% ± 1.59) *vs* HCs (5.95% ± 3.26, $p< 0.0001$)	In colon, ↑ MAIT cells in active UC patients (19.08 ± 0.76%) *vs* non-active patients *vs* 12.38 ± 1.45%, $p< 0.05$)	After PMA and ionomycin stimulation, ↑ IL-17-producing MAIT cells in UC (2.87 ± 0.57%) *vs* HCs (1.39 ± 0.28%, $p< 0.05$). No differences in IL-6- or TNF-α-producing MAIT cells. IL-18 levels correlated with expression levels of CD69 on MAIT cells ($r= 0.791$, $p= 0.0003$)	ND	↑ frequency of $CD69^+$ MAIT cells in UC *vs* HCs ($p< 0.05$). CD69 expression negatively correlated with frequency of MAIT cells in UC ($r= -0.391$, $p= 0.027$)	[94]
↓ in IBD patients *vs* HCs (both $p< 0.0001$). No differences in CD *vs* UC	↓ MAIT cells in UC colon (0.91 ± 0.62%) *vs* non-IBD colon (3.2 ± 2.7%, $p= 0.044$). ↓ MAIT cells in CD mucosae (1.35 ± 0.53%) *vs* non-IBD mucosae (4.93 ± 2.75, $p= 0.0093$)	No difference in % of IL-17- or IFN-γ-producing MAIT cells in IBD *vs* HCs. ↑ blood levels of IL-22 in UC (3.2 ± 2.5%) *vs* HCs (0.095 ± 0.019%, $p= 0.026$)	ND	ND	[87]

Table 6.1 Continued.

MAIT cell frequencies in peripheral blood	**MAIT cell frequencies at inflammation site**	**MAIT cell cytokines**	**MAIT cell phenotype**	**MAIT cell activation markers**	**Ref.**
↓ in CD (1.60 ± 0.20%) and UC (1.55 ± 0.55%) *vs* HCs (3.40 ± 0.30%, p <0.0001 and p= 0.0019, respectively)	↑ in the inflamed intestine of IBD patients (6.6 ± 1.4%) *vs* HCs (1.5 ± 0.3%, p= 0.002)	MAIT cells from CD and UC patients secreted ↑ IL-17 than HCs (both p< 0.05). Increased IL-17 production accompanied by ↓ IFN-γ secretion in CD patients only	↓ blood CD8α$^+$ MAIT cells in CD and UC patients *vs* HCs (p< 0.001 and p< 0.05, respectively)	ND	[95]
↓ in both CD and UC patients *vs* HCs (p< 0.05 and p< 0.005, respectively)	ND	↓ % of IFN-γ$^+$ MAIT cells in IBD patients *vs* HCs (p <0.05). IL-17$^+$ and TNF-α$^+$ MAIT cell levels comparable between IBD and HCs. ↓ MFIs of IFN-γ on MAIT cells in IBD *vs* HCs (p <0.05). MFIs of IL-17 and TNF-α on MAIT cell comparable between IBD and HCs	ND	Circulating MAIT cell deficiency accompanied by ↑ expression of CD69 (p< 0.0001) and annexin V (p< 0.05)	[346]

Abbreviations: HCs, healthy controls; UC, ulcerative colitis; CD, Crohn's disease;

In order to identify MAIT cells and study their characteristics, a flow cytometry method was developed and will be presented in this chapter. MAIT cells are phenotypically defined as $CD3^+$ $V\alpha7.2^+$ $CD161^{hi}$ cells, and are mostly $CD8^+$ (70-85%) or $CD4^-CD8^-$ double negative (DN) (10-20%). In adult blood, only a minor proportion of MAIT cells is $CD4^+$ (< 5%) [70, 71, 348].

MAIT cells are activated in a T cell receptor (TCR)-dependent manner by vitamin B metabolites produced by the gut microbiota or, in a TCR-independent manner, by IL-12, IL-15 and IL-18 cytokines [348, 349]. Vitamin B metabolites that activate MAIT cells are 6,7-dimethylribityl lumazine (RL-6,7-DiMe) and 5-amino-6-D-ribitylaminouracil (5-A-RU) [271]. The reaction of 5-A-RU with methylglyoxal (MG) forms the most potent MAIT cell activator 5-(2-oxopropylideneamino)-6-D-ribitylaminouracil (5-OP-RU), which will be used alone or in combination with GOS to stimulate MAIT cells within PBMCs [272].

To the best of the author's knowledge, the effects of vitamin B2 metabolites on other T cells subsets, such as T helper cells ($CD3^+$ $CD4^+$ lymphocytes) and cytotoxic T cells ($CD3^+$ $CD8^+$ lymphocytes), have not been explored yet. Other B vitamins were shown to affect T cell proliferation and to alter the proportions of T cell subsets. Supplementation with vitamin B6 increased the percentages of T cells and T helper cells in critically ill elderly individuals [350] and enhanced *ex-vivo* lymphocyte proliferation in young healthy women [351]. Vitamin B9 repletion of vitamin B9-deficient cells restored T cell proliferation and lowered the $CD4^+$ to $CD8^+$ T cell ratio *in vitro*, suggesting that vitamin B9 status is important in T cell immunity. It is plausible that also vitamin B2 derivatives affect T cell status. Therefore, the effects of 5-A-RU with methylglyoxal (MG), alone or combined with GOS, will be evaluated also on total lymphocytes, T cells, T helper cells and cytotoxic T cells.

Evidence suggests that unknown metabolites from dietary probiotics modulate T cell and MAIT cell functions [90, 91]. Soluble factors derived from lactobacilli decresed *Staphylococcus aureus*-induced activation of T helper cells and reduced the secretion of pro-inflammatory mediators by T cells [90]. Molecules present in lactobacilli cell-free supernatants directly dampened IFN-γ expression in immune-challenged MAIT cells *in vitro* [91]. GOS are prebiotics produced by the enzymatic transgalactosylation activity of various probiotic strains, including lactobacilli and bifidobacteria [190, 201]. Beside immunomodulation through the gut microbiota and their SCFAs, GOS exert direct effects on monocytes, macrophages and intestinal epithelial cells possibly via ligation to TLRs, as reviewed in [313]. The microbiota-independent effects of GOS on T cells and their subsets, including MAIT cells, are still under investigation.

Therefore, this work will assess whether GOS can modulate the functions of MAIT cells and other T cell subsets and whether these cells respond differently to vitamin B metabolites in presence of GOS. The effects of GOS and/or vitamin B metabolites will be assessed both in PBMCs from healthy donors and in PBMCs from Crohn's disease donors.

6.2 Aim and objectives

The first aim was to assess the effects of GOS on MAIT cells and other T cell subsets using PBMCs from healthy donors and those with Crohn's disease. The second aim was to evaluate whether these cells respond differently to vitamin B metabolite challenge in presence of GOS.

The specific objectives were to:

- Optimise a flow cytometry gating strategy to identify MAIT cells in PBMCs
- Perform LAL assay analysis of two vitamin B metabolites RL-6,7-DiMe and 5-A-RU prior to use in cell culture
- Assess the cytotoxicity of RL-6,7-DiMe, 5-A-RU and 5-A-RU + MG and choose the most potent activator for use in PBMC cultures
- Compare the baseline frequencies and functions of MAIT cells from healthy donors *vs* Crohn's disease donors in the response to GOS and/or chosen vitamin B metabolite
- Evaluate the effects of culturing with GOS and/or vitamin B metabolite on total PBMC viability and on the expression of surface markers (CD3, CD4, CD8, CD161, TCR Vα7.2), intracellular cytokines (IL-17A, IFN-γ) and CD69 by MAIT cells and other T cell subsets, using cells from healthy donors and those with Crohn's disease. Additionally, the effects of culturing with GOS and/or vitamin B metabolite on a panel of secreted cytokines chosen for their role in IBD (IL-1α, IL-1β, IL-1ra, IL-8, IL-10, IL-12p70, IL-17A, IFN-γ, TNF-α and granzyme B) will be assessed

Based on the results presented in previous chapters, it is hypothesised that GOS will induce activation of T cells and T cell subsets when tested in isolation. Additionally, based on the reviewed literature, it is expected that GOS will reduce MAIT cell activation induced by vitamin B metabolites.

6.3 Methods

B-GOS® batch C and vitamin B metabolites (RL-6,7-DiMe, 5-A-RU, 5-A-RU + MG) were prepared as detailed in section 2.3. LAL assay was carried out as described in section 2.9.2. Healthy PBMCs and Crohn's disease PBMCs were cultured as explained in section 2.3. Cell viability was measured by flow cytometry using a fixable viability stain (FVS780) as reported in section 2.5. Cell surface staining and intracellular staining by flow cytometry were performed as described in sections 2.7.2 and 2.7.3, respectively. A graphical summary of the methods used in this chapter is provided in Figure 6.1.

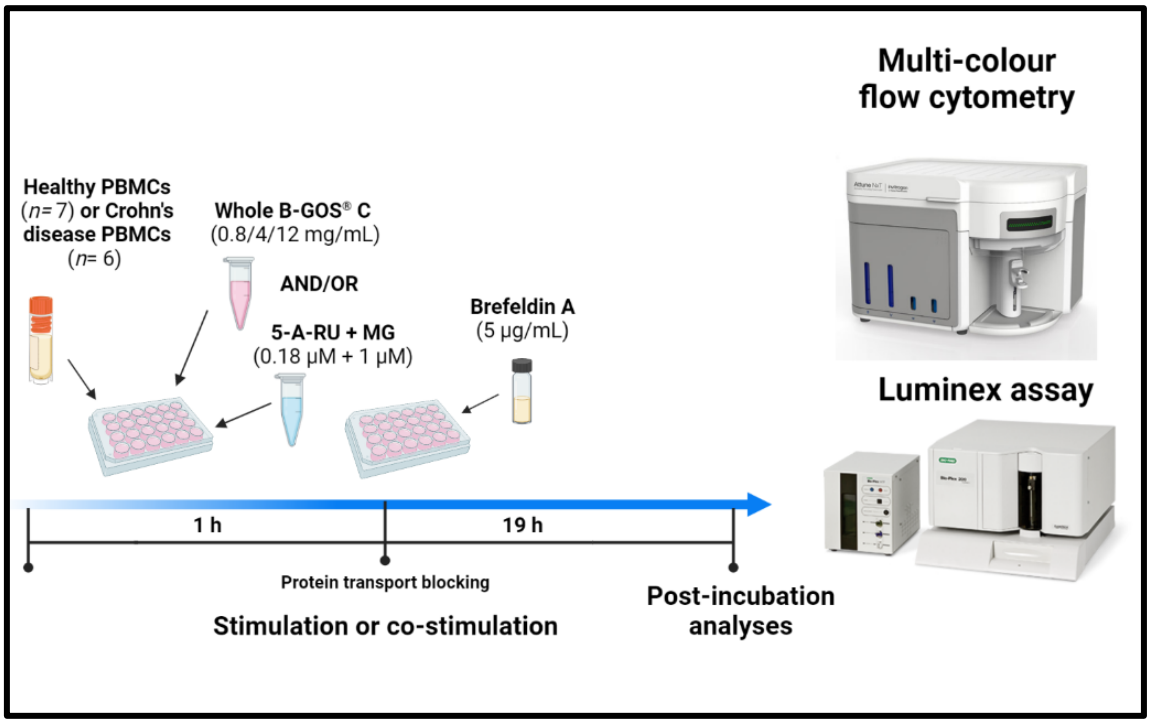

Figure 6.1 Graphical summary of the methods used for the assessment of the effects of culturing healthy and Crohn's disease PBMCs with GOS and/or a selected vitamin B metabolite on the frequencies and functions of MAIT cells and other T cell subsets.

6.4 Results

6.4.1 Optimisation of a flow cytometry gating strategy to identify MAIT cells in PBMCs

In order to acquire a sufficient number of events to allow identification of MAIT cells and their subsets, the number of events/sample was calculated based on Poisson statistics [352]. Acquisition of 300,000 events/sample was needed to maintain the coefficient of variation (CV) below 5% (CV= 2.7%). Figure 6.2 shows how MAIT cell numbers increased when 300,000 events/sample were recorded compared to the standard 10,000 events/sample.

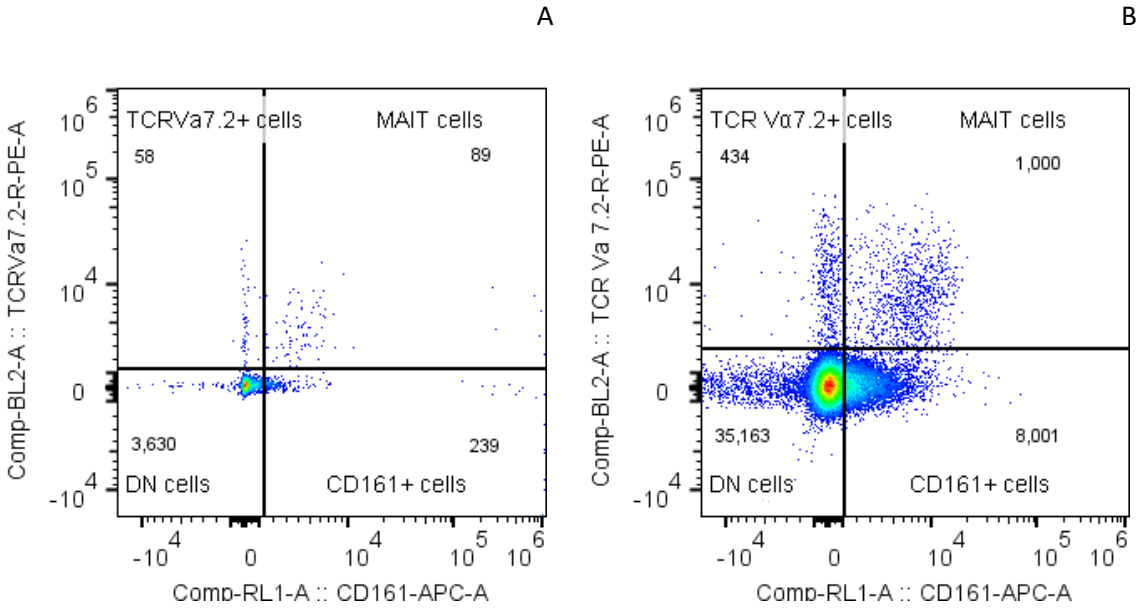

Figure 6.2 300,000 events/sample should be acquired when studying MAIT cells and subsets. A) MAIT cell numbers when 10,000 events/sample were collected; B) MAIT cell numbers when 300,000 events/sample were collected.

Pilot experiments were conducted to select the most informative markers for MAIT cell detection. Because MAIT cells are T lymphocytes that do not express TCRγδ, a dump channel was initially used to exclude TCRγδ$^+$ cells (Figure 6.3). Since only a very small percentage of lymphocytes was TCRγδ$^+$ (mean ± SD, 0.065 ± 0.006%; *n*= 4), the TCRγδ marker was not deemed informative and was not included in the final panel. This allowed having an additional detection channel for the study of intracellular cytokines.

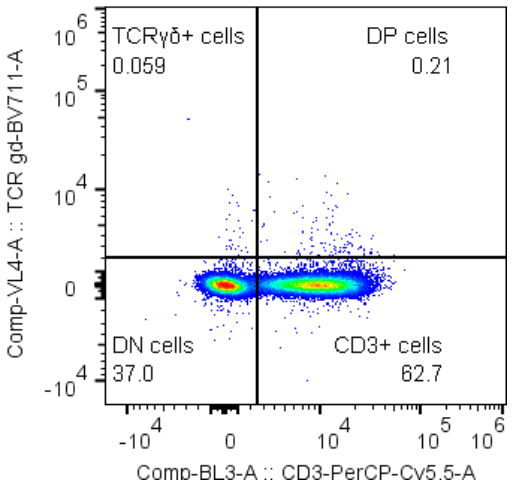

Figure 6.3 Only a very small percentage of lymphocytes was positive for TCRγδ marker, which was excluded from the final panel. TCRγδ$^+$ cells and CD3$^+$ cells were gated within the lymphocyte population after exclusion of dead PBMCs, debris and doublets.

Flow cytometry data were either displayed in FSC/SSC plots or in fluorescence plots and analysed using FlowJo Single Cell Analysis Software version 10.0 (FlowJo LLC). Unstained cells, isotype controls and fluorescence minus one (FMO) controls were used as indicated in section 2.7.2. Doublets were excluded on FSC-H *vs* FSC-A graphs using a polygonal gate. Within the singlets, a polygonal gate was drawn around PBMCs to exclude debris. Within the PBMC gate, a bisector gate was used to determine the percentages of live cells (FVS780$^-$) and dead cells (FVS780$^+$) in a FVS780-A histogram. Within the live PBMCs, lymphocytes were identified using a polygonal gate in a SSC-A *vs* FSC-A plot based on their size and complexity. Within the lymphocytes, T cells were identified as CD3$^+$ lymphocytes using a polygonal gate. MAIT cells were identified within the CD3$^+$ lymphocytes as those events positive for TCR Vα7.2 and CD161 markers using a quadrant gate. An example of how MAIT cells were gated using the TCR Vα7.2 and CD161 FMOs is shown in Figure 6.4.

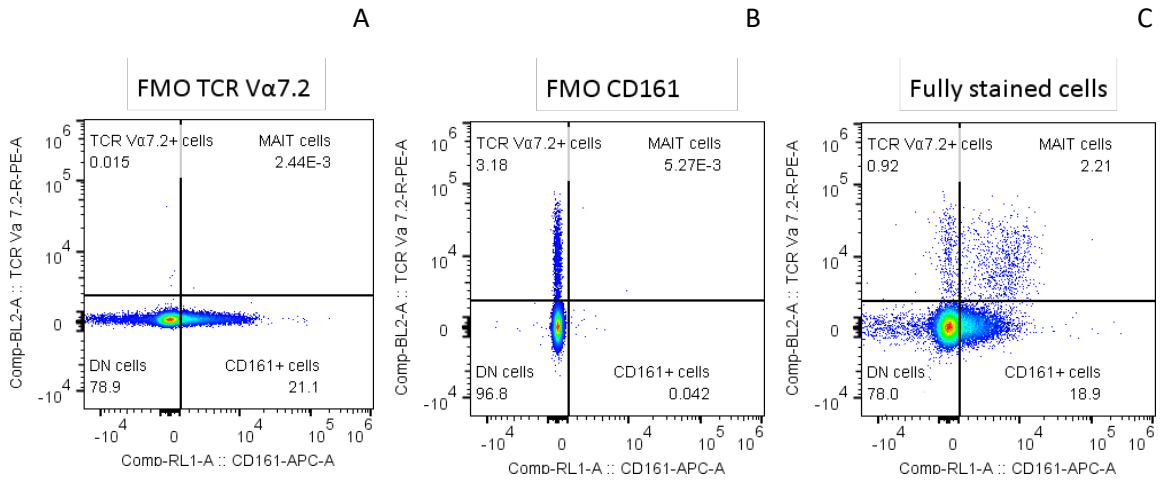

Figure 6.4 FMO controls used to set the positive and negative regions for MAIT cell staining. A) FMO TCR Vα7.2 contained all markers except TCR Vα7.2. B) FMO CD161 contained all markers except CD161. C) Fully stained sample.

To further investigate MAIT cells subsets, $CD4^+$ MAIT cells, $CD8^+$ MAIT cells, $CD4^-CD8^-$ (DN) MAIT cells and $CD4^+CD8^+$ (DP) MAIT cells were detected within MAIT cells using a quadrant gate. The frequencies of IFN-γ^+ cells or IL-$17A^+$ cells were calculated within MAIT cells and MAIT cell most abundant subsets ($CD8^+$ MAIT cells and DN MAIT cells) by applying a quadrant gate. $CD69^+$ MAIT cells and $CD69^+$ MAIT cell subsets ($CD69^+$ $CD8^+$ MAIT cells and $CD69^+$ DN MAIT cells) were identified by using a rectangular gate on a SSC-A *vs* CD69-APC-R700-A graphs. A summary of the gating strategy used in this work is reported in Figure 6.5. An example of flow cytometry graphs from a single donor co-stimulated with 5-A-RU + MG (0.18 µM + 1 µM) and B-GOS® batch C (0.8 mg/mL) is given in Figure 6.6 and Figure 6.7. Back-gating of MAIT cells was performed to ensure correct gate positioning (Figure 6.8).

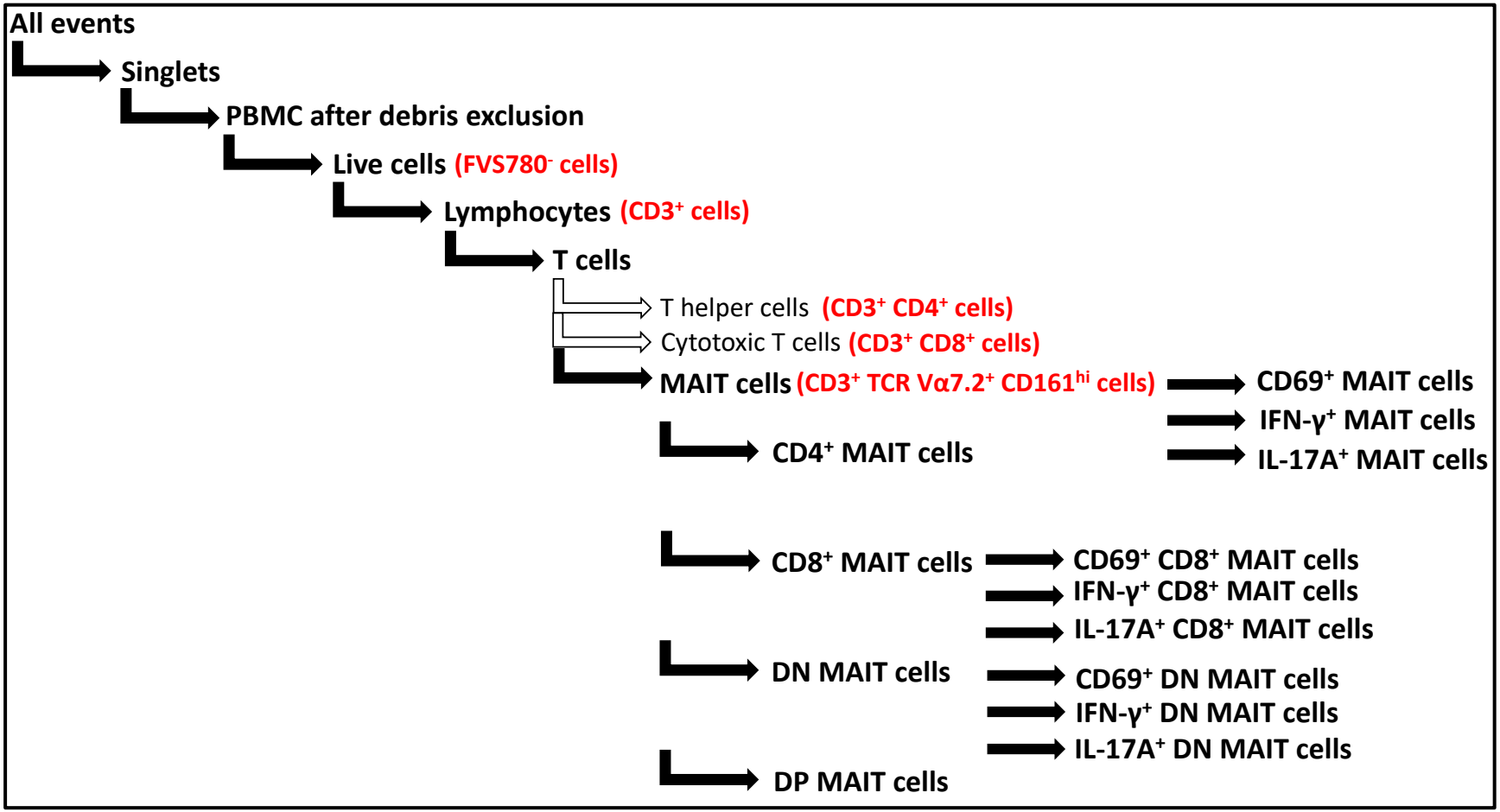

Figure 6.5 Summary of the gating strategy used to detect MAIT cells and their subsets.

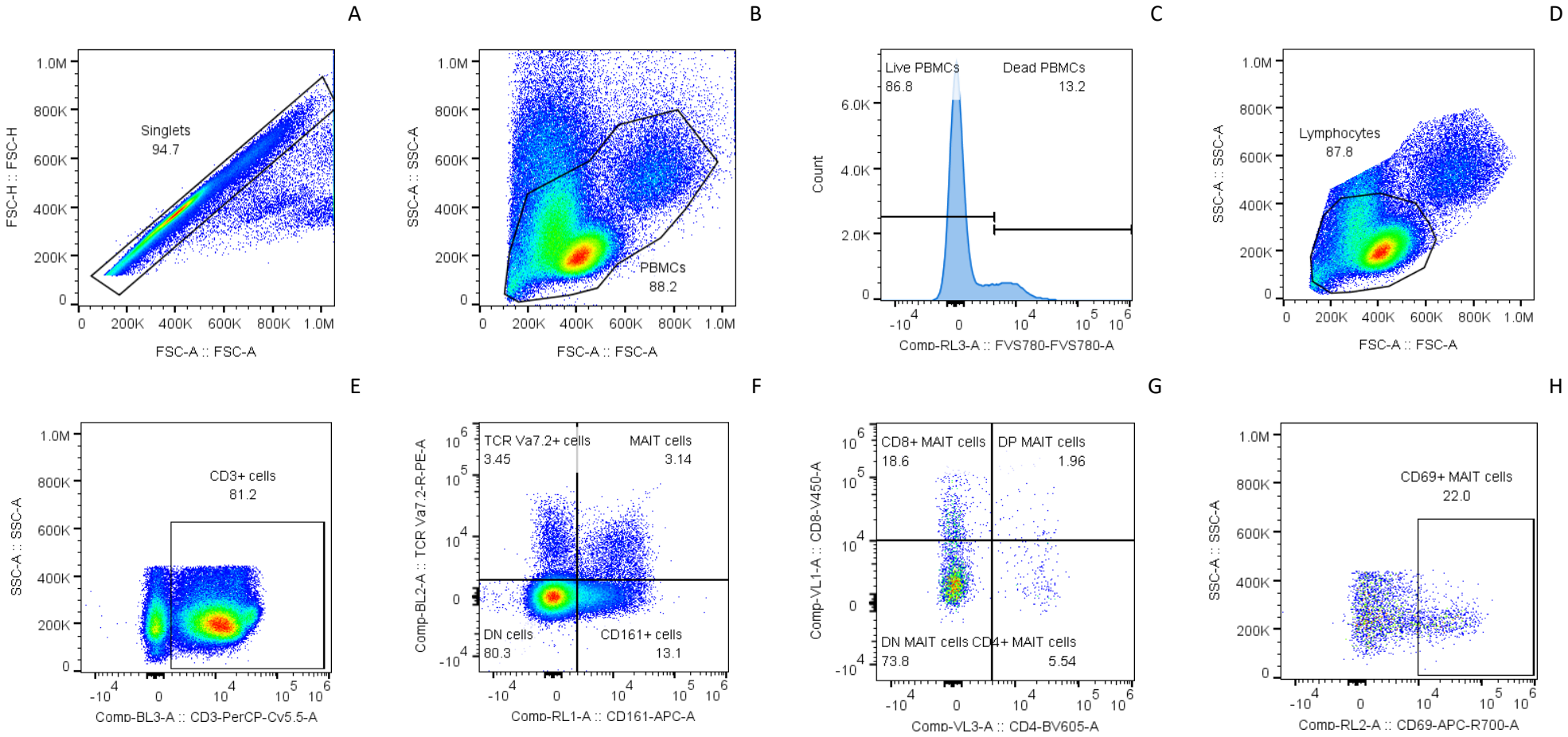

Figure 6.6 Example of flow cytometry graphs from a single donor co-stimulated with 5-A-RU + MG (0.18 µM + 1 µM) and B-GOS® batch C (0.8 mg/mL).A) Singlets, gated from all events; B) PBMCs gated from singlets; C) Live PBMCs, gated from PBMCs; D) Lymphocytes, gated from live PBMCs; E) $CD3^+$ cells, gated from lymphocytes; F) MAIT cells, gated from $CD3^+$ cells; G) $CD4^+$, $CD8^+$, DN and DP MAIT cells, gated from MAIT cells; H) $CD69^+$ MAIT cells, gated from MAIT cells.

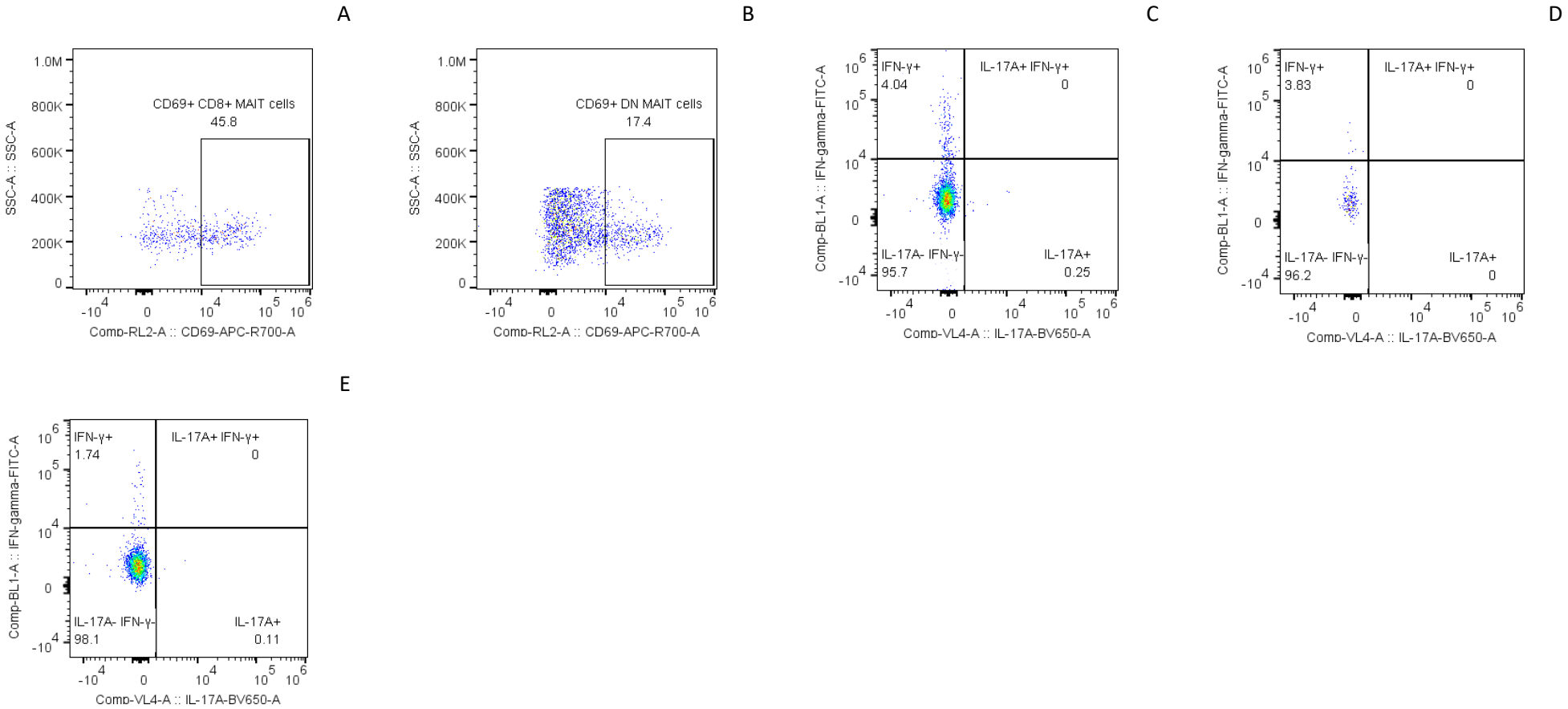

Figure 6.7 Example of flow cytometry graphs from a single donor co-stimulated with 5-A-RU + MG (0.18 µM + 1 µM) and B-GOS® batch C (0.8 mg/mL). A) $CD69^+$ $CD8^+$ MAIT cells, gated from $CD8^+$ MAIT cells; B) $CD69^+$ DN MAIT cells, gated from DN MAIT cells; C) IFN-γ^+, IL-$17A^+$ IFN-γ^+, IL-$17A^-$ IFN-γ^-, IL-$17A^+$ MAIT cells, gated from MAIT cells; D) IFN-γ^+, IL-$17A^+$ IFN-γ^+, IL-$17A^-$ IFN-γ^-, IL-$17A^+$ $CD8^+$ MAIT cells, gated from $CD8^+$ MAIT cells; E) IFN-γ^+, IL-$17A^+$ IFN-γ^+, IL-$17A^-$ IFN-γ^-, IL-$17A^+$ DN MAIT cells, gated from DN MAIT cells;

A B

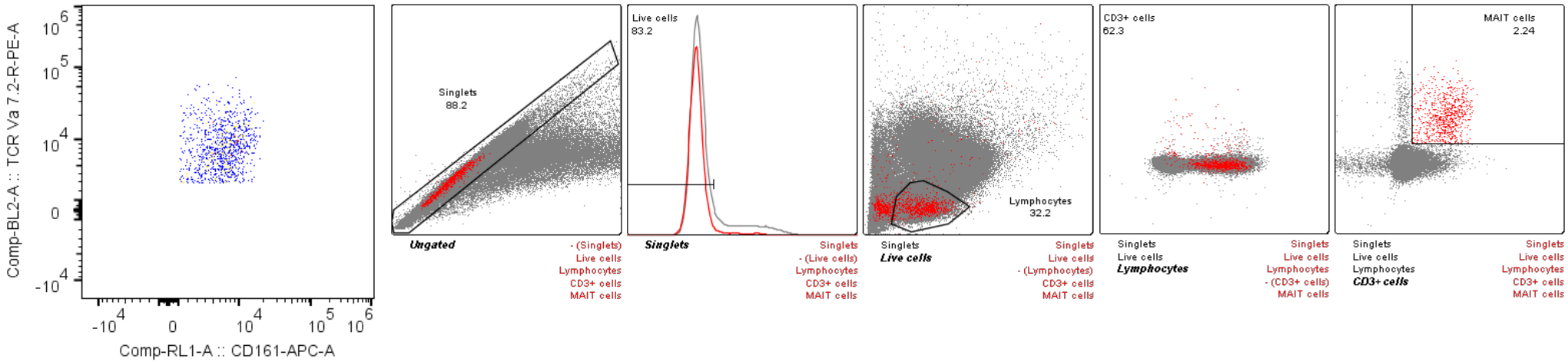

Figure 6.8 Confirmation of MAIT cell gate by back-gating. A) MAIT cells were identified as $CD3^+$ $V\alpha7.2^+$ $CD161^{hi}$ cells. B) Back-gating confirmed that the MAIT cell gate was placed correctly. MAIT cells were gated from $CD3^+$ cells, which were gated from lymphocytes/live PBMCs/singlets/all events.

Since during the optimisation phase illustrated in Section 6.4.1 IL-17A was not induced by B-GOS® stimulation, a pilot experiment using ConA as a T cell stimulus was conducted to ensure that IL-17A could be detected by intracellular staining. PBMCs from one single donor were stimulated for 5 h with ConA (5 µg/mL) in presence of the protein transport inhibitor brefeldin A (5 µg/mL). An IL-17A FMO control was used to set the gates for the detection of IL-17A$^+$ T cells. As illustrated in Figure 6.9, IL-17A$^+$ events were detected when ConA was used, indicating functional intracellular staining of IL-17A.

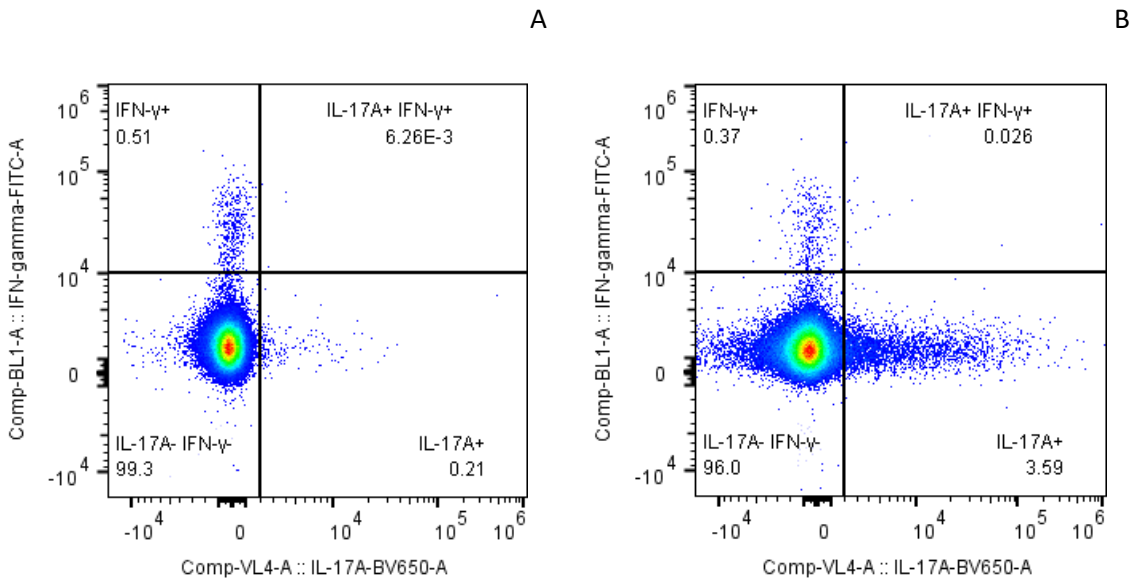

Figure 6.9 Example of flow cytometry graphs indicating positive staining of IL-17A$^+$ T cells after 5 h stimulation of healthy PBMCs from a single donor with ConA (5 µg/mL) in presence of brefeldin A (5 µg/mL). A) IL-17A FMO control for gating; B) Detection of IL-17A$^+$ T cells, which were gate from T cells/lymphocytes/live PBMCs/singlets/all events.

6.4.2 Assessment of LPS content in vitamin B metabolites

LAL assay was performed on vitamin B metabolites RL-6,7-DiMe and 5-A-RU before use in PBMC cultures because the compounds were not LPS-tested by the manufacturer. MG was supplied as a sterile reagent and thus not included in the LAL assay. RL-6,7-DiMe and 5-A-RU were tested at the same concentrations subsequently used in PBMC cultures (75 µM and 0.18 µM, respectively). A negative control (RPMI-1640 medium) and a positive control (LPS from *E. coli* O111:BA) were included. The positive control was diluted 10 times in LPS-free water prior to testing with a dilution factor determined by pilot experiments. Samples were tested in triplicate, and LPS concentrations (EU/mL) were interpolated from a standard curve in the 0.01-0.1 EU/mL range.

RL-6,7-DiMe and 5-A-RU presented levels of LPS below the 0.1 EU/mL limit for cell cultures, meaning that they can be used in direct contact with immune cells *in vitro*. The negative control did not contain any detectable LPS. The positive control presented quantities of LPS corresponding to 1.20 EU/mL ± 0.18 EU/mL (Figure 6.10).

A B

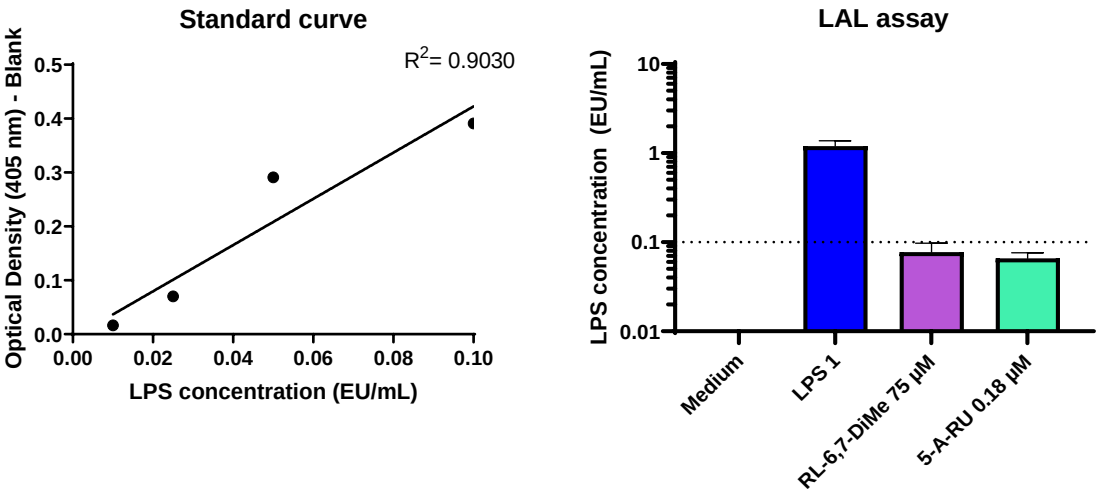

Figure 6.10 A) Standard curve in the 0.01-0.1 EU/mL range for the quantitation of LPS in samples by LAL assay. B) Levels of LPS in the vitamin B metabolites RL-6,7-DiMe and 5-A-RU. A negative control (RPMI-1640 medium) and a positive control (LPS from *E. coli* O111:BA) were included. LAL assay was conducted with technical replicates. Data are expressed as mean ± SD (*n*= 3). The dotted line at Y= 0.1 refers to the limit of LPS (EU/mL) for cell culture applications

6.4.3 Assessment of cytotoxicity and choice of vitamin B metabolite to use in PBMC cultures

PBMCs from healthy donors (*n*= 2) were stimulated for 20 h with RL-6,7-DiMe (75 µM) or 5-A-RU (0.18 µM) or 5-A-RU (0.18 µM) + MG (1 µM) to form the most potent activator 5-OP-RU. Unstimulated PBMCs were used as a negative control. MG-stimulated cells were included to ensure that the effects on MAIT cells were due to the formation of 5-OP-RU, and not to MG itself. Cells from each donor were plated in duplicate and brefeldin A (5 µg/mL) was added after 1 h incubation to half of the wells to allow the study of intracellular cytokines. Brefeldin A was not added to the remaining wells to enable the expression of the surface activation marker CD69, which is blocked in presence of brefeldin A [353, 354]. The concentrations of vitamin B metabolites and incubation times were chosen based on similar studies [85, 86, 279]. The effects of vitamin B metabolites on PBMC viability and on the expression of CD69 and intracellular IFN-γ and IL-17A by total lymphocytes, T cells ($CD3^+$), T helper cells ($CD3^+$ $CD4^+$), cytotoxic T cells ($CD3^+$ $CD8^+$), MAIT cells ($CD3^+$ $V\alpha7.2^+$ $CD161^{hi}$), $CD8^+$ MAIT cells ($CD3^+$ $CD8^+$ $V\alpha7.2^+$ $CD161^{hi}$) and DN MAIT cells ($CD3^+$ $CD4^-$ $CD8^-$ $V\alpha7.2^+$ $CD161^{hi}$) were evaluated by multi-colour flow cytometry. The viability of PBMCs exposed to RL-6,7-DiMe, 5-A-RU or 5-A-RU + MG with or without brefeldin A was measured to ensure that the chosen stimuli and concentrations were not cytotoxic.

Viability was above 80% for all the tested conditions, both in presence and in absence of brefeldin A (Table 6.2 and Table 6.3), indicating that PBMCs tolerated the treatments. Incubation of PBMCs with MG alone led to lower viability compared to the negative control, both without (p= 0.0065) and with (p= 0.0001) brefeldin A. This could be due to the pro-apoptotic effects of MG on leukocytes [355].

Table 6.2 Viability of PBMCs from healthy donors cultured for 20 h with RL-6,7-DiMe or 5-A-RU with or without methylglyoxal (MG) or MG alone in absence of brefeldin A.Unstimulated PBMCs were used as a negative control (NC). Cell viability was assessed by flow cytometry using a live/dead stain. Viability (%) values refer to the PBMC population following exclusion of doublets and debris. Results were considered significant if p< 0.05.

	NC	**MG**	**RL-6,7-DiMe**	**5-A-RU**	**5-A-RU + MG**	**One-way ANOVA *p* value**
	Mean ± SD (*n*= 2)	Mean ± SD (*n*= 2)	Mean ± SD (*n*= 2)	Mean ± SD (*n*= 2)	Mean ± SD (*n*= 2)	
Viability (%)	93.9 ± 1.3	82.9 ± 0.0**	91.9 ± 2.7	93.5 ± 2.1	91.6 ± 2.1	**0.0104**

**Significantly different from NC (Dunnett's *post-hoc* test, p= 0.0065)

Table 6.3 Viability of PBMCs from healthy donors cultured for 20 h with RL-6,7-DiMe or 5-A-RU with or without methylglyoxal (MG) or MG alone in presence of brefeldin A. Unstimulated PBMCs were used as a negative control (NC). PBMC viability was assessed by flow cytometry using a live/dead stain. Viability (%) values refer to the PBMC population following exclusion of doublets and debris. Results were considered significant if $p < 0.05$.

	NC + bref. A	**MG + bref. A**	**RL-6,7-DiMe + bref. A**	**5-A-RU + bref. A**	**5-A-RU + MG + bref. A**	**One-way ANOVA *p* value**
	Mean ± SD (*n*= 2)	Mean ± SD (*n*= 2)	Mean ± SD (*n*= 2)	Mean ± SD (*n*= 2)	Mean ± SD (*n*= 2)	
Viability (%)	92.7 ± 1.1	82.9 ± 0.0***	91.4 ± 0.4	92.6 ± 0.1	90.6 ± 1.1	**0.0002**

***Significantly different from NC (Dunnett's *post-hoc* test, $p = 0.0001$)

Following incubation with 5-A-RU + MG, but not with RL-6,7-DiMe or 5-A-RU, total lymphocytes ($p = 0.0203$), T cells ($p = 0.0034$), cytotoxic T cells ($p = 0.0009$), MAIT cells ($p = 0.0034$) and $CD8^+$ MAIT cells ($p = 0.0008$) presented higher CD69 (MFI) expression compared to the unstimulated control. Incubation with MG did not result in upregulated CD69 expression in PBMC subsets except for $CD8^+$ MAIT cells ($p = 0.0381$), which presented higher CD69 (MFI) values (Figure 6.11 and Figure 6.12). No changes in the percentages of any CD69-expressing cells were observed (Appendix F).

No changes in the percentages of IFN-γ-expressing lymphocytes, T cells, T helper cells or cytotoxic T cells were seen after stimulation with vitamin B metabolites (Figure 6.13). An increase in the percentages of MAIT cells and $CD8^+$ and DN MAIT cell subsets expressing IFN-γ was observed only after treatment with 5-A-RU + MG compared to control, although significance was not reached likely because of the limited sample size (Figure 6.14). Stimulation with the vitamin B metabolites did not affect the levels of IFN-γ (MFI) expression (Appendix F). No changes in the percentages of IL-17A-expressing cells nor in their IL-17A (MFI) expression levels were observed (Appendix F).

Overall, 5-A-RU + MG was well tolerated by PBMCs and induced the strongest activation in T lymphocytes and MAIT cells among the vitamin B metabolites tested. 5-A-RU + MG was therefore selected as the most potent stimulus to use in co-culture studies (section 6.4.5).

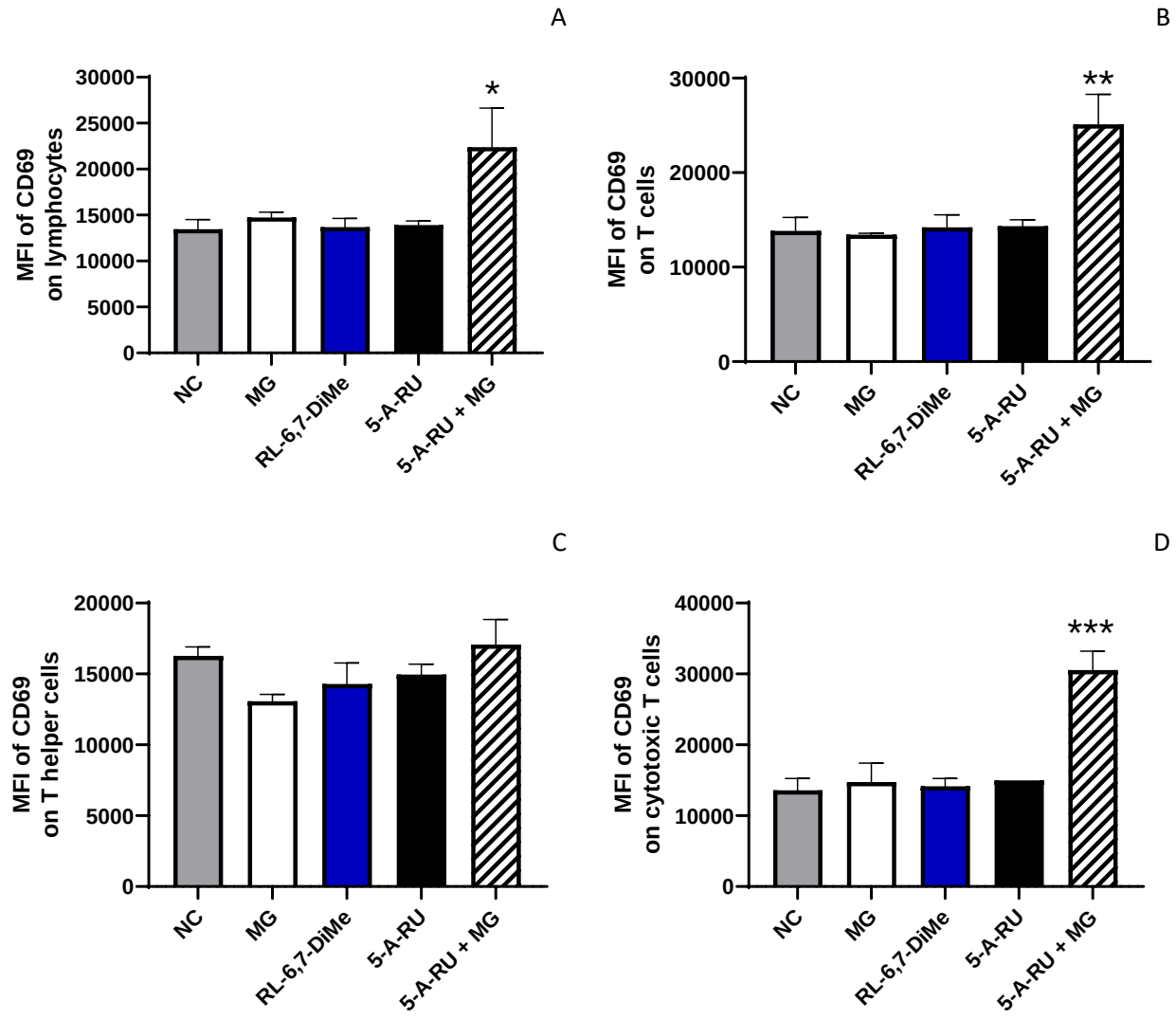

Figure 6.11 CD69 (MFI) expression on total lymphocytes, T cells, T helper cells and cytotoxic T cells after 20 h incubation with RL-6,7-DiMe or 5-A-RU with or without methylglyoxal (MG) or MG alone. Unstimulated PBMCs were used as a negative control (NC). Each sample was tested in duplicate (n= 2). Data are expressed as mean ± standard deviation (SD). One-way ANOVA followed by Dunnett's *post-hoc* test was performed. Results were considered significant if p< 0.05. *Significantly different from NC (Dunnett's post-hoc test, p< 0.005); **Significantly different from NC (Dunnett's post-hoc test, p< 0.005); ***Significantly different from NC (Dunnett's post-hoc test, p< 0.001).

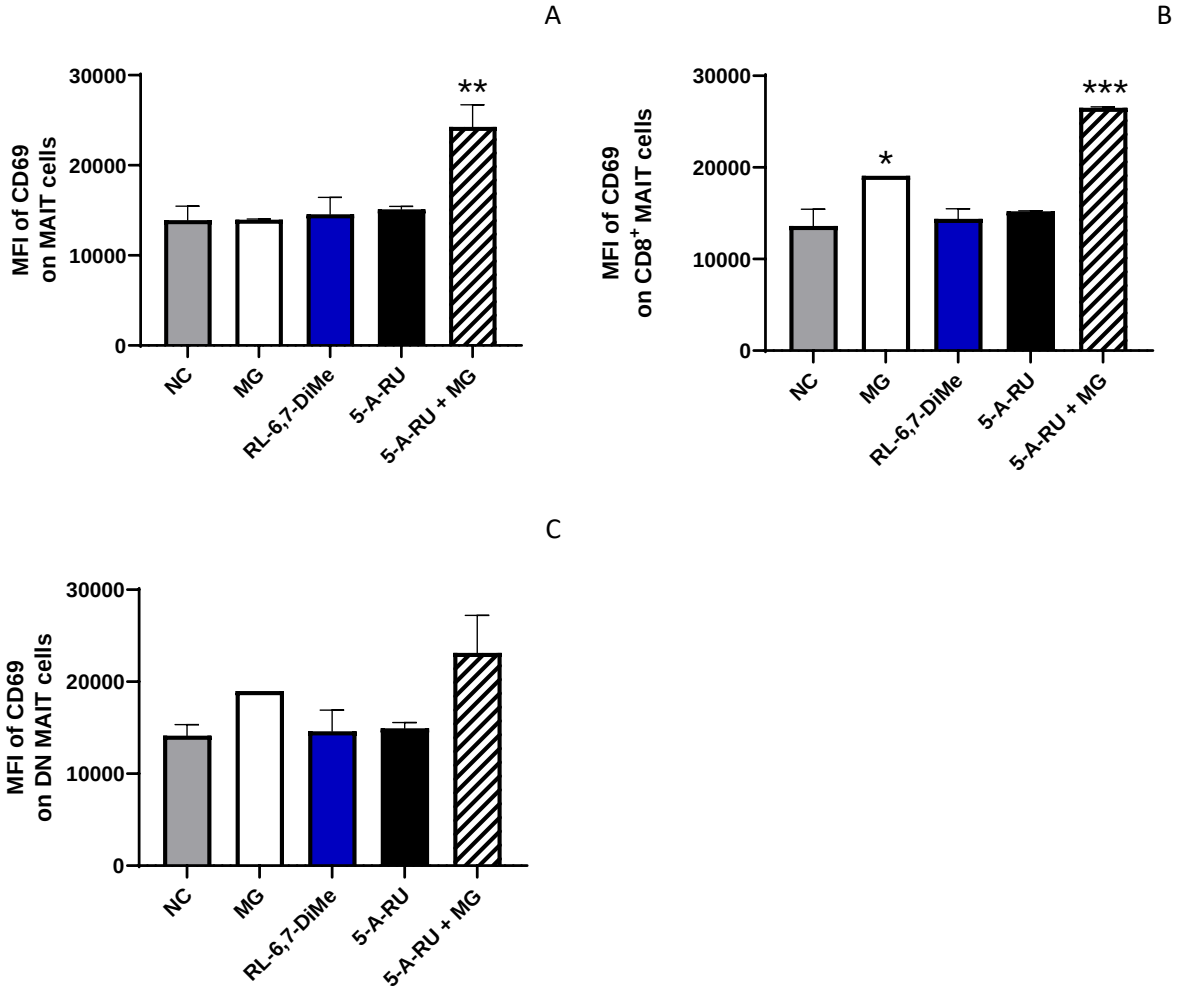

Figure 6.12 CD69 (MFI) expression on MAIT cells, $CD8^+$ MAIT cells and DN MAIT cells after 20 h incubation with RL-6,7-DiMe or 5-A-RU with or without methylglyoxal (MG) or MG alone. Unstimulated PBMCs were used as a negative control (NC). Each sample was tested in duplicate (n= 2). Data are expressed as mean ± standard deviation (SD). One-way ANOVA followed by Dunnett's *post-hoc* test was performed. Results were considered significant if $p< 0.05$. *Significantly different from NC (Dunnett's post-hoc test, $p< 0.005$); **Significantly different from NC (Dunnett's post-hoc test, $p< 0.005$); ***Significantly different from NC (Dunnett's post-hoc test, $p< 0.001$).

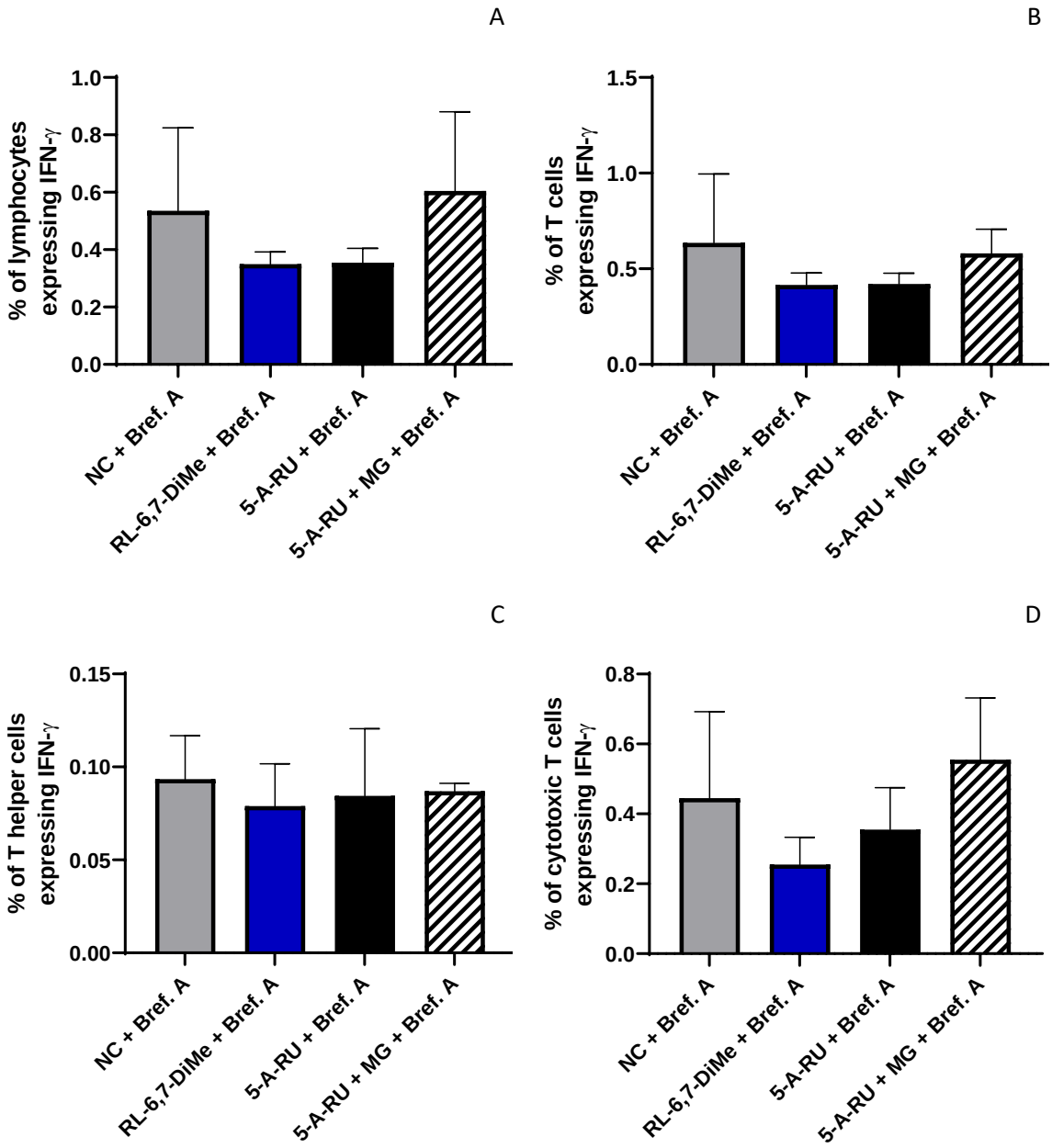

Figure 6.13 Percentages of lymphocytes and T cell subsets expressing IFN-γ after 20 h incubation with RL-6,7-DiMe or 5-A-RU with or without methylglyoxal (MG) or MG alone. Unstimulated PBMCs were used as a negative control (NC). Brefeldin A (5 µg/mL) was added after 1 h incubation. Each sample was tested in duplicate (*n*= 2). Data are expressed as mean ± standard deviation (SD).

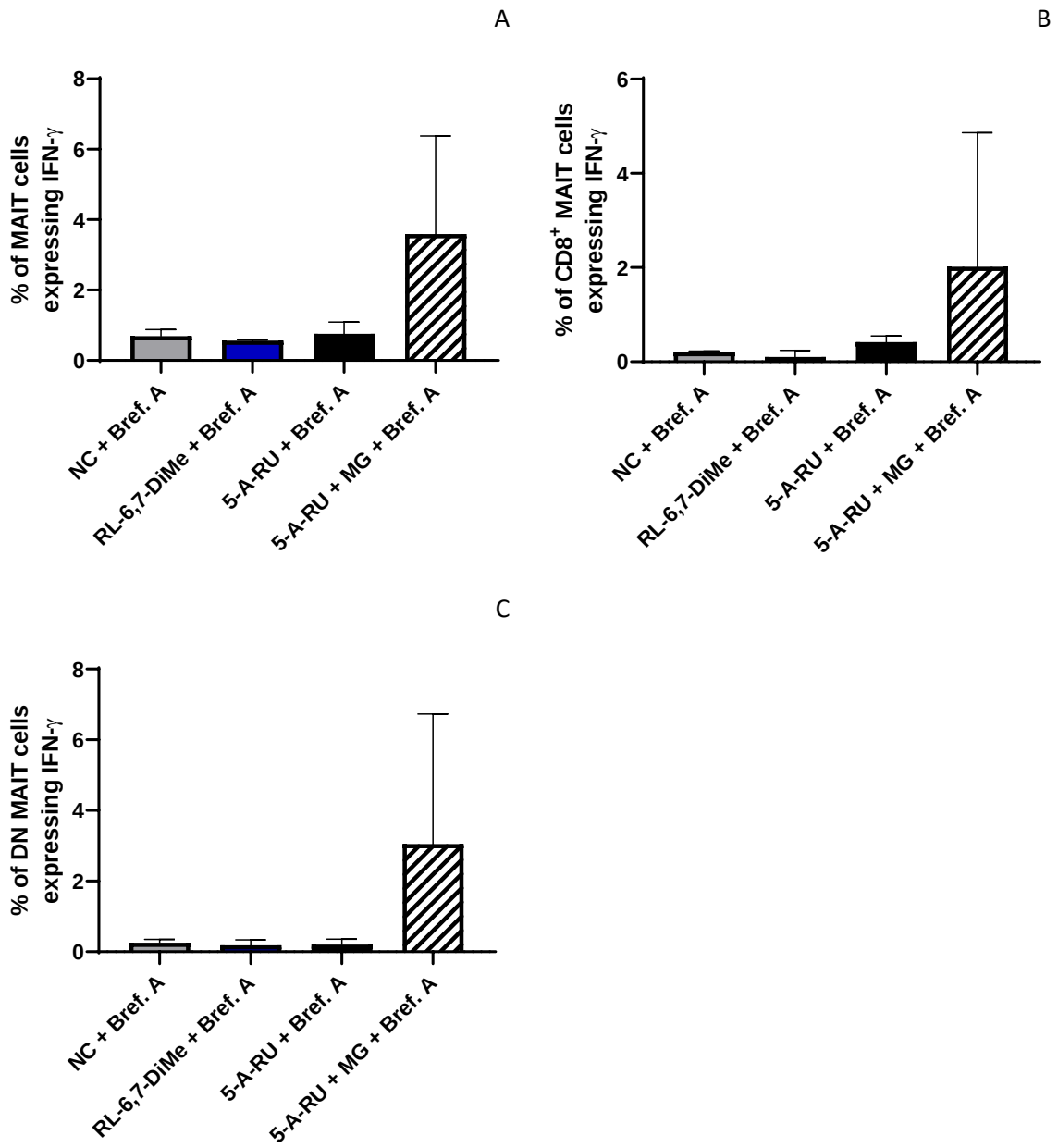

Figure 6.14 Percentages of MAIT cells and MAIT cell subsets expressing IFN-γ after 20 h incubation with RL-6,7-DiMe or 5-A-RU with or without methylglyoxal (MG) or MG alone. Unstimulated PBMCs were used as a negative control (NC). Brefeldin A (5 µg/mL) was added after 1 h incubation. Each sample was tested in duplicate (*n*= 2). Data are expressed as mean ± standard deviation (SD).

6.4.4 Baseline MAIT cell frequencies and functions in healthy donors *vs* Crohn's disease donors

Unstimulated PBMCs from healthy donors (*n*= 7) and Crohn's disease donors (*n*= 6) were incubated for 20 h in presence or absence of brefeldin A (5 μg/mL), according to the outcomes measured, as described in 6.4.3.

Because Crohn's disease PBMC viability was often <70% at baseline (section 6.4.5), which was likely due to Crohn's disease PBMCs being more fragile than healthy PBMCs, viability was coded as a covariate for both groups in order to allow comparisons, increase the power and remove the bias of having a confounding variable.

There were no differences in the frequencies of MAIT cells, $CD4^+$ MAIT cells, $CD8^+$ MAIT cells, DP MAIT cells or DN MAIT cells between unstimulated healthy PBMCs and Crohn's disease PBMCs (Table 6.4). As expected, the most abundant MAIT cell subsets were $CD8^+$ MAIT cells (healthy PBMCs, 45.7 ± 5.7% of MAIT cells; Crohn's disease PBMCs, 43.4 ± 18.6% of MAIT cells) and DN MAIT cells (healthy PBMCs, 32.3 ± 16.5% of MAIT cells; Crohn's disease PBMCs, 28.0 ± 13.3% of MAIT cells).

The expression levels of CD161 or TCR Vα7.2 on MAIT cells or of CD8 on $CD8^+$ MAIT cells were not different in Crohn's disease PBMCs compared to healthy PBMCs (Table 6.5).

There was a trend (*p*= 0.086) for lower percentages of DN MAIT cells expressing CD69 in Crohn's disease PBMCs (11.5 ± 8.4%) compared to healthy PBMCs (37.5 ± 16.6%). No differences in the expression of CD69 by total MAIT cells, $CD4^+$ MAIT cells, $CD8^+$ MAIT cells or DP MAIT cells were observed in Crohn's disease PBMCs compared to healthy PBMCs (Table 6.6).

IFN-γ and IL-17A expression of MAIT cells at baseline was low both in Crohn's disease PBMCs and in healthy PBMCs. Nevertheless, MAIT cells from Crohn's disease PBMCs expressed significantly higher levels of IL-17A compared to MAIT cells from healthy PBMCs (0.26 ± 0.35% *vs* 0.03 ± 0.06%, respectively; *p*= 0.011) (Table 6.7), in agreement with the literature [95].

Overall, Crohn's disease PBMCs and healthy PBMCs presented similar phenotype and activation status for most of the analysed subsets at baseline, but different expression levels of intracellular IL-17A.

Table 6.4 Frequencies of MAIT cells and MAIT cell subsets from unstimulated healthy PBMCs and Crohn's disease PBMCs after 20 h culture. Cell frequencies were measured by flow cytometry. Cell viability was coded as a covariate.

Cell frequencies	**Healthy PBMCs Unstimulated**	**Crohn's disease PBMCs Unstimulated**	**One-way ANCOVA *p* value**
	Mean ± SD (*n*= 7)	Mean ± SD (*n*= 6)	
MAIT cells (% of T cells)	2.6 ± 1.8	3.3 ± 2.3	0.122
$CD4^+$ MAIT cells (% of MAIT cells)	15.1 ± 10.6	17.3 ± 14.7	0.638
$CD8^+$ MAIT cells (% of MAIT cells)	45.7 ± 5.7	43.4 ± 18.6	0.592
DP MAIT cells (% of MAIT cells)	6.9 ± 7.5	11.2 ± 12.4	0.784
DN MAIT cells (% of MAIT cells)	32.3 ± 16.5	28.0 ± 13.3	0.913

Table 6.5 CD161, TCR Vα7.2 and CD8 (MFI) expression by MAIT cells and MAIT cell subsets from unstimulated healthy PBMCs and Crohn's disease PBMCs after 20 h culture. Cell frequencies were measured by flow cytometry. Cell viability was coded as a covariate.

Median fluorescence intensity (MFI)	**Healthy PBMCs Unstimulated**	**Crohn's disease PBMCs Unstimulated**	**One-way ANCOVA *p* value**
	Mean ± SD (*n*= 7)	Mean ± SD (*n*= 6)	
MFI of CD161 on MAIT cells	10,954 ± 2,335	10,271 ± 3,033	0.290
MFI of TCR Vα7.2 on MAIT cells	6,877 ± 760	6,895 ± 1,068	0.306
MFI of CD8 on $CD8^+$ MAIT cells	33,130 ± 13,133	30,051 ± 4,200	0.911

Table 6.6 Frequencies of CD69-expressing MAIT cells and MAIT cell subsets from unstimulated healthy PBMCs and Crohn's disease PBMCs after 20 h culture. Cell frequencies were measured by flow cytometry. Cell viability was coded as a covariate.

Cell frequencies	**Healthy PBMCs Unstimulated**	**Crohn's disease PBMCs Unstimulated**	**One-way ANCOVA *p* value**
	Mean ± SD (*n*= 7)	Mean ± SD (*n*= 6)	
% of MAIT cells expressing CD69	35.8 ± 16.8	13.7 ± 8.8	0.152
% of $CD4^+$ MAIT cells expressing CD69	4.4 ± 3.8	2.7 ± 1.9	0.649
% of $CD8^+$ MAIT cells expressing CD69	47.0 ± 17.4	17.5 ± 13.9	0.139
% of DN MAIT cells expressing CD69	37.5 ± 16.6	11.5 ± 8.4	0.086

Table 6.7 Frequencies of IFN-γ- and IL-17A- expressing MAIT cells from unstimulated healthy PBMCs and Crohn's disease PBMCs after 20 h culture. Brefeldin A (5 µg/mL) was added after 1 h incubation. Cell frequencies were measured by flow cytometry. Cell viability was coded as a covariate.

Cell frequencies	**Healthy PBMCs Unstimulated**	**Crohn's disease PBMCs Unstimulated**	**One-way ANCOVA *p* value**
	Mean ± SD (*n*= 7)	Mean ± SD (*n*= 6)	
% of MAIT cells expressing IFN-γ	1.2 ± 1.2	7.6 ± 16.1	0.152
% of MAIT cells expressing IL-17A	0.03 ± 0.06	0.26 ± 0.35	**0.011**

6.4.5 Effects of culturing healthy and Crohn's disease PBMCs with GOS and/or a selected vitamin B metabolite on the frequencies and functions of MAIT cells and other T cell subsets

Cell viability was measured to ensure that PBMCs tolerated 20 h culturing with B-GOS® batch C and/or with vitamin B metabolite 5-A-RU + MG at the chosen concentrations. Healthy PBMCs presented viability above 80% for all conditions tested, with no differences compared to unstimulated control, both in absence and in presence of brefeldin A (Table 6.8 and Table 6.9, respectively). On average, Crohn's disease PBMCs presented lower viability compared to healthy PBMCs, both in absence (60.6 ± 10.4 *vs* 84.4 ± 5.1) and in presence (63.9 ± 12.0 *vs* 88.7 ± 3.4) of brefeldin A (Table 6.10 and Table 6.11, respectively). No significant differences were observed

between stimulated and unstimulated Crohn's disease PBMCs in terms of cell viability, indicating that the culturing conditions were tolerated. Baseline differences in cell viability between healthy and Crohn's disease PBMCs were taken into account by including cell viability as a covariate in the statistical analyses, as previously anticipated in section 6.4.4.

Table 6.8 Viability of PBMCs from healthy donors cultured for 20 h with the vitamin B metabolite 5-A-RU + MG, B-GOS® batch C or a combination of the two in absence of brefeldin A.

	NC	**5-A-RU + MG**	**GOS C 0.8**	**GOS C 4**	**GOS C 12**	**5-A-RU + MG + GOS C 0.8**	**5-A-RU + MG + GOS C 4**	**5-A-RU + MG + GOS C 12**	**One-way ANOVA *p* value**
	Mean ± SD (*n*= 7)	Mean ± SD (*n*= 7)	Mean ± SD (*n*= 7)	Mean ± SD (*n*= 7)	Mean ± SD (*n*= 7)	Mean ± SD (*n*= 7)	Mean ± SD (*n*= 7)	Mean ± SD (*n*= 7)	
Viability (%)	84.9 ± 4.6	84.3 ± 4.0	85.3 ± 5.1	85.4 ± 4.8	83.8 ± 6.0	84.1 ± 5.4	84.4 ± 5.1	82.8 ± 5.8	0.9863

Table 6.9 Viability of PBMCs from healthy donors cultured for 20 h with the vitamin B metabolite 5-A-RU + MG, B-GOS® batch C or a combination of the two in presence of brefeldin A.

	NC	**5-A-RU + MG**	**GOS C 0.8**	**GOS C 4**	**GOS C 12**	**5-A-RU + MG + GOS C 0.8**	**5-A-RU + MG + GOS C 4**	**5-A-RU + MG + GOS C 12**	**One-way ANOVA *p* value**
	Mean ± SD (*n*= 6)	Mean ± SD (*n*= 6)	Mean ± SD (*n*= 6)	Mean ± SD (*n*= 6)	Mean ± SD (*n*= 6)	Mean ± SD (*n*= 6)	Mean ± SD (*n*= 6)	Mean ± SD (*n*= 6)	
Viability (%)	90.1 ± 3.5	88.9 ± 2.9	89.8 ± 3.7	89.5 ± 3.4	86.2 ± 4.5	89.0 ± 3.7	89.0 ± 3.2	87.0 ± 2.6	0.4832

Table 6.10 Viability of PBMCs from Crohn's disease donors cultured for 20 h with the vitamin B metabolite 5-A-RU + MG, B-GOS® batch C or a combination of the two in absence of brefeldin A.

	NC	**5-A-RU + MG**	**GOS C 12**	**5-A-RU + MG + GOS C 12**	**One-way ANOVA *p* value**
	Mean ± SD (*n*= 6)	Mean ± SD (*n*= 6)	Mean ± SD (*n*= 6)	Mean ± SD (*n*= 6)	
Viability (%)	67.3 ± 9.6	58.7 ± 10.0	62.4 ± 11.7	54.1 ± 10.3	0.1951

Table 6.11 Viability of PBMCs from Crohn's disease donors cultured for 20 h with the vitamin B metabolite 5-A-RU + MG, B-GOS® batch C or a combination of the two in presence of brefeldin A.

	NC	**5-A-RU + MG**	**GOS C 12**	**5-A-RU + MG + GOS C 12**	**One-way ANOVA *p* value**
	Mean ± SD (*n*= 5)	Mean ± SD (*n*= 6)	Mean ± SD (*n*= 6)	Mean ± SD (*n*= 6)	
Viability (%)	69.8 ± 14.9	64.2 ± 10.2	61.8 ± 11.1	59.6 ± 11.6	0.5494

While incubation of healthy PBMCs with GOS did not affect the frequencies of lymphocytes, T cell subsets or MAIT cell subsets, incubation with 5-A-RU + MG led to lower percentages of MAIT cells and $CD8^+$ MAIT cells (Figure 6.15 and Figure 6.16). MAIT cells from healthy PBMCs also expressed lower levels of TCR Vα7.2 on their surface after stimulation with 5-A-RU + MG (Figure 6.17). Similarly, when Crohn's disease PBMCs were cultured with 5-A-RU + MG, lower percentages of $CD8^+$ MAIT cells and slightly lower numbers of total T cells were seen, while higher percentages of DN MAIT were observed (Figure 6.18 and Figure 6.19). Incubation of Crohn's disease PBMCs with GOS did not alter T cell and MAIT cell frequencies (Figure 6.18 and Figure 6.19), nor did it induce changes in the expression levels of CD161 and TCR Vα7.2 on MAIT cells (Figure 6.20). Data were also reported in a table format and are available in Appendix F. Taken together, these results indicate that GOS do not alter T cell or MAIT cell frequencies in healthy PBMCs or in Crohn's disease PBMCs.

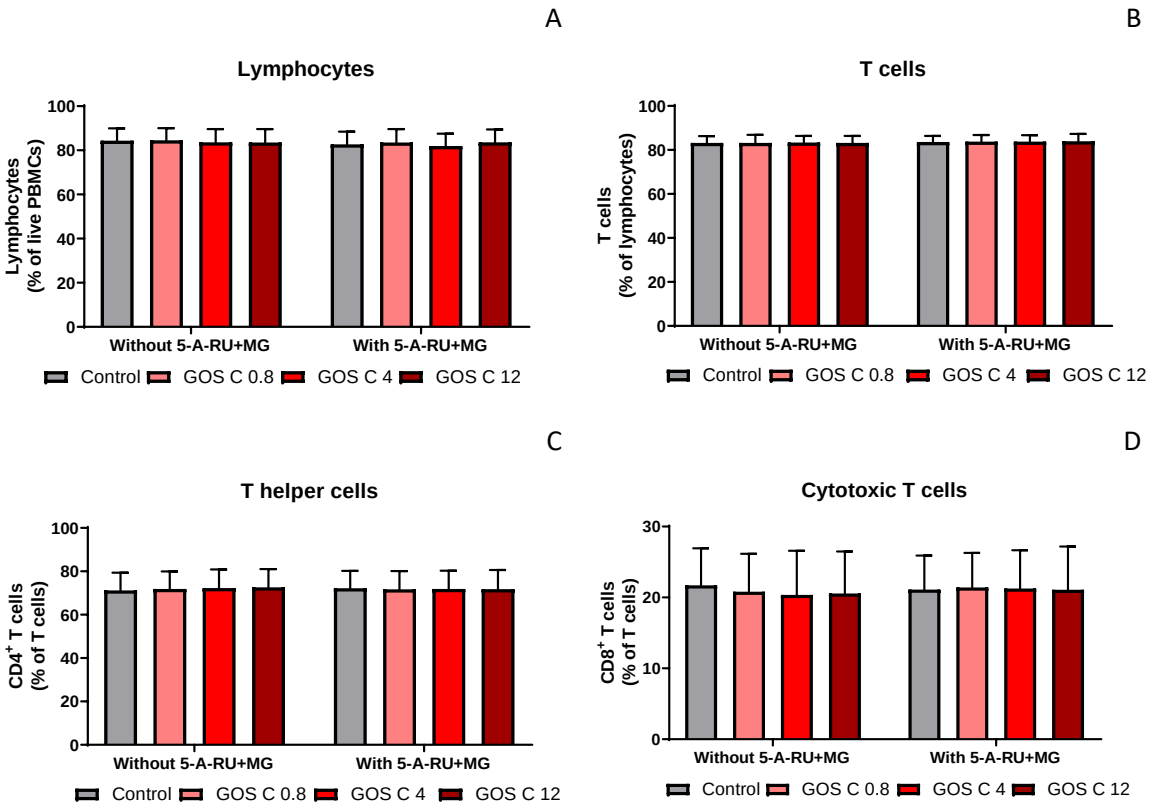

Figure 6.15 Frequencies of lymphocytes, T cells and T cell subsets from healthy PBMCs (*n*= 7) after 20 h culture with 5-A-RU + MG or B-GOS® batch C or after co-culture with both. Unstimulated PBMCs were used as a negative control. Cell frequencies were measured by flow cytometry. Data are expressed as mean ± standard deviation (SD).

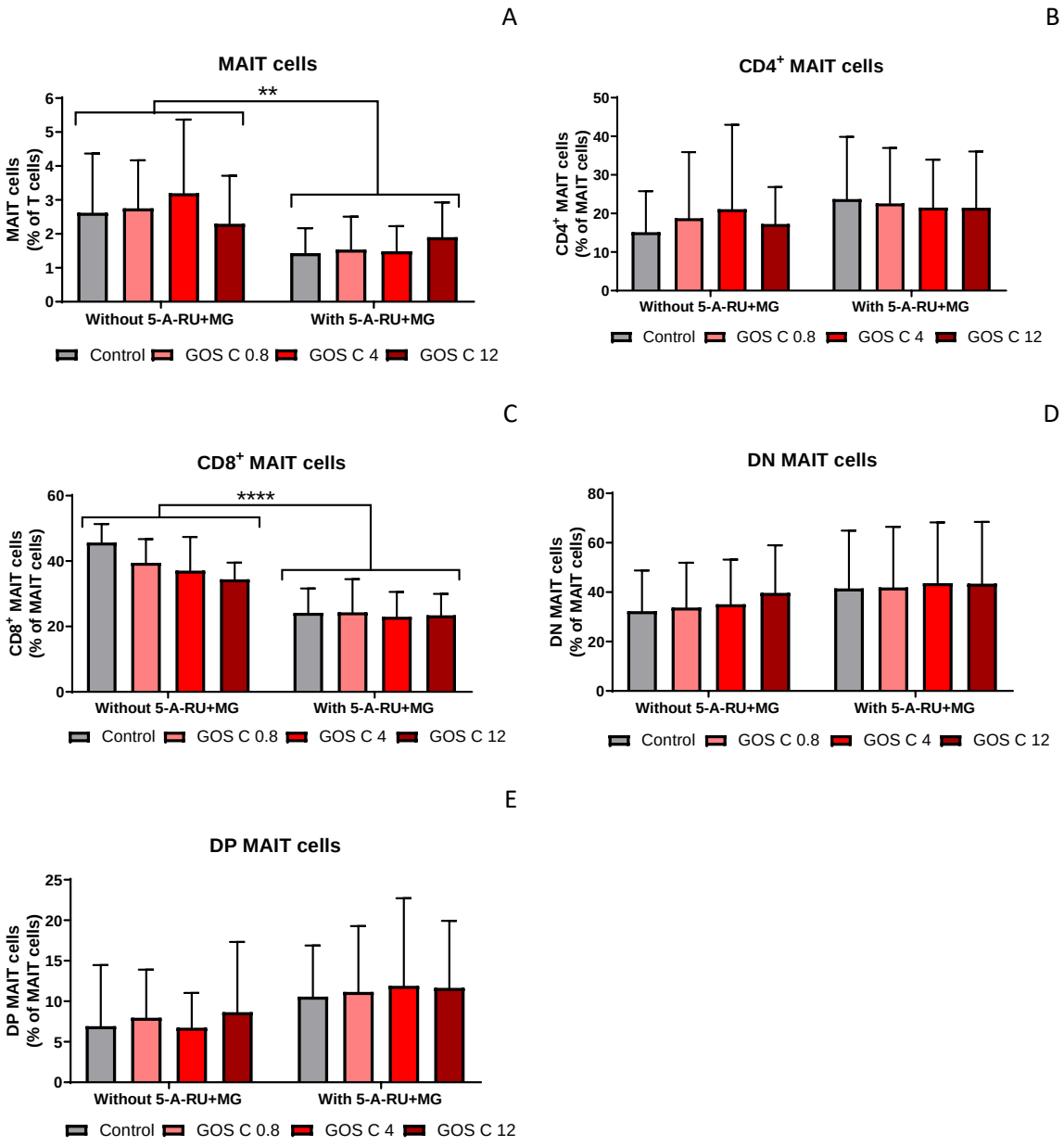

Figure 6.16 Frequencies of MAIT cells and MAIT cell subsets from healthy PBMCs (*n*= 7) after 20 h culture with 5-A-RU + MG or B-GOS® batch C or after co-culture with both. Unstimulated PBMCs were used as a negative control. Cell frequencies were measured by flow cytometry. Data are expressed as mean ± standard deviation (SD). Two-way ANCOVA followed by Bonferroni's *post-hoc* test was performed. Cell viability was coded as a covariate. Significant differences between 'without 5-A-RU + MG' *vs* 'with 5-A-RU + MG' are marked with an asterisk. A) ***p*= 0.005; C) *****p*< 0.0001.

A B

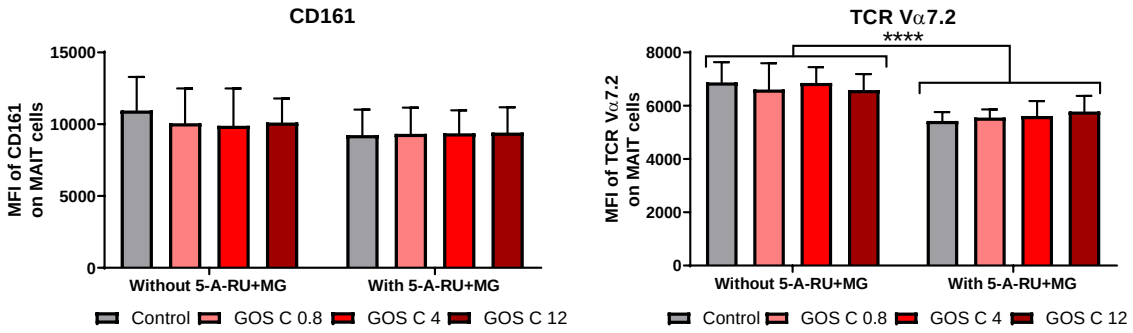

Figure 6.17 CD161 and TCR Vα7.2 expression (MFI) on MAIT cells from healthy PBMCs (*n*= 7) after 20 h culture with 5-A-RU + MG or B-GOS® batch C or after co-culture with both. Unstimulated PBMCs were used as a negative control. Cell frequencies were measured by flow cytometry. Data are expressed as mean ± standard deviation (SD). Two-way ANCOVA followed by Bonferroni's *post-hoc* test was performed. Cell viability was coded as a covariate. Significant differences between 'without 5-A-RU + MG' *vs* 'with 5-A-RU + MG' are marked with an asterisk. B) ****p< 0.0001.

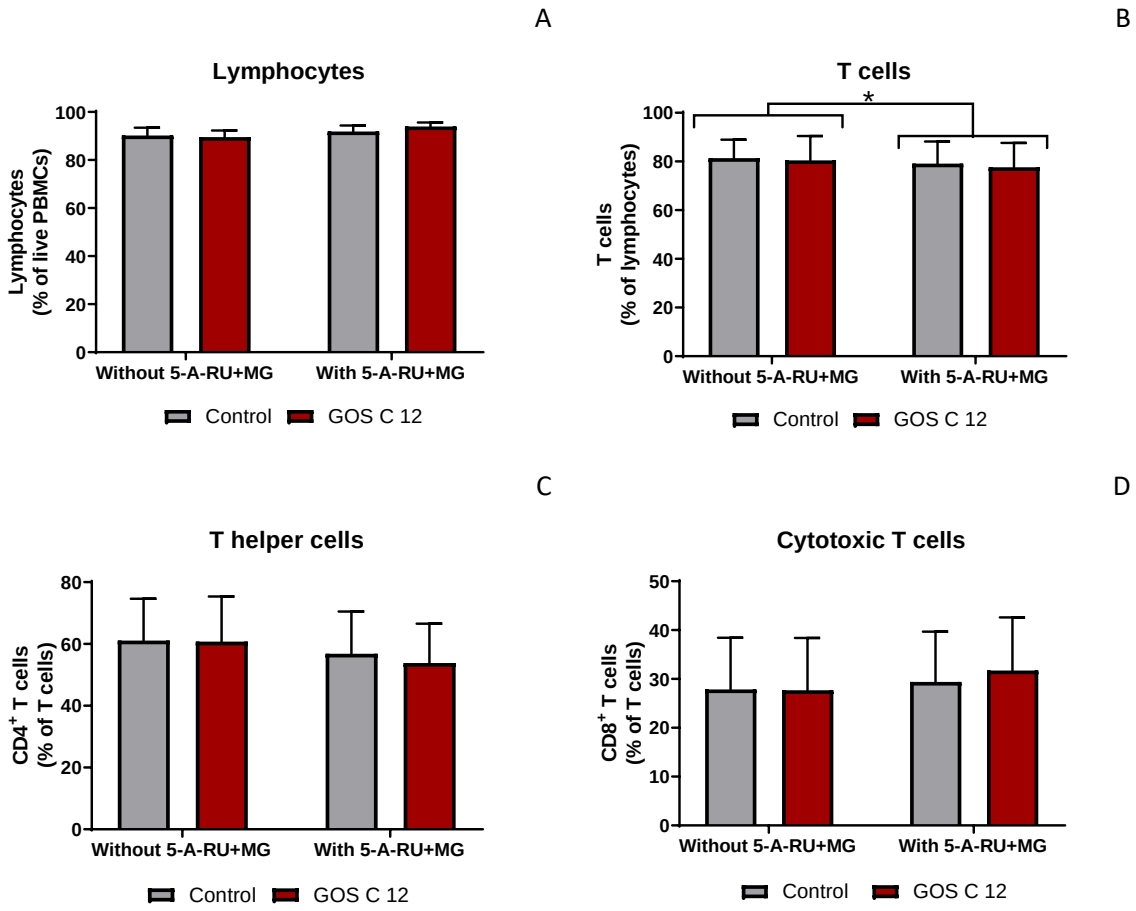

Figure 6.18 Frequencies of lymphocytes, T cells and T cell subsets from Crohn's disease PBMCs (*n*= 6) after 20 h culture with 5-A-RU + MG or B-GOS® batch C or after co-culture with both. Unstimulated PBMCs were used as a negative control. Cell frequencies were measured by flow cytometry. Data are expressed as mean ± standard deviation (SD). Two-way ANCOVA followed by Bonferroni's *post-hoc* test was performed. Cell viability was coded as a covariate. Significant differences between 'without 5-A-RU + MG' *vs* 'with 5-A-RU + MG' are marked with an asterisk. B) *p= 0.049.

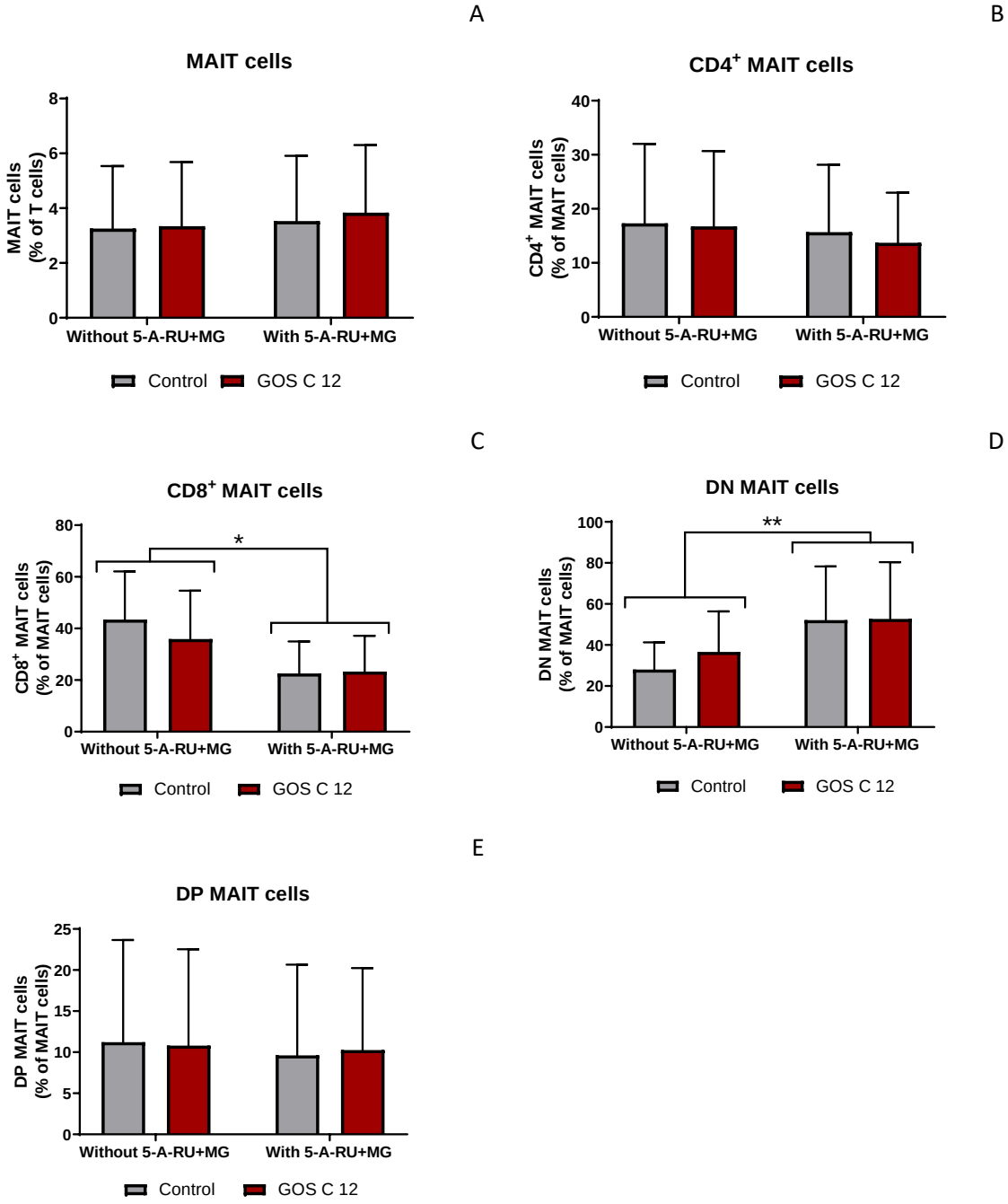

Figure 6.19 Frequencies of MAIT cells and MAIT cell subsets from Crohn's disease PBMCs (*n*= 6) after 20 h culture with 5-A-RU + MG or B-GOS® batch C or after co-culture with both. Unstimulated PBMCs were used as a negative control. Cell frequencies were measured by flow cytometry. Data are expressed as mean ± standard deviation (SD). Two-way ANCOVA followed by Bonferroni's *post-hoc* test was performed. Cell viability was coded as a covariate. Significant differences between 'without 5-A-RU + MG' *vs* 'with 5-A-RU + MG' are marked with an asterisk. C) **p*= 0.0049; D) ***p*= 0.007.

A B

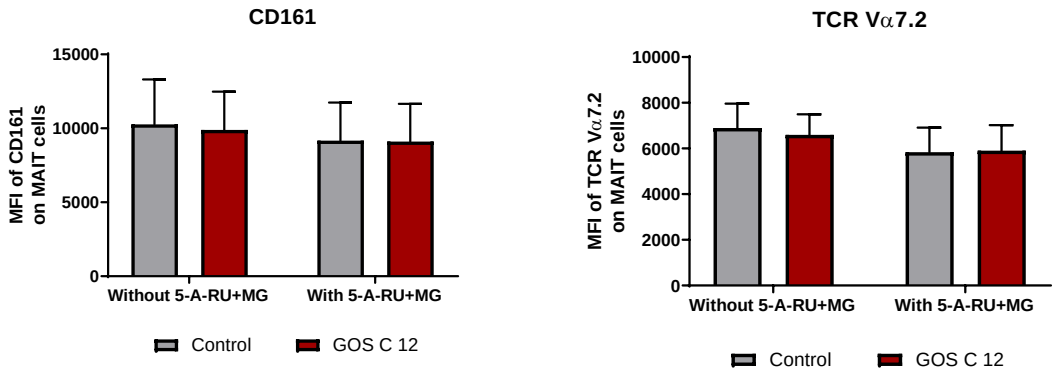

Figure 6.20 CD161 and TCR Vα7.2 expression (MFI) on MAIT cells from Crohn's disease PBMCs (*n*= 6) after 20 h culture with 5-A-RU + MG or B-GOS® batch C or after co-culture with both. Unstimulated PBMCs were used as a negative control. Cell frequencies were measured by flow cytometry. Data are expressed as mean ± standard deviation (SD).

Healthy PBMCs incubated with GOS presented higher frequencies of $CD69^+$ T helper cells compared to unstimulated control. A trend (p= 0.058) for higher frequencies of $CD69^+$ $CD8^+$ MAIT cells was seen when healthy PBMCs were cultured with 5-A-RU + MG compared to those incubated without 5-A-RU + MG (Figure 6.21 and Figure 6.22).

An increase in the expression of CD69 (MFI) on T cells, cytotoxic T cells, MAIT cells, $CD8^+$ MAIT cells and DN MAIT cells was observed when healthy PBMCs were stimulated with 5-A-RU + MG (Figure 6.23 and Figure 6.24). Conversely, stimulation with GOS alone did not affect CD69 expression on any T cell or MAIT cell subsets (Figure 6.23 and Figure 6.24). Co-culture of healthy PBMCs with GOS and 5-A-RU + MG resulted in lower CD69 expression by T cells and cytotoxic T cells compared to 5-A-RU + MG alone (Figure 6.23 and Figure 6.24).

Higher frequencies of $CD69^+$ T cells, $CD69^+$ T helper cells and $CD69^+$ cytotoxic T cells were found within Crohn's PBMCs cultured with GOS in absence of 5-A-RU + MG. The stimulatory effects of GOS on T cells and T cell subsets were lost when 5-A-RU + MG was present (Figure 6.25). As opposed to what observed in healthy PBMCs, lower frequencies of $CD69^+$ MAIT cells and $CD69^+$ DN MAIT cells were found in Crohn's disease PBMCs after incubation with 5-A-RU + MG compared to those incubated without 5-A-RU + MG (Figure 6.26). However, neither GOS nor 5-A-RU + MG caused any changes in CD69 (MFI) expression on T cells (Figure 6.27). Data presented in figures were also reported in a table format and are available in Appendix F.

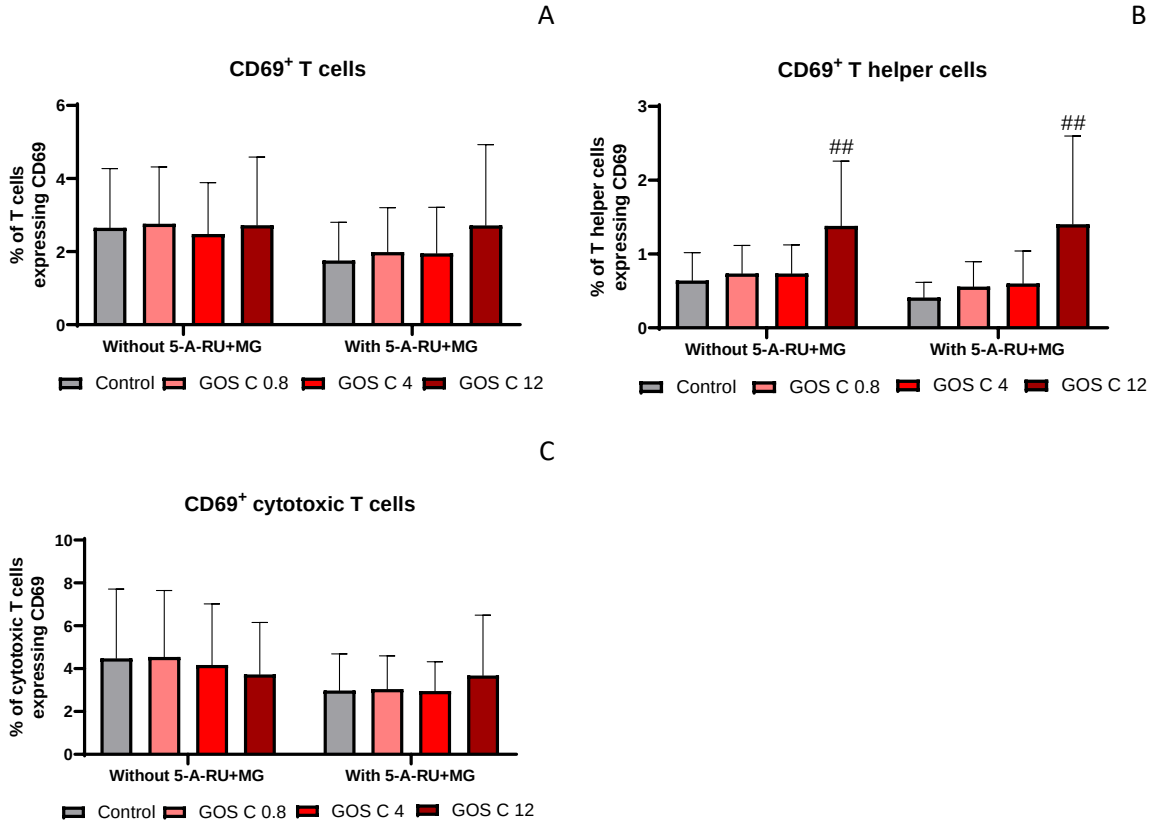

Figure 6.21 Frequencies of CD69-expressing T cells and T cell subsets from healthy PBMCs (*n*= 7) after 20 h culture with 5-A-RU + MG or B-GOS® batch C or after co-culture with both. Unstimulated PBMCs were used as a negative control. Cell frequencies were measured by flow cytometry. Data are expressed as mean ± standard deviation (SD). Two-way ANCOVA followed by Bonferroni's *post-hoc* test was performed. Cell viability was coded as a covariate. Significant differences between GOS *vs* control are marked with a hash. B) $^{\#\#}p$= 0.004.

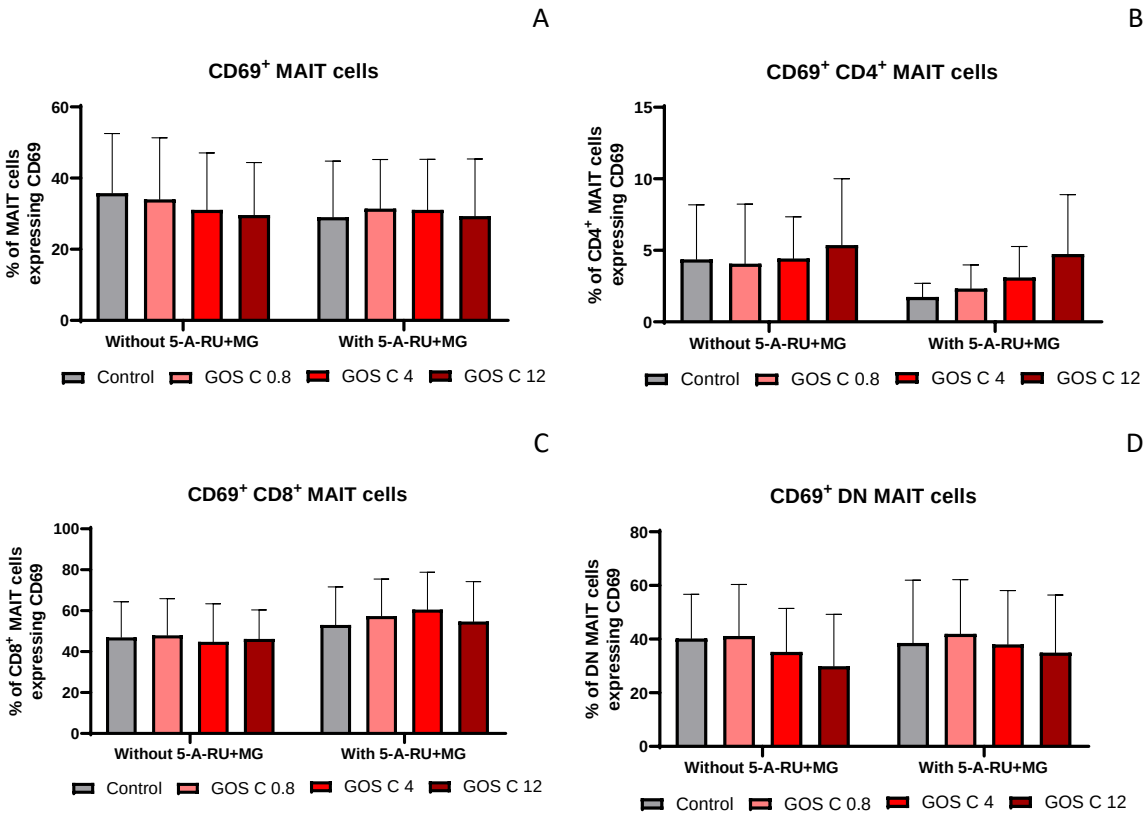

Figure 6.22 Frequencies of CD69-expressing MAIT cells and MAIT cell subsets from healthy PBMCs (*n*= 7) after 20 h culture with 5-A-RU + MG or B-GOS® batch C or after co-culture with both. Unstimulated PBMCs were used as a negative control. Cell frequencies were measured by flow cytometry. Data are expressed as mean ± standard deviation (SD).

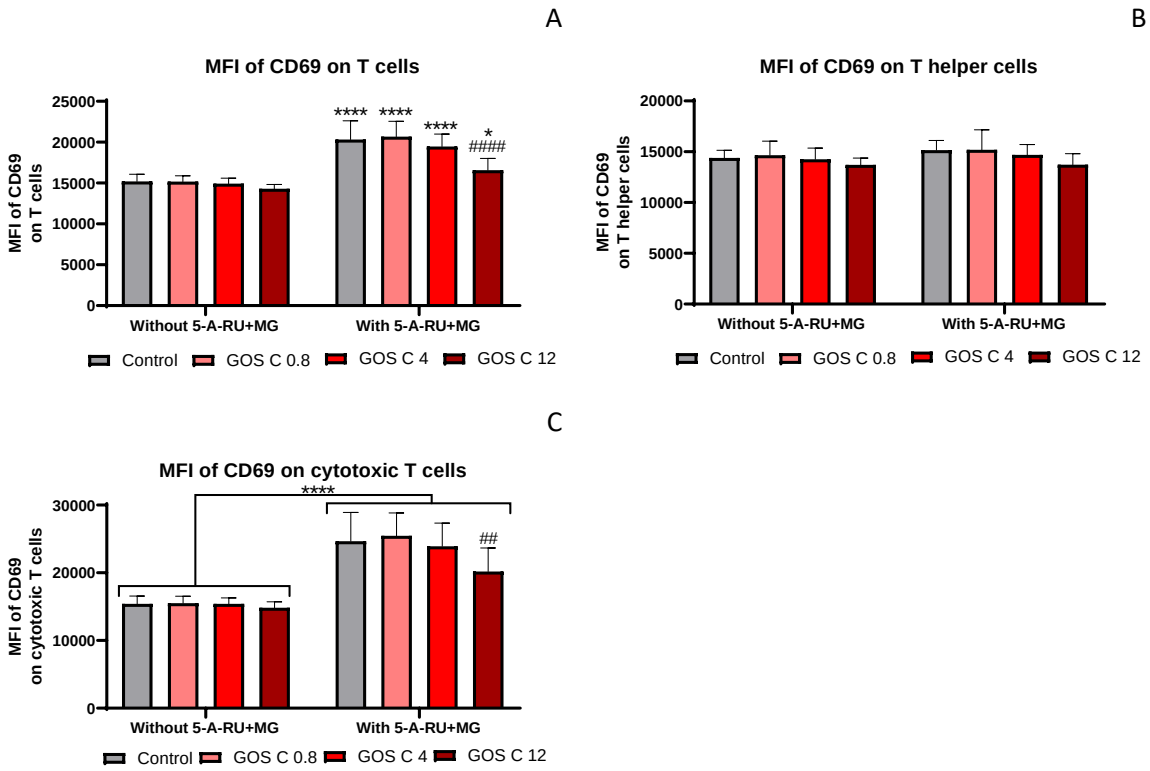

Figure 6.23 CD69 (MFI) expression on T cells and T cell subsets from healthy PBMCs (*n*= 7) after 20 h culture with 5-A-RU + MG or B-GOS® batch C or after co-culture with both. Unstimulated PBMCs were used as a negative control. Cell frequencies were measured by flow cytometry. Data are expressed as mean ± standard deviation (SD). Two-way ANCOVA followed by Bonferroni's *post-hoc* test was performed. Cell viability was coded as a covariate. Significant differences between 'without 5-A-RU + MG' *vs* 'with 5-A-RU + MG' are marked with an asterisk. Significant differences between GOS *vs* control are marked with a hash. A) ****p< 0.0001; *p= 0.0135; $^{\#\#\#\#}p$< 0.0001. C) ****p< 0.0001; $^{\#\#}p$= 0.0081.

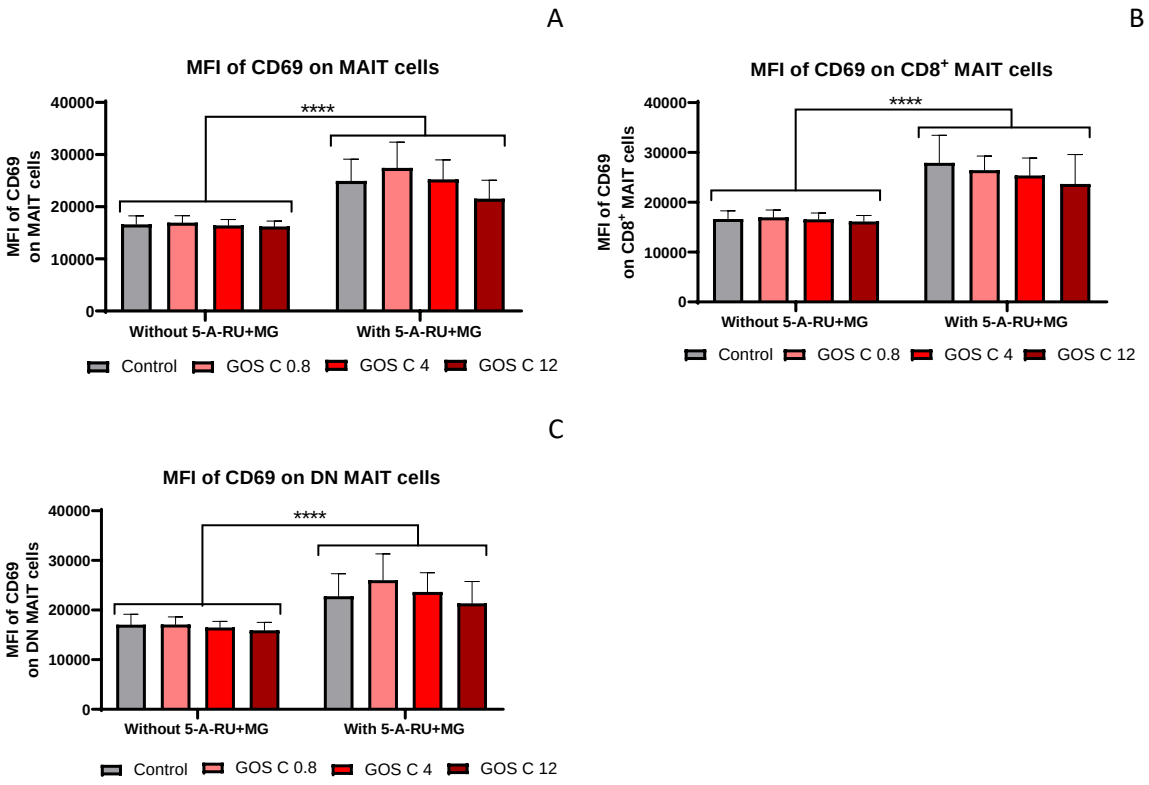

Figure 6.24 CD69 (MFI) expression on MAIT cells and MAIT cell subsets from healthy PBMCs (*n*= 7) after 20 h culture with 5-A-RU + MG or B-GOS® batch C or after co-culture with both. Unstimulated PBMCs were used as a negative control. Cell frequencies were measured by flow cytometry. Data are expressed as mean ± standard deviation (SD). Two-way ANCOVA followed by Bonferroni's *post-hoc* test was performed. Cell viability was coded as a covariate. Significant differences between 'without 5-A-RU + MG' *vs* 'with 5-A-RU + MG' are marked with an asterisk. All ****p< 0.0001.

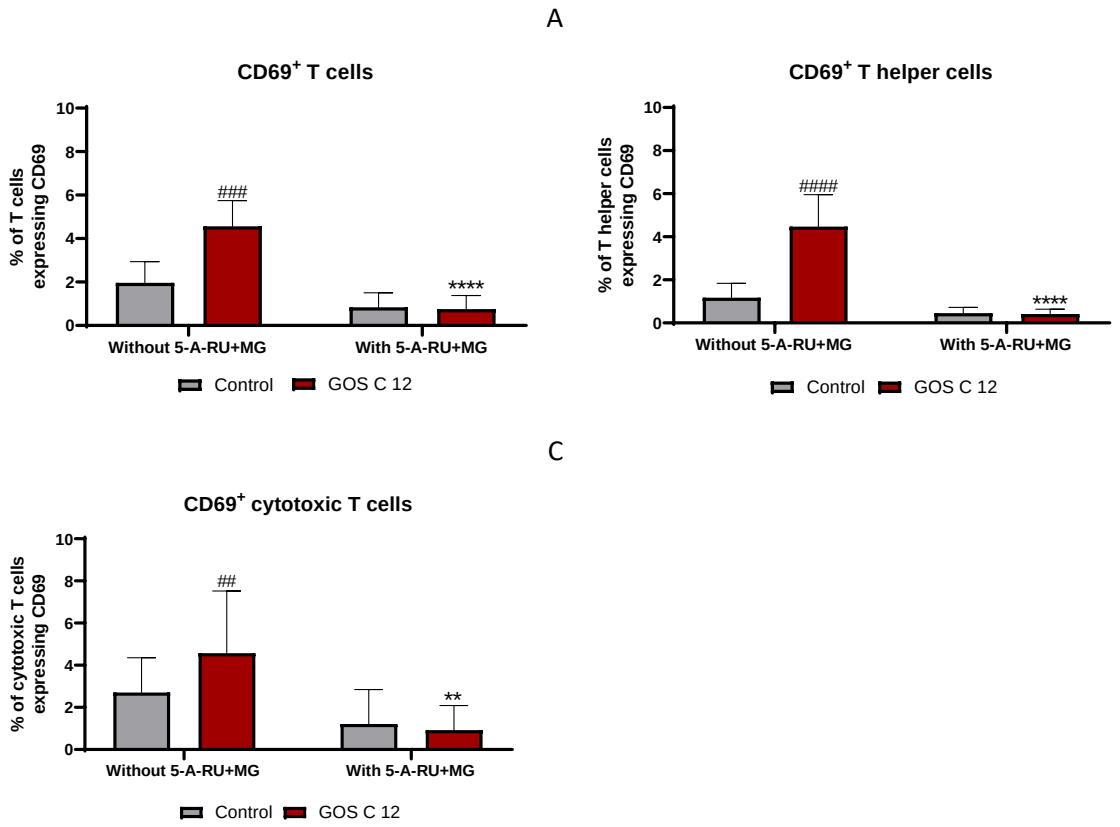

Figure 6.25 Frequencies of CD69-expressing T cells and T cell subsets from Crohn's disease PBMCs (*n*= 6) after 20 h culture with 5-A-RU + MG or B-GOS® batch C or after co-culture with both. Unstimulated PBMCs were used as a negative control. Cell frequencies were measured by flow cytometry. Data are expressed as mean ± standard deviation (SD). Two-way ANCOVA followed by Bonferroni's *post-hoc* test was performed. Cell viability was coded as a covariate. Significant differences between 'without 5-A-RU + MG' *vs* 'with 5-A-RU + MG' are marked with an asterisk. Significant differences between GOS *vs* control are marked with a hash. A) ****p< 0.0001; $^{\#\#\#\#}p$= 0.0001. B) ****p< 0.0001; $^{\#\#\#\#}p$= 0.0001. C) **p= 0.034; $^{\#\#}p$= 0.029.

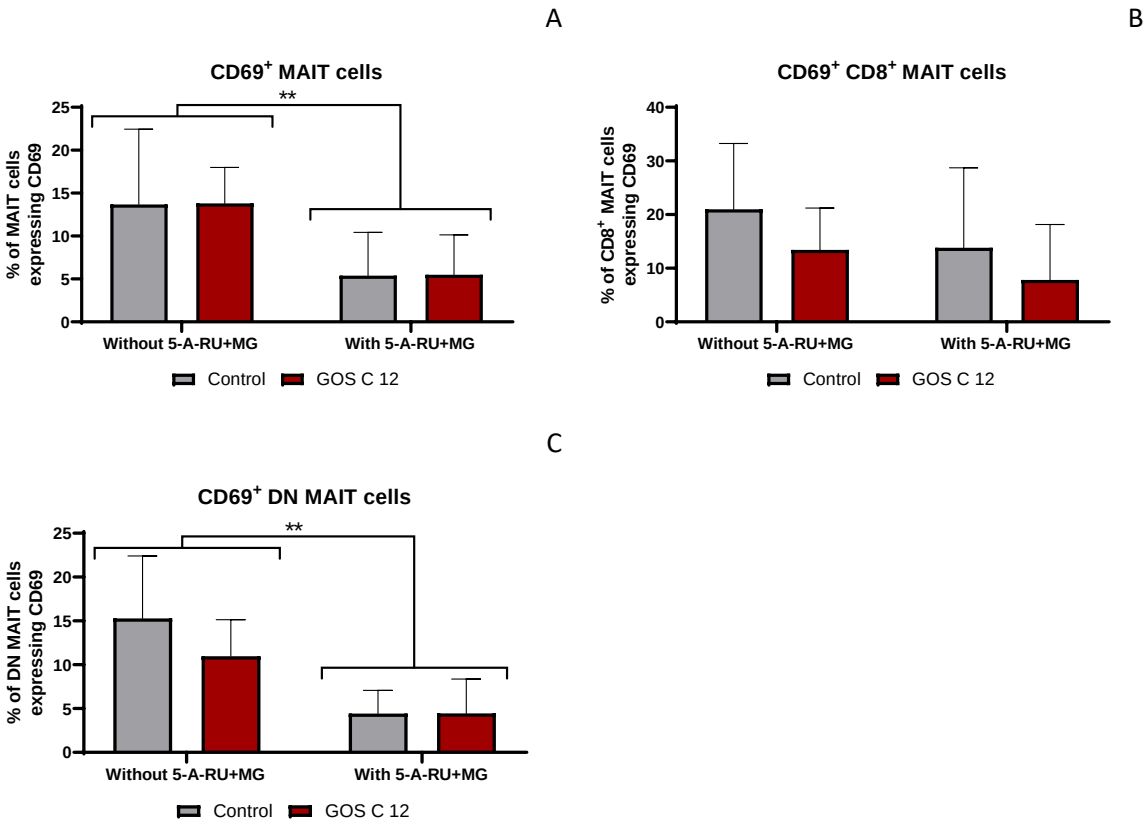

Figure 6.26 Frequencies of CD69-expressing MAIT cells and MAIT cell subsets from Crohn's disease PBMCs (*n*= 6) after 20 h culture with 5-A-RU + MG or B-GOS® batch C or after co-culture with both. Unstimulated PBMCs were used as a negative control. Cell frequencies were measured by flow cytometry. Data are expressed as mean ± standard deviation (SD). Two-way ANCOVA followed by Bonferroni's *post-hoc* test was performed. Cell viability was coded as a covariate. Significant differences between 'without 5-A-RU + MG' *vs* 'with 5-A-RU + MG' are marked with an asterisk. A) ***p*= 0.018. B) ***p*= 0.011.

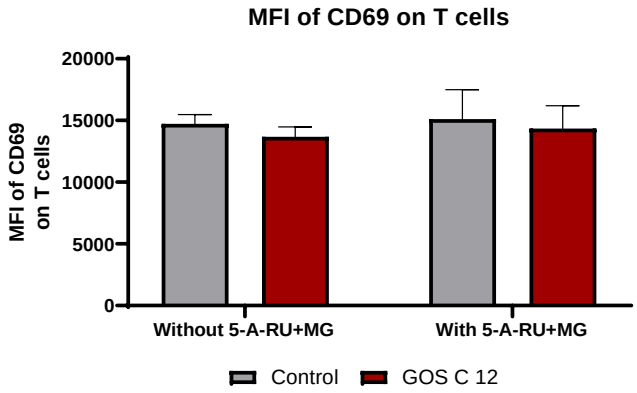

Figure 6.27 CD69 (MFI) expression on T cells from Crohn's disease PBMCs (*n*= 6) after 20 h culture with 5-A-RU + MG or B-GOS® batch C or after co-culture with both. Unstimulated PBMCs were used as a negative control. Cell frequencies were measured by flow cytometry. Data are expressed as mean ± standard deviation (SD).

In terms of intracellular cytokines, neither GOS nor 5-A-RU + MG or their combination affected the percentages of T cells and MAIT cells expressing IL-17A in healthy or in Crohn's disease PBMCs (Appendix F). In healthy PBMCs, higher percentages of T cells, cytotoxic T cells and MAIT cells expressed IFN-γ after stimulation with 5-A-RU + MG compared to those not incubated with the vitamin B metabolite, whereas GOS alone did not affect IFN-γ expression in any T cell subsets (Figure 6.28). No changes in the percentages of T cells or MAIT cells expressing IFN-γ were observed in Crohn's disease PBMCs after stimulation with GOS and/or 5-A-RU + MG (Figure 6.29).

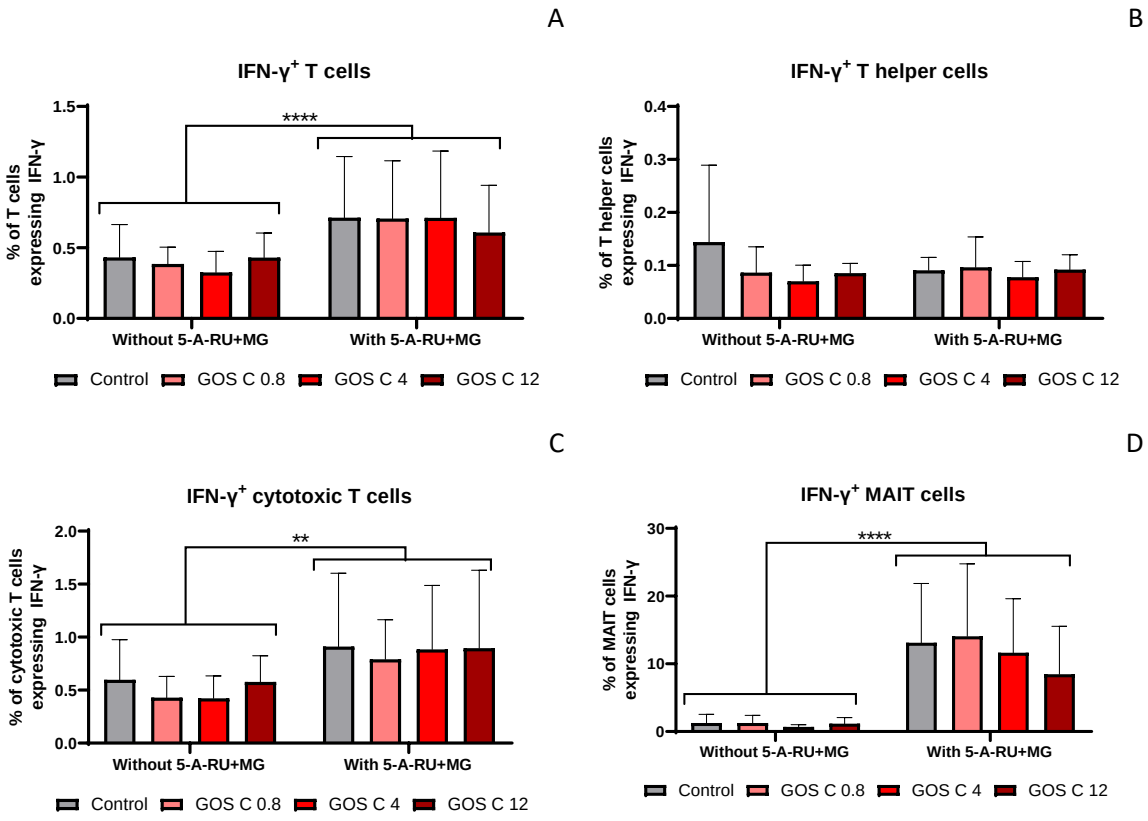

Figure 6.28 Frequencies of IFN-γ-expressing T cell subsets and MAIT cells from healthy PBMCs (*n*= 7) after 20 h culture with 5-A-RU + MG or B-GOS® batch C or after co-culture with both. Unstimulated PBMCs were used as a negative control. Brefeldin A (5 µg/mL) was added after 1 h incubation. Cell frequencies were measured by flow cytometry. Data are expressed as mean ± standard deviation (SD). Two-way ANCOVA followed by Bonferroni's *post-hoc* test was performed. Cell viability was coded as a covariate. Significant differences between 'without 5-A-RU + MG' *vs* 'with 5-A-RU + MG' are marked with an asterisk. A) ****p< 0.0001. C) **p= 0.003. D) ****p< 0.0001.

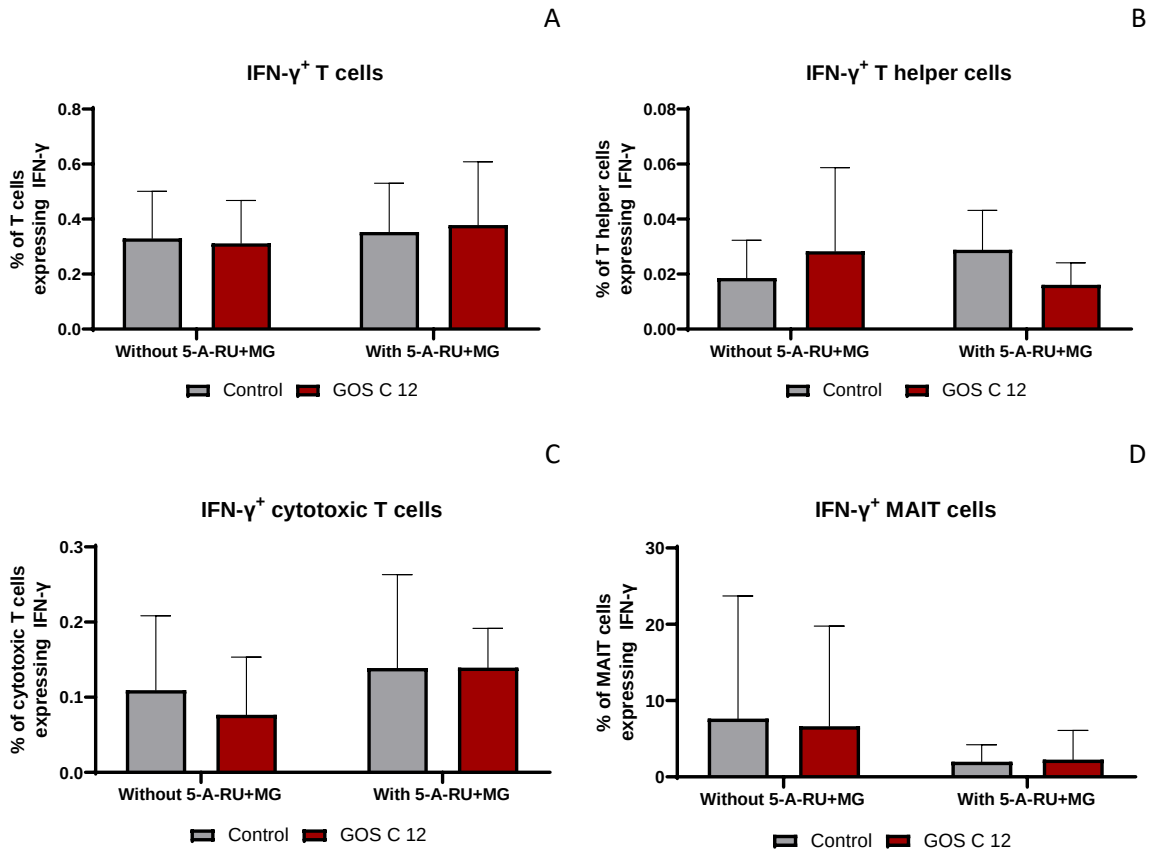

Figure 6.29 Frequencies of IFN-γ-expressing T cell subsets and MAIT cells from Crohn's disease PBMCs (*n*= 6) after 20 h culture with 5-A-RU + MG or B-GOS® batch C or after co-culture with both. Unstimulated PBMCs were used as a negative control. Brefeldin A (5 µg/mL) was added after 1 h incubation. Cell frequencies were measured by flow cytometry. Data are expressed as mean ± standard deviation (SD).

The effects of culturing healthy and Crohn's disease PBMCs with GOS and/or vitamin B metabolite were also assessed on a panel of secreted mediators chosen for their role in IBD (IL-1α, IL-1β, IL-1ra, IL-8, IL-10, IL-12p70, IL-17A, IFN-γ, TNF-α and granzyme B).

Healthy PBMCs incubated with 5-A-RU + MG secreted more IFN-γ and TNF-α compared to those incubated without the vitamin B metabolite (Figure 6.30). No differences were seen in the other soluble mediators assessed (Figure 6.31). Healthy PBMCs cultured with GOS secreted significantly higher levels of IL-8, both in presence and in absence of 5-A-RU + MG, compared to unstimulated control (Figure 6.32). Data were also summarised in a table format and presented in Appendix F.

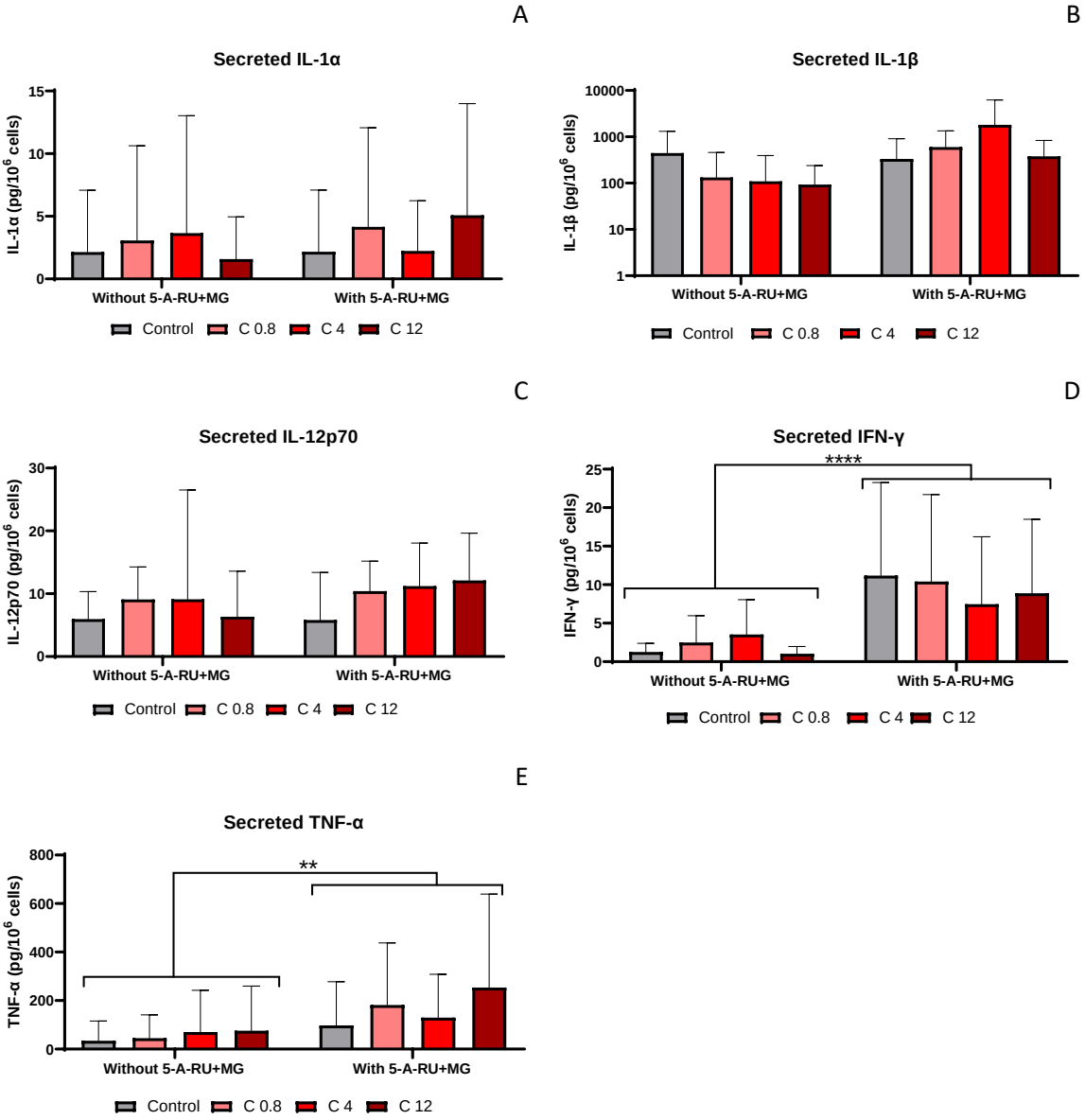

Figure 6.30 Th1 cytokines secreted by healthy PBMCs (*n*= 7) after 20 h culture with 5-A-RU + MG or B-GOS® batch C or after co-culture with both. Unstimulated PBMCs were used as a negative control (NC). Results were considered significant if $p < 0.05$. Secreted cytokines were measured by Luminex assay. Data are expressed as mean ± standard deviation (SD). Two-way ANCOVA followed by Bonferroni's *post-hoc* test was performed. Cell viability was coded as a covariate. Significant differences between 'without 5-A-RU + MG' *vs* 'with 5-A-RU + MG' are marked with an asterisk. D) ****$p < 0.0001$. E) **$p = 0.021$.

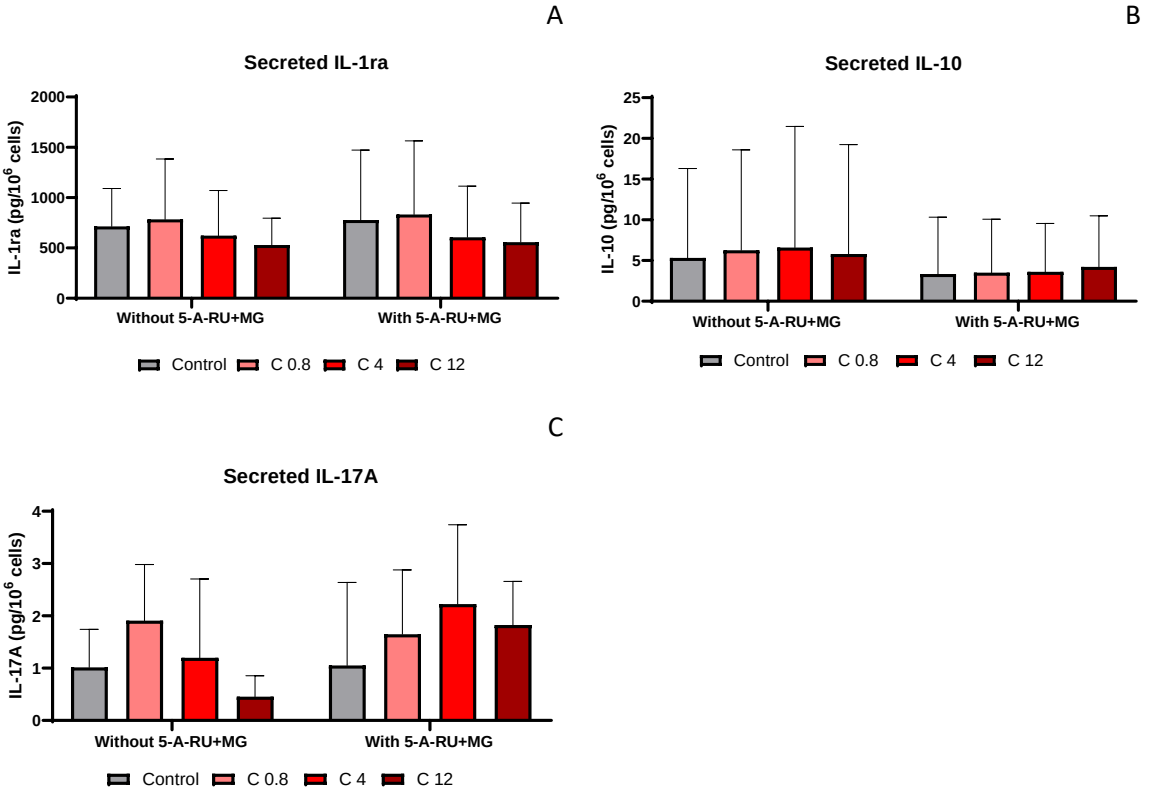

Figure 6.31 Th2 and Th17 cytokines secreted by healthy PBMCs (*n*= 7) after 20 h culture with 5-A-RU + MG or B-GOS® batch C or after co-culture with both. Unstimulated PBMCs were used as a negative control (NC). Results were considered significant if $p < 0.05$. Secreted cytokines were measured by Luminex assay. Data are expressed as mean ± standard deviation (SD).

A B

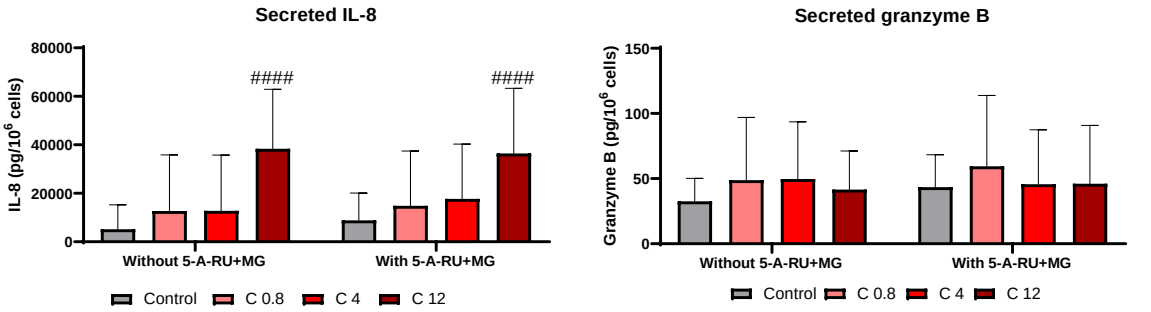

Figure 6.32 Chemokines (IL-8) and proteases (granzyme B) secreted by healthy PBMCs (*n*= 7) after 20 h culture with 5-A-RU + MG or B-GOS® batch C or after co-culture with both. Unstimulated PBMCs were used as a negative control (NC). Results were considered significant if $p< 0.05$. Secreted cytokines were measured by Luminex assay. Data are expressed as mean ± standard deviation (SD). Two-way ANCOVA followed by Bonferroni's *post-hoc* test was performed. Cell viability was coded as a covariate. Significant differences between GOS *vs* control are marked with a hash. A) $^{\#\#\#\#}p< 0.0001$.

Crohn's disease PBMCs cultured with GOS secreted higher levels of IL-1β, IL-8 and IFN-γ in absence of 5-A-RU + MG, compared to unstimulated control (Figure 6.33 and Figure 6.35). Crohn's disease PBMCs incubated with 5-A-RU + MG secreted less granzyme B and IL-1ra compared to those incubated without the vitamin B metabolite (Figure 6.34 and Figure 6.35). Data were also summarised in a table format and presented in Appendix F.

Overall, stimulation with GOS alone significantly increased the secretion of IL-8 in both healthy and Crohn's disease PBMCs. Additionally, GOS alone induced the release of higher levels of IL-1β and IFN-γ by Crohn's disease PBMCs. While incubation of healthy PBMCs with 5-A-RU + MG resulted in higher levels of intracellular and secreted IFN-γ, no changes in the levels of IFN-γ were seen in Crohn's disease PBMCs. Crohn's disease PBMCs were not as responsive as healthy PBMCs to 5-A-RU + MG challenge, as shown by their reduced ability to secrete granzyme B and IL-1ra after stimulation.

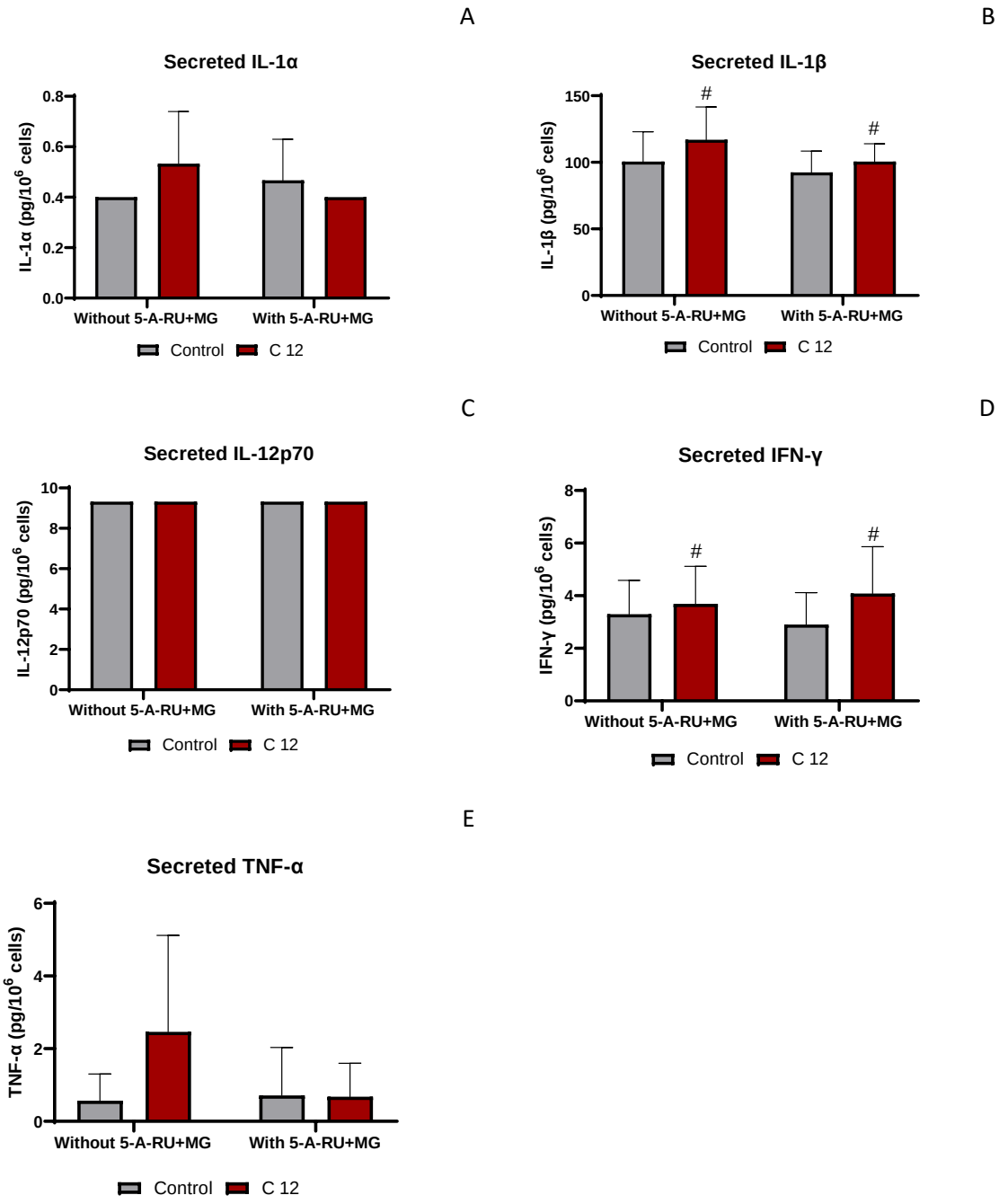

Figure 6.33 Th1 cytokines secreted by Crohn's disease PBMCs (*n*= 6) after 20 h culture with 5-A-RU + MG or B-GOS® batch C or after co-culture with both. Unstimulated PBMCs were used as a negative control (NC). Results were considered significant if $p< 0.05$. Secreted cytokines were measured by Luminex assay. Data are expressed as mean ± standard deviation (SD). Two-way ANCOVA followed by Bonferroni's *post-hoc* test was performed. Cell viability was coded as a covariate. Significant differences between GOS *vs* control are marked with a hash. B) $^{\#}p= 0.038$. D) $^{\#}p= 0.045$.

A

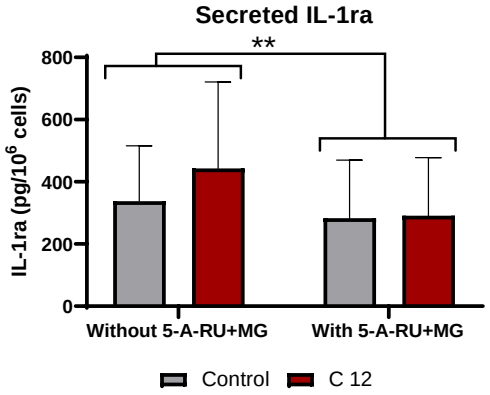

B

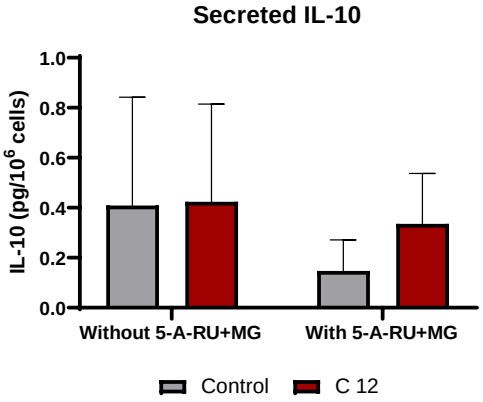

C

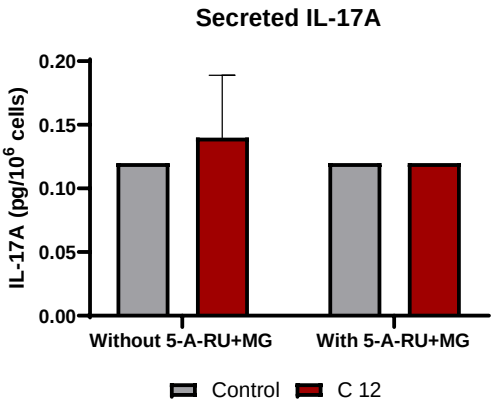

Figure 6.34 Th2 and Th17 cytokines secreted by Crohn's disease PBMCs (*n*= 6) after 20 h culture with 5-A-RU + MG or B-GOS® batch C or after co-culture with both. Unstimulated PBMCs were used as a negative control (NC). Results were considered significant if $p < 0.05$. Secreted cytokines were measured by Luminex assay. Data are expressed as mean ± standard deviation (SD). Two-way ANCOVA followed by Bonferroni's *post-hoc* test was performed. Cell viability was coded as a covariate. Significant differences between 'without 5-A-RU + MG' *vs* 'with 5-A-RU + MG' are marked with an asterisk. A) **p= 0.001.

A B

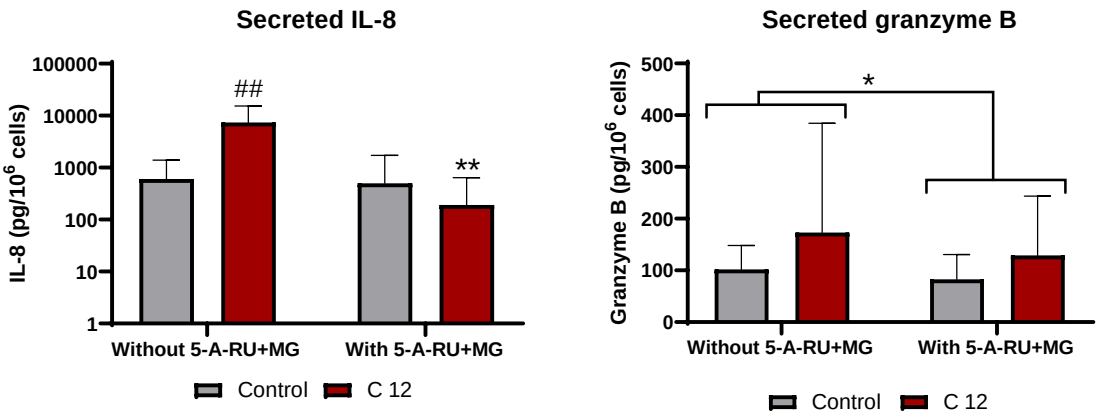

Figure 6.35 Chemokines (IL-8) and proteases (granzyme B) secreted by Crohn's disease PBMCs (*n*= 6) after 20 h culture with 5-A-RU + MG or B-GOS® batch C or after co-culture with both. Unstimulated PBMCs were used as a negative control (NC). Results were considered significant if $p< 0.05$. Secreted cytokines were measured by Luminex assay. Data are expressed as mean ± standard deviation (SD). Two-way ANCOVA followed by Bonferroni's *post-hoc* test was performed. Cell viability was coded as a covariate. Significant differences between 'without 5-A-RU + MG' *vs* 'with 5-A-RU + MG' are marked with an asterisk. Significant differences between GOS *vs* control are marked with a hash. A) $^{\#\#}p= 0.016$; $^{**}p= 0.0114$. B) $^{*}p= 0.044$.

6.5 Discussion

The first aim of this chapter was to assess the effects of GOS on MAIT cells and other T cell subsets using PBMCs from healthy donors and those with Crohn's disease. The second aim was to evaluate whether those cells respond differently to vitamin B metabolite challenge in presence of GOS.

A gating strategy has been successfully optimised to allow clear identification of MAIT cells within healthy and Crohn's disease PBMCs. Non-informative marker TCRγδ used during the optimisation process was excluded from the final panel to have an additional channel for the study of intracellular cytokines. Secondly, LAL assay performed on vitamin B metabolites confirmed that RL-6,7-DiMe and 5-A-RU contained levels of LPS below the 0.1 EU/mL limit for cell cultures and could therefore be used in direct contact with PBMCs.

Viability measurements were carried out to ensure that the vitamin B metabolites were not cytotoxic. Both healthy and Crohn's disease PBMCs tolerated treatment with RL-6,7-DiMe, 5-A-RU or 5-A-RU + MG in presence and in absence of brefeldin A, with no significant differences compared to unstimulated control. Among the tested stimuli, 5-A-RU + MG induced the strongest activation of T lymphocytes and MAIT cells. 5-A-RU + MG was therefore selected as the most potent stimulus to use in culture and co-culture studies.

In contrast with the reviewed literature (Table 6.1), Crohn's disease PBMCs and healthy PBMCs presented similar phenotype and activation status for most of the analysed subsets at baseline. However, in line with previous findings (Table 6.1), Crohn's disease PBMCs expressed higher levels of IL-17A compared to healthy PBMCs. Failure in detecting differences in the frequencies of several surface markers at baseline may be due to the heterogeneity of disease stages within Crohn's disease donors (*e.g.* in remission vs under medication), which correlate, for instance, with the extent of MAIT cell depletion in blood [346].

On average, Crohn's disease PBMCs presented lower viability compared to healthy PBMCs. This is likely due to Crohn's disease PBMCs being more fragile and inflamed compared to healthy PBMCs. Baseline differences in cell viability between healthy and Crohn's disease PBMCs were taken into account by including cell viability as a covariate in the statistical analyses.

Overall, 5-A-RU + MG alone led to a reduction in the frequencies of MAIT cells and $CD8^+$ MAIT cells in both healthy PBMCs and Crohn's disease PBMCs, likely due to the release of cytotoxic mediators following MR1-mediated activation [356]. Upon ligation of 5-A-RU + MG to the TCR, MAIT cells rapidly produce pro-inflammatory cytokines (e.g. IFN-γ, IL-17A, TNF-α) and cytotoxic factors (*e.g.* granzyme B, perforin), thus having a pivotal role in anti-microbial defence [356]. A

reduction in $CD8^+$ MAIT cell numbers could be due to the fact that $CD8^+$ MAIT cells are more sensitive and respond more strongly to stimulation with riboflavin derivatives compared to DN MAIT cells [357]. Stimulation of $CD8^+$ MAIT cells *in vitro* supports the accumulation and maintenance of the DN subpopulation, which can explain the higher frequencies of DN MAIT cells found after 5-A-RU + MG treatment in Crohn's disease PBMCs [357]. Since $CD8^+$ MAIT cells constitute up to 85% of MAIT cells [348], lower numbers of MAIT cells after incubation with 5-A-RU + MG are likely due to a decrease in the numbers of their most abundant subset.

5-A-RU + MG induced MAIT cell activation only in healthy PBMCs, as shown by CD69 upregulation and increased secretion of Th1 pro-inflammatory cytokines (IFN-γ and TNF-α). This was in line with previous findings [76], which showed increased expression of the activation marker CD69 after stimulation of MAIT cells with riboflavin derivatives. Conversely, stimulation of Crohn's disease PBMCs with 5-A-RU + MG did not alter CD69 expression levels on MAIT cells, but instead caused a decrease in the frequencies of $CD69^+$ MAIT cells. Generally, the frequencies of MAIT cells expressing the activation marker CD69 are higher in IBD patients compared to healthy controls, and even higher than those in remission [93]. It could be that some of the Crohn's disease PBMC donors analysed were in a remission stage, or under medication (*e.g.* anti-inflammatory drugs, corticosteroids), which may have affected their responsiveness to challenge with the riboflavin derivative.

As hypothesised at the beginning of the chapter, incubation of healthy and Crohn's disease PBMCs with GOS alone resulted in higher frequencies of T helper cells expressing CD69 and in an increased secretion of IL-8. Only in Crohn's disease PBMCs, stimulation with GOS led also to higher proportions of cytotoxic T cells expressing CD69 and to increased release of IL-1β and IFN-γ. Based on the results on secreted and intracellular IL-8 (Chapter 4) which indicated a significant increase in IL-8 expression by monocytes after stimulation with GOS and based on the available literature [358], monocytes are likely activated by GOS in a LPS-like manner via TLRs or via different pathways leading to NF-kB activation. Activated monocytes secrete IL-8, which in turn induces stimulatory effects on T cells. Indeed, incubation with GOS alone resulted in higher percentages of T helper cells expressing CD69, both in healthy and in Crohn's disease PBMCs. Overall, GOS seem to exert immunostimulatory effects on both healthy PBMCs and Crohn's disease PBMCs when tested in isolation, possibly via a direct effect on monocytes and consequent activation of T cells by their secreted mediators.

Co-culture with GOS and 5-A-RU + MG resulted in lower CD69 expression by T cells and cytotoxic T cells compared to the riboflavin derivative alone in healthy PBMCs. Similar results were found by Johansson *et al.* [91], who showed that unknown molecules present in cell-free supernatants from

cultured lactobacilli dampened *Staphylococcus aureus*-induced activation of T cells and MAIT cells. Since incubation with GOS alone resulted in higher percentages of T helper cells expressing CD69 in healthy PBMCs, and since T helper cells behave as regulatory T lymphocytes when expressing CD69 [359], there may have been cross talks between T cell types that led to the observed effects. It could also be that GOS directly interferes with 5-A-RU + MG signalling, although the exact mechanisms still require investigation.

Riboflavin metabolites are produced both by commensal (*e.g. Lactobacillus acidophilus*) and pathogenic (*e.g. Salmonella typhimurium*) bacteria and have a key role in promoting the development of MAIT cells and in activating MAIT cells' response against pathogens. Generally, Crohn's disease patients show increased gut permeability with potential translocation of bacterial products (including riboflavin metabolites) from the lumen, which lead to cell activation in the lamina propria. For this reason, it is advisable to use GOS without the addition of further riboflavin metabolites in Crohn's disease individuals. In healthy individuals, combinations of GOS with riboflavin metabolites may be beneficial to modulate cell activation. It is important to note that other bacterial compounds (*e.g.* SCFAs) that are known to affect the inflammatory status of immune cells in the gut and systemically have not been included in this model and could be explored in future studies.

Chapter 7 FINAL DISCUSSION AND CONCLUSIONS

7.1 Final conclusions

This research provides evidence for the microbiota-independent effects of GOS upon *ex-vivo* human PBMCs from healthy donors and from IBD patients. To date, no previous studies have investigated the effects of GOS on Crohn's disease PBMCs and this present a novelty of this work. Additionally, this is the first study to have investigated the effects of GOS upon MAIT cells and their subsets and to have determined the effects of isolated GOS fractions with different degree of polymerisation upon immune parameters of adult PBMCs.

Interestingly, the compounds contained in B-GOS® batches, namely GOS and the free sugars present as residues from GOS production, exerted opposing effects on immune cells *in vitro*. While the free sugars and in particular galactose promoted the release of pro-inflammatory mediators (*e.g.* IL-8) and upregulated CD69 expression on monocytes both in healthy PBMCs and IBD PBMCs, GOS displayed immunomodulatory effects by supporting the activation of T helper cells and inducing the secretion of a wider range of anti-inflammatory as well as pro-inflammatory mediators. In agreement with the literature [240], the effects of GOS were chain-length dependent, with lower DP fractions inducing the strongest responses compared to higher DP fractions. In contrast with other studies that observed an involvement of TLR4 in the release of cytokines after stimulation with prebiotics [241], no clear signalling via TLR4 was observed. This may indicate that GOS act via different receptors, among which TLR2 is a likely candidate based on the observed GOS effects and on similar studies in the literature [240].

On healthy PBMCs, GOS consistently exerted anti-inflammatory effects when combined with other immune challenges, including LPS, the riboflavin metabolite 5-A-RU+MG and poly(I:C), as measured by a reduction in both pro-inflammatory mediators and in the expression levels of activation markers. This situation is more likely to represent the real physiological conditions of the gut, where GOS is not found in isolation but in co-presence of other stimuli, such as microbial metabolites.

IBD PBMCs were less sensitive than healthy PBMCs to the effects of free sugars but more inflamed, as indicated by the lower numbers of monocytes expressing IL-8 but the higher intensity of its intracellular expression. Whereas in healthy PBMCs GOS showed clear anti-inflammatory properties when combined with LPS, 5-A-RU+MG or poly(I:C), it was not possible to study the same outcomes for IBD PBMCs, as some inflammatory stimuli (*e.g.* 5-A-RU+MG) failed to induce a strong response by Crohn's disease immune cells, including MAIT cells. This could be due by IBD

PBMCs having been exposed to constant inflammation and antigen stimulation, as indicated by their lower viability, higher percentages of activated cells and altered frequencies of NKT cells and T helper cells subsets at baseline, which suggest a recruitment of immune cells to the inflammation site. Taken together, these findings highlight the importance of performing immunophenotyping before assessing the immunological effects of prebiotics on PBMCs from diseased donors, as their inflammatory status at baseline may affect the response to stimuli.

In agreement with the initial hypothesis, the data from this study confirm for the first time that GOS exert immunological effects on *ex-vivo* adult PBMCs with mechanisms that are independent from the action of the gut microbiota. Furthermore, an insight into the cell types and potential pathways involved in their action was provided. As anticipated, B-GOS® promoted immunostimulation when tested alone, and the observed effects were mainly due to the free sugars contained in the product (*e.g.* galactose). In line with the hypothesis, lower DP fractions displayed the strongest immunological effects. Furthermore, GOS were shown to reduce inflammation induced by inflammatory stimuli when tested in co-cultures more representative of the physiological conditions found in the gut. While Crohn's disease PBMCs were more inflamed at baseline compared to healthy PBMCs, they presented features of exhaustion and responded more weakly to stimulation, in contrast to what was predicted. Finally, while GOS were expected to act via TLR4, no clear signalling via TLR4 was observed and TLR2 was, instead, proposed as a likely candidate.

A graphical summary of the main findings of this work is provided in Figure 7.1 for healthy PBMCs and Figure 7.2 for Crohn's disease PBMCs. The effects of pure GOS are distinguished from those of the free sugars by different colour-coded arrows, with grey arrows indicating the pure GOS' effects and blue arrows indicating the free sugars' effects. Dotted lines in Figure 7.1 refer to the inhibitory action of pure GOS on the pro-inflammatory effects of LPS, riboflavin metabolite and poly(I:C). Free sugars are likely to promote inflammation in both healthy and Crohn's disease PBMCs by signalling via TLR2 or alternative receptors (*e.g.* CLRs), resulting in increased amounts of secreted IL-6 and IL-8 by healthy PBMCs and of TNF-α and IL-8 by Crohn's disease PBMCs. Since the free sugars did not induce significant CD69 upregulation *per se*, it is proposed that pure GOS induce T cell activation in a direct manner, possibly via TLR2, on both healthy and Crohn's disease PBMCs. While B-GOS® exert immunostimulatory effects on both healthy and Crohn's disease PBMCs when tested alone, it decrease LPS-, riboflavin metabolite- and poly(I:C)- induced inflammation only on healthy PBMCs (Figure 7.1).

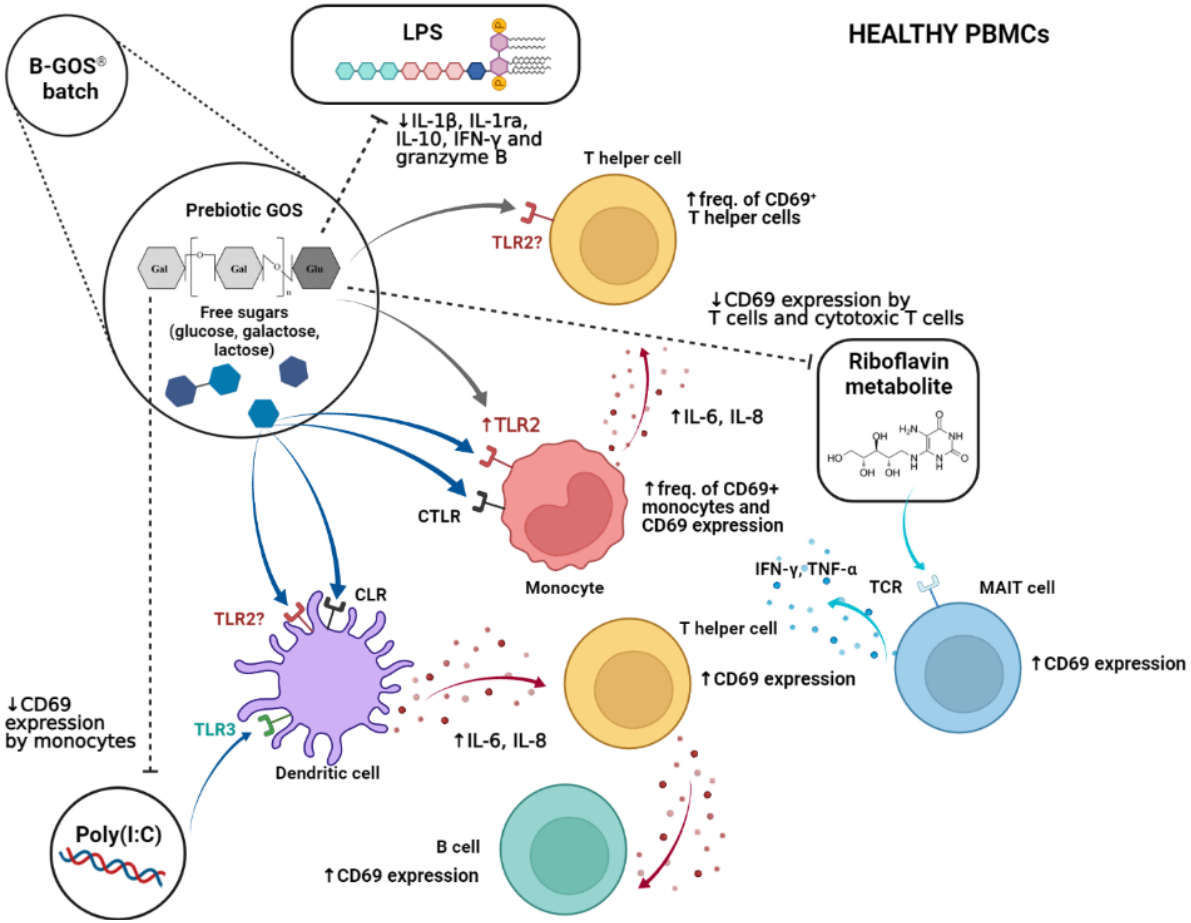

Figure 7.1 Proposed mechanism of GOS action in PBMCs from healthy donors.

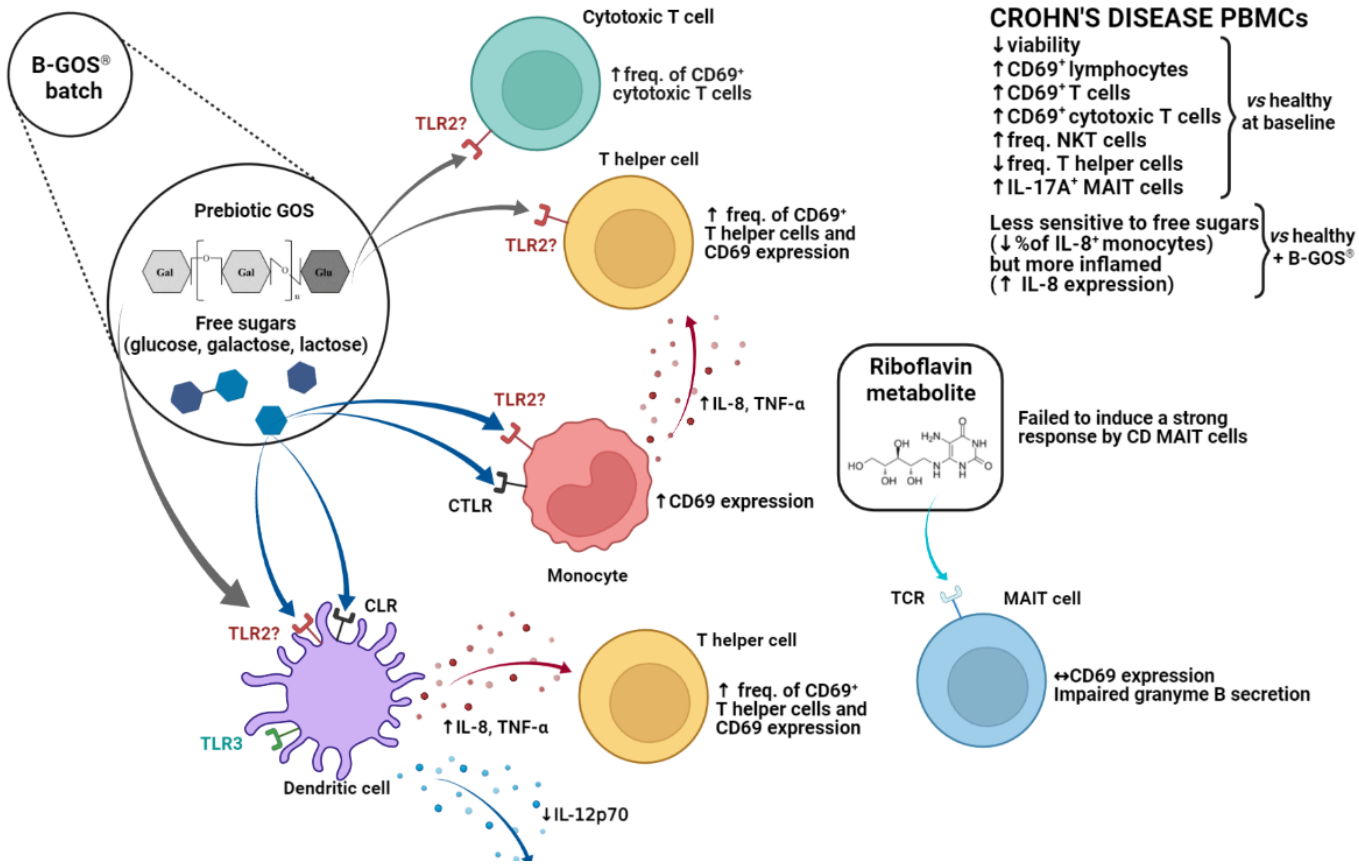

Figure 7.2 Proposed mechanism of GOS action in PBMCs from Crohn's disease donors.

7.2 Strengths and limitations

The first strength of this study was performing a thorough quality control of GOS batches and reagents before use in *ex-vivo* PBMCs cultures to identify potential LPS. While there are no such requirements when GOS are consumed orally, it is important to ensure that they do not contain LPS when in direct contact with immune cells in experimental settings as it may otherwise cause immunostimulation and lead to data misinterpretation, as has been previously noted for other prebiotic studies [307, 360].

Another strength was taking into account the contribution of the free sugars (particularly galactose) present as residues from GOS production, which were shown to exert pro-inflammatory effects on immune cells *per se*.

Additionally, GOS were tested in a wide range of conditions, including alone as a whole, alone as specific fractions, or in combination with other inflammatory stimuli. This helped providing a much greater insight into the action of GOS, which was shown to be dependent on both the structure of GOS as well as upon the environment around GOS (*e.g.* co-presence of other microbial products).

Another advantage of this model is that PBMCs were isolated from a living tissue and therefore more likely to capture the variability of human responses compared to standardised cell lines. Using *ex-vivo* PBMC cultures allowed exploration of the complex interplay between different cell subsets, which would have not been possible if isolated cell populations were used. On the other hand, this model may have introduced higher biological variability due to the intrinsic characteristics of human donors compared to cell lines, which may have led to lower statistical power during hypothesis testing.

Due to a lack of transportation studies on GOS, it was challenging to predict the exact amount of GOS that would transfer across the intestinal mucosa and enter in direct contact with immune cells. To address this issue, GOS were always tested at three different concentration based on similar studies in the literature [243], on the instructions for daily intake if orally consumed and on the hypothetical transfer rate of GOS across the gut [233, 234]. While most immunological effects were significant at the highest concentration of pure GOS used, dose-dependent patterns were seen both for activation markers and for most secreted mediators (*e.g.* IL-8, TNF-α). The only exception to this trend was IL-12p70, which was released by Crohn's disease PBMCs at lower levels only when lower concentrations of GOS were used.

B-GOS® batch C did not contain any detectable LPS, and was therefore chosen to study the immunological effects of GOS *in vitro*. PBMC stimulation with B-GOS® batch C led to increased T helper cell activation and higher cytokine secretion, either caused by GOS itself or by the free sugars contained in the product. Unfortunately, the available isolated GOS fractions contained levels of LPS which were above the limits for cell culture applications. While measures including pre-treatment with the antibiotic PMB were taken in place to neutralise LPS, and while it is likely that the observed immunological effects of GOS fractions were due to GOS rather than to LPS thanks to the agreement with previous experiments with the LPS-free B-GOS® batch C, it cannot be excluded that small amounts of LPS were still present.

When investigating the involvement of TLR4 in the secretion of soluble mediators by GOS-stimulated PBMCs, TLR4 antagonist was not tested at concentrations higher than the suggested maximum dose due to viability concerns. However, higher concentrations may have been more effective in blocking the potential signalling of GOS via TLR4. Moreover, the role of TLR4 was explored only on the release of IL-8, but not IL-6 and TNF-α, which were also produced by PBMCs after GOS stimulation. Assessing the levels of IL-6 and TNF-α may provide additional details about the involvement of TLR4 following culture with GOS.

While it was demonstrated that the increased levels of IL-8 after stimulation with B-GOS® batch were mainly attributable to the free sugars contained in the product, it was not possible to discriminate the effects of these sugars from those of GOS in case of IL-6 and TNF-α. It would be interesting to assess the levels of these mediators by conducting Luminex assays on PBMC supernatants in order to corroborate the findings on IL-8.

7.3 Future work

Overall, future research should firstly perform transportation studies on adults to determine more physiological concentrations of GOS, secondly identify the exact receptors and pathways involved in GOS action. The role of other receptors (*e.g.* TLR2, TLR5, TLR7, TLR8, CTLRs) on cytokine production by GOS-stimulated immune cells could be studied by using human TLR cell lines that have been either transfected to stably express a particular TLR gene or knocked out to prevent the expression of a specific TLR. Thirdly, future research should confirm the results presented in this thesis on more complex models. For instance, the effects of GOS could be studied on co-culture models mimicking the intestinal environment using Caco-2 cell monolayers and PBMCs or THP-1 cells. Germ-free mouse models are also suggested as an alternative approach to study the microbiota-independent effects of GOS in a more physiological manner, because they allow to take into account the real rate of transfer of GOS across the gut. Conversely, it is challenging to

assess the direct effects of GOS in a human intervention study for the impossibility to discern between the microbiota-mediated effects and the microbiota-independent effects. Finally, future product development work should focus on minimising the levels of free sugars contained in B-GOS® products, for example by improving the process of enzymatic conversion of lactose to GOS or by eliminating the disaccharide fractions by size-exclusion chromatography. This is particularly important for the potential use of GOS in IBD conditions, as Crohn's disease PBMCs showed increased cell activation following stimulation with the free sugars.

7.4 Novel findings

The key novelty of the work presented in this PhD thesis is an in-depth characterisation of the microbiota-independent effects of GOS on Crohn's disease PBMCs and on MAIT cells from both healthy and Crohn's disease donors. No previous work has demonstrated that GOS are able to induce activation of Crohn's disease T lymphocytes and to reduce the secretion of IL-12p70. These results can inform further nutritional studies on the potential use of prebiotic GOS as a supportive therapy for the management of inflammatory conditions, such as IBD. Furthermore, this study highlighted for the first time that galactose exerts pro-inflammatory effects on Crohn's disease monocytes and should be minimised in prebiotic products. Finally, this research showed for the first time that GOS is able to dampen the pro-inflammatory action of several stimuli, including LPS, poly(I:C) and a riboflavin metabolite, indicating a potential anti-pathogenic effect of GOS against bacterial or viral products.

Appendix A PBMC counts before and after washings to ensure optimal recovery after thawing

Table A-1 Recovery rates of PBMCs from healthy donors (*n*= 19) immediately after thawing and after the washing steps.

Status	Lot number	Expected cell counts ($X10^6$)	Cell counts after thawing ($X10^6$)	Cell counts after washing ($X10^6$)	Recovery rate after thawing (%)	Recovery rate after washing (%)	Average recovery rate after thawing (%)	Average recovery rate after washing (%)
Healthy	2011412001	100	77	87	77	113		
Healthy	1903040034	100	100	69	100	69		
Healthy	210172901C	100	210	94	210	45		
Healthy	20027130IC	100	120	81	120	68		
Healthy	2003425001	100	120	45	120	38		
Healthy	1805140180	100	110	65	110	59		
Healthy	1802210244	100	110	97	110	88		
Healthy	1805090103	100	83	59	83	71		
Healthy	1809140196	100	110	87	110	79		
Healthy	1804230207	100	100	76	100	76	119	79
Healthy	1807160152	100	92	57	92	63		
Healthy	1903060075	100	110	110	110	100		
Healthy	1910401003	100	93	93	93	100		
Healthy	1606200170	100	62	59	62	95		
Healthy	1702070039	100	174	260	174	149		
Healthy	1703170126	100	120	100	120	83		
Healthy	1707170061	100	210	100	210	48		
Healthy	1712130101	100	170	150	170	88		
Healthy	1903110116	100	98	74	98	75		

Table A-2 Recovery rates of PBMCs from IBD donors (*n*= 8) immediately after thawing and after the washing steps.

Status	Lot number	Expected cell counts ($X10^6$)	Cell counts after thawing ($X10^6$)	Cell counts after washing ($X10^6$)	Recovery rate after thawing (%)	Recovery rate after washing (%)	Average recovery rate after thawing (%)	Average recovery rate after washing (%)
IBD	1010113267	10	7	5	70	76	129	60
IBD	1010113278	10	14	11	140	77		
IBD	1010113287	10	11	8	110	69		
IBD	1010113291	10	12	5	121	45		
IBD	1010113300	10	16	11	158	66		
IBD	1010113306	10	18	8	180	44		
IBD	1010113308	10	13	7	133	50		
IBD	1010113318	10	12	6	121	50		

Appendix B Titration of viability dyes and validation experiments

BD Horizon™ Fixable Viability Stain 510 (FVS510) and BD Horizon™ Fixable Viability Stain 780 (FVS780) are viability stains that bind to cell-surface and intracellular amines and permeate into the cell membrane of dead cells. Titration of FVS510 and FVS780 was performed to determine the amount of dye needed to have the best separation between viable and non-viable cells. If too little stain is used, the cells do not stain as brightly as they could and they may not separate adequately from the negative cells. Too much antibody can increase non-specific binding, which increases the spread and background of the negative population. Both situations result in lower resolution of the measurement [361]. Dyes were reconstituted according to the manufacturer's instructions [282, 283] and then titrated at three different final concentrations in cell suspension (1:500/1:1000/1:2000). PBMCs (100 µL) were stained with 10 µL of dye at the three concentrations tested. To evaluate the ability of the dye to bind to dead cells, some PBMCs were treated with 20 µL of 70% ethanol (EtOH) before staining with the dye. Ethanol is known to have disruptive effects on the physical structure of cell membranes, which after treatment become permeable to the viability dye. Samples were washed as described in Chapter 2 section 2.5 and cell pellets were resuspended in PBS. PBMCs were analysed using an Attune NxT flow cytometer (Thermo Fisher Scientific). Doublets were excluded on FSC-H *vs* FSC-A graphs using a polygonal gate. Within the singlets, a polygonal gate was drawn around PBMCs to exclude debris. Within the PBMC gate, a bisector gate was used to determine the percentages of live cells ($FVS510^-$ or $FVS780^-$) and dead cells ($FVS510^+$ or $FVS780^+$) in a FVS510-A or FVS780-A histogram. To evaluate the results of staining, the Separation Index (SI) was calculated for each sample:

$$Separation\ Index\ (SI) = \frac{Median\ Positive - Median\ Negative}{(84\%\ Negative - Median\ Negative)/0.995}$$

The higher the Separation Index (SI) value, the better the separation between the positive and the negative populations [361]. Singlets from each tube of the titration were concatenated using FlowJo (FlowJo LLC). An example of titration data obtained for FVS780 is reported in Table B-1 and Figure B-1. All tested dilutions (1:500/1:1000/1:2000) of FVS780 showed separation between the positive and negative populations (SI= 10.8/10.8/11.0, respectively), with no significant changes among different concentrations. Whilst cells stained with FVS780 1:2000 did not display a positive

population as bright as that for cells stained with higher concentrations of the dye, PBMCs stained with FVS780 1:500 showed a very bright positive population and the staining of the negative population also increased if compared to the 1:1000 and 1:2000 dilutions. Therefore, the 1:1000 dilution for FVS780 and the 1:500 dilution for FVS510 were selected for flow cytometry experiments.

Table B-1 Example of separation index (SI) of PBMCs (*n*= 1) stained with 1:500-, 1:1000- and 1:2000-diluted BD Horizon™ Fixable Viability Stain 780 (FVS780).

Sample	Ancestry Subset Statistic For	Median Negative	Median Positive	84th Percentile Negative	Separation Index (SI)
PBMCs	Blank	22.0	20750	119	213
PBMCs	FVS780 1:500	375.0	13918	1628	10.8
PBMCs	FVS780 1:1000	214.0	7543	888	10.8
PBMCs	FVS780 1:2000	129.0	3782	458	11.0
Killed PBMCs	FVS780 1:1000	442.0	6723	811	16.9

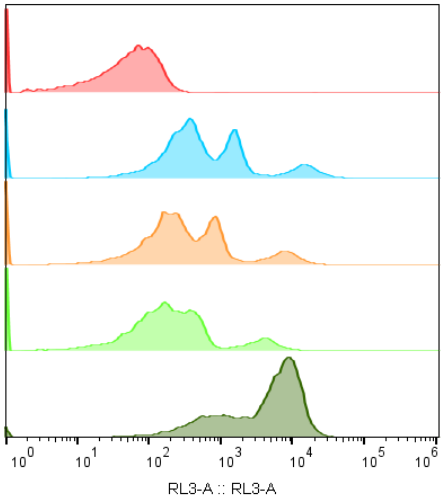

Figure B-1 Half offset overlay histogram reporting the percentage of live/dead cells for the following samples: blank (red), 1:500 FVS780 (blue), 1:1000 FVS780 (orange), 1:2000 FVS780 (light green) and 1:1000 FVS780 on ethanol-treated cells (dark green).

The level of correlation between the viability measures obtained by microscopy (trypan blue, TB) and flow cytometry (propidium iodide, PI) was calculated using matched samples to validate the use of flow cytometry. Both assays are based on the principle that viable cells display an intact membrane that excludes the dyes, which instead pass through the damaged plasma membranes of dead cells. Dead cells are distinguished from clear live cells using microscopy as their cytoplasm

becomes blue after TB staining. Viability assays by flow cytometry have the advantages of higher sensitivity due to increased sample size, and allow for inclusion in other assays such as immunophenotyping panels [281]. Staining of PBMCs with either TB or PI was performed as described in Chapter 2 section 2.5. FVS510 or FVS780 were used instead of PI in order to have more flexibility in multicolour flow cytometry panels and minimise spillover when using multiple fluorochromes. Overall, there was a positive linear relationship between TB and PI staining, with a high strength of correlation (r= 0.7236, p< 0.0001). Data spread was higher for samples stained with TB than for those stained with PI, as represented by the inter-quartile range (Figure B-2). This is likely to reflect the lower number of events collected by TB assay (approximately 100) compared to PI staining (10,000) and the human variability associated with TB measurements. Overall, the median viability was approximately equal for both TB- and PI-stained PBMCs, suggesting that the two methods correlated well. Viability dyes combined with flow cytometry were chosen for the experiments presented in this thesis.

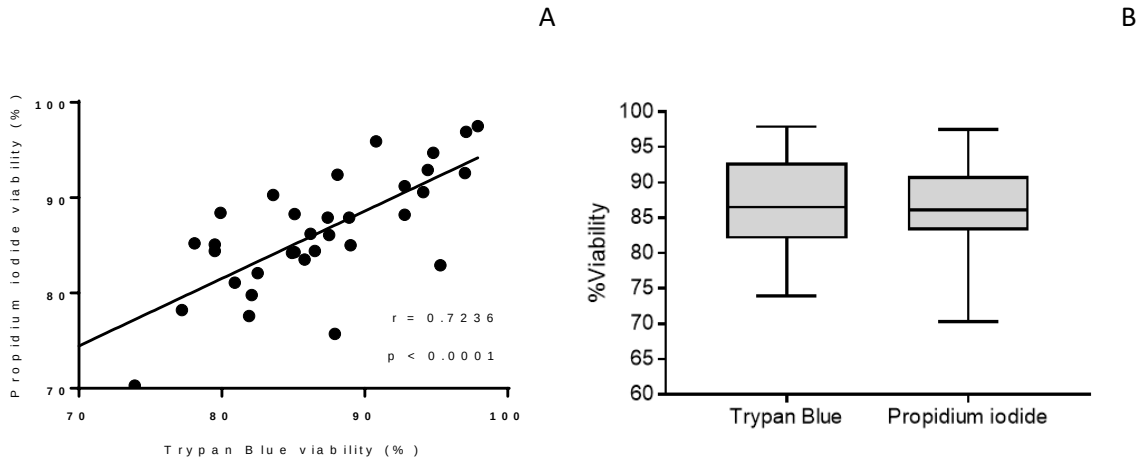

Figure B-2 A) Pearson's correlation test between propidium iodide (PI) and trypan blue (TB) staining methods (n= 33; significance level of p< 0.05). B) Box plot displaying the distribution of viability (%) for PBMCs stained with TB and PI (n= 33).

Appendix C Attune NxT instrument settings and compensation matrixes for flow cytometry experiments

Table C-1 Attune NxT instrument settings for the PBMC panel.

Excitation laser (nm)	Detector (nm)	Marker	Fluorochrome	Voltage
-	FSC	-	-	400
-	SSC	-	-	380
Blue (488)	BL1 (530/30)	CD25	BB515	380
	BL2 (574/26)	CD56	PE	410
	BL3 (695/40)	CD3	PerCP-Cy®5.5	480
	BL4 (780/60)	CD14	PE-Cy 7®	400
Violet (405)	VL2 (512/25)	CD8	BV510	400
	VL3 (603/48)	CD4	BV605	390
	VL4 (710/50)	CD19	BV711	500
Red (637)	RL2 (720/30)	CD69	APC-R700	400
	RL3 (780/60)	FVS780	FVS780	430

Table C-2 Compensation matrix applied for the PBMC panel.

	BL1	BL2	BL3	BL4	RL1	RL2	RL3	VL2	VL3	VL4
BL1	100.00	36.20	1.13	0.02	0.07	0.00	0.00	0.91	0.00	0.00
BL2	0.04	100.00	6.38	0.31	0.00	0.00	0.03	0.00	15.00	1.31
BL3	0.00	0.00	100.00	14.23	14.45	16.52	7.22	0.00	0.00	143.03
BL4	0.47	6.30	0.92	100.00	0.31	0.19	18.69	0.71	1.98	0.85
RL1	0.00	0.00	0.23	0.00	100.00	18.33	8.41	0.00	0.00	0.00
RL2	0.00	0.00	2.47	0.47	14.53	100.00	36.02	0.00	0.00	18.96
RL3	0.63	2.78	1.65	1.24	8.21	3.04	100.00	0.62	4.46	4.99
VL2	0.16	0.21	0.10	0.04	0.04	0.02	0.02	100.00	104.42	23.00
VL3	0.04	0.50	1.33	0.12	0.11	0.02	0.01	0.33	100.00	36.48
VL4	0.69	0.82	2.83	0.84	1.11	12.00	5.11	5.32	10.47	100.00

Table C-3 Attune NxT instrument settings for the MAIT cell panel.

Excitation laser (nm)	Detector (nm)	Marker	Fluorochrome	Voltage
-	FSC	-	-	400
-	SSC	-	-	380
Blue (488)	BL1 (530/30)	IFN-γ	FITC	500
	BL2 (574/26)	TCR Vα7.2	PE	420
	BL3 (695/40)	CD3	PerCP-Cy®5.5	500
	BL4 (780/60)	CD14	PE-Cy®7	400
Violet (405)	VL1 (440/50)	CD8	BV450	350
	VL2 (512/25)	IL-8	BV510	400
	VL3 (603/48)	CD4	BV605	390
	VL4 (710/50)	IL-17A	BV650	440
Red (637)	RL1 (670/14)	CD161	APC	450
	RL2 (720/30)	CD69	APC-R700	400
	RL3 (780/60)	FVS780	FVS780	450

Table C-4 Compensation matrix applied for the MAIT cell panel.

	BL1	BL2	BL3	BL4	RL1	RL2	RL3	VL1	VL2	VL3	VL4
BL1	100.00	6.10	0.26	0.02	0.00	0.00	0.00	0.00	0.51	0.18	0.00
BL2	2.28	100.00	8.10	0.35	0.01	0.00	0.00	0.00	0.00	10.02	0.32
BL3	0.75	0.07	100.00	10.09	11.03	12.14	7.70	0.19	0.08	0.33	32.82
BL4	1.87	4.88	0.80	100.00	0.13	0.20	27.10	0.26	0.13	0.53	0.10
RL1	0.00	0.00	0.69	0.04	100.00	15.64	9.88	0.00	0.00	0.04	1.48
RL2	0.07	0.00	3.48	0.47	14.55	100.00	52.00	0.00	0.00	0.00	5.70
RL3	0.00	0.24	0.22	0.58	3.96	1.52	100.00	0.68	0.34	0.42	0.26
VL1	0.20	0.02	0.02	0.00	0.00	0.01	0.00	100.00	7.21	1.05	0.03
VL2	0.82	0.11	0.01	0.00	0.00	0.00	0.00	27.72	100.00	105.63	7.59
VL3	0.05	0.57	2.07	0.12	0.09	0.02	0.01	13.59	0.29	100.00	12.32
VL4	0.06	0.02	3.26	0.14	71.33	17.09	8.72	65.21	1.54	51.39	100.00

Table C-5 Attune NxT instrument settings for the monocyte/TLR panel.

Excitation laser (nm)	Detector (nm)	Marker	Fluorochrome	Voltage
-	FSC	-	-	400
-	SSC	-	-	380
Blue (488)	BL1 (530/30)	IL-1β	FITC	500
	BL3 (695/40)	IL-10	BB700	460
	BL4 (780/60)	CD14	PE-Cy®7	420
Violet (405)	VL1 (440/50)	TLR4	BV421	300
	VL2 (512/25)	IL-8	BV510	400
Red (637)	RL1 (670/14)	TLR2	Alexa Fluor 647	480
	RL3 (780/60)	FVS780	FVS780	450

Table C-6 Compensation matrix applied for the monocyte/TLR panel.

	BL1	**BL3**	**BL4**	**RL1**	**RL3**	**VL1**	**VL2**
BL1	100.00	0.14	0.10	0.01	0.02	0.01	0.61
BL3	137.80	100.00	36.39	60.25	28.05	52.90	65.00
BL4	7.59	0.80	100.00	0.68	19.82	1.39	2.43
RL1	0.00	0.11	0.02	100.00	7.06	0.00	0.00
VL3	3.26	0.30	1.13	5.09	100.00	0.34	0.70
VL1	0.00	0.00	0.00	0.01	0.01	100.00	8.65
VL2	0.74	0.01	0.00	0.03	0.01	7.82	100.00

Appendix D Effects of protein transport inhibitors brefeldin A and monensin on PBMC viability

A pilot experiment using PBMCs from one healthy donor was performed to evaluate the effects of two protein transport inhibitors (brefeldin A and monensin) on PBMC viability. PBMCs (2.5 x 10^6 cells/mL) were stimulated for 5 h with con A (5 µg/mL or 50 µg/mL) in RPMI media containing either brefeldin A or monensin (both at 5 µg/mL). Following stimulation, cells were centrifuged at 300 x g for 10 minutes and supernatants were discarded. 100 µL cells were incubated with 10 µL of FVS780 for 15 minutes, protected from light. Cells were washed twice with a washing solution constituted by 1% BSA and 0.1% sodium azide in PBS, then centrifuged at 450 x g for 5 minutes and re-suspended in 300 µL PBS. Data were collected on an Attune NxT flow cytometer. Viability was expressed as a percentage of gated PBMCs following doublet and debris exclusion. Overall, brefeldin A was chosen over monensin because it was better tolerated by PBMCs under all culture conditions (control: 81.8% *vs* 78.4%; con A 5 µg/mL: 78.1% *vs* 74.6%; con A 50 µg/mL: 54.7% *vs* 39.6%), as shown in Figure D-1.

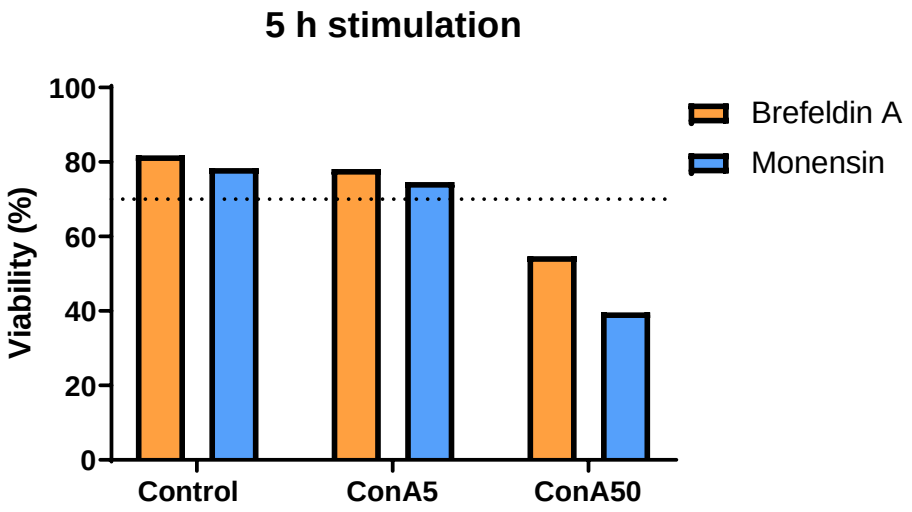

Figure D-1 Viability (%) of PBMCs from one healthy donor stimulated for 5 h with con A in presence of a protein transport inhibitor, as measured by flow cytometry.

Appendix E Supporting materials from Chapter 5

Table E-1 CD69 expression by T cell subsets and MAIT cell subsets from healthy PBMCs after 20 h culture with RL-6,7-DiMe (75 µM) or 5-A-RU (0.18 µM) or MG (1 µM) or 5-A-RU (0.18 µM) + MG (1 µM). Unstimulated PBMCs were used as a negative control (NC). Results were considered significant if $p < 0.05$.

	NC	**MG**	**RL-6,7-DiMe**	**5-A-RU**	**5-A-RU + MG**	**One-way ANOVA *p* value**
	Mean ± SD (*n*= 2)	Mean ± SD (*n*= 2)	Mean ± SD (*n*= 2)	Mean ± SD (*n*= 2)	Mean ± SD (*n*= 2)	
% of lymphocytes expressing CD69	1.4 ± 0.9	0.3 ± 0.2	1.3 ± 1.0	1.4 ± 0.8	3.2 ± 0.6	0.0894
MFI of CD69 on lymphocytes	13,474 ± 1,043	14,737 ± 569	13,687 ± 947	13,902 ± 464	22,396 ± 4,244*	**0.0274**
% of $CD3^+$ cells expressing CD69	1.2 ± 0.8	0.3 ± 0.2	1.0 ± 0.8	1.2 ± 0.7	1.8 ± 0.6	0.3955
MFI of CD69 on $CD3^+$ cells	13,829 ± 1,428	13,440 ± 150	14,215 ± 1,319	14,338 ± 685	25,116 ± 3,183**	**0.0039**
% of $CD4^+$ T cells expressing CD69	0.1 ± 0.1	0.3 ± 0.1	0.1 ± 0.1	0.1 ± 0.1	0.1 ± 0.1	0.4778
MFI of CD69 on $CD4^+$ T cells	16,277 ± 631	13,070 ± 494	14,293 ± 1,483	14,953 ± 743	17,071 ± 1,767	0.0855
% of $CD8^+$ T cells expressing CD69	3.1 ± 2.9	0.2 ± 0.1	2.7 ± 2.4	3.4 ± 2.4	6.4 ± 4.1	0.3792
MFI of CD69 on $CD8^+$ T cells	13,595 ± 1,660	14,753 ± 2,669	14,141 ± 1,097	14,977 ± 9.8	30,539 ± 2,664***	**0.0012**
% of MAIT cells expressing CD69	21.3 ± 21.8	2.2 ± 0.7	21.6 ± 21.2	23.8 ± 19.7	53.9 ± 6.2	0.1662
MFI of CD69 on MAIT cells	13,917 ± 1,539	13,973 ± 59	14,567 ± 1,881	15,120 ± 320	24,271 ± 2,454**	**0.0044**
% of $CD8^+$ MAIT cells expressing CD69	19.3 ± 19.8	2.5 ± 3.5	20.0 ± 19.9	23.2 ± 18.2	68.3 ± 17.5	0.0732
MFI of CD69 on $CD8^+$ MAIT cells	13,624 ± 1,807	19,089 ± 0*	14,376 ± 1,110	15,203 ± 68	26,506 ± 117***	**0.0011**
% of DN MAIT cells expressing CD69	24.3 ± 24.6	0.5 ± 0.7	23.5 ± 22.3	25.9 ± 23.0	52.7 ± 0.2	0.2189
MFI of CD69 on DN MAIT cells	14,139 ± 1,195	18,996 ± 0	14,606 ± 2,315	14,941 ± 634	23,149 ± 4,057	0.0764

*Significantly different from NC (Dunnett's *post-hoc* test, $p < 0.005$)

**Significantly different from NC (Dunnett's *post-hoc* test, $p < 0.005$)

***Significantly different from NC (Dunnett's *post-hoc* test, $p < 0.001$)

Table E-2 IFN-γ expression by T cell subsets and MAIT cell subsets from healthy PBMCs after 20 h culture with RL-6,7-DiMe (75 µM) or 5-A-RU (0.18 µM) or MG (1 µM) or 5-A-RU (0.18 µM) + MG (1 µM). Unstimulated PBMCs were used as a negative control (NC). Brefeldin A (5 µg/mL) was added after 1 h incubation. Results were considered significant if $p < 0.05$.

	NC + bref. A	**RL-6,7-DiMe + bref. A**	**5-A-RU + bref. A**	**5-A-RU + MG + bref. A**	**One-way ANOVA *p* value**
	Mean ± SD (*n*= 2)	Mean ± SD (*n*= 2)	Mean ± SD (*n*= 2)	Mean ± SD (*n*= 2)	
% of lymphocytes expressing IFN-γ	0.54 ± 0.29	0.35 ± 0.04	0.36 ± 0.05	0.61 ± 0.28	0.5519
MFI of IFN-γ on lymphocytes	25,729 ± 76	25,993 ± 706	23,973 ± 839	24,650 ± 496	0.0797
% of $CD3^+$ cells expressing IFN-γ	0.64 ± 0.36	0.42 ± 0.06	0.42 ± 0.06	0.58 ± 0.13	0.6214
MFI of IFN-γ on $CD3^+$ cells	26,532 ± 243	27,065 ± 301	24,946 ± 1,337	26,085 ± 1,182	0.2636
% of $CD4^+$ T cells expressing IFN-γ	0.09 ± 0.02	0.08 ± 0.02	0.08 ± 0.04	0.09 ± 0.00	0.9425
MFI of IFN-γ on $CD4^+$ T cells	N/A	N/A	N/A	N/A	N/A
% of $CD8^+$ T cells expressing IFN-γ	0.45 ± 0.25	0.26 ± 0.08	0.36 ± 0.12	0.56 ± 0.18	0.4287
MFI of IFN-γ on $CD8^+$ T cells	N/A	N/A	N/A	N/A	N/A
% of MAIT cells expressing IFN-γ	0.69 ± 0.18	0.57 ± 0.02	0.76 ± 0.33	3.59 ± 2.78	0.2351
MFI of IFN-γ on MAIT cells	N/A	N/A	N/A	N/A	N/A
% of $CD8^+$ MAIT cells expressing IFN-γ	0.21 ± 0.02	0.10 ± 0.14	0.42 ± 0.13	2.02 ± 2.85	0.5597
% of DN MAIT cells expressing IFN-γ	0.26 ± 0.09	0.18 ± 0.15	0.21 ± 0.15	3.05 ± 3.68	0.4207
MFI of IFN-γ on DN MAIT cells	N/A	N/A	N/A	N/A	N/A

Table E-3 IL-17A expression by T cell subsets and MAIT cell subsets from healthy PBMCs after 20 h culture with RL-6,7-DiMe (75 µM) or 5-A-RU (0.18 µM) or MG (1 µM) or 5-A-RU (0.18 µM) + MG (1 µM). Unstimulated PBMCs were used as a negative control (NC). Brefeldin A (5 µg/mL) was added after 1 h incubation. Results were considered significant if $p < 0.05$.

	NC + bref. A	**RL-6,7-DiMe + bref. A**	**5-A-RU + bref. A**	**5-A-RU + MG + bref. A**	**One-way ANOVA *p* value**
	Mean ± SD (*n*= 2)	Mean ± SD (*n*= 2)	Mean ± SD (*n*= 2)	Mean ± SD (*n*= 2)	
% of lymphocytes expressing IL-17A	0.11 ± 0.02	0.18 ± 0.04	0.56 ± 0.61	0.15 ± 0.07	0.5007
MFI of IL-17A on lymphocytes	4,774 ± 714	5,735 ± 1,133	7,697 ± 2,271	9,349 ± 4,815	0.4441
% of $CD3^+$ cells expressing IL-17A	0.10 ± 0.02	0.18 ± 0.06	0.56 ± 0.62	0.11 ± 0.03	0.4871
MFI of IL-17A on $CD3^+$ cells	4,381 ± 904	5,415 ± 1,267	7,348 ± 2,877	5,935 ± 546	0.4434
% of $CD4^+$ T cells expressing IL-17A	0.10 ± 0.02	0.15 ± 0.07	0.55 ± 0.61	0.11 ± 0.03	0.4774
MFI of IL-17A on $CD4^+$ T cells	N/A	N/A	N/A	N/A	N/A
% of $CD8^+$ T cells expressing IL-17A	0.08 ± 0.00	0.15 ± 0.04	0.46 ± 0.55	0.06 ± 0.02	0.5016
MFI of IL-17A on $CD8^+$ T cells	N/A	N/A	N/A	N/A	N/A
% of MAIT cells expressing IL-17A	0.11 ± 0.05	0.07 ± 0.09	0.37 ± 0.52	0.17 ± 0.08	0.7064
MFI of IL-17A on MAIT cells	N/A	N/A	N/A	N/A	N/A
% of $CD8^+$ MAIT cells expressing IL-17A	0.11 ± 0.16	0.00 ± 0.00	0.29 ± 0.40	0.48 ± 0.14	0.3025
MFI of IL-17A on $CD8^+$ MAIT cells	N/A	N/A	N/A	N/A	N/A
% of DN MAIT cells expressing IL-17A	0.11 ± 0.03	0.11 ± 0.16	0.43 ± 0.61	0.09 ± 0.13	0.6912
MFI of IL-17A on DN MAIT cells	N/A	N/A	N/A	N/A	N/A

Table E-4 Frequencies of lymphocytes, T cell subsets and MAIT cell subsets from healthy PBMCs after 20 h culture with 5-A-RU + MG, B-GOS® batch C or co-culture with both. Unstimulated PBMCs were used as a negative control. Cell frequencies were measured by flow cytometry. Cell viability was coded as a covariate.

Cell frequencies	**Control**		**GOS C 0.8**		**GOS C 4**		**GOS C 12**		**Two-way ANCOVA *p* value**		
	Mean ± SD (*n*= 7)		Mean ± SD (*n*= 7)		Mean ± SD (*n*= 7)		Mean ± SD (*n*= 7)				
	5-A-RU+MG		5-A-RU+MG		5-A-RU+MG		5-A-RU+MG		5-A-RU+MG	GOS C	5-A-RU+MG * GOS C
	-	+	-	+	-	+	-	+			
Lymphocytes (% of live PBMCs)	84.4 ± 5.6	82.7 ± 5.8	84.6 ± 5.6	83.5 ± 6.1	83.7 ± 6.0	82.0 ± 5.6	83.5 ± 6.1	83.6 ± 5.8	0.142	0.831	0.950
T cells (% of lymphocytes)	83.2 ± 3.0	83.6 ± 2.8	83.2 ± 3.7	83.8 ± 3.1	83.3 ± 3.1	83.8 ± 2.9	83.2 ± 3.2	83.9 ± 3.4	0.665	0.997	0.999
T helper cells (% of T cells)	71.2 ± 8.2	72.2 ± 8.0	71.9 ± 8.1	71.7 ± 8.4	72.3 ± 8.6	71.9 ± 8.4	72.6 ± 8.4	71.8 ± 8.8	0.935	0.992	0.994
Cytotoxic T cells (% of T cells)	21.7 ± 5.2	21.1 ± 4.8	20.8 ± 5.4	21.4 ± 4.9	20.4 ± 6.2	21.3 ± 5.4	20.6 ± 5.9	21.1 ± 6.1	0.981	0.964	0.988

Table E-4 Continued.

Cell frequencies	**Control**		**GOS C 0.8**		**GOS C 4**		**GOS C 12**		**Two-way ANCOVA *p* value**		
	Mean ± SD (*n*= 7)		Mean ± SD (*n*= 7)		Mean ± SD (*n*= 7)		Mean ± SD (*n*= 7)				
	5-A-RU+MG		5-A-RU+MG		5-A-RU+MG		5-A-RU+MG		5-A-RU+MG	GOS C	5-A-RU+MG * GOS C
	-	+	- +		-	+	-	+			
MAIT cells (% of T cells)	2.6 ± 1.8	1.4 ± 0.7	2.8 ± 1.4	1.5 ± 1.0	3.2 ± 2.2	1.5 ± 0.7	2.1 ± 1.4	1.7 ± 1.0	**0.005**	0.913	0.632
$CD4^+$ MAIT cells (% of MAIT cells)	15.1 ± 10.6	23.7 ± 16.1	18.8 ± 17.1	22.6 ± 14.4	21.1 ± 21.9	21.5 ± 12.4	17.3 ± 9.6	21.5 ± 14.6	0.261	0.990	0.918
$CD8^+$ MAIT cells (% of MAIT cells)	45.7 ± 5.7	24.2 ± 7.4	39.5 ± 7.2	24.3 ± 10.1	37.1 ± 10.3	23.0 ± 7.6	34.4 ± 5.1	23.4 ± 6.5	**<0.0001**	0.128	0.323
DN MAIT cells (% of MAIT cells)	32.3 ± 16.5	41.5 ± 23.4	33.8 ± 18.1	41.9 ± 24.5	35.1 ± 18.1	43.6 ± 24.6	39.7 ± 19.3	43.5 ± 25.0	0.210	0.946	0.987
DP MAIT cells (% of MAIT cells)	6.9 ± 7.5	10.6 ± 6.3	8.0 ± 5.9	11.2 ± 8.1	6.7 ± 4.3	11.9 ± 10.8	8.7 ± 8.7	11.7 ± 8.3	0.072	0.963	0.982

Significant main effect of *5-A-RU + MG* – Bonferroni's *post-hoc* test for multiple comparison:

MAIT cells – Without 5-A-RU + MG significantly different from with 5-A-RU + MG (p= 0.005)

$CD8^+$ MAIT cells – Without 5-A-RU + MG significantly different from with 5-A-RU + MG (p< 0.0001)

Table E-5 CD161 and TCR Vα7.2 expression (MFI) on MAIT cells from healthy PBMCs after 20 h culture with 5-A-RU + MG or B-GOS® batch C or after co-culture with both. Unstimulated PBMCs were used as a negative control. Cell frequencies were measured by flow cytometry. Cell viability was coded as a covariate.

Median fluorescence intensity (MFI)	**Control**		**GOS C 0.8**		**GOS C 4**		**GOS C 12**		**Two-way ANCOVA *p* value**		
	Mean ± SD (*n*= 7)		Mean ± SD (*n*= 7)		Mean ± SD (*n*= 7)		Mean ± SD (*n*= 7)				
	5-A-RU+MG		5-A-RU+MG		5-A-RU+MG		5-A-RU+MG		5-A-RU +MG	GOS C	5-A-RU+MG * GOS C
	-	+	-	+	-	+	-	+			
CD161 on MAIT cells	10,954 ± 2,335	9,244 ± 1,773	10,074 ± 2,424	9,332 ± 1,818	9,889 ± 2,600	9,365 ± 1,602	10,124 ± 1,668	9,417 ± 1,769	0.074	0.928	0.873
TCR Vα7.2 on MAIT cells	6,877 ± 760	5,428 ± 332	6,607 ± 99	5,556 ± 309	6,859 ± 594	5,614 ± 561	6,589 ± 601	5,781 ± 591	**<0.0001**	0.858	0.491

Significant main effect of *5-A-RU + MG* – Bonferroni's *post-hoc* test for multiple comparison:
TCR Vα7.2 on MAIT cells – Without 5-A-RU + MG significantly different from with 5-A-RU + MG ($p < 0.0001$)

Table E-6 Frequencies of lymphocytes, T cell subsets and MAIT cell subsets from Crohn's disease PBMCs after 20 h culture with 5-A-RU + MG, B-GOS® batch C or co-culture with both. Unstimulated PBMCs were used as a negative control. Cell frequencies were measured by flow cytometry. Cell viability was coded as a covariate.

Cell frequencies	**Control**		**GOS C 12**		**Two-way ANCOVA *p* value**		
	Mean ± SD (*n*= 6)		Mean ± SD (*n*= 6)				
	5-A-RU+MG		5-A-RU+MG		5-A-RU +MG	GOS C	5-A-RU +MG * GOS C
	-	+	-	+			
Lymphocytes (% of live PBMCs)	90.2 ± 3.3	91.9 ± 2.6	89.6 ± 2.7	93.9 ± 1.7	0.060	0.788	0.203
T cells (% of lymphocytes)	81.4 ± 7.6	79.2 ± 9.1	80.5 ± 10.0	77.7 ± 10.0	**0.049**	0.247	0.936
T helper cells (% of T cells)	61.1 ± 13.6	56.9 ± 13.6	60.8 ± 14.6	53.8 ± 12.8	0.618	0.968	0.803
Cytotoxic T cells (% of T cells)	27.9 ± 10.6	29.4 ± 10.3	27.7 ± 10.7	31.7 ± 10.9	0.742	0.743	0.740
MAIT cells (% of T cells)	3.3 ± 2.3	3.5 ± 2.4	3.3 ± 2.3	3.8 ± 2.5	0.089	0.306	0.907
$CD4^+$ MAIT cells (% of MAIT cells)	17.3 ± 14.7	15.7 ± 12.5	16.7 ± 14.0	13.7 ± 9.3	0.169	0.406	0.896
$CD8^+$ MAIT cells (% of MAIT cells)	43.4 ± 18.6	22.6 ± 12.4	35.9 ± 18.8	23.3 ± 13.9	**0.049**	0.705	0.547
DN MAIT cells (% of MAIT cells)	28.0 ± 13.3	52.1 ± 26.1	36.6 ± 19.8	52.7 ± 27.7	**0.007**	0.317	0.635
DP MAIT cells (% of MAIT cells)	11.2 ± 12.4	9.6 ± 11.0	10.8 ± 11.7	10.3 ± 10.0	0.280	0.621	0.891

Significant main effect of *5-A-RU + MG* – Bonferroni's *post-hoc* test for multiple comparison:
T cells – Without 5-A-RU + MG significantly different from with 5-A-RU + MG (*p*= 0.049)
$CD8^+$ MAIT cells – Without 5-A-RU + MG significantly different from with 5-A-RU + MG (*p*= 0.049)
DN MAIT cells – Without 5-A-RU + MG significantly different from with 5-A-RU + MG (*p*= 0.007)

Table E-7 CD161 and TCR Vα7.2 expression (MFI) on MAIT cells from Crohn's disease PBMCs after 20 h culture with 5-A-RU + MG or B-GOS® batch C or after co-culture with both. Unstimulated PBMCs were used as a negative control. Cell frequencies were measured by flow cytometry. Cell viability was coded as a covariate.

Median fluorescence intensity (MFI)	**Control**		**GOS C 12**		**Two-way ANCOVA *p* value**		
	Mean ± SD (*n*= 6)		Mean ± SD (*n*= 6)				
	5-A-RU+MG		5-A-RU+MG		5-A-RU +MG	GOS C	5-A-RU +MG * GOS C
	-	+	-	+			
CD161 on MAIT cells	10,271 ± 3,033	9,166 ± 2,580	9,899 ± 2,577	9,105 ± 2,557	0.126	0.141	0.813
TCR Vα7.2 on MAIT cells	6,895 ± 1,068	5,841 ± 1,069	6,595 ± 905	5,905 ± 1,115	0.429	0.482	0.573

Table E-8 Frequencies of CD69-expressing T cell subsets and MAIT cell subsets from healthy PBMCs after 20 h culture with with 5-A-RU + MG or B-GOS® batch C or after co-culture with both. Unstimulated PBMCs were used as a negative control (NC). Results were considered significant if $p < 0.05$.

Cell frequencies	**Control**		**GOS C 0.8**		**GOS C 4**		**GOS C 12**		**Two-way ANCOVA *p* value**		
	Mean ± SD (*n*= 7)		Mean ± SD (*n*= 7)		Mean ± SD (*n*= 7)		Mean ± SD (*n*= 7)				
	5-A-RU+MG		5-A-RU+MG		5-A-RU+MG		5-A-RU+MG		5-A-RU +MG	GOS C	5-A-RU+MG * GOS C
	-	+	-	+	-	+	-	+			
CD69⁺ T cells (% of T cells)	2.7 ± 1.6	1.8 ± 1.0	2.8 ± 1.6	2.0 ± 1.2	2.5 ± 1.4	2.0 ± 1.3	2.7 ± 1.9	2.7 ± 2.2	0.202	0.811	0.882
CD69⁺ T helper cells (% of T helper cells)	0.64 ± 0.38	0.41 ± 0.21	0.74 ± 0.38	0.56 ± 0.34	0.74 ± 0.39	0.60 ± 0.44	1.38 ± 0.88	1.40 ± 1.19	0.396	**0.003**	0.954
CD69⁺ cytotoxic T cells (% of cytotoxic T cells)	4.5 ± 3.2	3.0 ± 1.7	4.5 ± 3.1	3.0 ± 1.5	4.2 ± 2.9	3.0 ± 1.4	3.7 ± 2.4	3.7 ± 2.8	0.131	0.995	0.847

Significant main effect of *GOS C* – Bonferroni's *post-hoc* test for multiple comparison:
CD69⁺ T helper cells – GOS C 12 significantly different from NC (p= 0.004), GOS C 0.8 (p= 0.019) and GOS C 4 (p= 0.025)

Table E-8 Continued.

Cell frequencies	**Control**		**GOS C 0.8**		**GOS C 4**		**GOS C 12**		**Two-way ANCOVA *p* value**		
	Mean ± SD (*n*= 7)		Mean ± SD (*n*= 7)		Mean ± SD (*n*= 7)		Mean ± SD (*n*= 7)				
	5-A-RU+MG		5-A-RU+MG		5-A-RU+MG		5-A-RU+MG		5-A-RU +MG	GOS C	5-A-RU+MG * GOS C
	-	+	-	+	-	+	-	+			
CD69$^+$ MAIT cells (% of MAIT cells)	35.8 ± 16.8	29.0 ± 15.7	34.0 ± 17.3	31.4 ± 13.8	31.1 ± 16.0	31.1 ± 14.2	29.6 ± 14.7	29.3 ± 16.1	0.436	0.874	0.939
CD69$^+$ CD4$^+$ MAIT cells (% of CD4$^+$ MAIT cells)	4.4 ± 3.8	1.7 ± 0.9	4.1 ± 4.2	2.3 ± 1.7	4.4 ± 2.9	3.1 ± 2.2	5.4 ± 4.6	4.7 ± 4.1	0.068	0.408	0.852
CD69$^+$ CD8$^+$ MAIT cells (% of CD8$^+$ MAIT cells)	47.0 ± 17.4	53.1 ± 18.6	47.9 ± 17.9	57.4 ± 18.1	44.8 ± 18.6	60.5 ± 18.3	46.2 ± 14.2	54.7 ± 19.5	0.058	0.930	0.908
CD69$^+$ DN MAIT cells (% of DN MAIT cells)	37.5 ± 16.6	38.0 ± 21.4	37.8 ± 18.4	38.7 ± 20.4	32.9 ± 16.0	36.5 ± 18.8	30.0 ± 17.7	32.4 ± 20.8	0.792	0.699	0.997

Table E-9 CD69 (MFI) expression on T cell subsets and MAIT cell subsets from healthy PBMCs after 20 h culture with with 5-A-RU + MG or B-GOS® batch C or after co-culture with both. Unstimulated PBMCs were used as a negative control (NC). Results were considered significant if $p < 0.05$.

Median fluorescence intensity (MFI)	**Control**		**GOS C 0.8**		**GOS C 4**		**GOS C 12**		**Two-way ANOVA *p* value**		
	Mean ± SD (*n*= 7)		Mean ± SD (*n*= 7)		Mean ± SD (*n*= 7)		Mean ± SD (*n*= 7)				
	5-A-RU+MG		5-A-RU+MG		5-A-RU+MG		5-A-RU+MG		5-A-RU+MG	GOS C	5-A-RU+MG * GOS C
	-	+	-	+	-	+	-	+			
CD69 on T cells	15,205 ± 877	20,317 ± 2,303	15,173 ± 718	20,677 ± 1,867	14,923 ± 666	19,467 ± 1,528	14,300 ± 521	16,572 ± 1,439	**<0.0001**	**<0.0001**	**0.014**
CD69 on T helper cells	14,397 ± 747	15,157 ± 958	14,661 ± 1,389	15,193 ± 1,964	14,262 ± 1,088	14,684 ± 1,030	13,706 ± 674	13,724 ± 1,087	0.136	0.060	0.868
CD69 on cytotoxic T cells	15,417 ± 1,135	24,669 ± 4,249	15,506 ± 1,019	25,466 ± 3,366	15,422 ± 878	23,904 ± 3,436	14,831 ± 876	20,187 ± 3,485	**<0.0001**	**0.035**	0.124
CD69 on MAIT cells	16,631 ± 1,631	24,956 ± 4,166	16,953 ± 1,316	27,455 ± 4,934	16,404 ± 1,140	25,258 ± 3,739	16,203 ± 1,063	21,554 ± 3,514	**<0.0001**	0.054	0.182
CD69 on $CD8^+$ MAIT cells	16,634 ± 1,636	27,901 ± 5,558	16,996 ± 1,465	28,821 ± 5,850	16,584 ± 1,265	25,395 ± 3,497	16,144 ± 1,218	23,667 ± 5,920	**<0.0001**	0.229	0.457
CD69 on DN MAIT cells	17,059 ± 2,097	22,794 ± 4,528	17,077 ± 1,526	26,018 ± 5,312	16,491 ± 1,220	23,634 ± 3,895	15,923 ± 1,584	21,355 ± 4,396	**<0.0001**	0.427	0.682

Significant main effect of *5-A-RU + MG* – Bonferroni's *post-hoc* test for multiple comparison: CD69 on cytotoxic T cells – Without 5-A-RU + MG significantly different from with 5-A-RU + MG ($p < 0.0001$); CD69 on MAIT cells – Without 5-A-RU + MG significantly different from with 5-A-RU + MG ($p < 0.0001$); CD69 on $CD8^+$ MAIT cells – Without 5-A-RU + MG significantly different from with 5-A-RU + MG ($p < 0.0001$); CD69 on DN MAIT cells – Without 5-A-RU + MG significantly different from with 5-A-RU + MG ($p < 0.0001$). **Significant main effect of *GOS C* – Bonferroni's *post-hoc* test for multiple comparison:** CD69 on cytotoxic T cells – GOS 12 significantly different from NC ($p = 0.0081$). **Significant interaction *5-A-RU + MG*GOS C* – Dunnett's and Bonferroni's *post-hoc* tests for multiple comparison:** CD69 on T cells – GOS C 12 significantly different from NC ($p < 0.0001$) in presence of 5-A-RU + MG; NC significantly different from NC + 5-A-RU + MG ($p < 0.0001$); GOS C 0.8 significantly different from GOS C 0.8 + 5-A-RU + MG ($p < 0.0001$); GOS C 4 significantly different from GOS C 4 + 5-A-RU + MG ($p < 0.0001$); GOS C 12 significantly different from GOS C 12 + 5-A-RU + MG ($p = 0.0135$);

Table E-10 Frequencies of CD69-expressing T cell subsets and MAIT cell subsets from Crohn's disease PBMCs after 20 h culture with with 5-A-RU + MG or B-GOS® batch C or after co-culture with both. Unstimulated PBMCs were used as a negative control (NC). Results were considered significant if $p < 0.05$.

Cell frequencies	**Control**		**GOS C 12**		**Two-way ANOVA *p* value**		
	Mean ± SD (*n*= 6)		Mean ± SD (*n*= 6)				
	5-A-RU+MG		5-A-RU+MG		5-A-RU+MG	GOS C	5-A-RU+MG * GOS C
	-	+	-	+			
CD69⁺ T cells (% of T cells)	1.96 ± 0.98	0.83 ± 0.67	4.57 ± 1.18	0.76 ± 0.62	**<0.0001**	**<0.0001**	**<0.0001**
CD69⁺ T helper cells (% of T helper cells)	1.17 ± 0.66	0.46 ± 0.26	4.47 ± 1.49	0.41 ± 0.23	**<0.0001**	**<0.0001**	**<0.0001**
CD69⁺ cytotoxic T cells (% of cytotoxic T cells)	2.71 ± 1.64	1.21 ± 1.64	4.57 ± 2.95	0.92 ± 1.17	**0.034**	**0.029**	0.078
CD69⁺ MAIT cells (% of MAIT cells)	13.7 ± 8.8	5.4 ± 5.0	13.8 ± 4.2	5.5 ± 4.7	**0.018**	0.236	0.972
CD69⁺ CD8⁺ MAIT cells (% of CD8⁺ MAIT cells)	21.0 ± 12.3	13.8 ± 14.9	13.4 ± 7.8	7.8 ± 10.3	0.973	0.483	0.835
CD69⁺ DN MAIT cells (% of DN MAIT cells)	15.3 ± 7.1	4.4 ± 2.6	11.0 ± 4.2	4.4 ± 3.9	**0.011**	0.658	0.087

Significant main effect of *5-A-RU + MG* – Bonferroni's *post-hoc* test for multiple comparison:
CD69⁺ cytotoxic T cells – Without 5-A-RU + MG significantly different from with 5-A-RU + MG ($p = 0.034$)
CD69⁺ MAIT cells – Without 5-A-RU + MG significantly different from with 5-A-RU + MG ($p = 0.018$)
CD69⁺ DN MAIT cells – Without 5-A-RU + MG significantly different from with 5-A-RU + MG ($p = 0.011$)
Significant main effect of *GOS C* – Bonferroni's *post-hoc* test for multiple comparison:
CD69⁺ cytotoxic T cells – GOS C 12 significantly different from NC ($p = 0.029$)
Significant interaction *5-A-RU + MG*GOS C* – Bonferroni's *post-hoc* tests for multiple comparison:
CD69⁺ T cells – GOS C 12 significantly different from NC ($p = 0.0001$) in absence of 5-A-RU + MG; GOS C 12 without 5-A-RU + MG significantly different from GOS C 12 with of 5-A-RU + MG ($p < 0.0001$);
CD69⁺ T helper cells – GOS C 12 significantly different from NC ($p = 0.0001$) in absence of 5-A-RU + MG; GOS C 12 without 5-A-RU + MG significantly different from GOS C 12 with of 5-A-RU + MG ($p < 0.0001$);

Table E-11 CD69 (MFI) expression on T cells from Crohn's disease PBMCs after 20 h culture with with 5-A-RU + MG or B-GOS® batch C or after co-culture with both. Unstimulated PBMCs were used as a negative control (NC). Results were considered significant if $p < 0.05$.

Median fluorescence intensity (MFI)	**Control**		**GOS C 12**		**Two-way ANCOVA *p* value**		
	Mean ± SD (*n*= 6)		Mean ± SD (*n*= 6)				
	5-A-RU+MG		5-A-RU+MG		5-A-RU+MG	GOS C	5-A-RU+MG * GOS C
	-	+	-	+			
CD69 on T cells	14,723 ± 755	15,101 ± 2,399	13,681 ± 788	14,349 ± 1,842	0.192	0.379	0.848

Table E-12 Frequencies of IL-17A-expressing and IFN-γ-expressing T cell subsets and MAIT cells from healthy PBMCs after 20 h culture with with 5-A-RU + MG or B-GOS® batch C or after co-culture with both. Unstimulated PBMCs were used as a negative control (NC). Brefeldin A (5 µg/mL) was added after 1 h incubation. Results were considered significant if $p < 0.05$.

Cell frequencies	**Control**		**GOS C 0.8**		**GOS C 4**		**GOS C 12**		**Two-way ANCOVA *p* value**		
	Mean ± SD (*n*= 7)		Mean ± SD (*n*= 7)		Mean ± SD (*n*= 7)		Mean ± SD (*n*= 7)				
	5-A-RU+MG		5-A-RU+MG		5-A-RU+MG		5-A-RU+MG		5-A-RU+MG	GOS C	5-A-RU+MG * GOS C
	-	+	-	+	-	+	-	+			
% of T cells expressing IL-17A	0.09 ± 0.05	0.34 ± 0.36	0.64 ± 1.33	0.13 ± 0.08	0.15 ± 0.06	0.13 ± 0.08	0.10 ± 0.04	0.25 ± 0.32	0.844	0.624	0.217
% of T helper cells expressing IL-17A	0.09 ± 0.05	0.34 ± 0.34	0.61 ± 1.29	0.12 ± 0.09	0.15 ± 0.07	0.12 ± 0.08	0.10 ± 0.04	0.25 ± 0.32	0.829	0.638	0.219
% of cytotoxic T cells expressing IL-17A	0.08 ± 0.04	0.35 ± 0.41	0.61 ± 1.36	0.13 ± 0.06	0.14 ± 0.08	0.13 ± 0.08	0.09 ± 0.04	0.25 ± 0.32	0.951	0.673	0.265
% of MAIT cells expressing IL-17A	0.03 ± 0.06	0.38 ± 0.38	0.68 ± 1.17	0.39 ± 0.43	0.13 ± 0.10	0.46 ± 0.65	0.03 ± 0.04	0.35 ± 0.60	0.225	0.369	0.367

Table E-12 Continued.

Cell frequencies	**Control**		**GOS C 0.8**		**GOS C 4**		**GOS C 12**		**Two-way ANCOVA *p* value**		
	Mean ± SD (*n*= 7)		Mean ± SD (*n*= 7)		Mean ± SD (*n*= 7)		Mean ± SD (*n*= 7)				
	5-A-RU+MG		5-A-RU+MG		5-A-RU+MG		5-A-RU+MG		5-A-RU+MG	GOS C	5-A-RU+MG * GOS C
	-	+	-	+	-	+	-	+			
% of T cells expressing IFN-γ	0.41 ± 0.22	0.70 ± 0.40	0.36 ± 0.12	0.68 ± 0.38	0.33 ± 0.14	0.68 ± 0.44	0.41 ± 0.17	0.58 ± 0.32	**<0.0001**	0.986	0.812
% of T helper cells expressing IFN-γ	0.14 ± 0.13	0.09 ± 0.02	0.09 ± 0.04	0.09 ± 0.05	0.07 ± 0.03	0.08 ± 0.03	0.08 ± 0.02	0.09 ± 0.03	0.611	0.347	0.512
% of cytotoxic T cells expressing IFN-γ	0.53 ± 0.39	0.84 ± 0.66	0.39 ± 0.21	0.75 ± 0.36	0.41 ± 0.20	0.81 ± 0.59	0.52 ± 0.27	0.81 ± 0.71	**0.003**	0.760	0.976
% of MAIT cells expressing IFN-γ	1.17 ± 1.18	12.6 ± 8.1	1.16 ± 1.06	13.1 ± 10.1	0.70 ± 0.31	11.0 ± 7.4	1.00 ± 0.93	7.82 ± 6.69	**<0.0001**	0.778	0.577

Significant main effect of *5-A-RU + MG* – Bonferroni's *post-hoc* test for multiple comparison:

% of T cells expressing IFN-γ – Without 5-A-RU + MG significantly different from with 5-A-RU + MG ($p < 0.0001$)

% of cytotoxic T cells expressing IFN-γ – Without 5-A-RU + MG significantly different from with 5-A-RU + MG ($p = 0.003$)

% of MAIT cells expressing IFN-γ – Without 5-A-RU + MG significantly different from with 5-A-RU + MG ($p < 0.0001$)

Table E-13 Frequencies of IL-17A-expressing and IFN-γ-expressing T cell subsets and MAIT cells from Crohn's disease PBMCs after 20 h culture with with 5-A-RU + MG or B-GOS® batch C or after co-culture with both. Unstimulated PBMCs were used as a negative control (NC). Brefeldin A (5 µg/mL) was added after 1 h incubation. Results were considered significant if $p < 0.05$.

Cell frequencies and MFIs	**Control**		**GOS C 12**		**Two-way ANCOVA *p* value**		
	Mean ± SD (*n*= 7)		Mean ± SD (*n*= 7)				
	5-A-RU+MG		5-A-RU+MG		5-A-RU+MG	GOS C	5-A-RU+MG * GOS C
	-	+	-	+			
% of T cells expressing IL-17A	0.31 ± 0.29	0.60 ± 0.48	0.38 ± 0.31	0.44 ± 0.21	0.116	0.806	0.304
% of T helper cells expressing IL-17A	0.28 ± 0.28	0.57 ± 0.45	0.37 ± 0.29	0.41 ± 0.23	0.104	0.746	0.271
% of cytotoxic T cells expressing IL-17A	0.27 ± 0.22	0.50 ± 0.40	0.30 ± 0.26	0.40 ± 0.18	0.095	0.838	0.492
% of MAIT cells expressing IL-17A	0.33 ± 0.37	0.90 ± 1.27	0.57 ± 0.47	0.47 ± 0.36	0.544	0.692	0.391
% of T cells expressing IFN-γ	0.33 ± 0.17	0.35 ± 0.18	0.31 ± 0.16	0.38 ± 0.23	0.858	0.493	0.607
% of T helper cells expressing IFN-γ	0.02 ± 0.01	0.03 ± 0.01	0.03 ± 0.03	0.02 ± 0.01	0.644	0.470	0.188
% of cytotoxic T cells expressing IFN-γ	0.11 ± 0.10	0.14 ± 0.12	0.08 ± 0.08	0.14 ± 0.05	0.226	0.803	0.705
% of MAIT cells expressing IFN-γ	7.6 ± 16.1	2.0 ± 2.2	6.6 ± 13.1	2.3 ± 3.8	0.215	0.759	0.835

Table E-14 Levels of soluble mediators secreted by healthy PBMCs after 20 h culture with 5-A-RU + MG or B-GOS® batch C or after co-culture with both. Unstimulated PBMCs were used as a negative control (NC). Results were considered significant if $p < 0.05$.

Secreted cytokines (pg/10^6 cells)	**Control**		**GOS C 0.8**		**GOS C 4**		**GOS C 12**		**Two-way ANCOVA *p* value**		
	Mean ± SD (*n*= 7)		Mean ± SD (*n*= 7)		Mean ± SD (*n*= 7)		Mean ± SD (*n*= 7)				
	5-A-RU+MG		5-A-RU+MG		5-A-RU+MG		5-A-RU+MG		5-A-RU+MG	GOS C	5-A-RU+MG * GOS C
	-	+	-	+	-	+	-	+			
IL-1α	2.15 ± 4.93	2.17 ± 4.92	3.07 ± 7.56	4.16 ± 7.90	3.65 ± 9.38	2.23 ± 4.01	1.58 ± 3.38	5.08 ± 8.92	0.435	0.869	0.755
IL-1β	446.6 ± 864.4	333.2 ± 573.2	131.8 ± 325.9	601.9 ± 743.1	109.1 ± 285.8	1,809 ± 4,408	92.7 ± 146.8	379.2 ± 455.1	0.133	0.719	0.476
IL-8	5,187 ± 10,038	8,835 ± 11,238	12,690 ± 23,160	14,835 ± 22,572	12,782 ± 22,962	17,711 ± 22,604	38,371 ± 24,497	36,441 ± 26,866	0.411	**<0.0001**	0.968
IL-10	5.33 ± 10.96	3.35 ± 6.97	6.25 ± 12.35	3.50 ± 6.58	6.58 ± 14.87	3.62 ± 5.94	5.79 ± 13.44	4.22 ± 6.28	0.540	0.975	0.998
IL-12p70	5.97 ± 4.35	5.82 ± 7.57	9.09 ± 5.18	10.41 ± 4.77	9.12 ± 17.39	11.22 ± 6.84	6.33 ± 7.25	12.10 ± 7.53	0.217	0.492	0.796

Table E-14 Continued.

Secreted cytokines (pg/10^6 cells)	**Control**		**GOS C 0.8**		**GOS C 4**		**GOS C 12**		**Two-way ANOVA *p* value**		
	Mean ± SD (*n*= 7)		Mean ± SD (*n*= 7)		Mean ± SD (*n*= 7)		Mean ± SD (*n*= 7)				
	5-A-RU+MG		5-A-RU+MG		5-A-RU+MG		5-A-RU+MG		5-A-RU+MG	GOS C	5-A-RU+MG * GOS C
	-	+	-	+	-	+	-	+			
IL-17A	1.01 ± 0.73	1.05 ± 1.59	1.91 ± 1.07	1.65 ± 1.23	1.20 ± 1.51	2.22 ± 1.52	0.46 ± 0.40	1.83 ± 0.83	0.077	0.263	0.222
IFN-γ	1.26 ± 1.13	11.19 ± 12.07	2.49 ± 3.48	10.40 ± 11.30	3.54 ± 4.52	7.47 ± 8.76	1.03 ± 0.94	8.89 ± 9.60	**<0.0001**	0.979	0.764
TNF-α	34.60 ± 81.24	97.65 ± 179.95	45.02 ± 96.08	181.79 ± 255.92	70.64 ± 171.83	129.52 ± 179.09	75.58 ± 184.03	253.89 ± 384.96	**0.021**	0.426	0.802
Granzyme B	32.55 ± 17.63	43.50 ± 24.81	48.84 ± 48.10	59.44 ± 54.35	49.71 ± 43.86	45.63 ± 41.77	41.56 ± 29.67	46.09 ± 44.72	0.551	0.768	0.956

Significant main effect of *GOS C* – Bonferroni's *post-hoc* test for multiple comparison: IL-8 – GOS C 12 significantly different from NC ($p < 0.0001$), GOS C 0.8 ($p = 0.003$) and GOS C 4 ($p = 0.005$)

Significant main effect of *5-A-RU + MG* – Bonferroni's *post-hoc* test for multiple comparison: IFN-γ – Without 5-A-RU + MG significantly different from with 5-A-RU + MG ($p < 0.0001$); TNF-α – Without 5-A-RU + MG significantly different from with 5-A-RU + MG ($p = 0.021$).

Table E-15 Levels of soluble mediators secreted by Crohn's disease PBMCs after 20 h culture with 5-A-RU + MG or B-GOS® batch C or after co-culture with both. Unstimulated PBMCs were used as a negative control (NC). Results were considered significant if $p < 0.05$.

Secreted cytokines (pg/10^6 cells)	**Control**		**GOS C 12**		**Two-way ANCOVA *p* value**		
	Mean ± SD (*n*= 7)		Mean ± SD (*n*= 7)				
	5-A-RU+MG		5-A-RU+MG		5-A-RU+MG	GOS C	5-A-RU+MG * GOS C
	-	+	-	+			
IL-1α	0.40 ± 0.00	0.47 ± 0.16	0.53 ± 0.21	0.40 ± 0.00	0.818	0.436	0.080
IL-1β	100.6 ± 22.3	92.4 ± 16.0	116.9 ± 24.6	100.6 ± 13.3	0.562	**0.038**	0.567
IL-8	602.4 ± 786.7	500.4 ± 1,221.9	7,398.6 ± 7,922.5	191.2 ± 450.9	0.203	**0.016**	**0.028**
IL-10	0.41 ± 0.43	0.15 ± 0.12	0.42 ± 0.39	0.34 ± 0.20	0.262	0.508	0.499
IL-12p70	9.32 ± 0.00	9.32 ± 0.00	9.32 ± 0.00	9.32 ± 0.00	N/A	N/A	N/A
IL-17A	0.12 ± 0.00	0.12 ± 0.00	0.14 ± 0.05	0.12 ± 0.00	0.246	0.444	0.338
IFN-γ	3.30 ± 1.29	2.90 ± 1.21	3.69 ± 1.43	4.08 ± 1.78	0.285	**0.045**	0.461
TNF-α	0.57 ± 0.74	0.71 ± 1.32	2.46 ± 2.65	0.68 ± 0.92	0.667	0.065	0.125
Granzyme B	102.1 ± 46.2	82.5 ± 48.0	173.1 ± 211.2	128.8 ± 114.8	**0.044**	0.595	0.778
IL-1ra	337.5 ± 178.2	283.1 ± 16.3	442.8 ± 278.2	291.3 ± 186.2	**0.001**	0.745	0.407

Significant main effect of *GOS C* – Bonferroni's *post-hoc* test for multiple comparison: IL-1β – GOS C 12 significantly different from NC (p= 0.038); IFN-γ – GOS C 12 significantly different from NC (p= 0.045)**. Significant main effect of *5-A-RU + MG* – Bonferroni's *post-hoc* test for multiple comparison:** Granzyme B – Without 5-A-RU + MG significantly different from with 5-A-RU + MG (p= 0.044) IL-1ra – Without 5-A-RU + MG significantly different from with 5-A-RU + MG (p= 0.001); **Significant interaction *5-A-RU + MG*GOS C* – Bonferroni's *post-hoc* test for multiple comparison:** IL-8 — GOS C 12 significantly different from NC without 5-A-RU + MG (p= 0.016); GOS C 12 with 5-A-RU + MG significantly different from GOS C 12 without 5-A-RU + MG (p= 0.0114)

Appendix F Supporting materials from Chapter 6

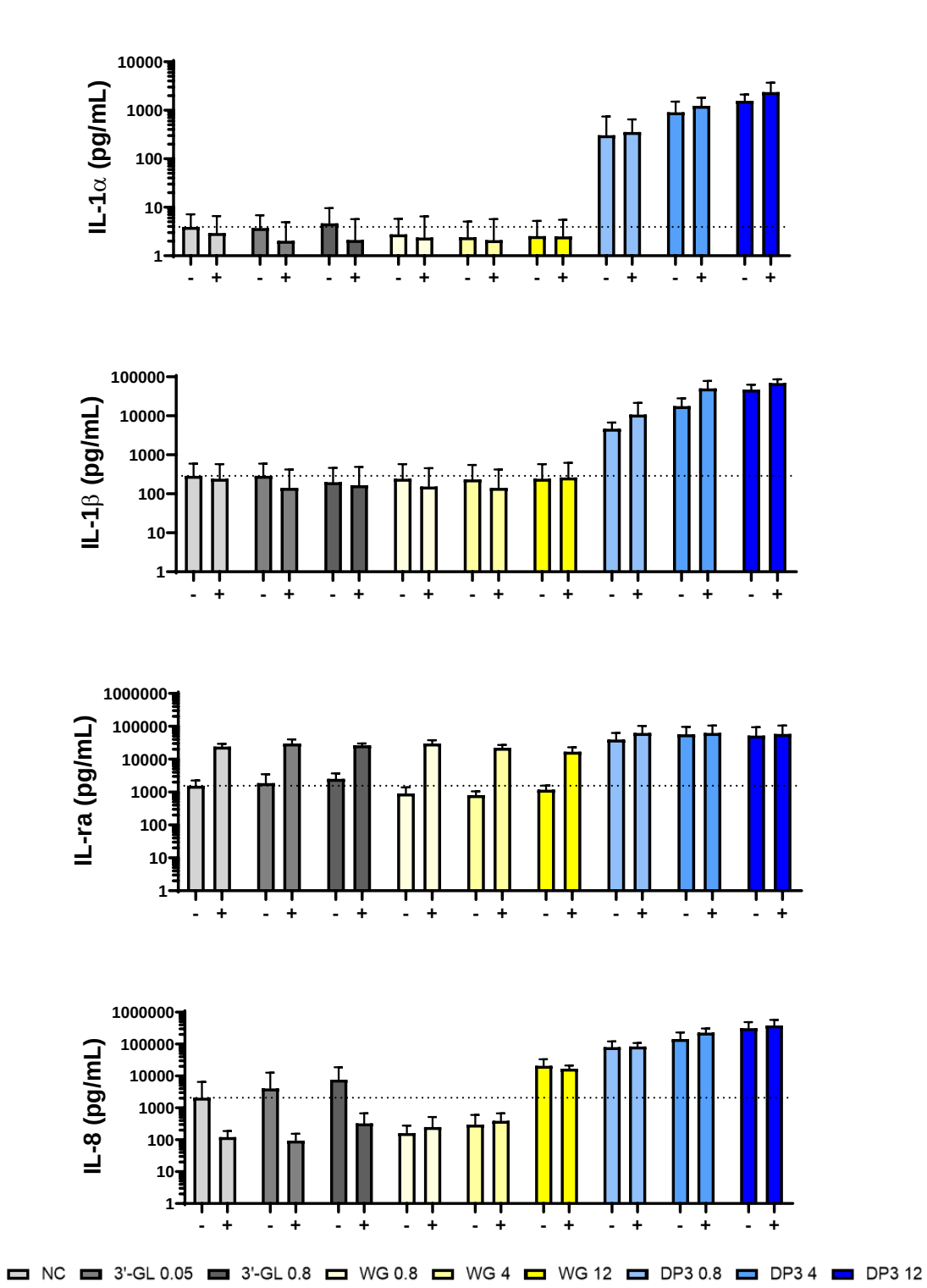

Figure F-1 Levels of IL-1α, IL-1β, IL-1ra and IL-8 secreted by healthy PBMCs (*n*= 5) after 1 h pre-incubation with DP2 – DP5 B-GOS® fractions, 3'-GL or whole B-GOS® followed by 24 challenge with (+) or without (-) poly(I:C). Unstimulated cells (NC) were used as control. Data are expressed as mean ± SD.

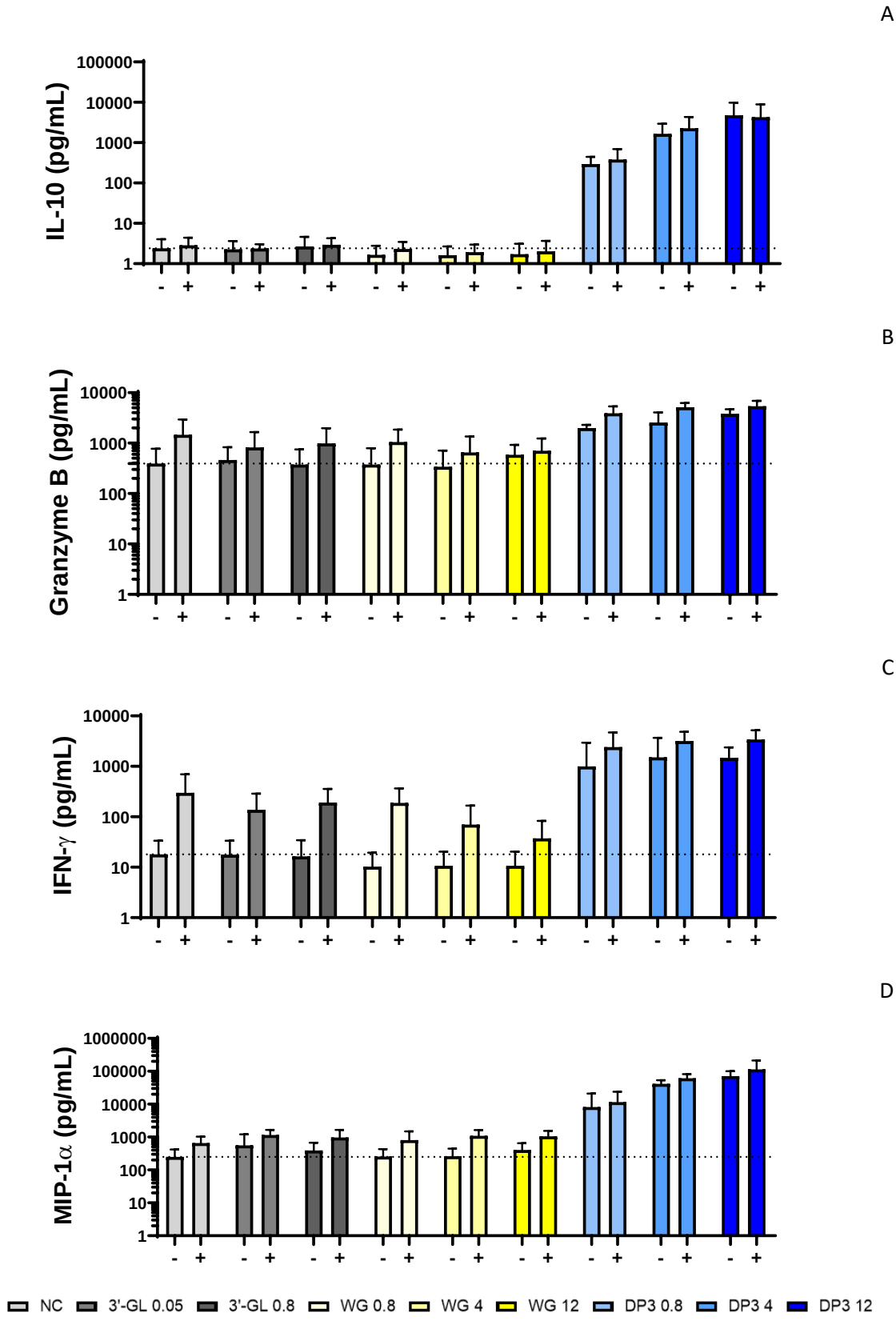

Figure F-2 Levels of IL-10, granzyme B, IFN-γ and MIP-1α secreted by healthy PBMCs (*n*= 5) after 1 h pre-incubation with DP2 – DP5 B-GOS® fractions, 3'-GL or whole B-GOS® followed by 24 challenge with (+) or without (-) poly(I:C). Unstimulated cells (NC) were used as control. Data are expressed as mean ± SD.

A

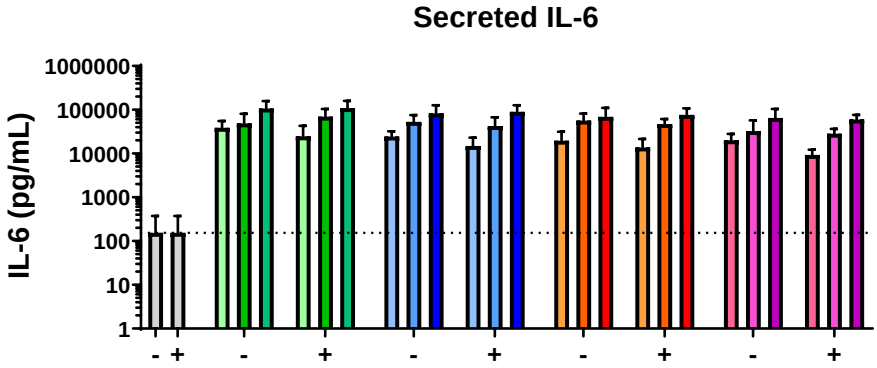

B

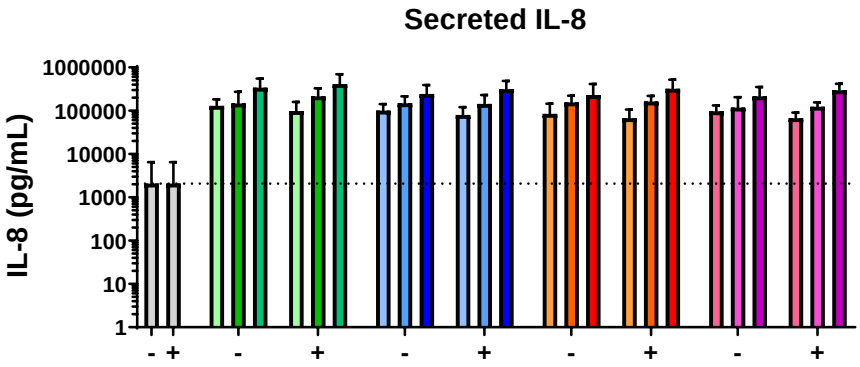

C

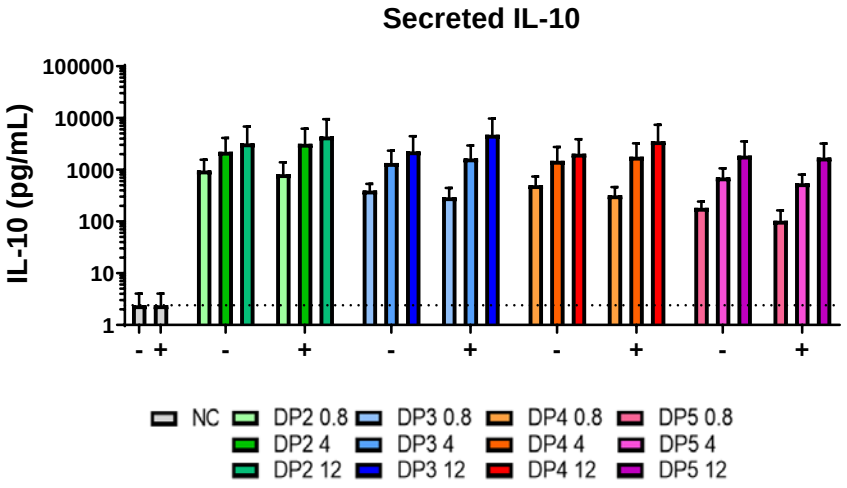

Figure F-3 Effects of stimulating healthy PBMCs (*n*= 5) for 24 h with B-GOS® DP2 – DP5 fractions with (+) or without (-) PMB pre-treatment on IL-6, IL-8 and IL-10. Unstimulated cells (NC) were used as control. Data are expressed as mean ± SD. Two-way ANOVA followed by Dunnett's *post-hoc* test was performed. All B-GOS® fractions caused a significant increase in all secreted mediators ($p < 0.05$).

A

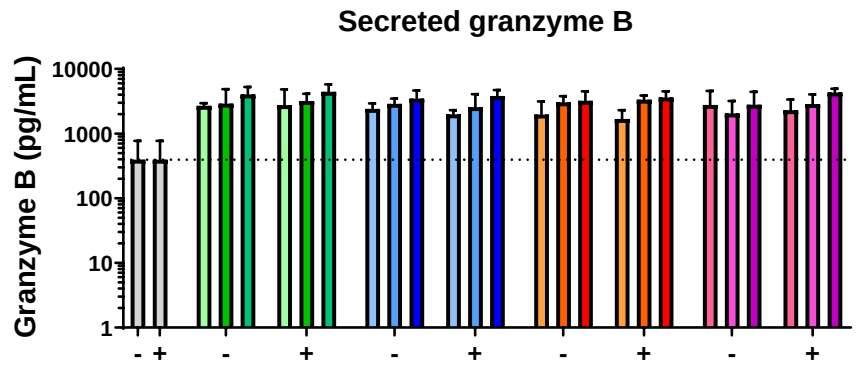

B

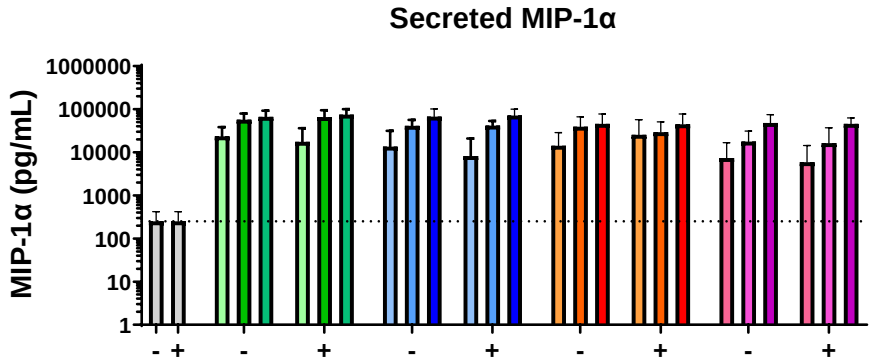

C

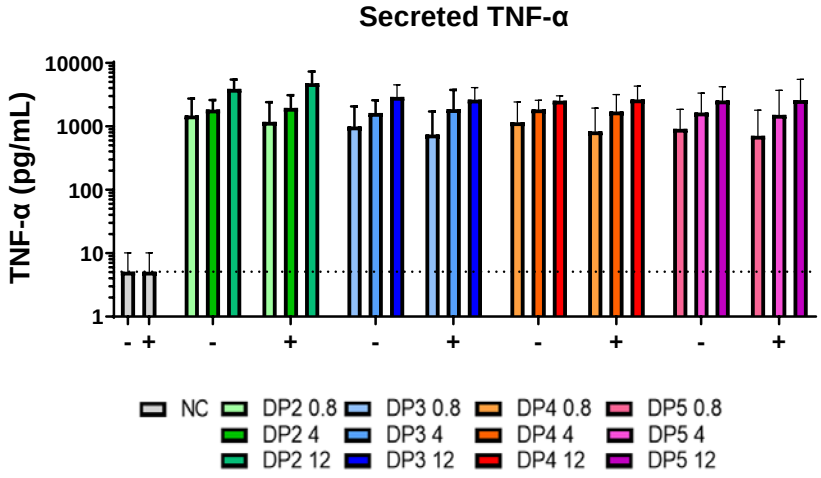

Figure F-4 Effects of stimulating healthy PBMCs (*n*= 5) for 24 h with B-GOS® DP2 – DP5 fractions with (+) or without (-) PMB pre-treatment on granzyme B, MIP-1α and TNF-α. Unstimulated cells (NC) were used as control. Data are expressed as mean ± SD. Two-way ANOVA followed by Dunnett's *post-hoc* test was performed. All B-GOS® fractions caused a significant increase in all secreted mediators ($p < 0.05$).

List of References

1. Liu, G. and Y. Zhao, *Toll-like receptors and immune regulation: their direct and indirect modulation on regulatory CD4+ CD25+ T cells.* Immunology, 2007. **122**(2): p. 149-156.

2. Medzhitov, R., *Recognition of microorganisms and activation of the immune response.* Nature, 2007. **449**(7164): p. 819-826.

3. Vénéreau, E., C. Ceriotti, and M.E. Bianchi, *DAMPs from Cell Death to New Life.* Frontiers in Immunology, 2015. **6**(422).

4. Amarante-Mendes, G.P., et al., *Pattern Recognition Receptors and the Host Cell Death Molecular Machinery.* Frontiers in Immunology, 2018. **9**(2379).

5. Kumar, H., T. Kawai, and S. Akira, *Pathogen recognition by the innate immune system.* International Reviews of Immunology, 2011. **30**(1): p. 16-34.

6. Willment, J.A. and G.D. Brown, *C-type lectin receptors in antifungal immunity.* Trends in Microbiology, 2008. **16**(1): p. 27-32.

7. Zhong, Y., A. Kinio, and M. Saleh, *Functions of NOD-Like Receptors in Human Diseases.* Frontiers in Immunology, 2013. **4**(333).

8. Rehwinkel, J. and M.U. Gack, *RIG-I-like receptors: their regulation and roles in RNA sensing.* Nature Reviews Immunology, 2020. **20**(9): p. 537-551.

9. Kawasaki, T. and T. Kawai, *Toll-Like Receptor Signaling Pathways.* Frontiers in Immunology, 2014. **5**(461).

10. Takeuchi, O. and S. Akira, *Pattern Recognition Receptors and Inflammation.* Cell, 2010. **140**(6): p. 805-820.

11. Sameer, A.S. and S. Nissar, *Toll-Like Receptors (TLRs): Structure, Functions, Signaling, and Role of Their Polymorphisms in Colorectal Cancer Susceptibility.* Biomed Res Int, 2021. **2021**: p. 1157023.

12. Raetz, C.R. and C. Whitfield, *Lipopolysaccharide endotoxins.* Annu Rev Biochem, 2002. **71**: p. 635-700.

13. Wassenaar, T.M. and K. Zimmermann, *Lipopolysaccharides in Food, Food Supplements, and Probiotics: Should We be Worried?* European Journal of Microbiology and Immunology, 2018. **8**(3): p. 63-69.

14. Xu, H., et al., *The modulatory effects of lipopolysaccharide-stimulated B cells on differential T-cell polarization.* Immunology, 2008. **125**(2): p. 218-228.

15. Plevin, R.E., et al., *The Role of Lipopolysaccharide Structure in Monocyte Activation and Cytokine Secretion.* Shock (Augusta, Ga.), 2016. **45**(1): p. 22-27.

16. Erridge, C., E. Bennett-Guerrero, and I.R. Poxton, *Structure and function of lipopolysaccharides.* Microbes and Infection, 2002. **4**: p. 837-851.

17. Akira, S., *Toll-like Receptors and Innate Immunity*, in *Advances in Immunology*, F.J. Dixon, Editor. 2001, Academic Press. p. 1-56.

18. Lu, Y.C., W.C. Yeh, and P.S. Ohashi, *LPS/TLR4 signal transduction pathway.* Cytokine, 2008. **42**(2): p. 145-151.

19. Vaure, C. and Y. Liu, *A Comparative Review of Toll-Like Receptor 4 Expression and Functionality in Different Animal Species.* Frontiers in Immunology, 2014. **5**(316).

20. McAleer, J.P. and A.T. Vella, *Understanding how lipopolysaccharide impacts CD4 T-cell immunity.* Critical reviews in immunology, 2008. **28**(4): p. 281-299.

21. de Oliviera Nascimento, L., P. Massari, and L. Wetzler, *The Role of TLR2 in Infection and Immunity.* Frontiers in Immunology, 2012. **3**(79).

22. Ferwerda, G., et al., *Dectin-1 synergizes with TLR2 and TLR4 for cytokine production in human primary monocytes and macrophages.* Cellular Microbiology, 2008. **10**(10): p. 2058-2066.

23. Parkin, J. and B. Cohen, *An overview of the immune system.* The Lancet, 2001. **357**(9270): p. 1777-1789.

24. Mold, C., H. Gewurz, and T.W. Du Clos, *Regulation of complement activation by C-reactive protein.* Immunopharmacology, 1999. **42**(1-3): p. 23-30.

25. Srinivasan, N., *Telling apart friend from foe: discriminating between commensals and pathogens at mucosal sites.* Innate Immun, 2010. **16**(6): p. 391-404.

26. Rakoff-Nahoum, S., et al., *Recognition of Commensal Microflora by Toll-Like Receptors Is Required for Intestinal Homeostasis.* Cell, 2004. **118**(2): p. 229-241.

27. Gonzalez, S., et al., *Conceptual aspects of self and nonself discrimination.* Self/nonself, 2011. **2**(1): p. 19-25.

28. Katsarou, A., et al., *Type 1 diabetes mellitus.* Nature Reviews Disease Primers, 2017. **3**(1): p. 17016.

29. Janeway, C.A., et al., *The immune system in health and disease*. 5th ed. Immunobiology. 2001, New York: Garland Science. 884.

30. Informed Health Online [Internet]. *What are the organs of the immune system?* 2006 14/01/2013 21/01/2019]; Available from: https://www.ncbi.nlm.nih.gov/books/NBK65083/.

31. Abbas, A.K., A.H. Lichtman, and S. Pillai, *Cellular and Molecular Immunology*. 8th ed. 2014, Philadelphia: Elsevier. 535.

32. Male, D., et al., *Immunology*. 7th ed. 2006, Philadelphia Elsevier. 563.

33. Constantinescu, C.S., R.I. Arsenescu, and V. Arsenescu, *Neuro-Immuno-Gastroenterology* 2016, Switzerland: Springer International Publishing. 345.

34. Calder, P.C. and A.D. Kulkarni, *Nutrition, Immunity, and Infection*. 2018, Boca Raton, Florida: CRC Press Taylor and Francis Group. 521.

35. Childs, C.E., *The effects of gender, pregnancy and diet upon rat tissue fatty acid composition and immune functions*, in *Faculty of Medicine, Health and Life Sciences*. 2009, University of Southampton: Southampton, UK. p. 379.

36. Chaplin, D.D., *Overview of the immune response.* Journal of Allergy and Clinical Immunology, 2010. **125**(2 Suppl 2): p. 1-41.

37. Ginhoux, F. and S. Jung, *Monocytes and macrophages: developmental pathways and tissue homeostasis.* Nature Review Immunology, 2014. **14**(6): p. 392-404.

38. Boyette, L.B., et al., *Phenotype, function, and differentiation potential of human monocyte subsets.* PLOS ONE, 2017. **12**(4): p. e0176460.

39. Vivier, E., et al., *Innate or adaptive immunity? The example of natural killer cells.* Science (New York, N.Y.), 2011. **331**(6013): p. 44-49.

40. Long, E.O., et al., *Controlling natural killer cell responses: integration of signals for activation and inhibition.* Annu Rev Immunol, 2013. **31**: p. 227-58.

41. Pennock, N.D., et al., *T cell responses: naive to memory and everything in between.* Advances in Physiology Education 2013. **37**(4): p. 273-283.

42. Pier, G.B., J.B. Lyczak, and L.M. Wetzler, *Immunology, Infection, and Immunity*. 2004, Washington, DC: ASM Press. 743.

43. Calder, P.C., et al., *Inflammatory disease processes and interactions with nutrition.* British Journal of Nutrition, 2009. **101** p. 1-45.

44. Afshar, R., B.D. Medoff, and A.D. Luster, *Allergic asthma: a tale of many T cells.* Clinical and Experimental Allergy, 2008. **38**(12): p. 1847-1857.

45. von Andrian, U.H. and C.R. Mackay, *T-cell function and migration. Two sides of the same coin.* The New England Journal of Medicine, 2000. **343**(14): p. 1020-1034.

46. Zhu, J., H. Yamane, and W.E. Paul, *Differentiation of effector CD4 T cell populations (*).* Annual Review in Immunology, 2010. **28**: p. 445-489.

47. Binder, C., et al., *CD2 Immunobiology.* Frontiers in Immunology, 2020. **11**(1090).

48. Mir, M.A., *Chapter 1 - Introduction to Costimulation and Costimulatory Molecules*, in *Developing Costimulatory Molecules for Immunotherapy of Diseases*, M.A. Mir, Editor. 2015, Academic Press. p. 1-43.

49. Bajnok, A., et al., *The Distribution of Activation Markers and Selectins on Peripheral T Lymphocytes in Preeclampsia.* Mediators of inflammation, 2017. **2017**: p. 8045161-8045161.

50. Machura, E., et al., *Expression of naive/memory (CD45RA/CD45RO) markers by peripheral blood CD4+ and CD8+ T cells in children with asthma.* Archivium Immunologiae et Therapiae Experimentalis (Warsz), 2008. **56**(1): p. 55-62.

51. Zidek, Z., P. Anzenbacher, and E. Kmonickova, *Current status and challenges of cytokine pharmacology.* British Journal of Pharmacology, 2009. **157**(3): p. 342-361.

52. Shield, M.A. and P.E. Mirkes, *Chapter 8 - Apoptosis*, in *Handbook of Developmental Neurotoxicology*, W. Slikker and L.W. Chang, Editors. 1998, Academic Press: San Diego. p. 159-188.

53. Wershil, B.K. and G.T. Furuta, *Gastrointestinal mucosal immunity.* Journal of Allergy and Clinical Immunology, 2008. **121**(2): p. 380-383.

54. Jung, C., J.P. Hugot, and F. Barreau, *Peyer's Patches: The Immune Sensors of the Intestine.* International Journal of Inflammation, 2010. **2010**: p. 1-12.

55. Mabbott, N.A., et al., *Microfold (M) cells: important immunosurveillance posts in the intestinal epithelium.* Mucosal Immunol, 2013. **6**(4): p. 666-677.

56. Turner, J.R., *Intestinal mucosal barrier function in health and disease.* Nature Reviews Immunology, 2009. **9**(11): p. 799-809.

57. Lewis, M.C., *The Gut-Associated Lymphoid System*, in *Nutrition, Immunity, and Infection*, P.C. Calder and A.D. Kulkarni, Editors. 2018, CRC Press Taylor and Francis Group: Boca Raton, Florida. p. 521.

58. Manzo, V.E. and A.S. Bhatt, *The human microbiome in hematopoiesis and hematologic disorders.* Blood, 2015. **126**(3): p. 311-318.

59. Nehra, V., E.V. Marietta, and J.A. Murray, *Chapter 12 - Celiac Disease and its Therapy: Current Approaches and New Advances*, in *Wheat and Rice in Disease Prevention and Health*, R.R. Watson, V.R. Preedy, and S. Zibadi, Editors. 2014, Academic Press: San Diego. p. 143-155.

60. Treiner, E., et al., *Selection of evolutionarily conserved mucosal-associated invariant T cells by MR1.* Nature, 2003. **422**(6943): p. 164-169.

61. Treiner, E., et al., *Mucosal-associated invariant T (MAIT) cells: an evolutionarily conserved T cell subset.* Microbes and Infection, 2005. **7**(3): p. 552-559.

62. Kawachi, I., et al., *MR1-Restricted V 19i Mucosal-Associated Invariant T Cells Are Innate T Cells in the Gut Lamina Propria That Provide a Rapid and Diverse Cytokine Response.* The Journal of Immunology, 2006. **176**(3): p. 1618-1627.

63. Le Bourhis, L., et al., *Antimicrobial activity of mucosal-associated invariant T cells.* Nature Immunology, 2010. **11**(8): p. 701-708.

64. Kurioka, A., et al., *MAIT cells: new guardians of the liver.* Clinical & Translational Immunology, 2016. **5**(8): p. 1-11.

65. Lee, O.J., et al., *Circulating mucosal-associated invariant T cell levels and their cytokine levels in healthy adults.* Experimental Gerontology, 2014. **49**: p. 47-54.

66. Novak, J., et al., *The decrease in number and change in phenotype of mucosal-associated invariant T cells in the elderly and differences in men and women of reproductive age.* Scand J Immunol, 2014. **80**(4): p. 271-5.

67. Reantragoon, R., et al., *Antigen-loaded MR1 tetramers define T cell receptor heterogeneity in mucosal-associated invariant T cells.* The Journal of Experimental Medicine, 2013. **210**(11): p. 2305-2320.

68. Gapin, L., *Where do MAIT cells fit in the family of unconventional T cells?* PLoS Biology, 2009. **7**(3): p. 435-438.

69. Dusseaux, M., et al., *Human MAIT cells are xenobiotic-resistant, tissue-targeted, CD161hi IL-17–secreting T cells.* Blood, 2011. **117**(4): p. 1250-1259.

70. Park, Y.W. and S.J. Kee, *Mucosal-associated Invariant T cells: A New Player in Innate Immunity.* Journal of Rheumatic Diseases, 2015. **22**(6): p. 337-345.

71. Gherardin, N.A., et al., *Human blood MAIT cell subsets defined using MR1 tetramers.* Immunol Cell Biol, 2018. **96**(5): p. 507-525.

72. Wakao, H., et al., *Mucosal-Associated Invariant T Cells in Regenerative Medicine.* Frontiers in Immunology, 2017. **8**: p. 1-11.

73. Napier, R.J., et al., *The Role of Mucosal Associated Invariant T Cells in Antimicrobial Immunity.* Frontiers in Immunology, 2015. **6**: p. 1-10.

74. Huang, S., et al., *MR1 antigen presentation to mucosal-associated invariant T cells was highly conserved in evolution.* Proceedings of the National Academy of Sciences, 2009. **106**(20): p. 8290.

75. Goldfinch, N., et al., *Conservation of mucosal associated invariant T (MAIT) cells and the MR1 restriction element in ruminants, and abundance of MAIT cells in spleen.* Vet Res, 2010. **41**(5): p. 62.

76. Hinks, T.S.C. and X.-W. Zhang, *MAIT Cell Activation and Functions.* Frontiers in Immunology, 2020. **11**(1014).

77. Leeansyah, E., et al., *Activation, exhaustion, and persistent decline of the antimicrobial MR1-restricted MAIT-cell population in chronic HIV-1 infection.* Blood, 2013. **121**(7): p. 1124-1135.

78. Ussher, J.E., et al., *TLR signaling in human antigen-presenting cells regulates MR1-dependent activation of MAIT cells.* European Journal of Immunology, 2016. **46**(7): p. 1600-1614.

79. Wallington, J.C., et al., *IL-12 and IL-7 synergize to control mucosal-associated invariant T-cell cytotoxic responses to bacterial infection.* The Journal of Allergy and Clinical Immunology, 2017: p. 1-20.

80. Sattler, A., et al., *IL-15 dependent induction of IL-18 secretion as a feedback mechanism controlling human MAIT-cell effector functions.* European Journal of Immunology, 2015. **45**(8): p. 2286-2298.

81. Liu, T., et al., *NF-κB signaling in inflammation.* Signal Transduction And Targeted Therapy, 2017. **2**: p. 17023.

82. Wong, E.B., T. Ndung'u, and V.O. Kasprowicz, *The role of mucosal-associated invariant T cells in infectious diseases.* Immunology, 2017. **150**(1): p. 45-54.

83. van Wilgenburg, B., et al., *MAIT cells are activated during human viral infections.* Nature Communications, 2016. **7**(1): p. 11653.

84. Reantragoon, R., et al., *Mucosal-associated invariant T cells in clinical diseases.* Asian Pacific Journal of Allergy and Immunology, 2016. **34**(1): p. 3-10.

85. Kjer-Nielsen, L., et al., *MR1 presents microbial vitamin B metabolites to MAIT cells.* Nature, 2012. **491**(7426): p. 717-723.

86. Corbett, A.J., et al., *T-cell activation by transitory neo-antigens derived from distinct microbial pathways.* Nature, 2014. **509**(7500): p. 361-365.

87. Hiejima, E., et al., *Reduced Numbers and Proapoptotic Features of Mucosal-associated Invariant T Cells as a Characteristic Finding in Patients with Inflammatory Bowel Disease.* Inflammatory Bowel Diseases, 2015. **21**(7): p. 1529-1540.

88. Veerapen, N., et al., *Chemical insights into the search for MAIT cells activators.* Molecular Immunology, 2021. **129**: p. 114-120.

89. Gapin, L., *Check MAIT.* The Journal of Immunology, 2014. **192**(10): p. 4475-4480.

90. Haileselassie, Y., et al., *Lactobacilli Regulate Staphylococcus aureus 161:2-Induced Pro-Inflammatory T-Cell Responses In Vitro.* PLOS ONE, 2013. **8**(10): p. e77893.

91. Johansson, M.A., et al., *Probiotic Lactobacilli Modulate Staphylococcus aureus-Induced Activation of Conventional and Unconventional T cells and NK Cells.* Frontiers in Immunology, 2016. **7**: p. 1-15.

92. Spaan, M., et al., *Frequencies of Circulating MAIT Cells Are Diminished in Chronic HCV, HIV and HCV/HIV Co-Infection and Do Not Recover during Therapy.* PLoS One, 2016. **11**(7): p. 1-13.

93. Tominaga, K., et al., *Possible involvement of mucosal-associated invariant T cells in the progression of inflammatory bowel diseases.* Biomedical Research, 2017. **38**(2): p. 111-121.

94. Haga, K., et al., *MAIT cells are activated and accumulated in the inflamed mucosa of ulcerative colitis.* Journal of Gastroenterology and Hepatology, 2016. **31**(5): p. 965-972.

95. Serriari, N.E., et al., *Innate mucosal-associated invariant T (MAIT) cells are activated in inflammatory bowel diseases.* Clinical & Experimental Immunology, 2014. **176**(2): p. 266-274.

96. Eyerich, K., V. Dimartino, and A. Cavani, *IL-17 and IL-22 in immunity: Driving protection and pathology.* European Journal of Immunology, 2017. **47**(4): p. 607-614.

97. Hueber, W., et al., *Secukinumab, a human anti-IL-17A monoclonal antibody, for moderate to severe Crohn's disease: unexpected results of a randomised, double-blind placebo-controlled trial.* Gut, 2012. **61**(12): p. 1693-700.

98. Parks, O.B., et al., *Interleukin-22 Signaling in the Regulation of Intestinal Health and Disease.* Frontiers in Cell and Developmental Biology, 2016. **3**(85).

99. U. Boehm, et al., *CELLULAR RESPONSES TO INTERFERON-γ.* Annual Review of Immunology, 1997. **15**(1): p. 749-795.

100. Ito, R., et al., *Interferon-gamma is causatively involved in experimental inflammatory bowel disease in mice.* Clinical and experimental immunology, 2006. **146**(2): p. 330-338.

101. Zheng, S.G., Z. Xu, and J. Wang, *A protective role of IFN-γ in T cell-mediated colitis by regulation of Treg/Th17 via induction of indoleamine-2,3-deoxygenase.* The Journal of Immunology, 2019. **202**(1 Supplement): p. 57.3-57.3.

102. Cibrian, D. and F. Sanchez-Madrid, *CD69: from activation marker to metabolic gatekeeper.* Eur J Immunol, 2017. **47**(6): p. 946-953.

103. Testi, R., et al., *The CD69 receptor: a multipurpose cell-surface trigger for hematopoietic cells.* Immunol Today, 1994. **15**(10): p. 479-83.

104. Radulovic, K. and J.H. Niess, *CD69 is the crucial regulator of intestinal inflammation: a new target molecule for IBD treatment?* Journal of immunology research, 2015. **2015**: p. 497056-497056.

105. Hasegawa, A., et al., *Crucial role for CD69 in the pathogenesis of dextran sulphate sodium-induced colitis.* PloS one, 2013. **8**(6): p. e65494-e65494.

106. Lauzurica, P., et al., *Phenotypic and functional characteristics of hematopoietic cell lineages in CD69-deficient mice.* Blood, 2000. **95**(7): p. 2312-2320.

107. Radulovic, K., et al., *CD69 regulates type I IFN-induced tolerogenic signals to mucosal CD4 T cells that attenuate their colitogenic potential.* J Immunol, 2012. **188**(4): p. 2001-13.

108. Neurath, M.F., *Cytokines in inflammatory bowel disease.* Nature Reviews Immunology, 2014. **14**(5): p. 329-342.

109. Illés, Z., et al., *Accumulation of Valpha7.2-Jalpha33 invariant T cells in human autoimmune inflammatory lesions in the nervous system.* Int Immunol, 2004. **16**(2): p. 223-30.

110. Miyazaki, Y., et al., *Mucosal-associated invariant T cells regulate Th1 response in multiple sclerosis.* Int Immunol, 2011. **23**(9): p. 529-35.

111. Hinks, T.S., *Mucosal-associated invariant T cells in autoimmunity, immune-mediated diseases and airways disease.* Immunology, 2016. **148**(1): p. 1-12.

112. Cho, J.-S., et al., *Lipopolysaccharide induces pro-inflammatory cytokines and MMP production via TLR4 in nasal polyp-derived fibroblast and organ culture.* PloS one, 2014. **9**(11): p. e90683-e90683.

113. Chiba, A., et al., *Activation status of mucosal-associated invariant T cells reflects disease activity and pathology of systemic lupus erythematosus.* Arthritis Research & Therapy, 2017. **19**(1): p. 58.

114. Annibali, V., et al., *CD161highCD8+T cells bear pathogenetic potential in multiple sclerosis.* Brain, 2011. **134**(2): p. 542-554.

115. Cho, Y.N., et al., *Mucosal-associated invariant T cell deficiency in systemic lupus erythematosus.* J Immunol, 2014. **193**(8): p. 3891-901.

116. Teunissen, M.B.M., et al., *The IL-17A-producing CD8+ T-cell population in psoriatic lesional skin comprises mucosa-associated invariant T cells and conventional T cells.* J Invest Dermatol, 2014. **134**(12): p. 2898-2907.

117. Dunne, M.R., et al., *Persistent changes in circulating and intestinal gammadelta T cell subsets, invariant natural killer T cells and mucosal-associated invariant T cells in children and adults with coeliac disease.* PloS One, 2013. **8**(10): p. 1-10.

118. Hinks, T.S., et al., *Steroid-induced Deficiency of Mucosal-associated Invariant T Cells in the Chronic Obstructive Pulmonary Disease Lung. Implications for Nontypeable Haemophilus influenzae Infection.* American Journal of Respiratory and Critical Care Medicine, 2016. **194**(10): p. 1208-1218.

119. Magalhaes, I., et al., *Mucosal-associated invariant T cell alterations in obese and type 2 diabetic patients.* J Clin Invest, 2015. **125**(4): p. 1752-62.

120. Booth, J.S., et al., *Mucosal-Associated Invariant T Cells in the Human Gastric Mucosa and Blood: Role in Helicobacter pylori Infection.* Front Immunol, 2015. **6**: p. 466.

121. Leung, D.T., et al., *Circulating mucosal associated invariant T cells are activated in Vibrio cholerae O1 infection and associated with lipopolysaccharide antibody responses.* PLoS Neglected Tropical Diseases, 2014. **8**(8): p. 1-8.

122. Le Bourhis, L., et al., *MAIT cells detect and efficiently lyse bacterially-infected epithelial cells.* PLoS Pathogens, 2013. **9**(10): p. 1-12.

123. Gold, M.C., et al., *Human mucosal associated invariant T cells detect bacterially infected cells.* PLoS Biology, 2010. **8**(6): p. 1-14.

124. Jiang, J., et al., *Mucosal-associated invariant T-cell function is modulated by programmed death-1 signaling in patients with active tuberculosis.* Am J Respir Crit Care Med, 2014. **190**(3): p. 329-39.

125. Szabo, P.A., et al., *CD1d- and MR1-Restricted T Cells in Sepsis.* Frontiers in Immunology, 2015. **6**(401).

126. Hengst, J., et al., *Nonreversible MAIT cell-dysfunction in chronic hepatitis C virus infection despite successful interferon-free therapy.* Eur J Immunol, 2016. **46**(9): p. 2204-10.

127. Eberhard, J.M., et al., *CD161+ MAIT cells are severely reduced in peripheral blood and lymph nodes of HIV-infected individuals independently of disease progression.* PLoS One, 2014. **9**(11): p. e111323.

128. Cosgrove, C., et al., *Early and nonreversible decrease of CD161++ /MAIT cells in HIV infection.* Blood, 2013. **121**(6): p. 951-61.

129. Sundstrom, P., et al., *Human Mucosa-Associated Invariant T Cells Accumulate in Colon Adenocarcinomas but Produce Reduced Amounts of IFN-γ.* The Journal of Immunology, 2015. **195**(7): p. 3472-3481.

130. Ling, L., et al., *Circulating and tumor-infiltrating mucosal associated invariant T (MAIT) cells in colorectal cancer patients.* Sci Rep, 2016. **6**: p. 20358.

131. Zabijak, L., et al., *Increased tumor infiltration by mucosal-associated invariant T cells correlates with poor survival in colorectal cancer patients.* Cancer Immunol Immunother, 2015. **64**(12): p. 1601-8.

132. Wallace, M.E., et al., *An emerging role for immune regulatory subsets in chronic lymphocytic leukaemia.* Int Immunopharmacol, 2015. **28**(2): p. 897-900.

133. Riva, A., et al., *Mucosa-associated invariant T cells link intestinal immunity with antibacterial immune defects in alcoholic liver disease.* Gut, 2018. **67**(5): p. 918-930.

134. Oo, Y.H., et al., *CXCR3-dependent recruitment and CCR6-mediated positioning of Th-17 cells in the inflamed liver.* J Hepatol, 2012. **57**(5): p. 1044-51.

135. Gerritsen, J., et al., *Intestinal microbiota in human health and disease: the impact of probiotics.* Genes & Nutrition, 2011. **6**(3): p. 209-240.

136. Esgalhado, M., et al., *Short-chain fatty acids: a link between prebiotics and microbiota in chronic kidney disease.* Future Microbiology, 2017. **12**(15): p. 1413–1425.

137. Weaver, C.M., *Diet, gut microbiome, and bone health.* Current Osteoporosis Reports, 2015. **13**(2): p. 125-130.

138. Wu, Z.A. and H.X. Wang, *A Systematic Review of the Interaction Between Gut Microbiota and Host Health from a Symbiotic Perspective.* SN Comprehensive Clinical Medicine, 2019. **1**(3): p. 224-235.

139. Humphreys, C., *19 - Intestinal Permeability*, in *Textbook of Natural Medicine (Fifth Edition)*, J.E. Pizzorno and M.T. Murray, Editors. 2020, Churchill Livingstone: St. Louis (MO). p. 166-177.e4.

140. Donaldson, G.P., S.M. Lee, and S.K. Mazmanian, *Gut biogeography of the bacterial microbiota.* Nature Reviews Microbiology, 2016. **14**(1): p. 20-32.

141. Rinninella, E., et al., *What is the Healthy Gut Microbiota Composition? A Changing Ecosystem across Age, Environment, Diet, and Diseases.* Microorganisms, 2019. **7**(1): p. 14.

142. Vlasova, A.N., et al., *Comparison of probiotic lactobacilli and bifidobacteria effects, immune responses and rotavirus vaccines and infection in different host species.* Veterinary immunology and immunopathology, 2016. **172**: p. 72-84.

143. Guinane, C.M. and P.D. Cotter, *Role of the gut microbiota in health and chronic gastrointestinal disease: understanding a hidden metabolic organ.* Therapeutic Advances in Gastroenterology, 2013. **6**(4): p. 295-308.

144. Silk, D.B., et al., *Clinical trial: the effects of a trans-galactooligosaccharide prebiotic on faecal microbiota and symptoms in irritable bowel syndrome.* Alimentary Pharmacology & Therapeutics, 2009. **29**(5): p. 508-518.

145. Thursby, E. and N. Juge, *Introduction to the human gut microbiota.* Biochemical Journal 2017. **474**(11): p. 1823-1836.

146. Bosco, N. and M. Noti, *The aging gut microbiome and its impact on host immunity.* Genes & Immunity, 2021. **22**(5): p. 289-303.

147. Yasmin, A., et al., *Prebiotics, gut microbiota and metabolic risks: Unveiling the relationship.* Journal of Functional Foods, 2015. **17**: p. 189-201.

148. Grimaldi, R., et al., *In vitro fermentation of B-GOS: impact on faecal bacterial populations and metabolic activity in autistic and non-autistic children.* FEMS Microbiology Ecology, 2017. **93**(2): p. 1-10.

149. Vieira, A.T., M.M. Teixeira, and F.S. Martins, *The role of probiotics and prebiotics in inducing gut immunity.* Frontiers in Immunology, 2013. **4**: p. 1-12.

150. Silva, Y.P., A. Bernardi, and R.L. Frozza, *The Role of Short-Chain Fatty Acids From Gut Microbiota in Gut-Brain Communication.* Frontiers in Endocrinology, 2020. **11**(25).

151. Frost, G., et al., *The short-chain fatty acid acetate reduces appetite via a central homeostatic mechanism.* Nature communications, 2014. **5**: p. 3611-3611.

152. Williams, E.A., J.M. Coxhead, and J.C. Mathers, *Anti-cancer effects of butyrate: use of micro-array technology to investigate mechanisms.* Proc Nutr Soc, 2003. **62**(1): p. 107-15.

153. Hosseini, E., et al., *Propionate as a health-promoting microbial metabolite in the human gut.* Nutrition Reviews, 2011. **69**(5): p. 245-258.

154. Rowland, I., et al., *Gut microbiota functions: metabolism of nutrients and other food components.* European Journal of Nutrition, 2018. **57**(1): p. 1-24.

155. Morowitz, M.J., E.M. Carlisle, and J.C. Alverdy, *Contributions of intestinal bacteria to nutrition and metabolism in the critically ill.* The Surgical clinics of North America, 2011. **91**(4): p. 771-viii.

156. Nel, I., et al., *MAIT cells, guardians of skin and mucosa?* Mucosal Immunology, 2021. **14**(4): p. 803-814.

157. Corrêa-Oliveira, R., et al., *Regulation of immune cell function by short-chain fatty acids.* Clinical & translational immunology, 2016. **5**(4): p. e73-e73.

158. Park, J., et al., *Short-chain fatty acids induce both effector and regulatory T cells by suppression of histone deacetylases and regulation of the mTOR–S6K pathway.* Mucosal Immunology, 2015. **8**(1): p. 80-93.

159. Zhu, X., et al., *Microbiota-gut-brain axis and the central nervous system.* Oncotarget 2017. **8**(32): p. 53829-53838.

160. Okumura, R. and K. Takeda, *Roles of intestinal epithelial cells in the maintenance of gut homeostasis.* Experimental & Molecular Medicine, 2017. **49**(5): p. e338-e338.

161. Doran, K.S., et al., *Concepts and mechanisms: crossing host barriers.* Cold Spring Harbor perspectives in medicine, 2013. **3**(7): p. a010090.

162. Park, B.S. and J.-O. Lee, *Recognition of lipopolysaccharide pattern by TLR4 complexes.* Experimental &Amp; Molecular Medicine, 2013. **45**: p. e66.

163. Glymenaki, M., et al., *Compositional Changes in the Gut Mucus Microbiota Precede the Onset of Colitis-Induced Inflammation.* Inflamm Bowel Dis, 2017. **23**(6): p. 912-922.

164. Frank, D.N., et al., *Molecular-phylogenetic characterization of microbial community imbalances in human inflammatory bowel diseases.* PNAS, 2007. **104**(34): p. 13780-13785.

165. Harris, L.A. and N. Baffy, *Modulation of the gut microbiota: a focus on treatments for irritable bowel syndrome.* Postgraduate Medicine, 2017. **129**(8): p. 872-888.

166. Williams, N.C., et al., *A prebiotic galactooligosaccharide mixture reduces severity of hyperpnoea-induced bronchoconstriction and markers of airway inflammation.* British Journal of Nutrition, 2016. **116**(5): p. 798-804.

167. Seyedian, S.S., F. Nokhostin, and M.D. Malamir, *A review of the diagnosis, prevention, and treatment methods of inflammatory bowel disease.* Journal of medicine and life, 2019. **12**(2): p. 113-122.

168. Ng, S.C., et al., *Worldwide incidence and prevalence of inflammatory bowel disease in the 21st century: a systematic review of population-based studies.* The Lancet, 2017. **390**(10114): p. 2769-2778.

169. Spiceland, C.M. and N. Lodhia, *Endoscopy in inflammatory bowel disease: Role in diagnosis, management, and treatment.* World journal of gastroenterology, 2018. **24**(35): p. 4014-4020.

170. Agrawal, M., et al., *Approach to the Management of Recently Diagnosed Inflammatory Bowel Disease Patients: A User's Guide for Adult and Pediatric Gastroenterologists.* Gastroenterology, 2021. **161**(1): p. 47-65.

171. Abegunde, A.T., et al., *Environmental risk factors for inflammatory bowel diseases: Evidence based literature review.* World journal of gastroenterology, 2016. **22**(27): p. 6296-6317.

172. Farrell, R.J. and M.A. Peppercorn, *Ulcerative colitis.* The Lancet, 2002. **359**(9303): p. 331-340.

173. Shanahan, F., *Crohn's disease.* The Lancet, 2002. **359**(9300): p. 62-69.

174. Maloy, K.J. and F. Powrie, *Intestinal homeostasis and its breakdown in inflammatory bowel disease.* Nature, 2011. **474**(7351): p. 298-306.

175. Strober, W. and I.J. Fuss, *Proinflammatory cytokines in the pathogenesis of inflammatory bowel diseases.* Gastroenterology, 2011. **140**(6): p. 1756-1767.

176. Triantafillidis, J.K., E. Merikas, and F. Georgopoulos, *Current and emerging drugs for the treatment of inflammatory bowel disease.* Drug design, development and therapy, 2011. **5**: p. 185-210.

177. Katz, J., *The Role of Probiotics in IBD.* Gastroenterology & hepatology, 2006. **2**(1): p. 16-18.

178. Carlson, J.L., et al., *Health Effects and Sources of Prebiotic Dietary Fiber.* Current Developments in Nutrition, 2018. **2**(3): p. 1-8.

179. Gibson, G.R., et al., *Expert consensus document: The International Scientific Association for Probiotics and Prebiotics (ISAPP) consensus statement on the definition and scope of prebiotics.* Nature Review Gastroenterology & Hepatology, 2017. **14**(8): p. 491-502.

180. Mano, M.C.R., et al., *Oligosaccharide biotechnology: an approach of prebiotic revolution on the industry.* Applied Microbiology and Biotechnology, 2017. **102**(1): p. 17-37.

181. Davani-Davari, D., et al., *Prebiotics: Definition, Types, Sources, Mechanisms, and Clinical Applications.* Foods (Basel, Switzerland), 2019. **8**(3): p. 1-27.

182. Mussatto, S.I. and I.M. Mancilha, *Non-digestible oligosaccharides: A review.* Carbohydrate Polymers, 2007. **68**(3): p. 587-597.

183. Rijnierse, A., et al., *Food-derived oligosaccharides exhibit pharmaceutical properties.* Eur J Pharmacol, 2011. **668 Suppl 1**: p. S117-23.

184. Lomax, A.R. and P.C. Calder, *Prebiotics, immune function, infection and inflammation: a review of the evidence.* British Journal of Nutrition, 2009. **101**(5): p. 633-658.

185. Meyer, T.S.M., et al., *Biotechnological Production of Oligosaccharides — Applications in the Food Industry*, in *Food Production and Industry*, H. Ayman and E. Amer, Editors. 2015, InTech: Rijeka, Croatia. p. 26-77.

186. Fernández, J., et al., *Healthy effects of prebiotics and their metabolites against intestinal diseases and colorectal cancer.* AIMS Microbiology, 2015. **1**(1): p. 48-71.

187. Vandamme, E.J. and W. Soetaert, *Biotechnical modification of carbohydrates.* FEMS Microbiology Reviews, 1995. **16**(2-3): p. 163-186.

188. Tzortzis, G. and J. Vulevic, *Galacto-Oligosaccharide Prebiotics*, in *Prebiotics and Probiotics Science and Technology*, D. Charalampopoulos and R.A. Rastall, Editors. 2009, Springer New York: New York, NY. p. 207-244.

189. Suárez, S., et al., *Effect of particle size and enzyme load on the simultaneous reactions of lactose hydrolysis and transgalactosylation with glyoxyl-agarose immobilized β-galactosidase from Aspergillus oryzae.* Process Biochemistry, 2018. **73**: p. 56-64.

190. Yu, L. and D.J. O'Sullivan, *Production of galactooligosaccharides using a hyperthermophilic β-galactosidase in permeabilized whole cells of Lactococcus lactis.* Journal of Dairy Science, 2014. **97**(2): p. 694-703.

191. Dawei, J., et al., *Production and identification of galacto-oligosaccharides from lactose using β-D-galactosidases from Lactobacillus leichmannii 313.* Carbohydrate Polymer Technologies and Applications, 2021. **2**: p. 100038.

192. Logtenberg, M.J., et al., *Touching the High Complexity of Prebiotic Vivinal Galacto-oligosaccharides Using Porous Graphitic Carbon Ultra-High-Performance Liquid Chromatography Coupled to Mass Spectrometry.* Journal of agricultural and food chemistry, 2020. **68**(29): p. 7800-7808.

193. He, Y., et al., *Human colostrum oligosaccharides modulate major immunologic pathways of immature human intestine.* Mucosal Immunology, 2014. **7**: p. 1326.

194. Newburg, D.S., et al., *Human Milk Oligosaccharides and Synthetic Galactosyloligosaccharides Contain 3'-, 4-, and 6'-Galactosyllactose and Attenuate Inflammation in Human T84, NCM-460, and H4 Cells and Intestinal Tissue Ex Vivo.* The Journal of Nutrition, 2016. **146**(2): p. 358-367.

195. Lehmann, S., et al., *In Vitro Evidence for Immune-Modulatory Properties of Non-Digestible Oligosaccharides: Direct Effect on Human Monocyte Derived Dendritic Cells.* PLoS One, 2015. **10**(7): p. 1-15.

196. Torres, D.P.M., et al., *Galacto-Oligosaccharides: Production, Properties, Applications, and Significance as Prebiotics.* Comprehensive Reviews in Food Science and Food Safety, 2010. **9**(5): p. 438-454.

197. Davis, L.M., et al., *Barcoded pyrosequencing reveals that consumption of galactooligosaccharides results in a highly specific bifidogenic response in humans.* PLoS One, 2011. **6**(9): p. e25200.

198. Scalabrin, D.M.F., et al., *New Prebiotic Blend of Polydextrose and Galacto-oligosaccharides Has a Bifidogenic Effect in Young Infants.* Journal of Pediatric Gastroenterology and Nutrition, 2012. **54**(3).

199. Vulevic, J., et al., *Modulation of the fecal microflora profile and immune function by a novel trans-galactooligosaccharide mixture (B-GOS) in healthy elderly volunteers.* American Journal of Clinical Nutrition, 2008. **88**: p. 1438-1446.

200. Vulevic, J., et al., *Influence of galacto-oligosaccharide mixture (B-GOS) on gut microbiota, immune parameters and metabonomics in elderly persons.* British Journal of Nutrition, 2015. **114**(4): p. 586-595.

201. Grimaldi, R., et al., *Fermentation properties and potential prebiotic activity of Bimuno® galacto-oligosaccharide (65% galacto-oligosaccharide content) on in vitro gut microbiota parameters.* British Journal of Nutrition, 2016. **116**(3): p. 480-486.

202. Searle, L.E., et al., *Purified galactooligosaccharide, derived from a mixture produced by the enzymic activity of Bifidobacterium bifidum, reduces Salmonella enterica serovar Typhimurium adhesion and invasion in vitro and in vivo.* Journal of Medical Microbiology, 2010. **59**(Pt 12): p. 1428-1439.

203. Drakoularakou, A., et al., *A double-blind, placebo-controlled, randomized human study assessing the capacity of a novel galacto-oligosaccharide mixture in reducing travellers' diarrhoea.* European Journal of Clinical Nutrition, 2009. **64**(2): p. 146-152.

204. Giddings, S.L., A.M. Stevens, and D.T. Leung, *Traveler's Diarrhea.* The Medical clinics of North America, 2016. **100**(2): p. 317-330.

205. Shoaf, K., et al., *Prebiotic galactooligosaccharides reduce adherence of enteropathogenic Escherichia coli to tissue culture cells.* Infect Immun, 2006. **74**(12): p. 6920-8.

206. Vulevic, J., et al., *Effect of a prebiotic galactooligosaccharide mixture (B-GOS®) on gastrointestinal symptoms in adults selected from a general population who suffer with bloating, abdominal pain, or flatulence.* Neurogastroenterology & Motility, 2018. **30**(11): p. e13440.

207. Bhatia, S., et al., *Galacto-oligosaccharides may directly enhance intestinal barrier function through the modulation of goblet cells.* Mol Nutr Food Res, 2015. **59**(3): p. 566-73.

208. Moro, G., et al., *A mixture of prebiotic oligosaccharides reduces the incidence of atopic dermatitis during the first six months of age.* Arch Dis Child, 2006. **91**(10): p. 814-9.

209. Grüber, C., et al., *Reduced occurrence of early atopic dermatitis because of immunoactive prebiotics among low-atopy-risk infants.* J Allergy Clin Immunol, 2010. **126**(4): p. 791-7.

210. Schouten, B., et al., *Oligosaccharide-induced whey-specific CD25(+) regulatory T-cells are involved in the suppression of cow milk allergy in mice.* J Nutr, 2010. **140**(4): p. 835-41.

211. Schouten, B., et al., *A potential role for CD25+ regulatory T-cells in the protection against casein allergy by dietary non-digestible carbohydrates.* British Journal of Nutrition, 2011. **107**(1): p. 96-105.

212. Vos, A.P., et al., *Dietary supplementation with specific oligosaccharide mixtures decreases parameters of allergic asthma in mice.* Int Immunopharmacol, 2007. **7**(12): p. 1582-7.

213. Schmidt, K., et al., *Prebiotic intake reduces the waking cortisol response and alters emotional bias in healthy volunteers.* Psychopharmacology, 2015. **232**(10): p. 1793-801.

214. EFSA Panel on Dietetic Products, N. and Allergies, *Scientific Opinion on the substantiation of a health claim related to "native chicory inulin" and maintenance of normal defecation by increasing stool frequency pursuant to Article 13.5 of Regulation (EC) No 1924/2006.* EFSA Journal, 2015. **13**(1): p. 3951.

215. Gourbeyre, P., S. Denery, and M. Bodinier, *Probiotics, prebiotics, and synbiotics: impact on the gut immune system and allergic reactions.* Journal of Leukocyte Biology, 2011. **89**(5): p. 685-695.

216. EFSA Panel on Dietetic Products, N.a.A.N., *Scientific Opinion on the substantiation of health claims related to galacto-oligosaccharides (GOS) and reduction of gastro-intestinal discomfort (ID 763) and decreasing potentially pathogenic microorganisms (ID 765) pursuant to Article 13(1) of Regulation (EC) No 1924/20061.* EFSA Journal, 2011. **9**(4): p. 1-15.

217. Huttenhower, C., et al., *Structure, function and diversity of the healthy human microbiome.* Nature, 2012. **486**(7402): p. 207-214.

218. Rios-Covian, D., et al., *Intestinal Short Chain Fatty Acids and their Link with Diet and Human Health.* Front Microbiol, 2016. **7**: p. 1-9.

219. Layden, B.T., et al., *Short chain fatty acids and their receptors: new metabolic targets.* Translational Research, 2013. **161**(3): p. 131-140.

220. Kamada, N., et al., *Control of pathogens and pathobionts by the gut microbiota.* Nature immunology, 2013. **14**(7): p. 685-690.

221. Pickard, J.M., et al., *Gut microbiota: Role in pathogen colonization, immune responses, and inflammatory disease.* Immunological reviews, 2017. **279**(1): p. 70-89.

222. Valentini, M., et al., *Immunomodulation by Gut Microbiota: Role of Toll-Like Receptor Expressed by T Cells.* Journal of Immunology Research, 2014. **2014**: p. 1-8.

223. Shokryazdan, P., et al., *Effects of prebiotics on immune system and cytokine expression.* Medical Microbiology and Immunology, 2017. **206**(1): p. 1-9.

224. Schley, P.D. and C.J. Field, *The immune-enhancing effects of dietary fibres and prebiotics.* Br J Nutr, 2002. **87 Suppl 2**: p. S221-S230.

225. Weaver, L.T., M.F. Laker, and R. Nelson, *Intestinal permeability in the newborn.* Archives of disease in childhood, 1984. **59**(3): p. 236-241.

226. Commare, C.E. and K.A. Tappenden, *Development of the infant intestine: implications for nutrition support.* Nutr Clin Pract, 2007. **22**(2): p. 159-73.

227. Michielan, A. and R. D'Incà, *Intestinal Permeability in Inflammatory Bowel Disease: Pathogenesis, Clinical Evaluation, and Therapy of Leaky Gut.* Mediators of Inflammation, 2015. **2015**: p. 1-10.

228. Fasano, A., *Gut permeability, obesity, and metabolic disorders: who is the chicken and who is the egg?* The American Journal of Clinical Nutrition, 2016. **105**(1): p. 3-4.

229. Vajro, P., G. Paolella, and A. Fasano, *Microbiota and gut-liver axis: their influences on obesity and obesity-related liver disease.* J Pediatr Gastroenterol Nutr, 2013. **56**(5): p. 461-8.

230. Vaarala, O., *Leaking gut in type 1 diabetes.* Curr Opin Gastroenterol, 2008. **24**(6): p. 701-6.

231. Nicoletti, A., et al., *Intestinal permeability in the pathogenesis of liver damage: From non-alcoholic fatty liver disease to liver transplantation.* World J Gastroenterol, 2019. **25**(33): p. 4814-4834.

232. Camilleri, M., et al., *Role for diet in normal gut barrier function: developing guidance within the framework of food-labeling regulations.* American journal of physiology. Gastrointestinal and liver physiology, 2019. **317**(1): p. G17-G39.

233. Gnoth, M.J., et al., *Investigations of the in vitro transport of human milk oligosaccharides by a Caco-2 monolayer using a novel high performance liquid chromatography-mass spectrometry technique.* The Journal of Biological Chemistry, 2001. **276**(37): p. 34363-34370.

234. Eiwegger, T., et al., *Prebiotic oligosaccharides: in vitro evidence for gastrointestinal epithelial transfer and immunomodulatory properties.* Pediatric Allergy and Immunology, 2010. **21**(8): p. 1179-1188.

235. Prieto, P.A., *In Vitro and Clinical Experiences with a Human Milk Oligosaccharide, Lacto-N-neoTetraose, and Fructooligosaccharides.* Food & Food Ingredients Journal of Japan, 2005. **210**(11): p. 1018-1030.

236. De Leoz, M.L., et al., *A quantitative and comprehensive method to analyze human milk oligosaccharide structures in the urine and feces of infants.* Anal Bioanal Chem, 2013. **405**(12): p. 4089-105.

237. Bode, L., et al., *Inhibition of monocyte, lymphocyte, and neutrophil adhesion to endothelial cells by human milk oligosaccharides.* Thrombosis and Haemostasis, 2004. **92**(6): p. 1402-1410.

238. Eiwegger, T., et al., *Human milk--derived oligosaccharides and plant-derived oligosaccharides stimulate cytokine production of cord blood T-cells in vitro.* Pediatric Research, 2004. **56**(4): p. 536-540.

239. Zenhom, M., et al., *Prebiotic oligosaccharides reduce proinflammatory cytokines in intestinal Caco-2 cells via activation of PPARgamma and peptidoglycan recognition protein 3.* J Nutr, 2011. **141**(5): p. 971-7.

240. Vogt, L., et al., *Immune Modulation by Different Types of β2→1-Fructans Is Toll-Like Receptor Dependent.* PLOS ONE, 2013. **8**(7): p. 1-12.

241. Capitan-Canadas, F., et al., *Prebiotic oligosaccharides directly modulate proinflammatory cytokine production in monocytes via activation of TLR4.* Molecular Nutrition & Food Research, 2014. **58**(5): p. 1098-1110.

242. Ortega-Gonzalez, M., et al., *Nondigestible oligosaccharides exert nonprebiotic effects on intestinal epithelial cells enhancing the immune response via activation of TLR4-NFkB.* Molecular Nutrition & Food Research 2014. **58**(2): p. 384-393.

243. Vendrig, J.C., L.E. Coffeng, and J. Fink-Gremmels, *In vitro evaluation of defined oligosaccharide fractions in an equine model of inflammation.* BMC Veterinary Research 2013. **9**(147): p. 1-10.

244. Lin, C.C., et al., *Rice bran feruloylated oligosaccharides activate dendritic cells via Toll-like receptor 2 and 4 signaling.* Molecules (Basel, Switzerland), 2014. **19**(4): p. 5325-5347.

245. Lin, C.C., et al., *Rice bran feruloylated oligosaccharides activate dendritic cells via Toll-like receptor 2 and 4 signaling.* Molecules, 2014. **19**(4): p. 5325-47.

246. Fransen, F., et al., *beta2-->1-Fructans Modulate the Immune System In Vivo in a Microbiota-Dependent and -Independent Fashion.* Front Immunol, 2017. **8**: p. 154.

247. Tucureanu, M.M., et al., *Lipopolysaccharide-induced inflammation in monocytes/macrophages is blocked by liposomal delivery of G(i)-protein inhibitor.* International journal of nanomedicine, 2017. **13**: p. 63-76.

248. Scaldaferri, F., et al., *Gut microbial flora, prebiotics, and probiotics in IBD: their current usage and utility.* Biomed Res Int, 2013. **2013**: p. 1-9.

249. Hedin, C., K. Whelan, and J.O. Lindsay, *Evidence for the use of probiotics and prebiotics in inflammatory bowel disease: a review of clinical trials.* Proc Nutr Soc, 2007. **66**(3): p. 307-15.

250. Damaskos, D. and G. Kolios, *Probiotics and prebiotics in inflammatory bowel disease: microflora 'on the scope'.* British journal of clinical pharmacology, 2008. **65**(4): p. 453-467.

251. Looijer-van Langen, M.A.C. and L.A. Dieleman, *Prebiotics in chronic intestinal inflammation.* Inflammatory bowel diseases, 2009. **15**(3): p. 454-462.

252. Akram, W., N. Garud, and R. Joshi, *Role of inulin as prebiotics on inflammatory bowel disease.* Drug Discoveries & Therapeutics, 2019. **13**(1): p. 1-8.

253. Wilson, B., et al., *Prebiotic Galactooligosaccharide Supplementation in Adults with Ulcerative Colitis: Exploring the Impact on Peripheral Blood Gene Expression, Gut Microbiota, and Clinical Symptoms.* Nutrients, 2021. **13**(10).

254. Valatas, V., G. Bamias, and G. Kolios, *Experimental colitis models: Insights into the pathogenesis of inflammatory bowel disease and translational issues.* European Journal of Pharmacology, 2015. **759**: p. 253-264.

255. Hartog, A., et al., *A potential role for regulatory T-cells in the amelioration of DSS induced colitis by dietary non-digestible polysaccharides.* The Journal of Nutritional Biochemistry, 2015. **26**(3): p. 227-233.

256. Welters, C.F., et al., *Effect of dietary inulin supplementation on inflammation of pouch mucosa in patients with an ileal pouch-anal anastomosis.* Dis Colon Rectum, 2002. **45**(5): p. 621-7.

257. Casellas, F., et al., *Oral oligofructose-enriched inulin supplementation in acute ulcerative colitis is well tolerated and associated with lowered faecal calprotectin.* Aliment Pharmacol Ther, 2007. **25**(9): p. 1061-7.

258. De Preter, V., et al., *Metabolic profiling of the impact of oligofructose-enriched inulin in Crohn's disease patients: a double-blinded randomized controlled trial.* Clinical and translational gastroenterology, 2013. **4**(1): p. 1-30.

259. Lindsay, J.O., et al., *Clinical, microbiological, and immunological effects of fructo-oligosaccharide in patients with Crohn's disease.* Gut, 2006. **55**(3): p. 348-55.

260. Benjamin, J.L., et al., *Randomised, double-blind, placebo-controlled trial of fructo-oligosaccharides in active Crohn's disease.* Gut, 2011. **60**(7): p. 923-9.

261. Hallert, C., M. Kaldma, and B.G. Petersson, *Ispaghula husk may relieve gastrointestinal symptoms in ulcerative colitis in remission.* Scand J Gastroenterol, 1991. **26**(7): p. 747-50.

262. Kanauchi, O., et al., *Treatment of ulcerative colitis patients by long-term administration of germinated barley foodstuff: multi-center open trial.* Int J Mol Med, 2003. **12**(5): p. 701-4.

263. Hanai, H., et al., *Germinated barley foodstuff prolongs remission in patients with ulcerative colitis.* Int J Mol Med, 2004. **13**(5): p. 643-7.

264. Mitsuyama, K., et al., *Treatment of ulcerative colitis with germinated barley foodstuff feeding: a pilot study.* Alimentary pharmacology & therapeutics, 1998. **12**(12): p. 1225-1230.

265. Stemcell. *Human Peripheral Blood Mononuclear Cells, Frozen*. [cited 2017 13 November]; Available from: https://www.stemcell.com/products/product-types/primary-and-cultured-cells/human-peripheral-blood-mononuclear-cells-frozen.html.

266. Cargnello, M. and P.P. Roux, *Activation and function of the MAPKs and their substrates, the MAPK-activated protein kinases.* Microbiology and molecular biology reviews : MMBR, 2011. **75**(1): p. 50-83.

267. Zhang, W. and H.T. Liu, *MAPK signal pathways in the regulation of cell proliferation in mammalian cells.* Cell Research, 2002. **12**(1): p. 9-18.

268. Ando, Y., et al., *Concanavalin A-mediated T cell proliferation is regulated by herpes virus entry mediator costimulatory molecule.* In Vitro Cellular & Developmental Biology - Animal, 2014. **50**(4): p. 313-320.

269. Hawkins, E.D., et al., *Quantal and graded stimulation of B lymphocytes as alternative strategies for regulating adaptive immune responses.* Nature Communications, 2013. **4**(1): p. 2406.

270. Ai, W., et al., *Optimal method to stimulate cytokine production and its use in immunotoxicity assessment.* International journal of environmental research and public health, 2013. **10**(9): p. 3834-3842.

271. Eckle, S.B., et al., *Recognition of Vitamin B Precursors and Byproducts by Mucosal Associated Invariant T Cells.* Journal of Biological Chemistry, 2015. **290**(51): p. 30204-30211.

272. Chen, Z., et al., *Mucosal-associated invariant T-cell activation and accumulation after in vivo infection depends on microbial riboflavin synthesis and co-stimulatory signals.* Mucosal Immunology, 2016. **10**: p. 58-68.

273. Alexopoulou, L., et al., *Recognition of double-stranded RNA and activation of NF-kappaB by Toll-like receptor 3.* Nature, 2001. **413**(6857): p. 732-8.

274. Damsgaard, C.T., et al., *Whole-blood culture is a valid low-cost method to measure monocytic cytokines - a comparison of cytokine production in cultures of human whole-blood, mononuclear cells and monocytes.* Journal of Immunological Methods, 2009. **340**(2): p. 95-101.

275. Katial, R.K., et al., *Cytokine Production in Cell Culture by Peripheral Blood Mononuclear Cells from Immunocompetent Hosts.* Clinical And Diagnostic Laboratory Immunology, 1998. **5**(1): p. 78-81.

276. Lomax, A.R., et al., *Inulin-Type beta2-1 Fructans have Some Effect on the Antibody Response to Seasonal Influenza Vaccination in Healthy Middle-Aged Humans.* Frontiers in Immunology, 2015. **6**: p. 1-8.

277. Childs, C.E., et al., *Xylo-oligosaccharides alone or in synbiotic combination with Bifidobacterium animalis subsp. lactis induce bifidogenesis and modulate markers of immune function in healthy adults: a double-blind, placebo-controlled, randomised, factorial cross-over study.* British Journal of Nutrition, 2014. **111**(11): p. 1945-1956.

278. Sullivan, K.E., et al., *Measurement of Cytokine Secretion, Intracellular Protein Expression, and mRNA in Resting and Stimulated Peripheral Blood Mononuclear Cells.* Clinical and Diagnostic Laboratory Immunology, 2000. **7**(6): p. 920-924.

279. Howson, L.J., et al., *MAIT cell clonal expansion and TCR repertoire shaping in human volunteers challenged with Salmonella Paratyphi A.* Nature Communications, 2018. **9**(1): p. 253.

280. Kunzmann, V., et al., *Polyinosinic-polycytidylic acid-mediated stimulation of human gammadelta T cells via CD11c dendritic cell-derived type I interferons.* Immunology, 2004. **112**(3): p. 369-377.

281. Avelar-Freitas, B.A., et al., *Trypan blue exclusion assay by flow cytometry.* Brazilian Journal of Medical and Biological Research, 2014. **47**(4): p. 307-315.

282. BD Biosciences. *Fixable viability stain 510*. [Technical data sheet 564406 Rev. 1] 21/03/2019]; Available from: http://www.bdbiosciences.com/ds/pm/tds/564406.pdf.

283. BD Biosciences. *Fixable viability stain 780* [Technical data sheet 565388 Rev. 2] 21/01/2019]; Available from: http://www.bdbiosciences.com/ds/pm/tds/565388.pdf.

284. Castillo-Hair, S. *FlowCal: Software for Analysis and Calibration of Flow Cytometry Data*. 2016 [cited 2019 04/03/2019]; Available from: https://benchling.com/pub/tabor-flowcal.

285. Abcam. *Flow cytometry immunophenotyping*. 2019 01/03/2019]; Available from: https://www.abcam.com/protocols/flow-cytometry-immunophenotyping.

286. Biolegend. *Intracellular Flow Cytometry Staining Protocol*. [cited 2021 19/02/2021]; Available from: https://www.biolegend.com/en-us/protocols/intracellular-flow-cytometry-staining-protocol.

287. R&D Systems. *Human Premixed Multi-Analyte Kit*. 2018 [cited 2019 06/03/2019]; Available from: https://resources.rndsystems.com/pdfs/datasheets/lxsahm.pdf.

288. Schultheiss, O.C. and S.J. Stanton, *Assessment of salivary hormones*, in *Methods in social neuroscience.* 2009, Guilford Press: New York, NY, US. p. 17-44.

289. Chung, K.F., *Chapter 27 - Cytokines*, in *Asthma and COPD (Second Edition)*, P.J. Barnes, et al., Editors. 2009, Academic Press: Oxford. p. 327-341.

290. Wurster, A.L. and M.J. Grusby, *Cytokines*, in *Encyclopedia of Biological Chemistry*, W.J. Lennarz and M.D. Lane, Editors. 2004, Elsevier: New York. p. 550-555.

291. FDA, *Guidance for Industry: Pyrogen and Endotoxins Testing: Questions and Answers*, U.S. Department of Health and Human Services, Editor. 2012: Online. p. 1-9.

292. GenScript. *What is Endotoxin?* 2002 [cited 2019 25/03/2019]; Available from: https://www.genscript.com/endotoxin-kits.html.

293. Thermo Fisher Scientific. *Pierce Chromogenic Endotoxin Quant Kit User Guide*. 2018 12/07/2018 26/02/2019]; Available from: https://www.thermofisher.com/document-connect/document-connect.html?url=https%3A%2F%2Fassets.thermofisher.com%2FTFS-Assets%2FLSG%2Fmanuals%2FMAN0017902_ChromogenicEndotoxinQuantKit_UG.pdf&title=VXNlciBHdWlkZTogUGllcmNlIENocm9tb2dlbmljIEVuZG90b3hpbiBRdWFudCBLaXQ=.

294. Thermo Fisher Scientific. *DetoxiGel Endotoxin Removing Gel Kit User Guide*. 2018 12/07/2018 26/02/2019].

295. Numis, A.L., et al., *Comparison of multiplex cytokine assays in a pediatric cohort with epilepsy.* Heliyon, 2021. **7**(3): p. e06445.

296. Vinolo, M.A.R., et al., *Regulation of inflammation by short chain fatty acids.* Nutrients, 2011. **3**(10): p. 858-876.

297. Elia, M., et al., *Evaluation of mannitol, lactulose and 51Cr-labelled ethylenediaminetetra-acetate as markers of intestinal permeability in man.* Clin Sci (Lond), 1987. **73**(2): p. 197-204.

298. Molis, C., et al., *Digestion, excretion, and energy value of fructooligosaccharides in healthy humans.* Am J Clin Nutr, 1996. **64**: p. 324-328.

299. Miner-Williams, W.M. and P.J. Moughan, *Intestinal barrier dysfunction: implications for chronic inflammatory conditions of the bowel.* Nutrition Research Reviews, 2016. **29**(1): p. 40-59.

300. Akbari, P., et al., *Characterizing microbiota-independent effects of oligosaccharides on intestinal epithelial cells: insight into the role of structure and size : Structure-activity relationships of non-digestible oligosaccharides.* Eur J Nutr, 2017. **56**(5): p. 1919-1930.

301. Bomhof, M., H. Skochylas, and R. Reimer, *Determining the gut microbiota-independent effects of prebiotic fiber in diet-induced obese rats.* The FASEB Journal, 2013. **27**(S1): p. 1056.6-1056.6.

302. Leppink, J., P. O'Sullivan, and K. Winston, *Effect size - large, medium, and small.* Perspectives on medical education, 2016. **5**(6): p. 347-349.

303. Lu, X.-X., et al., *Polymyxin B as an inhibitor of lipopolysaccharides contamination of herb crude polysaccharides in mononuclear cells.* Chinese Journal of Natural Medicines, 2017. **15**(7): p. 487-494.

304. Cardoso, L.S., et al., *Polymyxin B as inhibitor of LPS contamination of Schistosoma mansoni recombinant proteins in human cytokine analysis.* Microbial cell factories, 2007. **6**: p. 1-1.

305. Staples, K.J., et al., *IL-10 Induces IL-10 in Primary Human Monocyte-Derived Macrophages via the Transcription Factor Stat3.* The Journal of Immunology, 2007. **178**(8): p. 4779-4785.

306. Xiao, L., et al., *Human milk oligosaccharides promote immune tolerance via direct interactions with human dendritic cells.* European Journal of Immunology, 2019. **49**(7): p. 1001-1014.

307. Perdijk, O., et al., *Induction of human tolerogenic dendritic cells by 3'-sialyllactose via TLR4 is explained by LPS contamination.* Glycobiology, 2017. **28**(3): p. 126-130.

308. Weinberg, A., et al., *Viability and functional activity of cryopreserved mononuclear cells.* Clinical and diagnostic laboratory immunology, 2000. **7**(4): p. 714-716.

309. De Groote, D., et al., *Direct stimulation of cytokines (IL-1ß, TNF-α, IL-6, IL-2, IFN-γ and GM-CSF) in whole blood. I. Comparision with isolated PBMC stimulation.* Cytokine 1992. **4**(3): p. 239-248.

310. L. Jansky, P. Reymanova, and J. Kopecky, *Dynamics of Cytokine Production in Human Peripheral Blood Mononuclear Cells Stimulated by LPS or Infected by Borrelia.* Physiol. Res., 2003(52): p. 593-598.

311. Ngkelo, A., et al., *LPS induced inflammatory responses in human peripheral blood mononuclear cells is mediated through NOX4 and Gia dependent PI-3kinase signalling.* Journal of Inflammation, 2012. **9**(1): p. 1-7.

312. Mita, Y., et al., *Toll-like receptor 4 surface expression on human monocytes and B cells is modulated by IL-2 and IL-4.* Immunol Lett, 2002. **81**(1): p. 71-5.

313. Del Fabbro, S., P.C. Calder, and C.E. Childs, *Microbiota-independent immunological effects of non-digestible oligosaccharides in the context of inflammatory bowel diseases.* Proc Nutr Soc, 2020: p. 1-11.

314. De Marco, S., et al., *Probiotic Cell-Free Supernatants Exhibited Anti-Inflammatory and Antioxidant Activity on Human Gut Epithelial Cells and Macrophages Stimulated with LPS.* Evidence-based complementary and alternative medicine : eCAM, 2018. **2018**: p. 1756308-1756308.

315. Shomali, N., et al., *Harmful effects of high amounts of glucose on the immune system: An updated review.* Biotechnology and Applied Biochemistry, 2021. **68**(2): p. 404-410.

316. Calder, P.C., G. Dimitriadis, and P. Newsholme, *Glucose metabolism in lymphoid and inflammatory cells and tissues.* Curr Opin Clin Nutr Metab Care, 2007. **10**(4): p. 531-40.

317. Yeh, S.-L., et al., *Fructo-oligosaccharide attenuates the production of pro-inflammatory cytokines and the activation of JNK/Jun pathway in the lungs of D-galactose-treated Balb/cJ mice.* European journal of nutrition, 2014. **53**(2): p. 449-456.

318. Uddin, M.N., et al., *Toxic effects of D-galactose on thymus and spleen that resemble aging.* J Immunotoxicol, 2010. **7**(3): p. 165-73.

319. Paasela, M., et al., *Lactose inhibits regulatory T-cell-mediated suppression of effector T-cell interferon-γ and IL-17 production.* The British journal of nutrition, 2014. **112**(11): p. 1819-1825.

320. Miao, Y.-L., et al., *Gene expression profiles in peripheral blood mononuclear cells of ulcerative colitis patients.* World journal of gastroenterology, 2013. **19**(21): p. 3339-3346.

321. Sieber, G., et al., *Abnormalities of B-cell activation and immunoregulation in patients with Crohn's disease.* Gut, 1984. **25**(11): p. 1255-61.

322. Rabe, H., et al., *Distinct patterns of naive, activated and memory T and B cells in blood of patients with ulcerative colitis or Crohn's disease.* Clinical and experimental immunology, 2019. **197**(1): p. 111-129.

323. Funderburg, N.T., et al., *Circulating CD4(+) and CD8(+) T cells are activated in inflammatory bowel disease and are associated with plasma markers of inflammation.* Immunology, 2013. **140**(1): p. 87-97.

324. Kurakevich, E., et al., *Milk oligosaccharide sialyl(alpha2,3)lactose activates intestinal CD11c+ cells through TLR4.* Proc Natl Acad Sci U S A, 2013. **110**(43): p. 17444-9.

325. Ciesielska, A., M. Matyjek, and K. Kwiatkowska, *TLR4 and CD14 trafficking and its influence on LPS-induced pro-inflammatory signaling.* Cellular and molecular life sciences : CMLS, 2021. **78**(4): p. 1233-1261.

326. Tadema, H., et al., *Increased expression of Toll-like receptors by monocytes and natural killer cells in ANCA-associated vasculitis.* PloS one, 2011. **6**(9): p. e24315-e24315.

327. Liao, C.-M., M.I. Zimmer, and C.-R. Wang, *The functions of type I and type II natural killer T cells in inflammatory bowel diseases.* Inflammatory bowel diseases, 2013. **19**(6): p. 1330-1338.

328. Grose, R.H., et al., *Deficiency of invariant NK T cells in Crohn's disease and ulcerative colitis.* Dig Dis Sci, 2007. **52**(6): p. 1415-22.

329. Brailey, P.M., M. Lebrusant-Fernandez, and P. Barral, *NKT cells and the regulation of intestinal immunity: a two-way street.* The FEBS Journal, 2020. **287**(9): p. 1686-1699.

330. Lai, L.J., J. Shen, and Z.H. Ran, *Natural killer T cells and ulcerative colitis.* Cell Immunol, 2019. **335**: p. 1-5.

331. Holland, N., et al., *Reduced intracellular T-helper 1 interferon-gamma in blood of newly diagnosed children with Crohn's disease and age-related changes in Th1/Th2 cytokine profiles.* Pediatric research, 2008. **63**(3): p. 257-262.

332. Tindemans, I., M.E. Joosse, and J.N. Samsom, *Dissecting the Heterogeneity in T-Cell Mediated Inflammation in IBD.* Cells, 2020. **9**(1): p. 110.

333. Choy, M.C., et al., *P036 Expression of CD69 on peripheral lymphocytes predicts treatment response in Acute Severe ulcerative colitis.* Journal of Crohn's and Colitis, 2019. **13**(Supplement_1): p. S104-S104.

334. Radulovic, K., et al., *CD69 Regulates Type I IFN-Induced Tolerogenic Signals to Mucosal CD4 T Cells That Attenuate Their Colitogenic Potential.* The Journal of Immunology, 2012. **188**(4): p. 2001-2013.

335. Fuss, I.J., et al., *Both IL-12p70 and IL-23 are synthesized during active Crohn's disease and are down-regulated by treatment with anti-IL-12 p40 monoclonal antibody.* Inflamm Bowel Dis, 2006. **12**(1): p. 9-15.

336. Wright, E.M., M.n.G. Martín, and E. Turk, *Intestinal absorption in health and disease—sugars.* Best Practice & Research Clinical Gastroenterology, 2003. **17**(6): p. 943-956.

337. Bosshart, H. and M. Heinzelmann, *THP-1 cells as a model for human monocytes.* Annals of Translational Medicine, 2016. **4**(21): p. 22.

338. Dehus, O., T. Hartung, and C. Hermann, *Endotoxin evaluation of eleven lipopolysaccharides by whole blood assay does not always correlate with Limulus amebocyte lysate assay.* J Endotoxin Res, 2006. **12**(3): p. 171-80.

339. Depeint, F., et al., *Prebiotic evaluation of a novel galactooligosaccharide mixture produced by the enzymatic activity of Bifidobacterium bifidum NCIMB 41171, in healthy humans: a randomized, double-blind, crossover, placebo-controlled intervention study.* The American Journal of Clinical Nutrition, 2008. **87**: p. 785-791.

340. Gänzle, M.G., *Lactose and Oligosaccharides | Lactose: Galacto-Oligosaccharides*, in *Encyclopedia of Dairy Sciences (Second Edition)*, J.W. Fuquay, Editor. 2011, Academic Press: San Diego. p. 209-216.

341. Tzortzis, G., A.K. Goulas, and G.R. Gibson, *Synthesis of prebiotic galactooligosaccharides using whole cells of a novel strain, Bifidobacterium bifidum NCIMB 41171.* Applied Microbiology and Biotechnology, 2005. **68**(3): p. 412-416.

342. Ito, H., et al., *Degree of polymerization of inulin-type fructans differentially affects number of lactic acid bacteria, intestinal immune functions, and immunoglobulin A secretion in the rat cecum.* Journal of Agriculture and Food Chemistry, 2011. **59**(10): p. 5771-5778.

343. He, Y., N.T. Lawlor, and D.S. Newburg, *Human Milk Components Modulate Toll-Like Receptor-Mediated Inflammation.* Adv Nutr, 2016. **7**(1): p. 102-11.

344. He, Y., N.T. Lawlor, and D.S. Newburg, *Human Milk Components Modulate Toll-Like Receptor-Mediated Inflammation.* Advances in nutrition (Bethesda, Md.), 2016. **7**(1): p. 102-111.

345. Yañez-Ñeco, C.V., et al., *Galactooligosaccharide Production from Pantoea anthophila Strains Isolated from "Tejuino", a Mexican Traditional Fermented Beverage.* Catalysts, 2017. **7**(8): p. 242.

346. Ju, J.K., et al., *Activation, Deficiency, and Reduced IFN-γ Production of Mucosal-Associated Invariant T Cells in Patients with Inflammatory Bowel Disease.* Journal of Innate Immunity, 2020. **12**(5): p. 422-434.

347. Toubal, A., et al., *Mucosal-associated invariant T cells and disease.* Nature Reviews Immunology, 2019. **19**(10): p. 643-657.

348. Garner, L.C., P. Klenerman, and N.M. Provine, *Insights Into Mucosal-Associated Invariant T Cell Biology From Studies of Invariant Natural Killer T Cells.* Frontiers in Immunology, 2018. **9**(1478).

349. Patel, O., et al., *Recognition of vitamin B metabolites by mucosal-associated invariant T cells.* Nature Communications, 2013. **4**: p. 1-9.

350. Talbott, M.C., L.T. Miller, and N.I. Kerkvliet, *Pyridoxine supplementation: effect on lymphocyte responses in elderly persons.* The American Journal of Clinical Nutrition, 1987. **46**(4): p. 659-664.

351. Kwak, H.-K., et al., *Improved Vitamin B-6 Status Is Positively Related to Lymphocyte Proliferation in Young Women Consuming a Controlled Diet.* The Journal of Nutrition, 2002. **132**(11): p. 3308-3313.

352. Invitrogen. *Detecting rare events using flow cytometry: a step-by-step guide*. [cited 2021 27/04/2021]; Available from: https://www.thermofisher.com/uk/en/home/products-and-services/promotions/rare-events-guide.html.

353. Nylander, S. and I. Kalies, *Brefeldin A, but not monensin, completely blocks CD69 expression on mouse lymphocytes:: efficacy of inhibitors of protein secretion in protocols for intracellular cytokine staining by flow cytometry.* Journal of Immunological Methods, 1999. **224**(1): p. 69-76.

354. O'Neil-Andersen, N.J. and D.A. Lawrence, *Differential modulation of surface and intracellular protein expression by T cells after stimulation in the presence of monensin or brefeldin A.* Clinical and diagnostic laboratory immunology, 2002. **9**(2): p. 243-250.

355. Gawlowski, T., et al., *AGEs and methylglyoxal induce apoptosis and expression of Mac-1 on neutrophils resulting in platelet—neutrophil aggregation.* Thrombosis Research, 2007. **121**(1): p. 117-126.

356. Gebru, Y.A., et al., *Pathophysiological Roles of Mucosal-Associated Invariant T Cells in the Context of Gut Microbiota-Liver Axis.* Microorganisms, 2021. **9**(2).

357. Dias, J., et al., *The CD4(-)CD8(-) MAIT cell subpopulation is a functionally distinct subset developmentally related to the main CD8(+) MAIT cell pool.* Proc Natl Acad Sci U S A, 2018. **115**(49): p. E11513-e11522.

358. McGhee, J.R., et al., *Involvement of Mitogen-Activated Protein Kinase Pathways in Interleukin-8 Production by Human Monocytes and Polymorphonuclear Cells Stimulated with Lipopolysaccharide or Mycoplasma fermentans Membrane Lipoproteins.* Infection and Immunity, 1999. **67**(2): p. 688-693.

359. Vitales-Noyola, M., et al., *Patients with Systemic Lupus Erythematosus Show Increased Levels and Defective Function of CD69(+) T Regulatory Cells.* Mediators Inflamm, 2017. **2017**: p. 2513829.

360. Perdijk, O., et al., *The oligosaccharides 6'-sialyllactose, 2'-fucosyllactose or galactooligosaccharides do not directly modulate human dendritic cell differentiation or maturation.* PLOS ONE, 2018. **13**(7): p. e0200356.

361. UWCCC Flow Cytometry Laboratory. *Titrating Antibodies for Flow Cytometry*. 2016 05/05/2016 21/03/2019]; Available from: https://cancer.wisc.edu/research/wp-content/uploads/2017/03/Flow_TechNotes_Antibody-Titrations_20170918.pdf.